The impact of novel AMP-activated protein kinase (AMPK) activators and glucose variability on pancreatic α-cell function

Submitted by Katie Partridge to the University of Exeter as a thesis for the degree of *Doctor of Philosophy* in Medical Studies in April 2023.

Table of contents

Summary

The physiological maintenance of normal blood glucose levels (euglycaemia) and prevention of hypoglycaemia is controlled by the intricate process of hormone release from the pancreatic islets of Langerhans, including the secretion of glucose-raising hormone (glucagon) from the islet α-cells. The defective control of glucagon release is commonly associated with both hyperglycaemia and recurrent hypoglycaemia in individuals with diabetes mellitus (DM). There is increasing evidence that α-cells, alongside intra-islet and autonomic control, are directly glucose-sensing to control glucagon secretion, This is includes evidence to suggest the activation of a critical energy sensor, AMP-activated protein kinase (AMPK), is at least partly involved in the stimulation of glucagon release. The mechanisms behind how α-cells intrinsically regulate glucagon secretion, and how these defective regulatory mechanisms could contribute toward the pathophysiology of DM are relatively under-explored. Providing greater understanding of α-cell physiology can therefore aid the development of small molecule compounds to pharmacologically boost α-cell glucose sensing and restore the α-cell functionality observed in DM.

Here, the overarching aim of this thesis was to characterise the bioenergetic and secretory effects of pharmacological AMPK activation in pancreatic α-cells by using novel small molecules, including R481, O-304 and BI-9774. By doing so, this will widen the current knowledge on α-cell functional dynamics in both physiological and pathophysiological contexts, including recurrent hypoglycaemia. In addition to this, a literature review was conducted to highlight the putative role of AMPK and potential application of small molecule activators as a therapeutic avenue in cystic fibrosis-related diabetes (CFRD).

Evidence suggests that, for the first time, AMPK could be a potent modulator of α-cell metabolic function and substrate utilisation in nutrient-depleted conditions. Here, AMPK activator exposure differentially controlled the glucagon secretory response and total glucagon content in α-cells, suggesting a role of AMPK in regulating glucagon granule dynamics and mechanism-of-action of such small

molecules. Similarly, novel findings indicated that α-cells exposed to recurrent hypoglycaemic-like conditions (RLG) had intrinsic glycolytic and mitochondrial adaptations during low glucose and upon recovery, possibly to maintain energy status. The dysregulated intra-islet responses to glycaemia are similarly observed in other DM sub-types, such as CFRD, and contribute to worsened glucose tolerance. The author therefore discussed how the defective glucose-sensing in several tissues could contribute towards worsened glycaemia in CF/CFRD and postulated if the therapeutic application for small molecule AMPK activators could alleviate glucose-related complications, including inflammation, associated with CFRD.

Altogether, the themes in this thesis explored the complex and wide-ranging metabolic targets of small molecule AMPK activators in the pancreatic α-cell. Furthermore, evidence suggested α-cells metabolically respond and adapt, respectively, to acute and recurrent nutrient depletion, and thereby pose an important therapeutic avenue in restoring glucose homeostasis in DM.

List of figures

List of tables

Publications and conference proceedings arising from this thesis

Publications

Chapter 3

Cruz, A. M., **Partridge, K. M.,** Malekizadeh, Y., Vlachaki Walker, J. M., Weightman Potter, P. G., Pye, K. R., Shaw, S. J., Ellacott, K. L. J., and Beall, C. (2021) 'Brain Permeable AMP-Activated Protein Kinase Activator R481 Raises Glycaemia by Autonomic Nervous System Activation and Amplifies the Counterregulatory Response to Hypoglycaemia in Rats', *Frontiers in Endocrinology,* 12, p. 1630. Available at: https://doi.org/10.3389/FENDO.2021.697445/BIBTEX

Conference proceedings

Chapter 3

Partridge, K.M., Shaw, S.J., Morgan, N.G., Ellacott, K.L.J. and Beall, C. (2021) 'Novel AMP-activated protein kinase (AMPK) activator R481 promotes glucose and fat utilisation in pancreatic alpha cells', *Diabetic Medicine*, 38

Chapter 6

Partridge, K.M., Morgan, N.G., Ellacott, K.L.J. and Beall, C. (2022) 'Recurrent low glucose exposure (RLG) induces intrinsic metabolic adaptations in pancreatic alphaTC1. 9 cells', *Diabetologia,* 65:1, pp. S71-S72.

Author's Declaration

All work was conducted by the author, Katie Partridge, at both the University of Exeter Clinical and Biomedical Sciences (CBS) department and the University of Birmingham Institute of Metabolism and Systems Research in collaboration with Prof. David Hodson, with the exception of the following;

***Ex vivo* islet experiments (Chapter 3 and 4)**

Mouse islets were isolated with the assistance of Dr. Ana Miguel Cruz at the University of Exeter and Dr. Katrina Viloria at the University of Birmingham.

EndoC-βH1 culture (Chapter 3 and 4)

EndoC-βH1 β-cells were cultured with the assistance of Dr. Kaiyven Afi Leslie.

Chapter 4;

4.2.4.3: Dr. Ana Miguel Cruz conducted experiments and the author performed the relevant analysis.

4.2.6.1: Dr. Jiping Zhang ran the BD Accuri C6 Plus flow cytometer following sample generation, alongside assistance in data analysis.

4.2.8.2: Several glucagon measurements were generated with the assistance of Dr. Katrina Viloria (University of Birmingham).

4.2.9: Dr. Ana Miguel Cruz, Dr. Craig Beall and the author were involved in the AMPTT testing protocol and relevant endpoint measurements in STZ Sprague-Dawley rats. Dr. Ana Miguel Cruz performed the qPCR as well as the data analysis.

Chapter 7;

7.7, 7.9 – 7.11; written by Dr. Craig Beall as part of a collaborative literature review. Sections were edited by Katie Partridge.

These datasets were included in this thesis for completeness.

Abbreviations

For the convenience and ease for the reader, listed below is the commonly mentioned abbreviations given in this thesis.

Abbreviation	Definition
$[Ca^{2+}]_i$	Intracellular calcium concentration
µmol/l	Micromolar per litre
2-DG	2-deoxy-d-glucose
$5HT_{1F}$	5-hydroxytryptamine (serotonin) receptor 1F
AC	Adenylyl cyclase
ACC	Acetyl-CoA carboxylase
ADA	American Diabetes Association
ADaM	Allosteric drug and metabolite site
ADP	Adenosine diphosphate
AICAR	5-aminoimisazole-4-carboxamide riboside
AKT2	RAC-beta serine/threonine-protein kinase
AMP	Adenosine monophosphate
AMPK	AMP-activated protein kinase
AMPKTT	AMPK tolerance test
ANO1/2	Anoctamin 1/2
ANOVA	Analysis of variance
ANT	Adenine nucleotide translocase
APS	Ammonium persulfate
ATP	Adenosine triphosphate
AVP	Arginine vasopressin
BAT	Brown adipose tissue
BBB	Blood brain barrier
BMI	Body mass index
BSA	Bovine serum albumin
CaMKK2	Calcium-calmodulin-dependent protein kinase kinase-2
cAMP	Cyclic-adenosine monophosphate
CBS	Cystathionine beta-synthase
cDNA	Complementary DNA
CF	Cystic fibrosis
CFRD	Cystic fibrosis-related diabetes
CFTR	Cystic fibrosis transmembrane conductance regulator
CHI	Congenital hyperinsulinism
CoA	Coenzyme A
COVID-19	Coronavirus-19
CPT1a	Carnitine palmitoyltransferase-1A
CREB	Cyclic-AMP-response element binding protein
CRH	Corticotropin-release hormone
CRHR1	CRH receptor type 1
CRR	Counterregulatory response
DCDFA	Dichlorodihydrofluorescein diacetate

DHAP	Dihydroxyacetone phosphate
DIO	Diet induced obese
DKA	Diabetic ketoacidosis
DM	Diabetes mellitus
DMEM	Dulbecco's Modified Eagle's Medium
DMSO	Dimethyl sulfoxide
eATP	Extracellular ATP
ECAR	Extracellular acidification rate
ECM	Extracellular matrix
EDTA	Ethylenediaminetetraacetic acid
EGTA	Ethyleneglycol-bis(β-aminoethyl)-N,N,N',N'-tetraacetic Acid
ELISA	Enzyme-linked immunosorbent assay
ER	Endoplasmic reticulum
ETC	Electron transport chain
F 1,6BP	Fructose 1,6-bisphosphate
F6P	Fructose 6-phosphate
$FADH_2$	Flavin adenine dinucleotide (reduced)
FAO	Fatty acid oxidation
FBPase	Fructose-1,6-bisphosphatase
FBPase-2	Fructose 2,6-bisphosphatase-2
FBS	Fetal bovine serum
FCCP	Cyanide-p-trifluoromethoxyphenylhydrazone
FFA	Free fatty acid
G6P	Glucose-6-phosphatase
G6PDH	Glucose-6-phosphate dehydrogenase
GABA	Gamma-aminobutyric acid
$GABA_AR$	GABA type A receptor
GAD	Glutamic acid decarboxylase
GAPDH	Glyceraldehyde 3-phosphate dehydrogenase
GCGR	Glucagon receptor
GE	Glucose-excited
GEF	Guanine nucleotide exchange factor
GH	Growth hormone
GI	Glucose-inhibited
GI tract	Gastrointestinal tract
GIP	Glucose-dependent insulinotropic polypeptide
GIRK	G-protein inwardly rectifying potassium
GK	Glucokinase
GLP-1	Glucagon-like peptide 1
GLUT	Glucose transporter
GlycoPER	Glycolytic derived proton efflux rate
GSIS	Glucose stimulated insulin secretion
GTT	Glucose tolerance test
HAAF	Hypoglycaemia-associated autonomic failure
HEPES	4-(2-hydroxyethyl)-1-piperazineethanesulfonic acid
HFD	High fat diet

HGP	Hepatic glucose production
HHF7	Hyperinsulinaemic hypoglycaemic familial 7
HHS	Hyperglycaemic hyperosmolar state
Hiapp (tg)	Human islet amyloid polypeptide (transgenic) mice
HK	Hexokinase
HOMA-IR	Homeostatic model assessment for insulin resistance
HPA	Human primary astrocytes
HRP	Horseradish peroxidase
HRPT1	Hypoxanthine-guanine phosphoribosyltransferase-1
IAH	Impaired awareness of hypoglycaemia
IDF	International Diabetes Federation
iGluR	Ionotropic glutamate receptors
IGT	Impaired glucose tolerance
IMM	Inner mitochondrial membrane
IN	Intranasal
IR	Insulin receptor
K_{ATP}	ATP-sensitive potassium channel
KBH	Krebs' Ringer bicarbonate HEPES solution
LCFA	Long chain fatty acid
LCFA-CoA	Long-chain fatty acyl-Coenzyme A
LDH	Lactate dehydrogenase
LDHA	Lactate dehydrogenase-A
LDHB	Lactate dehydrogenase-B
LDL	Low-density lipoprotein
LKB1	Liver kinase B1
MCT	Monocarboxylate transporter
MDH	Malate dehydrogenase
mGPD	Mitochondrial glycerophosphate dehydrogenase
MMP	Metalloproteinase
MMTT	Mixed meal tolerance testing
MODY	Maturity onset diabetes of the young
mRNA	Messenger RNA
mTOR	Mammalian target of rapamycin
mTORC1	Mammalian target of rapamycin complex 1
NAD	Nicotinamide adenine dinucleotide
NAD+	Nicotinamide adenine dinucleotide (oxidised)
NADH	Nicotinamide adenine dinucleotide (reduced)
NADPH	Nicotinamide adenine dinucleotide phosphate
NAFLD	Non-alcoholic fatty liver disease
NaOH	Sodium hydroxide
NaPPi	Sodium pyrophosphate tetrabasic decahydrate
NF-κB	Inhibitor κB (IκB)/nuclear factor κB
NPY	Neuropeptide Y
NPY/AgRP	Neuropeptide Y/Agouti-related peptide

NTS	Nucleus of the tractus solaris
OAA	Oxaloacetate
OCR	Oxygen consumption rate
OCT-1	Organic cation uptake transporter-1
OGDH	α-ketoglutarate dehydrogenase
OGTT	Oral glucose tolerance test
OXPHOS	Oxidative phosphorylation
P1	Adenosine receptor class
P2X	Purinergic P2 X
P2Y	Purinergic P2 Y
PBS	Phosphate buffered saline
PC	Pyruvate carboxylase
PC2	Prohormone convertase 2
PCR	Polymerase chain reaction
PDC	Pyruvate dehydrogenase complex
PDH	Pyruvate dehydrogenase
PDK4	Pyruvate dehydrogenase kinase 4
PDP	Pyruvate dehydrogenase phosphatase
PEP	Phosphoenolpyruvate
PEPCK	Phosphoenolpyruvate carboxykinase
PERT	Pancreatic enzyme replacement therapy
PFK-1	Phosphofructokinase-1
PFK-2	Phosphofructokinase-2
PFKFB3	6-phosphofructo-2-kinase/fructose-2,6-biphosphatase 3 (PFK2/F2,6BP)
PGC-1α	Peroxisome proliferator-activated receptor γ coactivator-1α
PI3K	Phosphoinositide-3-kinase
PK	Pyruvate kinase
PKA	Protein kinase A
PKC	Protein kinase C
PLL	Poly-l-lysine
PMSF	Pyruvate kinase
PP	Pancreatic polypeptide
PP2A	Protein phosphatase 2A
PP2C	Protein phosphatase 2C
PSC	Pancreatic stellate cells
PVN	Paraventricular nucleus
qPCR	Quantitative PCR
RA	Receptor agonists
RD	Regular diet
RH	Recurrent hypoglycaemia
RIIH	Recurrent insulin-induced hypoglycaemia
RLG	Recurrent low glucose
ROS	Reactive oxygen species
Rot/AA	Rotenone and antimycin A
RPLP1	Ribosomal protein lateral stalk subunit P1
RT	Room temperature
SARS-CoV-2	Severe acute respiratory syndrome
SDH	Succinate dehydrogenase
SDHA	Succinate dehydrogenase a
SDS	Sodium dodecyl sulphate

SDS-PAGE	Sodium dodecyl sulphate polyacrylamide gel electrophoresis
Ser-79	Serine-79
Serotonin	5-hydroxytryptamine
SGLT	Sodium-glucose cotransporter
SH	Severe hypoglycaemia
SST	Somatostatin
SSTR2	SST receptor 2 isoform
STWS	Scott's tap water substitute
STZ	Streptozotocin
T1DM	Type 1 diabetes mellitus
T2DM	Type 2 diabetes mellitus
tATP	Total ATP
TBS	Tris buffered saline
TBS-T	Tris buffered saline with tween
TEMED	Tetramethylethylenediamine
TH	Tyrosine hydroxylase
Thr-172	Threonine-162
Tris	Trisaminomethane
TSC2	Tuberous Sclerosis Complex 2
TXNIP	Thioredoxin-interacting protein
UCP-2	Uncoupling protein 2
vATPase	Vacuolar-type ATPase
VDCC	Voltage dependent calcium channels
Veh	Vehicle
VMH	Ventromedial hypothalamus
VMN	Ventromedial nucleus of the hypothalamus
VRAC	Volume-regulated anion channels
WAT	White adipose tissue
ZDF	Zucker diabetic fatty (rat)
ZMP	AICAR 5'-monophosphate

Acknowledgements

Wow. From starting this PhD in Sept 2019, until April 2023, a great many significant events (both personal and global) have occurred that I otherwise could not have expected or anticipated. But alas, this has built resilience (!)

Firstly, to Craig, for your tireless support, encouragement and providing many exciting opportunities for me throughout this PhD. You always put another lens on a scenario to help me look at a problem at a different angle, and as such, making me a more critical thinker. Outside the lab, both your running advice and company in competing in duathlons helped me to see my potential that I would not have otherwise seen. So, to you, I thank you. I would like to thank my second and third supervisors throughout my PhD; Kate, Chloe and Noel. Your guidance, wealth of knowledge and training opportunities have made me a better scientist.

To the past and present members of the Exeter Neuroendocrine Group (i.e., the Beallacotts) and Level 4 RILD; the coffee, lab meeting snacks, lunches, conversations surrounding science (or not), and motivation have made my PhD journey in the RILD the nurturing and fantastic research environment that it is. To posthumously acknowledge Mohammad Baity, a kind friend and scientist who was taken too early. Thank you for your gentle wisdom in tissue culture. I'd like to thank Christine and Jess for (!) supplying the elusive chocolate to keep me going. A special thank you to Bec for telling me where the chocolate was kept, alongside your support in the form of motivational quotes and chats during trips to liquid nitrogen. For the lab, it's a privilege to be both your colleague and friend!

Thank you to the Wednesday circuits group, including our new member Charis, for keeping my motivation up and being a welcome break from work. To the outdoors adventures which provided a well-needed rest; to that I need to thank my hiking friends from Cardiff University. To acknowledge my development in confidence and leadership; 2nd Exeter (cub) scout group. A great bunch of strong, dedicated and resourceful friends.

To my family; Mum, Dad, Tom, Trina and Dominique. Your belief in me has never once been altered and I cannot acknowledge you all enough for nurturing a non-exhaustive list of values, including a strong work ethic, perseverance, positivity and most importantly; a “can do” attitude. Thank you for believing in me during times when I didn’t.

Lastly, I would like to posthumously dedicate this thesis to Delia and Richard Anderson. You showed me that no goal is out of reach. I endeavour to hope that you both are proud and continue to be proud of me in my achievements and values. Your drive and determination, in your memory, is what I strive to put in everything I do.

“The greatest glory in living lies not in never failing, but in rising every time we fall” ~ Nelson Mandela.

Chapter 1:

General introduction

1 General introduction

1.1 Diabetes mellitus (DM)

Diabetes mellitus (DM) is considered as a “silent” global epidemic, with the International Diabetes Federation (IDF) classifying DM as “…one of the largest global health emergencies in the 21st century” (*IDF Diabetes Atlas*, 2015; Bădescu *et al.*, 2016; Mobasseri *et al.*, 2020; Liu *et al.*, 2022). By 2045, DM prevalence will be up to 21.1 % (from 10.5% in 2021), with the greatest rise anticipated in middle-income countries (Sun *et al.*, 2021). In addition, the cost to the economy includes approximately £5.5 billion/year in the overall cost of hospital care surrounding diabetes and related complications (Stedman *et al.*, 2020). By 2045, the global cost is estimated to increase to a total of $1054 billion, emphasising the growing social and economic pressures of the disease (Sun *et al.*, 2021).

DM is a metabolic disease and is commonly diagnosed by chronic high blood glucose (hyperglycaemia) (Sapra and Bhandari, 2022). With increasing disease duration, the risk of severe peripheral and central complications is raised, as illustrated in Figure 1.1 (adapted from Tomic *et al.*, 2022). The high incidence of these complications, alongside chronic glucose variability, are significant causes of increased mortality and morbidity in individuals with DM (Forbes and Cooper, 2013). Furthermore, the rapid spread of novel severe acute respiratory syndrome coronavirus 2 (SARS-CoV-2), resulting in the coronavirus disease 2019 (COVID-19) pandemic, identified the greater risk of fatality in diabetes and related complications (Holman *et al.*, 2020). It is important to note, diabetes impacts both physical health and mental wellbeing (Anderson *et al.*, 2001; Pompili *et al.*, 2009). Depression is up to three-times higher in people with DM compared to individuals without, and thereby highlights the psychological and emotional strain of the disease (Roy and Lloyd, 2012).

Diabetes is highly heterogenous in pathogenesis (Karalliedde and Gnudi, 2016). The most prevalent subtypes include type 1 diabetes mellitus (T1DM), type 2

diabetes mellitus (T2DM) and gestational diabetes (Banday, Sameer and Nissar, 2020; Sapra and Bhandari, 2022). Other subtypes include secondary diabetes, monogenic and neonatal diabetes (Banday, Sameer and Nissar, 2020). Secondary diabetes is commonly diagnosed as a result of complications from pre-existing exocrine insufficient conditions, for instance cystic fibrosis-related diabetes (CFRD) and pancreatitis (commonly referred as “type 3c diabetes”) (Marshall *et al.*, 2005; Ewald *et al.*, 2012). The pathophysiological heterogeneity within DM sub-types range from age-of-onset, polygenic contribution from both multiple genetic predispositions to environmental factors (Padilla-Martínez *et al.*, 2020).

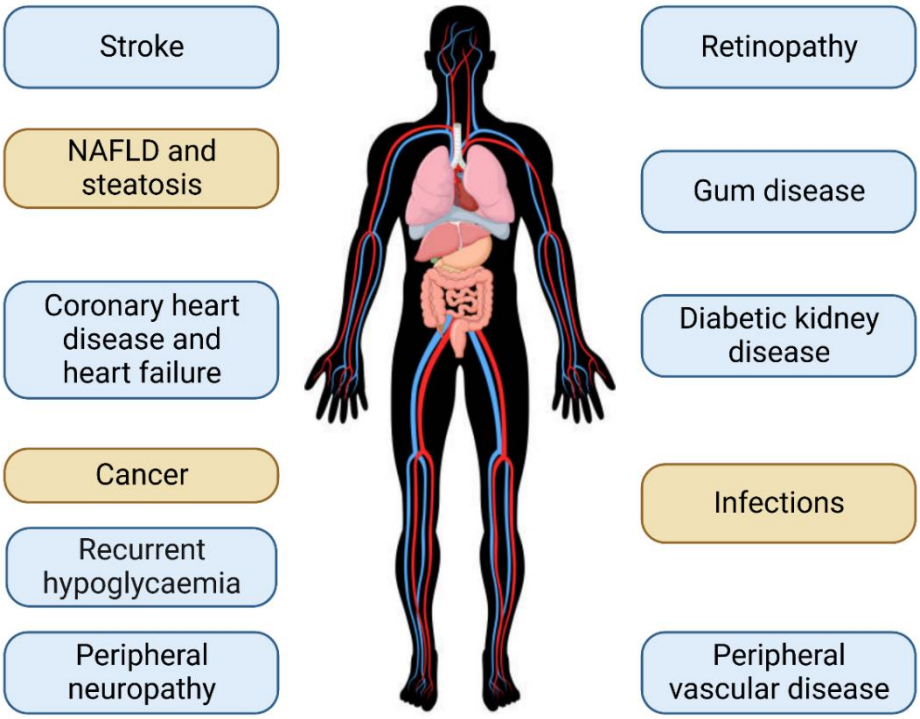

Figure 1.1: Common and emerging complications surrounding diabetes mellitus (DM)

Common complications (in blue) include stroke, retinopathy, gum disease, diabetic kidney disease (DKD), coronary heart disease and heart failure, recurrent hypoglycaemia, peripheral neuropathy and peripheral vascular disease. New and emerging complications include links to recurrent infections, cancer, and hepatic disease (including NAFLD and steatosis). Adapted from Tomic *et al.* 2022. Created using Biorender.com.

1.1.1 Type 1 diabetes mellitus (T1DM)

T1DM is characterised by the selective, chronic autoimmune attack and destruction of the insulin-producing β-cells in the pancreatic islets (Boldison and Wong, 2016; Nederstigt *et al.*, 2019). Prevalence is heritable, with up to 70% risk of developing T1DM in identical twin studies and up 9.0% risk of a child developing diabetes with a parent with diagnosed T1DM (Redondo *et al.*, 2008; DiMeglio, Evans-Molina and Oram, 2018). In 2021, up to 8.4 million people are living with T1DM with incidence rising worldwide by up to 5.0% (Gillespie *et al.*, 2004; Maahs *et al.*, 2010; Gregory *et al.*, 2022). The American Diabetes Association (ADA) clinical practice recommends T1DM diagnosis by either fasting plasma glucose levels (>7.0 mmol/l), plasma glucose 2 h post-OGTT, HbA1c (> 6.5%) (American Diabetes Association Professional Practice Committee, 2022b). Up to 85% of T1DM diagnosis occurs < 20 years, with significant evidence suggesting the heterogeneity of age-of-diagnosis is associated with distinct T1DM immune phenotypes (termed “endotypes”) (Maahs *et al.*, 2010). Children diagnosed typically present in clinic with polyuria (excessive urination), polydipsia (increased thirst), diabetic ketoacidosis (DKA) and profound weight loss (Duca *et al.*, 2017; Los and Wilt, 2023).

The clinical pathophysiology and progression of T1DM is illustrated in Figure 1.2, yet the aetiology of T1DM development is not fully understood (DiMeglio, Evans-Molina and Oram, 2018; Akil *et al.*, 2021). It is widely accepted that the activation of autoreactive $CD8^+$ T-cells lead to the destruction of the autoantigen-presenting β-cells, which potentiates an intra-islet inflammatory environment and insulitis characteristic of T1DM autoimmunity (Burrack, Martinov and Fife, 2017). In addition, autoantigen polymorphisms could also increase genetic predisposition to developing immune-mediated T1DM, as identified in monozygotic twin studies (Cooper *et al.*, 2008; Redondo *et al.*, 2008; Roep *et al.*, 2020). Possible environmental risk factors include viral-induced autoimmunity of the pancreatic islets, for instance, by enteroviral infection (Bodansky *et al.*, 1992; Boddu, Aurangabadkar and Kuchay, 2020; Norris, Johnson and Stene, 2020).

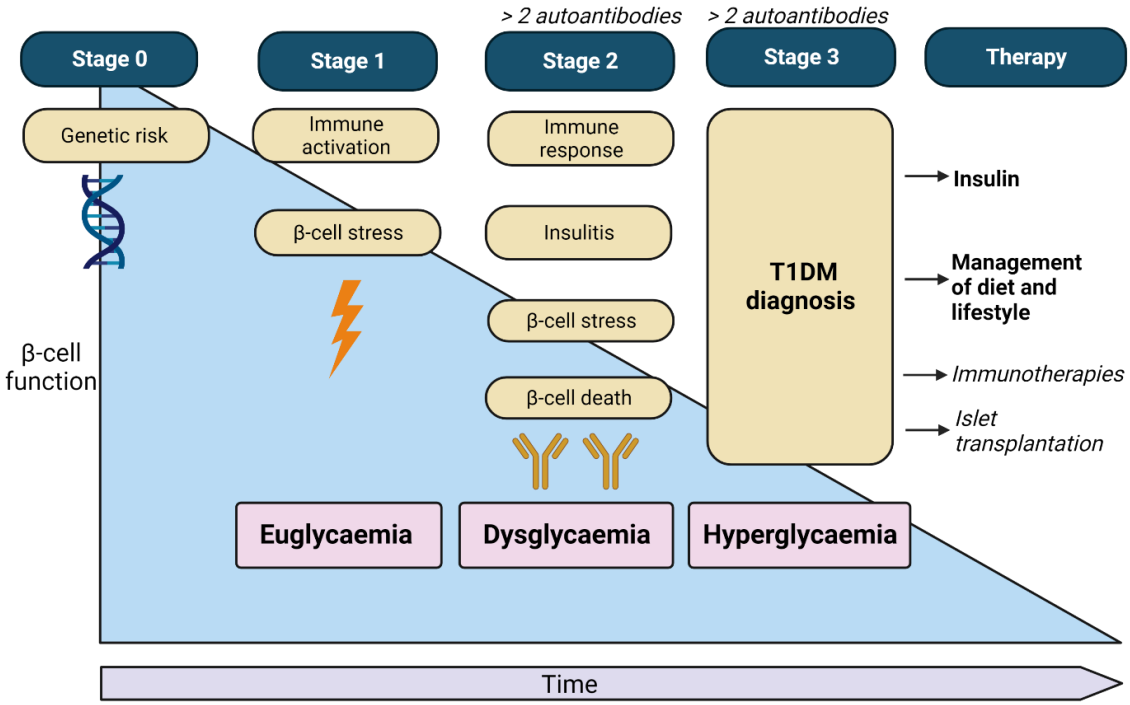

Figure 1.2: Schematic diagram of type 1 diabetes mellitus (T1DM) pathogenesis.

Increased genetic predisposition and putative environmental factors are associated with propagating the development of type 1 diabetes mellitus (T1DM). In stage 1, increased activation of the immune system leads to heightened β-cell stress response, but individuals display a retained blood glucose (euglycaemia) with no overt clinical symptoms. Over time, at stage 2, the presence of > 2 islet autoantibodies drive a heightened autoimmune response and inducing insulitis-associated β-cell dysfunction. At this stage, β-cell dysfunctionality enhances variable glycaemic status, but still without overt symptoms. Stage 3 is characterised by substantial β-cell loss and dysfunction, enhancing symptomatic hyperglycaemia and increasing the likelihood of a T1DM diagnosis. Standard (**in bold**) therapies for T1DM largely include careful management of diet and lifestyle to control glycaemia, exogenous insulin to attenuate hyperglycaemia. Emerging therapies (*in italics*) include immunotherapies and islet transplantation to help control glucose homeostasis in T1DM. Adapted from Akil *et al.* 2021 and DiMeglio *et al.* 2018. Created using Biorender.com.

1.1.2 Type 2 diabetes mellitus (T2DM)

90% of diagnosed DM cases are classified as type 2 diabetes mellitus (T2DM) and in 2019, it is estimated up to 1.0 million people in the UK are living with undiagnosed T2DM (Whicher, O'Neill and Holt, 2020; Regina, Mu'ti and Fitriany, 2022). IDF identified the global incidence of T2DM is estimated to rise from 415 million people in 2015, to 642 million by 2040 (*IDF Diabetes Atlas*, 2015; Unnikrishnan *et al.*, 2017). In particular, diabetes rates are exponentially rising in developing countries and by 2030 estimated DM rates will increase by 69% in developing countries compared to 20% in developed (*IDF Diabetes Atlas*, 2015). The aetiology of T2DM is clinical distinct from T1DM, as T2DM is associated with no β-cell autoimmunity but the remaining β-cells are defective in function (Zheng, Ley and Hu, 2017). Over time, dysfunctional β-cells drive insulin resistance and diminished glucose uptake from peripheral tissues, alongside increased β-cell death, further driving hyperglycaemia (Reaven, 1988; Weyer *et al.*, 1999; Zheng, Ley and Hu, 2017). T2DM is highly heterogeneous in clinical presentation due to both complex genetic-environmental interactions. Behavioural and lifestyle risk factors increase the likelihood of T2DM development, including a more sedentary lifestyle, obesity and poor dietary intake (Yuan and Larsson, 2020). Genetic risk variants also increase likelihood of T2DM development by 76%, as identified in monozygotic twin studies (Newman *et al.*, 1987; Kaprio *et al.*, 1992; Medici *et al.*, 1999). Impaired glucose tolerance (IGT) and abnormal glucose homeostasis is a major risk factor for subsequent diagnosis of T2DM and is commonly referred as "prediabetes" (Tabák *et al.*, 2012). 1 in 100 individuals with prediabetes develop T2DM within 10 years, with up to 70% of individuals with prediabetes eventually developingT2DM (Tabák *et al.*, 2012; Idowu *et al.*, 2022). Global prevalence of prediabetes is exponentially rising, with up to 8.3% of the world's population predicted to have prediabetes (*IDF Diabetes Atlas*, 2013). Early diagnosis of prediabetes is essential in implementing effective management strategies, including lifestyle changes, to reduce the development of overt T2DM. Meta-analysis of prediabetes found up to 54% lower risk of T2DM progression by

adjustment of lifestyle factors alone, identifying a potent non-pharmacological strategy to limit disease development (Glechner *et al.*, 2018).

1.1.3 Cystic fibrosis-related diabetes (CFRD)

Cystic fibrosis (CF) is a prevalent autosomal recessive disease, with pathogenesis caused by distinct mutations in the cystic fibrosis transmembrane conductance regulator (*CFTR*) gene (Scotet, L'hostis and Férec, 2020). The identification of the *CFTR* gene responsible for CF occurred over 30 years ago, and since then, further research has identified different *CFTR* mutations associated with CF to aid the development of precision-based therapy strategies (Kerem *et al.*, 1989; Riordan *et al.*, 1989; Rommens *et al.*, 1989; Scotet, L'hostis and Férec, 2020). The predominant clinical phenotype associated with CF includes excessive mucus build up in epithelial-lined tissues, such as the lungs, caused by defective chloride ion movement as a result of specific *CFTR* mutations (Balázs and Mall, 2019). Mucus plugging, especially in the lungs, increases the risk of *Staphylococcus aureus* and/or *Pseudomonas aeruginosa* colonisation, driving inflammation and further fibrotic damage (Yu and Sharma, 2022). The recurrent bouts of infection localised to the lungs are a prevalent driver of mortality in CF individuals (Zolin *et al.*, 2018). Other peripheral complications associated with CF are displayed in Figure 1.3. Common clinical presentations and diagnosis, in addition to lung manifestations, include low body mass index (BMI), compromised lung function, with low BMI resulting from pancreatic insufficiency and is commonly diagnosed by genetic testing (Farrell *et al.*, 2017; Chen, Shen and Zheng, 2021). In 1938, CF was first identified as a disease clinically distinct disease from coeliac disease, and where most individuals with CF died within a year of birth (Andersen, 1938). Now, the UK Cystic Fibrosis Registry reported 50% of individuals with CF born in 2021 will live to at least 53 years old (Cystic Fibrosis Trust, 2022). The increased survival rate, concurrent with heightened understanding and therapeutic targeting, has led to the identification of multiple whole-body complications which were otherwise undetected.

A common complication of CF is cystic fibrosis-related diabetes (CFRD), which affects up to 50% of CF individuals > 30 years old (Brennan *et al.*, 2004; Olesen *et al.*, 2020). CFRD is commonly referred to as “type 3c diabetes”, although the presence of CF makes CFRD a highly complex disease compared to pancreatitis alone (Gottlieb *et al.*, 2012). The likelihood of CFRD development can increase with corticosteroid treatment, which is commonly prescribed in CF to treat lung inflammation (Laguna, Nathan and Moran, 2010). Although CFRD shares clinical phenotypes of both T1DM and T2DM, it is regarded as a distinct condition. CFRD, unlike T1DM, is not characterised by autoimmune β-cell destruction but diagnosis is associated with diminished cell mass and insulin deficiency (Moheet and Moran, 2022). In addition, over disease duration, individuals with CFRD can develop insulin resistance and chronic hyperglycaemia, similar to T2DM aetiology (Calella *et al.*, 2018; Granados *et al.*, 2021). This is possibly due to reduced adipose depots and skeletal muscle for glucose uptake (Calella *et al.*, 2018; Granados *et al.*, 2021). The detailed pathophysiology and downstream impact of defective *CFTR* in CF is discussed in chapter 7.

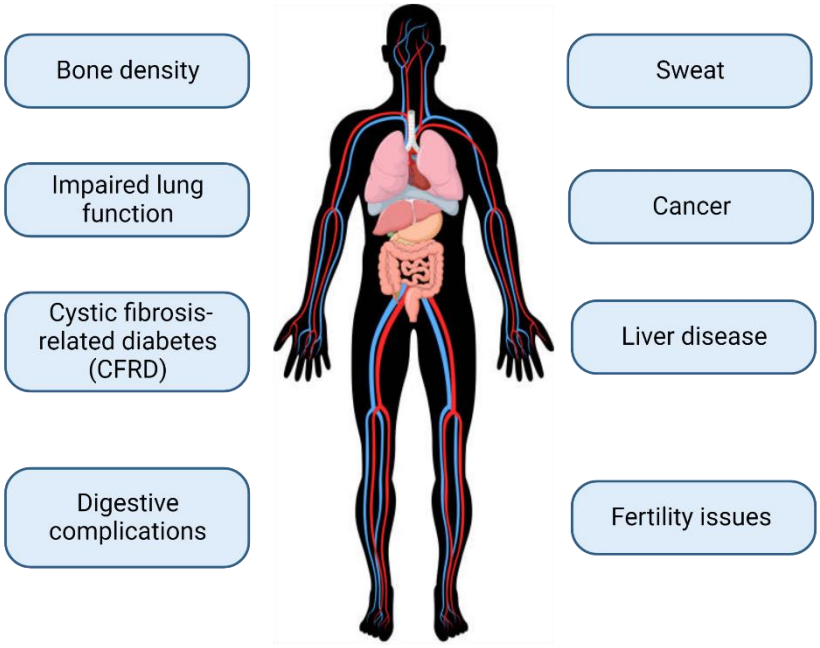

Figure 1.3: Complications of cystic fibrosis (CF)

A non-exhaustive list of complications from cystic fibrosis (CF) include compromised bone density/bone disorders, impaired lung function, cystic fibrosis-related diabetes (CFRD), digestive complications and exocrine insufficiency, altered sweat, cancer risk, liver disease, and fertility issues. Created using Biorender.com.

1.2 Hypoglycaemia and glucose counterregulation

Hypoglycaemia is a common, severe complication of insulin-treated T1DM and advanced T2DM (UK Prospective Diabetes Study (UKPDS) Group, 1998; Cryer, 2004). In 2017, the International Hypoglycaemia Study Group (IHSG) recently redefined the "clinical significance of biochemical hypoglycaemia" from the "frequency of detection of a glucose concentration < 3.0 mmol/l" to a level-based classification in order to sub-stratify hypoglycaemic events in clinical reporting, as summarised in Table 1.1 (Heller, 2017). Mild hypoglycaemic episodes have estimated to occur between 1 – 2 episodes/patient/week in T1DM and 0.3 – 0.7 episodes/patient/week in T2DM treated with insulin therapy (Frier, 2014). Severe hypoglycaemia (SH) is most often clinically referred to as requiring "third-party assistance", including hospital admittance. SH is highly prevalent over disease duration, with adults diagnosed with T1DM for >15 years have an increased incidence of SH with 3.2 episodes/patient/year (Heller *et al.*, 2007). If untreated, SH can lead to a coma and "death-in-bed" syndrome; with evidence suggesting SH is associated with a 3.4-fold increase in risk of mortality, after 5 years, in older individuals with diabetes (McCoy *et al.*, 2012). Imperfect insulin therapy and disease duration are two of the main contributors of hypoglycaemia in DM. The long-term mitigation of hypoglycaemia is a fine balance, but the recent advances in technologies (such as continuous glucose monitors and insulin pumps) with closed-loop systems provide a more integrated and sensitive approach (Kaur and Seaquist, 2023).

Table 1.1: Level-based classification of clinically-relevant hypoglycaemic events recommended by ADA and EASD workgroup.

Level	Glycaemic threshold
(1)	< 3.9 mmol/l
(2)	< 3.0 mmol/l; serious/clinically significant hypoglycaemia
(3)	Severe hypoglycaemia; cognitive dysfunction and third-party intervention

1.2.1 Physiological responses to acute hypoglycaemia

In a physiological context, blood glucose is maintained between 4.0 – 6.0 mmol/l (Mathew and Tadi, 2022). The fine interplay of both central and peripheral organs, such as the liver, skeletal muscle, pancreatic islets, adipose tissue and brain control glucose homeostasis by regulation of glucose production, uptake and/or glycogen breakdown. A reduction in blood glucose levels, between 4.4 – 4.7 mmol/l glucose, during exercise or fasted conditions, inhibit β-cell insulin secretion to result in an increase in hepatic glycogenolysis and both hepatic/renal gluconeogenesis (Muneer, 2021). As blood glucose continues to decrease (3.6 – 3.9 mmol/l), α-cells are stimulated to secrete glucagon by both direct and autonomic mechanisms as a second line of hypoglycaemia defence (Muneer, 2021). A similar glucose threshold also activates the sympathoadrenal response as a third line of defence, propagated by the cholinergic neurostimulation of the adrenal medulla for catecholamine secretion (Muneer, 2021). Both catecholamine and glucagon secretion stimulate hepatic/renal glycogenolysis and gluconeogenesis to restore euglycemia (Gerich *et al.*, 2001; Muneer, 2021). Epinephrine also limits glucose utilisation in both insulin-sensitive adipose tissue and skeletal muscle by activating the lipolytic pathway to generate carbon substrates required for gluconeogenesis (Dufour *et al.*, 2009). In addition, at 3.2 mmol/l blood glucose, growth hormone (GH) and cortisol are secreted after longer hypoglycaemic periods to stimulate hepatic ketogenesis and gluconeogenesis, but also induce epinephrine secretion (Sprague and María Arbeláez, 2011). Blood glucose less than 3.2 mmol/l activates behavioural defence mechanisms involving catecholamine-induced palpitations, acetylcholine-driven sweating, and hunger to drive recovery (Tesfaye and Seaquist, 2010). If blood glucose levels further decline (< 2.8 mmol/l), including no food ingestion, neuroglycopenic complications arise including a reduction in cognitive function and increasing risk of unconsciousness and/or seizure (Muneer, 2021). The homeostatic response to hypoglycaemia is summarised in Figure 1.4.

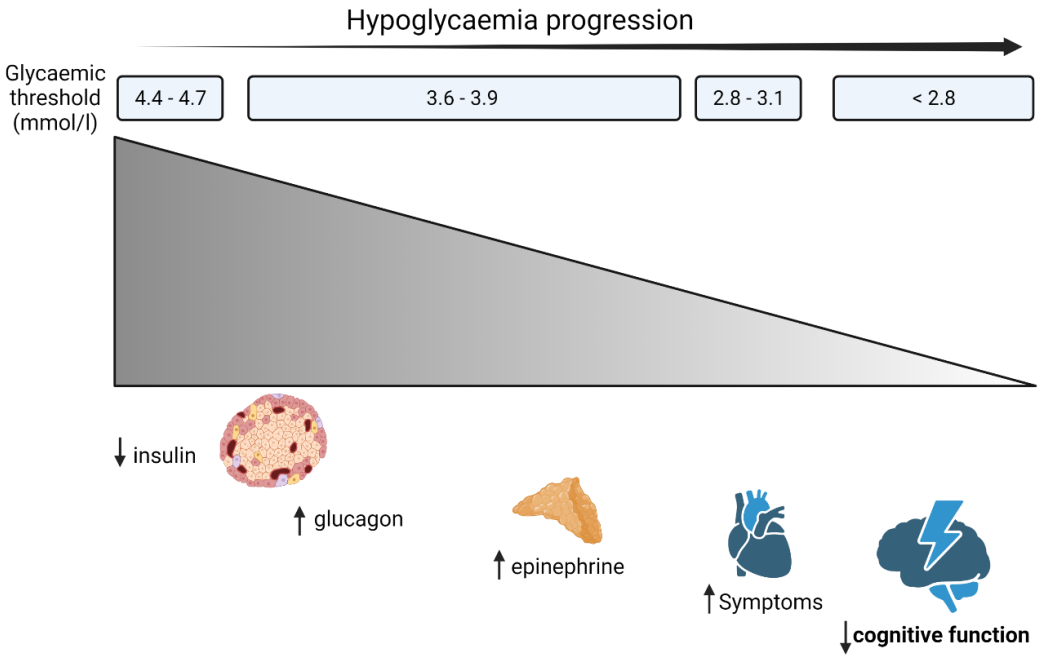

Figure 1.4: Physiological responses to hypoglycaemia.

As plasma [glucose] drops between 4.4 – 4.7 mmol/l glucose, β-cell insulin secretion is inhibited and thereby attenuates peripheral tissue glucose utilisation. As blood glucose drops further (3.6 – 3.9 mmol/l), counterregulatory hormone secretion (glucagon and epinephrine) is stimulated to promote hepatic gluconeogenesis. Glucose concentrations (2.8 – 3.1 mmol/l) promote sympathetic neural responses and thereby overt hypoglycaemic awareness, including sweating, hunger, heart palpitations and dizziness. If no actions are taken to prevent further hypoglycaemia, cognitive function declines and increase likelihood of unconsciousness. Created using Biorender.com.

.

1.2.2 Pathophysiological central and peripheral responses to recurrent hypoglycaemia

In T1DM, prior hypoglycaemic episodes lower the glycaemic threshold required to initiate an autonomic, symptomatic response to counteract hypoglycaemia, as described in Figure 1.5. Over disease progression, individuals with T1DM with a history of RH are at increased risk of impaired awareness of hypoglycaemia (IAH). In one study, SH reportedly affects over 50% of individuals with IAH with T1DM (Geddes *et al.*, 2008). IAH increases the risk of subsequent SH episodes and is associated with the increased mortality rate (McCoy *et al.*, 2012). IAH, in DM, is classified as the reduction or delay in onset of neurological and autonomic symptoms (including sweating, anxiety, palpitations, cognitive impairment) that appear at a much lower glucose threshold compared to individuals with retained hypoglycaemia counterregulation (Martín-Timón and Cañizo-Gómez, 2015). A maladaptive response to a recent, antecedent bout of hypoglycaemia contributes towards the defective autonomic counterregulatory hormone responses in response to glucose, commonly termed hypoglycaemia-associated autonomic failure (HAAF) (Cryer, 2001; Bisgaard Bengtsen, Møller and Bengtsen, 2022). HAAF involves the lack of stimulated epinephrine and glucagon response, alongside no reduction of plasma insulin levels (Cryer, 2001, 2005). Both defective glucose counterregulation and IAH further propel a vicious cycle for subsequent severe hypoglycaemic episodes in T1DM.

The mechanisms underlying the defective glucose counterregulatory response (CRR) following RH and/or IAH associated with HAAF is currently unclear. The development of several hypotheses focuses on the adaptations within brain glucose-sensing regions (e.g., the ventromedial hypothalamus, VMH) which could drive RH and lead to IAH over time. Evidence include glycogen supercompensation, blunted glucose-sensing, reduced glucose import, alteration in metabolic fuel utilisation and defective astrocyte-neurone communication in the ventromedial hypothalamus (VMH) (Martín-Timón and

Cañizo-Gómez, 2015; McCrimmon, 2022). These concepts are covered in greater depth in a recent review (McCrimmon, 2022).

Recent evidence suggests direct alterations to adrenal gland catecholamine release following RH (Ma *et al.*, 2018). Four recurrent insulin treatments abolished epinephrine secretion from isolated mouse adrenal chromaffin cells in response to hypoglycaemic conditions (Ma *et al.*, 2018). In addition, RH attenuated tyrosine hydroxylase (TH) immunoreactivity, an enzyme required for catecholamine synthesis, in comparison to single bout of hypoglycaemia (Ma *et al.*, 2018). Furthermore, RH-exposed mice had retained neuropeptide Y (NPY) immunoreactivity in the adrenal medulla, a neurotransmitter co-secreted in epinephrine vesicles, in comparison to one acute insulin treatment (Ma *et al.*, 2018). RH did not alter epinephrine secretion in mice with ablated NPY, suggesting the reduction in epinephrine secretion as a result of RH is driven by enhanced NPY inhibition of TH and thus limiting epinephrine vesicle stores in the adrenal gland (Ma *et al.*, 2018). Altogether, these data indicate the intrinsic secretory defects in catecholamine release in the adrenal medulla may contribute towards defective CRR. In comparison, little is currently known whether RH directly impacts α-cell glucagon secretion, identifying a significant gap in understanding on the peripheral effects of RH.

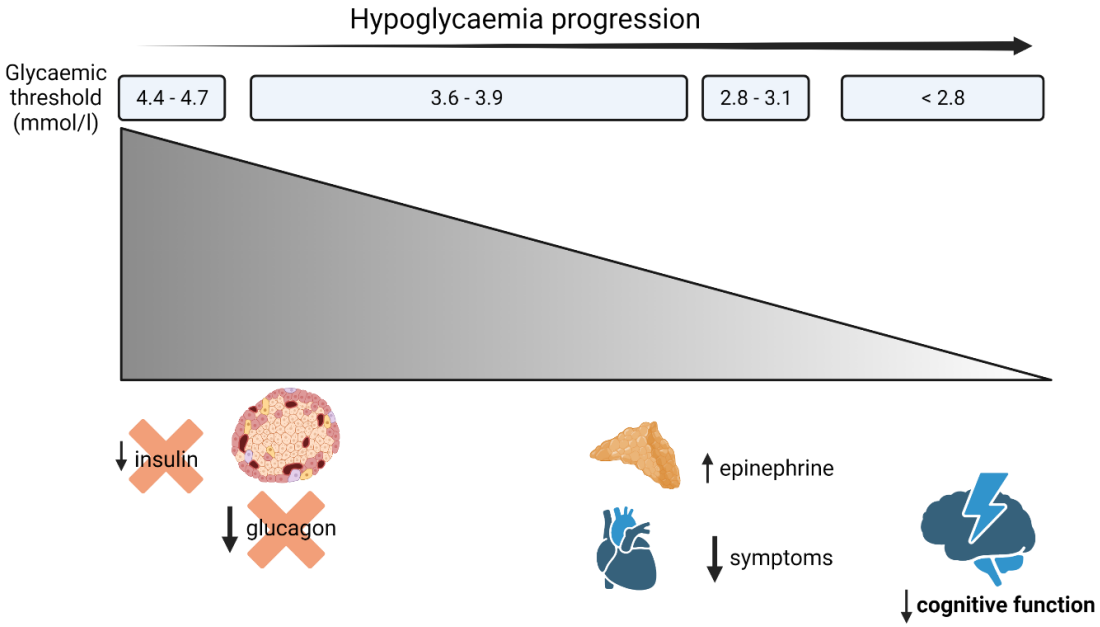

Figure 1.5: Pathophysiological responses to hypoglycaemia in T1DM.

In T1DM, the selective destruction of β-cells eliminates endogenous insulin secretion and thereby individuals require exogenous insulin therapy to maintain blood [glucose] levels. Therefore, despite a fall in blood glucose, plasma insulin can remain high. In addition, over disease progression, pancreatic α-cells are defective and do not adequately secrete glucagon in response to hypoglycaemia; thereby limiting hepatic gluconeogenesis. Individuals with impaired awareness of hypoglycaemia (IAH) have delayed corticosterone secretion in response to glycaemia, leading to reduction in autonomic symptoms and hypoglycaemia unawareness. The narrow glycaemic threshold for symptomatic presentation, or complete absence, increase the likelihood of severe cognitive decline and third-party intervention. Created using Biorender.com.

1.2.3 Key counterregulatory hormones

1.2.3.1 Insulin peripheral action

Insulin signalling cascade is mediated by insulin-insulin receptor (IR) binding, in which IR comprise of both α and β-subunits in a heterodimeric complex (Czech, 1985). IR β-subunits are abundantly expressed in skeletal muscle, adipose tissue, liver and pancreas (Yong and White, 2004). Insulin-IR binding activates downstream PI3K/PKB/Akt pathway to regulate hepatic gluconeogenesis, adipose lipolysis, skeletal muscle/hepatic glycogenolysis and GLUT-mediated glucose transport in adipose tissue/skeletal muscle (as described in Figure 1.6) (Hassan, Bourron and Hajduch, 2014).

In T1DM, β-cells are selectively destroyed and thereby abolishing endogenous insulin secretion over disease duration. Individuals with T1DM rely on exogenous insulin therapy, either by insulin pumps or by manual injections, to retain euglycaemia and stimulate postprandial glucose uptake from peripheral tissues to limit hyperglycaemia (Janež *et al.*, 2020). Hyperinsulinaemia, as a result of excessive insulin therapy, can increase the risk of multiple hypoglycaemic episodes and over time will increase likelihood of delayed behavioural and physiological counterregulation to hypoglycaemia (Cryer, 2010).

Insulin resistance is a causal factor for the development of obesity-related T2DM (Johnson, 2021). Insulin resistance is defined as the impaired downstream response to insulin-IR binding, including dysregulated glucose and lipid metabolism in key target tissues (Johnson, 2021). Chronic hyperglycaemia increases β-cell dysfunction, alongside the promotion of insulin resistance by the defective glucose disposal from peripheral tissues (Cerf, 2013). The widely regarded idea for β-cell dysfunction in T2DM is the β-cell “overcompensates” for tissue insulin insensitivity, by further driving hyperinsulinaemia, chronic hyperglycaemia and overtime, β-cell death (Cerf, 2013). In particular, insulin resistance pathophysiology involves increased gluconeogenesis, attenuated GLUT-4 mediated glucose uptake and enhanced adipocyte size in the liver,

skeletal muscle and adipose tissue respectively (Samuel and Shulman, 2016). These dysregulated metabolic processes in peripheral tissues are promoted by defective mitochondrial function and metabolic fuel inflexibility in response to hyperglycaemia, as further described in da Silva Rosa *et al.* 2020 (da Silva Rosa *et al.*, 2020). Recently, several studies alternatively suggest insulin resistance as a "adaptive defence mechanism" to protect insulin-targeted tissues from intracellular glucose overload and subsequent metabolic stress, but further research is required (Taegtmeyer *et al.*, 2013; Nolan *et al.*, 2015; Nolan and Prentki, 2019).

Individuals with T1DM can also develop insulin resistance in association with obesity and disease progression. Peripheral insulin therapy bypasses hepatic clearance, which endogenous insulin levels are limited by, and thereby the basal insulin levels are reportedly up to 2.5-fold greater than individuals without diabetes at similar blood [glucose] (Gregory *et al.*, 2019). This, therefore drives "iatrogenic hyperinsulinaemia" (Gregory *et al.*, 2019; Gregory, Cherrington and Moore, 2020). This is supported by the peripheral insulin insensitivity observed by induced hyperinsulinaemia in individuals without diabetes and healthy dogs in which basal insulin levels were to comparable to T1DM (Rizza *et al.*, 1985; Marangou *et al.*, 1986; Del Prato *et al.*, 1994; Gregory, Cherrington and Moore, 2020). Therefore, therapies to limit insulin insensitivity could include portal insulin therapy, as suggested by Gregory *et al.* 2020, to limit excessive peripheral insulin stimulation, and thereby attenuate the glycaemic variability associated with T1DM with reduced risk of insulin-induced hypoglycaemia (Gregory, Cherrington and Moore, 2020).

1.2.3.2 Glucagon peripheral action

Glucagon action is mediated by binding to G protein-coupled (GPCR) receptors (termed GCGRs) by stimulating both G_S-coupled signalling pathway to increase intracellular cAMP by adenylyl cyclase, and G_q-coupled pathway stimulating phospholipase C (PLC)-coupled $[Ca^{2+}]_I$ rises (Janah *et al.*, 2019). Glucagon receptor (GCGR) is abundantly expressed in the liver, but also expressed in

other glucose-sensitive tissues including white/brown adipose tissue, GI tract, and pancreatic β-cells to promote glucose and lipid-generating pathways (Figure 1.6) (Quesada *et al.*, 2008; Charron and Vuguin, 2015; Wendt and Eliasson, 2020).

Pancreatic α-cells, located in the islets of Langerhans, secrete glucagon in response to hypoglycaemia. Hypoglycaemic episodes in T1DM are promoted by the reduced autonomic stimulation of α-cell glucagon secretion, and thereby fuelling deeper, more severe hypoglycaemic episodes (Taborsky, Ahrén and Havel, 1998; Cryer, 2005). There is also evidence suggesting RH, at least in part with autonomic dysregulation, directly dysregulates the α-cell response to hypoglycaemia (Banarer, McGregor and Cryer, 2002). The mechanism by which this occurs is still unclear and is an area of ongoing research. To counteract hypoglycaemia, synthetic glucagon is commonly prescribed for individuals at high risk of level 2 hypoglycaemia and given when individuals are unable to swallow oral carbohydrates (e.g., unconsciousness) to raise blood glycaemia (American Diabetes Association, 2019). Glucagon therapy is limited in use by the known instability and insolubility of glucagon, meaning powdered glucagon requires reconstitution by a third-party (Thieu *et al.*, 2020). Altogether, understanding the mechanisms behind the defective α-cell function in DM is crucial for developing targeted and efficacious therapeutics to restore the counterregulatory response to hypoglycaemia.

In 1975, Unger and Orci classified DM as a “bi-hormonal disorder”, whereby the observed relative or complete insulin deficiency coincides with both hyperglucagonaemia and hyperglycaemia (Unger and Orci, 1975). Hyperglucagonaemia in DM is as result of excessive α-cell stimulation in fasted conditions, as well as defective postprandial suppression of glucagon secretion (Asadi and Dhanvantari, 2021). The development and release of the first intranasal (IN) glucagon by Eli Lilly in 2015 (BAQSIMI^{TM}), unlike intramuscular injections, can aid a glycaemia balance without causing “rebound” hyperglycaemia, alongside a lower bioavailability (Pontiroli *et al.*, 1989; Rosenfalck *et al.*, 1992; Dash *et al.*, 2018; Pontiroli and Tagliabue, 2019). This

evidence, alongside ease of use, provides a variety of advantageous benefits as an alternative to intramuscular therapy for individuals with DM and high glucose variability. In addition, hyperglucagonaemia increases the likelihood of DKA and further propels chronic hyperglycaemia in both T1DM and T2DM (Müller, Faloona and Unger, 1973; Reaven *et al.*, 1987; Mitrakou *et al.*, 2010; Meek *et al.*, 2015). The role of glucagon signalling in DM was evident by hepatic *GCGR* ablation in relevant rodent models. Previous studies demonstrated the loss of hepatic *GCGR* activity lowers hyperglycaemia and improves glucose tolerance in DM rodent models with retained β-cell mass, identifying a potential therapeutic target for excessive hepatic gluconeogenesis (Parker *et al.*, 2002; Gelling *et al.*, 2003; Kelly *et al.*, 2015; Wang *et al.*, 2015). Hepatic GCGR antagonism is, however, associated with α-cell hyperplasia, hyperaminoacidaemia, hepatic steatosis and raised low-density lipoprotein (LDL) levels which may limit the use of GCGR antagonists in clinic (Longuet *et al.*, 2013; Young H. Lee *et al.*, 2016; Galsgaard *et al.*, 2018). These findings, on the contrary, provide substantial evidence for a liver-α-cell feedback loop in regulating glucose homeostasis in physiology and in DM pathophysiology. The impaired hepatic glucagon signalling in DM, especially in individuals with hepatic steatosis, is commonly referred in published literature as “glucagon resistance” (Janah *et al.*, 2019). Glucagon resistance describes the defective hepatic amino acid uptake and reduction in glucagon signalling resulting in hyperaminoacidaemia which further potentiates a glucagon secretory response (i.e., hyperglucagonaemia) (Richter *et al.*, 2022). If, in DM, diminished hepatic glucagon signalling is potentiated by hepatic GCGR protein internalisation and/or downregulation is debated and therefore requires further research (Kramer *et al.*, 2021). Individuals with a rare *GCGR* inactivating mutation (Mahvash syndrome) demonstrated hyperaminoacidaemia, an unsuppressed glucagon secretory profile and in rare cases, α-cell hyperplasia, which is phenotypically similar to *GCGR*-ablated mice (Li *et al.*, 2018; Danielle Dean, 2020). These findings provide evidence towards the defective amino acid liver-α-cell axis in DM, potentiating excessive α-cell activity and hepatic glucagon

resistance commonly associated with T2DM and associated hepatic steatosis complications.

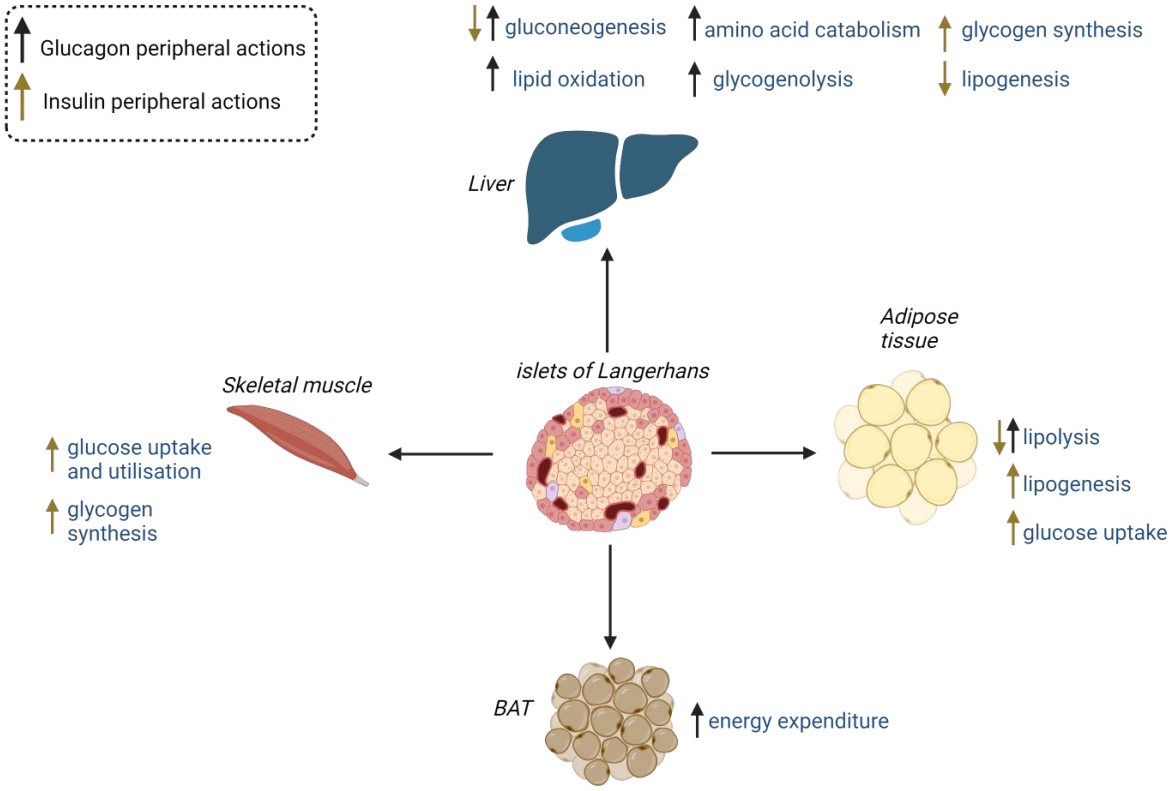

Figure 1.6: Peripheral actions of islet glucagon and insulin secretion.

Insulin primarily acts by stimulating glucose uptake in peripheral tissues and inhibits gluconeogenic/lipogenic pathways in the liver. Glucagon acts primarily on the liver by stimulating gluconeogenesis and amino acid catabolism in response to hypoglycaemia. Created using Biorender.com.

1.3 Intrinsic metabolic regulation of glycaemia

1.3.1 Gluconeogenesis and glycolysis

Hepatic glucagon-GCGR binding stimulate Gαs-coupled increases in cAMP levels leading to protein kinase-A (PKA) and cAMP response element-binding protein (CREB) activation. Phosphorylated CREB drive PEP carboxylkinase (*PEPCK*) and glucose-6-phosphatase (*G6PC*) gene expression by binding to cAMP response element (CRE) (Figure 1.7). Hepatic PEPCK activity drives oxaloacetate conversion to PEP for feeding into gluconeogenesis (illustrated in Figure 1.8), whereby G6PC catalyses the terminal gluconeogenic step for glucose-6-phosphate (G6P) conversion to glucose (Yang, Kalhan and Hanson, 2009; Sharma and Tiwari, 2021). Glucagon-mediated PKA activity stimulates other gluconeogenic pathways, independent of CREB, including PFK-2/fructose 2,6-bisphosphatase-2 (FBPase-2) phosphorylation (Rui, 2014). Glucagon-stimulated FBPase2 activity raises fructose 6-phosphate (F6P) levels drives glucose generation whilst reduced fructose 1,6-bisphosphate (F1,6BP) suppresses downstream glycolysis (Janah *et al.*, 2019). As glucagon-regulated gluconeogenesis is limited by transcriptional changes, glucagon signalling stimulates glycogenolysis to maintain euglycaemia during a period of acute fasting (Janah *et al.*, 2019). The glucagon/PKA cascade increases ATP-dependent phosphorylation of phosphorylase kinase and glycogen synthase, favouring hepatic glycogen breakdown to generate glucose (Janah *et al.*, 2019). Furthermore, PKA inactivates pyruvate kinase (PK), thereby limiting pyruvate generation and favouring F1,6BP generation. Glucagon influence on hepatic gluconeogenesis and glycolysis is summarised in both Figure 1.7 and Figure 1.8.

Glycolysis is a metabolic pathway required to generate ATP by supplying carbon substrate to the mitochondria and drive lactate production dependent on oxygen availability. Glycolytic rate is determined by glucose availability and activity of key rate-limiting enzymes. One of these, hexokinase (HK) IV/glucokinase (GK), drives glucose shuttling into the cell by relevant glucose transporters (GLUT) and/or sodium-glucose co-transporters (SGLT) and is

subsequently metabolised into G6P. The detailed mechanisms behind gluconeogenesis and glycolysis are summarised in Figure 1.8 (adapted from Cruz, 2019). The peach circles illustrate key rate-limiting enzymes of glycolysis.

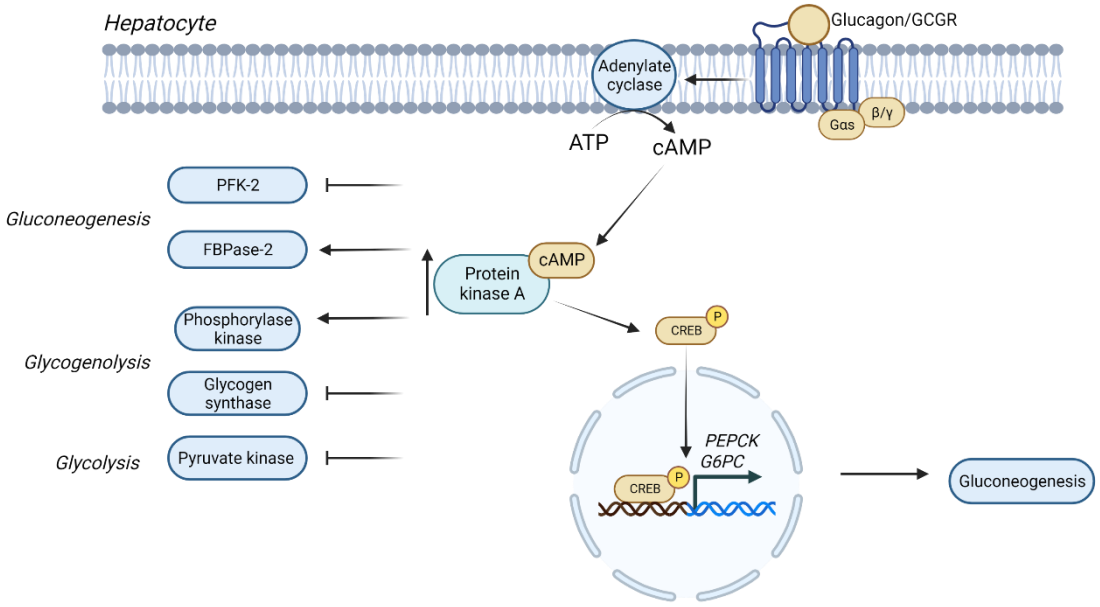

Figure 1.7: Glucagon/GCGR association and downstream mechanistic signalling pathways in hepatocytes.

Glucagon binding to the glucagon receptor (GCGR) stimulates the associated G-protein signalling cascade and the subsequent increase in intracellular cAMP levels. cAMP-stimulated protein kinase A (PKA) activation inhibits phosphofructokinase-2 (PFK-2), stimulates fructose 2,6-phosphatase-2 (FBPase-2) activity. Glucagon stimulates phosphorylase kinase activity and inhibits glycogen synthase by promoting glycogenolysis. In addition, glucagon inhibits pyruvate kinase activity and therefore limiting hepatic glycolytic rate. Glucagon increases cAMP/PKA activity and CREB phosphorylation/translocation to the nucleus for transcriptional upregulation of *PEPCK/G6PC*-dependent gluconeogenesis (CREB; cAMP response element-binding protein, PEPCK; phosphoenolpyruvate carboxylkinase, G6PC; glucose 6-phosphatase catalytic subunit). Created using Biorender.com.

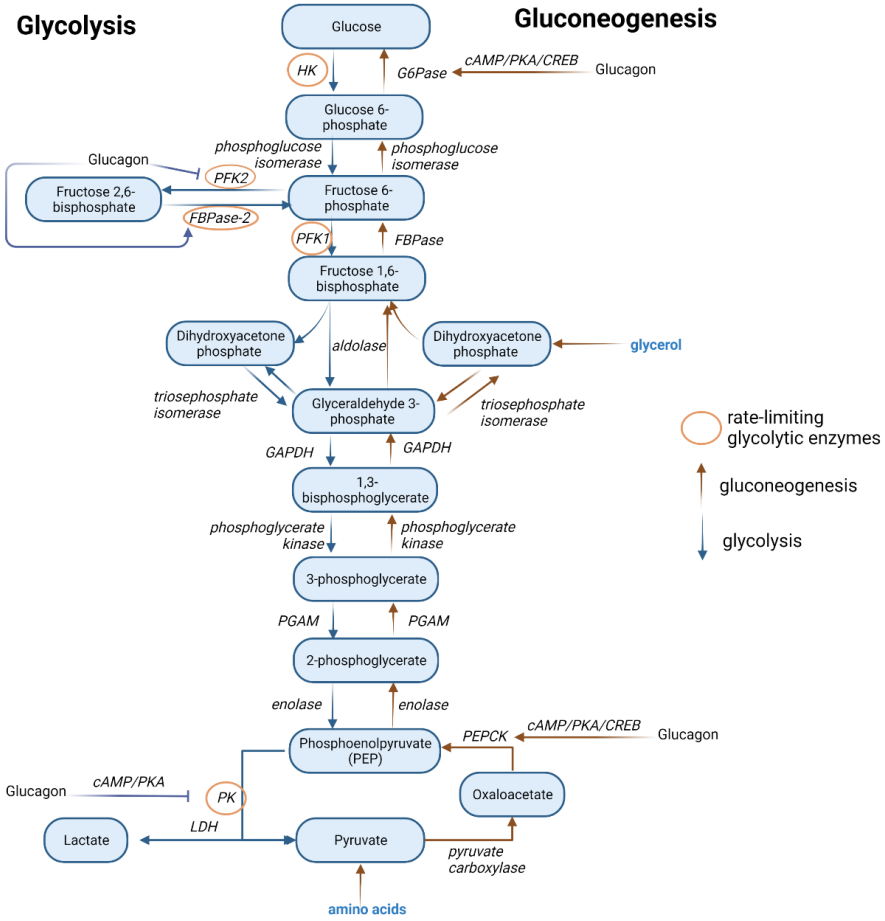

Figure 1.8: Glycolysis and gluconeogenic metabolic pathways.

The major enzymes and substrates responsible for glycolysis and gluconeogenesis. Glycolysis involves the conversion of imported glucose into a series of glycolytic intermediates to generate mitochondrial carbon substrate, pyruvate, for shuttling into the Krebs cycle. In certain tissues, dependent on fasted/fed status, pyruvate can be readily converted to lactate by lactate dehydrogenase (LDH) in anaerobic conditions. The peach circles identify rate-limiting enzymes for glycolysis, including pyruvate kinase (PK), phosphofructokinase-1 and -2 (PFK1/2), fructose 2,6-bisphosphatase (FBPase), and hexokinase (HK). Gluconeogenesis pathway involves the generation of “new” glucose from pyruvate carbon substrates. Amino acids, such as alanine, and glycerol generated from adipose tissue promote glucose generation in the liver. Glucagon can modulate different rate-limiting enzymes in both glycolysis and gluconeogenesis by stimulating cAMP/PKA pathway. Glucagon enhances cAMP/PKA signalling, thereby CREB transcriptional regulation, of key gluconeogenic genes (PEPCK and G6Pase). Elevated glucagon levels in the blood inhibit PFK-2 activity to reduce F 2,6-BP levels, as well as stimulating FBPase-2 activity. PGAM; phosphoglycerate mutase, PEPCK; phosphoenolpyruvate carboxylase, GAPDH; glyceraldehyde 3-phosphate dehydrogenase, G6Pase; glucose 6-phosphatase. Adapted from Cruz, 2019. Created using Biorender.com.

1.3.2 Oxidative respiration

Following glycolytic-derived pyruvate import into the mitochondria, pyruvate dehydrogenase (PDH) complex (PDC) facilitates pyruvate decarboxylation into acetyl-CoA, a key component in oxidative respiration. PDC complex links anaerobic glycolysis to mitochondrial oxidative respiration, driving metabolism in both fasted and postprandial conditions (Patel *et al.*, 2014). Pyruvate can enter the Krebs cycle also by carboxylation to oxaloacetate (OAA) by pyruvate carboxylase (PC). This anaplerotic pathway is required for hepatic OAA replenishment, fuelled by circulating amino acids and glycolytic end-products in order to regenerate intermediates for the Krebs cycle required for urea cycling to maintain hepatic redox state and gluconeogenesis (Cappel *et al.*, 2019). The Krebs cycle and related intermediates are summarised in Figure 1.9.

NADH and $FADH_2$ molecules, both generated from the Krebs cycle, enter the electron transport chain (ETC) by transferring electrons at both complex I (NADH : ubiquinone) and complex II (Nolfi-Donegan, Braganza and Shiva, 2020). Complex I transfer of electrons result in the extrusion of $4H^+$ across the inner mitochondrial membrane (IMM) (Nolfi-Donegan, Braganza and Shiva, 2020). Electrons from either complex I or II are transferred to complex III by reduced ubiquinol and leads to the extrusion of $2H^+$ (Nolfi-Donegan, Braganza and Shiva, 2020). Cytochrome c passes electrons to complex IV whereby both oxygen is a terminal electron acceptor to generate water (Nolfi-Donegan, Braganza and Shiva, 2020). Oxygen reduction to water result in protons being extruded by complex IV. Proton extrusion across the IMM space, as a result of electron transfer throughout the ETC, generates a protonmotive force commonly termed the mitochondrial membrane potential (Nolfi-Donegan, Braganza and Shiva, 2020). This protonmotive force couples electron transport and oxygen consumption to complex V (ATP synthase) and protons are subsequently imported back into the mitochondrial matrix. This protonmotive force drives, alongside a conformational rotation in complex V, ATP synthesis and is thereby called coupled respiration (Nolfi-Donegan, Braganza and Shiva, 2020; Ahmad, Wolberg and Kahwaji, 2022).

Uncoupled respiration is driven by adenine nucleotide translocase (ANT) and uncoupling protein (UCP) activity, which promotes mitochondrial proton leak from the IMM into the mitochondrial matrix (Nolfi-Donegan, Braganza and Shiva, 2020). Free fatty acids can act as mitochondrial uncouplers by stimulating UCP opening, and therefore have therapeutic significance in pathology. NAFLD-associated T2DM is characterised by hepatic and peripheral tissue oxidative stress, driving chronic low-grade inflammation as a result of hepatic lipid accumulation (Pinti *et al.*, 2019; Jakovljevic *et al.*, 2021). Pancreatic islets in T2DM are exposed to inflammatory mediators, driven by cytochrome c release and mitochondrial oxidative stress (Ma, Zhao and Turk, 2012; Janikiewicz *et al.*, 2015). As such, β-cells have dysfunctional antioxidant defences to inflammation by increases in intracellular reactive oxygen species (ROS) generation and compromised ER function, driving cell death (Sha, Hu and Bu, 2020). Little is known about α-cell mitochondrial function in DM. Several studies, including mathematical modelling and complex I knockout models, suggest decreased ATP-coupled respiration, possibly due to dysregulated complex I activity, further increases α-cell hyperplasia commonly associated with T2DM development (Grubelnik *et al.*, 2020a; Yu *et al.*, 2022).

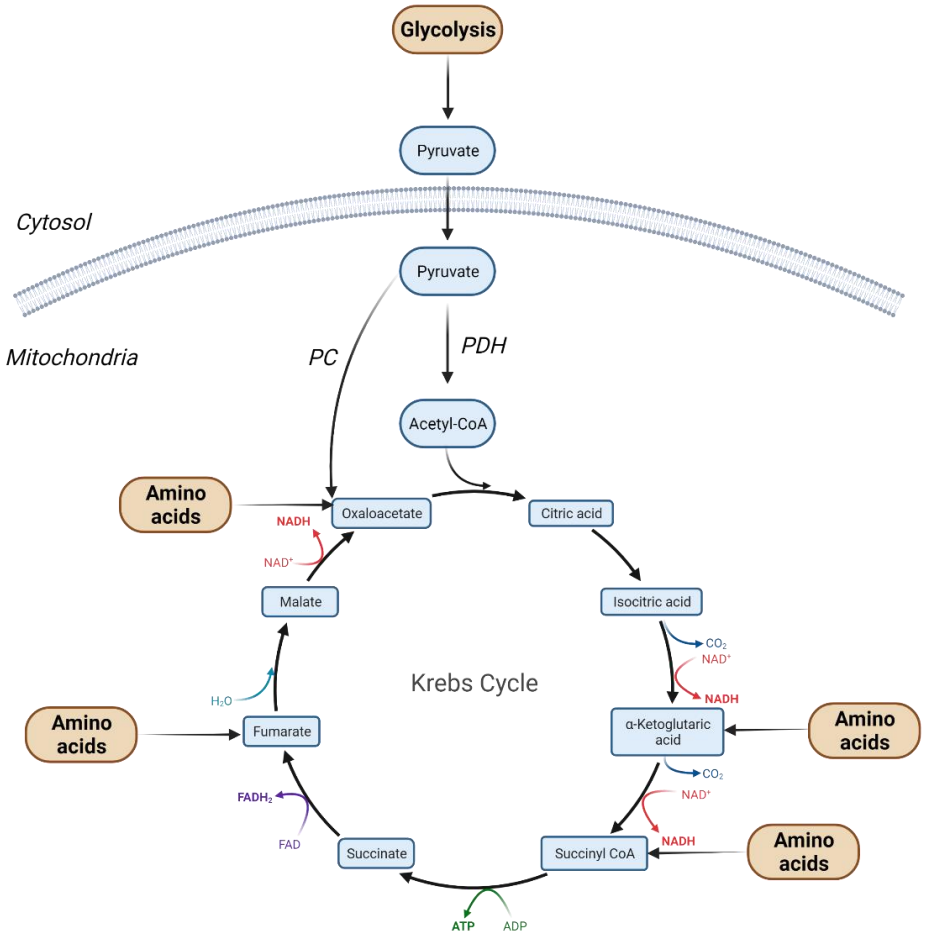

Figure 1.9: Mitochondrial pyruvate shuttling into the Krebs cycle.

Glycolytic end-product, pyruvate, is shuttled into the mitochondria to be converted to either acetyl-CoA or oxaloacetate by pyruvate dehydrogenase (PDH) or pyruvate carboxylase (PC) respectively. Citrate synthase catalyses the conversion of acetyl-CoA to citric acid and is regarded as the preliminary step of the Krebs cycle. Citric acid isomerised by aconitase to isocitric acid. Isocitric acid is decarboxylated to form NAD-dependent α-ketoglutaric acid, resulting in NADH generation. Amino acids, such as glutamine, can be metabolised to form α-ketoglutaric acid, further fuelling the Krebs cycle. α-ketoglutaric acid is further decarboxylated by α-ketoglutaric acid dehydrogenase; again, generating the cofactor NADH, to succinyl-CoA. Other amino acids, such as thymine, valine and isoleucine, fuel the generation of succinyl-CoA. Succinyl CoA is cleaved to result in succinate, an ATP-generating process. Succinate is oxidised to fumarate (a urea cycle end-product) by succinate dehydrogenase, generating the cofactor $FADH_2$. Fumarate can also be generated by several amino acids, including tyrosine and phenylalanine. Fumarate is hydrated to malate by fumarase, and malate is converted to oxaloacetate by malate dehydrogenase oxidation, generating $NADH_2$. This is considered the final step of the Krebs cycle, with the generation of cofactors $NADH_2$ and $FADH_2$ fuelling oxidative phosphorylation. Created using Biorender.com.

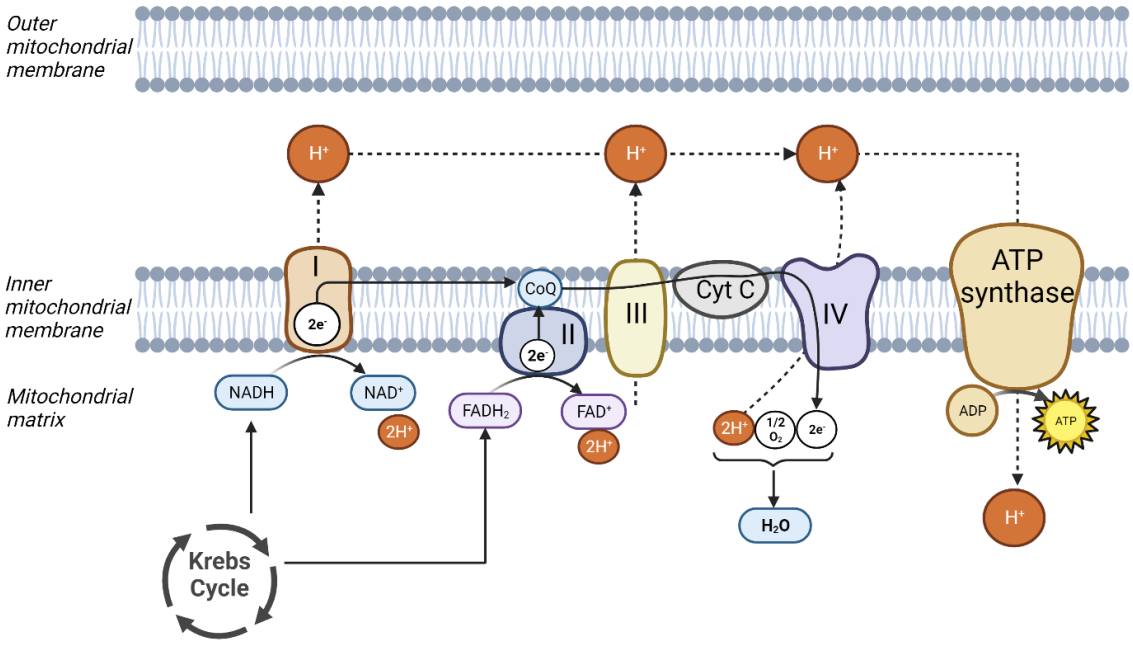

Figure 1.10: Schematic diagram illustrating mitochondrial oxidative phosphorylation.

NADH, a generated cofactor from the Krebs cycle, fuels complex I activity (ubiquinone oxidoreductase). Complex I comprise of NADH dehydrogenase, flavin mononucleotide (FMN) and iron-sulphur (Fe-S) clusters. NADH is converted to NAD by NADH dehydrogenase, transferring to 2 electrons ($2e^-$) from NADH to the flavin mononucleotide (FMN) and is accepted by succinate (complex II). 4 hydrogen ions (H^+) are extruded into the intermembrane space, setting a proton gradient within the mitochondria. Complex II accepts $2e^-$ generated from $FADH_2$ (generated from the Krebs cycle) catabolism, and is shuttled to coenzyme Q (CoQ), an electron carrier (in addition to complex I $2e^-$) to complex III. Complex III (cytochrome c reductase) can release 4 H^+ ions into the inner mitochondrial space, further driving the proton gradient. Cyt C (cytochrome C) transfer electrons into the mitochondrial matrix, by complex IV (cytochrome oxidase) to bind to oxygen (as well as H^+ ions) to generate H_2O. Complex V (ATP synthase) utilises the protonmotive force to form ATP via rotational conformational change of the complex and H^+ movement into the mitochondrial matrix. Created with Biorender.com.

1.3.3 Fatty acid oxidation (FAO)

In the liver, fasting periods require increased mitochondrial fatty acid oxidation (FAO) as an alternative metabolic pathway to sustain both ATP and NADH to fuel gluconeogenesis, and ketogenesis. In periods of glucose deprivation, hepatic FAO also regenerates acetyl-CoA to sustain oxidative respiration (Jieun Lee *et al.*, 2016). To allow mitochondrial import, fatty acids are activated by thioester modification with Coenzyme A dependent on acyl-CoA synthetases (Talley and Mohiuddin, 2023). Fatty acid acyl-CoA products are imported across the outer mitochondrial membrane (OMM) by carnitine palmitoyltransferase 1 (CPT1) by catabolising into acylcarnitine (Talley and Mohiuddin, 2023). Malonyl-CoA, generated by acetyl CoA carboxylase 1/2 (ACC1/2) catabolism of acetyl CoA, is an inhibitor of FAO by blocking CPT1 activity (Zu *et al.*, 2013). Acylcarnitine is then imported into the IMM by carnitine-acylcarnitine translocase (Talley and Mohiuddin, 2023). Acylcarnitine is converted back to acyl-CoA by CPT2 located on the IMM (Talley and Mohiuddin, 2023). Acyl-CoA is catalysed to acetyl-CoA and provides a carbon substrate for the Krebs cycle (Figure 1.11).

The reduced endogenous insulin production/action, as well as hyperglucagonaemia, in DM promotes hyperglycaemia by excessive hepatic gluconeogenesis, FAO, ketone body generation and impaired peripheral glucose uptake (Boden and Chen, 1999). The increased incomplete oxidation of FFAs result in the production and release of ketone bodies, including β-hydroxybutyrate (BHB) and acetoacetate, into the bloodstream resulting in DKA (Olpin, 2004). DKA is a severe complication commonly associated with insulin deficient T1DM and T2DM (Basu *et al.*, 1993). DKA is severe due to enhancing metabolic acidosis, as a result of reduced blood buffering capacity, a reduction in blood osmolarity (“hyperglycaemic hyperosmolar state”, HHS) and if not treated, can lead to renal failure (Gosmanov, Gosmanova and Kitabchi, 2021). DKA and HHS are further exacerbated by elevations in counterregulatory hormone secretion (glucagon, epinephrine) which further potentiate the hyperglycaemic state (Gosmanov, Gosmanova and Kitabchi, 2021). Therefore,

attention is needed towards treating DKA/HHS and modulating counterregulatory hormone secretion, as DKA is commonly the first overt symptom of DM (Fadini *et al.*, 2011; Ehrmann *et al.*, 2020).

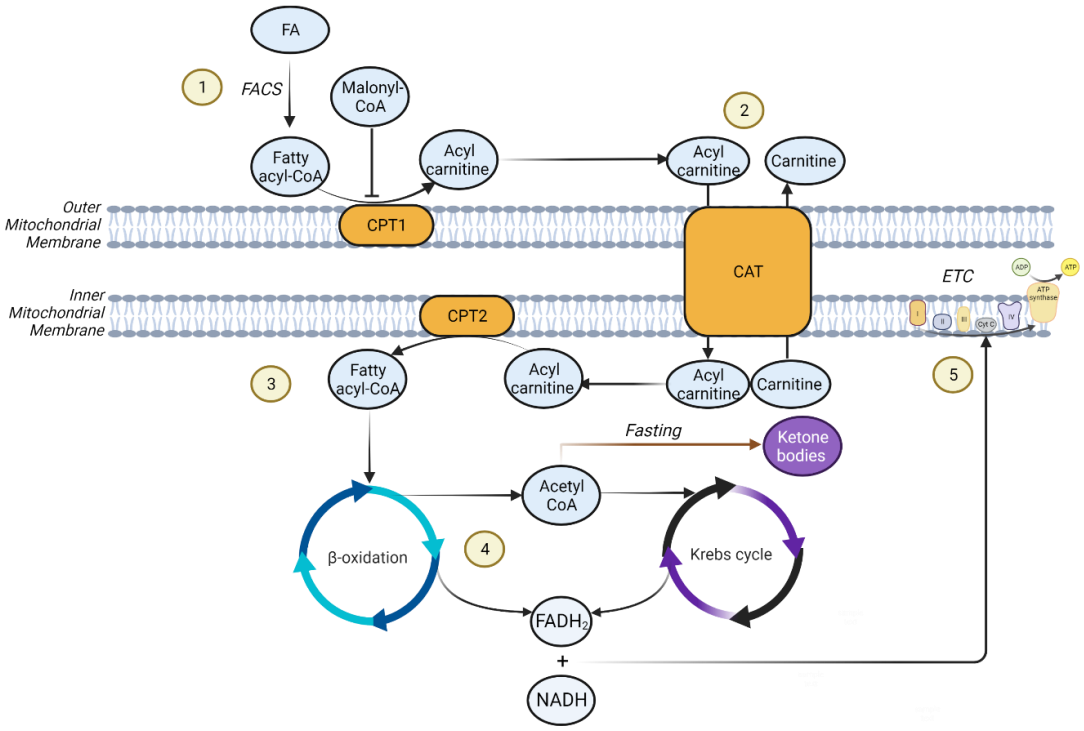

Figure 1.11: Schematic diagram of mitochondrial fatty acid oxidation (FAO).

(1) Long chain fatty acids (FAs) are esterified by long-chain fatty acyl-CoA synthetase (FACS) into fatty acyl-CoA whereby the FAs are “activated”. The mitochondrial membrane is impermeable to fatty acyl-CoA, and thereby they are converted to acyl-carnitine by carnitine palmitoyltransferase 1 (CPT1) located on the outer mitochondrial membrane (OMM). Malonyl CoA is an inhibitor of fatty acid oxidation (FAO) by limiting CPT1 activity and is inactivated by acetyl-CoA carboxylase (ACC) phosphorylation. (2) Acyl carnitine is imported into the mitochondrial matrix by carnitine translocase (CAT) alongside the extrusion of carnitine, known as the carnitine shuttle. (3) Acyl carnitine is converted back to fatty acyl-CoA by CPT2 localised to the inner mitochondrial membrane (IMM). (4) β-oxidation of fatty acyl-CoA generates acetyl CoA carbon substrates to feed the Krebs cycle and generate ketone bodies in periods of fasting following glycogen store depletion (in the liver). (5) Both the Krebs cycle and β-oxidation generates $FADH_2$/NADH to drive oxidative phosphorylation for coupled ATP synthesis. Created using Biorender.com.

1.4 Pancreatic α-cell regulation of glucagon secretion

Glucagon was first classified as a "contaminant" in pancreatic extracts when purifying insulin, due to the role of glucagon as a hyperglycaemic agent (Murlin *et al.*, 1923). Glucagon is accurately named from the label "**gluc**ose **agon**ist" for this reason (Banting and Best, 1922). The pioneering work by Unger and colleagues developed the first glucagon radioimmunoassay, in 1959, to measure sample glucagon content (Unger *et al.*, 1959). Since then, advanced understanding on glucagon processing have optimised reliable glucagon detection to exclude posttranslational proglucagon products (Holst and Albrechtsen, 2019). The proglucagon precursor is cleaved by prohormone convertase 2 (PC2) (α-cells) or PC1/3 (intestinal L cells), and in the islet generates glicentin-related pancreatic polypeptide (GRRP), glucagon, intervening peptide 1 (IP1) and major proglucagon fragment (MPGF) including GLP-1, IP2 and GLP-2 (Rix *et al.*, 2019).

1.4.1 Intrinsic low glucose stimulation

There is vast evidence to suggest a direct, low glucose-sensing ability of the α-cell to potentiate glucagon secretion. Pancreatic α-cells express the relevant glucose-sensing machinery to direct respond to a low glucose challenge, alongside extra-islet innervation (e.g., autonomic stimulation). Greater understanding, however, is required on both the importance and interplay of relevant glucose-sensing enzymes (e.g., AMPK) on α-cell function. In addition, it is debated in the published literature with regards to the role of ATP-sensitive potassium channel (K_{ATP}) activity and α-cell electrical activity, which is evaluated in greater depth in a recent review (Zhang, Dou and Rorsman, 2020). Figure 1.12 summarises the putative downstream metabolic alterations in response to low glucose (Tengholm and Gylfe, 2017; Zhang, Dou and Rorsman, 2020).

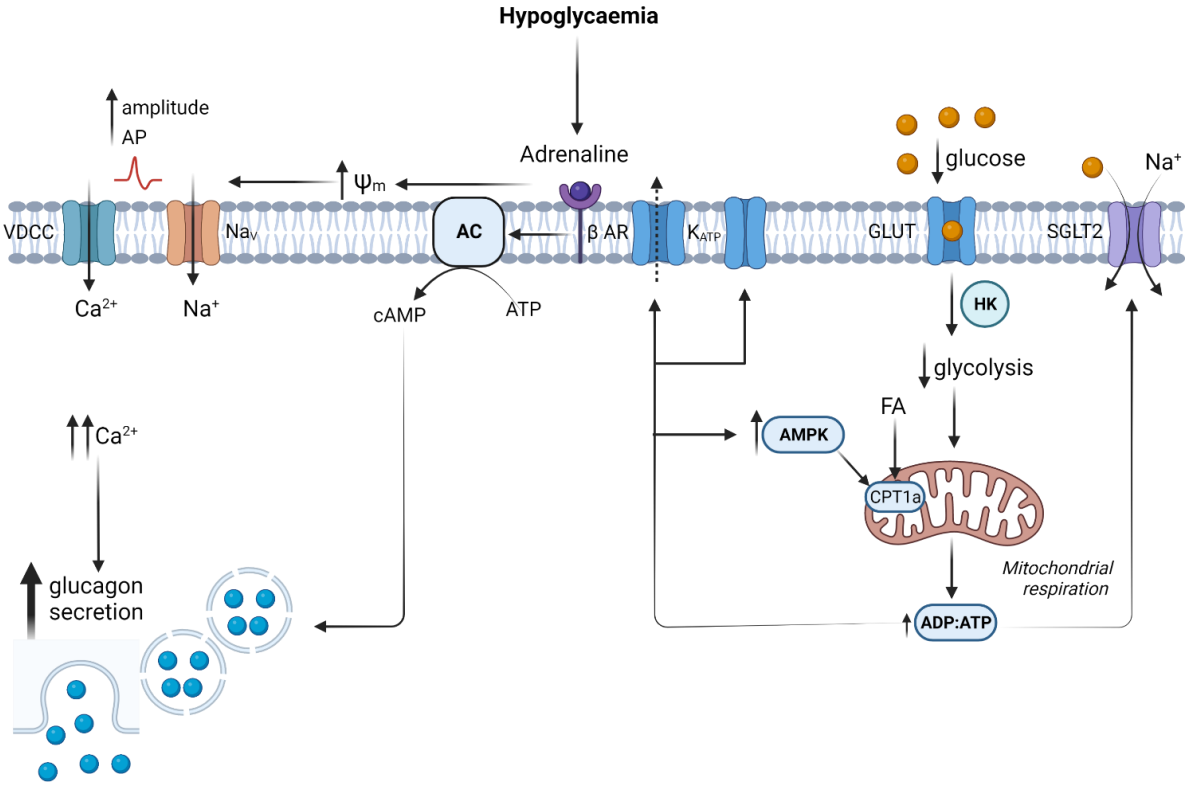

Figure 1.12: Low glucose-regulated glucagon secretion from pancreatic α-cells.

Low glucose concentrations enter by GLUT- and SGLT-mediated transport. The low intracellular glucose is then catabolised by the rate-limiting enzyme hexokinase-1 (HK-1) and oxidised to generate acetyl CoA for mitochondrial respiration. In addition, CPT1a-dependent FAO (most likely from endogenous FA) sustain ATP production to retain Na^+/K^+/ATPase activity and α-cell electrical activity under glucose-deprived conditions. Master energy sensor, AMP-activated kinase (AMPK), activity is high, and one could postulate AMPK-mediated ACC inactivation drives a glucagon secretory response via FAO. In addition, ADP:ATP ratio is low enough to close the majority of K_{ATP} channels, but K_{ATP} channel activity is not absent. Partial K_{ATP} channel activity maintains α-cell membrane sufficiently depolarised for voltage-gated Na^+ channel activation and thereby increasing action potential (AP) amplitude greater than the threshold for AP firing. The activation of voltage-gated calcium channels (VDCC), by high-amplitude APs facilitates a rise in $[Ca^{2+}]_I$, which further drives glucagon granule exocytosis. In addition, mitochondrial ATP production could drive increased intracellular cAMP (by adenylate cyclase, AC) and thereby glucagon exocytosis, but by what mechanism is relatively unclear. Autonomic counterregulatory secretion of adrenaline increases intracellular cAMP and potentiates low glucose-stimulated glucagon secretion. Created using Biorender.com.

1.4.2 Intra-islet regulation

1.4.2.1 β-cell

Glucose-stimulated insulin secretion (GSIS) from β-cells act as a paracrine "suppressor" of α-cell glucagon secretion to limit hyperglycaemia. Insulin receptors (IR) are expressed on the α-cell surface membrane, albeit at a lower level compared to β-cells (Takatani *et al.*, 2021). Insulin-IR binding can lower α-cell cAMP and thereby suppress glucagon secretion (Kawamori *et al.*, 2009; Elliott, Ustione and Piston, 2015). A recent study contested the direct insulin suppression of glucagon secretion, in which insulin stimulated δ-cell SGLT-mediated somatostatin secretion and therefore suppressed α-cell activity (Vergari *et al.*, 2019). Additional clarity if insulin or insulin secretagogues directly regulates α-cell secretion, is required. Insulin-containing granules contain transmitters such as GABA and zinc, and upon secretion, inhibit α-cell glucagon secretion (Franklin *et al.*, 2005; Xu *et al.*, 2006; Bailey, Ravier and Rutter, 2007; Kawamori *et al.*, 2009; Hardy *et al.*, 2011). The inhibitory neurotransmitter, GABA, binds to chloride channel $GABA_A$ receptor ($GABA_AR$) localised on the α-cell membrane, in which receptor translocation is increased in response to high glucose (Xu *et al.*, 2006). An increase in $GABA_AR$ opening, a chloride channel, hyperpolarises the α-cell, further limiting voltage-gated calcium channel (VDCC) opening and glucagon exocytosis (Xu *et al.*, 2006). Zinc is localised in β-cell insulin granules to regulate granule formation and insulin crystallisation by ZnT8-mediated zinc import into the granules (Qian *et al.*, 2000; Gee *et al.*, 2002). Zinc, when released, can reportedly inhibit α-cell glucagon secretion by K_{ATP} channel activation, and act as an "off signal" (Slucca *et al.*, 2010; Solomou *et al.*, 2015). It is important to note the action of zinc on α-cell function is contested due the high heterogeneity in ability to control α-cell glucagon secretion, possibly due to species differences (Slucca *et al.*, 2010; Solomou *et al.*, 2015). The β-cell secretion of serotonin, a known autocrine proliferative factor for β-cell growth, can suppress α-cell glucagon secretion at high glucose (Almaça *et al.*, 2016). Human α-cells express high levels of serotonin receptor $5HT_{1F,}$ in which serotonin binding attenuates crucial intracellular messenger cAMP and cAMP-mediated glucagon exocytosis (Almaça *et al.*, 2016).

1.4.2.2 δ-cell

Published research investigating δ-cell function and role in intra-islet signalling is increasing, due to the postulated δ-cell perturbations in insulin-induced hypoglycaemia (Klaff and Taborsky, 1987; Yue *et al.*, 2012; Karimian *et al.*, 2013). δ-cells are electrically excitable cells which secrete somatostatin (SST) in response to high glucose (Miranda *et al.*, 2022). SST inhibits both β-cell and α-cell activity, with α-cells expressing somatostatin receptor 2 isoform (SSTR2) on the cell surface membrane (Kailey *et al.*, 2012). It is thought that α-cell SST-SSTR2 colocalises to both L-type calcium channels and G-protein inwardly rectifying potassium (GIRK) channels, to promote α-cell hyperpolarisation and limit cAMP-dependent glucagon exocytosis (Gromada *et al.*, 2001). Interestingly, glucagon receptor ablation and loss of glucagon secretion abolished the SST response to increasing glucose availability, suggesting bi-hormonal (rather than unidirectional) feedback between α- and δ-cells (Svendsen and Holst, 2021).

1.4.3 Autonomic regulation and extraislet regulation

The autonomic innervation of the adrenal gland is responsible for stimulating adrenaline secretion (“fight or flight”) in response to hypoglycaemia. Adrenaline is a potent stimulator of α-cell glucagon secretion to raise blood glucose levels, by binding to cell surface α1 and β1-adrenoreceptors and increasing $[Ca^{2+}]_I$ (Vieira, Liu and Gylfe, 2004; De Marinis *et al.*, 2010). β-adrenergic activation raises α-cell $[Ca^{2+}]_I$ by stimulating two pore segment channel 2- (Tpc2) dependent calcium release from intracellular lysosomal stores, possibly by activation of exchange proteins activated by cAMP (EPAC2) and/or cAMP mobilisation (De Marinis *et al.*, 2010; Hamilton *et al.*, 2018).

Early studies suggested the postprandial release of glucose-dependent insulinotropic polypeptide (GIP) from intestinal K-cells inhibits glucagon secretion (Pederson and Brown, 1978). Recently, however, one study proposed an intestine-α-cell-β-cell axis for postprandial regulation of glycaemia (El *et al.*, 2021). The findings suggested GIP and the amino acid alanine additively

stimulate glucagon secretion, alongside direct β-cell GIP/GIPR binding, to potentiate the insulin response to limit postprandial hyperglycaemia (El *et al.*, 2021). During fasted conditions, although plasma GIP levels are low, GIP is a potent stimulator of α-cell glucagon secretion by increasing downstream cAMP/PKA signalling cascade and suppressing insulin secretion (Opara and Go, 1991; Christensen *et al.*, 2011; El *et al.*, 2021). The bi-hormonal action of GIP poses a valuable pharmacological target for restoring defective α-cell glucagon secretion in RH in response to a hypoglycaemic episode (El *et al.*, 2021).

1.4.4 Autocrine regulation

In response to low glucose, α-cells amplify the glucagon secretory response by autocrine potentiation. Autocrine stimulation by glucagon enhances the positive feedback loop by binding to surface glucagon receptors, further raising intracellular cAMP, thereby potentiating α-cell exocytosis and *Gcg* transcriptional expression (Ma *et al.*, 2005; Leibiger *et al.*, 2012). In addition, glutamate can act as an autocrine potentiator of glucagon secretion. Glutamate is colocalised in glucagon granules, and upon stimulation, bind onto ionotropic glutamate receptors (iGluRs) localised on the cell surface membrane, raising $[Ca^{2+}]_i$ to further enhance glucagon release (Yamada *et al.*, 2001; Cabrera *et al.*, 2008; Panzer, Tamayo and Caicedo, 2022). The defective glucagon release in response to hypoglycaemia in DM could be partially restored by pharmacological iGluR activation, however, this requires additional investigation.

1.5 Pancreatic β-cell regulation of insulin secretion

1.5.1 Glucose-stimulated insulin secretion (GSIS)

High glucose imported into the pancreatic β-cell, via GLUT transporters, is first metabolised by glucokinase (GK). The increase in intracellular glucose enhances glycolysis and therefore generation of pyruvate sustains mitochondrial-derived ATP generation. In addition, the increase in ATP drives rises in cAMP to further potentiate glucose-stimulated insulin secretion (GSIS). Low [ADP:ATP] levels inhibit β-cell K_{ATP} channel activity, further driving membrane depolarisation. Membrane depolarisation increases VDCC opening, raising $[Ca^{2+}]_I$ and potentiating insulin exocytosis. In theory, the low ADP:ATP ratio as a result of high glucose, would inhibit β-cell AMPK activity. Previous findings have shown the loss of catalytic AMPKα2-subunit diminished GSIS in mice, providing evidence for the importance of AMPK in sustaining β-cell function and glucose sensitivity (Beall *et al.*, 2010). Other metabolic coupling factors, such as NADPH, glutamate and PKC, also drive insulin granule exocytosis (Vega-Monroy *et al.*, 2011; Komatsu *et al.*, 2013).

1.5.2 Intra-islet regulation

1.5.2.1 α-cell

Glucagon release from neighbouring α-cells is crucial in sustaining basal insulin secretion. Glucagon and proglucagon products (including GLP-1) stimulate insulin secretion by binding GLP-1R and GCGR receptors on the β-cell surface membrane (Kilimnik *et al.*, 2010; Svendsen *et al.*, 2018). GLP-1R/GCGR stimulation increases intracellular cAMP, $[Ca^{2+}]_i$ and PKA/EPAC-mediated insulin exocytosis at high glucose levels (Meloni *et al.*, 2013).

In addition, acetylcholine is not just a neural β-cell stimulus. Acetylcholine is also secreted from α-cells, following a drop in glucose, to retain β-cell insulin response via muscarinic receptor activation (Rodriguez-Diaz *et al.*, 2011a). As acetylcholine can stimulate δ-cell SST secretion by M1 receptor binding, one review suggested acetylcholine acts a “feed forward” messenger to retain β-cell

sensitivity to subsequent changes in glycaemia and therefore limiting glycaemic variability (Rodriguez-Diaz *et al.*, 2020).

Interestingly, corticotropin-release hormone (*CRH*) transcript is abundantly expressed in α-cells (Benner *et al.*, 2014). CRH receptor type 1 (CRHR1) is expressed on the β-cell membrane and upon binding, canstimulate cAMP-mediated insulin release(Huising *et al.*, 2010). Further clarification into CRH-mediated insulin release is important to understand intra-islet regulation of β-cell function.

1.5.2.2 δ-cell

Urocortin-3 (UCN3) is co-released with insulin to stimulate δ-cell activity via UCN3-selective receptor, CRH2 (Van Der Meulen *et al.*, 2015). UCN3 is depleted in T2DM non-human and human β-cells, and cells lacking UCN3 have defective SST release and excessive GSIS response (Van Der Meulen *et al.*, 2015). UCN3 is therefore a potent regulator of β-cell insulin secretion to limit glycaemic variability and insulin-induced hypoglycaemia. In addition, SST via SST-5 binding inhibits cAMP-mediated insulin secretion by activating K_{ATP} and GIRK channels, reducing VDCC opening thereby attenuating Ca^{2+} influx (Ribalet and Eddlestone, 1995; Strowski *et al.*, 2000; Smith, Sellers and Humphrey, 2001). Altogether, these findings infer the importance of intra-islet regulation of hormone secretion.

1.5.3 Autonomic and extra-islet regulation

Noradrenaline activation by α_{2A}- adrenergic receptor binding, inhibits insulin secretory response by G-protein cascade activation (Zhao *et al.*, 2010). Noradrenaline can increase K_{ATP} channel activity up to two-fold, thereby inducing β-cell hyperpolarisation (Ying Zhao *et al.*, 2008). Overall, however, there is a lack of understanding on the neural control of β-cell insulin secretion. This is contributed by the differences between the localisation of sympathetic nerve endings in rodent and human islets due to contrasting islet architecture.

As mentioned, CRH can modulate insulin secretion from rodent islets (Huising *et al.*, 2010). One study showed AVP and CRH additively potentiate islet insulin secretion partially reliant on PKC pathway activation and regulation of $[Ca^{2+}]_I$ (O'Carroll *et al.*, 2008). CRH and AVP are neuropeptides that primarily act via the hypothalamic/pituitary/adrenal axis, identifying a possible new autonomic regulatory pathway for β-cell function (O'Carroll *et al.*, 2008).

The incretin regulation of insulin secretion has gained large focus in targeting therapeutics in T2DM. Postprandial release of GLP-1 from intestinal L-cells enhance GLP-1-GLP-1R β-cell binding and increases downstream cAMP signalling to stimulate GSIS (Jones *et al.*, 2018). A possible gut-vagal-islet neural loop for GLP-1 enhanced β-cell function has been proposed, but this needs to be further clarified (Krieger, Langhans and Lee, 2015). The action of GLP-1R agonists on GSIS is glucose-sensitive, and thereby these mimetics provide a valuable tool for lowering hyperglycaemia associated with DM without enhancing insulin-induced hypoglycaemia (Meloni *et al.*, 2013).

The paracrine and autonomic regulation of islet cell secretion is crucial in retaining appropriate glycaemic counterregulation and sustaining euglycaemia. The importance of intrinsic glucose-sensing to couple necessary hormone secretion is at least partly controlled by master energy sensor, AMP-activated protein kinase (AMPK). The pharmacology and tight regulation of AMPK activity is covered in greater depth in the next section.

1.6 AMPK

1.6.1 Structure and function

In mammals, AMPK is a master regulator of energy homeostasis whereby activity is increased dependent on low energy status. In turn, increased AMPK activity promotes catabolic pathway activation and inhibits anabolic pathways to sustain energy balance (Herzig and Shaw, 2018). AMPK is a heterotrimeric complex comprised of distinct α-, β- and γ-isoform combinations expressed in a tissue-specific manner (Yan *et al.*, 2018). The catalytic α-subunit (α1/2) contains the kinase domain (KD), in which threonine-172 residue (Thr-172) phosphorylation is required for full kinase activity (Hawley *et al.*, 1996). The β-subunit (β1/2) is regarded as a “scaffold” protein, but upon both N-terminus myristoylation and serine-108 (Ser-108) phosphorylation in the carbohydrate-binding module (CBM), regulates γ/α-subunit interaction and downstream AMPK activity (Oakhill *et al.*, 2010; Liang *et al.*, 2015). The γ (γ1/2/3) subunit contains 4 cystathionine-β-synthase (CBS) sites for the nucleotide binding (AMP, ADP and ATP) required for energy sensing and allosteric regulation of AMPK activity (Garcia and Shaw, 2017). The domains of AMPK are illustrated in Figure 1.13.

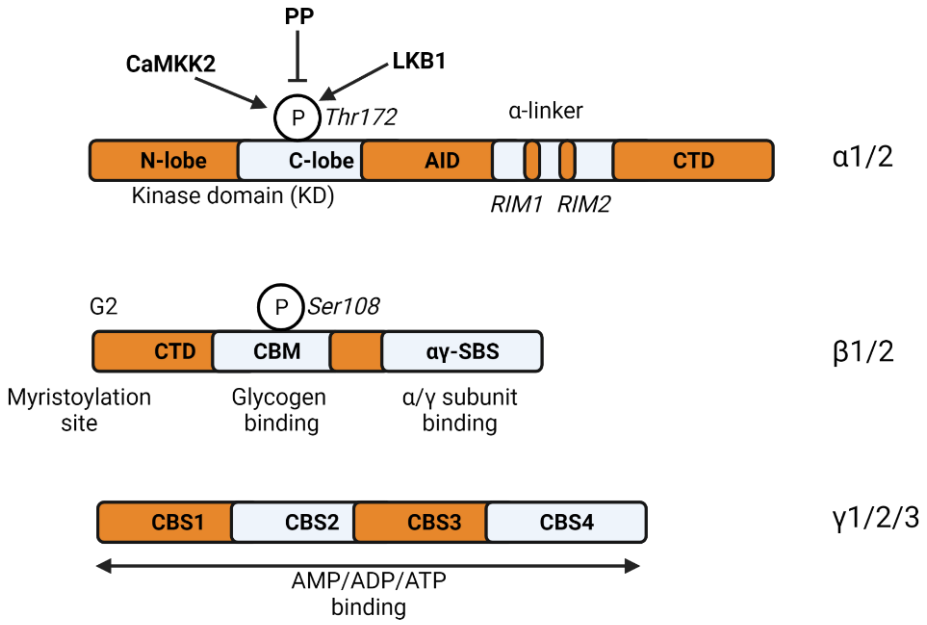

Figure 1.13: Structural domains of each AMPK subunit

The heterotrimeric AMPK complex is formed of three subunits (α, β, and γ), with the ability to form 12 different AMPK isoform-containing complexes. AMPK α1/2 contains the Thr-172 residue required for full kinase activity, housed in the C-lobe kinase domain (KD) and is further regulated by both upstream kinases (CaMKK2/LKB1) and protein phosphatases (PP); autoinhibitory domain (AID), RIM1 and RIM2 in the α-linker site (required for kinase conformational changes following binding of AMP on the γ-subunit) and C-terminal domain (CTD) site (required for β-unit binding). The AMPK β subunit contains a site, G2 at the N-terminus that when myristoylated, to potentiates allosteric AMP activation on the γ-subunit by altering AMPK complex conformation; carbohydrate binding domain (CBM) required for autoinhibitory serine-108 (Ser-108) phosphorylation on the β isoform to increase AMPK activity and glycogen binding/sensing and αγ subunit binding sequence (SBS) required for α/γ interaction and binding. The AMPK γ (1/2/3) subunit contains variable N-terminal domains (not shown) and four cystathionine β-synthase (CBS) repeats (forming two Bateman domains, CBS1/2, CBS3/4) containing four nucleotide binding sites. Created using Biorender.com.

1.6.2 Upstream kinase regulation

AMPK activity is upregulated by upstream kinases, including calcium/calmodulin dependent protein kinase kinase 2 (CaMKK2) and liver kinase B1 (LKB1). CaMKK2 is activated upon increased $[Ca^{2+}]_i$, and in turn, stimulates AMPKα Thr-172 phosphorylation (Hurley *et al.*, 2005). CaMKK2-dependent AMPK activation is at least partially mediated by hormonal stimulation (as covered in 1.6.4) (Gowans *et al.*, 2013).

LKB1 is a critical activator of AMPK and is enhanced by increased [AMP/ADP:ATP] binding to γ-subunit, especially in α2-containing tissues, such as the heart and skeletal muscle (Hawley *et al.*, 2003; Sakamoto *et al.*, 2005; Gowans *et al.*, 2013). The posttranslational modifications of LKB1 have been shown to promote association with lipid-containing membranes including lysosomes, Golgi, endoplasmic reticulum (ER), and cell surface membranes (Dogliotti *et al.*, 2017). Under nutrient-deprived conditions, LKB1 forms a complex assembly alongside AXIN, v-ATPase, Ragulator and AMPK, localised to the lysosomal membrane, to act as a direct sensor of glucose availability (Figure 1.14) (Ya Lin Zhang *et al.*, 2013; Hardie and Lin, 2017). The formation of the LKB1-AMPK-AXIN complex on the lysosomal membrane is greatly increased in glucose-deprived conditions (Ya Lin Zhang *et al.*, 2013). This complex can associate with lysosomal vacuolar-ATPase (vATPase), unoccupied aldolase and the Ragulator complex to facilitate LKB1-mediated AMPK activation (Hardie and Lin, 2017). LKB1-AXIN-AMPK binding is further enhanced upon allosteric AMP binding to AMPK (Zhang *et al.*, 2014). AXIN, as a scaffold protein, inhibits guanine nucleotide exchange factor (GEF) activity on the LAMTOR-Ragulator complex, promoting dissociation and inactivation of mTORC1 complex by Raptor phosphorylation (Zhang *et al.*, 2014). In addition, LKB1-AMPK activity limits TSC2 activity to further reduce mTORC1 activity in energy-depleted conditions (Demetriades, Plescher and Teleman, 2016). In addition, mTORC1-dependent inhibition of AMPKα2 is important for lysosomal translocation of AMPK, and thereby identifies a possible double feedback mechanism for lysosomal-associated AMPK signalling (Morrison *et al.*, 2022).

But what is the functional significance of AMPK activity localised to acidic stores? One idea could be an adaptive mechanism by the cell to “prepare” for prolonged nutrient starvation. Lysosomal vATPase is essential in maintaining granule acidification and cell autophagy, and activity is regulated by glucose availability (Song *et al.*, 2020; Sautin *et al.*, 2023). The lysosomal location of the glucose sensor and glycolytic enzyme, aldolase, could therefore “prime” AMPK to stimulate autophagic processes in periods of extended nutrient deprivation (Karabiyik *et al.*, 2021).

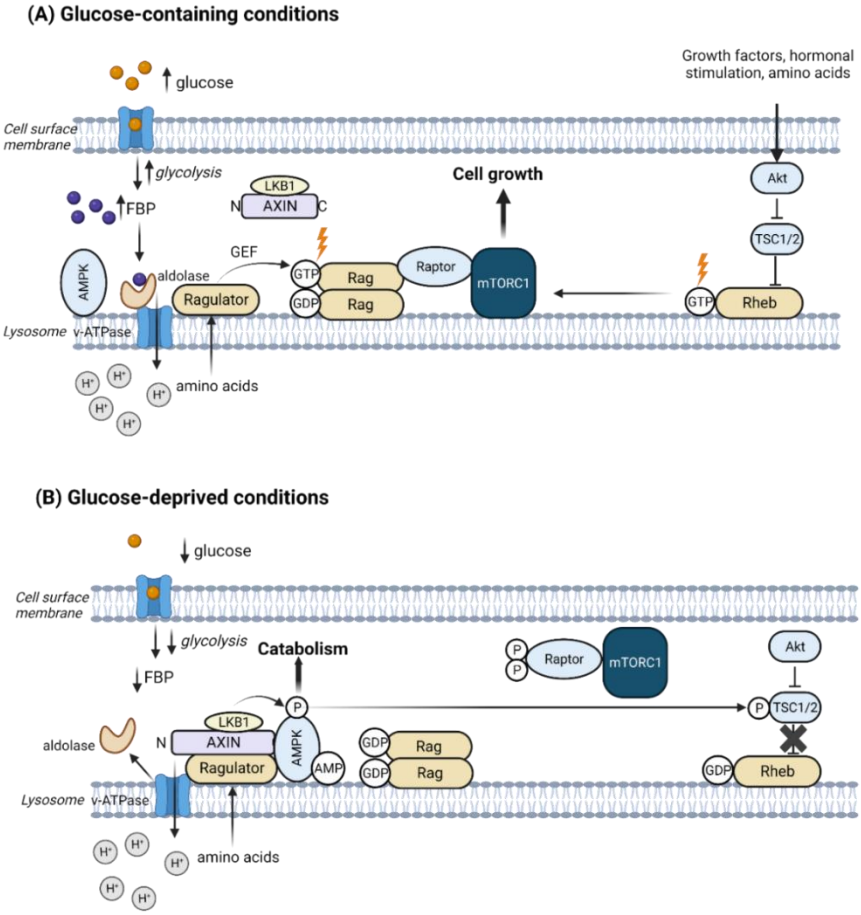

Figure 1.14: Hypothesised model for the lysosomal glucose/amino acid-sensing mechanism by AMPK-mTORC1 interactions.

(A) In glucose-containing conditions, increased cytosolic fructose 1,6-bisphosphate (F1,6BP) levels bind the corresponding glycolytic enzyme, aldolase, to vATPase proton pump and prevent LKB1/AXIN binding to the lysosomal membrane. Amino acids, released from the lysosome, can activate the Ragulator complex to increase guanine nucleotide exchange factor (GEF) activity on the Rag complex for activation by GTP binding. Rag activation promotes mTORC1 complex binding to the lysosomal surface, thereby promoting cell proliferation and growth. mTORC1 complex is further activated by PI3K/Akt activation by inhibiting TSC1/2 activity and promoting GTP-binding to Rheb. AMPK is inactivated but AMPK β-subunit is attached to the lipid lysosomal membrane by N-terminus myristoylation **(B)** Following glucose deprivation, aldolase dissociates away from lysosomal vATPase due to reduced levels of FBP. Aldolase dissociation facilitates LKB1-AXIN-AMPK binding to vATPase/Ragulator complex to limit mTORC1 activity. LKB1 stimulates AMPK activity, alongside rises in intracellular AMP, to promote catabolic pathway activation. AMPK activation promotes Raptor phosphorylation and TSC1/2 phosphorylation to limit mTORC1 complex activation in glucose-deprived conditions. To note, this model has been investigated in both mouse embryonic fibroblasts (MEFs) and human embryonic kidney (HEK-293) cell lines. Adapted from Hardie and Lin, 2017. Created using Biorender.com.

1.6.3 Allosteric regulation

Additionally from upstream kinases, AMPK is activated following rises in intracellular [AMP/ADP:ATP] in response to a depletion in energy status (ATP). AMP binding to the γ-subunit allosterically increases AMPK activity up to 10-fold compared to ADP, with greater AMP-dependent activity in γ1-containing complexes in the presence of physiological ATP concentrations (Gowans *et al.*, 2013; Ross, Jensen and Hardie, 2016). In addition, AMP and ADP increase α-Thr172 phosphorylation, and limit the dephosphorylation of α-Thr172 site by conformational changes in the α-kinase domain (Viollet *et al.*, 2010; Hardie, 2018; Steinberg and Carling, 2019). How AMP and ADP precisely modulate AMPK activity is not fully understood. CBS1 and 3 have a binding affinity for all adenosine nucleotides, but the binding affinities for CBS2/4 is currently uncertain (Xiao *et al.*, 2011, 2013; Ross, Jensen and Hardie, 2016). ATP competitive binding, compared to AMP, to the γ-subunit prevents interactions between the γ and α-kinase subunit (Xiao *et al.*, 2011; Carling, 2017). Altogether, the differential actions of adenosine nucleotides can regulate the conformational state of AMPK at least partly dependent on tissue-specific expression of the γ-isoform in accordance with tissue function.

1.6.4 Hormonal regulation

Leptin, a satiety hormone, increases AMPK activity and promote catabolic pathway activation in peripheral tissues (Minokoshi *et al.*, 2002; Steinberg, Rush and Dyck, 2003; Lee *et al.*, 2004; Yu *et al.*, 2004). Central actions of leptin however inhibit AMPK activity, highlighting the fundamental differences between central and peripheral AMPK actions. Leptin is thought to potentiate p70S6-mTOR mediated AMPKα2 serine-491 (Ser491) phosphorylation in the hypothalamus, activating AMPK, and thereby limiting food intake (Dagon *et al.*, 2012; Jeon, 2016). Ghrelin, on the other hand, following a calorie-restricted diet, stimulates substantia nigra (SN) AMPK activity by likely AMPK β subunit modifications (Bayliss *et al.*, 2016). In addition, the binding of ghrelin to GHSR1a receptor stimulates hypothalamic AMPK activity by Ca^{2+}-induced

CaMKK2 stimulation (Kola *et al.*, 2005). Therefore, the central action of satiety hormones relies on upstream regulation of AMPK activity to sustain energy balance.

Similar to leptin, GLP-1 can regulate AMPK activity in a tissue-specific manner. GLP-1R agonist, exenatide, increased acute AMPK/PI3K-Akt/nitric oxide synthase (NOS) activity in endothelial cells (Wei *et al.*, 2016). Similarly, GLP-1-enhanced AMPK activation by inhibiting key diabetogenic enzyme activity in a high cholesterol-exposed β-cell line (R. Li *et al.*, 2021a). On the other hand, GLP-1 exposure decreased hypothalamic AMPK activation and α2 levels in fasted rats (Seo *et al.*, 2008). In addition, GLP-1 agonist liraglutide inhibited food intake by reducing hypothalamic AMPK activity and BAT thermogenesis to increase energy expenditure, highlighting key functional differences in GLP-1/AMPK signalling between brain and peripheral tissues (Beiroa *et al.*, 2014).

1.7 Small molecule AMPK activators

1.7.1 Indirect AMPK activators

1.7.1.1 Metformin-like activators

The use of small molecules and natural derivatives to pharmacologically activate AMPK have well-characterised therapeutic effects in T2DM, especially in alleviating hyperglycaemia (Coughlan *et al.*, 2014). Metformin, an indirect AMPK activator, is a widely prescribed and the "preferred initial pharmacological agent" to lower hyperglycaemia and improve insulin sensitivity observed in T2DM for over 70 years (Salpeter *et al.*, 2008; Pernicova and Korbonits, 2014; American Diabetes Association Professional Practice Committee, 2022a). It is well characterised that metformin's ability to lower blood glucose is mainly through inhibition of hepatic gluconeogenesis (Stumvoll *et al.*, 1995; Madiraju *et al.*, 2014). If metformin **1)** activates hepatic AMPK to reduce hepatic gluconeogenesis and **2)** whether metformin, independent from hepatic action, can enhance insulin-stimulated skeletal muscle and adipose tissue glucose uptake is not fully understood (McIntyre *et al.*, 1991; Yuan *et al.*, 2019) Interestingly, metformin has been highlighted to have both an AMPK-

independent and - dependent action on hepatocytes. Metformin does not directly bind to purified AMPK, but indirectly activates AMPK by increasing [AMP:ATP] levels (Zhou *et al.*, 2001). After organic cation uptake transporter (OCT-1) dependent hepatocyte import, metformin is thought to inhibit both mitochondrial complex I and mitochondrial glycerophosphate dehydrogenase (mGPD) thereby enhancing hepatic AMP-dependent AMPK activation [(El-Mir *et al.*, 2000; Zhou *et al.*, 2001; Detaille *et al.*, 2002; Madiraju *et al.*, 2014; Pernicova and Korbonits, 2014). Other suggestions include metformin modulating gene transcription and altering mitochondrial redox state (Zhong *et al.*, 2016; Cameron *et al.*, 2018). The Sakamoto group identified that fructose-bisphosphate-1 (FBP-1), a key hepatic gluconeogenic enzyme, is allosterically inhibited by AMP (Hunter *et al.*, 2018). By using an AMP-insensitive FBP-1 knock-in mouse model, findings identified that AMPK is not required for metformin-induced lowering of hepatic glucose production, but instead postulated metformin-induced changes in liver energy charge drives rises in $[AMP]_i$ and thereby inhibition of FBP-1-dependent gluconeogenesis (Hunter *et al.*, 2018). Metformin-treated *in vitro* hepatocyte culture models supported these findings, where metformin was shown to lower G6P, a downstream substrate for hepatic gluconeogenic pathways, at least partly mediated by upstream substrate FBP-1 levels (Moonira *et al.*, 2020). A similar trend, although not significant, was seen in FBP-2 knockout mice (Park *et al.*, 2020). These findings therefore identify a nucleotide-dependent, rather than AMPK-dependent, mechanism of action of metformin as a hyperglycaemia-lowering agent.

Novel AMPK activators, R419 and R481, developed by Rigel Pharmaceuticals (CA, USA) are thought to have metformin-like mechanistic actions by mildly inhibiting oxidative respiration (unpublished data from Rigel Pharmaceuticals). R481 activates AMPK in a neuronal cell line, at a low [drug], compared to metformin, with both drugs having high brain permeability (Moreira, 2014; Cruz *et al.*, 2021). R481-stimulation of AMPK can improve hypoglycaemia-induced counterregulation, as peripheral R481 infusion attenuated glucose infusion rate (GIR) and increased plasma [glucagon] in hyperinsulinaemic-hypoglycaemic

rats (Cruz *et al.*, 2021). Unlike R481, R419 does not cross the blood-brain barrier (BBB) and is thought to have peripheral-localised actions *in vitro*, such as myotubes, macrophages, hepatocytes and skeletal muscle (Jenkins *et al.*, 2013; Boß *et al.*, 2016). R419 has therapeutic efficacy in improving peripheral insulin sensitivity in obese mouse models, but possibly in an AMPK-independent, AMP-sensitive manner (Jenkins *et al.*, 2013; Boß *et al.*, 2016). Similar to metformin, R419 reduced oxidative respiration, redox state and potentiates the [AMP/ADP:ATP] ratio in hepatocytes (Jenkins *et al.*, 2013). Altogether, some indirect activators could exert several therapeutically beneficial actions, including glucose sensitivity, by AMP-, rather than AMPK-, dependent actions (Jenkins *et al.*, 2013).

1.7.2 Direct AMPK activators

1.7.2.1 Pan- and ADaM site binding activators

AMPK can be directly activated by specific small molecules, that bind to the AMPK complex to either 1) induce a conformational change to promote α-Thr172 phosphorylation, or 2) by inhibiting α-Thr172 dephosphorylation, propagated by direct AMPK β/γ association (Kim *et al.*, 2016). A-769662 was the first “direct” AMPK small molecule activator identified (Kim *et al.*, 2016). A-769662 binds to a unique allosteric drug and metabolite (ADaM) site, a binding pocket located between the β- and α-subunit, to protect against α-subunit dephosphorylation and promote allosteric AMP binding to the γ-subunit (Aledavood *et al.*, 2019). In addition, certain agonists binding to the ADaM site have β-isoform selectivity, with A-769662 and salicylate preferentially stimulating AMPK complexes containing the β1 isoform (Sanz, Rubio and Garcia-Gimeno, 2013). Since then, multiple small molecules have been classified as ADaM-site agonists, including 991, MK8722 and PF-739, and have potent effects on peripheral glucose uptake (Olivier, Foretz and Viollet, 2018). As such, ADaM site agonists have possible anti-hyperglycaemic actions in individuals with T2DM.

Another small molecule, 991, binds to the ADaM site in AMPK, but is additionally classified as a “pan”-AMPK activator. “Pan” refers to being able to

stimulate all 12 heterotrimeric AMPK complex combinations, and thereby such activators have greater potential for whole-body AMPK activation. The development of synthetic pan-AMPK activator, O-304, by Betagenon (Sweden) increased AMPK activity in multiple cell types. O-304 can suppress the dephosphorylation of the αThr172 residue and requires upstream kinase stimulation (namely LKB1) to potentiate downstream AMPK activity (Steneberg *et al.*, 2018). These characteristics possibly highlight O-304 as an ADaM site activator, but the precise binding site is unclear (Steneberg *et al.*, 2018). In addition, O-304 has large potential as a clinical AMPK activator for T2DM therapeutics. In humans with T2DM and T2DM rodent models, O-304 treatment attenuated fasting hyperglycaemia and increased skeletal muscle glucose uptake, similar to other direct AMPK activators (Bultot *et al.*, 2016; Myers *et al.*, 2017; Steneberg *et al.*, 2018). The clinical efficacy is compromised in pan-AMPK activator, MK-8722, which was found to cause cardiac hypertrophy after short-term administration in non-human primates (Myers *et al.*, 2017). O-304, unlike MK-8722, improved adverse cardiovascular complications in individuals with T2DM and T2DM rodent models (Steneberg *et al.*, 2018). This is possibly due the first clinical purposing of O-304 as a PCSK9 inhibitor to treat peripheral arterial disease (*The Small molecule AMPK activator O304 acts as an oral PCSK9 inhibitor - Betagenon AB*, 2015). Altogether, AMPK activator O-304 has large therapeutic potential for treating complications and restoring glucose homeostasis in DM.

1.8 Project aims, objectives and hypotheses.

Over the last 17 years, there has been a rapid increase in publications focused on understanding α-cell function in health and disease. It is relatively unexplored how α-cells metabolically and functionally respond to changes in glucose availability. In addition, by understanding the therapeutic potential of AMPK activators in DM, it is not known if pharmacologically targeting AMPK in the α-cell could restore defective glucagon secretion observed in DM and diabetes-related complications. Therefore, the aims for this thesis were to characterise and examine the role of AMPK activity, by exposure to small molecule AMPK activators (R419, R481, O-304 and BI-9774) in regulating α-cell bioenergetics, including glycolysis and mitochondrial respiration. In addition, experimental studies examined the impact of pharmacological AMPK activation on α-cell glucagon secretion in response to glucose availability. These aims were primarily explored in the α-cell line, αTC1.9, and mouse *ex vivo* islets. Furthermore, a literature review examined the relationship between AMPK and CFTR, and potential applicability in both CF and CFRD development. The aims and hypotheses of this thesis are also covered in Figure 1.15.

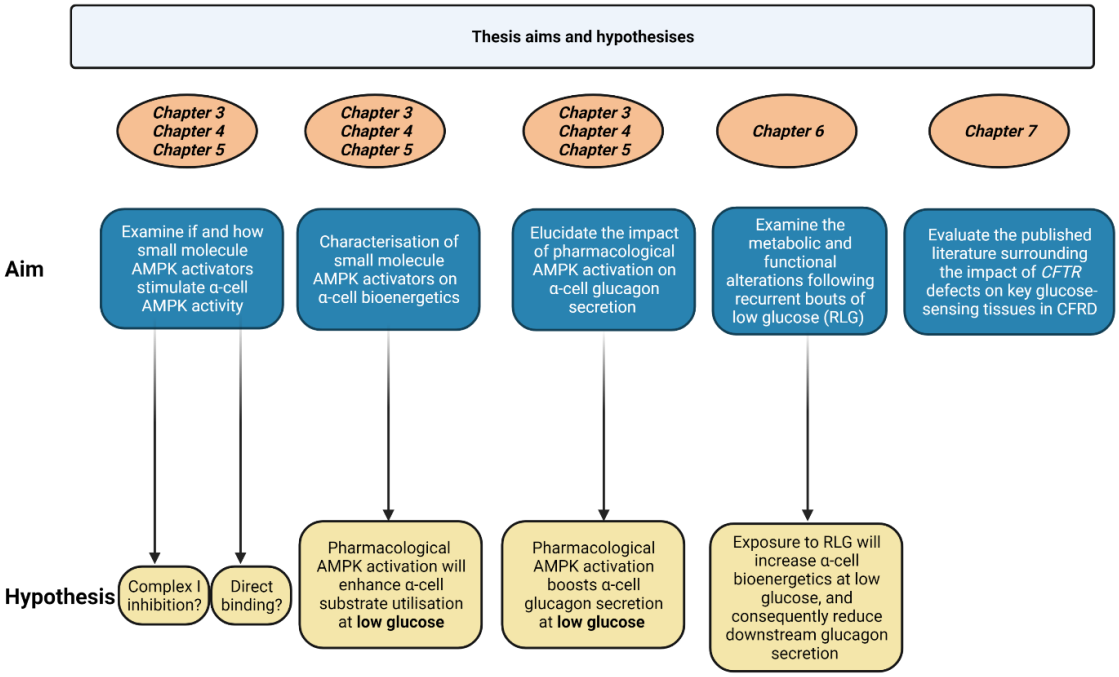

Figure 1.15: Schematic diagram illustrating the aims and hypotheses covered in this thesis.

This thesis explored the role of AMPK and novel AMPK activators in α-cell responses to glucose availability. In addition, this thesis evaluated the mechanistic role of AMPK and CFTR in glucose-sensing tissues during CFRD development. Created using Biorender.com.

Chapter 2

Materials and Methods

2 Materials and methods

2.1 Materials

2.1.1 Table of chemicals

Table 2.1: Chemicals

Chemical	Manufacturer	Catalogue number
0.05% (w/v) Trypsin-EDTA	Thermo Fisher	25300-062
100% ethanol (for RNA extraction)	Fisher Scientific	E/0650DF/17
2',7'-dichlorodihydrofluorescein diacetate (DCDFA)	Cayman/Cambridge Bioscience	20656
50 X MEM, 172 mmol/l	Thermo Fisher	11130036
96-well PCR plate (No skirt)	Sarstedt	72.1978
Acrylamide/Bisacrylamide (37.5:1, 30%)	Fisher Scientific/Alfa Aesar	J61505
Aprotinin	Merck	A1153
ATP:ADP ratio kit	Sigma-Aldrich	MAK135
ATPLite luminescence assay system	PerkinElmer	6016947
AZ PFKB3 67 (AZ-67)	Biotechne	5742
Benzamidine	Sigma-Aldrich	12072
BI-9774	OpnMe/Boehringer Ingelheim	N/A
Bio-Rad protein assay dye reagent	Bio-Rad	500-0006
BioTrace NT Nitrocellulose membrane	Pall/VWR	66485
Bovine serum albumin (BSA), lyophilised powder	Sigma-Aldrich	A2153
Bovine serum albumin (fraction V, fatty-acid free)	Merck	10775835001
Bromophenol blue sodium salt	Sigma-Aldrich	B5525
BSA-palmitate FAO substrate	Agilent	10270-100
Calcium chloride	Sigma-Aldrich	C7902
Chloroform	Fisher Scientific	C/4920/08
Collagenase Type XI	Merck	C 7657
DAKO REAL EnVision™ Detection System	Agilent	K500711-2
DEPC-treated water	Fisher Scientific	R0601
D-glucose	Sigma-Aldrich	G7021
Dimethyl Sulfoxide HYBRI-MAX (DMSO)	Sigma-Aldrich	D2650
D-mannitol	Sigma-Aldrich	M4125
DMEM (EndoC-βH1)	Gibco	41965039
DMEM no glucose	Fisher Scientific/Gibco	11966-025

DMEM, no glucose or phenol red	Fisher Scientific/Gibco	A14430-01
DPX	Sigma-Aldrich	06522
Epinephrine	Sigma-Aldrich	E4250
Ethylene glycol-bis(β-aminoethyl ether)-N,N,N′,N′-tetraacetic acid (EGTA)	Melford	E1102
Ethylenediaminetetraacetic acid disodium salt (EDTA)	Sigma-Aldrich	E1644
Evoscript cDNA synthesis set	LifeScience/Roche	07912374001
EvoScript Universal cDNA Master	Roche	07912374001
Extracellular matrix (ECM)	Sigma-Aldrich	E1270
Fibronectin (bovine plasma)	Sigma-Aldrich	P4333
Foetal bovine serum (FBS)	SeraLabs/Gibco	A201009/10270106
Fructose	Sigma-Aldrich	F3510
Galactose	Sigma-Aldrich	G0750
Glucagon ELISA	Mercodia	10-1281-01
Glycine	Melford	G0709
Glycolytic rate assay kit	Agilent	103346-100
Haematoxylin	Sigma-Aldrich	51275
HBSS	Gibco	14175
HEPES (solution/powdered)	Sigma-Aldrich	H0877/H3357
HEPES-buffered XF medium (pH 7.4)	Agilent	103575-100
Histo-Clear II	SLS	HS-202
Histopaque-1077	Merck	10771
Hydrochloric acid (HCl) (1M/1N solution)	Fisher Scientific	J/4320/15
Indinavir	Sigma-Aldrich	SML0189
Isopropanol	Fisher Scientific	BP2618-1
L-glutamine	Fisher Scientific	25030-024
L-lactate assay system	Cayman/Cambridge Bioscience	700510
Lumit™ Glucagon Immunoassay	Promega	W8020/W8022
Lumit™ Insulin Immunoassay	Promega	N/A
Magnesium chloride ($MgCl_2$) solution	Sigma-Aldrich	63069
Magnesium sulphate heptahydrate ($MgSO_4$)	Sigma-Aldrich	M2773
MEM	Merck	M2279
Methanol	Sigma-Aldrich	34860
Mito Stress test kit	Agilent	103015-100
Monosodium phosphate (NaH_2PO_4)	Sigma-Aldrich	S0751
N,N,N′,N′-Tetramethylethylenediamine (TEMED)	Sigma-Aldrich	T7024

Newborn Calf Serum (NCS)	Merck	N4637
Nicotinamide	Sigma-Aldrich	N3376
O-304	Cayman/Cambridge Bioscience/MedChemExpress	100757965/HY-112233
Penicillin-streptomycin	Sigma-Aldrich/Fisher	P4333/15070-063
Phenylmethanesulfonyl fluoride (PMSF)	Sigma-Aldrich	P7626
Phosphate buffered saline (PBS) tablets	Oxoid/Fisher Scientific	10209252
Poly-L-lysine hydrobromide (PLL)	Sigma-Aldrich	P1274
Ponceau S solution red	Sigma-Aldrich	P7170
Potassium chloride	Sigma-Aldrich	P5405
Propidium iodide (PI)	Sigma-Aldrich	P4864
Quantikine® Glucagon immunoassay	Biotechne/R&D systems	DGCG0
R419	Rigel Pharmaceuticals	N/A
R481	Rigel Pharmaceuticals	N/A
RNAse-Free DNase set	Qiagen	79254
RNeasy Plus	Qiagen	74134
RPMI-1640	Merck	R8758
RPMI-1640	Merck	R8758
SBI-0206965	Cayman	18477
SeeBlue plus 2 pre-stained protein standard	Life Technologies	LC5925
Skimmed milk powder	Sigma-Aldrich	70166
Sodium bicarbonate	Sigma-Aldrich	S5761
Sodium Chloride (NaCl)	Sigma-Aldrich	S7653
Sodium dodecyl sulphate (SDS)	Melford	B2008
Sodium Fluoride (NaF)	Sigma-Aldrich	S7920
Sodium hydroxide (NaOH)	Sigma-Aldrich	55881
Sodium Orthovanodate ($NaVO_4$)	Sigma-Aldrich	S6508
Sodium Pyrophosphate Tetrabasic Decahydrate (NaPPi)	Sigma-Aldrich	S6422
Sodium pyruvate	Sigma-Aldrich	P5280
Sodium selenite	Sigma-Aldrich	214485
Sterile water for injections	Medisave	WIA210
Streptozotocin (STZ)	Sigma-Aldrich	S0130
Sucrose	Melford	S0809
TaqMan Universal Mastermix II	ThermoFisher	4440043
TaqMan™ Gene Expression Assay	ThermoFisher	4331182 S
Transferrin	Sigma-Aldrich	T8158
TRI® Reagent	Invitrogen	M9738
Tris	Melford	B2005
Triton X100	VWR	M143
Triton X100	VWR	M143

Tween®-20	Sigma-Aldrich	P2287
UltraPure™ DNase/RNase-free distilled water	Gibco	10977035
β-mercaptoethanol (BME)	Sigma-Aldrich	M3148
β-Nicotinamide adenine dinucleotide sodium salt	Sigma-Aldrich	N0632

2.1.2 Table of general equipment

Table 2.2: General equipment

Equipment	Supplier
Accu-Check glucose meter	Roche
Odyssey CLx	LI-COR Biosciences
PHERAstar FS microplate reader	BMG Labtech
Seahorse XFe96 analyser	Agilent
BD Accuri C6 Plus	BD Biosciences
HirschmannTM counting chamber (8100103)	Fisher Scientific
Nikon 50i Eclipse brightfield microscope	Nikon
Zeiss Primovert microscope	3842002950, Zeiss
Leica S9e dissection microscope	Leica-microsystems
QuantStudio™ 12K Flex	Thermo Fisher Scientific
Mini-PROTEAN® Tetra system	Bio-Rad

2.1.3 Table of cell culture materials

Table 2.3: Cell culture materials

Equipment	Supplier/Manufacturer	Catalogue number
T-25	Sarstedt	83.3910.002
T-75	Sarstedt	83.3911.002
T-175	Sarstedt	83.3912.002
60 mm3 dish (suspension)	Fisher	11369273
35 mm^3 dish (suspension)	Sarstedt	83.3900.500
60 mm^3 dish (adherent)	Sarstedt	83.3901
12-well plate	Sarstedt	83.3921
48-well plate	Sarstedt	83.3923
96-well plate (white-coated)	Greiner Bio-One	655074
384-well plate (white-coated)	Greiner Bio-One	781074

2.1.4 Table of software

Table 2.4: Software

Software	Supplier
ImageJ/Fiji 1.53q (64-bit)	ImageJ/Java
Wave	Agilent
Image Studio Lite Ver5.2	LI-COR Biosciences
GraphPad Prism 9.5.1	GraphPad Software

2.1.5 Table of antibodies

2.1.5.1 Primary antibodies

Table 2.5: Primary antibodies

Antibody	Catalogue number	Supplier
p-AMPKα1/2 (Thr172)	2535	CST
p-ACCα/β (Ser79)	3661	CST
AMPKα (F6)	2793	CST
AMPKβ1 (71C10)	4178	CST
AMPKβ2	4148	CST
GLUT1	07-1401	Millipore
GLUT4 (1F8)	2213	CST
β-actin	NB600-501/66009-1-Ig	Biotechne/Proteintech

2.1.5.2 Secondary antibodies

Table 2.6: Secondary antibodies

Antibody	Catalogue number	Supplier
Alexa Fluor™ 680 goat anti-mouse IgG	A21057	Invitrogen
DyLight™ 800 goat anti-rabbit polyclonal Ab IgG	ROCK611-145-122	VWR/Rockland

2.2 Methods

2.2.1 Cell culture

Aseptic cell culture was followed to prevent contamination. The cells and islets were incubated at 37 degrees in a humidified atmosphere containing 95% air and 5.0% CO_2. Cells were confirmed mycoplasma-free through selective luciferase assay (MycoAlert, LT07-318).

2.2.1.1 αTC1.9 cell culture

AlphaTC1 Clone 9 (αTC1.9, CRL-2350^{TM}) is a murine pancreatic α cell line generated from an adenoma harvested from a transgenic C57BL/6J x DBA/2J mouse expressing viral SV40 large T (LT) antigen oncogene driven by the rat preproglucagon promoter control (Powers *et al.*, 1990). αTC1.9 cells were kindly gifted from Dr. Hannah Welters and originally sourced from the American Type Culture Collection (ATCC). αTC1.9 cells were used between passages 7 and 30. For all experiments, αTC1.9 cells were seeded a day prior to experimentation in full, stock medium (Table 2.7) and incubated at 37 degrees, 5.0% CO_2 overnight.

The general αTC1.9 cell culture required cell passage every 2-3 days with media addition (1-2 ml) or replacement if necessary and maintained at up to 80% confluency. For experimental purposes only, plasticware used were coated with reconstituted poly-L-lysine (PLL) at a working concentration of 4 µg/ml for > 30 minutes in a 5% CO_2 incubator. Any excess PLL was washed using phosphate-buffered saline (PBS). αTC1.9 cells were passaged, media aspirated, washed with PBS, and detached with 0.05% (w/v) trypsin-EDTA (1 - 2 ml for T-25, 3 ml for T-75, 6 - 7 ml for T-175 flasks) for up to 5 min at 37 degrees. To cease trypsinisation, stock medium was added (T25; 1.5 - 2 ml, T75; 3 - 4 ml, T175; 6 - 7 ml). Cells were pelleted by centrifugation at 1000 rpm for 5 min and resuspended by gentle pipetting and split either in a 1:2 or 1:3 ratio, dependent on cell confluency and viability. When cells were thawed from liquid nitrogen stores, αTC1.9 cells were cultured for additional two passages before experimental use.

Table 2.7: ***In vitro* cell culture medium constituents.**

Krebs' Ringer bicarbonate HEPES (KBH) solution was prepared in accordance with the protocol from Leclerc *et al.*, 2011.

Description	Cell Line	Medium	Supplements
Full	EndoC-βH1	DMEM (31885023)	1.0 g/l glucose 2.0 mmol/l L-glutamine 100U/ml penicillin and 100 µg/ml streptomycin 50 µmol/l β-2-mercaptoethanol 10 mmol/l nicotinamide 5.5 µg/ml transferrin 6.6 ng/ml sodium selenite 2% fatty acid free BSA
Coating medium	EndoC-βH1	DMEM (41965039)	100U/ml penicillin and 100 µg/ml streptomycin 2 µg/ml fibronectin 1% extracellular matrix (ECM)
Full	αTC1.9	DMEM (11966-025)	5.5 mmol/l glucose 0.02% fatty acid free BSA 1.0 mmol/l sodium pyruvate 10% FBS (A201009/10270-106) 2.0 % penicillin and streptomycin 15 mmol/l HEPES 0.1 mmol/l MEM (11130-051)
Krebs' Ringer bicarbonate HEPES (KBH), buffer for measuring glucagon secretion	αTC1.9	N/A	130 mmol/l NaCl 3.6 mmol/l KCl 1.5 mmol/l $CaCl_2$ 0.5 mmol/l KH_2PO_4 0.5 mmol/l $MgSO_4$ 2.0 mmol/l Na_2CO_3 10 mmol/l HEPES 0.1% fatty acid free BSA

2.2.1.2 EndoC-βH1 cell culture

EndoC-βH1 are a clonal human beta cell line created by transducing foetal pancreatic buds with a lentiviral vector which expressed SV40LT antigen driven by the insulin promoter (Ravassard *et al.*, 2011). These transfected buds were implanted into SCID mice and differentiated into β-cell insulinomas. β-cells were subsequently extracted, transfected with hTERT, further grafted in SCID mice for expansion, and dissociated to generate an *in vitro* cell line (Ravassard *et al.*, 2011). EndoC-βH1 have close homogeneity to human islet β-cells in regard to the cells' glucose- and incretin-stimulated insulin secretory response and therefore recognised as a valid model of human β-cell function (Tsonkova *et al.*, 2018). Cells were used until passage 66.

EndoC-βH1 cells, a kind gift from Prof. Noel Morgan, were cultured in T25 flasks pre-coated with ECM (1.0%) and fibronectin (2.0 µg/ml) in high glucose-containing DMEM (Gibco) for at least 1 h (Table 2.7). The coating medium was subsequently discarded and replenished with full culture medium described in Table 2.7. For experimental purposes, all cell culture consumables were precoated with ECM/fibronectin-mixture prior to cell seeding.

Both cell lines used (αTC1.9 and EndoC-βH1) were seeded for experiments according to Table 2.8.

Table 2.8: Experimental seeding density for each cell culture vessel.

Flask/Plate	Seeding Density
T75	1.0 million cells/flask
12-well plate	100,000 – 200,000 cells/well
48-well plate	150,000 cells/well
60 mm^3 dish	400,000 – 1.5 million cells/dish
96-well plate	750 cells/well
96-well plate (Seahorse)	16,000 – 30,000 cells/well

2.2.2 In vivo studies

All experimental procedures described using animals were conducted under a Home Office Project License and alongside Home Office regulations (UK), University of Exeter, University of Birmingham and the Animals (Scientific Procedures) Act 1986. Animal welfare was closely monitored with the assistance from staff at the Biological Services Unit, Hatherly and Living Systems Institute (LSI, University of Exeter).

The *in vivo* procedures described in this thesis used 8 – 12-week-old CD-1/ICR male mice and Sprague Dawley Rats (50 - 75 g) purchased from Charles River Laboratories (Margate, UK). Rodents were maintained at 22 – 23 degrees and 55 % humidity in group housing (between two – four animals). Animals were fed *ad libitum,* standard chow diet and had constant access to water. Circadian timing was regulated at a 12-hour light and dark cycle.

2.2.2.1 *In vivo* AMPK activator Tolerance Test (AMPKTT)

The measurements for basal non-fasting blood glucose were taken from Sprague Dawley rats prior to intra-peritoneal (i.p.) streptozotocin (STZ) (125 mg/kg) injection (dissolved in HBSS) to induce diabetes. Blood glucose was measured the following day to confirm rat diabetic status, with only diabetic rats (classified as blood glucose greater than 10 mmol/l at baseline) being included in this study. On Day 3, rats underwent an AMPK tolerance test (AMPKTT). These experimental rats were fasted for 5 h prior to blood glucose sampling

from the tail vein. Immediately post-blood glucose sampling, STZ-treated rats were i.p. injected with either vehicle (5.0 % DMSO solution) or O-304 (HY-112233) (10 mg/kg, 5.0% DMSO) and blood glucose measurements were taken at 30, 60 and 120 minutes post-i.p. injection. These animals were subsequently humanely sacrificed using a lethal dose of anaesthetic (Pentoject^{TM}). Terminal plasma was collected following exsanguination via cardiac puncture and tissues were subsequently collected for further analysis. Terminal blood was centrifuged at 3000 rpm for 15 min at 4.0 degrees, with the collected plasma collected distributed to multiple Eppendorf tubes and frozen at - 80 degrees for long-term storage.

2.2.3 Ex vivo islet isolation and culture

Briefly, CD-1 mice were euthanised using cervical dislocation and death was confirmed using femoral artery lesion. Collagenase, reconstituted in minimum essential medium (MEM) or RPMI-1640 medium, (1.0 mg/ml) was injected into the bile duct following clamping the ampulla of Vater. These pancreata were extracted and collagenase digestion was activated at 37 degrees, for up to 12 min (dependent on collagenase lot and brand). These pancreata were washed with RPMI-1640 (1) solution and pelleted at 1500 rpm for 1 min. Supernatant was removed and pellet was resuspended with RPMI-1640 (1) solution. Reconstituted pellet was shaken vigorously using a vortex-mixer for 30 x 10 seconds to ensure full pancreata dissociation. Pancreata was then pelleted at 1500 rpm for 1.0 min and washed twice with RPMI-1640 (1) solution. To ensure the removal of undigested tissue, the resuspended islets were filtered using 425 µm steel mesh and pelleted again at 1500 rpm (1.0 min). Media was removed, pellets were resuspended using Histopaque® 1077 (Merck) and layered with RPMI-1640 (1) medium. Data collected from University of Birmingham used both Histopaque® 1119 and 1083 for islet purification. Reconstituted pancreata were centrifuged at 1950 x g for 24 min (slow acceleration, 1, no brake, 0) at 10 degrees. Pancreatic islets appeared as a “ring” interphase between the Histopaque ® 1077 and RPMI-1640 (1) solution, and further washed at least twice.

These islets were resuspended with RPMI-1640 (2) medium and hand-picked to purify viable islets into an appropriate cell culture dish, dependent on islet number collected. Islets for static incubation experiments were recovered for at least 12 h prior to experimental use and were only included in experiments for up to 48 h post-harvesting at 37 degrees, 5% CO_2 incubator. The dish media was replaced every 2 – 3 days if required. On the experimental day, ten islets were hand-picked using a dissection microscope (Leica S9e) and size-matched (five larger and five smaller islets) into low-bind protein tubes. The medium constituents for islet culture are described in Table 2.9.

Table 2.9: Mouse islet culture medium and constituents.

ATP-BSA buffer is described in Viloria *et al.* 2020.

Solutions	Components	Purpose
RPMI-1640 (1)	RPMI-1640 1 % penicillin/streptomycin 10 % NCS	Wash
RPMI-1640 (2)	RPMI-1640 1 % penicillin/streptomycin 10 % FBS	Culture
ATP-BSA buffer	120 mmol/l NaCl 4.8 mmol/l KCl 24 mmol/l $NaHCO_3$ 0.5 mmol/l Na_2HPO_4 5 mmol/l HEPES 2.5 mmol/l $CaCl_2$ 1.2 mmol/l $MgCl_2$ 0.1% BSA (normal or fatty-acid free)	Static hormone secretion
Acid-ethanol	0.1% Triton-X 75% ethanol 15 mmol/l HCl	Lysis for hormone content

2.2.4 Pharmacological and glucose-sensitive studies

All compounds included in this thesis were dissolved in 100% DMSO and diluted in appropriate buffer for experiment. If a concentration response was being examined, all drug concentrations contained the same total percentage of DMSO in comparison to the largest concentration.

2.2.4.1 Cell lysate preparation and media collection

αTC1.9 experiments consisted of up to 2 h serum-free period (in stated glucose), with all treatments were conducted in serum-starved conditions (0 % FBS) and conditioned media were collected in respective Eppendorf tubes. Post-treatment, cells were exposed to a cold PBS wash to prevent further AMPK activation. PBS was replaced by ice-cold 1X lysis buffer (as described in Table 2.10) and was prepared using stock lysis buffer (Table 2.11) containing permeabilising and chelating agents alongside the addition of respective protease inhibitors. Plates were placed on ice, lysis buffer added, cells were scraped for mechanical dislodging and lysates were collected. All samples were frozen between – 20 and - 80 dependent on analysis.

Table 2.10: **1 x lysis buffer containing specific protease inhibitors.**

Note: PMSF was added last (max. 5 min prior to lysis) due to inhibitor instability.

Reagent	Final concentration in lysis buffer	Purpose
1 x lysis buffer	1 ml	N/A
Na_3VO_4	1.0 mmol/l (2.0 µl/ml)	Competitive phosphotyrosyl phosphatase (PTP) inhibitor
Benzamide	1.0 mmol/l (2.0 µl/ml)	Protease inhibitor
2-Mercaptoethanol	0.1 % v/v (1.0 µl/ml)	RNase deactivation
Sucrose	92.0 mg/ml	Osmolarity buffer
PMSF	0.1 mmol/l (2.0 µl/ml)	Serine phosphatase inhibitor

Table 2.11**: Stock lysis buffer constituents**

Reagent	[Stock]	[Final], 1X lysis buffer	Purpose
NaPPi	50 mmol/l	10.0 mmol/l	Phosphatase inactivation
Tris HCl pH 7.4	1M	25.0 mmol/l	Osmolarity and pH buffer
NaF	750 mmol/l	50.0 mmol/l	Serine/threonine phosphatase inhibitor
NaCl	4.0 M	0.1 M	Retain protein solubility and ionic strength
EDTA pH 8.0	0.5 M	1.0 mmol/l	Metal chelating agent, high affinity for $[Ca^{2+}]$, buffer
EGTA pH 8.0	0.2 M	5.0 mmol/l	Metal chelating agent, high affinity for $[Mg^{2+}]$, buffer
Triton X100	100%	1%	Permeabilises cell membranes

2.2.4.2 Protein content estimation

Respective lysates were thawed on ice and centrifuged at 14,800 rpm at 4 degrees for 20 min to remove cell debris. Supernatant was removed and placed into new Eppendorf tubes. Total protein was measured by Bradford assay method using a dye-based approach (Bradford, 1976).

In summary, 0.5 – 1.0 µl of sample was added in triplicate to each well in a clear 96-well plate. The corresponding standards (between 0 – 4.0 mg/ml) of bovine serum albumin (BSA) were diluted in the relevant lysis buffer volume. Bradford Assay Reagent (BioRad, 200 µl) was added (diluted 1:5 from stock with double-distilled water, ddH_2O). This solution was thoroughly mixed prior to measurement using orbital shaking at 500 rpm for 5 min at room temperature. The well absorbance was measured at 595 nm using PheraStar® *FS* plate reader (BMG LabTech). Protein content was estimated using the known standard absorbance subtracted by blank absorbance (i.e., buffer alone) and interpolation from calculated standard curve. All protein quantification results were also normalised to blank sample. For equal protein loading for western blotting, protein samples were diluted in 1X lysis buffer and diluted sample buffer (Table 2.14)

Table 2.12: **Western blot calculations to load 10.0 µg/protein/well in respective lysis buffer and sample buffer dilutions.**

Normalised protein (mg/ml)	Lysate volume (µl)	Lysis buffer (µl)	4 X sample buffer (µl)	Total (µg)	Total (µl)	Protein/well
A	C= B/A	E – D – C	D = B/4	B	E	10 µg loading/well

2.2.4.3 Composition of hand cast gels

Hand-cast acrylamide gels were prepared according to Table 2.13 (mini-PROTEAN ® Tetra, BioRad). Both TEMED and 20% ammonium persulphate (APS) compounds were added last to initiate acrylamide polymerisation. Once the resolving gel was added into the casting apparatus, ddH_2O was added to accurately level the gel and remove bubbles on the surface. ddH_2O was subsequently removed and stacking gel was added in either a 10- or 15- well comb. Gels included SDS to denature protein 3D secondary and tertiary structures, therefore linearising and coating protein in negative charge in proportion to protein length (Brunelle and Green, 2014). Gels are comprised of upper “stacking” gel has a lower acrylamide proportion compared to below resolving gel to facilitate fast protein movement in order to “stack” and form a compressed band of protein before moving through the higher percentage acrylamide resolving gel (Brunelle and Green, 2014).

Table 2.13: Hand-cast SDS-PAGE acrylamide gel composition.

Note; APS and TEMED were added last for gel polymerisation.

Reagent (2X gels)	Stacking (4 % acrylamide)	10 % acrylamide	Purpose
ddH_2O	2.8 ml	4.15 ml	Diluent
0.5 M Tris pH 6.8	1.25 ml	-	pH alters rate of protein migration and stacking
1.5 M Tris pH 8.8	-	3.15 ml	
30% acrylamide	850.0 µl	3.75 ml	Polymerises to form gel pores required for protein electrophoresis
10% SDS	50.0 µl	110.0 µl	Denatures proteins, coats protein in negative charge for electrophoresis
20% APS	50.0 µl	55.4 µl	Oxidising agent, initiates acrylamide polymerisation
TEMED	5.35 µl	11.0 µl	Aids free radical formation, initiates acrylamide polymerisation

2.2.4.4 SDS-PAGE protein electrophoresis

Laemmli, 1970 developed sodium dodecyl sulphate polyacrylamide gel (SDS-PAGE) electrophoresis to separate proteins according to individual molecular weights (Laemmli, 1970). In this thesis, proteins were heated at 37 degrees, for 10 min, before loading 10 µg protein/well. To run through the stacking gel, 90 volts (V) were applied for at least 15 min until samples have run through the stacking gel, and subsequently increased to 150V for up to 115 min dependent on acrylamide percentage gel used. The components of SDS-PAGE buffers for immunoblotting are covered in Table 2.14.

Table 2.14: SDS-PAGE electrophoresis buffers.

Buffer	Constituents
Sample buffer	125.0 mmol/l Tris-HCl (pH 6.8) 20.0% (v/v) glycerol 4.0% (w/v) SDS Bromophenol blue containing 0.1% (v/v) 2-Mercaptoethanol
Running buffer	25.0 mmol/l Tris 192.0 mmol/l glycine 0.1 % SDS
Transfer buffer	20% (v/v) methanol 48.0 mmol/l Tris-base 39.0 mmol/l glycine pH 8.3
TBS-T	150.0 mmol/l NaCl 20.0 mmol/l Tris-HCl pH 7.4 0.05% (v/v) Tween-20

2.2.4.5 Nitrocellulose protein transfer

The electrotransfer using transfer buffer was used to transfer SDS-PAGE gel-embedded proteins onto permeabilised nitrocellulose membranes. The transfer buffer constituents are displayed in Table 2.14. To facilitate efficient protein transfer, the sandwich method was applied. The sandwich method comprised of a nitrocellulose membrane placed onto the gel, sandwiched between filter paper and fibre pads on both sides, placed into a cassette and into a filled tank. Electrical current was applied at 100 V for up to 95 mins. Nitrocellulose membrane matrix was used as it has a high affinity for protein binding. To prevent tank heating, surrounding transfer buffer was cooled by ice packs and surrounding ice if necessary. Ponceau-S Red staining, a reversible protein dye, was applied to check efficacy of protein transfer and subsequently repeatedly washed with 0.1% Tris-buffered saline-tween (TBS-T) to remove excess dye.

2.2.4.6 Immunodetection

At all times, membranes were gently rocked to ensure even membrane-liquid coverage. Membranes were subsequently blocked in 5 % (w/v) dried skimmed milk diluted in TBS-T at room temperature for 1 h. The blocking step limits non-specific antibody binding to open pore sites. Excess milk was washed using TBS-T until milk was removed and applied respective primary antibody dilution for either 1 h or overnight at 4 degrees.

Following incubation, primary antibodies were removed and frozen for future use. Membranes were washed using 6 x 5 min washes with TBS-T and applied light-sensitive secondary antibody diluted in TBS-T (Table 2.15) at room temperature (1 h) protected from light. Secondary antibodies used are conjugated to fluorophores for highly sensitive, multiplex imaging. Following incubation, membranes were washed up to 6 x 10 min TBS-T washes. The suppliers, catalogue numbers and antibody preparations are shown in Table 2.15. The protein fluorescence in each blot was immunodetected using Odyssey® CLx (LI-COR).

Table 2.15: Primary antibody preparation.

Antibody	Diluent	Dilution	Species	Incubation time and temperature
p-AMPKα1/2 (Thr-172)	2.5 % (v/v) BSA/TBS-T	1:1000	Rabbit	4 degrees, overnight
AMPKα (F6)	2.5 % (v/v) BSA/TBS-T	1:1000	Mouse	4 degrees, overnight
p-AMPKβ1 (Ser-182)	2.5 % (v/v) BSA/TBS-T	1:1000	Rabbit	4 degrees, overnight
AMPKβ1	2.5 % (v/v) BSA/TBS-T	1:1000	Rabbit	4 degrees, overnight
AMPKβ2	2.5 % (v/v) BSA/TBS-T	1:1000	Rabbit	4 degrees, overnight
p-ACCα/β (Ser-79)	2.5 % (v/v) BSA/TBS-T	1:1000	Rabbit	4 degrees, overnight
GLUT1	2.5 % (v/v) BSA/TBS-T	1:1000	Rabbit	4 degrees, overnight
GLUT4 (1F8)	2.5 % (v/v) BSA/TBS-T	1:1000	Mouse	4 degrees, overnight
β-actin	2.5 % (v/v) BSA/TBS-T or TBS-T only	1:10,000	Mouse	4 degrees, 1 h

Table 2.16: Secondary antibody preparation

Antibody	Diluent	Dilution	Species	Incubation time and temperature
Alexa Fluor 680 goat anti-mouse IgG	TBS-T	1:10,000	Mouse	1 h, room temperature
DyLightTM 800 goat anti-rabbit polyclonal Ab IgG	TBS-T	1:10,000	Rabbit	1 h, room temperature

2.2.4.7 Western blot analysis

Densitometric analysis was conducted using Image Studio™ Lite V.5.2 (LI-COR) software by selecting proteins of interest (determined by a known molecular weight protein ladder, SeeBlue; LC5925) using drawn boxes by eliminating background signal. Signal was measured using pixel intensity. Protein phosphorylation was either normalised to total protein of interest or β-actin. In addition, β-actin was used as a loading control. The control sample in cohort was normalised to a value of 1 and relative changes in phosphorylation were determined by fold-change from the designated control sample.

2.2.5 Immunohistochemical (IHC) staining

Wax-embedded C57/BL6 mouse pancreata were sliced at 4.0 µm thickness. Wax was removed and washed twice using solvent Histo-Clear (NAT1334, Fisher/SLS) for 5 min. Respective sections were rehydrated in decreasing ethanol concentrations for 1 min each. All slides were then washed with 100 % methanol for 1 min, and rehydrated in ddH_2O for 5 min. The slices were antigen-retrieved in citrate buffer (pH 6.0), at a high heat for 20 min and sections were cooled for an additional 20 min. The sections were subsequently blocked using normal goat serum (1:20) in 1 x TBS for 5 min. In addition, sections were incubated with respective primary antibody dilutions (up to 1:750) overnight. Sections were washed in 1 X Tris-Buffered Saline. DAKO REAL peroxidase blocking solution (S2023) was applied to sections for 5 min in 1 X TBS. DAKOReal Envision HRP (Anti-Rabbit) was applied to sections for 30 min, and subsequently washed in 1 X TBS. DAB substrate working solution was prepared, using DAKO REAL DAB^+ Chromogen/DAKO REAL substrate buffer and incubated with the sections for 10 min. Sections were subsequently washed in ddH_2O. Sections were stained in haematoxylin for 5 min, washed in ddH_2O, stained in Scott's Tap Water Substitute (STWS), washed in ddH_2O, incubated in 2 % copper sulphate in 0.9 % saline for 5 min, and finally washed in ddH_2O. Sections were dehydrated increasing ethanol concentrations (50 – 90 %, 5 min) and 100 % ethanol twice for 5 min. Finally, sections were washed in Histo-Clear and Histo-Clear II (Fisher/SLS, NAT1334) for 5 min and fixed with coverslips using DPX. The respective buffer constituents are displayed in Table 2.17.

Table 2.17: Immunohistochemical (IHC) staining buffers.

Buffer	Constituents	1X	10X	pH
Citrate buffer	Citric acid, ddH_2O	1.92 g	19.2 g	6.0 (adjusting using 2N NaOH)
Tris-Buffered Saline (TBS)	Tris Base	6.1 g (50 mmol/l)	61 g (0.5 M)	pH 7.6
	NaCl	9 g (0.9%)	90 g (9%)	
	ddH_2O	1 L		
0.5% copper sulphate in 0.9% saline solution	Copper sulphate	5 g	N/A	N/A
	NaCl	9 g		
	ddH_2O	1L		
Scott's Tap Water Substitute (STWS)	Sodium bicarbonate (Sigma, S5761)	3.5 g (40 mmol/l)	N/A	N/A
	Magnesium sulphate (Sigma, M7506)	20 g (170 mmol/l)		
	ddH_2O	Up to 1 L		
	Sodium azide	0.05 %		

2.2.6 Glucagon secretion

Static hormone secretion was normalised to either total lysed protein using 1X lysis buffer or by total glucagon content as stated. Epinephrine (5.0 µmol/l) was used as a positive control for α-cell glucagon secretion. All samples were collected and placed on ice to minimise hormone degradation, and frozen at -80 degrees for further analysis.

2.2.6.1 αTC1.9 glucagon secretion

On the day of experimentation, following serum-free incubation (2 h), cells were exposed to Krebs' Ringer bicarbonate HEPES (KBH) or 1 X ATP-BSA buffer solution containing respective glucose concentrations ± respective AMPK activator for 1 h. To optimise the measurement of glucagon, aprotinin (~ 0.025 mg/ml) was added to supernatants and lysates in the O-304 study. KBH and 1 x ATP-BSA buffer constituents are covered in Table 2.7 and Table 2.9.

2.2.6.2 Islet glucagon secretion

Mouse islets were pre-incubated in 1 X ATP-BSA buffer containing 11.7 mmol/l glucose for 1 h at 37 degrees. Islets were either washed in 3.0 mmol/l or 0.5 mmol/l glucose-containing 1 X ATP-BSA buffer and replaced with respective glucose conditions for 1 h. Supernatant was removed, islets were washed with cold 1 X ATP-BSA buffer and subsequently lysed using acid-ethanol (Table 2.9). Aprotinin (~ 0.025 mg/ml) was added to all collections.

2.2.7 Glucagon analysis

2.2.7.1 Quantikine® Glucagon Immunoassay

Enzyme-linked immunosorbent assays (ELISAs) were performed according to manufacturer's instructions. In brief, samples and standards (31.3 pg/ml - 2000 pg/ml) were loaded onto the plate and incubated at room temperature (3 h). Cold glucagon antibody conjugate was incubated for 1 h at 2 – 8 degrees. Substrate solution was subsequently added for 30 min at room temperature and reaction was stopped to ensure colour change (blue to yellow). The optical density was measured within 30 min and wavelength correction (450 – 540 nm)

applied to all samples/standards. The glucagon content in supernatants were interpolated from standard curve using applied cubic spline regression.

2.2.7.2 Mercodia glucagon immunoassay

Mercodia glucagon immunoassay (10-1281-01) was performed under the manufacturer's instructions. In brief, samples and standards were plated in duplicate in a white-coated 96-well plate. Enzyme conjugate (1X) solution was added to each well, mixed (700 – 900 rpm) overnight at 4 degrees for up to 22 h. The following day, samples were washed with 1X wash buffer six times. Samples were incubated with Substrate TMB for 30 min at room temperature, and reaction was stopped by adding a Stop solution. Optical density was measured at 450 nm and was read within 30 min. Samples were interpolated from a standard curve generated by four parameter logistical testing with $1/y^2$ weighting.

2.2.7.3 Promega Lumit™ glucagon immunoassay

Cell and islet glucagon supernatant/content were measured using the Promega Lumit™ Glucagon immunoassay and modified from the manufacturer's instructions. In summary, lysates (total glucagon content) samples were sonicated for 5 min. Supernatants from monolayer cells were centrifuged between 100 – 200 x g to remove cellular debris. Table 2.18 indicates sample dilutions and standard curve reference.

Samples and standards (displayed in Table 2.19) were plated in at least technical triplicates in a white-coated 384-well plate (Greiner Bio-One). Sample:antibody master mix:detection substrate was added in 1:1:0.5 ratio respectively. Antibody master mix (Table 2.20) was added per well, plate was shaken at 300 rpm for 3 min and kept at room temperature for 1 h to ensure antibody binding. The detection buffer was added, and luminescence (RLU) was read within 10 min using PheraSTAR plate reader. An overview of the experimental protocol is displayed in Figure 2.1.

Table 2.18: Promega Lumit™ glucagon immunoassay dilutions

Samples	Model	Dilution
Secretion	αTC1.9	1:100
	Islet	No
Content	αTC1.9	1:1500
	Islet	1:1000

Table 2.19: Respective standards for the Promega Lumit™ glucagon immunoassay

	[Glucagon] pM	[Glucagon] pg/ml
#12	2000	6800
#11	1000	3400
#10	500	1700
#9	250	850
#8	125	425
#7	63	5213
#6	31	106
#5	16	53
#4	8	27
#3	4	13
#2	2	7
#1 (ATP buffer only)	0	0

Table 2.20: Antibody and detection buffer preparation for Promega Lumit™ glucagon immunoassay

	Component	Dilution
Antibody Mix	Anti-Glucagon mAb-SmBit	1:200 or 1:400
	Anti-Glucagon mAb-LgBit	1:200 or 1:400
	Antibody Dilution Buffer B	
Lumit™ Detection Reagent	Detection Buffer B	1 in 20
	Detection Substrate B	

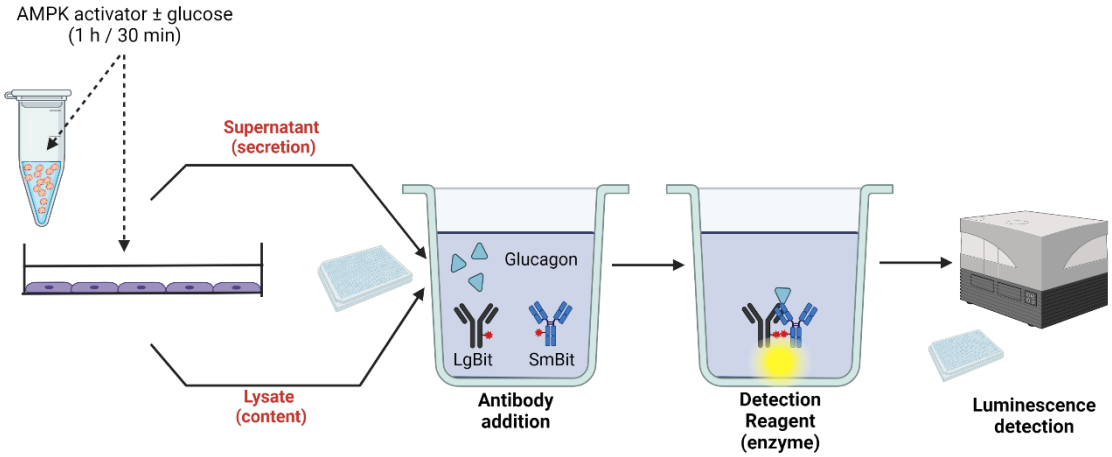

Figure 2.1: Schematic diagram of the Promega Lumit™ glucagon immunoassay.

2.2.8 Recurrent Low Glucose (RLG)

αTC1.9 cells were serum-starved in 5.5 mmol/l glucose-containing DMEM media for 2 h and subsequently incubated in either 0.5 (antecedent and recurrent low glucose; RLG) or 5.5 (control/acute low glucose) mmol/l glucose-containing media for 3 h. Cells were subsequently recovered in normal culture medium overnight, following a PBS wash, for up to 16 h. This protocol occurred for three full days. At the end of the third day, cells were recovered for 2 h prior to seeding into respective PLL-coated culture dish at a specific seeding density dependent on experimental question asked. The general RLG protocol is illustrated in Figure 2.2.

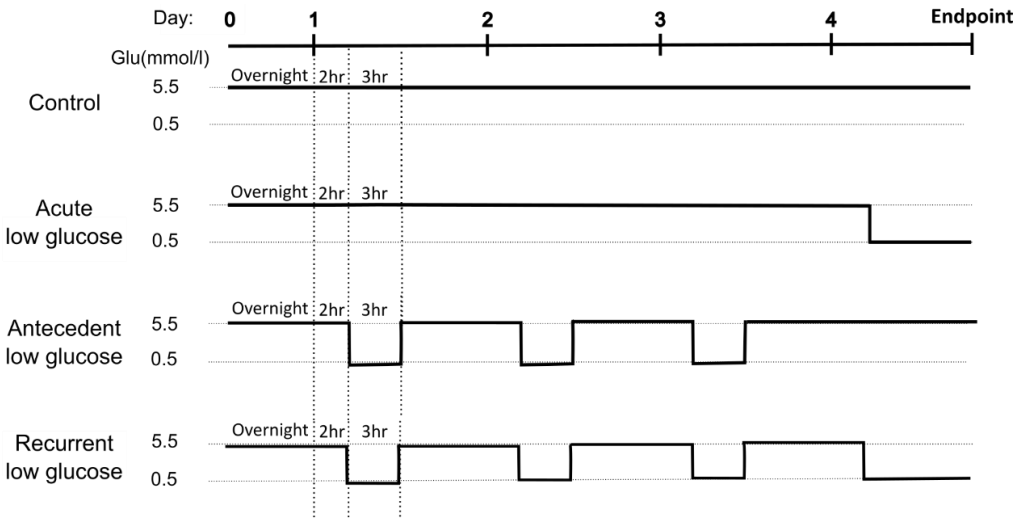

Figure 2.2: Schematic diagram of the *in vitro* recurrent low glucose (RLG) model.

The recurrent low glucose (RLG) *in vitro* model was developed to accurately represent hypoglycaemia episodes observed in diabetes mellitus (DM). In brief, following seeding and overnight acclimatisation, αTC1.9 cells were exposed to 2 h bouts of serum-free medium containing 5.5 mmol/l glucose prior to glucose challenge or retained euglycaemic-like conditions. Following serum-starvation (2 h), the antecedent and recurrent low glucose (RLG)-treated groups were exposed to 0.5 mmol/l glucose for 3 h. The control and acute low glucose (ALG) groups were incubated in 5.5 mmol/l glucose for 3 h; both in serum-free conditions. All cells were recovered in 5.5 mmol/l glucose, full media overnight. This protocol occurred for 3-days. At the end of the third day, cells were recovered in 5.5 mmol/l glucose-containing full medium for 2 h prior to seeding for the respective experiment. On Day 4, both ALG and RLG-treated cells were exposed to low glucose (0.5 mmol/l). The control and antecedent-treated groups were incubated in 5.5 mmol/l glucose, with both treatments occurring for up to 1 h dependent on experiment.

2.2.9 Bioenergetic measurements

Cellular bioenergetics were assessed using real-time, live-cell oxidative respiration (oxygen consumption rate, OCR) and extracellular pH (extracellular acidification rate, ECAR) measurements using Seahorse XFe96 analyser. OCR and ECAR quantify mitochondrial and glycolytic respiration, respectively, through using high thorough-put oxygen and proton-quenching fluorophores bound to XFe cartridge individual probes, demonstrated in the schematic diagram. During measurement cycles, XFe cartridge is lowered and contained within a small, cell microchamber. In this small area, cell oxygen consumption and media acidification (H^+) were detected precisely by bound fluorophores (Pelgrom, van der Ham and Everts, 2016).

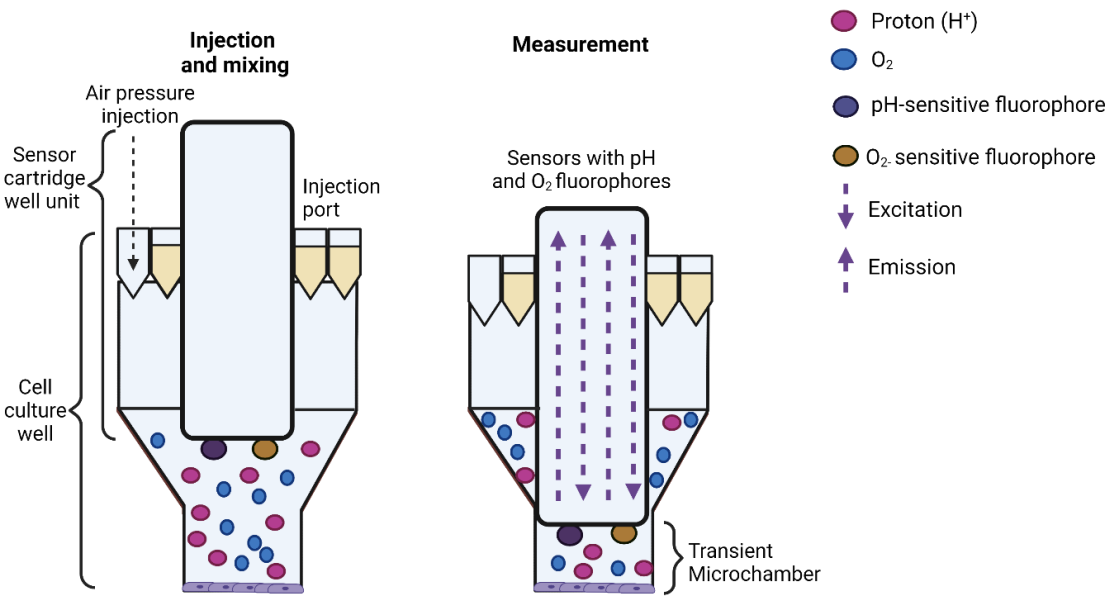

Figure 2.3: Seahorse XFe96 well microchamber and assay microdynamics.

During injection and mixing, the cartridge sensor containing bound fluorophores and relevant pH sensors are unloaded into the well. The respective compound is injected into the medium following port injection. Oxygen consumption rate (OCR) and extracellular acidification rate (ECAR) are measured following sensor “docking” into the cell culture well, creating a transient microchamber for the oxygen and pH-bound fluorophores to measure H+ and oxygen. The respective fluorescent emission signal, following fluorophore excitation, is measured by each well in a highly dynamic microfluidic system. Figure adapted from Pelgrom *et al.*, 2016.

In brief, cells were seeded in full media overnight, and the sensor cartridge was hydrated in ddH_2O overnight. On the experimental day, cells were washed up to two times in low-buffered (HEPES, 5.0 mmol/l) Seahorse XF DMEM media (pH 7.4, Agilent) containing 2.5 mmol/l sodium pyruvate and 2.0 mmol/l L-glutamine. To note, this buffer and constituents are referred to as “standard” Seahorse XF DMEM media throughout this thesis. Galactose and fructose utilisation studies included washes in Seahorse XF pH 7.4 media without such additives. Pharmacological AMPK activator/inhibitor treatment was either included during the degassing period (1 h) or acutely injected through Port A prior to assay. The degassing period removes artificial CO_2 and O_2 sources in the medium, therefore removing CO_2-controlled buffering and subsequent pH alterations (Traba *et al.*, 2016). During this time, cartridge ports were loaded with respective compounds, dependent on the study, and cartridge hydrant was replaced with either ddH_2O or calibrant. The cartridge was equilibrated, and sensors calibrated prior to use. The cell culture plate was also equilibrated and calibrated to 37 degrees prior to metabolic measurements for ~ 12 min. All assays, unless otherwise stated, had 3 min mix and 3 min measure per cycle, with number of cycles dependent on experiment. Following assay, cells were lysed using 50 mmol/l NaOH and protein content was quantified using Bradford assay method. Metabolic measurements were normalised to total protein, unless otherwise stated.

2.2.9.1 Glycolytic rate assay

The glycolytic rate protocol is summarised in Table 2.21 and Figure 2.4, with detailed experimental conditions provided in respective studies. Baseline measurements were taken following between four - eight measurement cycles and subsequent four measurement cycles after rotenone/antimycin A (Rot/AA, 1:1) (well concentration; 0.5 µmol/l) and 2-deoxyglucose (2-DG) (well concentration; 50 mmol/l) injection. Rot/AA inhibits complex I and III respectively to block mitochondrial-derived extracellular CO_2 acidification. 2-DG is a competitive glucose analogue which inhibits glycolytic rate by preventing rate-limiting enzyme hexokinase (HK) activity. 2-DG-dependent reduction in

proton efflux rate (PER) confirms glycolytic-derived PER (glycoPER). The definitions of bioenergetic parameters analysed and analysis calculations are summarised in Table 2.22.

Table 2.21: Glycolytic rate assay test protocol steps.

Mix	Measure	Cycles
3 min	3 min	4 – 8 basal 4 measurements (Rot/AA) 4 measurements (2-DG)

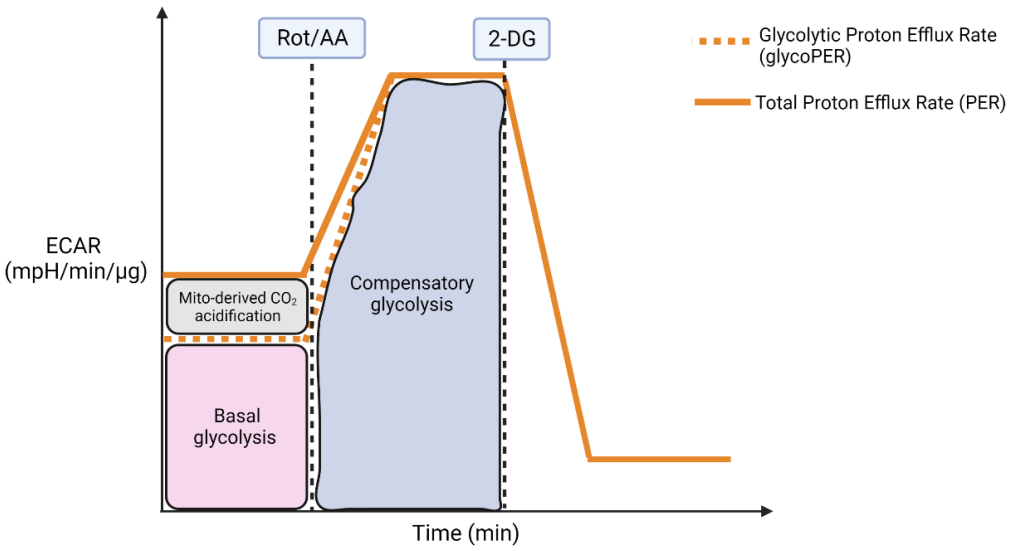

Figure 2.4: Glycolytic rate assay protocol.

To measure glycolytic rate, rotenone/antimycin A (Rot/AA) was first injected (0.5 µmol/l) to inhibit mitochondrial respiration and subsequently 2-deoxyglucose (2-DG) (50 mmol/l). Basal glycolysis was calculated by subtracting total proton efflux rate (PER) by mitochondrial CO_2 acidification. Compensatory glycolysis was calculated by total glycolytic PER between Rot/AA injection and 2-DG injection. Adapted from (*Agilent Technologies Seahorse XF Glycolytic Rate Assay Kit User Guide*, no date)

Table 2.22: Seahorse XFe96 parameter definitions and respective calculations.

Experiment	End point	Calculation	Definition
Glucose dose response	ΔECAR/OCR_{MAX}	Maximum measurement post injection – average baseline measurements	Measurement of cell's ability to utilise extracellular glucose available
	Basal	Average baseline measurements	
Glycolytic Rate	Proton Efflux Rate (PER)	PER (pmol H+/min) = ECAR (mpH/min) x BF (mmol/l/pH) x Geometric Volume (µl) x Kvol	Number of protons extruded into the extracellular medium over time (pmol/lmin)
	Compensatory Glycolysis	Maximum glycoPER measurement after Rot/AA injection	Glycolytic rate post-Complex I/III inhibition, inhibiting mitochondrial respiration and allow cells to rely on glycolysis as a primary energy producer
	Basal glycolysis	Last glycoPER measurement before first injection	Glucose → lactate
	GlycoPER	Proton efflux rate eliminated CO_2-dependent acidification from mitochondrial respiration.	Proton efflux rate (PER) derived from glycolysis and is an indicator of extracellular lactate production
MitoStress	ATP-linked respiration	(Last rate measurement before oligomycin injection) – (minimum rate measurement after oligomycin injection)	ATP synthase inhibition (via. Oligomycin) indicates proportion of cellular respiration required to promote ATP production.
	Proton leak	(Minimum rate measurement after oligomycin injection) – (non-mitochondrial respiration)	Basal respiration not driving ATP production
	Maximal respiration	(Maximum rate measurement after FCCP injection) – (non-mitochondrial respiration)	Uncoupling the mitochondrial proton gradient through FCCP stimulates electron transport chain to achieve maximum respiration the cell can feasibly achieve
	Basal respiration	(Last rate measurement before first injection) – (non-mitochondrial respiration rate)	Oxygen consumption (OCR) meeting cellular ATP demand after mitochondrial proton leak
	Spare respiratory capacity (%)	(Maximal Respiration)/(Basal Respiration) *100	Cell capability to respond to energy demand and therefore considered an indicator of cellular fitness
	Coupling efficiency	ATP production rate/ (basal respiration rate) * 100	

2.2.9.2 Buffer capacity assay

To both accurately determine the quantitative PER, rather than qualitative ECAR, and determine whether drugs alter media buffer capacity, a cell-free assay were conducted by removing each Seahorse XFe96 components (i.e., sensors, microplate, medium) to calculate the media buffer factor (BF). BF is calculated by quantifying proton extrusion into the medium to alter the pH by 1 pH unit, and in doing so, ECAR measurements can be converted into proton efflux rate (PER), as advised by Agilent Technologies (*Agilent Technologies Seahorse XF Buffer Factor Protocol Quick Reference Guide*, no date). Full culture media was incubated overnight and on the experimental day, plate medium was degassed for 1 h prior to assay. The well buffer factor was determined by titrating 5.0 mmol/l HCl or media through port A – C respectively and calculated using equation illustrated in Table 2.22. In summary, buffer factor is $[H^+]$ required to alter 1.0 pH unit (mmol/l/pH). A representative pH trace is displayed in Figure 2.5, with Table 2.23 stating the calculated buffer factor of each respective treatment.

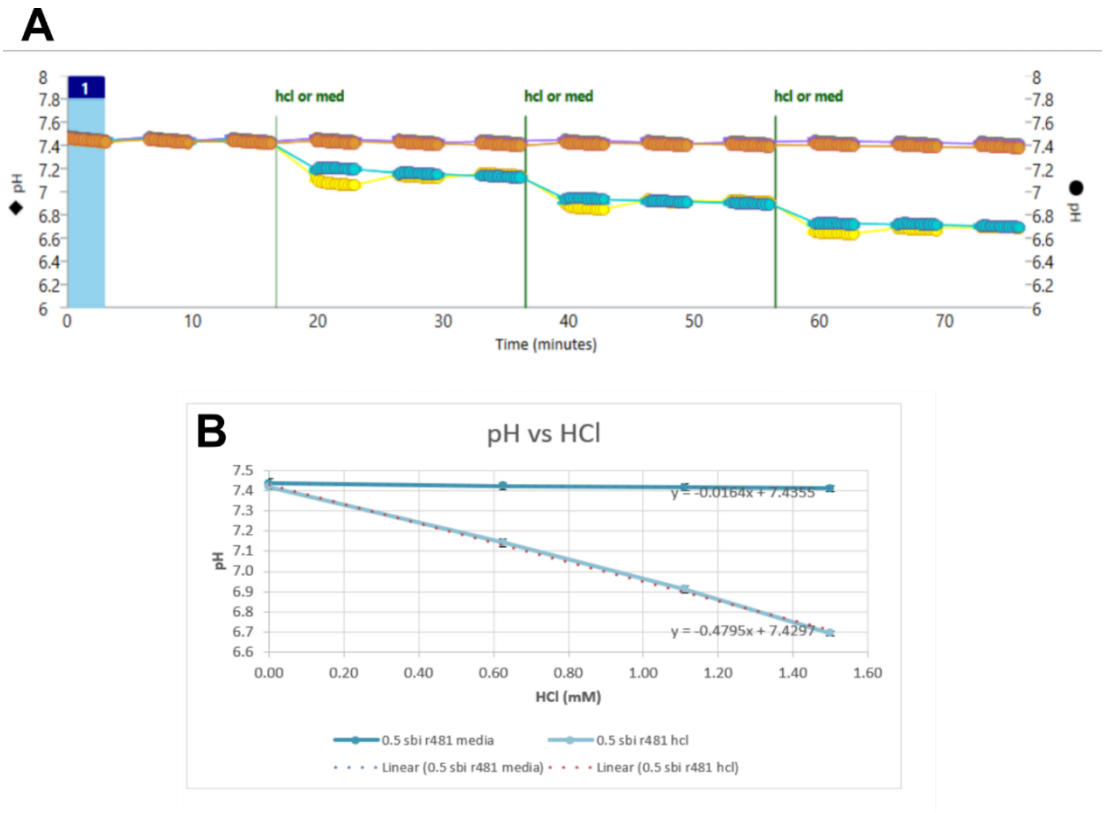

Figure 2.5: Representative X-Y trace for determining the condition buffer factor.

(A) Multiple injections of normal, full media or titrations of HCl (5.0 mmol/l) into the well medium to test buffer capacity. (B) Representative buffer factor calculation of well medium by increasing [HCl].

Table 2.23: Condition buffer factor readings (mM/pH)

Condition	Buffer factor (mM/pH)
0.5/Vehicle	2.2
11.7/Vehicle	2.3
0.5/R481	2.2
11.7/R481	2.2
0.5/SBI	2.2
11.7/SBI	2.2
0.5/SBI + R481	2.2
11.7/SBI + R481	2.2

2.2.9.3 Mitochondrial stress (MitoStress) assay

Mitochondrial function was assessed using standard mitochondrial stress (MitoStress) kit according to manufacturer instructions (Agilent, UK), displayed in Figure 2.6 . Table 2.24 summarises experimental design. The optimal oligomycin and FCCP-induced OCR changes were determined by individual titration assays between 0.5 – 2.5 µmol/l oligomycin and 0.125 – 2.0 µmol/l FCCP, as displayed in Figure 2.7.

The titration assay determined optimal oligomycin and FCCP concentration being 1.5 µmol/l and 1.0 µmol/l respectively. Further MitoStress assays, experimental design included three basal measurements (~14 minutes) and three ECAR/OCR measurements were taken in-between each inhibitor (oligomycin, 1.5 µmol/l; FCCP, 1.0 µmol/l and Rot/AA, 0.5 µmol/l) injection (Table 2.24). Oligomycin binds to the proton channel ATP synthase (complex V of electron transport chain), blocking ATP synthase activity and therefore accumulating extracellular protons to rapidly hyperpolarise the mitochondrial membrane to limit cell oxygen consumption (Hearne *et al.*, 2020). Carbonyl cyanide-p-trifluoromethoxyphenylhydrazone (FCCP) uncouples mitochondrial oxidative metabolism by blocking proton transport across the mitochondrial inner membrane, allowing maximal cell oxygen consumption (To *et al.*, 2010). Rot/AA, as described previously, blocks remaining mitochondrial respiration.

Table 2.22 illustrates how ECAR/OCR measurements were analysed to provide parameters of α-cell mitochondrial function.

Table 2.24: Mitochondrial stress test protocol

Mix	Measure	Cycles
3 min	3 min	3 basal 3 measurements (oligomycin) 3 measurements (FCCP) 3 measurements (2-DG)

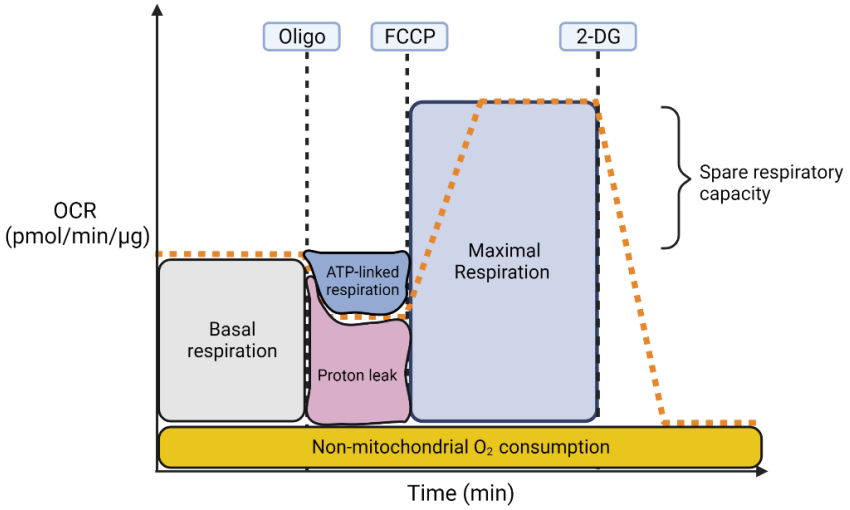

Figure 2.6: MitoStress assay protocol.

Basal respiration is calculated by removing non-mitochondrial oxygen consumption, following 2-deoxyglucose (2-DG) inhibition of glycolysis. Proton leak is calculated from the OCR between oligomycin (Oligo) and FCCP injection. ATP-linked respiration is calculated by the drop in OCR following Oligo injection. Maximal respiration is derived from OCR readings between FCCP and 2-DG injection, and spare respiratory capacity is the difference between maximal respiration and ATP-linked respiration. Adapted from (*Agilent Technologies Seahorse XF Cell Mito Stress Test Kit User Guide 103015-100*, no date)

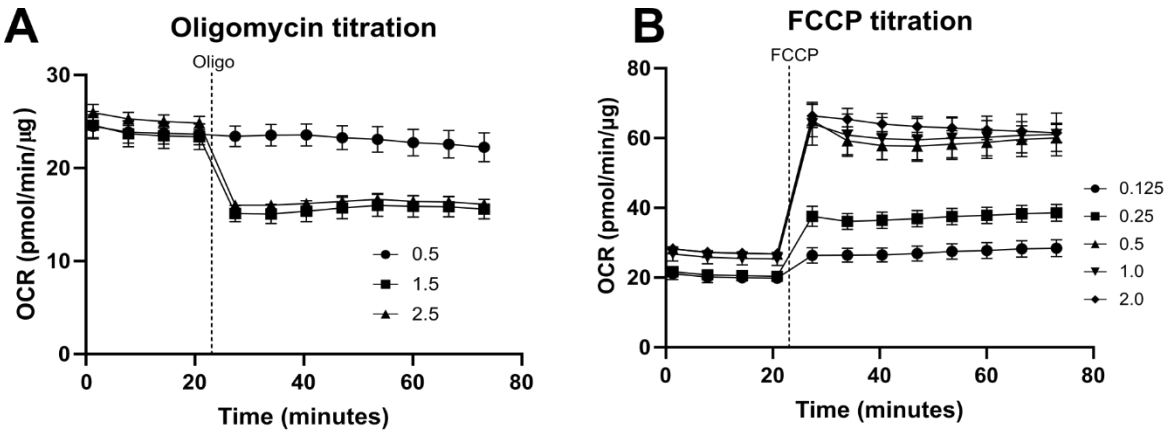

Figure 2.7: Oligomycin and FCCP titration assays.

Four basal measurements were recorded prior to either oligomycin (Oligo, 0.5 – 2.5 µmol/l) or FCCP (0.125 – 2.0 µmol/l) injection and eight measurements were taken following inhibitor addition (one individual plate, n = 8).

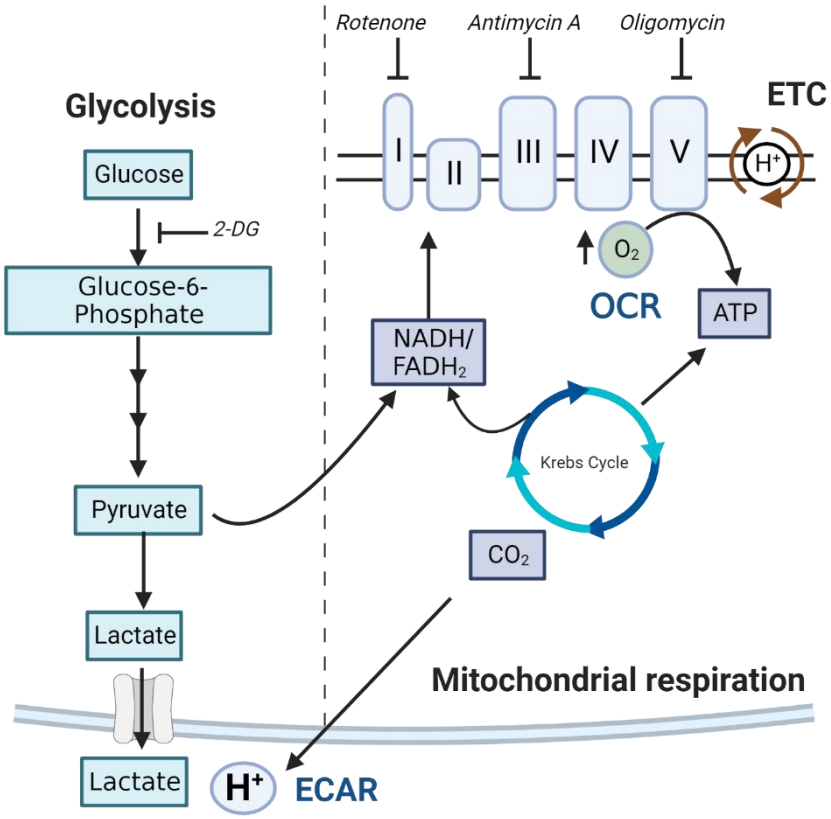

Figure 2.8: Key inhibitor actions to determine specific bioenergetic parameters.

2-deoxyglucose (2-DG) acts as a competitive inhibitor of glycolysis, reducing production of glucose-6-phosphate. Rotenone and antimycin A inhibit complex I and III, respectively, required for oxidative respiration. Complex V (ATP synthase) inhibition, by oligomycin, inhibit ATP-linked respiration. The inhibition of specific bioenergetic pathways facilitate the accurate calculation of glycolysis and oxidative respiration. Created with Biorender.com.

2.2.9.4 Recurrent low glucose

On Day 4 of RLG, αTC1.9 cells were washed twice with standard Seahorse XF DMEM media and subsequently exposed to a final bout of 0.5 mmol/l or 5.5 mmol/l dependent on treatment group for 30 - 60 min ± AMPK activator either during or post-degassing. Dependent on study, cells were either kept in same [glucose] ± AMPK activator or replaced with glucose-free Seahorse XF pH 7.4 DMEM media for glycolytic reactivation studies. In recurrent AMPK activator/inhibitor treatment, drug was incubated alongside or before specified 3 h 0.5 mmol/l treatment.

2.2.10 Nucleotide measurements

2.2.10.1 [ADP:ATP] ratio

αTC1.9 cells were seeded into white-coated 96-well plates (Greiner Bio-One). The following day, cells were exposed to respective experimental conditions for 30 min (post-2 h serum-free period) and [ADP:ATP] was measured.

[ADP:ATP] ratio kit (Sigma-Aldrich) measures [ADP] and [ADP] through a luciferase-based assay. Briefly, cells are lysed to release intracellular ATP and ADP into the working solution. Luciferase present in the ATP reagent solution reacts with ATP present and reacts with D-luciferin substrate to produce light. Light intensity is a measure of $[ATP]_i$. Following the addition of ATP reagent, ADP is converted to ATP through an enzyme reaction which consequently reacts in the same way as $[ATP]_I$ measurements. The second luminescent reading is indicative of total [ADP] and [ATP]. All readings were measured by PHERAstar FS microplate reader. This is summarised in Figure 2.9. To calculate the [ADP:ATP], Figure 2.10 depicts the respective calculation.

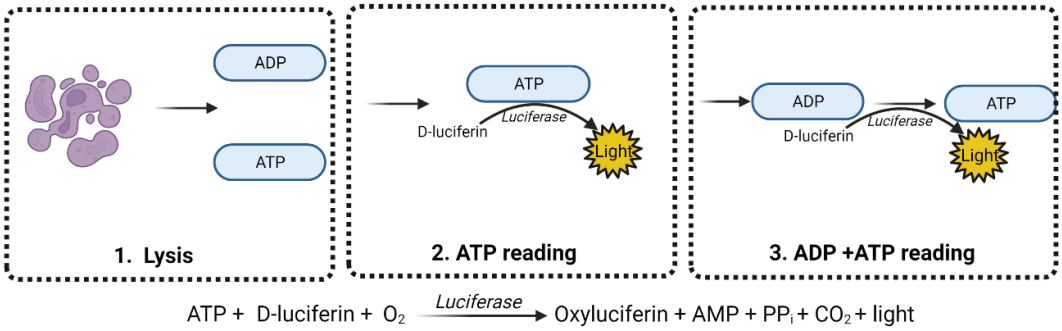

Figure 2.9: [ADP:ATP] ratio assay.

(1) Cells were first lysed and released intracellular ADP/ATP into the surrounding medium. (2) D-luciferin, added in ATP reagent mixture, reacts with ATP using the added luciferase enzyme to produce a luminescent light signal. This is proportional to total ATP/well. (3) ADP was converted to ATP, which then reacts with D-luciferin in the same reaction as (2), producing luminescence. This was indicative of total ADP and ATP within the well. Created using Biorender.com.

$$\text{ADP:ATP ratio} = \frac{RLU_C - RLU_B}{RLU_A}$$

Figure 2.10: [ADP:ATP] ratio calculation.

ATP luminescence (RLU_A) was divided from total ADP/ATP signal (RLU_C) minus background residual ATP signal (RLU_B). Created using Biorender.com.

2.2.10.2 Total and extracellular ATP

Total and extracellular ATP were measured by a luciferase-based luminescence reaction and performed according to manufacturer's instructions. Cells were lysed with mammalian lysis buffer (MLB) and mixed at 700 rpm for 5 min on an orbital shaker. Substrate solution was then added, plate was dark adapted for 5 minutes and mixed for 5 min using orbital shaking at 700 rpm. Gain adjustment (90%) was according to the highest standard (10.0 µM). Extracellular ATP was measured from collected supernatants and normalised to total protein to calculate ATP secretion.

2.2.11 L-lactate secretion

αTC1.9 cells were treated for up to 2 h ± AMPK activator, after 30 min pre-treatment ± AMPK inhibitor, dependent on experiment. Samples were processed according to manufacturer's instructions (Cayman Chemical, 700510). Briefly, samples were centrifuged at 1000 x g for 10 min at 4.0 degrees to remove floating cells. The collected supernatants were acidified using 0.5 M metaphosphoric acid (MPA) to inactivate residual lactate dehydrogenase (LDH). The supernatant was centrifuged again at 10,000 x g for 5 min at 4 degrees to pellet supernatant proteins and subsequently the pH was neutralised using potassium carbonate. To remove precipitated salts, supernatants were again centrifuged at 10 min for 5 minutes at 4 degrees, and assay samples were frozen at - 80 to prevent L-lactate degradation. To quantify L-lactate levels, known standards (up to 1000 µM) were ran alongside unknown samples to generate a standard curve with standard readings subtracted from blank (0 µM). The concentration of L-lactate in each sample were interpolated from the standard curve, quantified by fluorescence at excitation of 585 nm and emission at 610 nm. Lactate secretion was calculated by normalisation of total supernatant lactate levels divided by total protein (Figure 2.11).

$$\text{L-lactate } (\mu M) = \left(\frac{\text{CF - (y-intercept)}}{\text{Slope}} \right) \text{ x DPD x Sample dilution}$$

Figure 2.11: L-lactate quantification.

CF; corrected fluorescence, DPD; deproteination dilution.

2.2.12 Cell viability

2.2.12.1 Flow cytometry

Flow cytometry utilises multiple lasers to determine single cell size by measuring forward light scatter (FSC) and cell granularity by side light scatter (SSC), as identified in Figure 2.12 (Epstein, Watson and Smith, 1988). Flow cytometer can do this through fluidics, optics and electronic analysis. **A.** Fluidics comprise of a buffered solution (sheath fluid) to mobilise sample to lasers, **B.** Optics containing excitation lasers and photomultiplier tubes to generate both visible (cell size, granularity measurements) and fluorescent signals diluted through dichroic filters to detect specific fluorescent wavelength, **C.** Electronics convert fluorescent signals into quantitative events (Givan, 2011). Propidium iodide (PI) is a membrane impermeable nucleic acid dye that can only fluorescently binds to cell DNA and RNA in disrupted cell membranes (Rosenberg, Azevedo and Ivask, 2019). PI stain can therefore be used to exclude viable cells (Rosenberg, Azevedo and Ivask, 2019) and fluorescent "events" plotted as a histogram.

2.2.12.2 Methodology

On the experimental day, cells were stimulated with respective conditions in DMEM for 1 h. Supernatant was transferred to FACS tubes (Sarstedt), cells were detached and placed in respective flow tubes. Cells and media were pelleted using 1000 rpm for 5 min centrifugation. Pellet was resuspended in propidium iodide (PI) solution comprised of FACS buffer (2.0% FBS, 2.0% propidium iodide, PBS) comprising of DMEM with FACS buffer (1:2). The resuspended pellets were kept cold for 10 min prior flow cytometry. Positive control cells used for gating were kept in full media prior to resuspension in PI solution and heated to 60 degrees for 30 min. Flow cytometry was conducted using BD C6 Accuri Flow Cytometer.

2.2.12.3 Flow cytometry analysis

To exclude cellular debris, gating preferences was applied in accordance with the relevant positive control at 70.6 % cell death, to result in relevant fluorescent

events (Figure 2.12). The resulting fluorescence intensity (PE-A) calculated the percentage cell number with the respective fluorescent intensity. VL-R determined PI-stained cells and thereby interpreted as dead cells, and V1-L are unstained cells, hence cells with intact cell membranes (i.e., live cells). Data was analysed using BD CSampler Plus Software, as a percentage of total cell death.

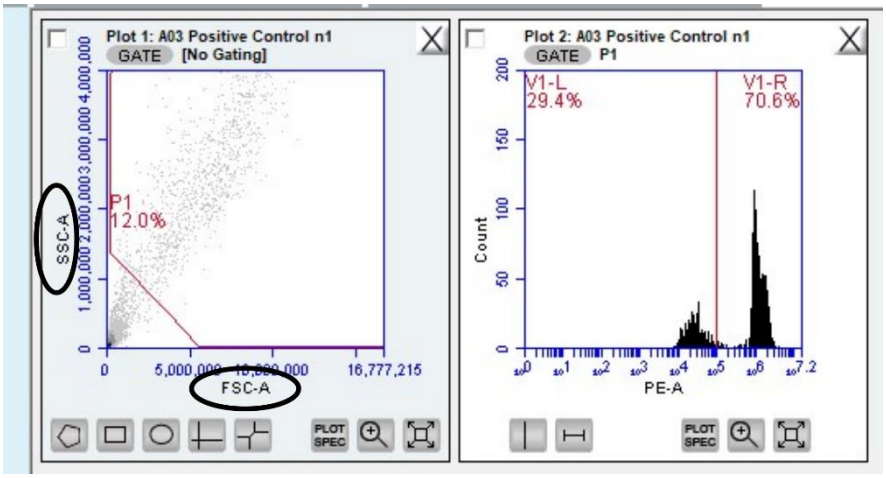

Figure 2.12: Flow cytometry gating strategy

The gating preferences applied for all samples were in accordance with the respective positive control (70.6 % cell death, 60 degrees heat, 30 min). The cellular debris (left hand corner, Plot 1) was removed in accordance with low forward scatter (FSC) and side scatter (SSC), as circled. The remaining cell population in the allocated “gate” was further analysed dependent on propidium iodide (PI) cell uptake (by V1-R population), determining cell apoptosis. V1-L cell population indicate unstained cells, and therefore alive cells.

2.2.13 Reactive Oxygen Species (ROS)

The following day post-cell seeding, cells were washed, serum-starved and subsequently incubated in 5.5 mmol/l glucose-containing DMEM with respective AMPK activator for 1 h. Cells were washed with 1 X PBS and stained with 2',7'-dichlorodihydrofluorescein diacetate (DCDFA) for 30 min to measure well fluorescence. Cells were subsequently washed (three times) in 1 X PBS and placed in fresh 1 X PBS. The plate fluorescence was read at 480/520 nm using a gain of adjustment at 50 % from the full plate.

2.2.14 Quantitative Polymerase Chain Reaction (qPCR) experimental pipeline

Prior to quantifying tissue gene expression, several preparatory steps are conducted to limit contamination and prepare sufficient cDNA input (Figure 2.13).

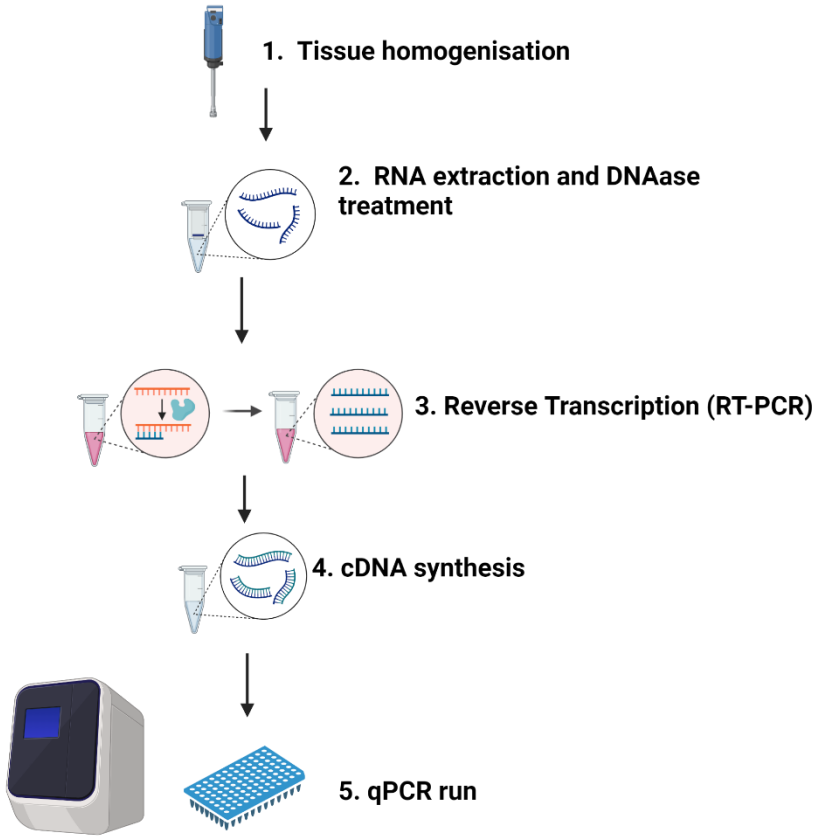

Figure 2.13: Quantitative PCR (qPCR) sample preparation pipeline.

A schematic diagram illustrating the steps required for sample preparation, including 1) tissue (i.e., liver), 2) RNA extraction and decontamination, 3) reverse transcription PCR (RT-PCR) and 4) cDNA synthesis for the final qPCR run to quantify liver gene expression.

2.2.14.1 RNA extraction

Trizol reagent (TRI®) and magnesium ($MgCl_2$) was added to 50 – 100 mg liver tissue and homogenised using Retsch homogeniser (30.0 Hz) for 10 min. Samples were spun at 12,000 rpm for 20 min at 4 degrees and subsequently the pink TRI® layer was transferred (DNA and protein) to a clean tube. Chloroform was then added to each sample and vigorously shaken for 15 seconds prior to 5 min incubation at room temperature. Homogenised samples were spun at 14,800 rpm for 20 min at 4 degrees. Aqueous phase was transferred (RNA) and GlycoBlue was added to aid pellet visualisation. Isopropanol was added to the aqueous phase (RNA) and samples were mixed and incubated at 10 min (room temperature). Samples were spun again at 14,800 rpm for 10 min at 4 degrees. Supernatant was removed and 75% molecular-grade ethanol was added to wash the pellet and vortexed. Sample was spun at 14,800rpm for 30 min at 4 degrees (1). Pellet was washed again with 75% molecular-grade ethanol and vortexed. Samples were again centrifuged as describe in (1), with ethanol removed and pellet allowed to air dry for up to 15 min. Each pellet was resuspended in TE buffer (Sigma-Aldrich) Sample RNA concentration was quantified using Nanodrop 8000, with 260:280 ratio (purification) accepted between 1.8 – 2.0.

2.2.14.2 DNA digestion

In accordance with manufacturer's instructions, all samples were treated to remove genomic DNA contamination (detected via Nanodrop), by mixing with Buffer RDD (RNeasy Mini, Qiagen), DNase I and RNase-free water and incubated on the benchtop at room temperature for 10 min.

2.2.14.3 RNA cleanup

Buffer RLT was added to sample and gently mixed with ethanol. Sample was transferred to RNeasy Mini spin column and centrifuged for 15 seconds at ≥10,000 rpm (2). Flow through was removed, Buffer RPE was added and centrifuged as described in (2). Flow through was again removed and washed with Buffer RPE and centrifuged for 2 min at ≥10,000 rpm. RNase-free water

was added directly to the spin column membrane and further centrifuged for 1 min ≥10,000 rpm to elute RNA. [RNA] was checked using Nanodrop 8000.

2.2.14.4 cDNA synthesis

RNA samples were prepared for cDNA synthesis according to Table 2.25 (EvoScript cDNA synthesis, 07912374001) in a 96-well plate and incubated at 4.0 degrees for 5 min to facilitate primer-RNA annealing. Enzyme mix (10 X) was added to catalyse cDNA synthesis and remove sample RNA scaffolds after cDNA synthesis for effective PCR primer-cDNA binding. The reverse transcription (RT) thermal profile is shown in Table 2.26. The samples were further diluted in RNA/DNase – free water (1:2) and stored at 4.0 degrees for quantitative PCR (qPCR) analysis.

Table 2.25: EvoScript RNA preparation for cDNA synthesis protocol.

Component	Volume	[Final]
Water, PCR Grade	0 µl	-
Reaction Buffer, [5X]	4.0 µl	1 X
Template RNA	14.0 ul	2.5 µg
Total volume	18.0 µl	

Table 2.26: Thermocycler thermal profile for cDNA synthesis

Step	Temperature (°C)	Time (min)
1	42	30
2	85	5
3	65	15
4	4	Hold

2.2.14.5 qPCR

Prior to qPCR, all cDNA samples and probes were thoroughly mixed. Total mastermix (TaqMan™ Universal Mastermix II, 4440043; TaqMan™ Gene Expression Assay, 4331182 S) was prepared according to Table 2.27 (A/B) and added to each corresponding well in a 384-well plate. Sample cDNA (in nuclease-free water) was first added to each well in a 96-well mixing plate, pulse centrifuged to pellet at > 3000 rpm, gently vortexed and lastly repeated pulse centrifuged. Samples were transferred to the 384-well plate and sealed using a heat-sealing non-adhesive film. The plate was pulse centrifuged, as described previously, and qPCR was ran using (QuantStudio™ 12K Flex) (Table 2.28).

Table 2.27: TaqMan™ Gene Expression Assay

(A) Probe and primer concentrations.

Forward primer	Reverse primer	Probe
20 X	20X	20X
18 µM	18 µM	5 µM

(B) MasterMix™ components/well.

	Per well (µl)
TaqMan® Universal MasterMix	2.5
TaqMan® Probe (20X)	0.25
ddH_2O	1.25
cDNA (ng/ul)	1
TOTAL	5

**Table 2.28: Quantitative Polymerase Chain Reaction (qPCR) thermal profile (TaqMan™ Universal Master Mix II standard profile). ***standard cycling mode

Step	Temperature (°C)	Time*	Cycles
Enzyme activation	95	10 min	1
Denature	95	15 seconds	40
Anneal/Extend	60	1 min	

1.1.1.1.1. qPCR analysis

Data analysis was conducted using the $2^{-\Delta\Delta Ct}$ method, as previously described, and normalised to relevant housekeeping genes (*Hrpt1, Sdha, Rplp1*) (Livak and Schmittgen, 2001). Housekeeping gene expression is displayed in Figure 2.14 and gene information is described in Appendix A, Table 9.1.

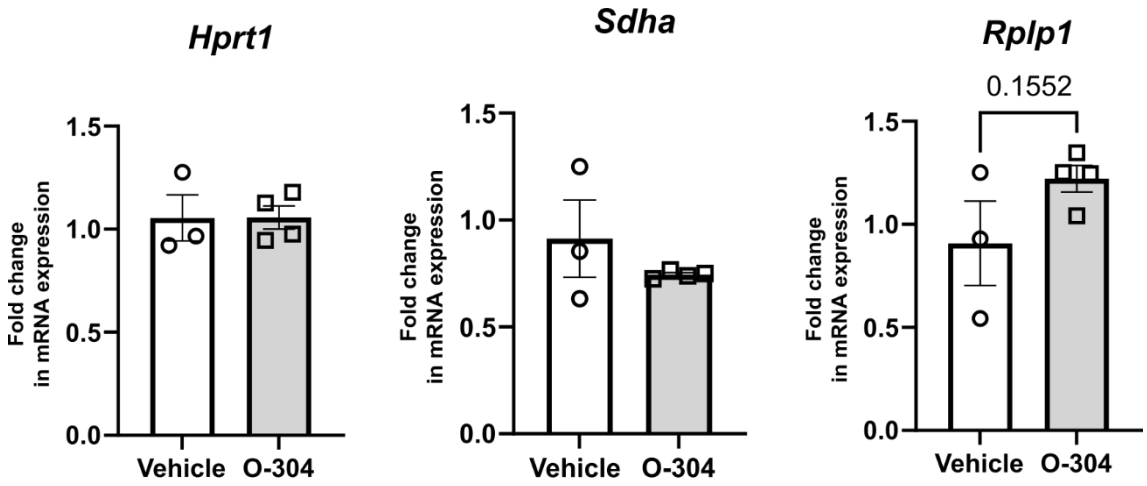

Figure 2.14: Housekeeping liver gene expression in vehicle/O-304-treated diabetic Sprague-Dawley rats.

Hypoxanthine-guanine phosphoribosyltransferase 1 (*Hrpt1*), succinate dehydrogenase a (*Sdha*), and ribosomal protein lateral stalk subunit P1 (*Rplp1*) housekeeping gene expression quantified using qPCR for normalisation of results (unpaired two-tailed t-test, n = 3 – 4).

2.2.15 Statistical analysis

Statistical significance between groups was classified as a p value < 0.05 and displayed as mean ± standard error of the mean (SEM). If comparing two groups, unpaired two-tailed t-tests were used. When comparing more than three groups, One-Way ANOVA was used. Repeated measures Two Way ANOVA analysis was used when comparing groups over a specific time course, represented in an X-Y graph. An appropriate multiple comparisons test was conducted, dependent on data normality and experimental question being tested. All statistical tests were conducted by GraphPad Prism 9.5.1 software.

Chapter 3

Investigation into the role of endogenous AMPK activity and by R481, on glucose-dependent metabolism in pancreatic α-cells.

3 Investigation into the role of endogenous AMPK activity, and by R481, on glucose-dependent metabolism in pancreatic α-cells.

3.1 Introduction

α-cells are the second most abundant cell type in the islets of Langerhans, accounting for approximately 30 – 40% of cell area (Cabrera *et al.*, 2006; Da Silva Xavier, 2018). In healthy individuals, α-cells are under tight paracrine control from the surrounding β- and δ-cells which are postprandially active to prevent hyperglycaemia further propagated by improper glucagon secretion (Acreman and Zhang, 2022). In DM, the glucagon response to glycaemia is dysregulated, with diminished glucagon secretion at low glucose and excess glucagon secretion in hyperglycaemic conditions. In T1DM, α-cells are the predominant cell type in the islet due to selective β-cell loss (Rahier, Goebbels and Henquin, 1983). It is still relatively poorly understood, compared to β-cell counterparts, on the mechanisms are behind α-cell glucagon secretion. Impaired glucagon secretion is predominantly attributed to the loss of centrally-regulated and paracrine inhibition (Taborsky, Ahrén and Havel, 1998; Hoffman *et al.*, 2021). However, Brissova *et al.* 2018 recently provided evidence for intrinsic α-cell defect (s) in T1DM, where α-cells were found to have differentially expressed genes required for adequate hypoglycaemia-stimulated glucagon secretion (Brissova *et al.*, 2018). This chapter, therefore, explores if (and how) pharmacologically modulating AMPK activity, a known α-cell glucose sensor, could be a potential target in restoring diminished α-cell glucagon secretion commonly seen in T1DM.

Profiling the expression of AMPK subunit isoforms in the islet is key to selecting an appropriate small molecule measure both AMPK activity and hormone secretion. Both α- and β-cells express both α-isoforms required for full kinase activity (Beall *et al.*, 2010; Leclerc *et al.*, 2011; Sun *et al.*, 2015). In addition, dominant negative expression (α1 D157A) of α-cell AMPKα1 abolished low glucose-stimulated glucagon secretion (Leclerc *et al.*, 2011). Furthermore, constitutively active AMPKα1^{312} enhanced glucagon secretion at low glucose,

alongside a lack of suppression of glucagon secretion at high glucose in αTC1.9 cells and mouse islets (Leclerc *et al.*, 2011). Moreover, α-cell specific AMPKα1 and upstream kinase LKB1 knockout mouse islets had attenuated low glucose (3.0 mmol/l) sensitive glucagon secretion (Sun *et al.*, 2015). Altogether, these findings infer endogenous AMPKα1/LKB1 activity appears to be important in low glucose-stimulated glucagon secretion.

AMPKβ isoform expression is tissue specific and corresponds to cell function. For instance, AMPKβ1$^{-/-}$ hepatocytes displayed abolished insulin attenuation of gluconeogenic gene expression and enhanced triglyceride formation (Oakhill *et al.*, 2010). AMPKβ1 expression is relatively ubiquitously expressed, with highest expression in both the liver and brain (Thornton, Snowden and Carling, 1998). Whereas AMPKβ2 expression is abundant in skeletal muscle, in which AMPKβ2$^{-/-}$ mice have reduced skeletal muscle glycogen at both fed and fasted states (Thornton, Snowden and Carling, 1998; Dasgupta *et al.*, 2023). Mouse and human islets express both AMPKβ1 and β2 isoforms, with β1 being the most predominant at 64 – 71 % relative expression (Scott *et al.*, 2015). β2 expression is most likely localised to the β-cell. Whole-body AMPKβ2 knockout mice displayed fasting hyperinsulinaemia, corroborating findings by the same author using a selective β2 inhibitor (MT47-100) which enhanced supernatant insulin at high glucose in a β2-dependent manner (Scott *et al.*, 2015). Additionally, cytosol/nucleus β2 antibody injection enhanced MIN6 insulin promoter activity regardless of [glucose] (Da Silva Xavier *et al.*, 2000). Additional evidence suggests glucose deprivation and rises in AMP-γ-subunit binding can promote β-subunit myristoylation and membrane association, in turn promoting upstream kinases (such as LKB1) to stimulate α-Thr-172 phosphorylation and downstream kinase activity (Oakhill *et al.*, 2010; Neopane *et al.*, 2022). Little is known about α-cell AMPK β isoform expression and more specifically, if such activity (alongside AMPKα1) is important for glucose-sensitive α-cell glucagon secretion.

AMPK activity is, in part, driven by increased intracellular [AMP:ATP] resultant from glucose deprivation. In turn, AMPK activation stimulates catabolic, ATP-

producing pathways to restore intracellular energy balance. One such pathway is glycolysis, whereby increased short term increased AMPK activity can drive glycolytic flux in certain cell types where glucose deprivation is common, such as cancer cells (Hu *et al.*, 2019). AMPK can directly modulate glycolytic enzyme activity, such as increasing PFKFB3 phosphorylation (also referred to in the literature as “PFK2”, or “PFKFB”) as a result of AMP depletion (Marsin *et al.*, 2002). PFKFB3 is an isoform of the bidirectional PFK-2 family, whereby enzymes contain both a phosphatase and kinase domain (hence, PFK-2 is also commonly interchanged with “PFK-2/FBPase2” in the wider literature) (Sakakibara *et al.*, 1997). PFKFB3 generates a potent allosteric activator of phosphofructokinase-1 (PFK-1), which catalyses the conversion of fructose-6-phosphate (F6P) to fructose 1,6-bisphosphate (F1,6-BP) (Merrins *et al.*, 2012) (Figure 1.8). PFKFB3 does this by increasing fructose 2,6 bisphosphate (F2,6BP) levels catalysed from F6P (Merrins *et al.*, 2012). Similar to AMPK, PFK-1 is allosterically modulated by AMP and ATP levels making it a crucial sensor of intracellular energy depletion (Van Schaftingen *et al.*, 1982). Thereby PFKFB3 is comparable to PFK-1, as a key target in modulating cell glycolytic flux. PFKFB kinase activity is also dependent on how glycolytic-dependent the tissue is. Human and mouse islets express both PFKFB2 and PFKFB3, and when both were silenced glucose-stimulated F2,6BP levels and insulin secretion were attenuated in a β-cell model (Arden *et al.*, 2008). PFK-2/FBPase2 activity is thought to be metabolically “paired” with glucokinase (GK) activity at high glucose in various PFK-2/FBPase2-overexpressed β-cell lines, which similarly drives β-cell glucose utilisation at [glucose] required for GK activity (Massa *et al.*, 2004; Baltrusch *et al.*, 2006). Similarly, genetically altering phosphatase and/or kinase activity on PFKFB2 altered mouse islet calcium oscillatory activity required for hormone granule exocytosis (Merrins *et al.*, 2012). Glucagon (via PKA-dependent mechanisms) can modulate PFK-2/FBPase2-GK colocalization and subcellular localisation in hepatocytes, with α-cell rate-limiting GK activity and glycolysis-derived lactate production being greatest at high glucose (Sekine *et al.*, 1994; Cullen *et al.*, 2014; Zaborska *et*

al., 2020; Wang *et al.*, 2021). Although speculative, these findings can provide the possibility for AMPK-PFKFB3 controlled α-cell glycolysis at high glucose.

At high glucose levels, α-cells predominantly drive anaerobic glycolysis whereby the majority of pyruvate generation is most likely converted to lactate (Sanchez *et al.*, 2021; Cuozzo *et al.*, 2022). The reason being is that human α-cells highly express both *LDHA* and monocarboxylate transporters (MCT2/4) required for lactate generation and transport (Sekine *et al.*, 1994; Zaborska *et al.*, 2020). Similarly, mitochondrial glucose oxidation is limited in comparison to β-cells at high glucose availability (Schuit *et al.*, 1997; Sanchez *et al.*, 2021; Cuozzo *et al.*, 2022). Lactate may not just be a glycolytic end-product, as the import of exogenous lactate has been reported to diminish low glucose-stimulated glucagon secretion, most likely through greater K_{ATP} channel opening, thereby hyperpolarising the α-cell membrane and inactivating voltage-gated sodium/calcium channels, reducing action potential amplitude (Zaborska *et al.*, 2020). These findings could indicate that targeting endogenous lactate production may directly influence α-cell glucose-sensing and function.

Recent evidence suggests impaired islet cell metabolism is a driver of dysfunctional hormone secretion observed in DM. For instance, T2DM islets showed impaired mitochondrial and glycolytic protein expression, alongside attenuated glucose utilisation (Anello *et al.*, 2005; Haythorne *et al.*, 2019). In addition, key rate-limiting glycolytic enzymes (e.g., PFK, FBPase and aldolase) were enhanced in both diabetic mouse islets with an inducible gain-of-function K_{ATP} channel mutation and chronically hyperglycaemic β-cell line (Brereton *et al.*, 2014; Haythorne *et al.*, 2022). α-cells similarly present altered metabolic responses in T2DM. Chronic hyperglycaemia associated with the genetic ablation of fumarase (a key enzyme for Krebs cycle propagation), promoted α-cell mitochondrial dysfunction and abolished glucose-sensitive glucagon secretion from mouse islets (Knudsen *et al.*, 2019). Similarly, increased transcript expression of certain mitochondrial complexes are essential for electron transport in T2DM α-cells (Dai *et al.*, 2022). Glucose-sensing may similarly be altered, as glucokinase (GCK) activation in α-cells attenuated HFD-

associated hyperglucagonaemia (Bahl *et al.*, 2021). T1DM is similarly indicative of impaired α-cell metabolic and glucagon secretory function. Although the small sample size, Brissova *et al.* 2018 confirmed in RNAseq analysis downregulation of genes associated with glucose metabolism (e.g. *PFKP, PDHA1, SLC5A1*) (Brissova *et al.*, 2018). Similarly, T1DM-predisposed human islets ($GADA^+$) appear to show gene downregulation associated with glucose-sensing and glycolysis, including highly enriched *GCK* and *LDHA* (Heimberg *et al.*, 1996; Basco *et al.*, 2018; Sanchez *et al.*, 2021; Doliba *et al.*, 2022). Altogether, these data suggest glucose-sensitive glucagon secretion from α-cells is at least partially determined by intrinsic metabolic function, in which the latter appears to be dysregulated in both T1DM and T2DM.

Under recurrently hypoglycaemic conditions, certain glucose-sensing cells (e.g., astrocytes) require the use of alternative substrates to sustain energy supply and function (Weightman Potter *et al.*, 2019). Similarly to astrocyte metabolic adaptations, computational modelling found ATP production in pancreatic α-cells to be significantly higher than β-cells, suggesting α-cells could promote alternative substrate catabolism to retain function at low glucose (Grubelnik *et al.*, 2020a). More recently, Briant *et al.* 2018 demonstrated fatty acid oxidation (FAO) inhibition or silencing by CPT1a attenuated glucagon secretion regardless of extracellular glucose in both mouse/human islets and an α-cell line (Briant *et al.*, 2018a). The authors suggested CPT1a-mediated glucagon secretion is maintained by fuelling α-cell sodium-potassium pump ATPase activity, limiting ion channel inactivation and sustaining action potential amplitude (Briant *et al.*, 2018a). In addition, a transcriptomic analysis suggested high expression of FAO indicator *PDK4* in healthy α-cells, supporting the Briant *et al.* hypothesis of α-cell metabolic switching (Dorajoo *et al.*, 2017). AMPK can similarly upregulate FAO by decreasing malonyl-CoA inhibition of CPT1a by inactivation of ACC2; postulating a role for AMPK-CPT1a in α-cell metabolic switching at low glucose (O'Neill, Holloway and Steinberg, 2013). However, without examining the metabolic impact of exogenous free fatty acids (FFA), these findings rely on the idea that CPT1a-dependent activity in the α-cell is at least partially dependent on endogenous FA stores to maintain glucagon

secretion. Treatment with high levels of the saturated FFA, palmitate, enhanced mouse islet glucagon secretion regardless of extracellular glucose availability (Olofsson *et al.*, 2004). In addition, α-cells exposed to longer term (2-days) treatment with palmitate stimulated glucagon secretion, similarly at high concentrations (Piro *et al.*, 2010). These datasets have relevance to DM, a pathophysiological condition commonly associated with high circulating FFAs and hyperglucagonaemia. Whether physiological [FFAs] are utilised by the α-cell, in an AMPK-dependent manner, to sustain α-cell function at low glucose has not been explored.

Recurrent glucose deprivation is associated with diminished endogenous low glucose-stimulated AMPK activation in the hypothalamus and attenuated counterregulatory responses (Alquier *et al.*, 2007). As mentioned, α-cells are intrinsically glucose-sensing and so it is reasonable to suggest recurrent hypoglycaemic episodes could directly blunt glucose-sensitive AMPK activity in the α-cell. α-cell AMPK activity has been previously linked to glucagon secretion although the mechanisms are not well understood (Sun *et al.*, 2015). Prior research has mainly focused on using indirect AMPK activators, providing conflicting results. For instance, well-used AMPK activator and AMP mimetic AICAR failed to stimulate αTC1.9 AMPK activity (Leclerc *et al.*, 2011). In addition, acute exposure to high metformin concentrations enhanced AMPK activity and glucagon secretion regardless of glucose availability (Leclerc *et al.*, 2011). Similar findings were observed in healthy human participants, whereby metformin enhanced serum glucagon before and throughout hypoglycaemic clamp studies (Fruehwald-Schultes *et al.*, 2001). Elevated metformin concentrations, especially *in vitro* cell cultures, increase likelihood of AMP-dependent, AMPK-independent off-target effects (Miller *et al.*, 2013; Hunter *et al.*, 2018; Johanns, Hue and Rider, 2023). Although AMPKβ1-selective AMPK activator A-769662 similarly enhanced α-cell glucagon secretion, this appeared to be at least partially glucose-sensitive, possibly due to enhanced inhibition of AMPK by high glucose levels (Leclerc *et al.*, 2011). Altogether, these findings suggest the need for allosteric AMPK activators to better interrogate how AMPK activity regulates α-cell function.

Novel AMPK-activating small molecules, R481 and R419, are thought to have a metformin-like mechanism of action by mildly inhibiting complex I (Jenkins *et al.*, 2013). R419 can regulate AMPK-dependent substrate utilisation, including FAO and glucose uptake, in both glucose-sensing hepatocytes and skeletal muscle respectively (Jenkins *et al.*, 2013). Similarly, in rodent hyperinsulinaemic-hypoglycaemic clamp studies, Cruz *et al.* showed peripheral R481 administration enhanced plasma glucagon levels and reduced the need for exogenous glucose during hypoglycaemia, indicating increased glycaemic counterregulation (Cruz *et al.*, 2021). Since R481 was peripherally administrated, it is possible that R481 could have direct actions on α-cell glucagon secretion in hypoglycaemic conditions.

Altogether, these findings provide a potential role of glucose-sensitive AMPK activity in regulating α-cell glucagon secretion. Therefore, the author sought to test the hypothesis that pharmacologically amplifying AMPK activity using R419/R481 (Rigel Pharmaceuticals) could modulate fuel utilisation to boost α-cell glucagon secretion in response to hypoglycaemic-like conditions. This hypothesis was examined using the mouse α-cell line, αTC1.9, with the following experimental objectives;

1. Does R419/R481 modulate α-cell AMPK activity?
2. Does amplifying AMPK activity modify α-cell substrate utilisation? If so, how?
3. Does increased AMPK activity alter α-cell alternative substrate usage dependent on glucose availability?
4. If so, how does this impact downstream glucagon secretion?

3.2 Results

3.2.1 Characterisation of the αTC1.9 cell line

3.2.1.1 Glucose-dependent AMPK activation

AMPK is an energy stress marker and as such, is activated in glucose-deprived conditions. Glucose deprivation increases $[AMP]_i$ and by binding to AMPK γ subunit, subsequently enhances Thr-172 phosphorylation of AMPK α and kinase activity (Mitchelhill *et al.*, 1997). Serine-79 residue phosphorylation, thereby inactivation, of ACC is a well-established marker of upstream AMPK activation (Munday *et al.*, 1988). Here, endogenous AMPK activation (pAMPK, Thr-172 and pACC, Ser-79) was measured following αTC1.9 exposure to a glucose concentration range (0.1 – 11.7 mmol/l) for 1 h. All fold changes stated are in comparison to the high glucose (11.7 mmol/l).

αTC1.9 cells exposed to lower [glucose] had a trend towards, but not significantly, enhanced AMPKα-Thr-172 phosphorylation compared to α-cells exposed to high glucose treatment (0.1; 2.002 ± 0.4469, $P = 0.1248$, 0.5; 1.837 ± 0.6156, 1.0, 1.291 ± 0.2979, 3.0; 1.063 ± 0.2322, 5.5; 0.6589 ± 0.1029) (fold change) (Figure 3.1B). Low glucose-stimulated AMPK activation was similarly demonstrated by measured ACC phosphorylation; with low [glucose] availability stimulating ACC-Ser-79 phosphorylation compared to high extracellular glucose (fold change) (0.1; 3.229 ± 0.2250, $P = 0.0001$, 0.5; 1.871 ± 0.2749, $P = 0.0401$, 1.0; 1.496 ± 0.2928, 3.0; 1.506 ± 0.2001, 5.5; 0.04400) (Figure 3.1C).

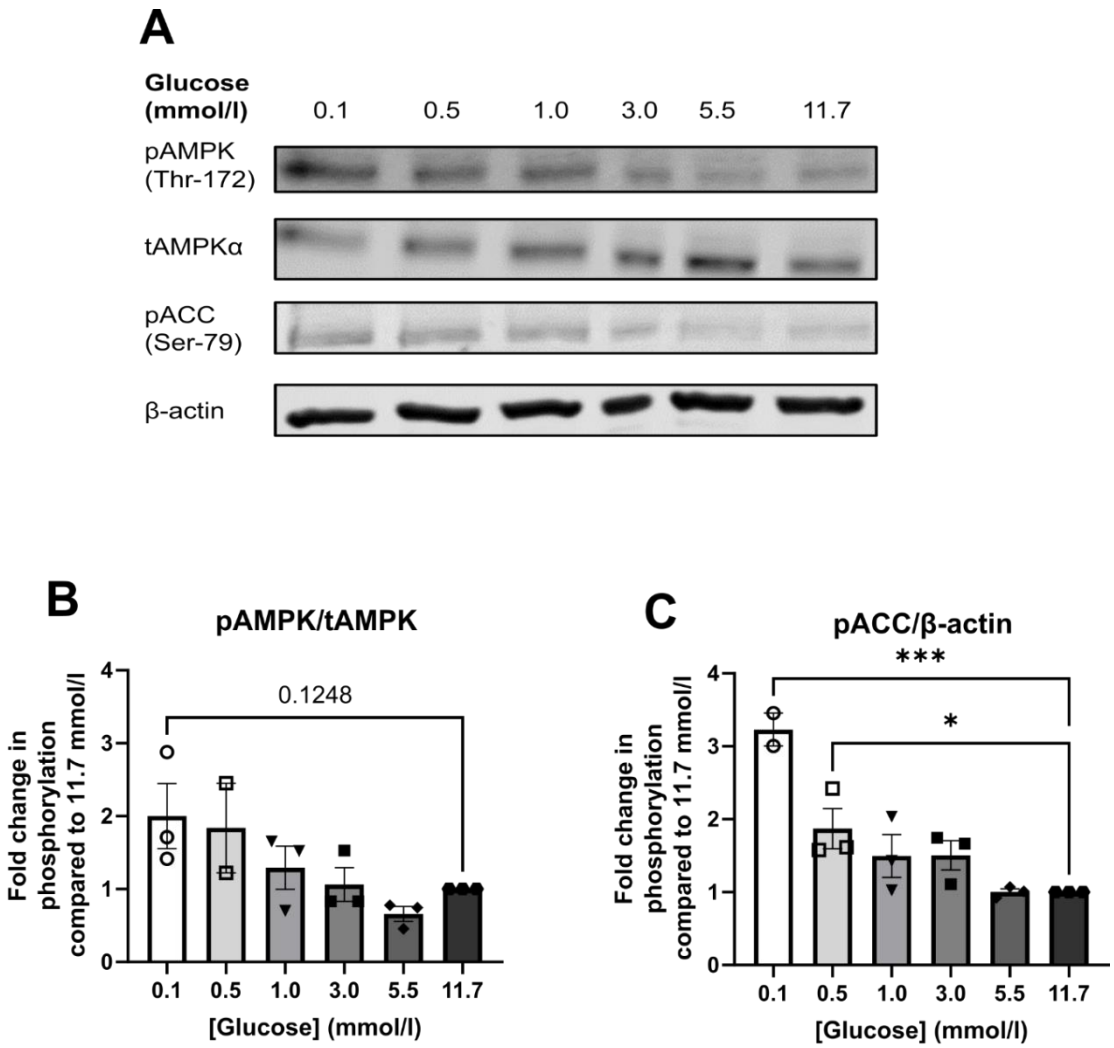

Figure 3.1: Glucose-sensitive AMPK signalling activation in αTC1.9 cells.

αTC1.9 cells were incubated in 0.1 - 11.7 mmol/l glucose for 1 h in KBH (Krebs-Buffered HEPES) solution **A.** Representative immunoblots were probed for phosphorylated AMPK (Thr-172, pAMPK), phosphorylated ACC (Ser-79, pACC), total AMPKα (tAMPK), and β-actin (loading control). Densitometric analysis of mean pooled data for **B.** pAMPK and **C**. pACC normalised to t-AMPK and beta-actin respectively (n = 2 – 3, One-Way ANOVA with Tukey Multi-Comparison test, *P<0.05, ***P<0.001)

3.2.1.2 Glucose-sensitive glucagon secretion

Here, to corroborate published findings, αTC1.9 cells were exposed to 5.5 mmol/l glucose-containing medium prior to incubating cells with between 0.1 – 11.7 mmol/l glucose to observe αTC1.9 cell glucose sensitivity.

αTC1.9 cells had significantly increased glucagon secretion at low glucose availability (0.1 mmol/l) when compared to high glucose (11.7 mmol/l) (pg/µg) (0.1; 8.678 ± 1.580, *P = 0.0420,* 0.5; 6.861 ± 1.156, 1.0; 6.470 ± 0.9539, 3.0; 3.960 ± 0.2950, 5.5; 5.152 ± 1.060, 11.7; 3.998 ± 1.160) (Figure 3.2).

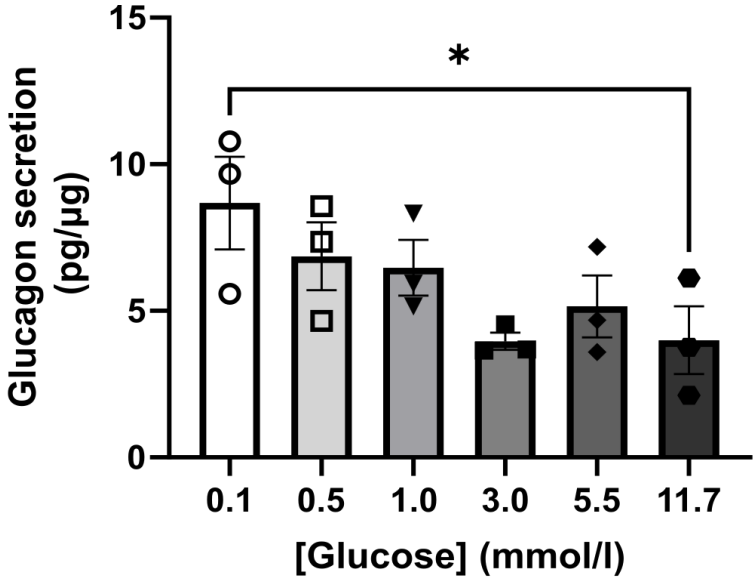

Figure 3.2: αTC1.9 glucose-sensitive glucagon secretion.

αTC1.9 cells were exposed to 5.5 mmol/l glucose for 2 h prior to incubated cells with between 0.1 – 11.7 mmol/l glucose-containing Krebs-Buffered HEPES (KBH) solution for 1 h. Supernatant glucagon was measured using Quantikine® glucagon immunoassay and normalised to total protein to calculate glucagon secretion (n = 3, One-Way ANOVA with Dunnetts multiple comparison test compared to 11.7 mmol/l only, *P<0.05)

3.2.1.3 GLUT transporter expression

Pancreatic islets express a variety of glucose transporters (GLUTs) to facilitate glucose entry for glycolysis, including GLUT4 in the α-cells (Bähr *et al.*, 2012). Both GLUT1 and GLUT4 transporter expression was characterised in αTC1.9 cells following the exposure to R419/R481 (50 nmol/l) in 1.0 – 11.7 mmol/l glucose-containing media for 1 h. The findings found αTC1.9 cells expressed GLUT1 and GLUT4 protein, and expression appears to be unaltered following AMPK activator and/or glucose exposure (Figure 3.3:

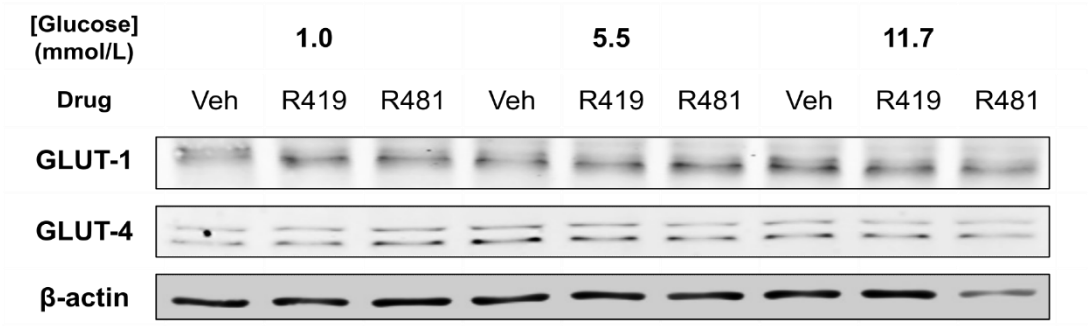

Figure 3.3: GLUT1 and GLUT4 protein expression in αTC1.9 cells.

αTC1.9 cells were incubated with 1.0 – 11.7 mmol/l glucose-containing DMEM ± R419/R481 (50 nmol/l) for 1 h. Representative immunoblot of GLUT1, GLUT4, β-actin protein expression (immunoblotting courtesy of Ms. Valentina Abba, n = 1).

3.2.2 AMPK β isoform expression

AMPK β isoforms are selectively expressed in a tissue-specific manner. However, little is known about isoform localisation in specific pancreatic islet endocrine cells.

3.2.2.1 AMPK β1 is the primary β-isoform expressed in αTC1.9 cells.

Here, for the first time, AMPK β1/2 protein expression was examined in α-cells following differing glucose availability. AMPK β1 was highly expressed in α-cells, compared to no AMPK β2 expression observed (Figure 3.4).

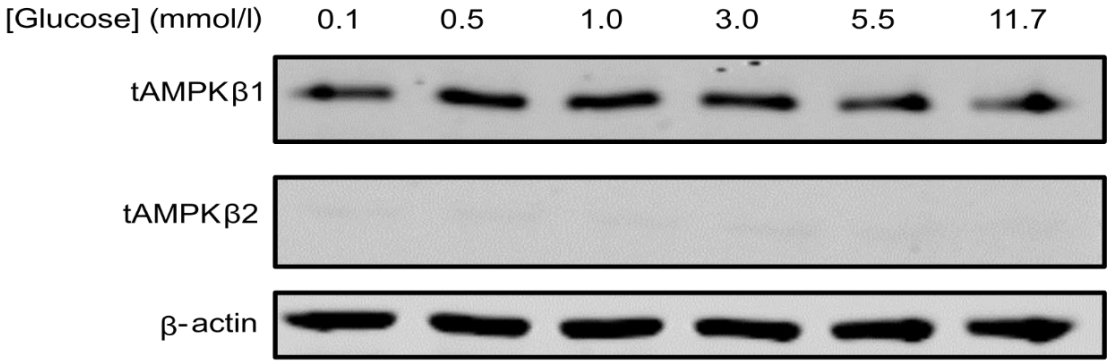

Figure 3.4: AMPKβ1 is the primary isoform protein expressed in αTC1.9 cells.

αTC1.9 cells were incubated with between 0.1 – 11.7 mmol/l glucose-containing Krebs Buffered Hepes (KBH) solution for 1 h prior to lysis. Representative immunoblot for total AMPKβ1 (tAMPKβ1, 4178), total AMPKβ2 (tAMPKβ2, 4148, n = 3).

3.2.2.2 AMPK β1 is primarily expressed in wild-type C57/BL6 mouse islets.

Pancreatic islets and β-cells express both AMPK β1/2 isoforms (Scott *et al.*, 2015). Therefore, fixed C57/BL6 pancreatic tissue (kindly donated by Dr. Jessica Hopkinson and Mr. Josan Gandawijaya) were immunostained with AMPK β1 or AMPK β2 antibodies. As observed, mouse pancreatic islets exhibit high AMPK β1 immunostaining relative to AMPK β2 immunostaining (Figure 3.5).

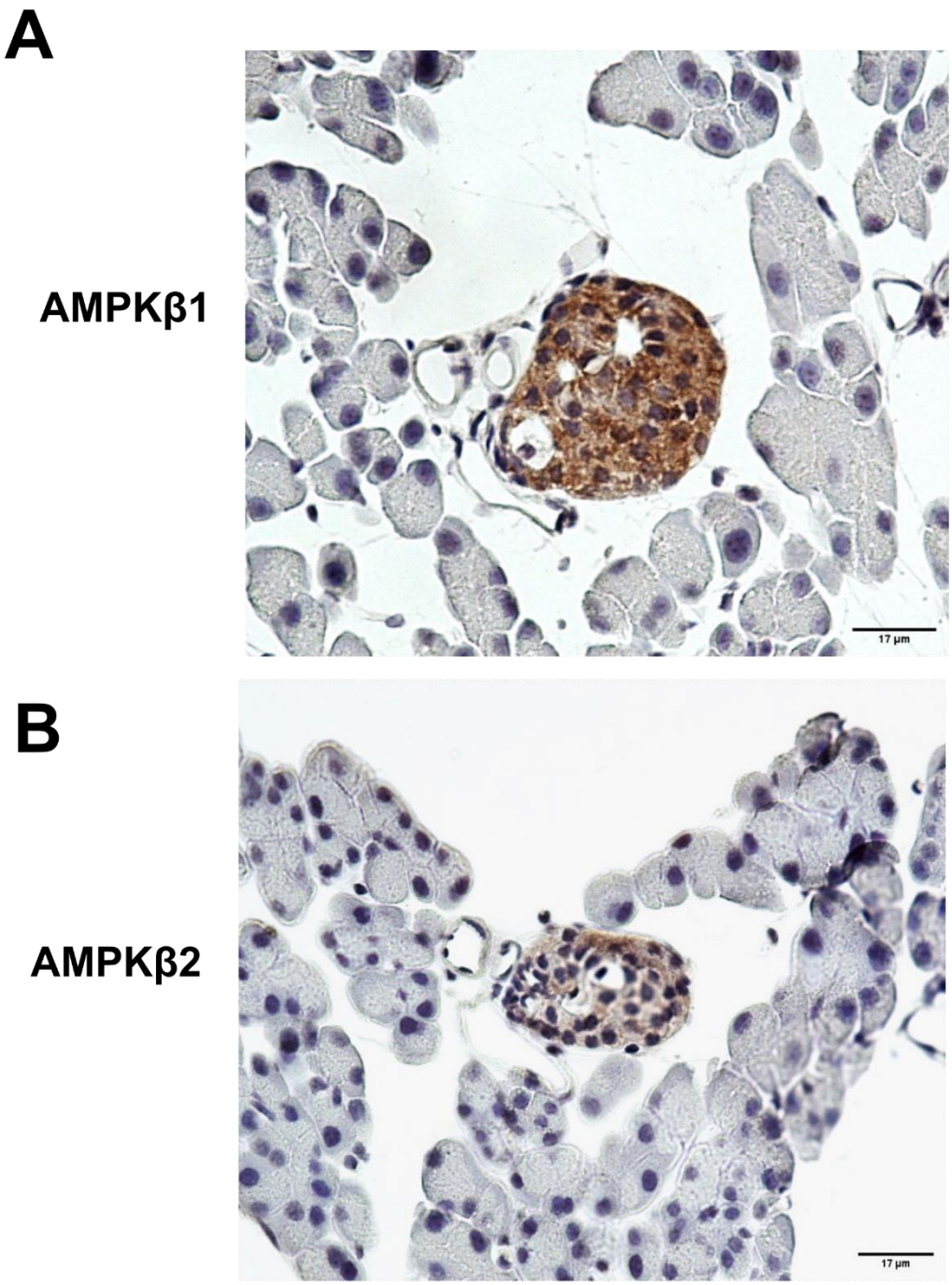

Figure 3.5: Mouse pancreatic islets exhibit high AMPK β1 immunostaining relative to AMPK β2.

AMPKβ isoform expression was measured using immunohistochemical staining (IHC) on C57/BL6 wax-embedded mouse pancreatic slices. AMPK β1 (1 in 500) and AMPK β2 (1 in 250) are shown in Panel A and Panel B respectively at 40X magnification (Nikon 50i, brightfield microscope, n = 1 animal).

3.2.3 Indirect AMPK activator (R419 and R481) experiments

3.2.3.1 R419 and R481 increased α-cell AMPK signalling cascade activation.

R419 and R481 can indirectly activate AMPK in mouse neuronal cell line and skeletal muscle (Marcinko *et al.*, 2015; Cruz *et al.*, 2021). To examine if both compounds will similarly stimulate AMPK activation, α-cells were exposed to R419/R481 (50 nmol/l) for 1 h in media containing 1.0 – 11.7 mmol/l glucose.

R481 enhanced α-cell AMPK phosphorylation, not R419, at 1.0 mmol/l glucose compared to vehicle control (fold change) (Vehicle; 1.378 ± 0.1245, R419; 1.641 ± 0.1848, R481; 2.027 ± 0.1615, *P = 0.0339*) (Figure 3.6Bi). Similarly, at 5.5 mmol/l glucose, R481 stimulated AMPK phosphorylation, not R419 (fold change) (Vehicle; 1.378 ± 0.1245, R419; 1.641 ± 0.1848, R481; 2.027 ± 0.1615, *P = 0.0267*) (Figure 3.6Bii). At 11.7 mmol/l glucose, both R419 and R481 failed to enhance AMPK phosphorylation (fold change) (R419; 1.731 ± 0.3465, R481; 1.875 ± 0.3811, *P = 0.1358*) (Figure 3.6Biii).

R481, but not R419, increased ACC phosphorylation when incubated with 1.0 mmol/l glucose (fold change) (Vehicle; 1.192 ± 0.0946, R419; 1.619 ± 0.1545, R481; 2.138 ± 0.3709, *P = 0.0242*) (Figure 3.6Ci). At 5.5 mmol/l glucose, both R419 and R481 enhanced ACC phosphorylation (fold change) (Vehicle; 0.9931 ± 0.03722, R419; 1.514 ± 0.09168, *P = 0.0666,* R481; 2.159 ± 0.2395, *P = 0.0014*) (Figure 3.6Cii). Similarly, both R419 and R481 enhanced ACC inactivation at 11.7 mmol/l glucose (fold change) (R419; 1.702 ± 0.08586, *P = 0.0151,* R481; 1.928 ± 0.2665, *P = 0.0071*) (Figure 3.6Ciii).

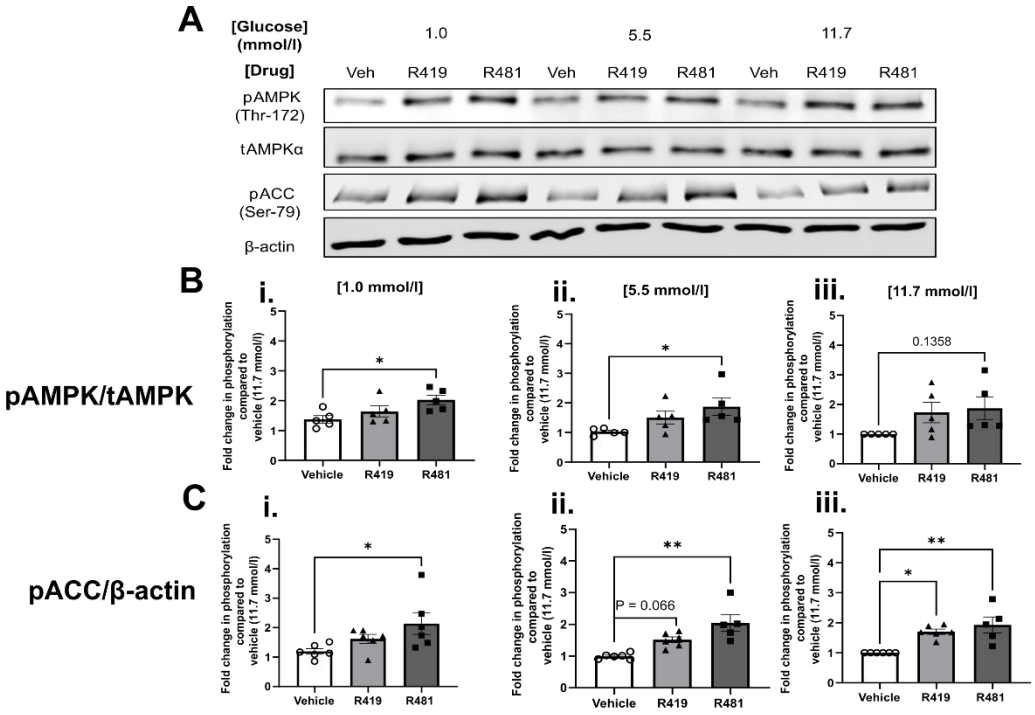

Figure 3.6: AMPK activators R419 and R481 increased AMPK signalling cascade activation.

αTC1.9 cells were incubated with R419 or R481 (50 nmol/l) for 1 h in DMEM containing 1.0 – 11.7 mmol/l glucose. **A.** Representative immunoblots for phosphorylated AMPK (pAMPK, Thr-172), total AMPKα (tAMPK), phosphorylated ACC (pACC, Ser-79) and housekeeping protein beta-actin (β-actin). Densitometric analysis for **B i-iii.** p-AMPK/t-AMPK (**B i**. One-Way ANOVA with Tukey's multiple comparison test **B ii.** Kruskal-Wallis test with Dunn's multiple comparisons test, **B iii.** One-Way ANOVA with Tukey's multiple comparison test) and **C i – iii.** p-ACC/β-actin, n = 5) and **C i-iii**. p-ACC/β-actin (**C i-iii.** Kruskal-Wallis test with Dunn's multiple comparison test, n = 5 - 6) (*P<0.05, **P<0.01, ***P<0.001)

3.2.4 R481 and α-cell glycolytic rate

3.2.4.1 α-cell glucose utilisation is increased in a glucose-dependent manner.

αTC1.9 cells show glucose-sensitive AMPK activation and glucagon secretion. However, there are no published findings characterising αTC1.9 glucose-dependent glycolysis. Therefore, αTC1.9 cells were exposed to standard Seahorse XF DMEM medium (containing 2.0 mmol/l L-glutamine, 2.5 mmol/l sodium pyruvate supplements) containing no glucose for 1 h prior to being acutely incubated with 0.1 – 11.7 mmol/l glucose for ~ 40 min. To note, the data displayed in Figure 3.7 is derived from the same data (vehicle) displayed in Figure 3.8 and Figure 3.9.

Here, increasing [glucose] acute injection subsequently increased glucose utilisation (% $\Delta ECAR_{MAX}$) (0.1; 21.53 ± 1.144, *0.1 vs 0.5, P < 0.0001,* 0.5; 57.08 ± 1.417, *0.5 vs 1.0, P < 0.0001,* 1.0; 78.86 ± 1.754, *1.0 vs 3.0, P < 0.0001,* 3.0; 92.84 ± 1.816, *3.0 vs 5.5, P = 0.1821,* 5.5; 98.46 ± 1.717, *5.5 vs 11.7, P = 0.0060,* 11.7; 107.4 ± 2.345) (Figure 3.7B).

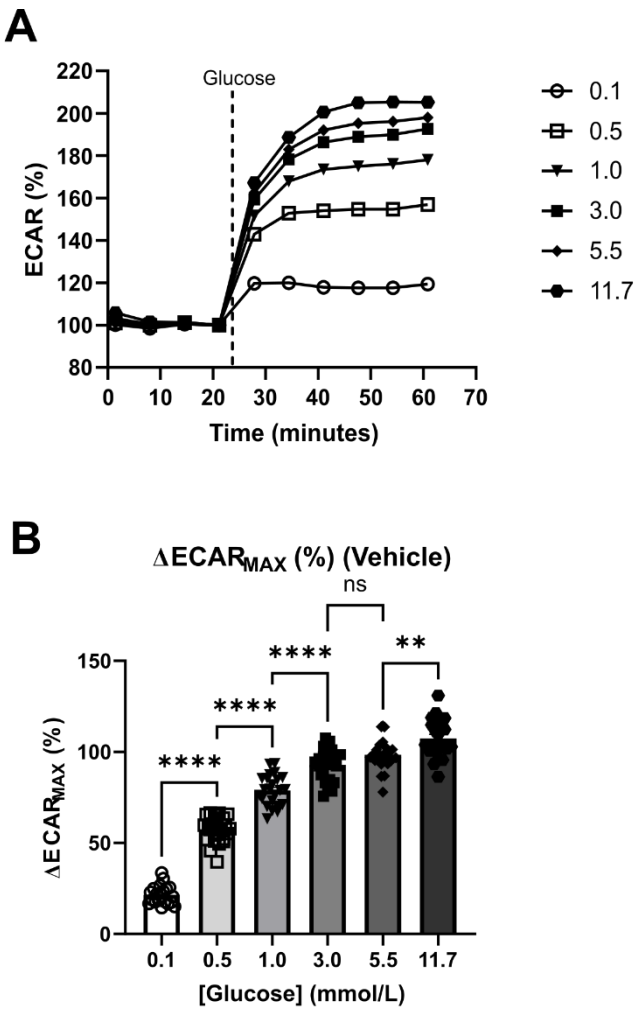

Figure 3.7: αTC1.9 glucose utilisation was enhanced in a concentration-dependent manner.

αTC1.9 cells were exposed to standard Seahorse XF DMEM media in glucose-absent conditions for 1 h. **A.** Representative traces depicting changes in αTC1.9 extracellular acidification rate (ECAR) following increasing [glucose] (0.1 – 11.7 mmol/l) injections (~ 24 min) into surrounding standard Seahorse XF DMEM medium (%). **B.** Glucose utilisation was measured by percentage increase in ECAR ($\Delta ECAR_{MAX}$), calculated from maximum ECAR measurement post-glucose injection minus baselined ECAR reading prior to injection (100%) (One-Way ANOVA with Tukey's multiple comparison test, **P<0.01, ****P<0.0001, n = 20 – 24, three separate plates)

3.2.4.2 R481 enhanced α-cell glucose utilisation in a concentration-dependent manner.

Activation of AMPK promotes catabolic processes for ATP production, including glycolysis (Doménech *et al.*, 2015). Here, R481 (50 nmol/l) was incubated for 1 h in standard Seahorse XF DMEM medium prior to between 0.1 – 11.7 mmol/l glucose acute injection, to examine if pharmacological AMPK activation will influence α-cell glycolytic rate.

R481 did not alter basal ECAR prior to glucose injection (mpH/min/µg) (Vehicle; 3.419 ± 0.05993, R481; 3.404 ± 0.06108) (Figure 3.8A). However, similarly to metformin, R481 attenuated basal OCR (pmol/min/µg) (Vehicle; 50.19 ± 0.9651, R481; 47.11 ± 0.8853, *P = 0.0385*) (Figure 3.8B)

After 0.1 mmol/l glucose acute injection, R481 did not alter $\Delta ECAR_{MAX}$ in αTC1.9 cells (mpH/min/µg) (Vehicle; 0.8450 ± 0.02914, R481; 0.8703 ± 0.03731). However, at 0.5 mmol/l glucose, R481 enhanced $\Delta ECAR_{MAX}$ (Vehicle; 2.039 ± 0.1028, R481; 2.501 ± 0.09250, *P = 0.0017*). Similarly, R481 continued to increase $\Delta ECAR_{MAX}$ at 1.0 mmol/l glucose (Vehicle; 2.583 ± 0.1228, R481; 3.419 ± 0.1405, *P < 0.0001*). At 3.0 mmol/l glucose injection, R481 stimulated $\Delta ECAR_{MAX}$ (Vehicle; 3.059 ± 0.1301, R481; 4.721 ± 0.2551, *P < 0.0001*). R481 enhanced 5.5 mmol/l glucose $\Delta ECAR_{MAX}$ (Vehicle; 2.930 ± 0.1156, R481; 5.126 ± 0.2794, *P < 0.0001*). At 11.7 mmol/l glucose, R481 continued to increase $\Delta ECAR_{MAX}$ (Vehicle; 3.231 ± 0.1555, R481; 4.986 ± 0.2316, *P < 0.0001*). $\Delta ECAR_{MAX}$ was derived from representative X-Y ECAR graphs displayed in Figure 3.9Ai-Fi.

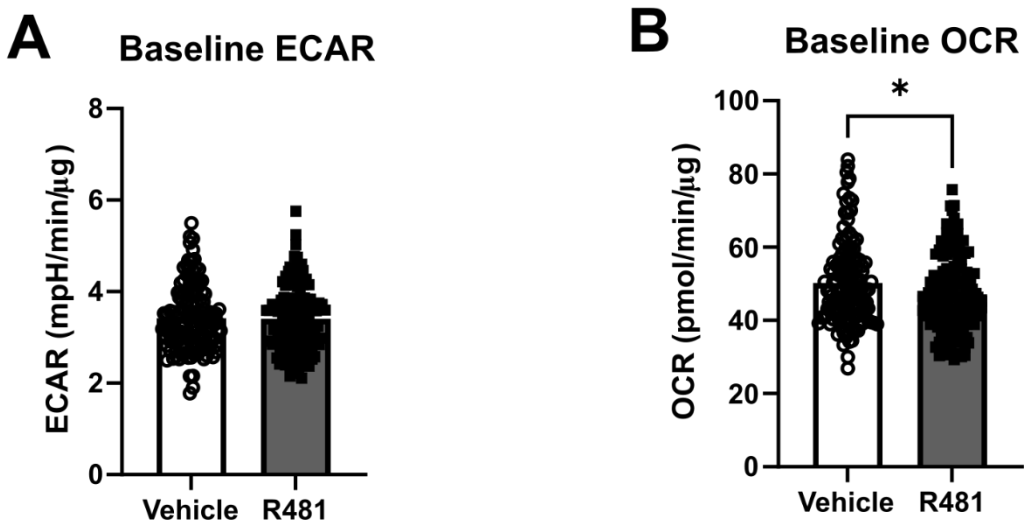

Figure 3.8: R481 attenuated basal OCR in α-cells.

αTC1.9 cells were exposed to R481 (50 nmol/l) in standard Seahorse XF DMEM media in glucose-absent conditions for 1 h. **A.** Baseline ECAR and **B.** OCR was calculated from average measurements prior to glucose injection (Mann-Whitney test, *P<0.05, n = 136, three separate plates)

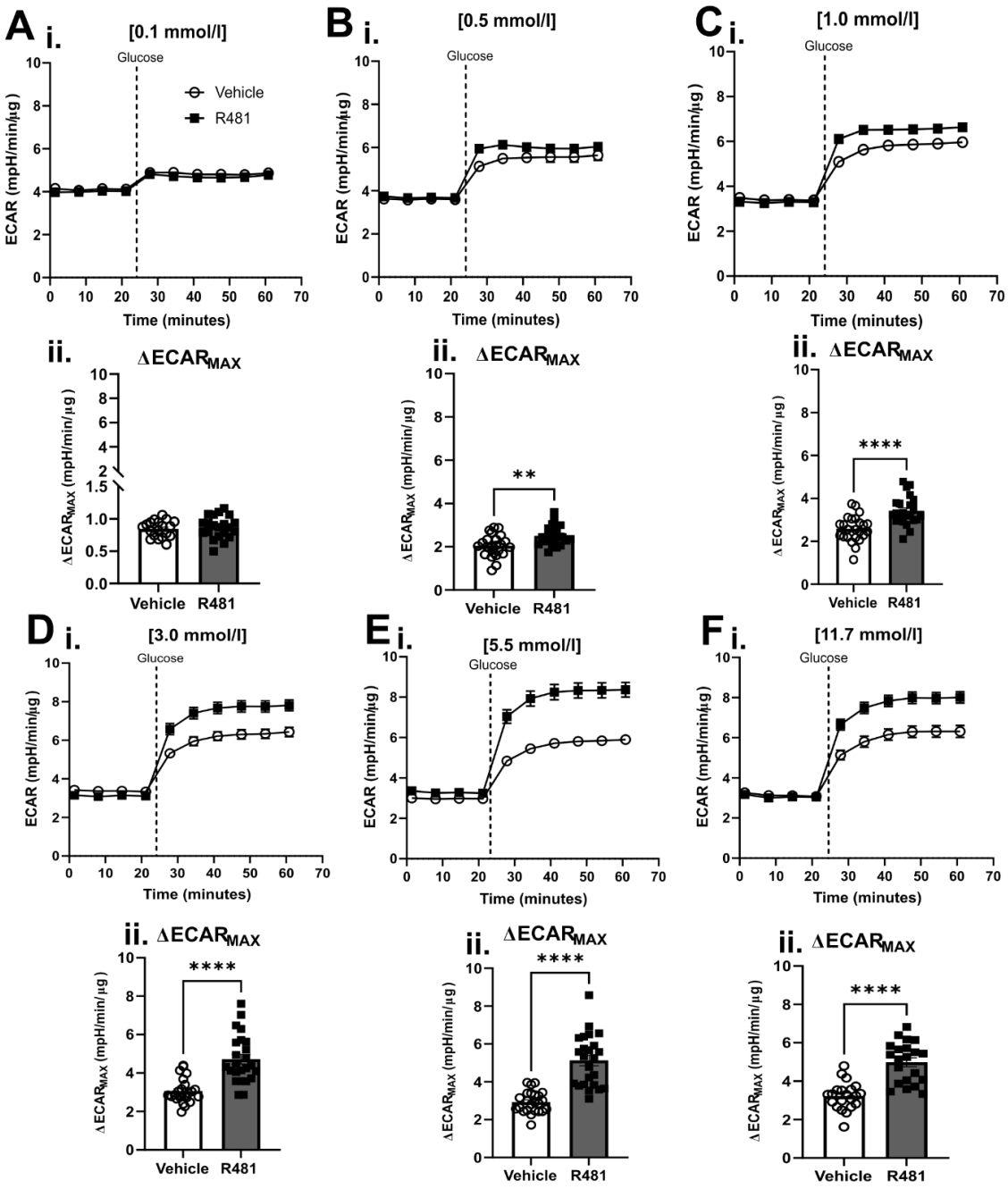

Figure 3.9: R481 enhanced α-cell glucose utilisation in a concentration-dependent manner.

αTC1.9 cells were incubated in R481 (50 nmol/l) in standard Seahorse XF DMEM media in glucose-free conditions for 1 h. **A – F i.** Representative traces depicting changes in αTC1.9 extracellular acidification rate (ECAR) following increasing [glucose] (0.1 – 11.7 mmol/l) injections (~24 min) into surrounding standard Seahorse XF DMEM medium (mpH/min/µg). Glucose utilisation was measured by **A – F ii**. $\Delta ECAR_{MAX}$, calculated from maximum ECAR measurement post-glucose injection minus average baseline ECAR readings prior to injection (**A – C**., **E – F**., unpaired two-tailed t-test, **B.** Mann-Whitney test. **P < 0.01, ****P < 0.0001, n = 19 – 24, three separate plates)

3.2.4.3 α-cell glycolytic rate was increased following R481 exposure in an SBI-sensitive manner.

Here, experiments sought to test if R481-enhanced glucose utilisation was AMPK-dependent by exposing α-cells to SBI-0206967 (SBI, 30.0 µmol/l) and R481 for 1 h in 0.5 – 11.7 mmol/l glucose prior to performing a glycolytic rate assay to quantitatively measure glycolysis (glycoPER).

SBI inhibited glycolytic parameters in the presence or absence of R481, whereas R481 had an effect in the absence of SBI for basal glycolysis (pmol/min/µg) (Figure 3.10A; Vehicle; 9.668 ± 0.6678, R481; 13.49 ± 0.6877, *Vehicle vs R481, P < 0.0001,* SBI; 5.271 ± 0.4545, *Vehicle vs SBI, P < 0.0001,* SBI + R481; 7.740 ± 0.4836, *R481 vs SBI + R481, P < 0.0001*) and PER alone (%) ((Figure 3.10D; Vehicle; 36.33 ± 1.690, R481; 46.87 ± 0.9455, *Vehicle vs R481, P < 0.0001,* SBI; 22.96 ± 1.311, *Vehicle vs SBI, P < 0.0001,* SBI + R481; 33.81 ± 1.037, *R481 vs SBI + R481, P < 0.0001*). Both SBI and R481 treatment, however R481 alone did not, attenuate compensatory glycolysis at 0.5 mmol/l glucose (Vehicle; 18.23 ± 0.9639, R481; 20.30 ± 0.8728, SBI; 14.32 ± 0.6899, *Vehicle vs SBI, P = 0.0041,* SBI + R481; 15.31 ± 0.6375, *R481 vs SBI + R481, P = 0.0001*) (Figure 3.10C).

Similarly in Figure 3.11, at 11.7 mmol/l glucose, SBI inhibits compensatory glycolysis and PER in the presence of absence of R481 (Basal Glycolysis; Vehicle; 28.00 ± 1.599, R481; 34.51 ± 1.560, *P = 0.1282,* SBI; 20.91 ± 1.715, *Vehicle vs SBI, P = 0.0227,* SBI + R481; 28.54 ± 2.069, *R481 vs SBI + R481, P = 0.0639)* (Compensatory glycolysis; Vehicle; 86.25 ± 4.653, R481; 85.67 ± 3.436, SBI; 43.34 ± 3.166, *Vehicle vs SBI, P < 0.0001,* SBI + R481; 45.62 ± 3.095, *R481 vs SBI + R481, P < 0.0001*) (Figure 3.11B and Figure 3.11C). Whereas, R481 only increases PER (%) in the absence of SBI (Vehicle; 64.69 ± 0.7108, R481; 73.31 ± 0.7946, *Vehicle vs R481, P < 0.0001,* SBI; 56.09 ± 1.612, *Vehicle vs SBI, P = 0.0055,* SBI + R481; 67.40 ± 1.518) (Figure 3.11D).

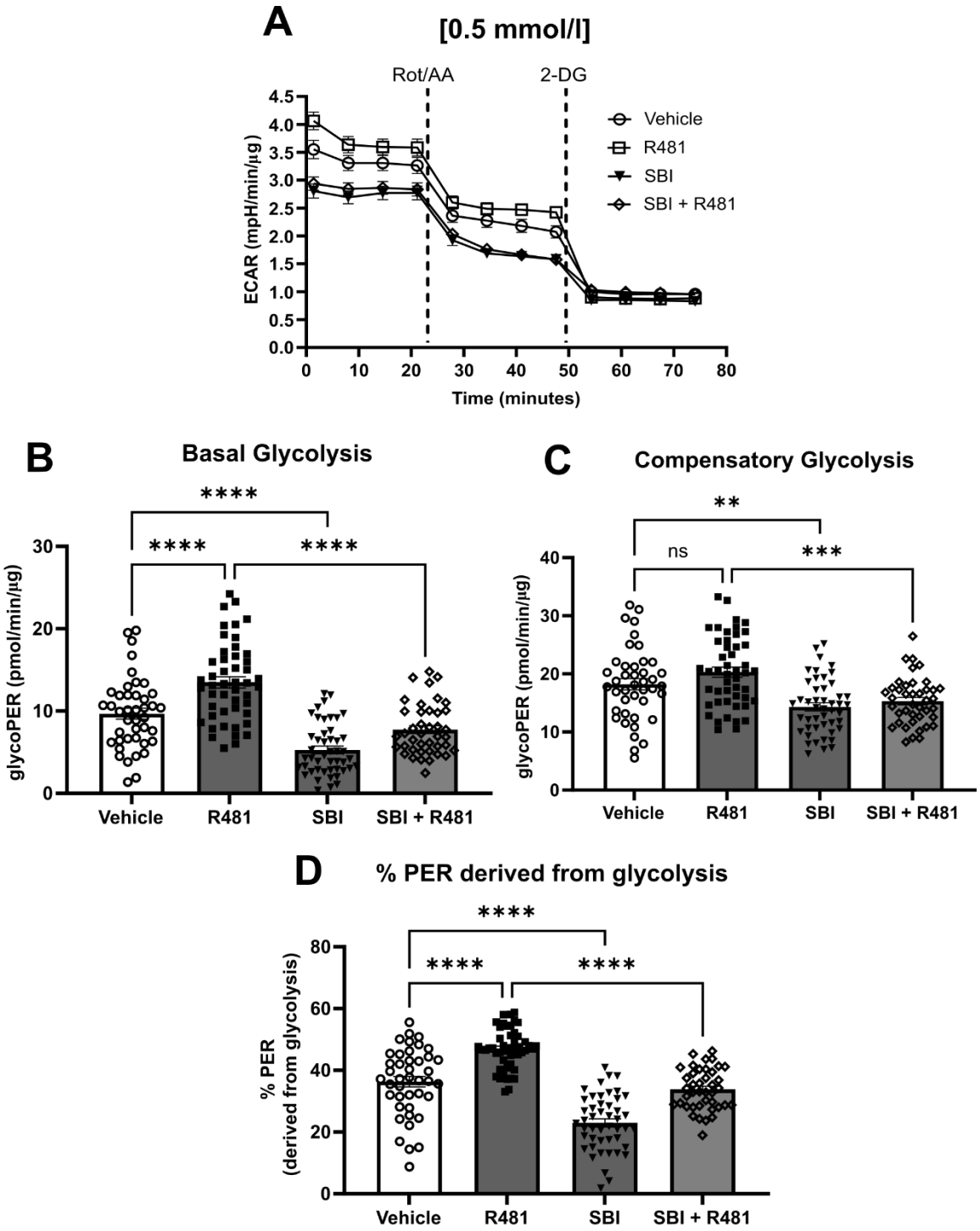

Figure 3.10: R481 enhanced SBI-sensitive glycolysis at acute low glucose in α-cells.

αTC1.9 cells were exposed to SBI-0206967 (30.0 µmol/l) ± R481 (50 nmol/l) in 0.5 mmol/l glucose (50 nmol/l) in standard Seahorse XF DMEM medium. **A.** Representative extracellular acidification rate (ECAR) trace following rotenone/antimycin A (Rot/AA) and 2-deoxyglucose (2-DG) injections. **B.** Basal glycolysis (One-Way ANOVA with Tukey's multiple comparison test), **C.** compensatory glycolysis (One-Way ANOVA with Tukey's multiple comparison test), and **D**. % proton efflux rate derived from glycolysis (% PER) were calculated from glycolytic proton efflux rate (glycoPER) (Kruskal-Wallis test with Dunn's multiple comparison test) (n = 41 – 48, *P<0.05, **P<0.01, ***P<0.001, ****P<0.0001, four separate plates)

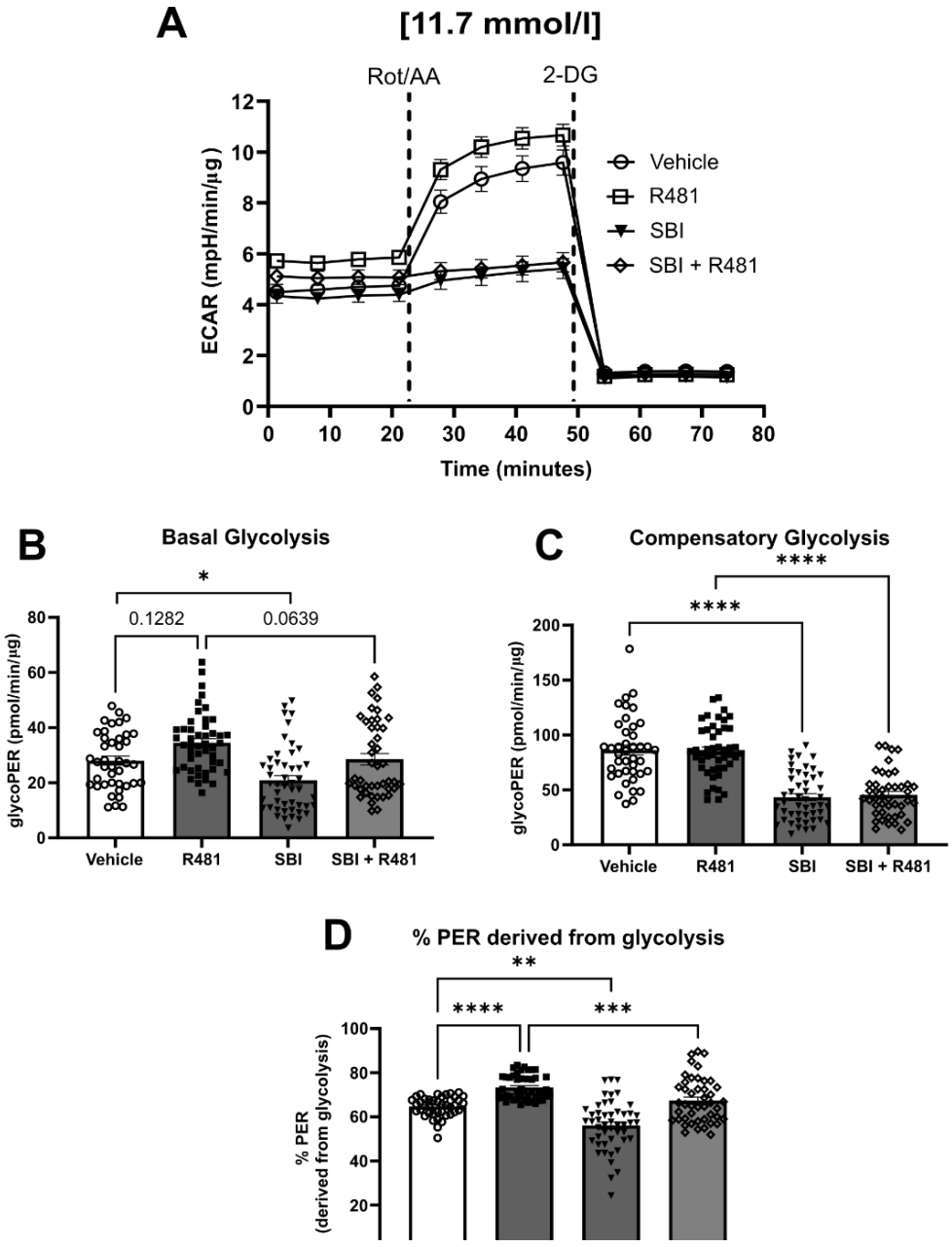

Figure 3.11: R481 enhanced SBI-sensitive glycolysis at high extracellular glucose in α-cells.

αTC1.9 cells were exposed to SBI-0206967 (30.0 µmol/l) ± R481 (50 nmol/l) in 11.7 mmol/l glucose (50 nmol/l) in standard Seahorse XF DMEM medium. **A.** Representative extracellular acidification rate (ECAR) trace following rotenone/antimycin A (Rot/AA) and 2-deoxyglucose (2-DG) injections. **B.** Basal glycolysis, **C.** compensatory glycolysis and **D.** % proton efflux rate derived from glycolysis (% PER) were calculated from glycolytic proton efflux rate (glycoPER) (Kruskal-Wallis test with Dunn's multiple comparison test) (n = 43 – 48, *P<0.05, **P<0.01, ***P<0.001, ****P<0.0001, four separate plates)

3.2.5 Lactate secretion

3.2.5.1 R481 increased α-cell lactate secretion in a glucose-sensitive manner.

To determine whether R481-enhanced glycolytic flux correlates proportional to changes in lactate secretion, αTC1.9 lactate secretion was measured following R481 treatment for 2 h. This time point was chosen to correspond with the incubation time in the metabolic flux analyses.

L-lactate secretion was significantly increased by R481 treatment in a glucose-sensitive manner (µM/µg) (0.5: vehicle; 95.565 +/- 6.349, R481; 122.212 ± 11.889, 5.5: vehicle; 198.987 ± 23.116, R481; 402.587 ± 48.137, 11.7: vehicle; 225.010 ± 25.613, R481; 556.819 ± 48.576) (Figure 3.12).

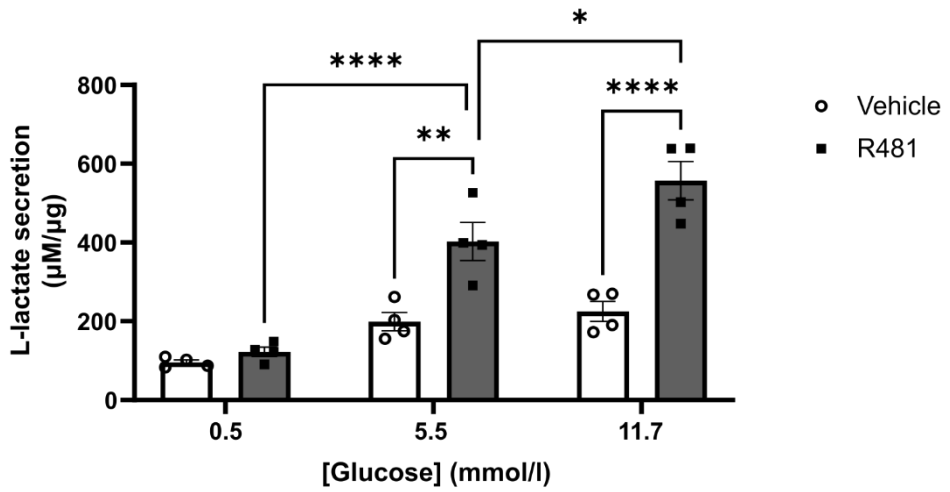

Figure 3.12: R481 increased α-cell L-lactate secretion in a glucose-sensitive manner.

αTC1.9 cells were exposed to R481 (50 nmol/l) and between [0.5 – 11.7 mmol/l] glucose for 2 h and supernatant was removed for measuring L-lactate secretion (n = 4, **P>0.01,****P>0.0001) and normalised to total protein (Two-Way ANOVA with Tukey's multiple comparison test) (n= 4, *P > 0.05, **P>0.01, ****P>0.0001).

3.2.6 R481 and α-cell fatty acid oxidation

Fatty acid oxidation (FAO) is a catabolic metabolic process to sustain ATP production. The αTC1.6 cell line, a less differentiated clonal cell line than αTC1.9, previously showed intrinsic FAO is enhanced at low vs high glucose exposure; corresponding to glucose-sensitive glucagon secretion (Briant *et al.*, 2018a). AMPK stimulates FAO by ACC inactivation (Munday *et al.*, 1988). It is therefore plausible that endogenous AMPK activation, at low glucose, could stimulate palmitate-induced FAO specifically at low glucose to retain ATP generation and glucose sensitivity.

3.2.6.1 α-cells increased palmitate oxidation, regardless of [glucose], in a concentration-dependent manner.

Optimal [palmitate] was determined by measuring ΔOCR_{MAX} following 0 – 150 µmol/l BSA-palmitate injection following 1 h incubation of 0.5/11.7 mmol/l glucose incubation in standard Seahorse XF DMEM medium. At 0.5 mmol/l glucose, increasing [palmitate] acute injection enhanced ΔOCR_{MAX} and levelled at 100 µmol/l (pmol/min) (BSA; 8.016 ± 3.123, 50; 10.08 ± 0.1443, *50 vs 100, P = 0.0086,* 100; 22.42 ± 1.940, *BSA vs 100, P = 0.0023,* 150; 26.00 ± 2.860, *BSA vs 150, P = 0.0002*) (Figure 3.13Aii). However, at 11.7 mmol/l glucose, 150 µmol/l [palmitate] continued to enhance αTC1.9 ΔOCR_{MAX} (BSA; -1.065 ± 1.562, 50; 3.859 ± 0.9119, 100; 6.575 ± 1.623, *BSA vs 100, P = 0.0055,* 150; 14.33 ± 1.539, *BSA vs 150, P < 0.0001, 100 vs 150, P = 0.0071*) (Figure 3.13Bii). Therefore, palmitate-BSA (150.0 µmol/l) was used for the subsequent study.

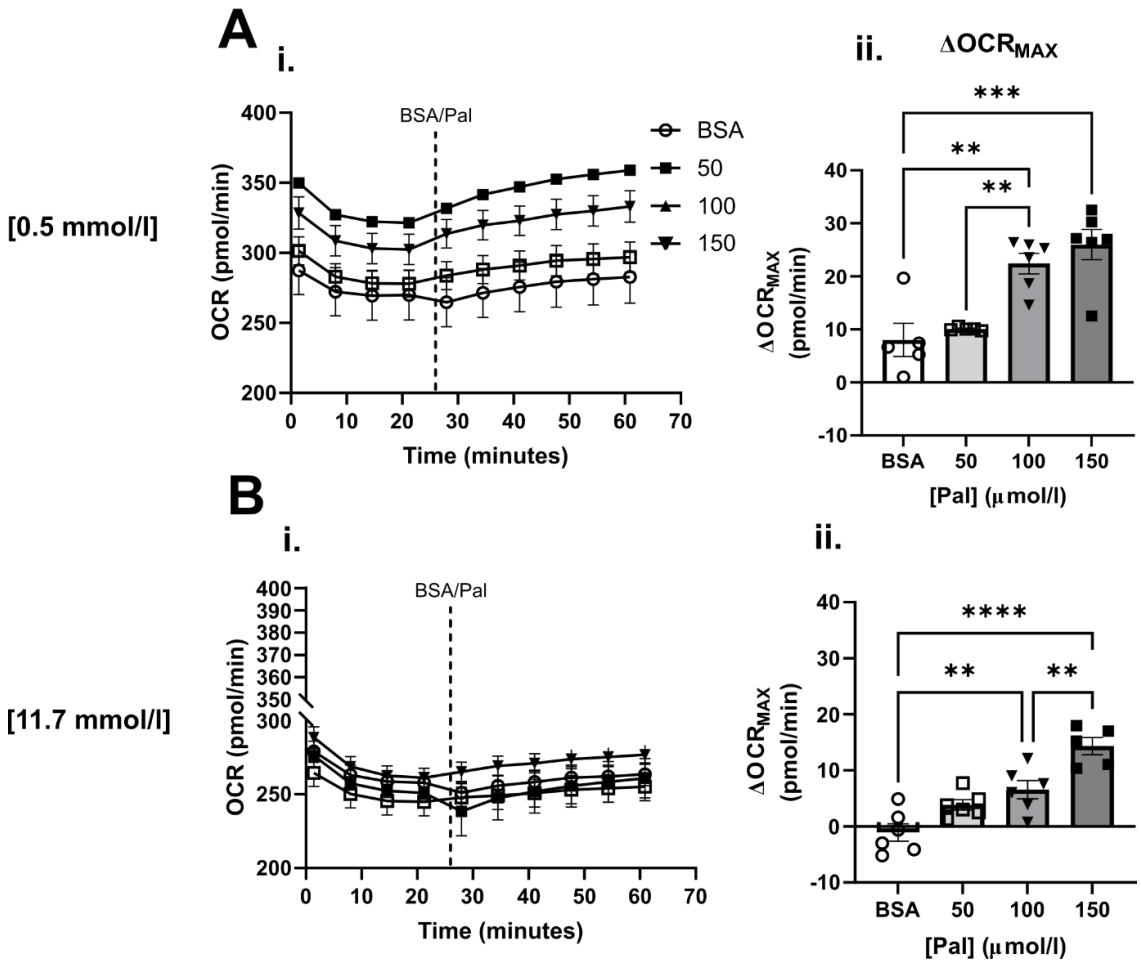

Figure 3.13: α-cells oxidised palmitate in a concentration-dependent manner.

αTC1.9 cells were preincubated in standard Seahorse XF DMEM medium and either 0.5 or 11.7 mmol/l glucose for 1 h. **A i**. 0.5 mmol/l **B i.** 11.7 mmol/l glucose representative oxygen consumption rate (OCR, pmol/min/µg) traces, with BSA:palmitate (0 - 150 µmol/l) injection at ~24 min. **C i-ii**. Palmitate oxidation was determined by ΔOCR_{MAX}, measured by maximum OCR reading post-palmitate/BSA injection subtracted by average baseline OCR measurements prior to injection (One-Way ANOVA with Tukey's multiple comparisons test, **P<0.01, ***P<0.001 ****P<0.0001, n = 5 – 6, one plate)

3.2.6.2 R481 enhanced α-cell palmitate oxidation at low, but not high, glucose availability.

To examine the impact on α-cell oxidative metabolism following exogenous AMPK activation, α-cells were preincubated with AMPK activator R481 (50 nmol/l) alongside 0.5/11.7 mmol/l glucose-containing standard Seahorse XF medium for 1 h prior to being acutely exposed to palmitate (150.0 µmol/l) (Figure 3.14A-B). R481 enhanced ΔOCR_{MAX} induced by palmitate at 0.5 mmol/l, but not at 11.7 mmol/l glucose (0.5: vehicle; 27.198 ± 1.554, R481; 33.948 ± 0.975, *0.5 vehicle vs 0.5 R481, P = 0.0016,* 11.7: vehicle; 24.999 ± 1.060, R481; 27.950 ± 1.451, *0.5 R481 vs 11.7 R481, P = 0.0063*) (Figure 3.14C).

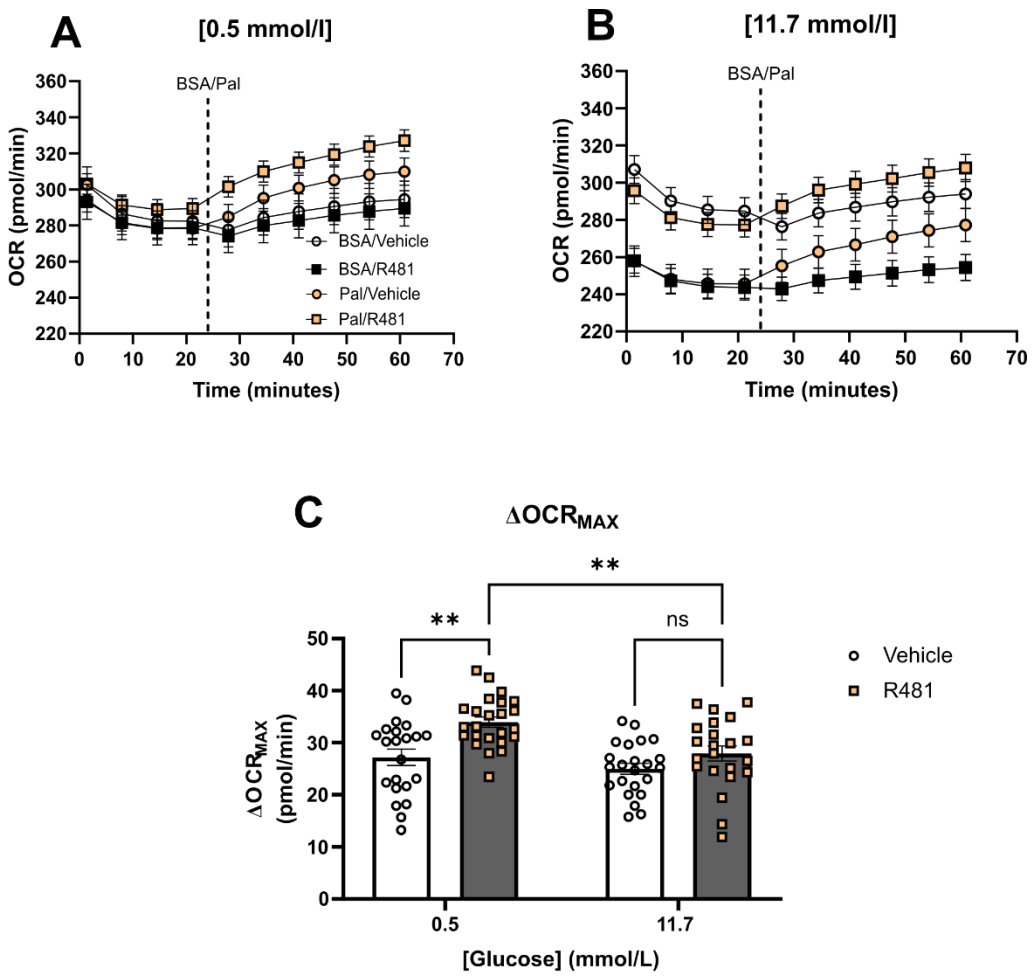

Figure 3.14: R481 enhanced α-cell palmitate-induced oxidative metabolism at low, but not high, glucose.

αTC1.9 cells were preincubated with ± R481 (50 nmol/l) in standard Seahorse XF DMEM medium and 0.5/11.7 mmol/l glucose for 1 h. **A - B**. Representative oxygen consumption rate (OCR, pmol/min/µg) traces, with BSA:palmitate (150.0 µmol/l) injection at ~24 min. **C.** Palmitate oxidation was determined by ΔOCR_{MAX}, measured by maximum OCR reading post-palmitate/BSA injection subtracted by average baseline OCR measurements prior to injection (Two-Way ANOVA with Tukey's multiple comparisons test, **P<0.01, n = 22 - 24, two separate plates, ns; not significant)

3.2.7 Intracellular nucleotide charge

3.2.7.1 R481 increased α-cell [ADP:ATP] in a glucose-dependent manner.

R481 is a metformin-like compound that indirectly activates AMPK by mildly inhibiting oxidative metabolism, as displayed earlier in this thesis. Metformin-induced AMPK phosphorylation is driven indirectly by rises in [AMP:ATP] ratio (Hawley *et al.*, 2010). To examine if R481 increased [ADP:ATP], α-cells were incubated with R481 (50 nmol/l) in standard Seahorse XF media containing 0.5 – 11.7 mmol/l glucose for 30 min prior to [ADP:ATP] assay.

R481 enhanced α-cell [ADP:ATP] ratio compared to vehicle at 0.5 mmol/l (fold change) (R481; 1.719 +/- 0.2736) (Figure 3.15A). Similarly, at 5.5 mmol/l glucose, R481 increased [ADP:ATP] ratio (R481; 1.293 ± 0.02734) (Figure 3.15B). At 11.7 mmol/l glucose, a trend was observed (although not statistically significant) in R481 enhanced [ADP:ATP] ratio (R481; 1.662 ± 0.3319) (Figure 3.15C).

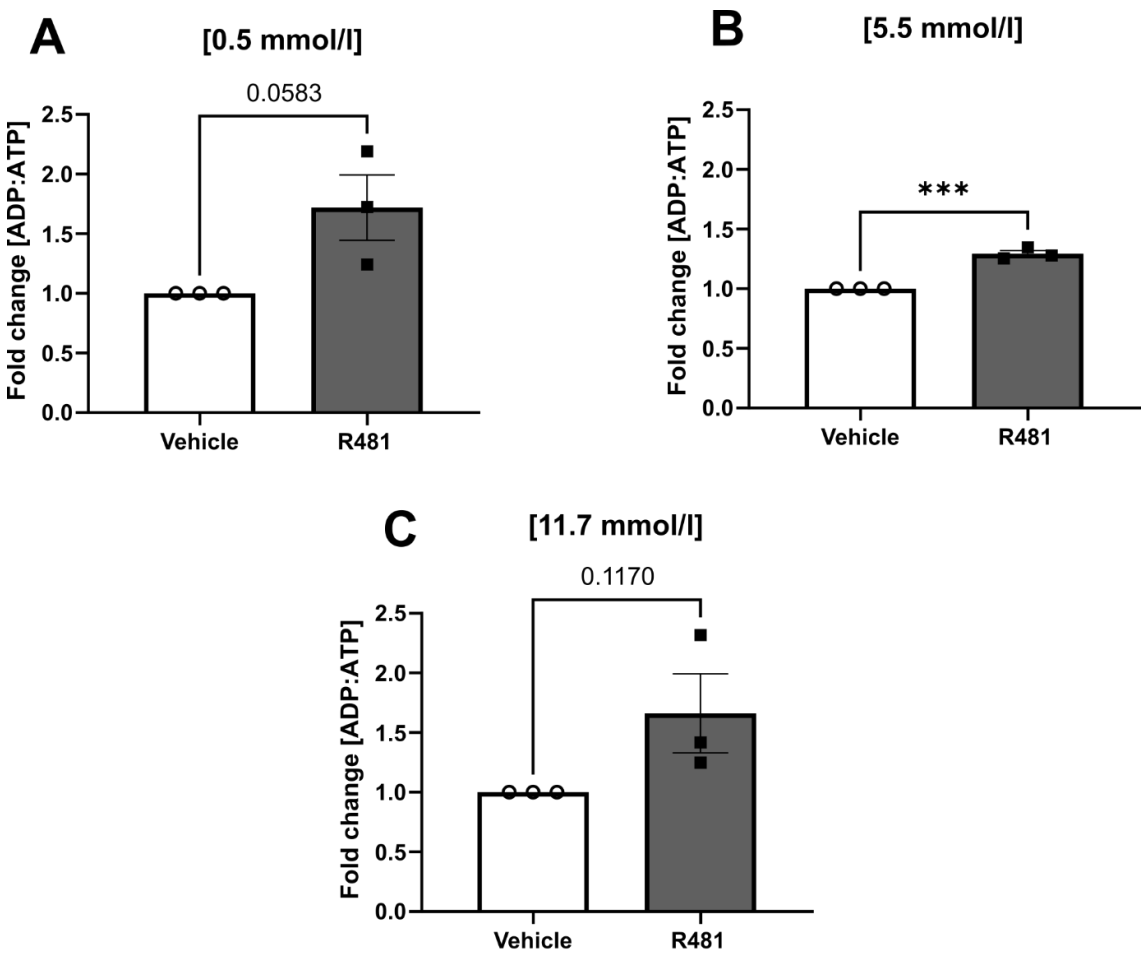

Figure 3.15: R481 increased [ADP: ATP] ratio in α-cells.

αTC1.9 cells were incubated with ± R481 (50 nmol/l) in standard Seahorse XF DMEM media containing **A.** 0.5, **B.** 5.5 or **C.** 11.7 mmol/l glucose for 30 min and subsequently measured cellular [ADP:ATP] using a luminescence-based assay (Sigma-Aldrich) (Two-tailed unpaired t-test, *P<0.05, ***P<0.001, n = 3) (study conducted by Ms. Valentina Abba).

3.2.7.2 R481 attenuated α-cell total ATP (tATP) in a glucose-dependent manner.

As showed previously, R481 attenuated oxidative respiration. To examine if R481 inhibited oxidative respiration would reflect diminished total ATP (tATP). αTC1.9 cells were incubated with R481 (50 nmol/l) in medium containing 2.5 mmol/l sodium pyruvate, 2.0 mmol/l L-glutamine, to mimic conditions in bioenergetic studies, and 0.5/11.7 mmol/l glucose for 30 min prior to tATP analysis.

R481 reduced α-cell tATP at 0.5 mmol/l glucose (µmol/ml) (Vehicle; 1.706 ± 0.1962, R481; 1.145 ± 0.1214, *P = 0.0289*) (Figure 3.16A). At 5.5 mmol/l glucose, R481 did not alter tATP levels (Vehicle; 1.755 ± 0.2529, R481; 1.461 ± 0.1635) (Figure 3.16B). Similarly, at 11.7 mmol/l glucose, R481 did not modulate tATP levels (Vehicle; 1.580 ± 0.2046, R481; 1.472 ± 0.1331) (Figure 3.16C).

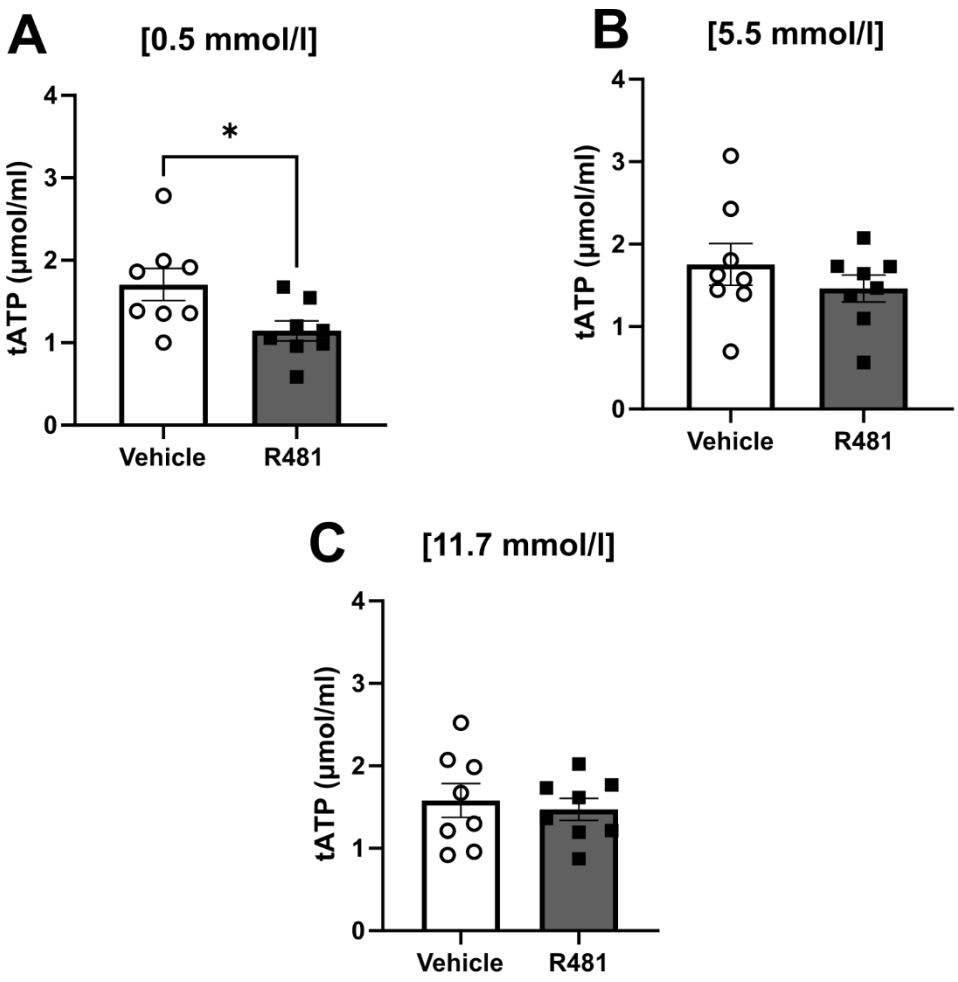

Figure 3.16: R481 lowered α-cell total ATP (tATP) levels in a glucose-sensitive manner.

αTC1.9 cells were incubated ± R481 (50 nmol/l) for up to 1 h at **A.** 0.5, **B**. 5.5 and **C.** 11.7 mmol/l glucose. Total ATP (tATP) (µM/ml) was quantified using ATPlite™ luminescence assays (Two-tailed unpaired t-test, *P<0.05, n = 8)

3.2.7.3 R481 did not alter αTC1.9 ATP secretion at any [glucose].

β-cells co-secrete ATP and insulin, with exogenous ATP stimulating synchronous $[Ca^{2+}]_I$ and insulin secretion in human and murine β-cells and therefore thought to act as an autocrine feedback mechanism to drive pulsatile insulin secretion (Jacques-Silva *et al.*, 2010; Wuttke, Idevall-Hagren and Tengholm, 2013; Khan *et al.*, 2014; Tengholm, 2014; Hauke *et al.*, 2022). α-cells express ATP-stimulated P2X and P2Y receptors (Coutinho-Silva *et al.*, 2003; Tudurí *et al.*, 2008). Similarly, to β-cells, exogenous ATP attenuated $[Ca^{2+}]$ oscillations and glucagon secretion at low glucose in mouse islets (Tudurí *et al.*, 2008). Little is known, however, if α-cells secrete ATP. To examine α-cell ATP secretion following R481 exposure, α-cells were incubated with R481 (50 nmol/l) alongside 0.5 – 11.7 mmol/l glucose for 1 h prior to examining supernatant ATP. ATP secretion was measured by extracellular ATP normalised to total protein.

At 0.5 mmol/l glucose, R481 does not alter ATP secretion by αTC1.9 cells (μM/mg) (Vehicle; 4.327 ± 2.089, R481; 4.190 ± 1.241) (Figure 3.17A). R481 did not modulate ATP secretion at 1.0 mmol/l glucose (Vehicle; 4.875 ± 1.532, R481; 5.473 ± 2.454) (Figure 3.17B). Similarly, ATP secretion was not altered at 5.5 mmol/l glucose following R481 incubation (Vehicle; 5.166 ± 1.427, R481; 5.384 ± 0.7668) (Figure 3.17C). R481 did not affect ATP secretion at 11.7 mmol/l glucose (Vehicle; 8.559 ± 2.199, R481; 5.784 ± 0.8166) (Figure 3.17D).

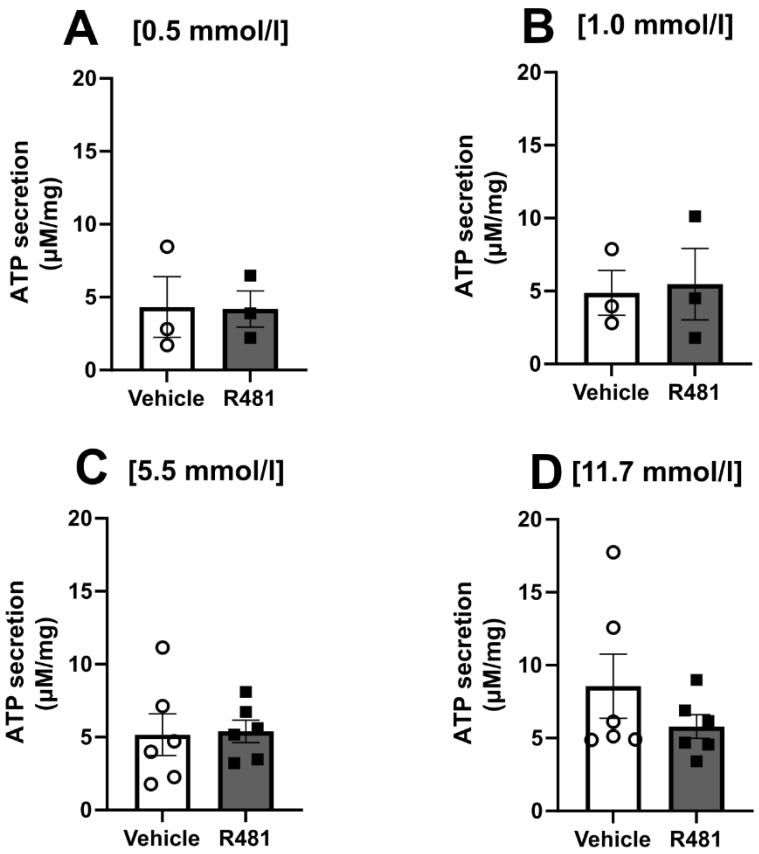

Figure 3.17: R481 did not alter α-cell ATP secretion at any extracellular [glucose].

αTC1.9 cells were serum-starved with 5.5 mmol/l glucose-containing DMEM media for 2 h, and subsequently stimulated with R481 (50 nmol/l) with **A.** 0.5, **B**. 5.5, **C.** 11.7 mmol/l glucose for 1 h. ATP secretion (µmol/mg) was quantified using ATPlite™ luminescence assays and normalised to total cellular protein (mg) (Unpaired two-tailed t-test, n = 3 – 6).

3.2.8 Indirect AMPK activators and glucagon secretion

3.2.8.1 α-cell glucagon secretion was unaffected by either R419/R481 exposure.

To investigate if indirect AMPK activators modulate α-cell glucagon secretion, αTC1.9 cells were exposed to 5.5 mmol/l glucose for 2 h prior to being incubated with R419/R481 (50 nmol/l) for 1 h in 0.5 – 11.7 mmol/l glucose-containing media.

R419 and R481 did not alter glucagon secretion at 0.5 mmol/l (pg/µg) (Vehicle; 10.06 ± 1.590, R419; 8.733 ± 0.7218, R481; 7.670 ± 0.7554). Similarly, R419/R481 did not modulate glucagon secretion at 5.5 mmol/l glucose (Vehicle; 10.35 ± 2.013, R419; 7.078 ± 1.405, R481; 6.907 ± 1.159). At 11.7 mmol/l glucose, glucagon secretion was not altered following R419/R481 exposure (Vehicle; 8.875 ± 1.277, R419; 9.080 ± 2.106, R481; 8.032 ± 0.9971).

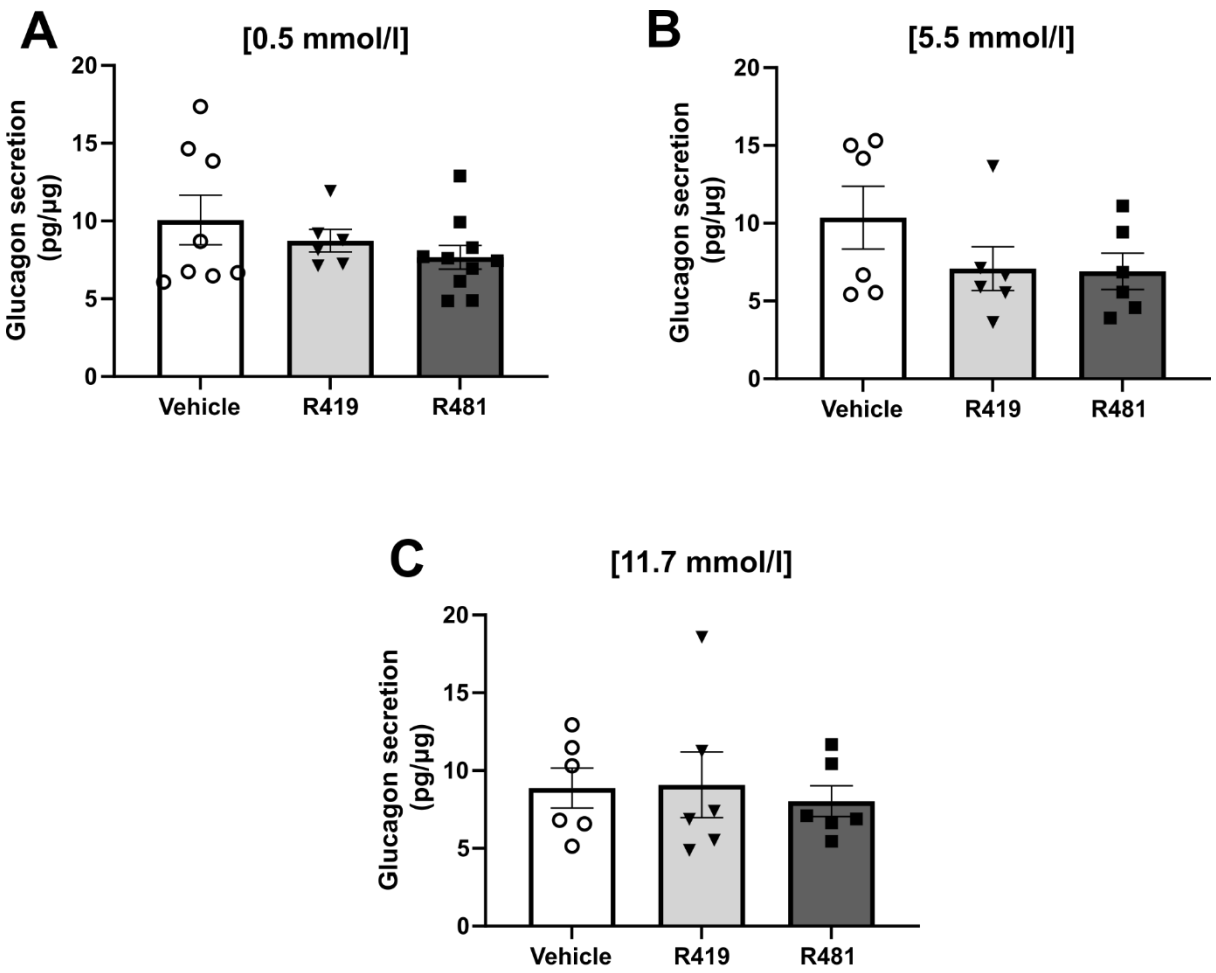

Figure 3.18: α-cell glucagon secretion was unaffected by either R419 or R481 exposure.

αTC1.9 cells were incubated ± R419/R481 (50 nmol/l) in Krebs Buffered HEPES media (KBH) for 1 h in either **A.** 0.5 (One-Way ANOVA with Dunnett's multiple comparison test), **B.** 5.5 (One-Way ANOVA with Dunnett's multiple comparison test) or **C.** 11.7 mmol/l glucose (Kruskal-Wallis test with Dunn's multiple comparison test) containing Krebs Buffered HEPES (KBH) solution, following a 2 h serum starvation period in 5.5 mmol/l glucose. Glucagon secretion was measured using Mercodia Glucagon ELISA and normalised to lysed total cell protein (pg/µg) (n = 6 – 10)

3.2.8.2 R481 did not alter islet glucagon secretion.

Studies involving monolayer α-cell line have benefits for examining intrinsic mechanistic changes. However, due to the absence of paracrine innervation, the α-cell glucose threshold for glucagon secretion is lowered (Le Marchand and Piston, 2010; Asadi and Dhanvantari, 2021). Therefore, mouse *ex vivo* islets were exposed to 11.7 mmol/l glucose-containing ATP buffer prior to decreasing or retained glucose availability to 0.5/11.7 mmol/l glucose.

R481 did not alter islet glucagon secretion at 0.5 mmol/l glucose (% content) (Vehicle; 0.03367 ± 0.002705, R481; 0.03208 ± 0.004212) (Figure 3.19Ai). Similarly, 11.7 mmol/l glucose, R481 did not modulate islet glucagon secretion (Vehicle; 0.04267, R481; 0.03387 ± 0.002795) (Figure 3.19Bi). Glucagon content was also measured, with no difference following R481 treatment at 0.5 mmol/l glucose (µg) (Vehicle; 0.5638 ± 0.153, R481; 0.5468 ± 0.1704) (Figure 3.19Aii). R481 did not alter glucagon content at 11.7 mmol/l glucose (Vehicle; 0.3200 ± 0.1117, R481; 0.5997 ± 0.1845) (Figure 3.19Bii).

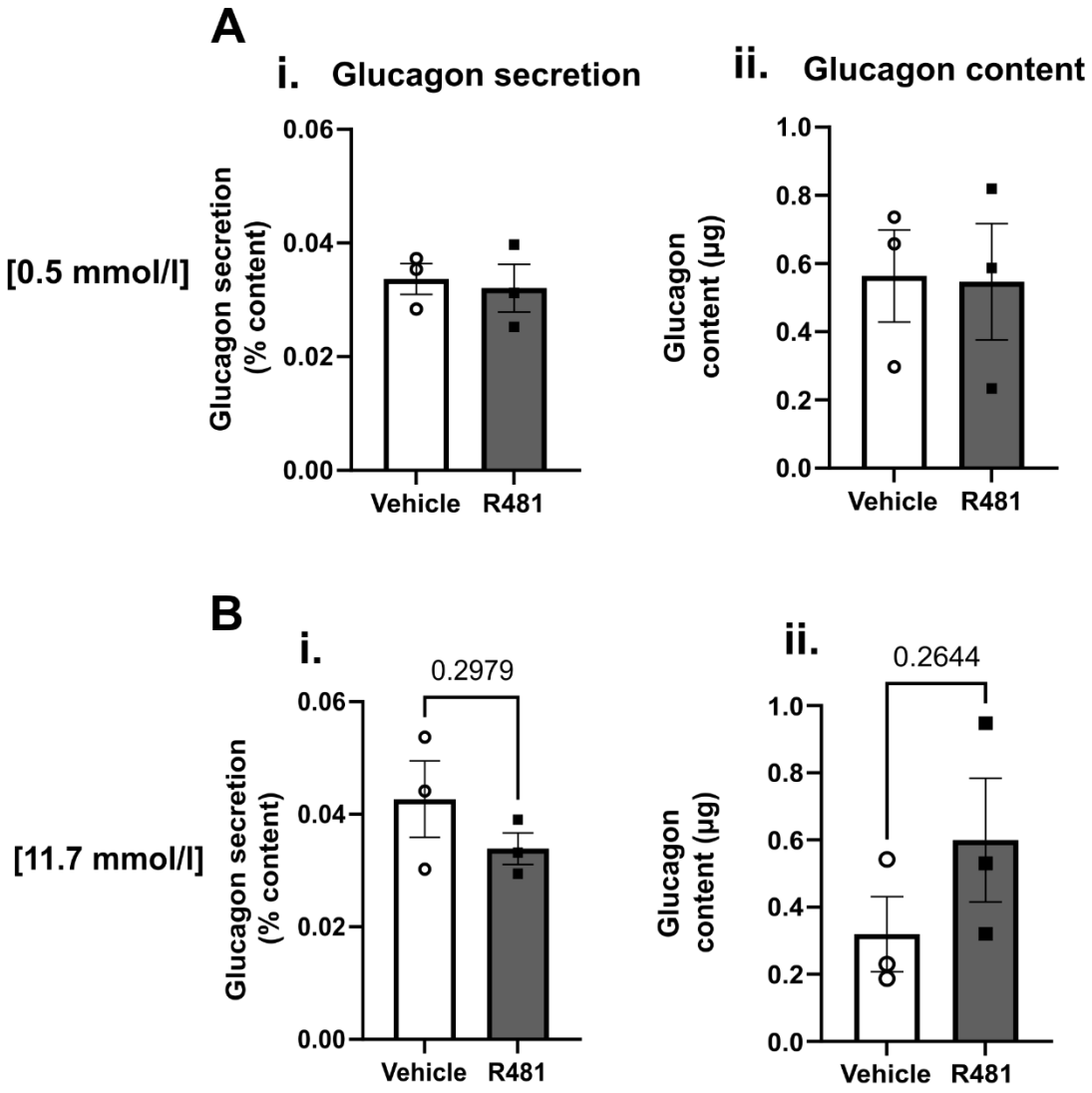

Figure 3.19: R481 treatment did not affect mouse islet glucagon secretion nor content.

Ex vivo mouse islets were incubated in 11.7 mmol/l glucose-containing ATP-buffer for 1 h, prior to being stimulated with low glucose (0.5 mmol/l) for an additional 1 h. Supernatant was collected, and islets were lysed in acid-ethanol for glucagon content. **A - B i.** Glucagon secretion normalised to **A - B ii.** total glucagon content using Promega Glucagon Lumit™ immunoassay (n = 3, unpaired two-tailed t-test)

3.2.9 R481 and β-cell glucose utilisation

High glucose increases oxidative phosphorylation in β-cells, but not α-cells, in intact islets (Wang *et al.*, 2021). The depletion of β-cell LKB1, an upstream AMPK activator, compromised islet mitochondrial function and high glucose-induced ATP generation (Swisa et al., 2015). To examine whether R481 modulated glycolysis-derived glucose utilisation in β-cells in comparison to α-cells, R481 (50 nmol/l) was preincubated in standard, glucose-free Seahorse XF DMEM media for 1 h. 0.5 – 11.7 mmol/l glucose was injected into media to measure glucose utilisation.

3.2.9.1 R481 enhanced EndoC-βH1 glucose utilisation in a concentration-dependent manner.

R481 did not alter basal ECAR prior to glucose injection (mpH/min/µg) (Vehicle; 1.328 ± 0.04673, R481; 1.357 ± 0.04550) (Figure 3.20A). R481 induced a trend, although not significant, to reduce basal OCR (pmol/min/µg) (Vehicle; 14.85 ± 0.3581, R481; 13.88 ± 0.4720, *P = 0.0791*) (Figure 3.20B). At 0.5 mmol/l glucose, R481 did not alter $\Delta ECAR_{MAX}$ in EndoC-βH1 cells (Vehicle; 0.09480 ± 0.06328, R481; - 0.009458 ± 0.03904) (Figure 3.21Aii). R481 did, however, enhance β-cell $\Delta ECAR_{MAX}$ at 5.5 mmol/l glucose (Vehicle; 0.4308 ± 0.04390, R481; 0.6631 ± 0.02866, *P = 0.0002*) (Figure 3.21Bii). Following 11.7 mmol/l glucose injection, R481 did not alter $\Delta ECAR_{MAX}$ (Vehicle; 0.8080 ± 0.06592, R481; 0.9390 ± 0.08115) (Figure 3.21Cii).

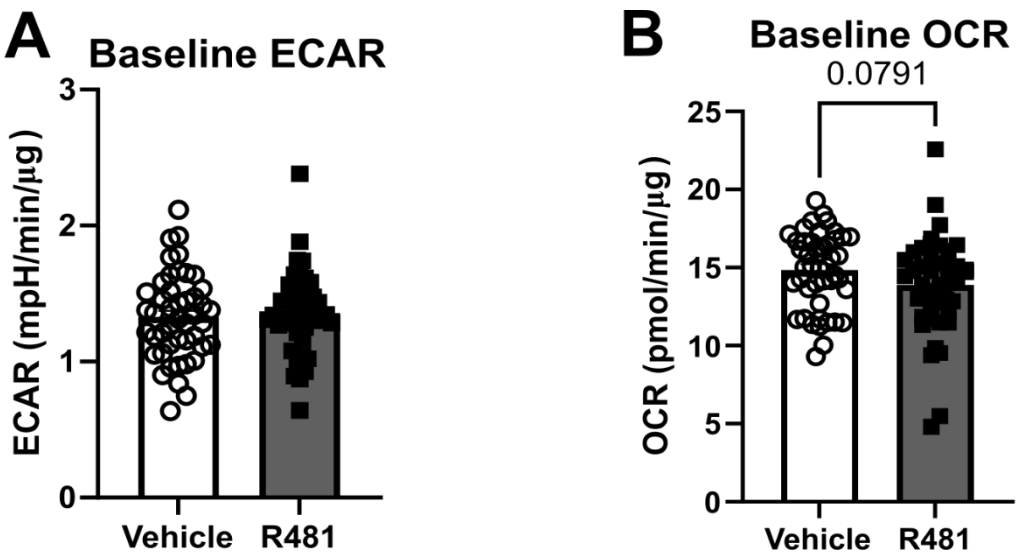

Figure 3.20: Basal human β-cell oxidative and glycolytic metabolism following R481 treatment.

EndoC-βH1 cells were exposed ± R481 (50 nmol/l) for 1 h. **A.** Baseline ECAR (mpH/min/µg) (Unpaired two tailed t-test) and **B**. OCR (pmol/min/µg) (Mann-Whitney test) was calculated from the last three measurements prior to glucose injection (n = 44 – 46, two separate plates).

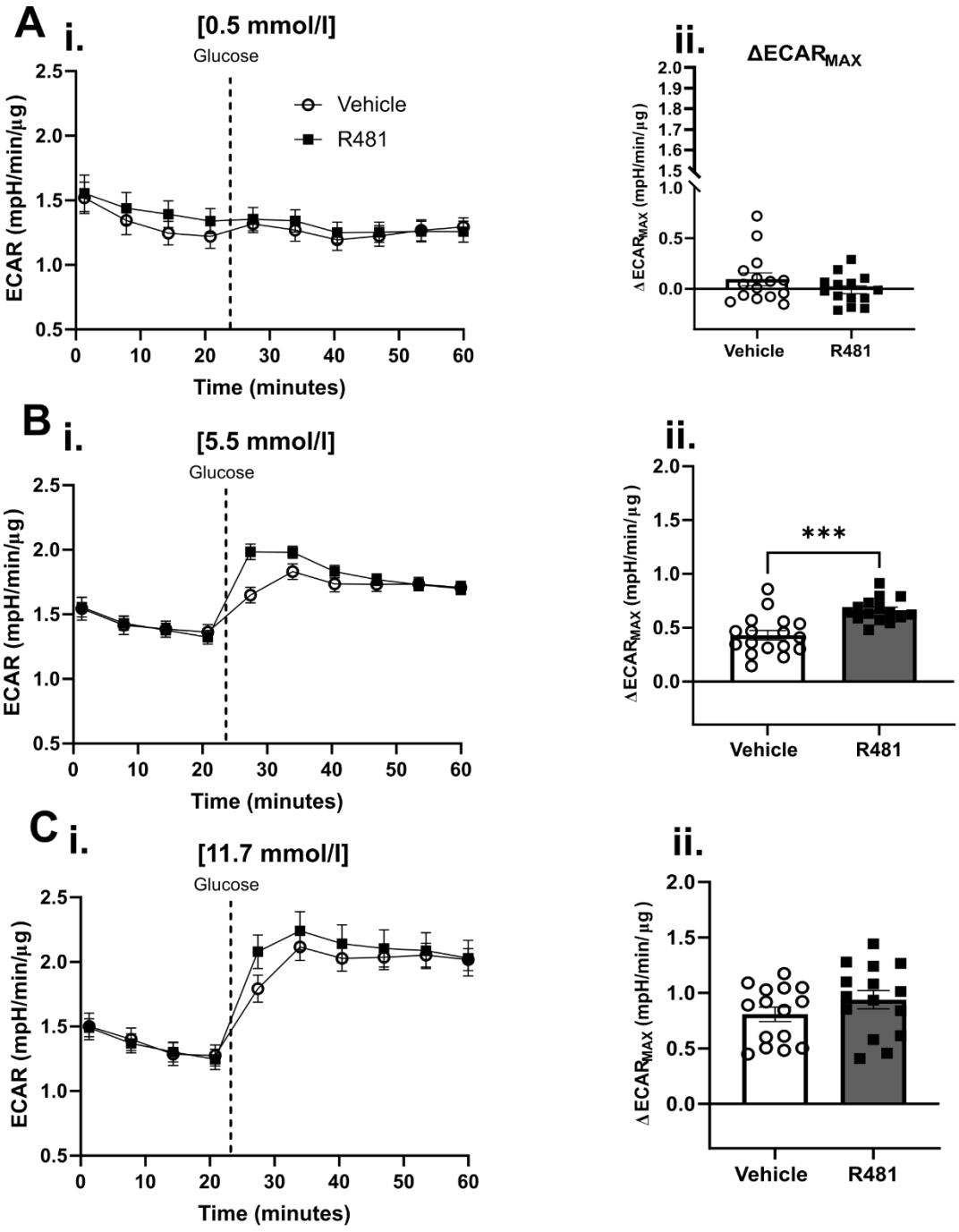

Figure 3.21: R481 increased human EndoC-βH1 β-cell glycolysis in a glucose-sensitive manner.

EndoC-βH1 cells were incubated in R481 (50 nmol/l) in standard Seahorse XF DMEM media in glucose-free conditions for 1 h. **A – F i.** Representative traces depicting changes in EndoC-βH1 extracellular acidification rate (ECAR, mpH/min/µg) following increasing [glucose] (0.5 – 11.7 mmol/l) injections (~ 24 min) into surrounding standard Seahorse XF DMEM medium (mpH/min/µg). **A-C ii**. $\Delta ECAR_{MAX}$ was calculated from maximal ECAR measurement post-injection minus average last three baseline measurements prior to injection (**A ii.** Mann-Whitney test, **B – C ii.** Unpaired two-tailed t-test) (n = 14 - 16, two separate plates).

3.3 Discussion

3.3.1 Assessing glucose-sensitive AMPK activity in the αTC1.9 cell line

Here, αTC1.9 cells increased AMPK pathway activation at 0.1 – 0.5 mmol/l low glucose. Allosteric activation of AMPK does not necessarily require α-Thr-172 phosphorylation, with the reported partial reliance in changes to the activation loop conformation (Yan *et al.*, 2019). Thereby, downstream substrate (ACC) phosphorylation is a more reliable marker of AMPK activity and one can be confident low glucose (0.1 – 0.5 mmol/l) stimulated AMPK activation in αTC1.9 cells. A proposed model for allosteric activation of AMPK is illustrated in Figure 3.22, adapted from De Souza Almeida Matos *et al.*, 2019; Scott *et al.*, 2014. It is well-regarded that glucose-sensing in cell lines require low glucose concentrations to increase AMPK activity. For instance, the hypothalamic cell line GT1.7, required a low glucose concentration (0.1 – 1.0 mmol/l) to exhibit enhanced AMPK activity, dependent on glucose alone, and low glucose-induced hyperpolarisation (Beall *et al.*, 2012). Similarly, Salt *et al.* 1998 showed the mouse β-cell line, INS-1, had an IC_{50} for AMPK activity was 1.9 – 3.1 mmol/l glucose, with AMPK activity beginning to attenuate between 0.1 – 1.0 mmol/l glucose (Salt *et al.*, 1998). These findings collectively illustrate that the classification of “low” glucose required for increased AMPK activity occurs between 0.1 – 1.0 mmol/l glucose and additionally provides further evidence that α-cell AMPK activity is regulated by glucose-deprivation.

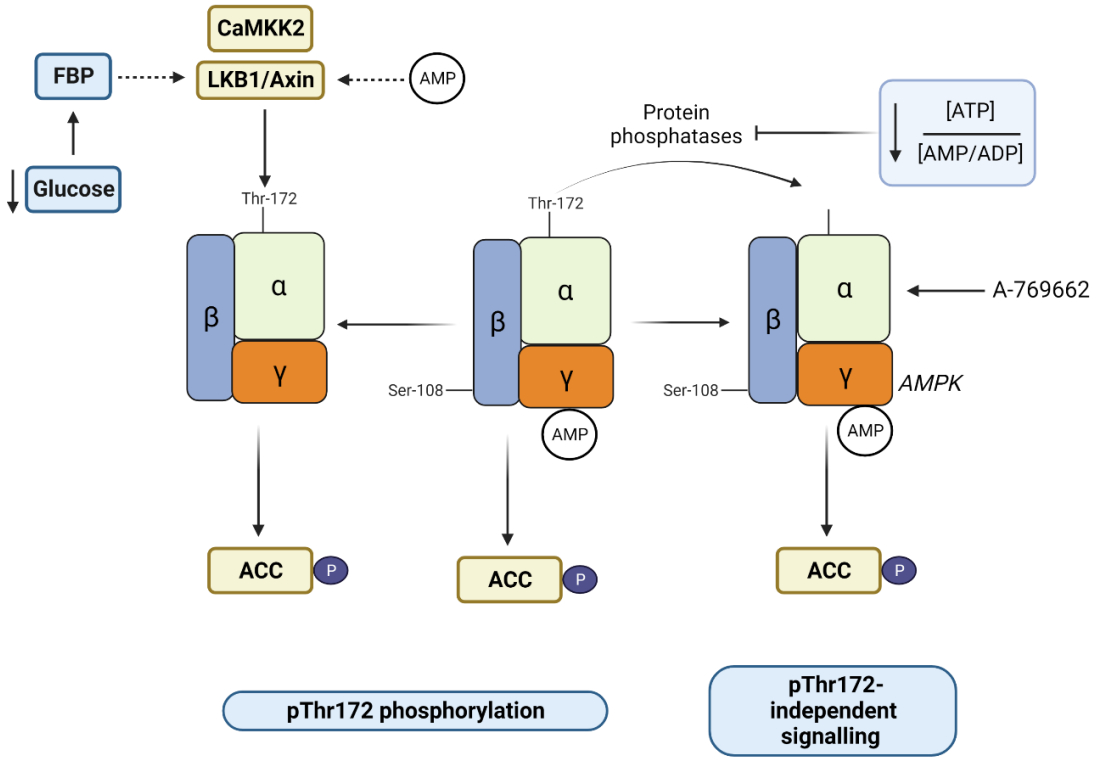

Figure 3.22: Proposed model for the allosteric regulation of AMPK activity and downstream targets.

The increased AMPK activity is regulated three separate mechanism **1.** α-Thr-172 phosphorylation by upstream kinases (e.g., LKB1/CaMKK2) (pThr-172 phosphorylation-dependent signalling), **2.** suppression of α-Thr-172 phosphorylation by protein phosphatase activity (inhibited by decreased ATP: AMP/ADP) and **3.** direct allosteric nucleotide binding (AMP/ADP). The rapid dephosphorylation of α-Thr-172, alongside retained β-Ser108 phosphorylation can still enhance AMPK activation and downstream signalling, as evidenced by work involving the synergistic actions of both A-769662 and AMP (pThr-172-independent signalling). This is independent of changes in upstream signalling. Created using Biorender.com.

Leclerc *et al.* 2011 showed 0.1 mmol/l glucose stimulated glucagon secretion in αTC1.9 cells, agreeing with evidence provided in this thesis (Leclerc *et al.*, 2011). This is supported by previous published work showing [glucose] less than ~ 1.0 mmol/l stimulated glucagon secretion in a concentration-dependent manner; with the greatest glucagon secretory response being between 0 – 0.5 mmol/l glucose (Ravier and Rutter, 2005). β-cells similarly have a left-shifted insulin response to glucose in clonal cell lines but also islets cultured in high glucose and in human islets compared to mouse (Rabuazzo *et al.*, 1997; Erion *et al.*, 2015; Pingitore *et al.*, 2017). αTC1.9 glucose metabolism appeared to also be left-shifted, with the greatest increase in glucose utilisation (> 2-fold) when increasing from 0.1 to 0.5 mmol/l glucose availability. Several papers suggested this was because αTC1.9 cells have increased hexokinase (*HK*) expression, and thereby increased glycolytic activity at low glucose due to the lower K_M compared to glucokinase (Ravier and Rutter, 2005; Leclerc *et al.*, 2011). In addition, it would be plausible to speculate that αTC1.9 cells may have decreased expression of another critical energy sensor, AMPK, in comparison to islet counterparts. This is because αTC1.9 cells are highly sensitive to low glucose-stimulated AMPK activation, with AMPK activity becoming attenuated/abolished at > 1.0 mmol/l glucose, as evidenced here. The regulation of AMPK activity could be involved in glucose-regulated glucagon secretion, after constitutively active (CA) and dominant negative (DN) AMPK mutants displayed loss of glucose-controlled glucagon secretion between 0.1 – 17.0 mmol/l glucose in αTC1.9 cells (Leclerc *et al.*, 2011). Altogether, this evidence may provide a glucose-sensing explanation on why the maximal inhibitory glucagon response to glucose is achieved at > 1.0 mmol/l glucose and consequently why αTC1.9 cells have a considerably lower glucose threshold for downstream secretory function.

AMPK activity is also regulated by AMPKβ subunit myristoylation and Ser-108 phosphorylation (Oakhill *et al.*, 2010). AMPKβ subunit acts as a scaffold, modulating AMP binding and subcellular localisation (Oakhill *et al.*, 2010). As previously mentioned, β isoform expression is tissue-specific, with expression of AMPK heterotrimeric complexes directly relating to cell function (Sanz, Rubio

and Garcia-Gimeno, 2013). No published literature, to date, has examined which β isoform is expressed by the α-cells. Here, αTC1.9 cells demonstrated high β1 expression compared to the β2 isoform, which was completely absent in this study. Published findings indicate that the pancreas and islets predominantly express β1 relative to β2 (Scott *et al.*, 2015). Similarly, evidence from this thesis indicated AMPKβ1 mouse islet staining is greater than β2, confirming findings from Scott *et al.*, 2015. The evidence provided here did not clarify AMPKβ isoform colocalisation to glucagon-positive α-cells and insulin-positive β-cells in islets, which is an important consideration for future experiments. Interestingly, AMPKβ isoforms both contain a carbohydrate binding motif (CBM) located on the N terminus which facilitates glycogen binding (Janzen, Whitfield and Hoffman, 2018). The CBM of the β2 subunits contains a Thr-101 insertion which is likely to be contribute to β2 having a greater glycogen and oligosaccharide affinity, with such an insertion reported to be absent in the β1 CBM (Koay *et al.*, 2010; Bieri *et al.*, 2012). In addition, β-cells contain glycogen stores, and have the enzymatic capacity to generate glycogen, but the functional role of glycogen in β-cell metabolism and function is controversial (Malaisse, 2016; Mir-Coll *et al.*, 2016; Nagy *et al.*, 2018). Chronic hyperglycaemia associated with T2DM has been reported to drive glycogen accumulation within β-cells by impairing oxidative metabolism, leading to K_{ATP} channel opening, diminished insulin secretion and enhancing β-cell apoptosis (Brereton *et al.*, 2016). Similarly, human islets derived from one donor and exposed to hyperglycaemic-like conditions, had upregulated *Prkab1* transcript expression, the gene encoding AMPKβ1 (Brun *et al.*, 2020). In α-cells, glycogen is undetectable in diabetic animal and human islets (Graf and Klessen, 1981; Brereton *et al.*, 2016). No published evidence has indicated if α-cells lack glycogen-related enzyme machinery, including glycogen synthase and phosphorylase, for glycogen storage. One can speculate the absence of α-cell glycogen can be evidenced by the lack of expression of the high glycogen-affinity isoform AMPKβ2, as stated previously. Additionally, β2 isoform staining observed in mouse islets is most likely derived from non-α-cell endocrine cells (β/δ cells), possibly relating to the capability for glycogen storage in β-cells.

Altogether, a number of future considerations arise from this speculation, including; 1) newly diagnosed individuals with T1DM still retain functional β-cells (Steele *et al.*, 2004), so does increased glycogen cytotoxicity contribute to progressive β-cell loss in T1DM disease progression? 2) if, and how, does specific AMPK β isoform expression impact islet cell hormone secretion? and 3) does AMPK β isoform expression alter in DM? The latter question can be answered by the analysis of publicly available RNAseq datasets, an important consideration for further investigation.

3.3.2 R481 as a potent activator of AMPK in the α-cell

The efficacy of AMPK activating compounds, R419 and R481, to increase α-cell AMPK activity was assessed in low (1.0 mmol/l), normal (5.5 mmol/l) and high (11.7 mmol/l) glucose. Here, R481 robustly increased AMPK activity, regardless of glucose availability in α-cells. R481 is a brain permeable AMPK-activating compound and is highly potent by concentrations in the nmol/l range. This data was supported by R481 dose-dependently stimulating AMPK activity in the glucose-sensing hypothalamic neuronal cell line, GT1.7 (Cruz *et al.*, 2021). On the other hand, R419 increased α-cell AMPK activity, but perhaps in a glucose-sensitive and variable manner. A concentration response using increasing [R419] up to 50 nmol/l similarly demonstrated variable efficacy in activating AMPK in GT1.7 cells (Beall *et al.*, 2012). Although speculative, the contrasting AMPK activity by both compounds could be attributed to differences in biochemical structure. Altogether, due to the potent and reliable actions of R481 enhancing α-cell AMPK activity, R481 was subsequently used for further work examining AMPK involvement in α-cell function.

3.3.3 R481 stimulated α-cell glycolysis

Evidence from collaborators at Rigel Pharmaceuticals, who generously gifted R481 and R419, previously suggested R481 indirectly activates AMPK by mildly inhibiting mitochondrial respiration, similar to metformin (Jenkins *et al.*, 2013; Vial, Detaille and Guigas, 2019). There is consensus that metformin indirectly activates AMPK by increasing [AMP/ADP:ATP] ratio as a consequence of mild

mitochondrial inhibition (Vial, Detaille and Guigas, 2019). All studies described found R481 robustly demonstrated attenuation of oxygen consumption rate (OCR), an indicator of mitochondrial respiration, and increased [ADP:ATP] in α-cells, confirming these findings. R481, therefore, may allosterically increase α-cell AMPK activity by rises in energy charge, similar to metformin.

The known role of AMPK in glycolysis could suggest R481 would promote α-cell glycolysis in an AMPK-dependent manner*.* Firstly, evidence implied R481 stimulated α-cell glucose utilisation, demonstrated by $\Delta ECAR_{MAX}$, at [glucose] greater than 0.1 mmol/l glucose. Similarly, additional work using the AMPK inhibitor SBI-0206965 (SBI) suggested these findings could be AMPK-dependent, as SBI attenuated α-cell glucose utilisation following R481 treatment at both low and high glucose availability. In skeletal muscle, glucose uptake is partially regulated by thioredoxin-interacting protein (TXNIP) (Parikh *et al.*, 2007). TXNIP is an α-arrestin binding protein involved in maintaining cellular redox balance by limiting thioredoxin (TXN) reducing capacity (Patwari *et al.*, 2006). As TXNIP is predominantly expressed in highly metabolic tissues, for instance, liver and skeletal muscle, it a key modulator of glucose uptake by attenuating GLUT-1 mRNA expression alongside promoting GLUT-1 internalisation to limit glucose uptake (Schwartz and Blouet, 2011; DeBalsi *et al.*, 2014; Noblet *et al.*, 2021; Qayyum *et al.*, 2021). Wu *et al.* 2013 demonstrated glucose deprivation increased AMPK-dependent degradation of TXNIP, promoted GLUT-1 activity and prevented transporter internalisation (Wu *et al.*, 2013). In one study, small molecule TXNIP inhibitor (SRI-37330) and TXNIP knockdown in αTC1.6 cells reduced glucagon secretion, confirming reduced serum glucagon in fasted and TXNIP-inhibited mice (Thielen *et al.*, 2020). Similarly the GLUT1 inhibitor, phloretin, enhanced glucagon secretion by 1.7-fold in mouse islets, perhaps mimicking low intracellular glucose (Suga *et al.*, 2019). Transcriptional profiling of human islets suggest TXNIP is expressed in α-cells, but further work is required to confirm this (Segerstolpe *et al.*, 2016). αTC1.9 cells express GLUT1 protein, corroborating prior research in αTC cells, with protein expression seemingly unaffected by pharmacological AMPK activation (Suga *et al.*, 2019). Protein expression, however, cannot discount if

R481 can modulate transporter endocytosis and glucose uptake. It would be interesting to suggest that pharmacological AMPK activation, by R481, could increase α-cell glucose utilisation by limiting TXNIP-mediated GLUT1 internalisation. Measuring α-cell glucose uptake and GLUT1/AMPK co-localisation following R481 treatment would be interesting to explore in the future.

Insulin-stimulated glucose uptake is predominantly due to GLUT4, where transporter expression is primarily localised to insulin-responsive tissues such as skeletal muscle and adipose tissue (Bähr *et al.*, 2012). Islet expression of GLUT4 is relatively unexplored, but published work suggests GLUT4 expression is restricted to both human and rodent islets, as well as abundant expression throughout the pancreas (Heimberg *et al.*, 1995; Kobayashi *et al.*, 2004). In addition, this thesis showed αTC1.9 cells do express GLUT4 and GLUT1, corresponding to previous findings (Bähr *et al.*, 2012). In addition, *GLUT4* gene expression in the α-cell appeared to be regulated by glucose-sensing intrinsic and paracrine regulation (Bähr *et al.*, 2012). In adipose and skeletal muscle, GLUT4 translocation to the cell surface membrane is stimulated by insulin-insulin receptor (IR) binding and PI3K/Akt pathway activation, increasing glucose uptake (Honzawa, Fujimoto and Kitamura, 2019). Both mouse and human α-cells express insulin receptors, and upon insulin binding, attenuates the cAMP-PKA pathway which inhibits glucagon secretion (Franklin *et al.*, 2005; Kawamori *et al.*, 2009; Elliott, Ustione and Piston, 2015). It is therefore interesting to speculate that intra-islet insulin could increase insulin-mediated GLUT4 translocation on the α-cell membrane, thereby enhancing glycolysis-derived lactate production, α-cell hyperpolarisation to suppress glucagon secretion.

R481 similarly increased lactate secretion from αTC1.9 cells dependent on glucose availability, corresponding with R481 increasing glucose utilisation and basal glycolysis. The lack of changes in lactate secretion at low glucose can be explained by the majority of pyruvate generated from glycolysis feeding mitochondrial oxidative respiration, to maintain ATP production. Human α-cells,

unlike β-cells, have highly enriched *LDHA* expression (Sanchez *et al.*, 2021; Cuozzo *et al.*, 2022). At high glucose, α-cells predominantly metabolise glucose by anaerobic glycolysis to produce lactate (by increased LDH activity) as an end-product derived from pyruvate (Schuit *et al.*, 1997). Interestingly, lactate transport in α-cells is controlled by bidirectional monocarboxylate transporters (MCTs) expressed on the cell surface membrane (Zaborska *et al.*, 2020). Exogenous lactate can similarly hyperpolarise human and mouse α-cell membrane potential, attenuating glucagon secretion by activating the K_{ATP} channel (Zaborska *et al.*, 2020). As R481 mildly attenuates oxidative metabolism and increases [ADP:ATP], one could speculate R481-exposed α-cells require increased glycolytic-derived lactate production to sustain and manage intracellular ATP levels. Although evidence from this chapter suggests R481 attenuated total ATP levels only at low glucose, this unexpected finding could be attributed to the diminished ATP generation derived from mildly inhibited oxidative respiration, on which α-cells rely on for sustaining energy levels at low glucose.

From an intra-islet perspective, albeit at much lower levels, human β-cells predominantly express *LDHB* isoform of LDH which has higher affinity for lactate than pyruvate (Ždralević *et al.*, 2018; Cuozzo *et al.*, 2022). Hyperinsulinaemic hypoglycaemic familial 7 (HHF7) individuals are characterised by an MCT-1 gain-of-function mutation in β-cells, facilitating lactate import and conversion to pyruvate stimulating glucose-insensitive insulin secretion (Otonkoski *et al.*, 2007). It would be interesting to investigate if HHF7 individuals are associated with increased MCT lactate import into the α-cell, leading to hyperpolarisation-derived suppression of glucagon secretion (alongside strong paracrine influence) associated with hypoglycaemia (Zaborska *et al.*, 2020). In addition, high islet lactate levels could suppress the glucagon secretory response to reduce the risk for hyperglucagonaemia, which therefore supports the clinical absence of glucagon secretion in HHF7, contrasting with other types of DM.

3.3.4 R481 and alternative substrate utilisation at low glucose

Glucose-sensing cells, including hypothalamic neuronal cells, enhance AMPK-dependent fatty acid oxidation (FAO) at low glucose, but not at high glucose (Taïb *et al.*, 2013). In addition, glucose sensing α-cells have been postulated to drive counterregulatory glucagon secretion by increased FAO-derived ATP production at low glucose (Briant *et al.*, 2018a). Therefore, the work presented here examined if pharmacological AMPK activation, by R481, would drive FAO under glucose deficit. Here, αTC1.9 cells were exposed to an acute bout of saturated fatty acid, palmitate, following low and high glucose incubation alongside R481 treatment. R481 enhanced α-cell palmitate oxidation under glucose-deprived conditions, demonstrated for the first time. AMPK activation inhibits ACC activity and thereby attenuates malonyl-CoA inhibition of CPT1a-dependent FAO (Lipovka and Konhilas, 2015). Recent evidence from Briant *et al.* 2018 discovered α-cell-specific CPT1a knockout diminished glucagon secretion at low glucose in both murine islets and αTC1.6 cells (Briant *et al.*, 2018a). FAO can increase ROS generation, which is buffered by uncoupling protein-2 (UCP-2) activity to prevent oxidative stress (Andrews *et al.*, 2008). In addition to CPT1a, α-cell UCP-2 expression is thought to retain adequate low glucose-sensitive glucagon secretion, perhaps by limiting cytotoxic oxidative stress (Diao *et al.*, 2008; Allister *et al.*, 2013). Both attenuating UCP-2 or CPT1a expression in rodent models attenuated plasma glucagon and glucagon secretion under glucose-deprived conditions (Diao *et al.*, 2008; Allister *et al.*, 2013; Briant *et al.*, 2018a). AMPK-CPT1a-UCP-2 axis is postulated to be important in stimulating orexigenic food intake, in response to the “hunger hormone” ghrelin, which secretion is raised in glucose deprivation, including fasting (De Morentin *et al.*, 2011). One could therefore postulate that the AMPK-CPT1a-UCP-2 link in the α-cell could drive glucagon secretion under periods of low glucose. Recurrent hypoglycaemia, associated with T1DM, can drive FA usage and dependence in glucose-sensing human primary astrocytes (HPA), which the authors suggest promoted a degree of mitochondrial flexibility (Weightman Potter *et al.*, 2019). It is increasingly thought the diminished counterregulatory glucagon secretion observed in T1DM is at least partially

attributed to intrinsic defects in α-cell glucose-sensing machinery. It would therefore be interesting to speculate if impaired α-cell AMPK-CPT1a-UCP-2 axis could potentially be pharmacologically targeted to stimulate/retain glucagon secretion in recurrent hypoglycaemia associated with T1DM.

3.3.5 R481 and α-cell glucagon secretion

To examine the impact of pharmacological AMPK activation on glucagon secretion, both αTC1.9 cells and *ex vivo* murine islets were exposed to R481 alongside either low or high glucose levels to measure glucagon secretion. As R481 potently enhanced α-cell metabolism and lactate secretion, it would be interesting to speculate that R481 exposure would attenuate the α-cell glucagon secretory response. Experimental findings suggested R481 did not alter α-cell glucagon secretion, both in an intra-islet and isolated environment. Previous findings using other indirect AMPK activators suggested otherwise, with metformin exposure reducing glucose-mediated suppression of glucagon secretion in αTC1.9 cells (Leclerc *et al.*, 2011). Therefore, this evidence suggests neither R481 nor R419 alter α-cell glucagon secretion.

3.3.6 R481 and β-cell glucose utilisation

The role of AMPK activation in β-cell function and secretory capacity is somewhat debated. As previously shown, R481 potently stimulated SBI-sensitive αTC1.9 glycolysis and lactate release. Further experiments therefore examined if R481 increased bioenergetics in β-cells in a similar manner. Here, R481-incubated human EndoC-βH1 β-cells increased glucose utilisation following euglycaemic-like [glucose] availability, in which the effect appeared relatively short-lasting at ~ 15 min post injection. Human islet β-cells express relatively low levels of *LDHA* and *LDHB* and are considered “disallowed” genes. Human β-cells do not express MCTs required for lactate transport, which may suggest any β-cell derived lactate production is converted back to pyruvate to feed the Krebs cycle (Sekine *et al.*, 1994; Andersson *et al.*, 2015; Cuozzo *et al.*, 2022). It is important to note that clonal β-cell line EndoC-βH1 has previously showed increased lactate secretion and expression of known “disallowed”

genes *LDHA* and *SLC16A1* (MCT-1) which has been suggested to be, in part, behind the small threshold range for GSIS in monolayer cell cultures (Pullen *et al.*, 2010; Andersson *et al.*, 2015; Tsonkova *et al.*, 2018). EndoC-βH1 bioenergetic signatures may therefore not be replicable of human islets and data provided should be taken with caution. There could, similarly, be an explanation for this as the increased MCT expression associated with cultured β-cells could be contributed by a slightly enhanced hypoxic phenotype. One recent study found reducing medium volume (100.0 µl to 33.0 µl) enhanced adipocyte function alongside increasing mitochondrial-derived glucose oxidation to sustain ATP generation (Tan *et al.*, 2022). As β-cells primarily perform aerobic glucose oxidation at high glucose, it would be interesting to see if reduced medium culture conditions could abolish anaerobic-like signatures seen here in EndoC-βH1 cells.

To summarise, for the first time, enhancing α-cell AMPK activity by R481, modulated metabolic substrate utilisation dependent on glucose availability (illustrated in Figure 3.23). Mildly enhancing FAO, by targeting α-cell AMPK activity, may therefore be beneficial in the context of T1DM, in order to retain glucagon exocytosis following recurrent hypoglycaemia. Additional bioenergetic studies, to clarify secretion findings, could use human islets and/or co-culture models to reliable mimic the human α-cell paracrine environment.

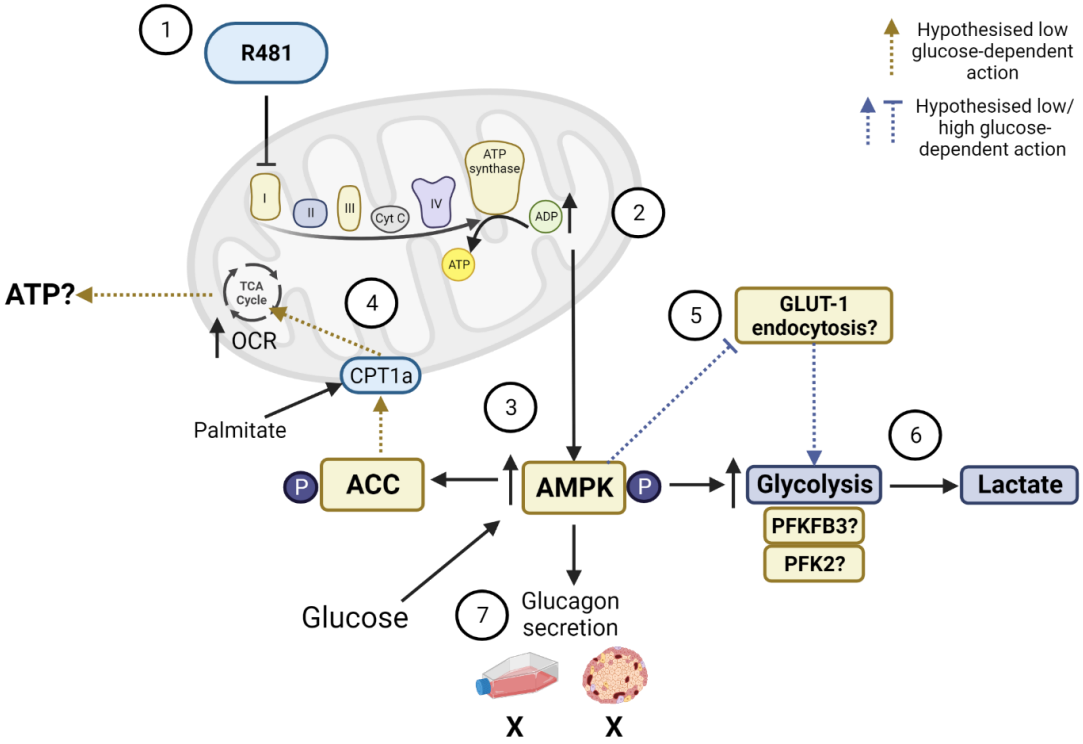

Figure 3.23: Summary of Chapter 3 findings and hypothesised actions.

1. R481 is thought to be a potent indirect AMPK activator, and similarly to metformin, by mildly inhibiting mitochondrial oxidative respiration. **2.** R481 enhanced α-cell [ADP:ATP] ratio, with both findings indicating R481 mildly inhibit α-cell mitochondrial respiration. **3.** R481 increased α-cell AMPK activity independent of glucose availability. **4.** Additionally, R481 increased low glucose-stimulated palmitate oxidation which could be driven by increased AMPK-dependent ACC inactivation. If this would have an impact on intracellular ATP would need to be clarified. **5.** Increased AMPK activity has been linked with modulate GLUT trafficking to the cell surface membrane. **6.** R481 increased α-cell glycolysis regardless of glucose availability, parallel to observed L-lactate secretion. One suggested mechanism of R481 enhancing α-cell glycolytic rate could be by upregulated AMPK-dependent glycolytic enzyme machinery (for instance, PFKFB3 and/or PFK-2) and/or suppressing GLUT1 endocytosis. **7.** Altogether, this chapter observed no significant changes in glucagon secretion by either mouse islets or αTC1.9 cells. Created using Biorender.com.

Chapter 4

Investigation into the effect of O-304 exposure on α-cell function and glucose homeostasis

4 Investigation into the effect of O-304 exposure on α-cell function and glucose homeostasis

4.1 Introduction

Previously, chapter 3 discussed how the indirect AMPK activator, R481, increased low glucose-dependent glycolysis independent of any changes to α-cell glucagon secretion. Findings from chapter 3 implied R481 mildly inhibits α-cell mitochondrial oxidative respiration, similarly to metformin. These findings are important in understanding the mechanistic, downstream impact of AMPK activator application. The preclinical development of new indirect AMPK activators, which activate AMPK by altering cell energy status (i.e., increase in intracellular AMP), is often impaired due to the risk of lactic acidosis, especially noted in clinical use of R118 (Brass and Hoppel, 2015; Low Wang, Galinkin and Hiatt, 2015). Due to the risk of off-target actions by AMP-dependent pathways, there is significant research interest to create compounds that directly bind and activate the AMPK complex (Olivier, Foretz and Viollet, 2018). If so, similarly to metformin, do the respective direct small molecules have therapeutic efficacy in restoring glucose homeostasis in DM?

Direct AMPK activators can be classified by molecule binding site; **1.** γ-subunit binding, **2.** ADaM site binding (including β-selective and pan-AMPK activators), **3.** β-isoform modification (Olivier, Foretz and Viollet, 2018). Stenberg and colleagues identified O-304 as a small molecule, direct AMPK activator with therapeutic potential in diabetes (Steneberg *et al.*, 2018). In cell-free assays containing human recombinant AMPKα, -β, and -γ trimers, the authors showed robust AMPK phosphorylation (similarly to ADP) in the presence and absence of ATP (Steneberg *et al.*, 2018). These studies also suggested O-304 can prevent AMPKα Thr-172 dephosphorylation without inhibiting protein phosphatase 2C (PP2C) activity and therefore acting similarly to AMP/ADP whilst not reducing total ATP (Steneberg *et al.*, 2018). Additionally, these findings suggest O-304 as a pan-AMPK activator in AMPKα1/β1/γ1 and AMPKα2/β1/γ1 trimer complexes. However, the “pan” description may need to

be taken with caution as there are no published data examining O-304-dependent AMPK activity in other β and γ-subunit isoform-containing heterotrimeric complexes. Altogether, these data pose several questions for future work; **1.** Does O-304 allosterically activate AMPK through rises in $[AMP]_i$ and **2.** Does O-304 selectively activate β1/2-containing complexes, similarly to other AMPK activators? AMPK subunit isoform expression is tissue-specific, largely dependent on regulatory function (Birk and Wojtaszewski, 2006; Ross, Jensen and Hardie, 2016). By answering these questions, this will clarify which binding site O-304 utilises to modulate AMPK complex activity, and therefore inform future tissue-specific therapeutic avenues.

The successful completion of phase II clinical trials for direct AMPK activators, O-304 and PXL770, has opened the possibility for safe AMPK-focused therapeutics (Steneberg *et al.*, 2018; Cusi *et al.*, 2021). These findings, focused on O-304, reported a reduction in fasting blood glucose after 6 weeks in both diet-induced obese (DIO) and type 2 diabetic (hIAPPtg) mice (Steneberg *et al.*, 2018). Interestingly, T2DM mice fed a HFD for 9 weeks and a subsequent 6 weeks HFD supplemented with O-304 had a lower fasting blood glucose than animals exposed to HFD alone for 15 weeks (Steneberg *et al.*, 2018). Preclinical evidence suggested O-304 reduced heart glycogen but did not change heart weight and improved cardiovascular function in DIO mice (Steneberg *et al.*, 2018). Cardiac hypertrophy is a side effect observed in some preclinical AMPK activators, identifying O-304 potentially having no cardiac toxicity in humans (Myers *et al.*, 2017). A 27-day phase IIa clinical trial with O-304 was therefore performed and similarly showed a reduced fasting plasma glucose associated with O-304 treatment in individuals with metformin-treated T2DM (Steneberg *et al.*, 2018). These data suggest O-304 may reverse hyperglycaemia commonly associated with metabolism-related disorders.

Type 2 diabetes development is associated with diminished glucose uptake, associated with insulin resistance, in peripheral tissues (i.e. liver and skeletal muscle), and furthermore increasing the metabolic phenotype of hyperglycaemia and hyperinsulinaemia (Defronzo and Tripathy, 2009; Jaspers

et al., 2017). Insulin resistance can be, albeit controversially, associated with obesity and long-term insulin treatment in T1DM. Evidence suggests a 12 – 61% reduction in skeletal muscle insulin sensitivity in populations with T1DM, with the main proposed mechanisms being inhibition of insulin signalling resultant from chronic hyperglycaemia (Kaul, Apostolopoulou and Roden, 2015). Pharmacological modulators that both target insulin-dependent and independent metabolic dysregulation have the sought potential to attenuate both hyperinsulinaemia and hyperglycaemia (Cokorinos *et al.*, 2017). In HFD-fed mice, O-304 increased glucose uptake in calf and thigh skeletal muscle, which can be partially explained by the attenuation of O-304-stimulated glucose uptake in AMPKα1/2 silenced rodent myotubes (Steneberg *et al.*, 2018). DIO and hiAPPtg mice displayed reduced fasting insulin and insulin resistance (HOMA-IR) after 6-7 weeks treatment, suggesting improved insulin sensitivity (Steneberg *et al.*, 2018). These data correspond with other findings involving direct ADaM site-binding AMPK activators (991, SC4, PF-739), which are associated with enhanced glucose uptake in skeletal muscle in physiological contexts (Lai *et al.*, 2014; Bultot *et al.*, 2016; Cokorinos *et al.*, 2017; Myers *et al.*, 2017; Ngoei *et al.*, 2018). Pan AMPK activators PF739 and MK-8722 have similarly reduced hyperglycaemia in diabetic rodent and non-human primate models by increasing skeletal muscle glucose uptake (Cokorinos *et al.*, 2017; Myers *et al.*, 2017). How O-304 can stimulate peripheral glucose uptake can be partially explained by increased AMPKα1/2 activation, but if downstream metabolic processes (i.e., glycolysis and mitochondrial respiration) are affected by O-304 exposure in an AMPK- and glucose-dependent manner is unknown.

AMPK activation is controlled by carbohydrate metabolism, for instance, AMPKβ subunit contains a carbohydrate-binding motif (CBM) for glycogen binding and sensing (Oligschlaeger *et al.*, 2016). The growing rise in high fructose-containing diets have been attributed to the increased hepatic lipid accumulation and insulin resistance; major risk factors for type 2 diabetes development (Geidl-Flueck *et al.*, 2021). Both fructose and glucose are monosaccharides and once consumed, are absorbed into hepatocytes using GLUT transporter-mediated uptake (Wu, Fritz and Powers, 1998). Hepatic

fructose metabolism generates glyceraldehyde 3-phosphate (G3P) and feeds into glycolytic generation of pyruvate by pyruvate kinase (PK); bypassing key glycolytic rate limiting enzymes (glucokinase, PFK-1) (Campbell *et al.*, 2014). Fructose-derived metabolites also include dihydroxyacetone phosphate (DHP) which drive *de novo* lipogenesis and lipid droplet formation (Campbell *et al.*, 2014; Mortera, Bains and Gugliucci, 2019; Taskinen, Packard and Borén, 2019) (Figure 4.1). Hepatic fructose metabolism is less glycolytically regulated by hormones (i.e. insulin/glucagon) and substrate availability compared to glucose, and therefore high-fructose diets can drive hepatic insulin resistance in the context of T2DM. Importantly, hepatic AMPK and downstream activation are decreased in high-fructose diet fed mice and AMPKγ-activating mutant mice have reduced hepatic triglyceride accumulation (Choi, Abdelmegeed and Song, 2017; Woods *et al.*, 2017). Similarly, a review suggested “bursts” of fructose consumption limits allosteric activation by AMP on AMPKγ subunit binding sites, limiting AMPK activation (Gugliucci, 2016; Johanns, Hue and Rider, 2023).

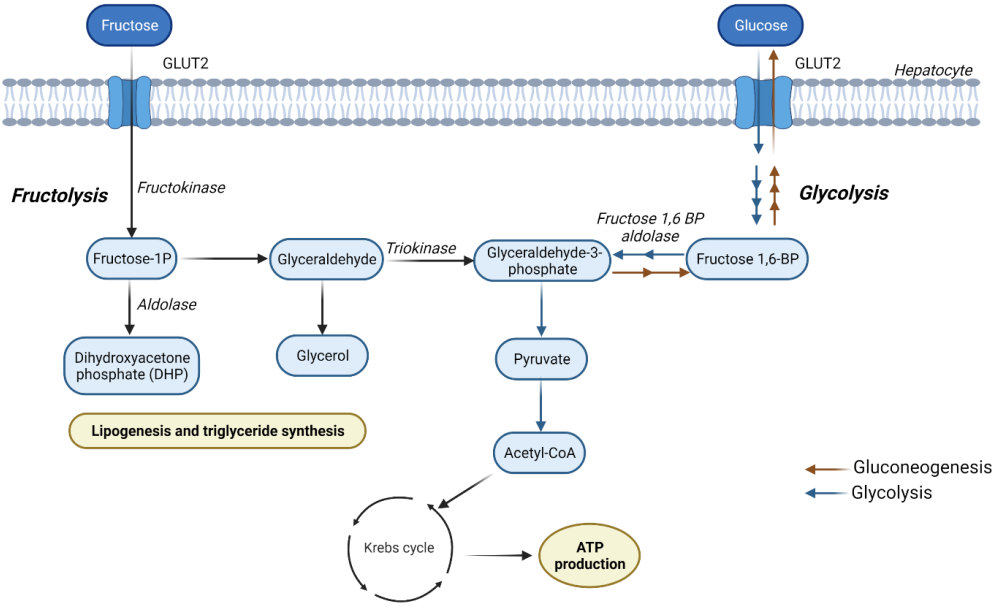

Figure 4.1: Fructose metabolism in the liver.

Fructose is imported into the hepatocytes by GLUT-2 mediated fructose transport, similar to glucose. Fructose is catabolised to intermediated fructose-1-phosphate (fructose-1P) by fructokinase. Fructokinase is a highly fructose-sensing enzyme, as is crucial to fructose metabolism. Fructose-1P is metabolised to dihydroxyacetone phosphate (DHP) by aldolase B to enhance lipogenesis. In addition, fructose-1P is metabolised to glyceraldehyde (for glycerol formation required for triglyceride synthesis) and further modified by triokinase for glyceraldehyde-3-phosphate generation. Glyceraldehyde-3-phosphate is metabolised to pyruvate, thereby entering glycolysis (blue arrows), and therefore accelerating acetyl-CoA generation to increase ATP production. The generation of glyceraldehyde-3-phosphate can be utilised as a substrate for gluconeogenesis (brown arrows). Adapted from (Tappy and Le, 2010).

Galactose, similarly, is a monosaccharide commonly found in fruits (Gross and Acosta, 1991). Comparable to fructose, galactose is imported into the liver by GLUT-mediated diffusion and can be glycolytically metabolised after conversion from UDP-galactose to UDP-glucose via the Leloir pathway (Qi and Tester, 2019; Conte *et al.*, 2021). UDP-galactose is also substrate for glycosylation of macromolecules and glycosphingolipid generation; the latter being associated with increased insulin resistance and mitochondrial stress (Balram, Thapa and Chatterjee, 2022). Additional work is required to determine how alternative sugars are utilised by other GLUT-expressing peripheral tissues and whether, if any, effects are AMPK-mediated.

Hyperglycaemia metabolically impacts multiple peripheral tissues other than skeletal muscle, including the liver and adipose tissue. Increased hepatic gluconeogenesis, compared to glycogenolysis, contributes to hyperglycaemia associated with diabetes (Jiang *et al.*, 2020). The findings from published literature primarily agree that increases in skeletal muscle glucose uptake are the primary therapeutic target to reduce hyperglycaemia (Zierath and Kawano, 2003). Metformin is the most commonly used therapeutic for T2DM, as it reduces hepatic gluconeogenesis without impacting β-cell insulin secretion (Yki-Järvinen, 1997; Nishitani *et al.*, 2002; Merz and Thurmond, 2020). The underlying mechanisms remain controversial in the literature. More recently, the AMPK-independent actions of metformin suggested increased AMP, PFK-1 activation, and FBPase-1 inhibition, are causal factors for the observed clinically reduced hepatic gluconeogenesis (Foretz *et al.*, 2010; Hunter *et al.*, 2018; Moonira *et al.*, 2020; Johanns *et al.*, 2022). The direct AMPK activator, 991, has been identified as a β1-selective activator in cell-free assays (Xiao *et al.*, 2013). Johanns *et al.* 2022 findings suggested 991 reduced lactate and pyruvate-dependent, glucagon-dependent glucose production in rodent hepatocytes (Johanns *et al.*, 2022). Although 991 is a direct AMPK activator, compared to metformin, Johanns *et al.* 2022 similarly demonstrate both AMPK dependent (via AMPKβ1) and independent (MPC/GPD2 inhibition) actions on hepatic gluconeogenesis (Johanns *et al.*, 2022). Similarly, other direct AMPK activators (MK8722, PF739) reduced both glucagon-dependent and independent glucose

production (derived from both lactate and pyruvate) in wild type hepatocytes, corresponding with reduced glucagon-induced PKA activation (Johanns *et al.*, 2022). Such effects were diminished in AMPKβ1 KO hepatocytes, implying AMPK-dependent actions on hepatic gluconeogenesis (Johanns *et al.*, 2022). The allosteric AMPK activator, C24, also reduced AMPK-dependent glucose production by downregulation of key gluconeogenic genes *PEPCK* and *G6Pase*, in both hepatocytes and db/db mice (Li *et al.*, 2013). Although O-304 (10.0 µmol/l) did not alter hepatic lactate/pyruvate-derived glucose production, regardless of glucagon stimulation, O-304 reduced glucagon-dependent PKA activity in an AMPK-β1 independent manner (Johanns *et al.*, 2022). These findings suggest O-304 has the capacity to attenuate hepatic glucagon signalling, but if O-304 treatment has gluconeogenic capability needs to be explored in a more replete model. Both T1DM and T2DM are largely attributed to the dysregulation of glucagon secretion over time, and therefore, modulating glucagon-regulated gluconeogenesis by small molecular AMPK activators is a potential therapeutic target.

In T2DM, over time, β-cells become unable to respond to hyperglycaemia by compensating with pathological second-phase insulin secretion and consequently increase ER stress (’T Hart *et al.*, 2000; Laybutt *et al.*, 2007). Pharmacological modulators that promote β-cell “rest” and not stress are important to help mitigate β-cell failure commonly observed in T2DM (van Raalte and Verchere, 2017). The pharmacological increase in skeletal muscle glucose uptake, by using AMPK activators, would therefore limit hyperglycaemia-associated β-cell stress. AMPK activator O-304 reduced pancreas amyloid (IAPP) deposition, a hallmark feature of β-cell failure in type 2 diabetes, and improved arginine-stimulated insulin secretion (first-phase) in HFD-fed mice (Steneberg *et al.*, 2018). Furthermore, O-304 reduced high glucose-exacerbated islet amyloid deposits in humanised IAPP expressing (hiAPPtg) islets (Steneberg *et al.*, 2018). The authors suggest, although speculative, O-304 can improve β-cell function in pathological contexts indirectly by increasing AMPK-dependent glucose uptake in skeletal muscle, thereby ameliorating hyperglycaemia.

There is considerable evidence, however, that AMPK activation directly regulates islet function. However, published findings examining the functional impact of endogenous/exogenous AMPK activation are conflicting and widely debated (Nguyen-Tu *et al.*, 2022). Published experimental findings involving small molecules to activate β-cell AMPK are considerably variable due to, length of treatment, AMPK activator and experimental model used (Nguyen-Tu *et al.*, 2022). Endogenous AMPK activation is required for normal β-cell glucose sensing, which was evident in mouse AMPKα2 islet electrophysiological work (Beall *et al.*, 2010). O-304 directly increased AMPK signalling cascade activation in mouse, human and hiAPPtg islets (Steneberg *et al.*, 2018). Furthermore, there are preliminary indications that O-304 alters islet metabolic function. Genome and transcriptional analysis of HFD-fed mice found 1621 differentially regulated genes vs mice fed regular diet (RD) (López-Pérez *et al.*, 2021). 1495 of those genes are not differentially regulated in islets derived from both HFD and O-304-exposed mice relative to RD, suggesting O-304 can protect islet gene signature associated with HFD (López-Pérez *et al.*, 2021). O-304 appeared to reduce islet mitochondrial metabolism (PDK4) and fatty acid oxidation (CD36, CPT1A, CPT1B) transcript expression in HFD mice, compared to RD (López-Pérez *et al.*, 2021). In addition, O-304 normalised insulin (*Ins1*) and glucose transporter (*Slc2a2)* gene expression changes associated with HFD in mouse islets (López-Pérez *et al.*, 2021). These data could suggest O-304 has the capability to directly alter islet cell function by activation of AMPK.

LKB1, an upstream kinase of AMPK, can couple murine β-cell glucose metabolism to insulin secretion (Hardie and Alessi, 2013; Fu *et al.*, 2015). The β-cell-specific knockout of LKB1 in pancreatic islets displayed a diminished glucose-dependent response in OCR and ECAR and coincided with reduced high glucose dependent insulin secretion (Fu *et al.*, 2015). These findings similarly showed a reduced glutamine flux in LKB1-silenced MIN6 cells, in addition to LKB1 knockout β-cells displaying increased tolbutamide-induced action potential firing frequency and increased calcium influx (Fu *et al.*, 2015). Similarly, global AMPKα1 and RIP-Cre α2 specific knockout β-cells had both dysregulated GSIS, alongside a lack of low glucose-dependent electrical

responsivity and therefore glucose sensitivity (Beall *et al.*, 2010). A reduction in *UCP-2* mRNA levels were observed in AMPKα1/RIP-Creα2 KO mice, and thereby suggests UCP-2 activity as being important in limiting β-cell ROS production (characteristically observed in pathological conditions characterised by chronic hyperglycaemia by lowering mitochondrial membrane potential (Zhang *et al.*, 2001; Elksnis *et al.*, 2019). These data suggest an important role of AMPK in β-cell glucose sensing and hormone secretion. However, there is a lack of knowledge on how (or whether) AMPK may have a role in glucose-sensitive hormone secretion in other islet cell types.

In insulin-treated diabetes, α-cell glucagon secretion becomes dysregulated with increasing disease duration. Alterations in the glucagon response in T1DM and T2DM include unsuppressed and defective low-glucose-dependent glucagon secretion (Meek *et al.*, 2015; Gilon, 2020; Panzer and Caicedo, 2021). One suggestion for the dysregulated α-cell counterregulation to hypoglycaemia could be diminished intrinsic glucose-sensing. Both AMPK α isoforms and related upstream kinases are expressed in α-cells (Leclerc *et al.*, 2011; Sun *et al.*, 2015). Mouse isolated α-cells express primarily AMPKα1, rather than α2 (Sun *et al.*, 2015). In addition, mouse α-cells have increased LKB1 expression compared to β-cells (Sun *et al.*, 2015). The LKB1-AMPKα axis has been implicated in α-cell function. For instance, preproglucagon promoter deletion in LKB1 knockout mice reduced fasted plasma glucagon, alongside lowering fasting blood glucose (Sun *et al.*, 2015). Similarly, both αAMPKα1 and αLKB1 knockout mice had enhanced glucose infusion rates in hypoglycaemic-hyperinsulinaemic clamp studies, suggesting diminished whole-body glucose sensitivity (Sun *et al.*, 2015). αLKB1 knockout islets had reduced 3.0 mmol/l-stimulated glucagon secretion, with no change at lower (0.1 mmol/l) or higher (17 mmol/l) glucose. On the other hand, either individual or double α-cell specific knockout of AMPKα1 or AMPKα2 does not significantly alter mouse islet low glucose-dependent glucagon secretion (Sun *et al.*, 2015). The discrepancies highlighted in Sun *et al.*, 2015 can be contributed to the low genetic knockout efficiency (~45% α-cells were selectively deleted for such alleles), and variable reduction in AMPK activity (40%; αLKB1; 32% αAMPKα1;

27%; αAMPKα2). The overexpression of active AMPKα1^{312} (Thr172) limited suppression of glucagon secretion at high glucose, whereas, downregulation using kinase-dead mutant (α1 D157A) diminished low glucose-stimulated glucagon secretion (Leclerc *et al.*, 2011) These findings, altogether, could identify AMPK a key “switch” in activating or inhibiting the α-cell glucagon secretory response.

The pharmacological activation of AMPK offers possible therapeutic avenues to ameliorate the defective α-cell glucagon response to hypoglycaemia which is commonly associated with insulin-treated diabetes. However, published *in vitro* work offers discrepancies. Metformin (500 µmol/l) treatment diminished low glucose-stimulated glucagon secretion and impaired the suppression of high glucose in αTC1.9 cells (Leclerc *et al.*, 2011). In contrast, the ‘direct’ AMPK activator A-769662 (500 µmol/l) increased glucagon secretion regardless of glucose availability. This study, however, has some limitations. For example, metformin and A-769662 have AMPK-independent actions on cellular processes, such as mild mitochondrial inhibition, glucose uptake and electrical activity in a tissue-specific manner (Owen, Doran and Halestrap, 2000; Vlachaki Walker *et al.*, 2017; Kopietz *et al.*, 2021; Said *et al.*, 2022). More in-depth investigation is required, therefore, to examine whether and how next generation direct AMPK activators’ influence α-cell function in the context of diabetes.

In this chapter, O-304 was used to test the overarching hypothesis that α-cell AMPK activation will enhance glucose-dependent metabolism and downstream glucagon secretion. AMPK activity, bioenergetics and hormone secretion were assessed in two *in vitro* islet cell lines (Endo-CβH1, αTC1.9). Glucagon secretion was also measured in *ex vivo* mouse islets. Finally, a preliminary study was conducted in streptozotocin (STZ) Sprague Dawley rats to examine the hypothesis that O-304 will enhance the glucagon secretory response to limit hyperglycaemia in a rodent model of T1DM. The questions investigated in this study include;

1. Can O-304 exposure stimulate AMPK activation in the α-cell?
2. Does O-304 enhance α-cell substrate utilisation, measured by changes in glycolysis and mitochondrial respiration, in an AMPK-dependent manner?
3. If any, does O-304 exposure regulate downstream glucagon secretion from islets and isolated α-cells?

4.2 Results

4.2.1 O-304 and AMPK signalling cascade activation at different [glucose]

4.2.1.1 O-304 activates the AMPK signalling cascade in α-cells

To identify an optimal [O-304] to stimulate α-cell AMPK activation, α-cells were incubated in high glucose-containing media (11.7 mmol/l) ± O-304 (0 – 10.0 µmol/l) for 1 h.

[O-304] treatment enhanced AMPKα-Thr172 phosphorylation in comparison to vehicle; with a notable additional four-fold increase in AMPK phosphorylation at 10.0 µmol/l compared to 5.0 µmol/l O-304 (fold change in densitometry) (2.5; 1.345 ± 0.05065, 5.0; 2.432 ± 0.362, p = 0.1872, 10.0**;** 9.876 ± 1.076, p = 0.0086) (Figure 4.2Bi). ACC phosphorylation was similarly increased, in line with phosphorylation of AMPK, in a concentration manner; with both 5.0 and 10.0 µmol/l treatment enhancing ACC phosphorylation compared to vehicle (fold change in densitometry) (2.5; 1.464 ± 0.02187, 5.0; 3.095 ± 0.2022, p = 0.0118, 10.0; 11.62 ± 0.6479, p <0.0001) (Figure 4.2Bii). For subsequent work, either a concentration of 5.0 or 10.0 µmol/l O-304 was used.

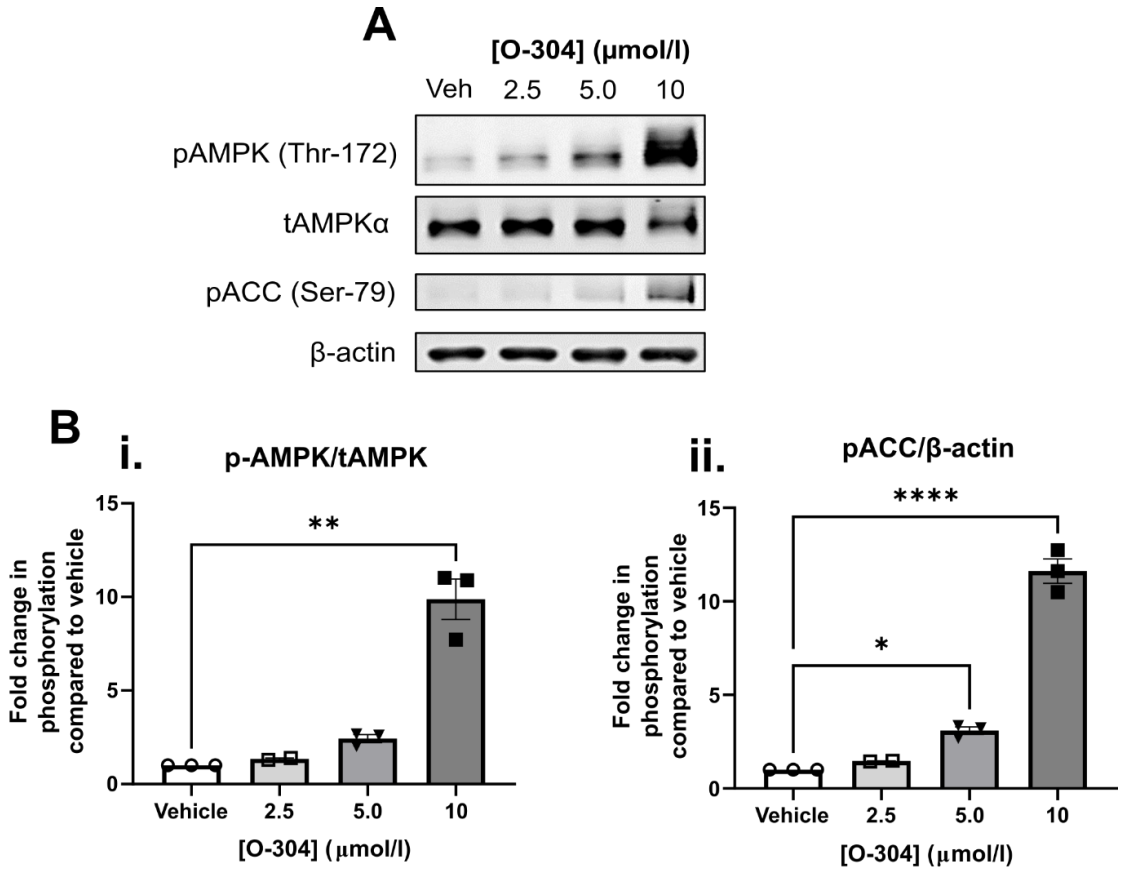

Figure 4.2: Increasing [O-304] enhanced AMPK signalling cascade activation.

αTC1.9 cells were incubated with 11.7 mmol/l glucose-containing Krebs Buffered HEPES solution (KBH) ± O-304 (2.5 – 10 µmol/l) for 1 h. **A.** Representative immunoblot for phosphorylated AMPKα1/2 (pAMPK, Thr172), total AMPKα1/2 (tAMPK), phosphorylated ACC (pACC, Ser79) and beta-actin (β-actin). **B.** Densitometric analysis for i. pAMPK normalised to tAMPK (Kruskal-Wallis test with Dunn's multiple comparison test) ii. pACC normalised to β-actin (One-Way ANOVA with Dunnett's multiple comparison test) (n = 2- 3, *P<0.05, **P<0.01, ****P<0.001)

4.2.1.2 SBI attenuated O-304-stimulated ACC phosphorylation, dependent on extracellular glucose.

To investigate if O-304 stimulated α-cell glycolysis and oxidative respiration by activating AMPK, α-cells were incubated with AMPK/ULK-1 inhibitor, SBI-0206965 (SBI, 30.0 µmol/l), at euglycaemic-like conditions (5.5 mmol/l) prior to O-304 (5.0 µmol/l) exposure ± SBI- for an additional 1 h in differing [glucose]-containing media.

After 0.5 mmol/l glucose exposure, the O-304 enhanced ACC phosphorylation was prevented by SBI pre-treatment (fold change in densitometry) (Vehicle; 1.711 ± 0.2967, O-304; 3.707 ± 0.6374, *Vehicle vs O-304*; p = 0.0259, SBI; 0.4280 ± 0.09595, SBI + O-304; 1.801 ± 0.2936, *O-304 vs SBI + O-304;* p = 0.0325) (Figure 4.3Bii) . In contrast, AMPK phosphorylation (Thr-172) was elevated in the presence of SBI (fold change in densitometry) (Vehicle; 1.388 ± 0.1745, O-304; 3.182 ± 0.2480, SBI; 2.547 ± 0.8207, SBI + O-304; 4.996 ± 1.504) (Figure 4.3Bi).

Following 5.5 mmol/l glucose incubation, a trend (although not statistically significant) towards O-304 enhanced ACC phosphorylation was seen and a non-significant reduction in ACC phosphorylation was observed following SBI incubation (fold change in densitometry) (Vehicle; 1.321 ± 0.1396, O-304; 2.382 ± 0.2678, SBI; 0.5046 ± 0.0450, SBI + O-304; 1.910 ± 0.3730) (Figure 4.4A/Bii). On the contrary, O-304 + SBI additively enhanced AMPK Thr-172 phosphorylation by >2-fold with O-304 alone (fold change in densitometry) (Vehicle; 1.135 ± 0.2088, O-304; 2.018 ± 0.4424, SBI; 3.129 ± 0.7891, SBI + O-304; 4.810 ± 0.684, p = 0.0335) (Figure 4.4Bi).

Similarly, at high glucose (11.7 mmol/l) , O-304 and SBI- additively enhanced AMPK Thr-172 phosphorylation (fold change in densitometry) (O-304; 2.310 ± 0.2936, SBI; 2.111 ± 0.4041, SBI + O-304; 5.553 ± 0.7287, *O-304 vs SBI + O-304, p = 0.0029, SBI vs SBI + O-304, p = 0.0020*) (Figure 4.5Bi). O-304 continued to enhance ACC Ser-79 phosphorylation, but the effect was attenuated with SBI treatment. Interestingly, SBI- treatment alone reduced

endogenous ACC phosphorylation (fold change in densitometry) (O-304; 2.285 ± 0.1783, *Vehicle vs O-304, p < 0.0001,* SBI; 0.2762 ± 0.07149, *Vehicle vs SBI, p = 0.0038,* SBI + O-304; 1.150 ± 0.04978, *O-304 vs SBI + O-304, p = 0.0002)* (Figure 4.5Bii). Altogether, O-304 enhanced AMPK activity in an SBI- and glucose-sensitive manner.

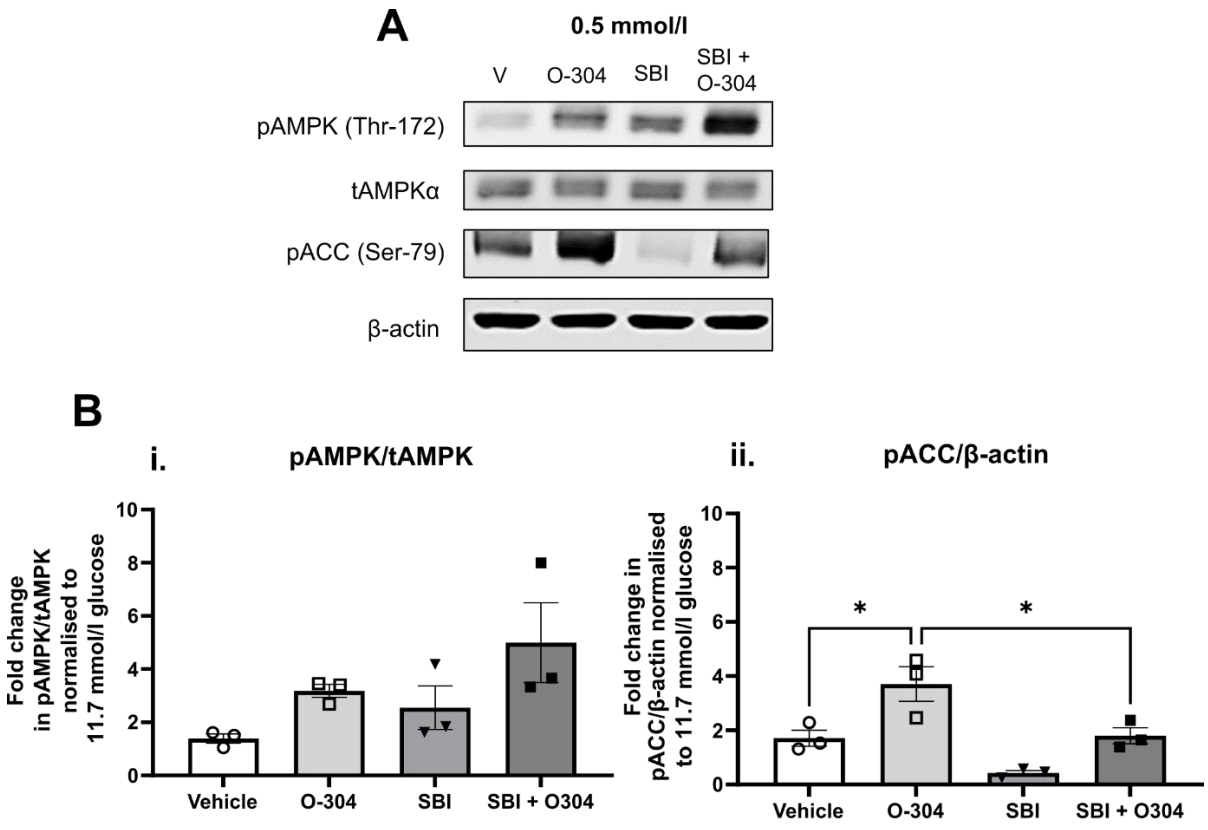

Figure 4.3: O-304 increased α-cell AMPK signalling cascade activation at low glucose.

αTC1.9 cells were incubated with 5.5 mmol/l glucose and preincubated with SBI-0206965 (SBI-, 30.0 µmol/l) for 30 min. Cells were subsequently incubated with 5.0 µmol/l O-304 ± SBI- for 1 h. **A.** Representative immunoblot for [0.5 mmol/l] glucose for phosphorylated AMPKα1/2 (pAMPK, Thr172), total AMPKα1/2 (tAMPK), phosphorylated ACC (pACC, Ser79) and beta-actin (β-actin). **B.** Densitometric analysis for **i.** pAMPK normalised to tAMPK (One-Way ANOVA with Tukeys multiple comparison test) **ii.** pACC normalised to β-actin (vehicle, 11.7 mmol/l) (One-Way ANOVA with Tukeys multiple comparison test) (n = 3, *P<0.05)

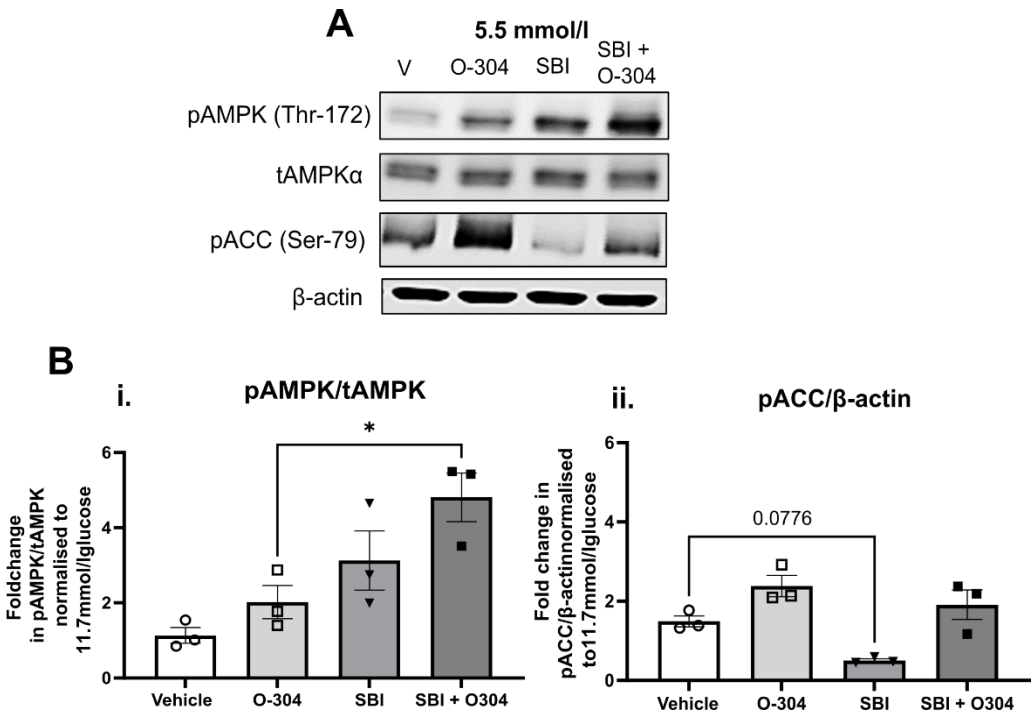

Figure 4.4: O-304 reduced α-cell AMPK signalling cascade activation at euglycaemic-like conditions.

αTC1.9 cells were incubated with 5.5 mmol/l glucose and preincubated with SBI-0206965 (SBI, 30 µmol/l) for 30 min. Cells were then subsequently exposed to 5.0 µmol/l O-304 for 1 h and lysate was harvested. **A.** Representative immunoblot for [5.5 mmol/l] glucose for phosphorylated AMPKα1/2 (pAMPK, Thr172), total AMPKα1/2 (tAMPK), phosphorylated ACC (pACC, Ser79) and beta-actin (β-actin). **B.** Densitometric analysis for **i.** pAMPK normalised to tAMPK (One-Way ANOVA with Tukeys multiple comparison test) **ii.** pACC normalised to β-actin at [11.7 mmol/l] glucose (One-Way ANOVA with Tukeys multiple comparison test) (n = 3, *P<0.05, **P<0.01)

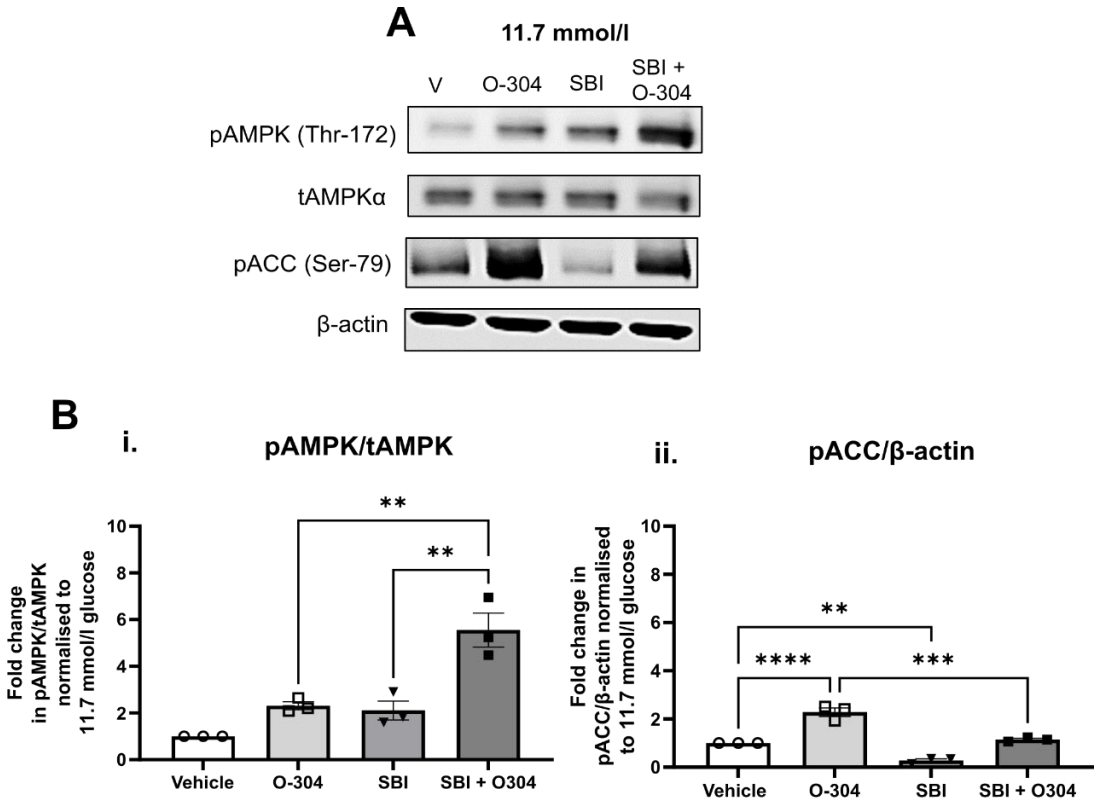

Figure 4.5: O-304 enhanced α-cell AMPK signalling cascade activation at hyperglycaemic-like conditions.

αTC1.9 cells were incubated with 5.5 mmol/l glucose and preincubated with SBI-0206965 (SBI-, 30 µmol/l) for 30 min. Cells were subsequently incubated with 5.0 µmol/l O-304 for 1 h. **A.** Representative immunoblot for [11.7 mmol/l] glucose for phosphorylated AMPKα1/2 (pAMPK, Thr172), total AMPKα1/2 (tAMPK), phosphorylated ACC (pACC, Ser79) and beta-actin (β-actin). **B.** Densitometric analysis for **i.** pAMPK normalised to tAMPK (One-Way ANOVA with Tukeys multiple comparison test) **ii.** pACC normalised to β-actin at [11.7 mmol/l] glucose (One-Way ANOVA with Tukeys multiple comparison test) (n = 3, *P<0.05, **P<0.01, ***P<0.001, ****P<0.0001)

4.2.2 Glucose utilisation

4.2.2.1 O-304 and SBI- concentration-dependent actions on α-cell bioenergetics.

To determine an optimal [O-304] and [SBI] to use in further metabolic studies, SBI was preincubated (0 – 100 µmol/l, ~30 min) prior to O-304 acute injection (0 – 5.0 µmol/l) (at ~18 min following start of assay) and following high glucose acute injection (11.7 mmol/l) (at ~42 min following start of assay).

4.2.2.2 O-304 and SBI influence α-cell bioenergetics in glucose-free conditions.

SBI, at all concentrations used, lowered basal extracellular acidification rate (ECAR) (mpH/min/µg) (-; 2.524 ± 0.07752, 30; 2.099 ± 0.08460, - *vs 30, p = 0.0008,* 50; 2.085 ± 0.08901, - *vs 50, p = 0.0002,* 100; 1.923 ± 0.05786, - *vs 100, p < 0.0001*) (Figure 4.6A). SBI- also reduced basal OCR compared to vehicle (-) in glucose-free, standard Seahorse XF DMEM medium (containing pyruvate and L-glutamine) (pmol/min/µg) (-; 36.53 ± 0.8140, 30; 30.18 ± 0.9027, - *vs 30, p < 0.0001,* 50; 31.28 ± 0.8100, - *vs 50, p = 0.0002,* 100; 28.72 ± 0.5628, - *vs 100, p < 0.0001*) (Figure 4.6B).

Acute O-304 injection concentration-dependently enhanced both glucose utilisation ($\Delta ECAR_{MAX}$) (mpH/min/µg) (Vehicle; -0.08517 ± 0.04248, 1.0; 0.6218 ± 0.07987, *Vehicle vs 1.0, p < 0.0001,* 2.5; 1.029 ± 0.06358, *Vehicle vs 2.5, p > 0.0001, 1.0 vs 2.5*:, *p = 0.0005,* 5.0; 1.211 ± 0.07436, *Vehicle vs 5.0, p > 0.0001*) (Figure 4.6D). In addition, acute O-304 injection concentration-dependently increased mitochondrial respiration (ΔOCR_{MAX}) in standard Seahorse XF DMEM medium, as mentioned above (pmol/min/µg) (Vehicle; -1.185 ± 0.2200, 1.0; 9.150 ± 0.8411, *Vehicle vs 1.0, p < 0.0001,* 2.5; 15.58 ± 0.8451, *Vehicle vs 2.5, p < 0.0001, 1.0 vs 2.5, p < 0.0001,* 5.0; 17.49 ± 0.5917, *Vehicle vs 5.0, p < 0.0001*) (Figure 4.6C).

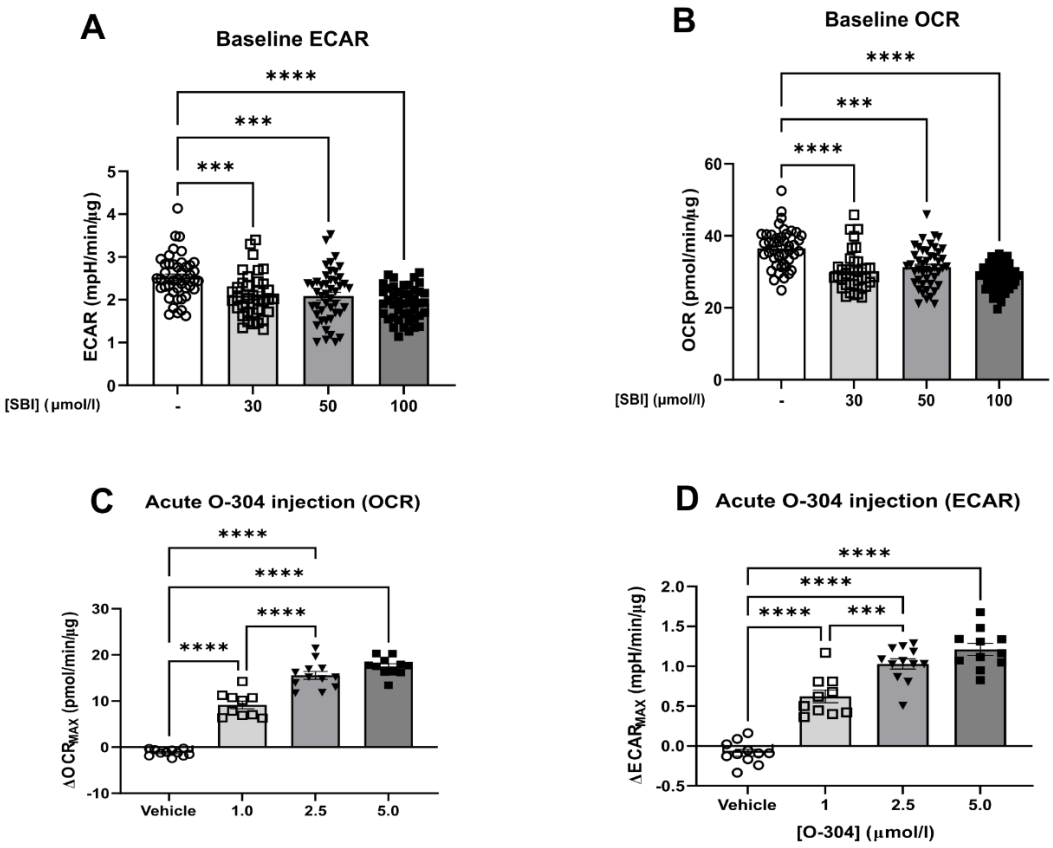

Figure 4.6: Both AMPK activation and AMPK inhibition regulate α-cell glycolysis and oxidative respiration in glucose-free conditions.

αTC1.9 cells were preincubated in standard Seahorse XF DMEM medium with SBI-0206965 (SBI; 0 – 100 µmol/l) for ~ 27 minutes prior to O-304 (0 - 5.0 µmol/l) and subsequent glucose (11.7 mmol/l) injection. **A.** Baseline ECAR (One-Way ANOVA with Dunnetts multiple comparison test) **B.** OCR prior to O-304 injection (Kruskal-Wallis with Dunn's multiple comparison test). **C.** acute ΔOCR_{MAX} post-O-304 (0 - 5.0 µmol/l) injection and **D.** Acute $\Delta ECAR_{MAX}$ post-O-304 (0 - 5.0 µmol/l) injection calculated from maximal ECAR – average baseline (One-Way ANOVA with Tukey's multiple comparison test) (n = 10 -12, two separate plates, *P ≤ 0.05, **P≤ 0.01, ***P≤0.001, ****P≤0.0001).

4.2.2.3 SBI- ameliorates O-304-dependent glucose utilisation in a concentration-dependent manner.

Increasing [SBI] did not alter O-304 (1.0 µmol/l) enhanced α-cell $\Delta ECAR_{MAX}$ after 11.7 mmol/l glucose injection (mpH/min/µg) (-; 0.6218 ± 0.07987, 30; 0.5836 ± 0.06069, 50; 0.7021 ± 0.07945, 100; 0.6633 ± 0.0764) (Figure 4.7C). Similarly, [SBI] did not change ΔOCR_{MAX} (-; 9.150 ± 0.8411, 30; 8.322 ± 0.8740, 50; 8.420 ± 0.5014, 100; 7.340 ± 0.7284) (Figure 4.7D). Post-glucose injection, 100 µmol/l SBI- significantly reduced maximum OCR (OCR_{MAX}) (pmol/min/µg) (-; 44.67 ± 2.213, 30; 40.72 ± 3.2, 50; 40.03 ± 1.679, 100; 34.73 ± 1.695, - *vs 100, p = 0.0046*) (Figure 4.7F). However, 100 µmol/l did not influence maximal ECAR ($ECAR_{MAX}$) (-; 7.298 ± 0.9064, 30; 6.597 ± 0.7128, 50; 6.309 ± 0.8106, 100; 5.686 ± 0.5930) (Figure 4.7E). 100 µmol/l SBI also did not influence $\Delta ECAR_{MAX}$ (-; 3.921 ± 0.07192, 30; 3.575 ± 0.573, 50; 3.287 ± 0.5466, 100; 3.038 ± 0.5108) (Figure 4.7G).

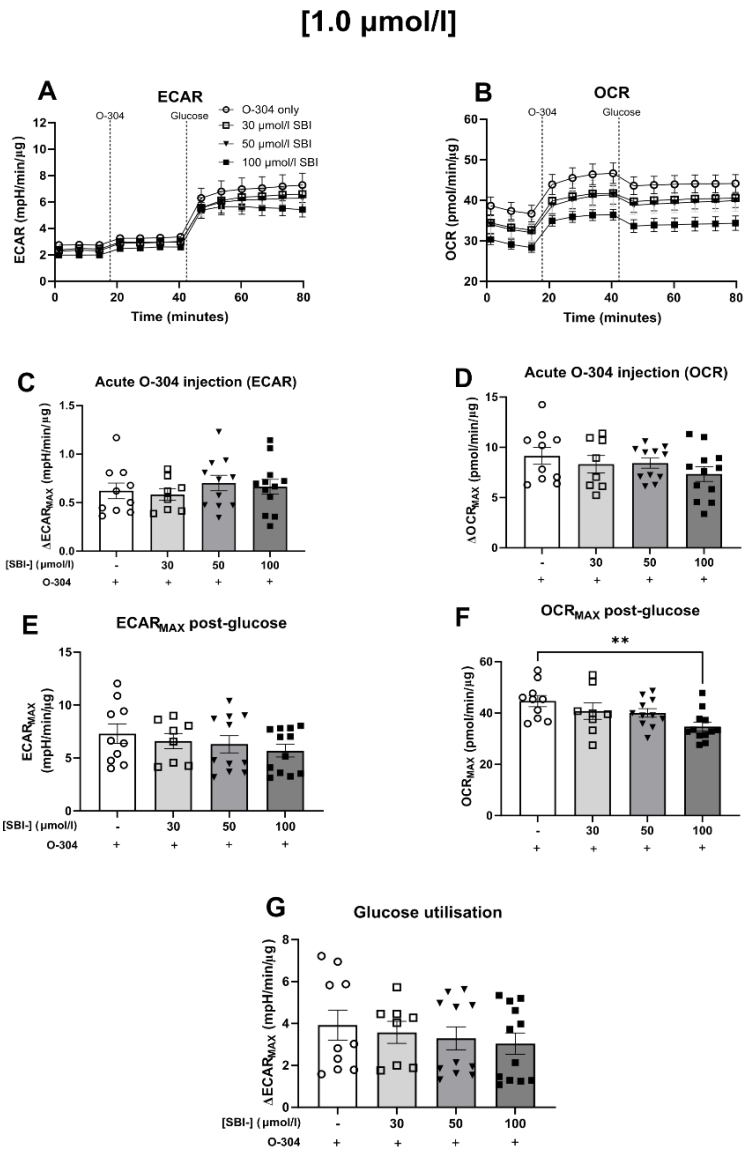

Figure 4.7: Increasing [SBI-0206965] does not alter 1.0 µmol/l O-304-enhanced α-cell glycolysis and oxidative metabolism.

αTC1.9 cells were preincubated in standard Seahorse XF DMEM medium with SBI-0206965 (SBI, 30.0 – 100 µmol/l) for ~ 30 minutes prior to O-304 (1.0 µmol/l) and subsequent glucose (11.7 mmol/l) injection. **A.** Representative extracellular acidification rate (ECAR, mpH/min/µg) and **B.** oxygen consumption rate (OCR, pmol/min/µg) traces **C.** $\Delta ECAR_{MAX}$ (maximal ECAR – average baseline) (One-Way ANOVA with Dunnetts multiple comparison test) and **D.** ΔOCR_{MAX} (maximal OCR – average baseline) (One-Way ANOVA with Dunnetts multiple comparison test) changes were calculated post O-304 injection. **E.** Maximal ECAR ($ECAR_{MAX}$) post glucose injection and **F.** Maximal OCR (OCR_{MAX}) post glucose injection (One-Way ANOVA with Dunnetts multiple comparison test) was calculated, alongside **G.** glucose utilisation from $ECAR_{MAX}$ post-glucose measurements – average $ECAR_{MAX}$ measurements post-O-304 injection (Kruskal-Wallis test with Dunns multiple comparison test) (n = 8 - 12, **P≤ 0.01)

After 2.5 µmol/l O-304 acute injection, only 100 µmol/l SBI- reduced O-304-enhanced $\Delta ECAR_{MAX}$ in α-cells (-; 1.029 ± 0.06358, 30; 0.9278 ± 0.05156, 50; 0.9647 ± 0.05649, 100; 0.7599 ± 0.08968, - *vs 100, p = 0.0179*) (Figure 4.8B). This effect was similarly displayed in ΔOCR_{MAX} (-; 15.58 ± 0.8451, 30; 12.73 ± 1.124, 50; 13.04 ± 0.9114, 100; 9.694 ± 1.085, - *vs 100, p = 0.0003*) (Figure 4.8D). Representative X-Y ECAR and OCR depicts significantly lower α-cell bioenergetics, dependent on [SBI]-, pre- and post-O-304 (2.5 µmol/l) treatment (Figure 4.8A-B). Post-glucose injection, increasing [SBI]-concentration-dependently reduced $ECAR_{MAX}$ (-; 8.138 ± 0.4671, 30; 6.498 ± 0.2802, - *vs 30, p = 0.0228,* 50; 6.037 ± 0.4816, - *vs 50, p = 0.0016,* 100; 5.169 ± 0.2987, - *vs 100, p < 0.0001*) (Figure 4.8E). Similarly, increased [SBI]- incubation concentration-dependently reduced OCR_{MAX} post-glucose injection (-; 50.79 ± 1.937, 30; 40.82 ± 2.342, - *vs 30, p = 0.0193,* 50; 43.63 ± 2.220, - *vs 50, p = 0.0957,* 100; 37.10 ± 3.058, - *vs 100, p = 0.0006*) (Figure 4.8F). $\Delta ECAR_{MAX}$ following glucose injection similarly inhibited with increased [SBI]- preincubation (-; 4.619 ± 0.4110, 30; 3.643 ± 0.2908, - *vs 30, p = 0.1647,* 50; 3.119 ± 0.387, - *vs 50, p = 0.0111,* 100; 2.610 ± 0.307, - *vs 100, p = 0.0006*) (Figure 4.8G).

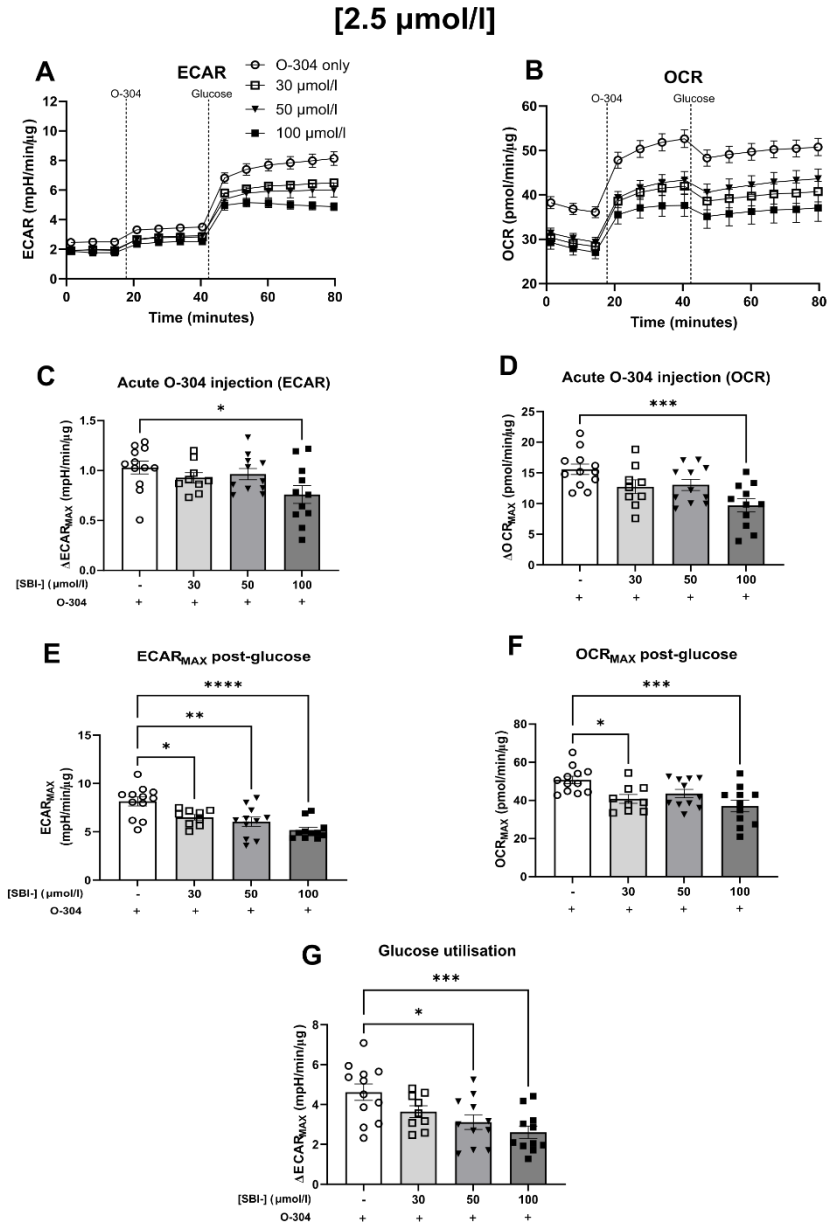

Figure 4.8: Increasing [SBI-0206965] reduced 2.5 µmol/l O-304-enhanced α-cell glycolysis and oxidative metabolism.

αTC1.9 cells were preincubated in standard Seahorse XF DMEM medium with SBI-0206965 (30 – 100 µmol/l) for ~ 30 minutes prior to O-304 (2.5 µmol/l) and subsequent glucose (11.7 mmol/l) injection. **A.** Representative extracellular acidification rate (ECAR, mpH/min/µg) and **B.** oxygen consumption rate (OCR, pmol/min/µg) traces **C.** $\Delta ECAR_{MAX}$ (maximal ECAR – average baseline) (One-Way ANOVA with Dunnetts multiple comparison test) and **D.** ΔOCR_{MAX} (maximal OCR – average baseline) (One-Way ANOVA with Dunnetts multiple comparison test) changes were calculated post O-304 injection. **E.** Maximal ECAR ($ECAR_{MAX}$) post glucose injection and **F.** Maximal OCR (OCR_{MAX}) post glucose injection (One-Way ANOVA with Dunnetts multiple comparison test) was calculated, alongside **G.** glucose utilisation from $ECAR_{MAX}$ post-glucose measurement – $ECAR_{MAX}$ measurement post-O-304 injection (One-Way ANOVA with Dunnetts multiple comparison test) (n = 9 - 12, *P ≤ 0.05, **P≤ 0.01, ***P≤0.001, ****P≤0.0001)

Increasing [SBI] preincubation reduced ΔOCR_{MAX} following O-304 (5.0 µmol/l) exposure in glucose-free conditions (-; 17.49 ± 0.5917, 30; 13.50 ± 0.9135, - *vs 30, p = 0.0102*, 50; 15.27 ± 0.8593, 100; 11.19 ± 1.130) (Figure 4.9D). Similarly, 5.0 µmol/l O-304 acute-enhanced $\Delta ECAR_{MAX}$ was attenuated with increasing [SBI]- (-; 1.211 ± 0.07436, 30; 0.940 ± 0.06124, - *vs 30, p = 0.0553,* 50; 1.139 ± 0.05642, 100; 0.9506 ± 0.1071, - *vs 100, p = 0.0567*) (Figure 4.9C). Representative X-Y ECAR (Figure 4.9A) and OCR (Figure 4.9B) traces are displayed in Figure 4.9A-B. Furthermore, all [SBI]- treatments reduced 5.0 µmol/l O-304-dependent $ECAR_{MAX}$ (-; 9.442 ± 0.4306, 30; 7.619 ± 0.4914, - *vs 30, p = 0.0256,* 50; 7.447 ± 0.4737, - *vs 50, p = 0.0093,* 100; 6.505 ± 0.4486, - *vs 100, p = 0.0002)* (Figure 4.9E). All [SBI]- reduced O-304-dependent OCR_{MAX} (-; 54.67 ± 1.70, 30; 44.62 ± 2.095, - *vs 30, p = 0.0122,* 50; 43.63 ± 2.220, - *vs 50, p = 0.0044,* 100; 36.53 ± 2.850, - *vs 100, p < 0.0001*) (Figure 4.9F). Although a not statistically significant trend in $\Delta ECAR_{MAX}$ was observed at 50.0 µmol/l SBI-, only 100 µmol/l SBI- attenuated O-304-enhanced $\Delta ECAR_{MAX}$ (-; 5.554 ± 0.4898, 30; 4.489 ± 0.4501, 50; 4.046 ± 0.4471, - *vs 50, p = 0.0922,* 100; 3.522 ± 0.491, - *vs 100, p = 0.0289*) (Figure 4.9G).

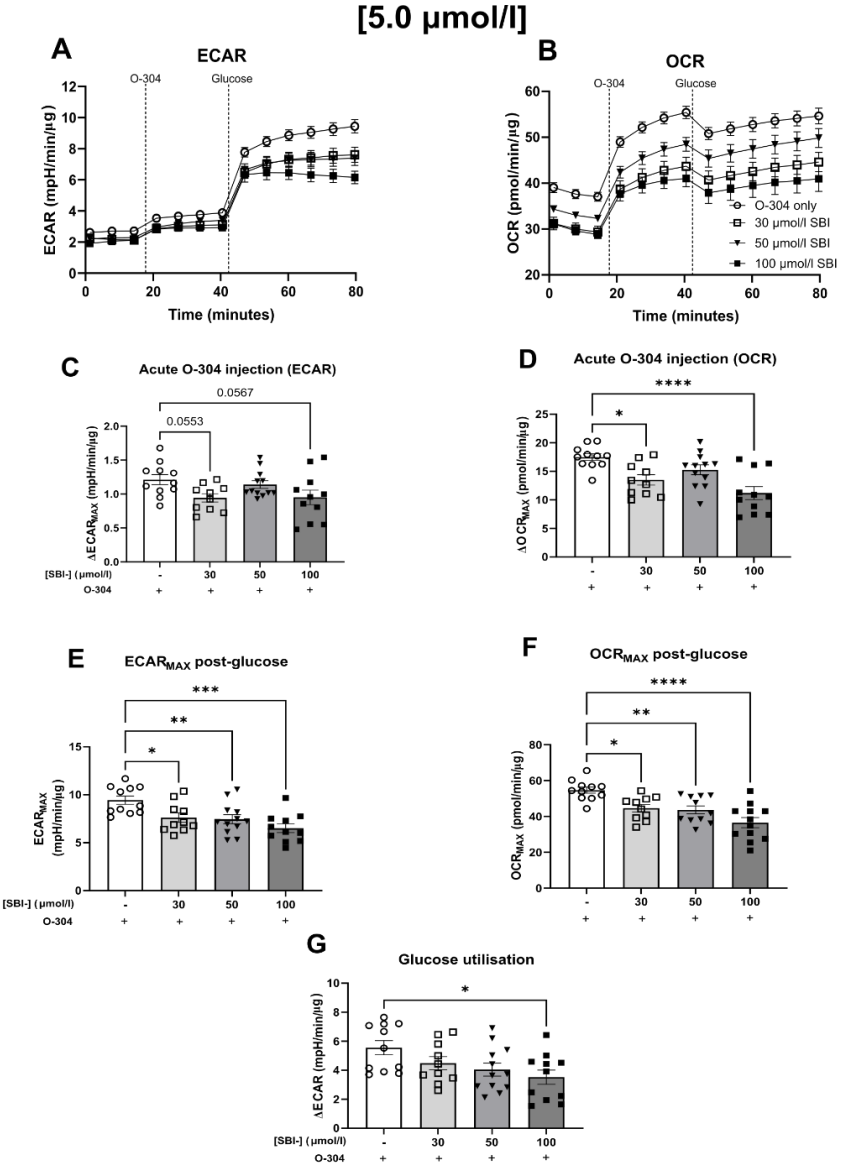

Figure 4.9: Increasing [SBI-0206965] significantly reduced 5.0 µmol/l O-304-enhanced α-cell glycolysis and oxidative metabolism.

αTC1.9 cells were preincubated in standard Seahorse XF DMEM medium with SBI-0206965 (30 – 100 µmol/l) for ~ 30 minutes prior to O-304 (5.0 µmol/l) and subsequent glucose (11.7 mmol/l) injection. **A.** Representative extracellular acidification rate (ECAR, mpH/min/µg) and **B.** oxygen consumption rate (OCR, pmol/min/µg) traces **C.** $\Delta ECAR_{MAX}$ (maximal ECAR – average baseline) (One-Way ANOVA with Dunnetts multiple comparison test) and **D.** ΔOCR_{MAX} (maximal OCR – average baseline) (One-Way ANOVA with Dunnetts multiple comparison test) changes were calculated post O-304 injection. **E.** Maximal ECAR ($ECAR_{MAX}$) post glucose injection and **F.** Maximal OCR (OCR_{MAX}) post-glucose injection (One-Way ANOVA with Dunnetts multiple comparison test) was calculated, alongside **G.** glucose utilisation from $ECAR_{MAX}$ post-glucose measurement – maximum ECAR measurement post-O-304 injection (Kruskal-Wallis test with Dunn's multiple comparison test) (n = 10 - 12, *P ≤ 0.05, **P≤ 0.01, ***P≤0.001, ****P≤0.0001)

4.2.2.4 O-304 acute injection did not affect media pH

To eliminate the possibility of O-304 acidifying the extracellular media and altering ECAR values, rather than direct α-cell metabolic regulation, pH measurements were analysed from blank (no cells, n = 1) and cell-containing wells (n = 3) that had no SBI- treatment and ± 5.0 µmol/l O-304 injection from one plate. Representative X-Y pH trace showed vehicle vs O-304 measurements (± cells) (Figure 4.10A). Figure 4.10B found no significant media pH changes post-O-304 injection in cell-containing wells (Vehicle; 7.386 ± 0.01397, O-304; 7.373 ± 0.005321).

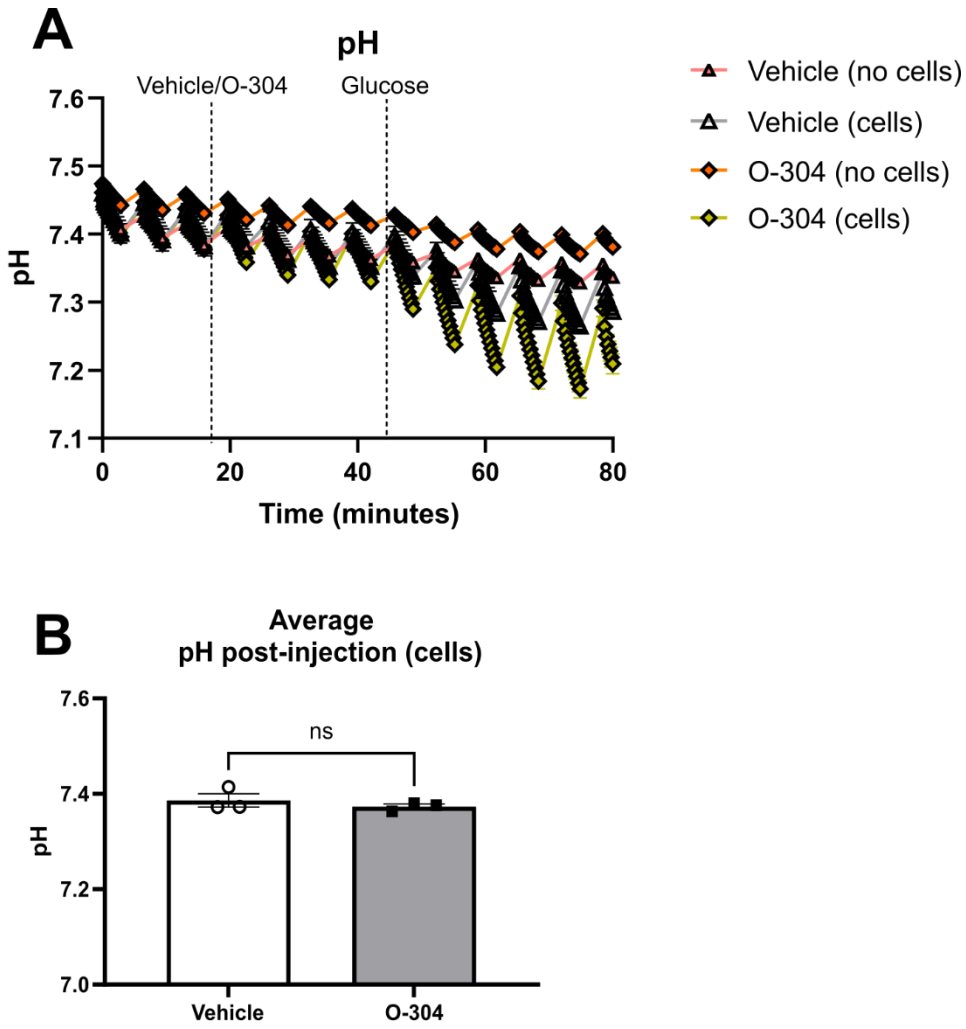

Figure 4.10: Acute injection of O-304 and α-cell extracellular media pH.

αTC1.9 cells were preincubated vehicle (no SBI-0206965) for 30 min in normal glucose conditions, and subsequently exposed to O-304 (5.0 µmol/l) for 1 h. **A.** Representative trace depicting pH changes in extracellular media (vehicle, no cells; O-304, no cells, n =1 each; vehicle, cells; O-304; cells, n = 3) over experiment time, **B.** Mean pH post-O-304 injection (n = 3, Unpaired two-tailed t-test, n/s; not significant)

4.2.2.5 O-304 enhanced α-cell glucose utilisation in a glucose-dependent and AMPK-dependent manner

α-cells were exposed to SBI (30.0 µmol/l, 30 min) in 5.5 mmol/l glucose-containing standard Seahorse XF DMEM medium, prior to O-304 (5.0 µmol/l) ± SBI addition for 1 h in glucose-free standard Seahorse XF medium. O-304 enhanced, compared to vehicle, basal ECAR in the absence of glucose and standard Seahorse XF DMEM medium (mpH/min/µg) (Vehicle; 1.850 ± 0.1364, O-304; 3.572 ± 0.1742, *Vehicle vs O-304,* $p < 0.0001$, SBI; 1.613 ± 0.07746, SBI + O-304; 3.497 ± 0.1585) (Figure 4.11C). O-304 similarly enhanced baseline OCR ≥ 2-fold prior to glucose injection in an SBI-insensitive manner (pmol/min/µg) (Vehicle; 27.69 ± 1.438, O-304; 65.31 ± 3.252, SBI; 26.58 ± 1.057, SBI + O-304; 58.21 ± 2.997) (Figure 4.11D). O-304 did not alter $\Delta ECAR_{MAX}$ after 0.5 mmol/l glucose injection, however, it is attenuated following [SBI-] pre-treatment (mpH/min/µg) (Vehicle; 0.3711 ± 0.04928, O-304; 0.4447 ± 0.07927, SBI; 0.1791 ± 0.0369, *Vehicle vs SBI, $p = 0.0745$*, SBI + O-304; 0.01705 ± 0.04183, *O-304 vs SBI + O-304, $p < 0.001$*) (Figure 4.11Ai-ii). In the presence of high (11.7 mmol/l) extracellular glucose, O-304 significantly enhanced $\Delta ECAR_{MAX}$ and SBI- ameliorates this effect (mpH/min/µg) (Vehicle; 1.266 ± 0.1290, O-304; 3.812 ± 0.3510, *Vehicle vs O-304, $p < 0.0001$,* SBI; 0.9527 ± 0.06362, SBI + O-304; 2.425 ± 0.2156, *O-304 vs SBI + O-304, $p = 0.0003$*) (Figure 4.11Bi-ii).

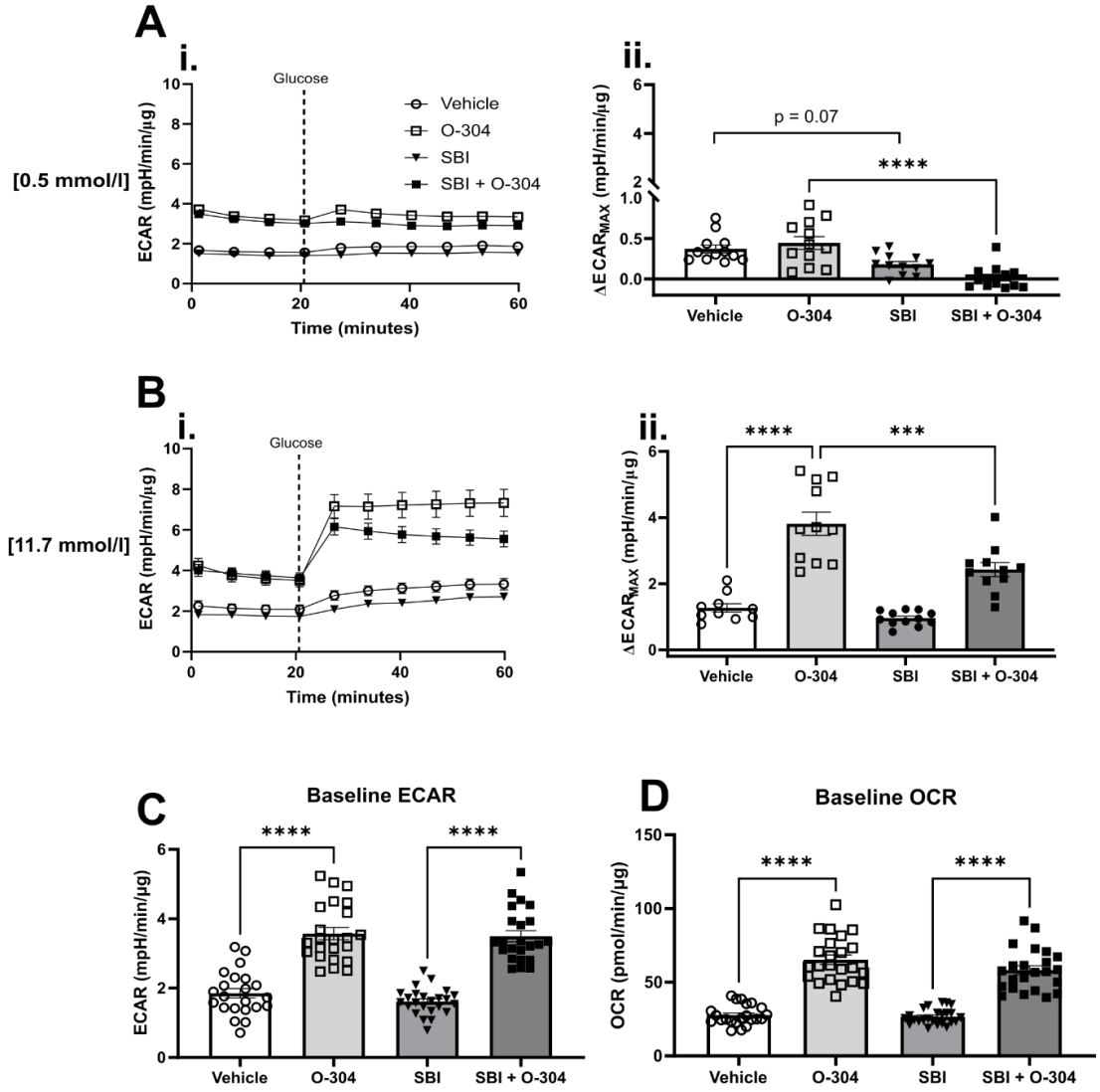

Figure 4.11: O-304 enhanced α-cell glucose utilisation in both a glucose- and AMPK-sensitive manner.

αTC1.9 cells were preincubated with SBI-0206965 (SBI; 30.0 µmol/l) in glucose-containing, standard Seahorse XF DMEM media (5.5 mmol/l) for 30 min and subsequently exposed to O-304 (5.0 µmol/l) in the absence of glucose for 1 h. **A-B i.** Normalised representative traces depicting changes extracellular acidification rate (ECAR) following glucose injection (0.5 – 11.7 mmol/l) injections into surrounding extracellular media at the indicated time point **A-B ii.** $\Delta ECAR_{MAX}$, or glucose utilisation, was calculated from maximum ECAR reading ($ECAR_{MAX}$) following glucose injection minus average baseline ECAR readings (One Way ANOVA with Tukey's multiple comparison test) **C.** Normalised average baseline ECAR prior to glucose injection (Kruskal-Wallis test with Dunn's multiple comparison test) **D.** Normalised average baseline OCR prior to glucose injection (Kruskal-Wallis test with Dunn's multiple comparison test) (n = 10 - 12 (two separate plates), ***P ≤ 0.001, ****P ≤ 0.0001)

4.2.2.6 β-cell glycolysis and oxidative metabolism is enhanced by O-304 exposure but did not influence glucose utilisation.

To assess whether O-304 would influence glucose utilisation in another islet cell type, human β-cell line EndoC-βH1 cells were incubated ± O-304 (5.0 µmol/l) for 1 h in standard Seahorse XF DMEM medium prior to acute injection of increasing [glucose] (0.5 – 11.7 mmol/l) into the surrounding extracellular media.

O-304 enhanced baseline ECAR in β-cells (mpH/min/µg) (Vehicle; 1.237 ± 0.07215, O-304; 1.790 ± 0.07455, $p < 0.0001$) (Figure 4.12A). Furthermore, O-304 increased basal OCR by up to 1.5-fold in glucose-free conditions (pmol/min/µg) (Vehicle; 15.54 ± 0.5945, O-304; 24.26 ± 1.122) (Figure 4.12B). O-304 did not significantly $\Delta ECAR_{MAX}$ after 0.5 – 11.7 mmol/l acute injection (Figure 4.13A-Cii). Normalised ECAR traces are displayed in Figure 4.13A-Ci (0.5: Vehicle; - 0.04785 ± 0.048, O-304; -0.05971 ± 0.04069, 5.5: Vehicle; 0.3796 ± 0.01715, O-304; 0.3690 ± 0.05542, 11.7: Vehicle; 0.7529 ± 0.04501, O-304; 0.7139 ± 0.07286).

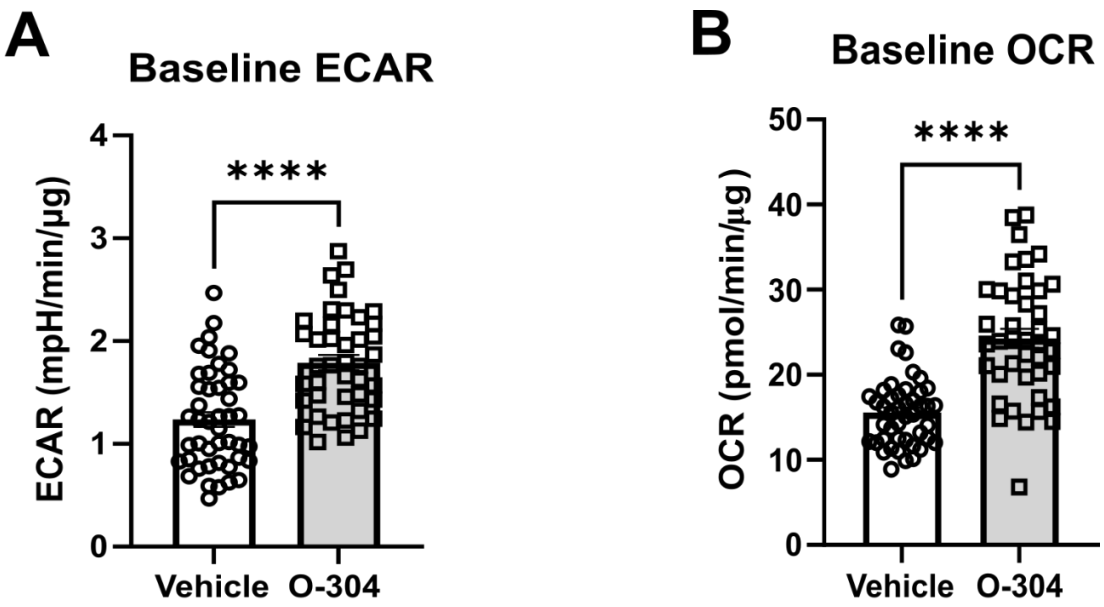

Figure 4.12: O-304 increased human β-cell basal ECAR and OCR.

EndoC-βH1 cells were exposed to O-304 (5.0 µmol/l) in standard Seahorse XF DMEM media for 1 h. Baseline **A.** ECAR and **B.** OCR were calculated from average three baseline measurements prior to injection (Unpaired two-tailed t-test, n = 41 – 45, two separate plates, ****P<0.0001)

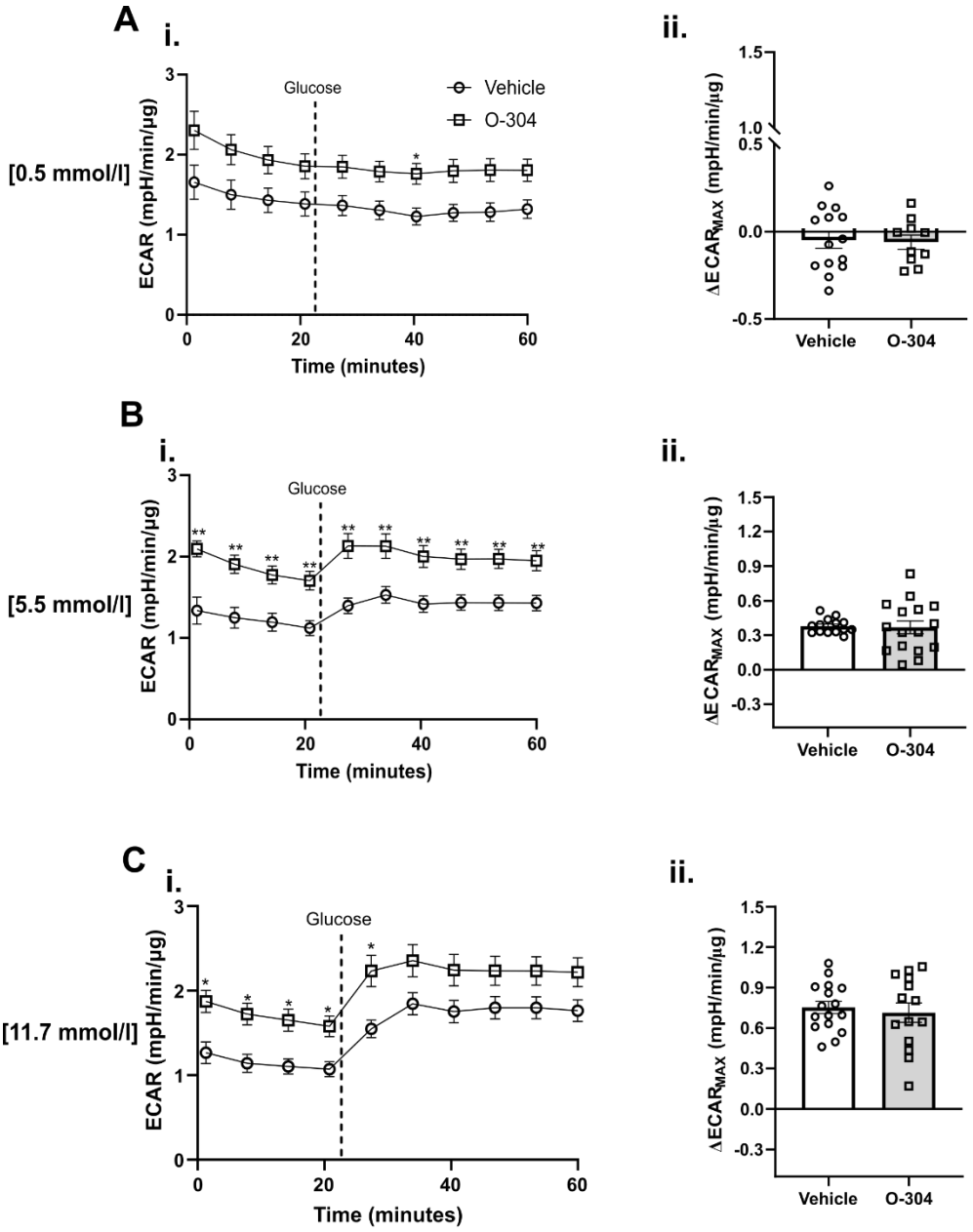

Figure 4.13: O-304 increased human β-cell ECAR, but not glucose utilisation.

EndoC-βH1 cells were exposed to O-304 (5.0 µmol/l) in standard Seahorse XF DMEM media for 1 h and after ~ 24 min, either **A.** 0.5, **B.** 5.5 or **C.** 11.7 mmol/l glucose was injected into the extracellular media. **A-C i**. Representative extracellular acidification rate (ECAR, Multiple unpaired t-tests with Holm-Šídák multiple comparison test) traces and **A-C ii.** $\Delta ECAR_{MAX}$ was calculated from maximal ECAR measurement post-injection minus average three baseline measurements prior to injection (Unpaired two-tailed t-test) (n = 10 - 16, two separate plates, *P < 0.05).

4.2.3 Lactate secretion

4.2.3.1 Lactate secretion was increased upon O-304 treatment in a glucose-dependent manner.

Lactate is both a glycolytic end product for energy generation and potential autocrine regulator of α-cell glucagon secretion cellular signalling is lactate. Monocarboxylate transporters (MCTs) expressed on the plasma membrane export lactate after glycolytic generation, resulting in media extracellular acidification. Extracellular acidification rate (ECAR) is an indicator of lactate-derived acidification and mitochondrial proton export, with the buffer capacity of the medium can contribute to measured ECAR (Zaborska *et al.*, 2020). Therefore, to determine if O-304-driven glycolysis alters lactate secretion, extracellular L-lactate was measured following 2 h (a similar time duration to study 4.2.2.5) ± O-304 (5.0 µmol/l) and L-lactate secretion was measured by normalisation to total protein. O-304 treatment (2 h) enhanced L-lactate secretion in a glucose-sensitive manner (µM/µg) (0.5: Vehicle; 152.38 ± 17.116, O-304; 364.085 ± 18.963, $p < 0.0001$, 11.7: Vehicle; 56.012 ± 0.849, *0.5 Vehicle vs 11.7 Vehicle P = 0.0010,* O-304; 65.135 ± 4.960) (Figure 4.14).

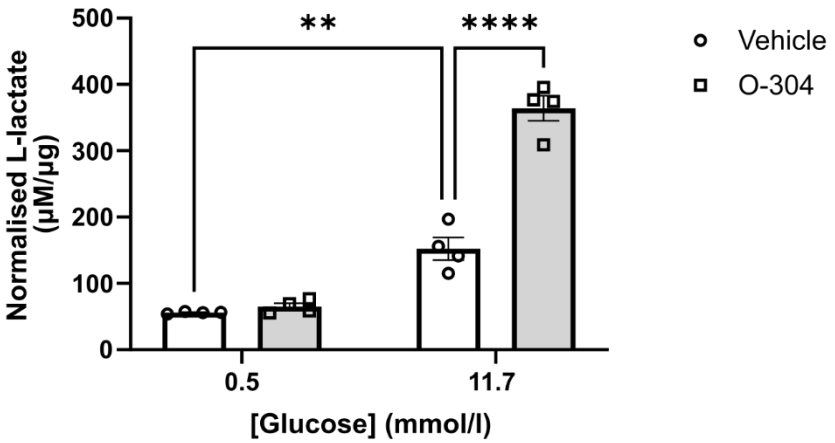

Figure 4.14: O-304 increased α-cell L-lactate secretion in a glucose-dependent manner after 2 h treatment.

αTC1.9 cells were exposed to O-304 (5.0 µmol/l) for 2 h and supernatant was removed for measuring extracellular L-lactate and normalised to total protein to calculate L-lactate secretion (Two-Way ANOVA with Tukey's multiple comparisons test) (n= 4, ** P > 0.01, ****P>0.0001).

4.2.3.2 O-304 enhanced α-cell glucose-dependent lactate secretion, in an AMPK-dependent manner.

To determine whether the observed increases in lactate secretion following O-304 exposure are AMPK-dependent, media supernatants were collected from O-304 treatment for 1 h) for lactate analysis. Similarly, O-304 did not alter L-lactate secretion after 0.5 mmol/l glucose exposure (µM/µg) (Vehicle; 84.922 ± 7.304, O-304; 97.577 ± 12.822, SBI; 82.688 ± 10.652, SBI + O-304; 84.758 ± 5.845). At 5.5 mmol/l glucose, O-304 enhanced L-lactate secretion was attenuated by SBI- preincubation (µM/µg) (Vehicle; 138.866 ± 7.891, O-304; 186.608 ± 20.778, *Vehicle vs O-304, p = 0.0114,* SBI; 87.586 ± 6.966, *Vehicle vs SBI, p = 0.0063,* SBI + O-304; 93.7 ± 11.613, *O-304 vs SBI + O-304, p < 0.0001*). Further rises in extracellular [glucose] availability (11.7 mmol/l) increased O-304-dependent L-lactate secretion and was similarly inhibited by SBI- treatment (µM/µg) (Vehicle; 133.435 ± 5.471, O-304; 228.148 ± 8.613, *Vehicle vs O-304, p < 0.0001,* SBI; 88.517 ± 2.492, *Vehicle vs SBI, p = 0.0183,* SBI + O-304; 95.744 ± 4.603, *O-304 vs SBI + O-304, p < 0.0001*) (Figure 4.15).

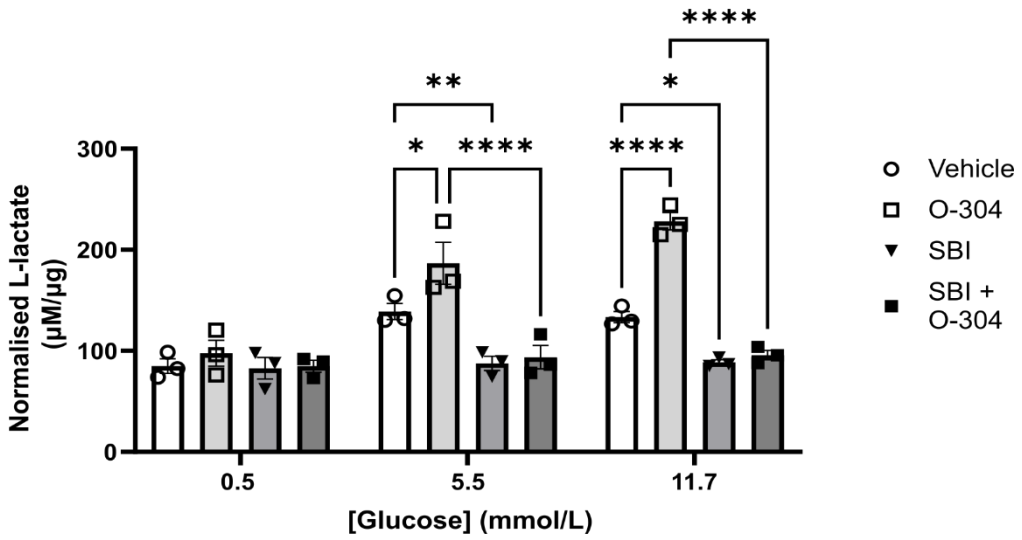

Figure 4.15: O-304 enhanced α-cell L-lactate secretion in an AMPK and glucose-dependent manner after 1 h.

αTC1.9 cells were exposed to 5.5 mmol/l glucose and preincubated with SBI-0206965 (SBI, 30 µmol/l) for 30 min. Cells were exposed with 5.0 µmol/l O-304 for 1 h and supernatant was removed for measuring extracellular L-lactate and normalised to total protein to calculate L-lactate secretion (n = 3, Two-Way ANOVA with Tukey's multiple comparison test, *P>0.05, **P>0.01, ***P>0.001, ****P>0.0001)

4.2.4 Alternative substrate utilisation

4.2.4.1 Glutamine and pyruvate utilisation

Previous studies described in this chapter have demonstrated O-304 treatment can enhance basal glycolysis and oxidative metabolism in glucose-free and glutamine/pyruvate-containing conditions. To test the idea that O-304 will enhance acute pyruvate and L-glutamine utilisation in α-cells, cells were incubated in no glucose, glutamine or pyruvate for > 1 h prior to acute glutamine (2.0 mmol/l) or pyruvate (2.5 mmol/l) injection.

4.2.4.2 O-304 did not alter α-cell acute pyruvate or glutamine utilisation.

Comparing substrate utilisation using vehicle alone data, α-cells have greater ΔOCR_{MAX} after acute pyruvate, compared to glutamine, reintroduction ($p < 0.0001$) (Figure 4.16B).

O-304 and SBI pre-treatment did not influence basal ECAR prior to substrate injection (mpH/min/µg) (Vehicle; 0.6994 ± 0.06224, O-304; 0.6985 ± 0.05598, SBI; 0.6886 ± 0.07192, SBI + O-304; 0.6821 ± 0.06731) (Figure 4.17C). In addition, O-304 or SBI did not alter α-cell acute pyruvate-derived $\Delta ECAR_{MAX}$ (mpH/min/µg) (Vehicle; 0.5393 ± 0.04491, O-304; 0.4874 ± 0.05541, SBI-; 0.5211 ± 0.06896, SBI + O-304; 0.5822 ± 0.06919) (Figure 4.17Bii). Glutamine-derived $\Delta ECAR_{MAX}$ displayed as a control for cell-independent, media acidification (mpH/min/µg) (Vehicle; - 0.02358 ± 0.08524, O-304; -0.2233 ± 0.04342, SBI; -0.09077 ± 0.06713, SBI + O-304; -0.1756 ± 0.03127) (Figure 4.17Bi). Representative ECAR traces are displayed in Figure 4.17Ai-ii.

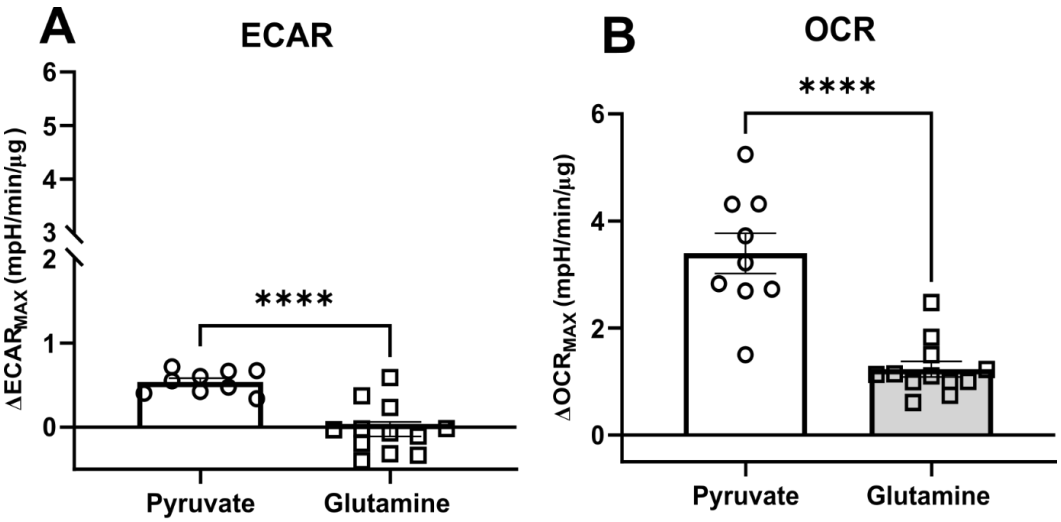

Figure 4.16: Pyruvate is a preferred substrate for α-cell glycolysis and oxidative metabolism, in comparison to L-glutamine.

αTC1.9 cells were pre-incubated with no glucose, pyruvate or L-glutamine-containing media for 1 h and both glutamine (2.0 mmol/l) or pyruvate (2.5 mmol/l) were injected into the extracellular media. **A.** $\Delta ECAR_{MAX}$ and **B.** ΔOCR_{MAX} were calculated from maximal ECAR/OCR measurement post-injection minus average baseline readings (Two-tailed unpaired t-test, ****P<0.0001, n = 9 – 12)

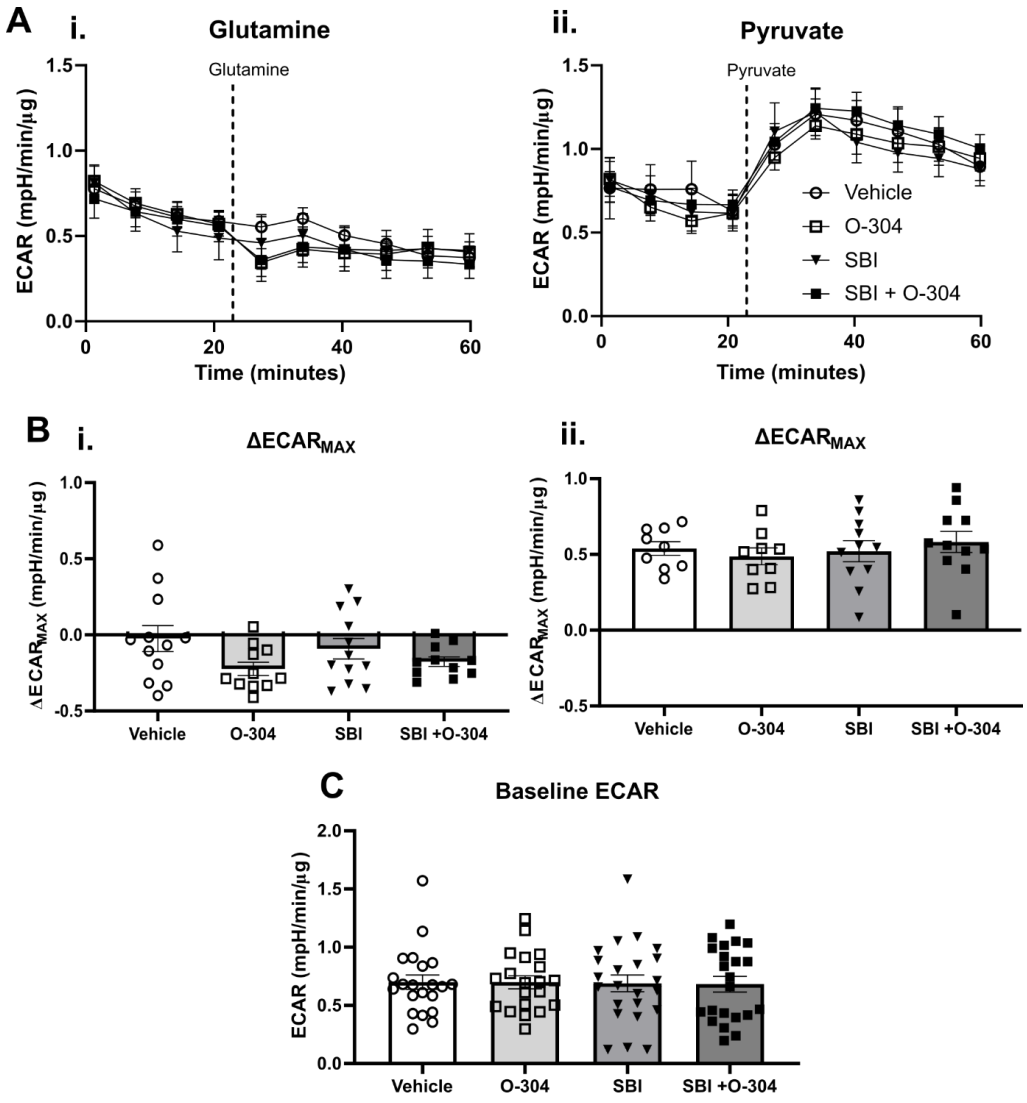

Figure 4.17: O-304 did not alter α-cell glycolysis following L-glutamine or pyruvate injection.

αTC1.9 cells were pre-incubated with SBI-0206965 (SBI, 30.0 µmol/l) for 30 min in 5.5 mmol/l glucose. Media was replaced with no glucose, pyruvate or L-glutamine-containing media ± O-304 (5.0 µmol/l) and SBI for an additional 1 h and both **A.** i. glutamine- and **A. ii.** pyruvate-induced extracellular acidification rate (ECAR) were injected into the media and subsequent B. $\Delta ECAR_{MAX}$ (maximum ECAR value post injection minus average baseline, n = 9 - 12) for **i.** pyruvate and **ii.** glutamine injection were calculated (One-Way ANOVA with Tukey's multiple comparison test). **C**. Baseline ECAR (average ECAR measurements prior to injection) were calculated (One-Way ANOVA with Tukey's multiple comparison test, n = 21 - 23) (two seperate plates)

Furthermore, O-304 did not modulate acute glutamine ΔOCR_{MAX} (Vehicle; 1.231 ± 0.1456, O-304; 1.088 ± 0.1712, SBI; 1.782 ± 0.3354, SBI + O-304; 1.407 ± 0.2625) (Figure 4.18Bi). SBI and O-304 exposure had an additive increase on pyruvate ΔOCR_{MAX} (Vehicle; 3.396 ± 0.3748, O-304; 3.520 ± 0.3513, *O-304 vs SBI + O-304, p = 0.0942,* SBI; 3.957 ± 0.2739, SBI + O-304; 4.631 ± 0.3129, *Vehicle vs SBI + O-304, p = 0.0522*) (Figure 4.18Bii). SBI increased basal OCR prior to substrate addition, however, SBI-enhanced OCR was attenuated by O-304 exposure (Vehicle; 8.264 ± 0.3804, O-304; 8.109 ± 0.3561, SBI; 10.19 ± 0.4973, *Vehicle vs SBI, p = 0.0055,* SBI + O-304; 8.522 ± 0.3407, *SBI vs SBI + O-304, p = 0.0192*) (Figure 4.18C).

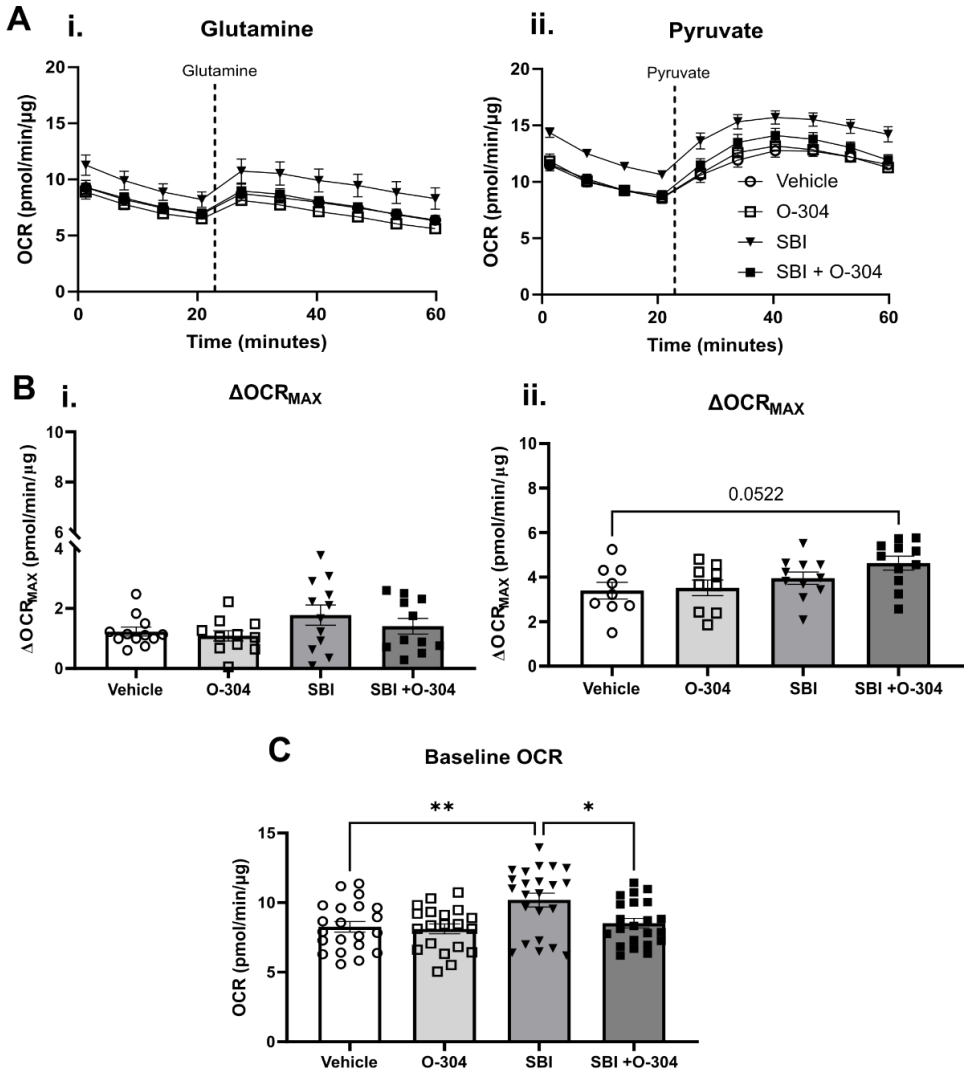

Figure 4.18: O-304 does not alter α-cell L-glutamine- or pyruvate-enhanced mitochondrial respiration.

αTC1.9 cells were pre-incubated with SBI-0206965 (SBI, 30.0 µmol/l) for 30 min in 5.5 mmol/l glucose. Media was replaced with no glucose, pyruvate or L-glutamine-containing media ± O-304 (5.0 µmol/l) and SBI-0206965 (SBI, 30 µmol/l) for an additional 1 h and both **A. i.** glutamine- and **A. ii.** pyruvate-induced oxygen consumption rate (OCR) was injected into the media and subsequent **B.** ΔOCR_{MAX} (maximum OCR value post injection minus average baseline, n = 21 -23) for **i.** pyruvate and **ii.** glutamine injections were calculated (One-Way ANOVA with Tukey's multiple comparison test). **C.** Baseline OCR (average OCR measurements prior to injection) were calculated (One-Way ANOVA with Tukey's multiple comparison test, *P>0.05, **P>0.01, n = 9 - 12, two separate plates).

4.2.4.3 Fructose and galactose utilisation

In hexokinase-expressing tissues (such as skeletal muscle and adipose tissue), fructose can be catabolised by glycolysis (Dholariya and Orrick, 2022). Similarly, galactose is primarily metabolised to glucose-6-phosphate in galactokinase (GALK-1)-expressing tissues, such as the liver, for glycogen synthesis (Holden, Rayment and Thoden, 2003; Sellick, Campbell and Reece, 2008).

Pilot work conducted by Dr. Ana Miguel Cruz examined whether **a.** α-cells utilise galactose and fructose for glycolysis and downstream oxidative metabolism and if so, **b.** whether O-304 modulates individual substrates' utilisation.

4.2.4.4 Fructose enhanced ECAR, in a concentration-dependent manner, by α-cells, compared to galactose.

Data provided in Figure 4.19 are the vehicle groups displayed in Figure 4.21 and Figure 4.22. Fructose, unlike galactose, increased α-cell $\Delta ECAR_{MAX}$ in a concentration-dependent manner (mpH/min/µg) (*2.5 Fruct vs 5.5 Fruct, p = 0.0025, 5.5 Fruct vs 11.7 Fruct, p < 0.0001)* (Figure 4.19). In addition, the magnitude of this increase in $\Delta ECAR_{MAX}$, at a high concentration, is relatively small in comparison to glucose (Figure 4.20) (mpH/min/µg) (Galactose; 0.2472 ± 0.05939, *galactose vs glucose, P < 0.0001,* Fructose; 1.150 ± 0.1391, *fructose vs glucose, P = 0.0008,* Glucose; 2.499 ± 0.2848).

0.5, 5.5 and 11.7 mmol/l fructose enhanced α-cell $\Delta ECAR_{MAX}$ greater than galactose at the same concentration (mpH/min/µg) (0.5: galactose; 0.128 ± 0.039, fructose; 0.347 ± 0.054, *0.5 Gal vs 0.5 Fruct, p = 0.0565,* 5.5: galactose; 0.309 ± 0.048, fructose; 0.643 ± 0.041, *5.5 Gal vs 5.5 Fruct, p < 0.0001,* 11.7: galactose; 0.247 ± 0.059, fructose; 1.150 ± 0.139, *11.7 Gal vs 11.7 Fruct, p < 0.0001*) (Figure 4.19).

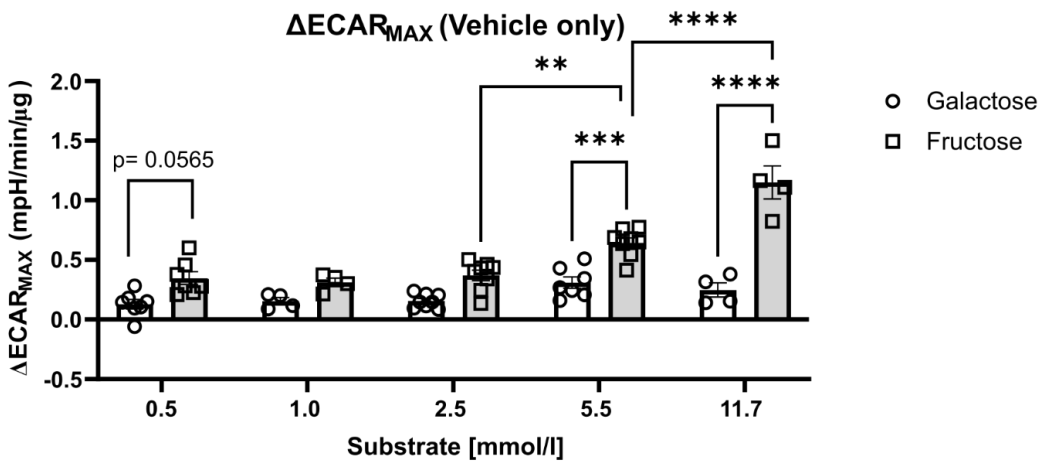

Figure 4.19: Fructose increased α-cell glycolysis greater than galactose.

αTC1.9 cells were incubated in standard Seahorse XF DMEM media for 1 h and subsequently between 0 – 11.7 mmol/l fructose or galactose was injected into the extracellular media after loading into Seahorse XFe96 metabolic analyser. Fructose and galactose utilisation (vehicle only) was calculated by $\Delta ECAR_{MAX}$ (Two-Way ANOVA with Tukey's multiple comparisons test) from maximum ECAR measurement post-glucose injection minus average baseline ECAR readings (**P<0.01, ***P<0.001, ****P<0.0001, n = 4 – 8, one – two individual plates).

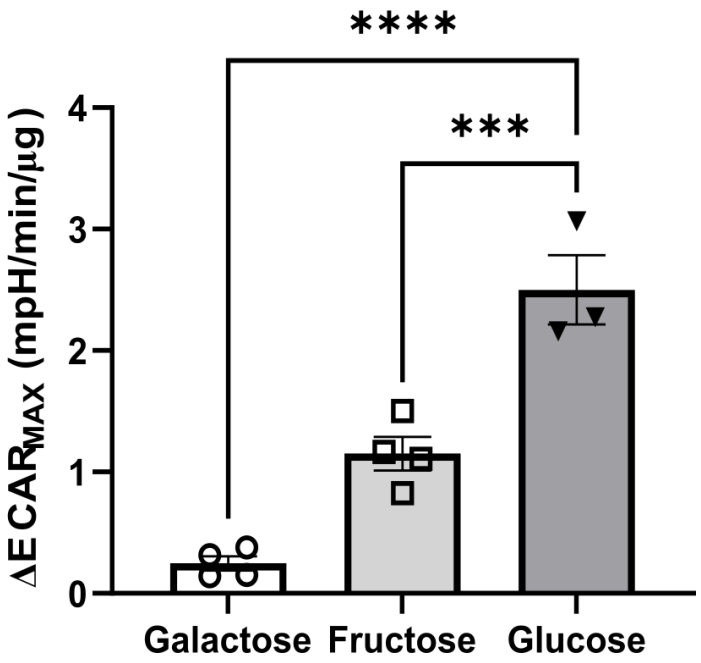

Figure 4.20: The magnitude of fructose and galactose increase in α-cell $\Delta ECAR_{MAX}$ is less than glucose.

αTC1.9 cells were incubated in standard Seahorse XF DMEM media for 1 h and subsequently between 11.7 mmol/l galactose, fructose and glucose were injected into the extracellular media after loading into Seahorse XFe96 metabolic analyser. Fructose and galactose utilisation (vehicle only) was calculated by $\Delta ECAR_{MAX}$ (One Way ANOVA with Dunnett's multiple comparisons test) from maximum ECAR measurement post-glucose injection minus average baseline ECAR readings (***P<0.001, ****P<0.0001, n = 3 – 4, one individual plate).

4.2.4.5 O-304 enhanced both α-cell fructose- and galactose-dependent glycolysis

O-304 enhanced fructose α-cell $\Delta ECAR_{MAX}$ in a fructose concentration-dependent manner (mpH/min/µg) (2.5: Vehicle; 0.370 ± 0.04388, O-304; 0.6763 ± 0.1328, $p = 0.0460$, 5.5: vehicle; 0.6431 ± 0.04149, O-304; 1.344 ± 0.08769, $p < 0.0001$, 11.7: vehicle; 1.150 ± 0.1391, O-304; 1.943 ± 0.1846, $p = 0.0378$) (Figure 4.21Aii-Eii). O-304 similarly increased galactose $\Delta ECAR_{MAX}$, in a galactose concentration-dependent manner (mpH/min/µg) (0.5: vehicle; -0.05997 ± 0.03906, O-304; -0.05784 ± 0.3770, $p = 0.0530$, 2.5: Vehicle; 0.1559 ± 0.02052, O-304; 0.5565 ± 0.1449, $p = 0.0161$, 5.5: vehicle; 0.3089 ± 0.04755, O-304; 0.7185 ± 0.2088, $p = 0.080$ 11.7: vehicle; 0.2472 ± 0.05939, O-304; 0.7346 ± 0.1323, $p = 0.0152$) (Figure 4.22Aii-Eii).

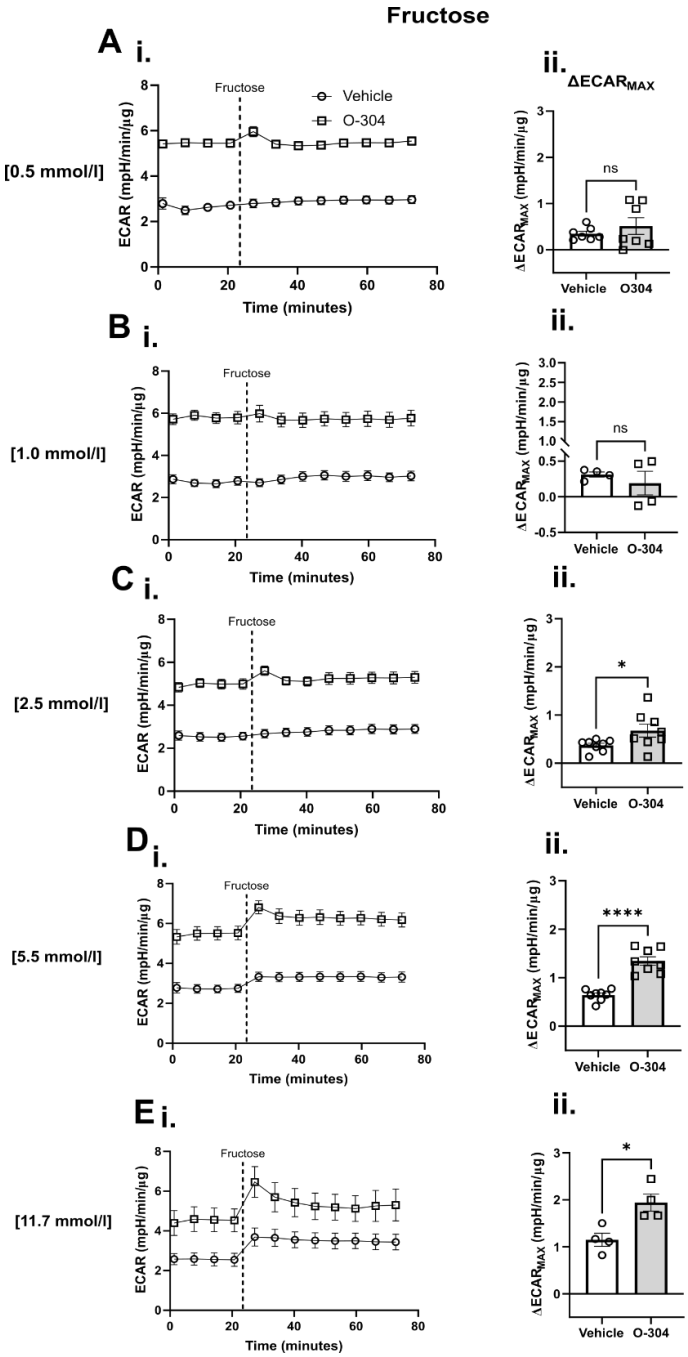

Figure 4.21: O-304 enhanced concentration-dependent fructose glycolytic utilisation in α-cells.

αTC1.9 cells were incubated ± O-304 (10.0 µmol/l) in standard Seahorse XF media for 1h and subsequently between 0 – 11.7 mmol/l fructose was injected into the extracellular media after loading into Seahorse XFe96 metabolic analyser. Representative extracellular acidification rate (ECAR) traces from **A i.** 0.5, **B i.** 1.0, **C i.** 2.5, **D i.** 5.5, **E i**. 11.7 mmol/l fructose acute injections at ~20 min. Fructose utilisation was calculated by **A – E ii.** $\Delta ECAR_{MAX}$ (maximum ECAR measurement post-glucose injection minus average baseline ECAR readings, mpH/min/µg) (A-E ii. Unpaired two-tailed t-test)

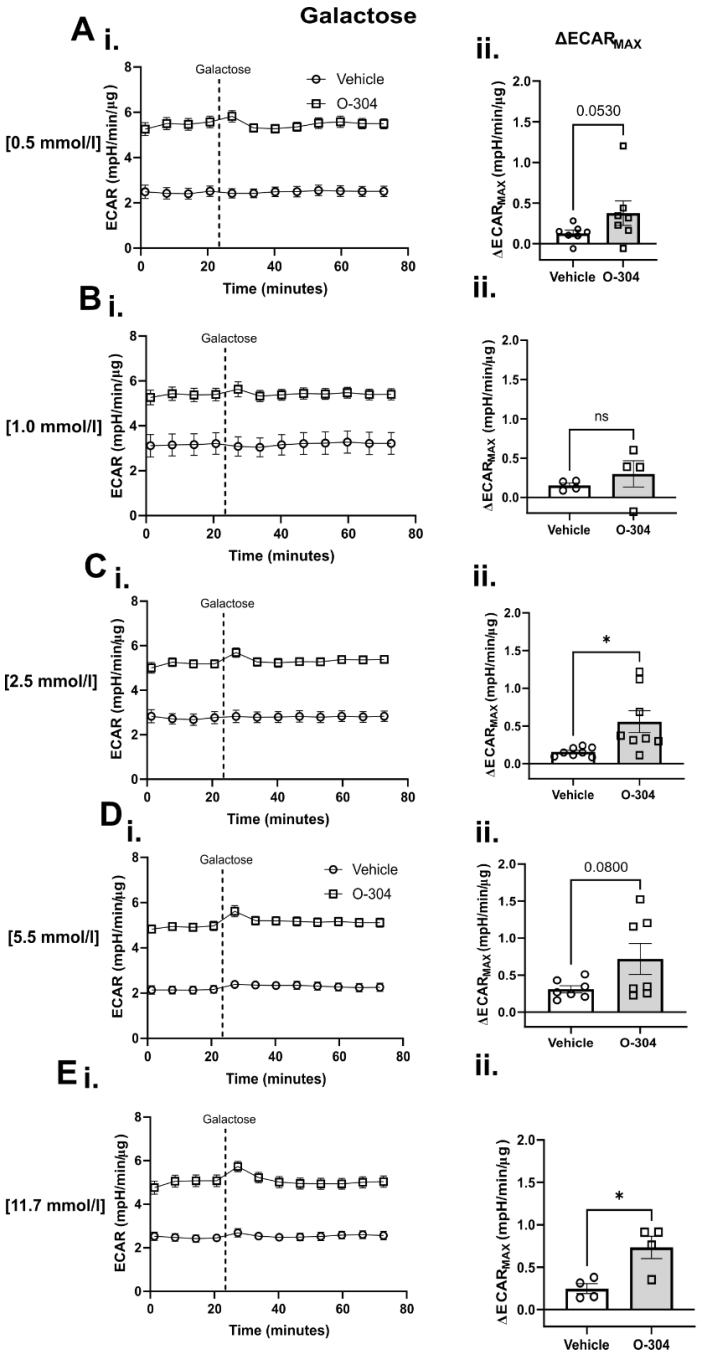

Figure 4.22: O-304 increased concentration-dependent galactose glycolytic utilisation in α-cells.

αTC1.9 cells were incubated ± O-304 (10 µmol/l) in standard Seahorse XF DMEM media for 1 h and subsequently between 0 – 11.7 mmol/l galactose was injected into the extracellular media after loading into Seahorse XFe96 metabolic analyser. Representative extracellular acidification rate (ECAR) traces from **A i.** 0.5, **B i.** 1.0, **C i.** 2.5, **D i.** 5.5, **E i.** 11.7 mmol/l galactose acute injections at ~20 min. Galactose utilisation was calculated by **A – E ii.** $\Delta ECAR_{MAX}$ (maximum ECAR measurement post-glucose injection minus average baseline ECAR readings, mpH/min/µg) **(A - B ii.** Two-tailed Mann-Whitney test, **C – E ii.** Unpaired two-tailed t-test, *P<0.05, **P<0.01, ***P<0.001, ****P<0.0001, n = 4 – 8, one – two individual plates).

4.2.4.6 O-304 enhanced α-cell fructose- or galactose-dependent mitochondrial respiration

O-304 increased fructose-dependent ΔOCR_{MAX} (pmol/min/µg) (0.5: Vehicle; 0.4988 ± 0.2190, O-304; 8.595 ± 2.128, *p = 0.0026,* 2.5: Vehicle; 0.370 ± 0.04388, O-304; 0.6763 ± 0.1328, *p = 0.0104,* 5.5: vehicle; 0.6431 ± 0.04149, O-304; 1.344 ± 0.08769, *p = 0.0009,* 11.7: vehicle; 1.150 ± 0.1391, O-304; 1.943 ± 0.1846, *p = 0.0378*) (Figure 4.23Aii-Eii).

O-304 similarly enhanced galactose-driven ΔOCR_{MAX} (pmol/min/µg) (0.5: vehicle; -1.132 ± 0.4362, O-304; 7.318 ± 2.159, *p = 0.0024,* 1.0: Vehicle; -1.387 ± 0.2810, O-304; 8.830 ± 2.689, *p = 0.0286,* 2.5: vehicle; -0.8826 ± 0.1471, O-304; 10.04 ± 1.834, *p = 0.0002,* 5.5: Vehicle; -0.6960 ± 0.1824, O-304; 9.576 ± 2.672, *p = 0.0024,* 11.7: vehicle; -0.5661 ± 0.1391, O-304; 5.927 ± 1.574, *p = 0.0063*) (Figure 4.24Aii-Eii).

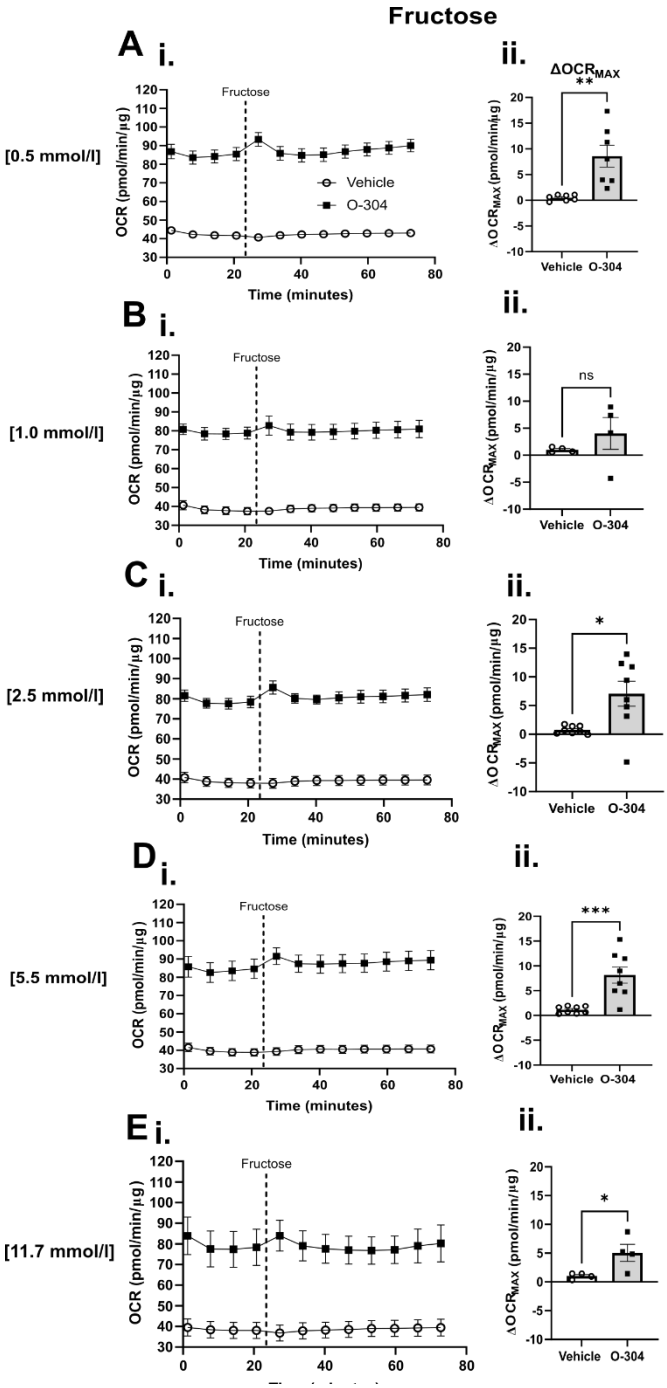

Figure 4.23: O-304 enhanced fructose-induced oxidative respiration in α-cells.

αTC1.9 cells were incubated ± O-304 (10.0 µmol/l) in standard Seahorse XF media for 1h and subsequently between 0 – 11.7 mmol/l fructose was injected into the extracellular media after loading into Seahorse XFe96 metabolic analyser. Representative oxygen consumption rate (OCR) traces from **A i.** 0.5, **B i**. 1.0, **C i.** 2.5, **D i.** 5.5, **E i.** 11.7 mmol/l fructose acute injections at ~32 min. Fructose utilisation was calculated by **A – E ii.** ΔOCR_{MAX} (maximum OCR measurement post-glucose injection minus average baseline OCR readings, mpH/min/µg) (A ii. Unpaired two-tailed t-test, **B - C ii.** Two-tailed Mann-Whitney test, **D - E ii**. Unpaired two-tailed t-test, *P<0.05, **P<0.01, ***P<0.001, ****P<0.0001, n = 4 – 8, one – two individual plates).

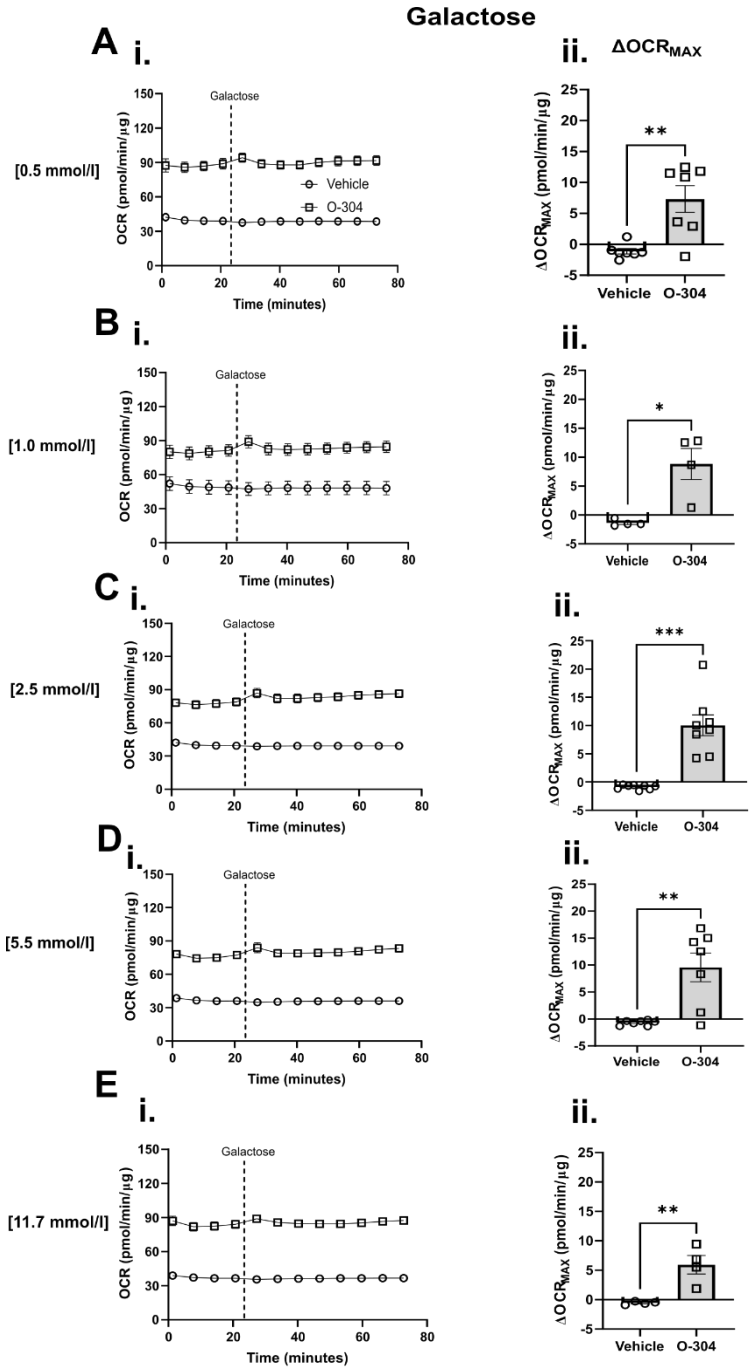

Figure 4.24: O-304 increased concentration-dependent galactose-induced oxidative respiration in α-cells.

αTC1.9 cells were incubated ± O-304 (10 µmol/l) in standard Seahorse XF DMEM media for 1h and subsequently between 0 – 11.7 mmol/l galactose was injected into the extracellular media after loading into Seahorse XFe96 metabolic analyser. Representative oxygen consumption rate (OCR) traces from **A i**. 0.5, **B i.** 1.0, **C i.** 2.5, **D i.** 5.5, **E i.** 11.7 mmol/l galactose acute injections at ~20 min. Galactose utilisation was calculated by **A – E ii.** ΔOCR_{MAX} (maximum OCR measurement post-glucose injection minus average baseline OCR readings, mpH/min/µg) (**A ii.** Unpaired two-tailed t-test, **B - C ii.** Two-tailed Mann-Whitney test, **D – E ii.** Unpaired two-tailed t-test, *P<0.05, **P<0.01, ***P<0.001, ****P<0.0001, n = 4 – 8, one – two individual plates).

4.2.5 Mitochondrial function

As previously demonstrated, O-304 enhanced α-cell oxidative metabolism in both glucose-free and -containing conditions. To investigate whether acute O-304 treatment could drive α-cell mitochondrial oxidative metabolism, α-cells were incubated in 0.5 – 11.7 mmol/l glucose ± O-304 (5.0 µmol/l) for 1 h prior to measuring mitochondrial function.

ATP-linked respiration, proton leak and coupling efficiency mitochondrial parameters, calculations derived from the oligomycin-induced reduction of OCR, were measured from one experiment. Three experiments, including the one mentioned were included in the analysis in calculating basal respiration, maximal respiration, spare respiratory capacity and non-mitochondrial oxygen consumption. The optimal oligomycin and FCCP inhibitor concentrations were determined by a titration assay (Figure 2.7).

4.2.5.1 In α-cells, O-304 reduced ATP-linked oxidative respiration in a glucose- and SBI-insensitive manner.

At 0.5 mmol/l glucose, O-304 reduced ATP-linked respiration (pmol/min/µg) (Vehicle; 12.98 ± 0.9405, O-304; 7.385 ± 1.040, *Vehicle vs O-304, p = 0.0032,* SBI; 13.02 ± 0.3986, SBI + O-304; 10.40 ± 0.5170) (Figure 4.25C). O-304 similarly attenuated SBI-insensitive mitochondrial coupling efficiency (% OCR) (Vehicle; 47.98 ± 0.7947, O-304; 9.350 ± 1.373, SBI; 43.73 ± 0.4052, SBI + O-304; 12.27 ± 0.2697) (Figure 4.25E). Furthermore, O-304 enhanced SBI-insensitive proton leak (pmol/min/µg) (Vehicle; 13.98 ± 0.7550, O-304; 72.06 ± 2.042, *Vehicle vs O-304, p = 0.0005,* SBI; 16.80 ± 0.6643, SBI + O-304; 74.25 ± 2.613 *SBI vs SBI + O-304, p = 0.0401*) (Figure 4.25D)

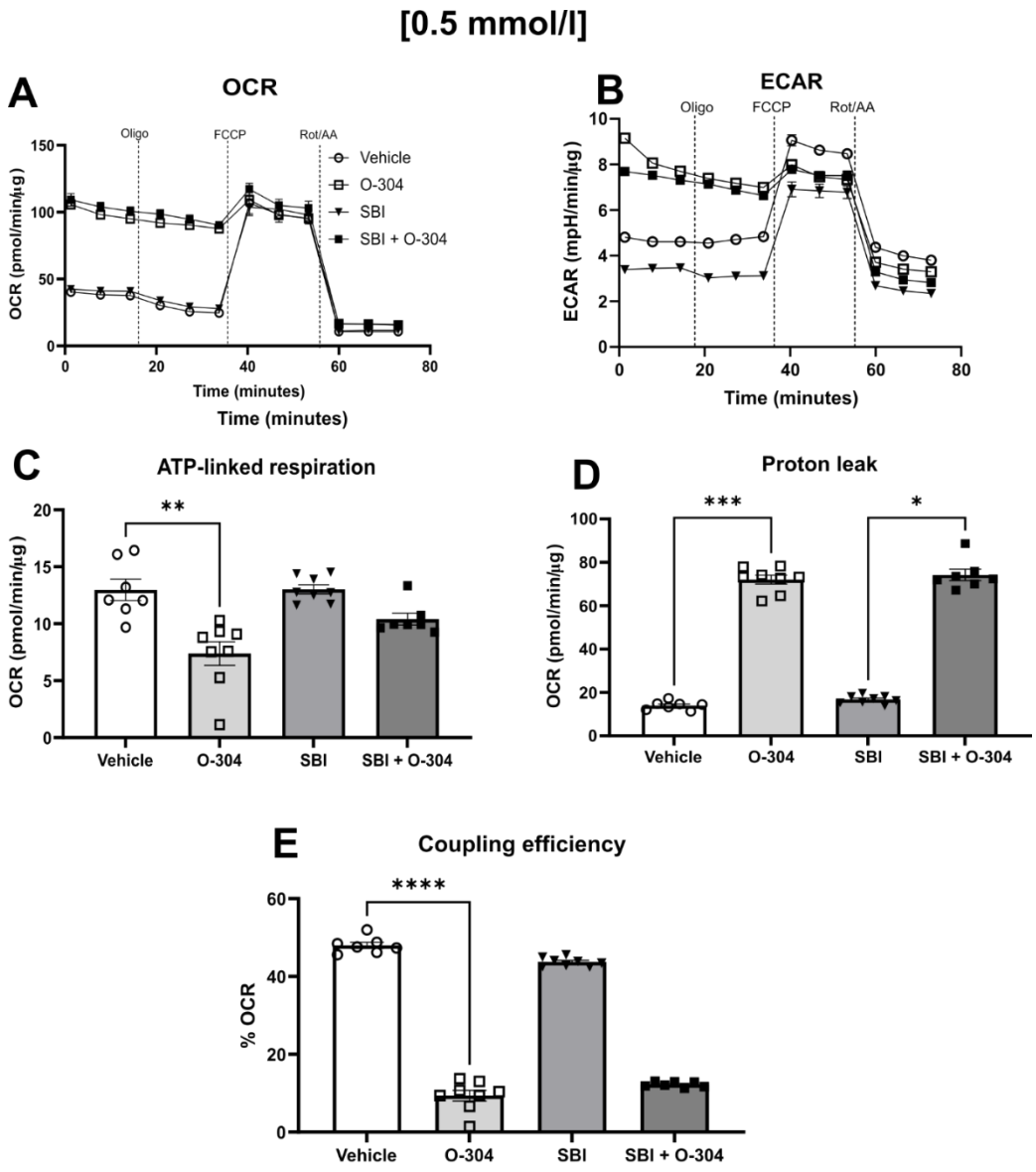

Figure 4.25: O-304 reduced α-cell mitochondrial ATP-linked respiration, coupling efficiency and enhanced proton leak in an SBI-insensitive manner at low glucose.

αTC1.9 cells were preincubated with SBI-0206965 (SBI) (30 µmol/l) for 30min in normal glucose conditions, and subsequently exposed to O-304 (5.0 µmol/l) at 0.5 mmol/l glucose for 1 h. **A.** Respective oxygen consumption rate (OCR, pmol/min/µg) trace and **B.** extracellular acidification rate (ECAR, mpH/min/µg) at baseline and after acute injection of oligomycin (oligo) (1.5 µmol/l), FCCP (1.0 µmol/l) and rotenone/antimycin A (Rot/AA) (1:1, 0.5 µmol/l). Trace was used to determine; **C.** ATP-linked respiration (Kruskal-Wallis test with Dunn's multiple comparison test) **D.** Proton leak (Kruskal-Wallis test with Dunn's multiple comparison test) **E.** Coupling efficiency (Kruskal-Wallis test with Dunn's multiple comparison test) (one plate, n = 7 - 8, *P<0.05, **P<0.01, ***P<0.001, ****P<0.0001)

Likewise, at 5.5 mmol/l glucose, O-304 continued to reduce SBI-insensitive ATP-linked respiration (pmol/min/µg) (Vehicle; 14.07 ± 0.3047, O-304; 2.936 ± 0.3451, *Vehicle vs O-304, p < 0.0001,* SBI; 11.28 ± 0.5711, SBI + O-304; 4.04 ± 0.5994) (Figure 4.26B). O-304 similarly attenuated coupling efficiency, regardless of SBI- treatment (%OCR) (Vehicle; 51.36 ± 0.8833, O-304; 3.626 ± 0.4075, *Vehicle vs O-304, p < 0.0001,* SBI; 45.26 ± 0.7825, SBI + O-304; 4.628 ± 0.5784) (Figure 4.26E). However, SBI alone reduced ATP-linked respiration and coupling efficiency (ATP-linked respiration; *Vehicle vs SBI, p = 0.0023,* Coupling efficiency; *Vehicle vs SBI, p < 0.0001*) (Figure 4.26C/E). O-304 enhanced proton leak regardless of SBI pre-treatment (pmol/min/µg) (Vehicle; 13.34 ± 0.3685, O-304; 77.67 ± 2.487, *Vehicle vs O-304; p < 0.0001,* SBI; 13.64 ± 0.6980, SBI + O-304; 80.58 ± 3.445) (Figure 4.26D).

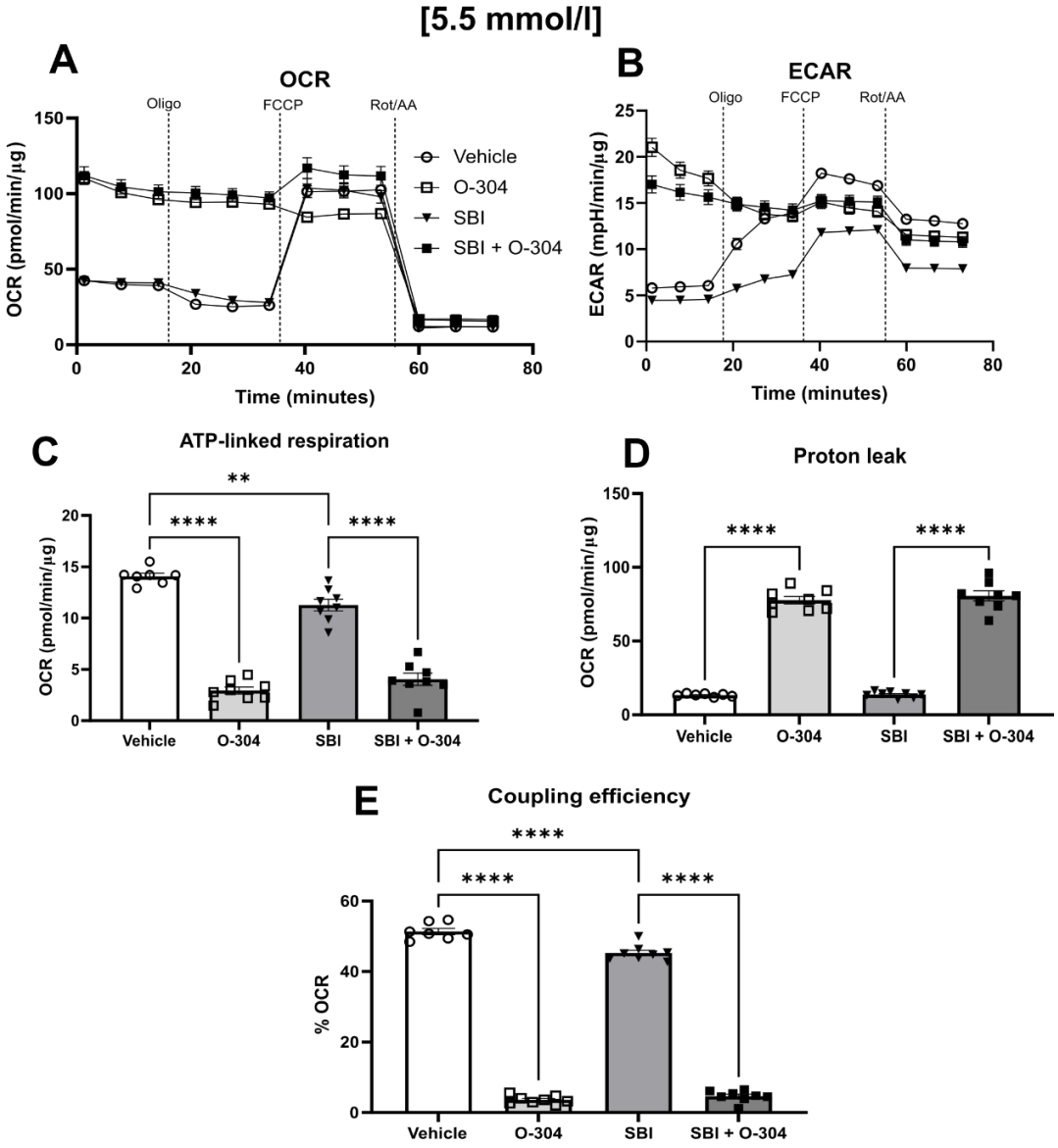

Figure 4.26: O-304 reduced α-cell mitochondrial ATP-linked respiration, coupling efficiency and enhanced proton leak in an SBI-sensitive manner at euglycaemic-like conditions.

αTC1.9 cells were preincubated with SBI-0206965 (SBI) (30 µmol/l) for 30min in normal glucose conditions, and subsequently exposed to O-304 (5.0 µmol/l) at 5.5 mmol/l glucose for 1 h. **A.** Respective oxygen consumption rate (OCR, pmol/min/µg) and **B.** extracellular acidification rate (ECAR, mpH/min/µg) traces at baseline and after acute injection of oligomycin (oligo) (1.5 µmol/l), FCCP (1.0 µmol/l) and rotenone/antimycin A (Rot/AA) (1:1, 0.5 µmol/l). Trace was used to determine; **C.** ATP-linked respiration (One-Way ANOVA with Tukey's multiple comparison test) **D.** Proton leak (One-Way ANOVA with Tukey's multiple comparison test) **E**. Coupling efficiency (One-Way ANOVA with Tukey's multiple comparison test) (one plate, n = 7 - 8, *P<0.05, **P<0.01, ***P<0.001, ****P<0.0001)

At high glucose (11.7 mmol/l), O-304 attenuated SBI-insensitive ATP-linked respiration (pmol/min/µg) (Vehicle; 15.01 ± 0.4835, O-304; 1.211 ± 0.1061, *Vehicle vs O-304, p < 0.0001,* SBI; 11.74 ± 0.6365, SBI + O-304; 2.040 ± 0.8163) (Figure 4.27C). O-304 similarly reduced coupling efficiency, regardless of SBI pre-treatment (%OCR) (Vehicle; 52.42 ± 0.9102, O-304; 1.413 ± 0.1231, *Vehicle vs O-304, p < 0.0001,* SBI; 45.40 ± 0.6779, SBI + O-304; 2.423 ± 1.004) (Figure 4.27E). SBI treatment alone continued to reduce ATP-linked respiration and coupling efficiency (ATP-linked respiration: *Vehicle vs SBI, p = 0.0024,* Coupling efficiency: *Vehicle vs SBI; p < 0.0001*) (Figure 4.27C/E).

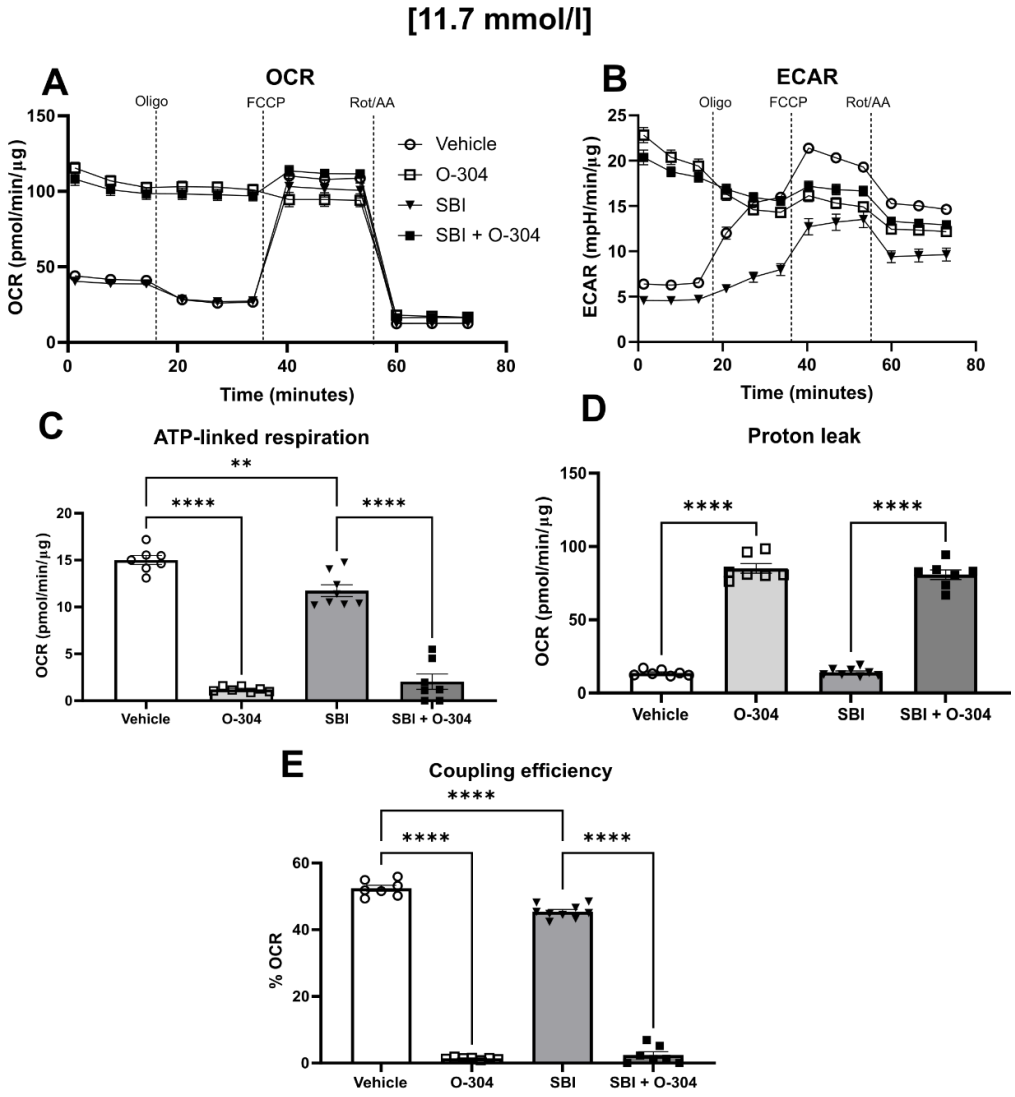

Figure 4.27: O-304 reduced α-cell mitochondrial ATP-linked respiration, coupling efficiency and enhanced proton leak in an SBI-insensitive manner at high glucose.

αTC1.9 cells were preincubated with SBI-0206965 (SBI) (30 µmol/l) for 30min in normal glucose conditions, and subsequently incubated with O-304 (5.0 µmol/l) at 11.7 mmol/l glucose for 1 h. **A.** Respective oxygen consumption rate (OCR, pmol/min/µg) and **B.** extracellular acidifcation rate (ECAR, mpH/min/µg) traces at baseline and after acute injection of oligomycin (oligo) (1.5 µmol/l), FCCP (1.0 µmol/l) and rotenone/antimycin A (Rot/AA) (1:1, 0.5 µmol/l). Traces were used to determine; **C.** ATP-linked respiration (One-Way ANOVA with Tukey's multiple comparison test) **D.** Proton leak (One-Way ANOVA with Tukey's multiple comparison test) **E.** Coupling efficiency (One-Way ANOVA with Tukey's multiple comparison test) (one plate, n = 7 - 8, *P<0.05, **P<0.01, ***P<0.001, ****P<0.0001)

4.2.5.2 O-304 increased α-cell basal oxidative metabolism and non-mitochondrial oxygen consumption in a glucose- and SBI-insensitive manner

At 0.5 mmol/l glucose, O-304 increased α-cell spare respiratory capacity (pmol/min/µg) (Vehicle; 68.01 ± 2.560, O-304, 19.67 ± 2.076, *Vehicle vs O-304, $p < 0.0001$,* SBI; 65.42 ± 2.408, SBI + O-304; 22.03 ± 1.952) (Figure 4.28C). O-304 enhanced basal respiration (pmol/min/µg) (Vehicle; 25.78 ± 0.8257, O-304; 76.24 ± 1.873, *Vehicle vs O-304, $p < 0.0001$,* SBI; 26.05 ± 1.032, SBI + O-304; 73.73 ± 2.679) (Figure 4.28D). Similarly, O-304 increased non-mitochondrial consumption (pmol/min/µg) ((Vehicle; 10.96 ± 0.4274, O-304; 14.83 ± 0.3240, *Vehicle vs O-304, $p < 0.0001$,* SBI; 10.63 ± 0.4894, SBI + O-304; 14.66 ± 0.5118) (Figure 4.28F). All O-304-enhanced parameters were SBI-insensitive. O-304 did not affect α-cell maximal respiration (pmol/min/µg) (Vehicle; 93.78 ± 2.948, O-304; 95.86 ± 2.296, SBI; 91.47 ± 3.014, SBI + O-304; 95.79 ± 2.917) (Figure 4.28E).

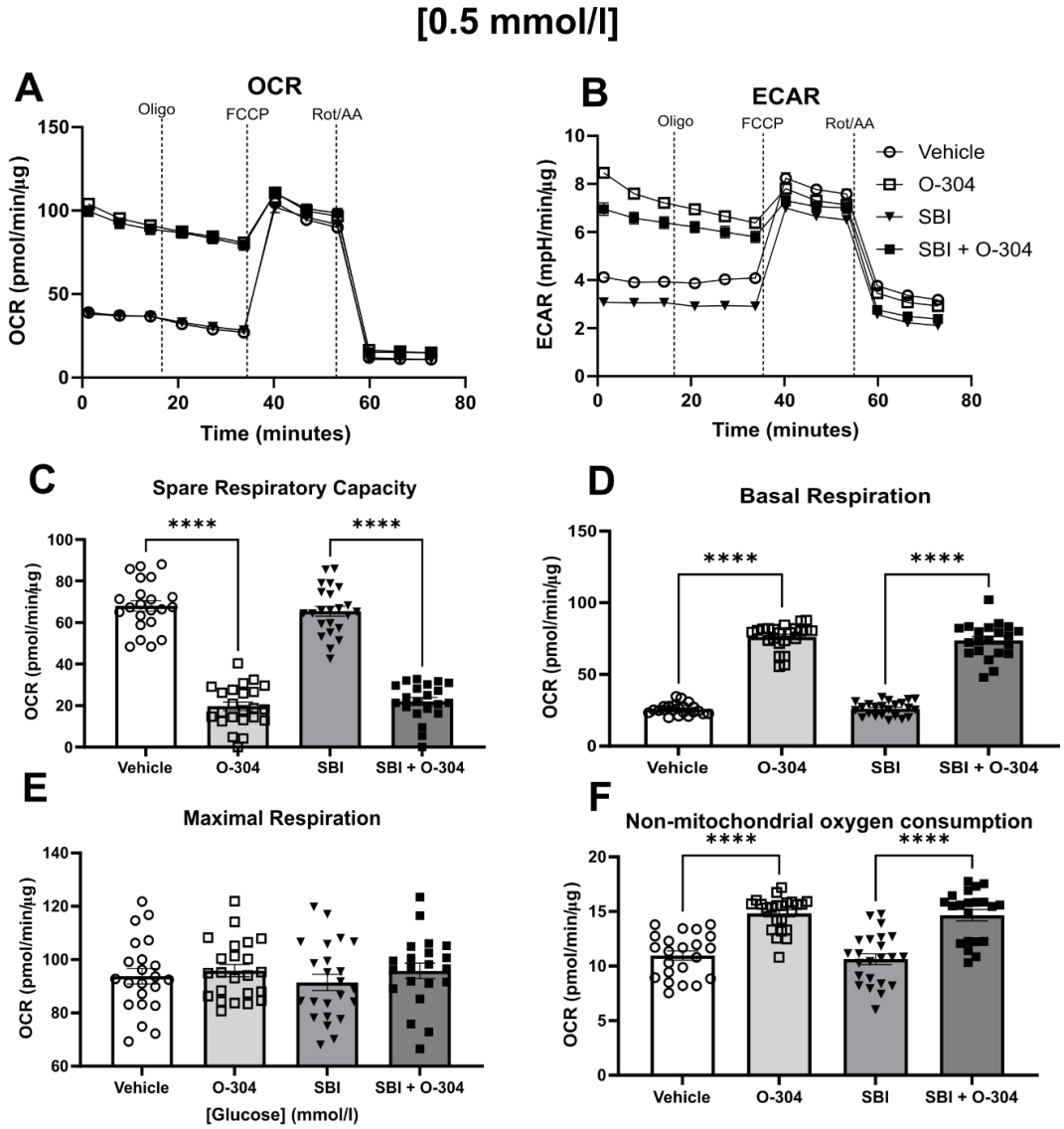

Figure 4.28: O-304 reduced α-cell spare respiratory capacity and mitochondrial respiration in an SBI-insensitive manner during acute low glucose.

αTC1.9 cells were preincubated with SBI-0206965 (SBI) (30.0 µmol/l) for 30min in normal glucose conditions, and subsequently exposed to O-304 (5.0 µmol/l) at 0.5 mmol/l glucose for 1 h. **A.** Respective oxygen consumption rate (OCR, pmol/min/µg) and **B.** extracellular acidification rate (ECAR, mpH/min/µg) traces at baseline and after acute injection of oligomycin (oligo) (1.5 µmol/l), FCCP (1.0 µmol/l) and rotenone/antimycin A (Rot/AA) (1:1, 0.5 µmol/l). Both traces were used to determine; **C.** Spare respiratory capacity (One-Way ANOVA with Tukey's multiple comparison test) **D.** Basal respiration (Kruskal-Wallis test with Dunn's multiple comparison test) **E.** Maximal respiration (One Way ANOVA with Tukey's multiple comparison test) **F.** Non-mitochondrial oxygen consumption rate (One-Way ANOVA with Tukey's multiple comparison test) (three individual plates, n = 21 – 23, *P<0.05, **P<0.01, ***P<0.001, ****P<0.0001)

At 5.5 mmol/l glucose, O-304 attenuated SBI-insensitive spare respiratory capacity (Vehicle; 63.80 ± 2.299, O-304; 1.538 ± 0.6174, *Vehicle vs O-304, p < 0.0001,* SBI; 66.75 ± 2.916, SBI + O-304; 21.94 ± 1.498) (Figure 4.29C). O-304 similarly reduced maximal respiration, with SBI restoring this reduction (Vehicle; 89.34 ± 3.175, O-304; 74.08 ± 1.950, *Vehicle vs O-304, p = 0.0028, O-304 vs SBI + O-304, p < 0.0001*, SBI; 90.39 ± 3.559, SBI + O-304; 96.93 ± 2.436) (Figure 4.29E). O-304, regardless of SBI treatment, enhanced basal respiration (Vehicle; 24.73 ± 0.9584, O-304; 77.34 ± 1.747, *Vehicle vs O-304, p < 0.0001,* SBI; 23.63 ± 0.7429, SBI + O-304; 74.99 ± 2.374) (Figure 4.29D). Furthermore, O-304 increased non-mitochondrial oxygen consumption (Vehicle; 10.85 ± 0.5904, O-304; 14.61 ± 0.5216, *Vehicle vs O-304, p < 0.0001,* SBI; 11.05 ± 0.4515, SBI + O-304; 14.38 ± 0.5460) (Figure 4.29F).

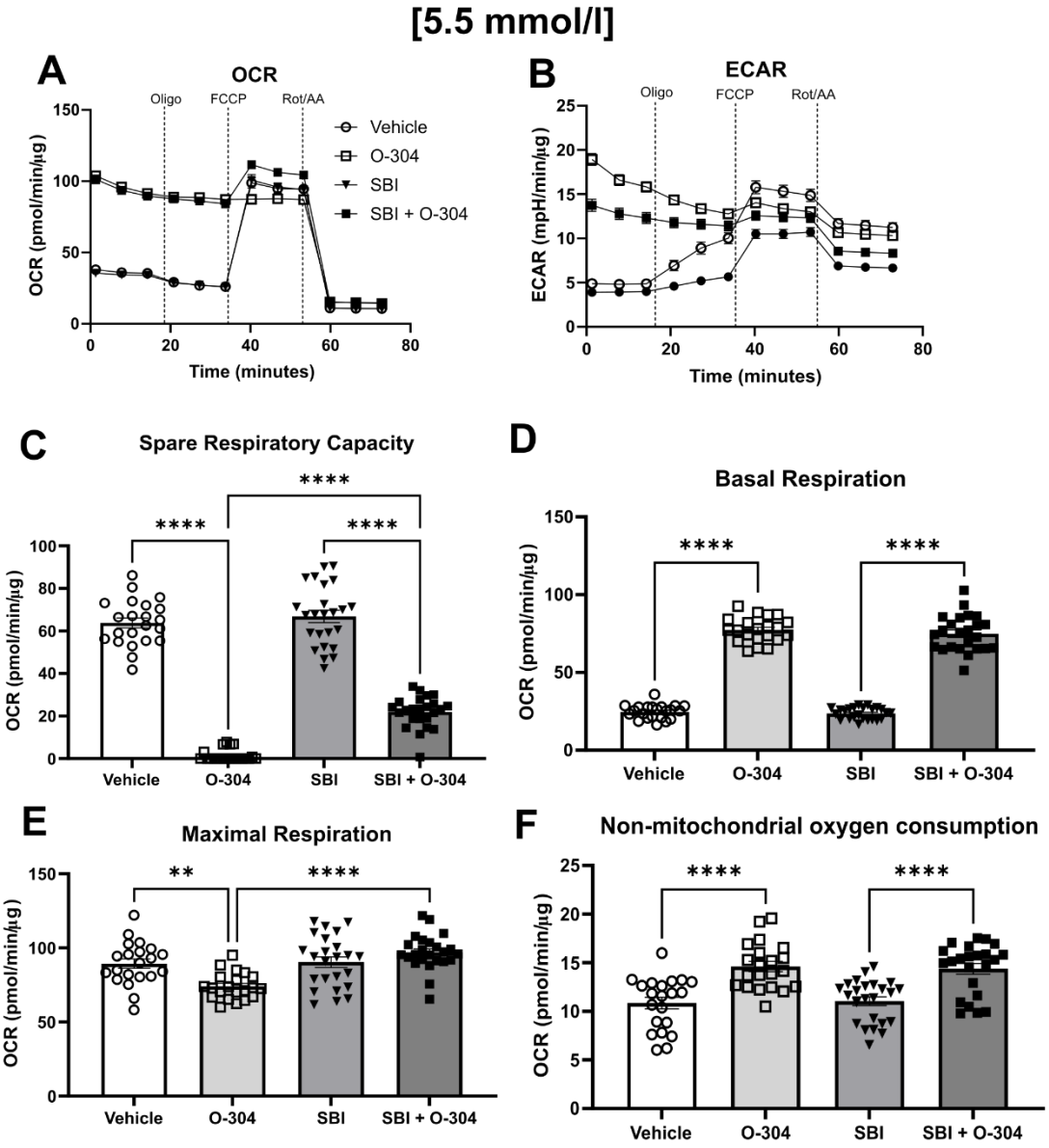

Figure 4.29: O-304 reduced α-cell metabolic respiratory parameters in an SBI-insensitive manner at euglycaemic-like conditions.

αTC1.9 cells were preincubated with SBI-0206965 (SBI) (30 µmol/l) for 30 min in normal glucose conditions, and subsequently exposed to O-304 (5.0 µmol/l) at 5.5 mmol/l glucose for 1 h. **A.** Respective oxygen consumption rate (OCR, pmol/min/µg) and **B.** extracellular acidification rate (ECAR, mpH/min/µg) traces at baseline and after acute injection of oligomycin (oligo) (1.5 µmol/l), FCCP (1.0 µmol/l) and rotenone/antimycin A (Rot/AA) (1:1, 0.5 µmol/l). Both traces were used to determine; **C.** Spare respiratory capacity (One-Way ANOVA with Tukey's multiple comparison test) **D.** Basal respiration (Kruskal-Wallis test with Dunn's multiple comparison test) **E.** Maximal respiration (One Way ANOVA with Tukey's multiple comparison test) **F.** Non-mitochondrial oxygen consumption (One-Way ANOVA with Tukey's multiple comparison test) (three individual plates, n = 22 – 24, *P<0.05, **P<0.01, ***P<0.001, ****P<0.0001)

At 11.7 mmol/l glucose, O-304 continued to reduce α-cell spare respiratory capacity, however this was partially recovered by SBI treatment (Vehicle; 63.20 ± 3.087, O-304; *Vehicle vs O-304, p < 0.0001,* 1.689 ± 0.5340, SBI; 69.45 ± 3.914, SBI + O-304; 15.55 ± 1.226, *O-304 vs SBI + O-304, p = 0.0336*) (Figure 4.30C). Maximal respiration, following SBI exposure, was not different in SBI control but was greater in O-304 cells (Vehicle; 88.63 ± 4.168, O-304*;* 75.77 ± 2.558, *Vehicle vs O-304, p = 0.1,* SBI; 93.68 ± 4.898*, SBI vs O-304, p = 0.0081,* SBI + O-304; 92.86 ± 3.411, *SBI + O-304 vs O-304, p = 0.0081*) (Figure 4.30E). O-304 treatment enhanced non-mitochondrial oxygen consumption but was unaffected by SBI pre-treatment (Vehicle; 11.41 ± 0.6720, O-304; 14.96 ± 0.4686, *Vehicle vs O-304, p = 0.0004,* SBI; 11.60 ± 0.5598, SBI + O-304; 15.18 ± 0.66) (Figure 4.30F).

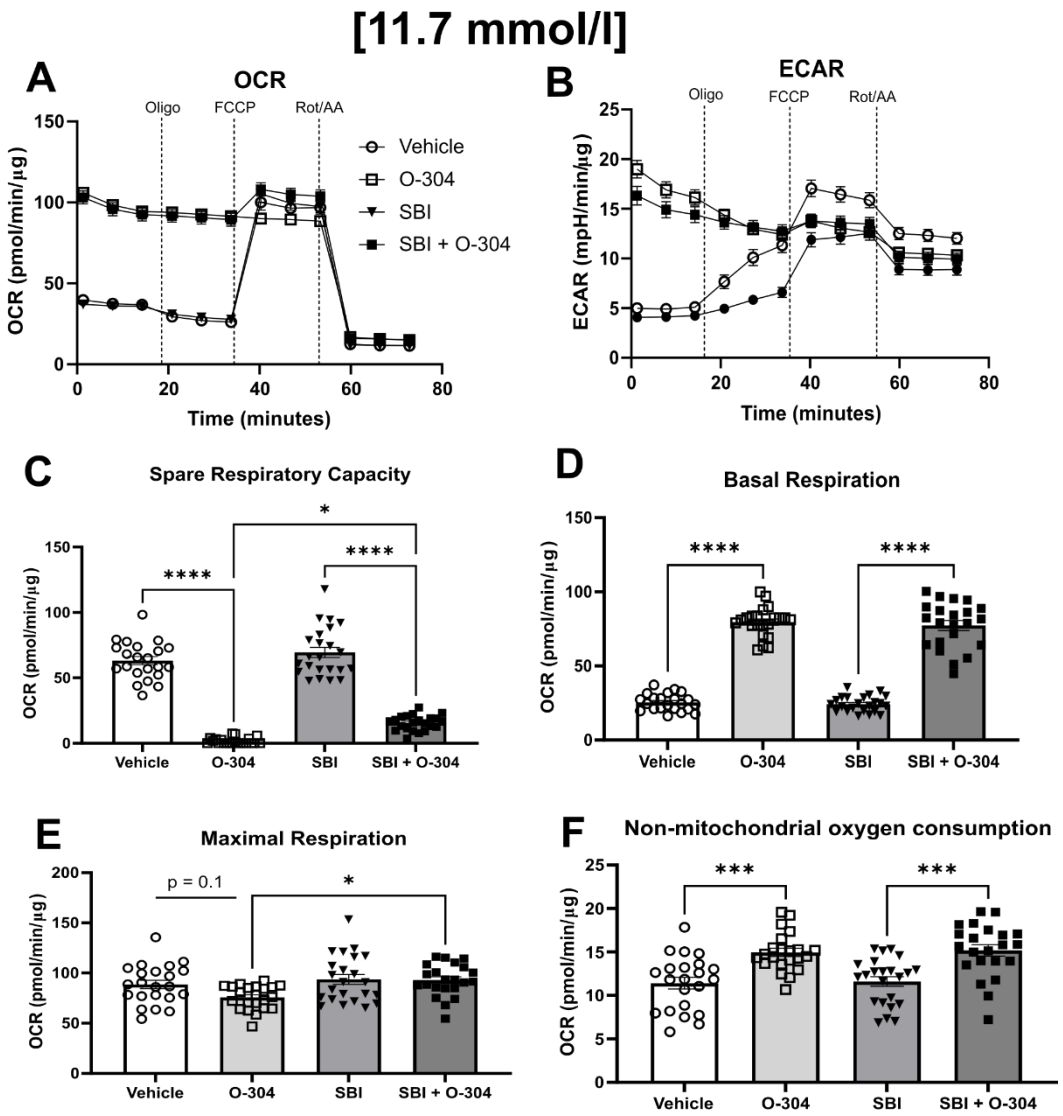

Figure 4.30: O-304 reduced α-cell spare respiratory capacity but increased basal respiration at hyperglycaemic-like conditions.

αTC1.9 cells were preincubated with SBI-0206965 (SBI) (30.0 µmol/l) for 30 min in normal glucose conditions, and subsequently exposed to O-304 (5.0 µmol/l) at 11.7 mmol/l glucose for 1 h. **A.** Respective oxygen consumption rate (OCR, pmol/min/µg) and **B.** extracellular acidification rate (ECAR, mpH/min/µg) traces at baseline and after acute injection of oligomycin (oligo) (1.5 µmol/l), FCCP (1.0 µmol/l) and rotenone/antimycin A (Rot/AA) (1:1, 0.5 µmol/l). Both traces were used to determine; **C.** Spare respiratory capacity (Kruskal-Wallis test with Dunn's multiple comparison test) **D.** Basal respiration (Kruskal-Wallis test with Dunn's multiple comparison test) **E**. Maximal respiration (One Way ANOVA with Tukey's multiple comparison test) **F**. Non-mitochondrial oxygen consumption (One Way ANOVA with Tukey's multiple comparison test) (three separate plates, n = 22 – 23, *P<0.05, **P<0.01, ***P<0.001, ****P<0.0001)

4.2.6 Cell viability and reactive oxygen species (ROS) generation

4.2.6.1 O-304 treatment did not alter α-cell viability.

The work described in this chapter highlighted O-304 exposure reduced coupled mitochondrial respiration. To access the possibility O-304 can acutely impair α-cell viability, cell death was measured using the same experimental treatment time (1 h), following exposure to O-304 (0 – 5.0 µmol/l) and 0.5/11.7 mmol/l glucose.

O-304 did not significantly alter α-cell death at any concentration used at 0.5 mmol/l glucose (% cell death) (Vehicle; 4.743 ± 1.364, 1.0; 3.953 ± 0.7182, 2.5; 4.970 ± 0.7863, 5.0; 5.323 ± 1.587) (Figure 4.31A). No change in cell viability was similarly seen at 11.7 mmol/l glucose (% cell death) (Vehicle; 5.227 ± 1.339, 1.0; 4.407 ± 0.07030, 2.5; 4.680 ± 0.9277, 5.0; 4.817 ± 0.7659) (Figure 4.31B).

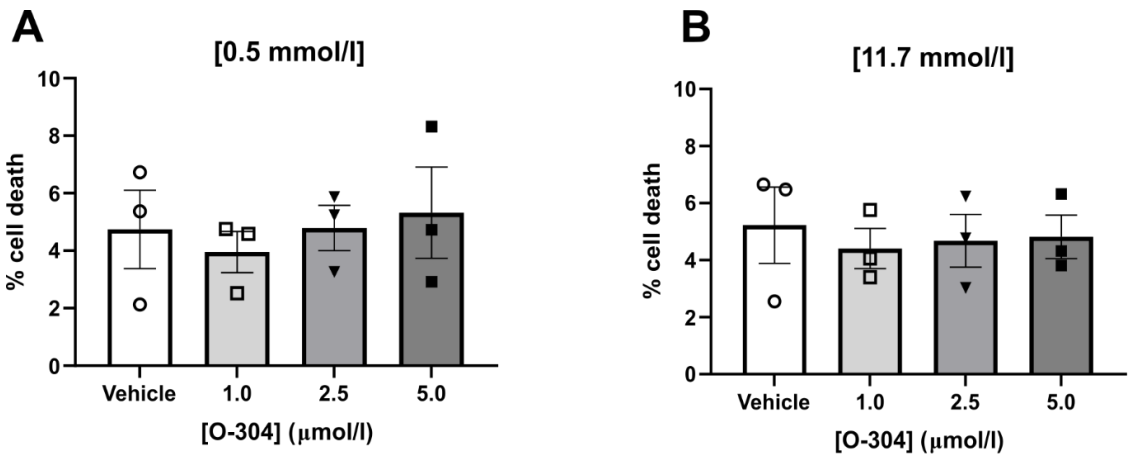

Figure 4.31: α-cell viability is unaffected by acute O-304 treatment.

αTC1.9 cells were exposed to either **A.** 0.5 or **B.** 11.7 mmol/l glucose containing between 1.0 – 5.0 µmol/l O-304 for 1h. Cell death was measured using propidium iodide staining and flow cytometry, gated against positive control (One-Way ANOVA with Dunnetts multiple comparison test, n = 3).

4.2.6.2 α-cell ROS production was increased upon O-304 treatment, compared to R481.

To test whether O-304 enhanced oxidative metabolism correlated with increased ROS generation, α-cells were incubated in 0 – 5.0 µmol/l O-304 for 1 h prior to ROS luminescence stain (DCDFA) loading. Data suggests a trend, although not statistically significant, towards an O-304 concentration-dependent fold increase in relative light units (RLU) (1.0; 1.242 +/- 0.1844, 2.5; 1.492 ± 0.1947, *p = 0.1092,* 5.0; 1.459 ± 0.1741, *p = 0.1423*) (Figure 4.32). Furthermore, to compare alongside indirect AMPK activator R481 (50 nmol/l), O-304 (5.0 µmol/l) enhanced fold change in RLU (O-304; 1.148 ± 0.1334, *Vehicle vs O-304, p = 0.0565,* R481; 1.186 ± 0.1171) (Figure 4.33).

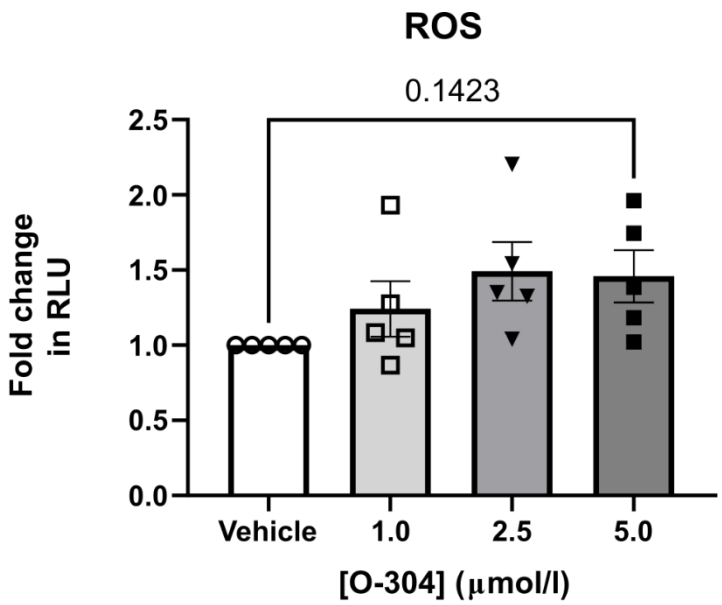

Figure 4.32: α-cell ROS production following O-304 exposure.

αTC1.9 cells were preincubated with 5.5 mmol/l glucose-containing media ± O-304 (1.0 – 5.0 µmol/l) for 1h. Cells were subsequently stained with DCDFA (10.0 µmol/l) for 30 min. DCDFA luminescence was measured at 480/520nm excitation/emission (relative luminescence units, RLU) and is an indication of total [ROS] calculated as fold change vs control (One-Way ANOVA with Dunnett's multiple comparison test)

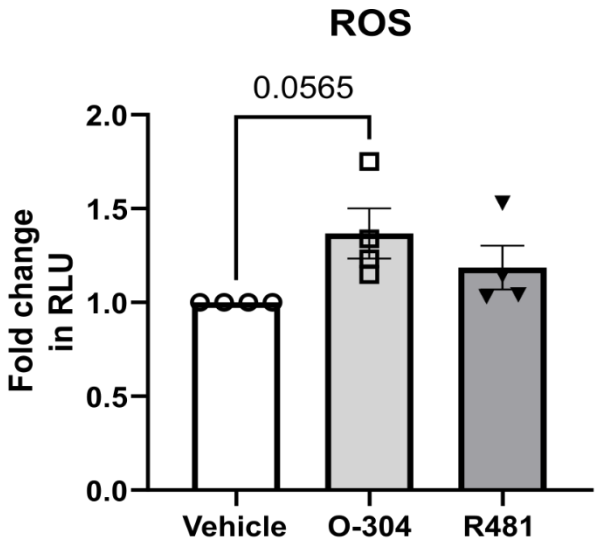

Figure 4.33: O-304, but not R481, enhanced α-cell reactive oxygen species (ROS) production.

αTC1.9 cells were preincubated with 5.5 mmol/l glucose-containing media ± R481 (50 nmol/l) or O-304 (5.0 µmol/l) for 1 h. Cells were subsequently stained with DCDFA (10.0 µmol/l) for 30 min. DCDFA luminescence was measured at 480/520nm excitation/emission (relative luminescence units, RLU) and is an indication of total [ROS] calculated as fold change vs control (One-Way ANOVA with Dunnett's multiple comparison test)

4.2.7 Nucleotide measurements

4.2.7.1 O-304 reduced α-cell total ATP in a glucose-sensitive manner.

To examine whether O-304 treatment is altering α-cell energy status, cells were incubated in O-304 (5.0 µmol/l) and glucose-containing medium for 30 min, and total ATP (tATP) was measured. tATP measurements include both extracellular and intracellular ATP and was displayed as fold change in RLU. O-304 significantly reduced fold change in total ATP at 0.5 mmol/l glucose (fold change) (O-304; 0.7207 ± 0.06909, $p = 0.0024$) (Figure 4.34A). Similarly, at 5.5 mmol/l glucose, O-304 attenuated fold change in tATP (O-304; 0.7882 ± 0.09216, $p = 0.0444$) (Figure 4.34B). However, at 11.7 mmol/l glucose, O-304 did not alter tATP (fold change) (O-304; 0.8947 ± 0.1683) (Figure 4.34C).

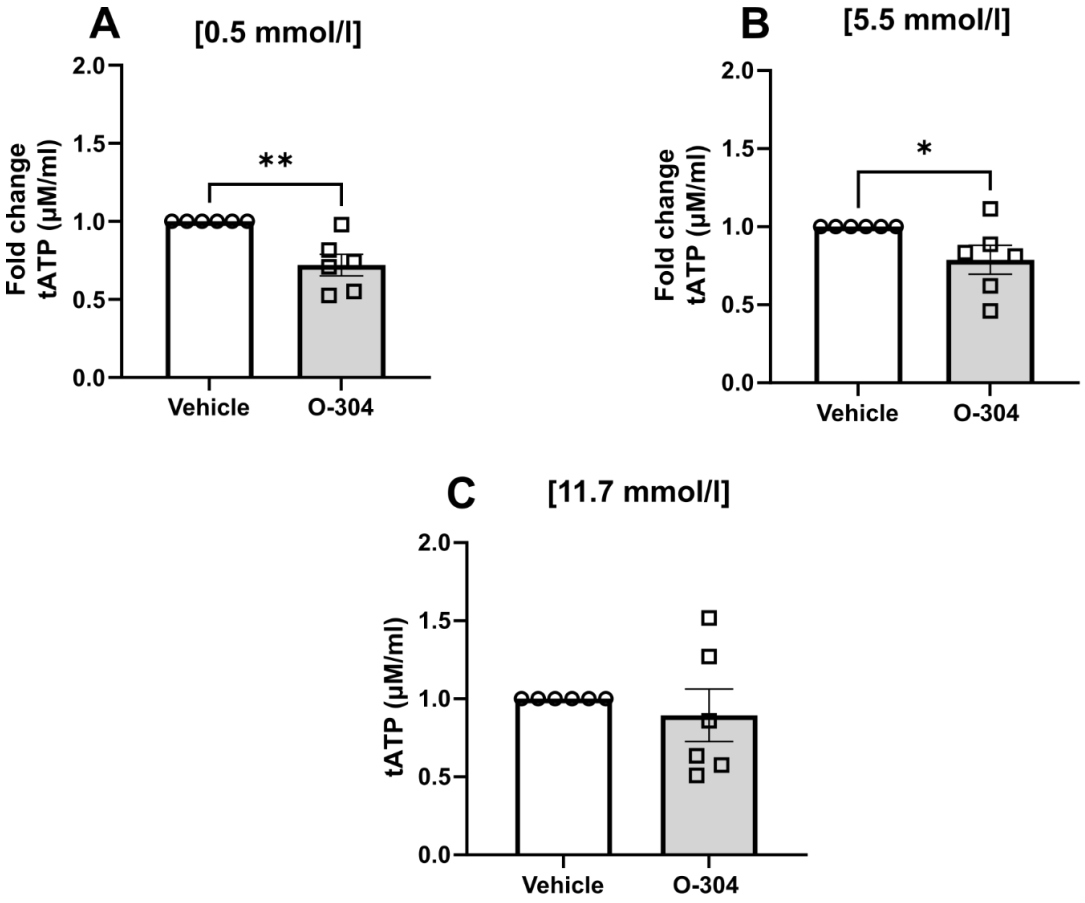

Figure 4.34 α-cell total ATP (tATP) was reduced following O-304 exposure in a glucose-dependent manner.

αTC1.9 cells were exposed to O-304 (5.0 µmol/l) ± 5.5 mmol/l glucose for 30 min, and further incubated in 0.5 – 11.7 mmol/l glucose ± O-304 for a further 30 min. **A**. 0.5 **B**. 5.5 and **C.** 11.7 mmol/l glucose, with total ATP (tATP) represented as fold change (Two-tailed unpaired t-test, *P<0.05, **P<0.01)

4.2.7.2 ATP secretion was not altered following O-304 exposure.

ATP is co-secreted with insulin, from β-cells, in response to high glucose and can act as an autocrine messenger of β-cell function by binding to cell surface purinergic receptors (Richards-Williams *et al.*, 2008). α-cells have previously been described to express purinergic receptors, and exposure to ATP limits glucagon release at low glucose (Coutinho-Silva *et al.*, 2003; Tudurí *et al.*, 2008). Therefore, a study conducted by Ms. Isabel Burn investigated whether O-304, by AMPK activation, regulated α-cell ATP secretion as a form of purinergic signalling. α-cells were exposed to 2.5 – 50 µmol/l O-304 for 30 min and ATP secretion was measured. Increasing [O-304] did not influence α-cell ATP secretion (µM/mg) (Vehicle; 52.05 ± 17.70, 2.5; 64.69 ± 28.03, 5.0; 43.48 ± 14.23,10.0; 62.88 ± 10.66, 25.0; 56.88 ± 8.861, 50.0; 52.33 ± 4.737) (Figure 4.35).

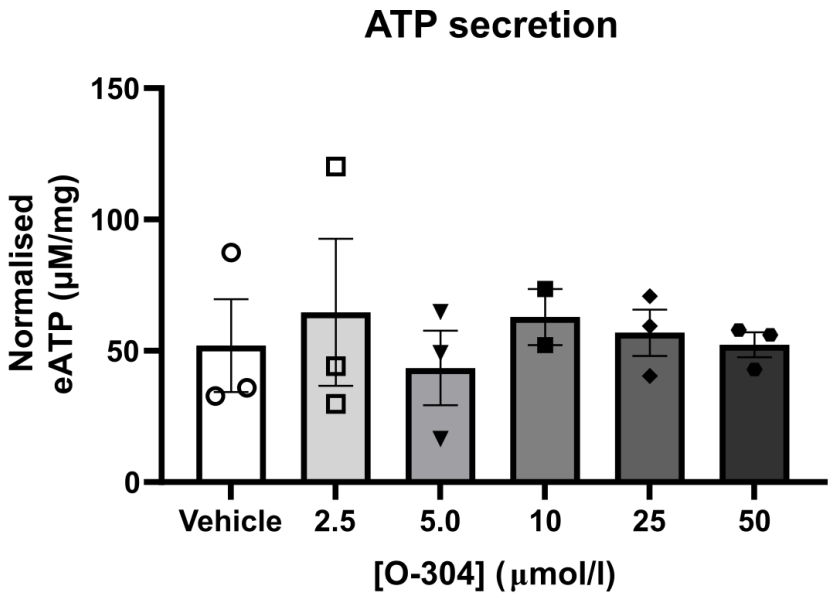

Figure 4.35: Increasing [O-304] does not alter αTC1.9 extracellular ATP secretion.

αTC1.9 cells were exposed to 5.5 mmol/l glucose ± O-304 (2.5 – 50 µmol/l) for 30 min. Cells were subsequently lysed for total protein and supernatant was used to measure extracellular ATP using a luminescence-based assay (Perkin-Elmer). Supernatant was normalised to total protein (µM/mg) (One-Way ANOVA with Dunnett's multiple comparison test, n = 2 – 3)

4.2.8 Hormone secretion

4.2.8.1 O-304 enhanced α-cell glucagon secretion in a concentration-dependent manner

To investigate whether O-304-enhanced α-cell bioenergetics is consequently enhancing downstream glucagon secretion, α-cells were exposed to O-304 (0 – 5.0 µmol/l) ± glucose (0.1/11.7 mmol/l glucose) for 1 h following a 30 min incubation with high (11.7 mmol/l) glucose.

O-304 increased glucagon secretion at 0.1 mmol/l glucose (% glucagon secretion) (Vehicle; 7.220 ± 2.162, 1.0; 11.22 ± 5.746, 2.5; 7.349 ± 1.70, 5.0; 28.04 ± 4.406, *Vehicle vs 5.0, p = 0.0132*) (Figure 4.36Ai). Similarly, O-304 increased glucagon secretion, in a concentration dependent manner, at 11.7 mmol/l glucose (% secretion) (Vehicle; 6.736 ± 1.124, 1.0; 8.135 ± 1.097, 2.5; 11.68 ± 2.219, 5.0; 22.30 ± 4.217, *Vehicle vs 5.0, p = 0.006*) (Figure 4.36Bi). At 11.7 mmol/l glucose, O-304-enhanced glucagon secretion and reduced total α-cell glucagon content at 5.0 µmol/l only (µg) (Vehicle; 0.1733 +/- 0.01519, 1.0; 0.1752 ± 0.01673, 2.5; 0.1674 ± 0.01252, 5.0; 0.1129 ± 0.01108, *Vehicle vs 5.0, p = 0.0397*) (Figure 4.36Bii). This was not seen at 0.1 mmol/l glucose (µg) (Vehicle; 0.1530 ± 0.01652, 1.0; 0.2164 ± 0.03029, 2.5; 0.2029 ± 0.007279, 5.0; 0.1289 ± 0.01025) (Figure 4.36Aii).

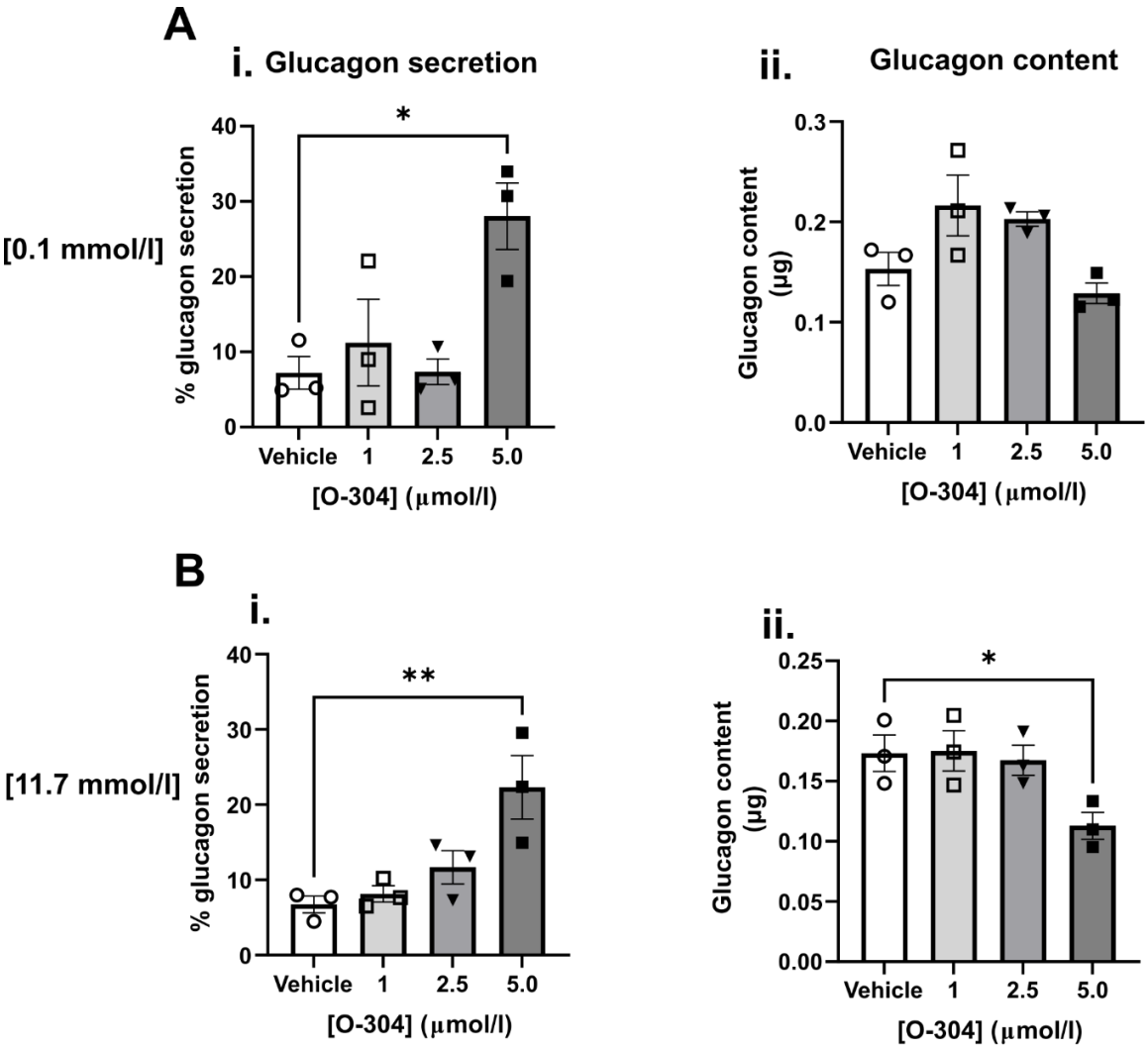

Figure 4.36: O-304 increased isolated α-cell glucagon secretion.

αTC1.9 cells were preincubated with 0 – 5.0 µmol/l O-304 for 30 min and 11.7 mmol/l glucose prior to replacing extracellular [glucose] with either **A**. 0.1 or **B.** 11.7 mmol/l glucose ± O-304 for 1 h. **A - Bi.** Glucagon secretion was normalised to **ii.** total glucagon content (One-Way ANOVA with Dunnetts multiple comparison test, n = 3, *P<0.05, **P<0.01)

4.2.8.2 O-304 reduced mouse islet glucagon content at low glucose but did not alter glucagon secretion.

Islet glucagon secretory measurements were pooled from data collected at University of Birmingham, in collaboration with Prof. David Hodson's group, and data from the University of Exeter. Similar glucagon secretion (% content) values were observed at each [glucose] in both data sets.

Data suggests a non-significant reduction in islet glucagon secretion at 0.5 mmol/l glucose following O-304 exposure (% glucagon secretion) (Vehicle; 0.1925 ± 0.03161, O-304; 0.1306 ± 0.01912, $p = 0.1357$) (Figure 4.37Ai). No significant difference was seen at 11.7 mmol/l glucose treatment (% glucagon secretion) (Vehicle; 0.1347 ± 0.02021, O-304; 0.1301 ± 0.01745) (Figure 4.37Bi). Similarly, O-304 reduced glucagon content at 0.5 mmol/l glucose (µg) (Vehicle; 0.1512 ± 0.02147, O-304; 0.09417 ± 0.01253, $p = 0.0462$) (Figure 4.37Aii). O-304 did not alter total glucagon content at 11.7 mmol/l glucose (µg) (Vehicle; 0.09827 ± 0.01487, O-304; 0.1055 ± 0.01478) (Figure 4.37Bii).

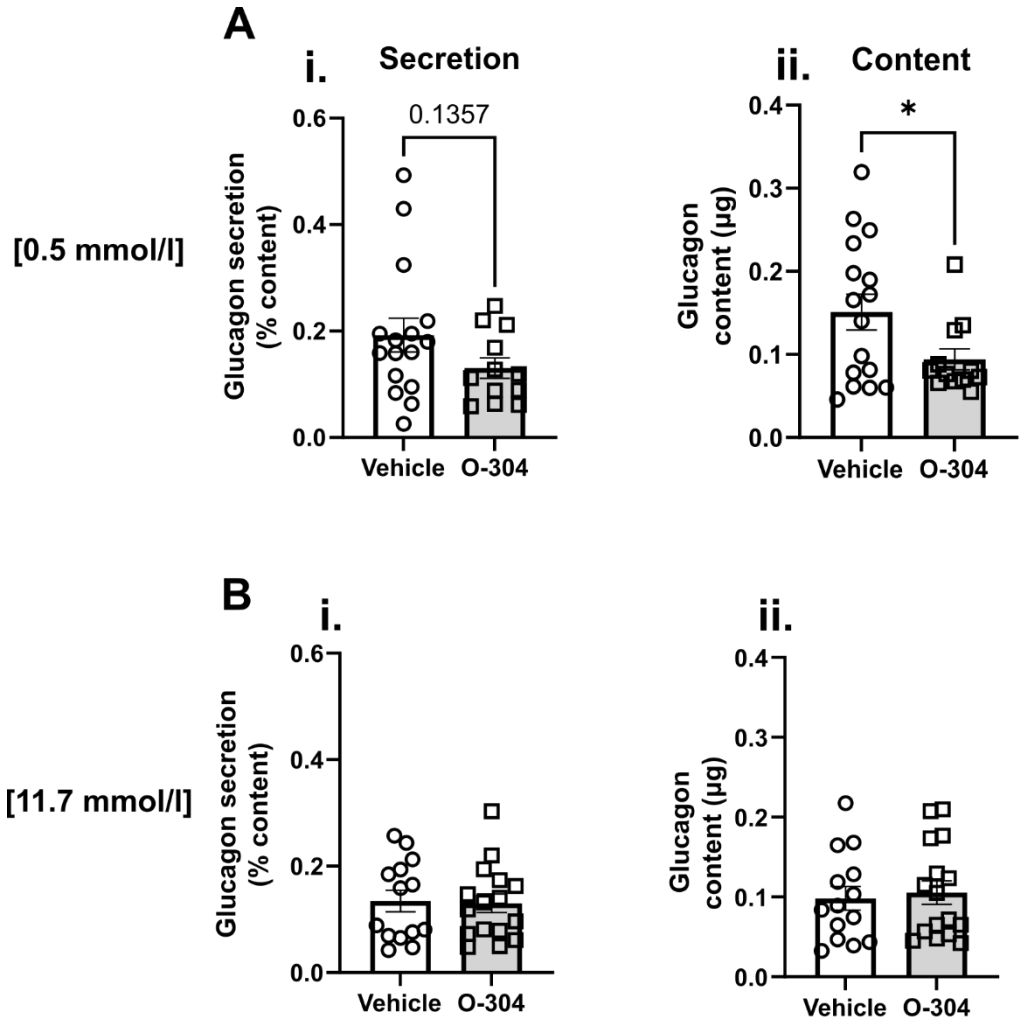

Figure 4.37: O-304 reduced mouse islet glucagon content but not secretion in a glucose-dependent manner.

Mouse *ex vivo* islets exposed to 11.7 mmol/l glucose-containing ATP buffer for at least 1 h prior to stimulation with **A.** 0.5 (**i.** secretion and **ii.** content; unpaired two-tailed t test) **B.** 11.7 mmol/l glucose (**i.** secretion and **ii.** content; unpaired two-tailed t test) ± O-304 (5.0 µmol/l) for an additional 1 h. Glucagon secretion measurements were normalised to total glucagon content (% content) (n = 12 – 16, *P < 0.05)

4.2.9 AMPK activator tolerance test (AMPKTT) in diabetic rats

To investigate if the direct AMPK activator (O-304) would lower hyperglycaemia in diabetic rats, an AMPK tolerance test (AMPKTT) was performed in STZ rats as described in Figure 4.38A and parameters including blood glucose, plasma glucagon and hepatic gluconeogenic gene expression were measured. This pilot *in vivo* study was conducted by Dr. Ana Miguel Cruz, Ms Katie Partridge and Dr. Craig Beall.

4.2.9.1 O-304 trended to reduced plasma blood glucose and hepatic *PEPCK* gene expression in diabetic rats.

Blood glucose was measured over 120 min and measurements taken every 30 – 60 min. A reduction in blood plasma glucose at 120 min post-O-304 injection was observed in STZ rats (mmol/l) (Vehicle; 22.10 ± 2.055, O-304; 12.48 ± 4.384, $p = 0.1385$) (Figure 4.38Bi-ii). O-304 did not alter endpoint plasma glucagon (pmol/l) (Vehicle; 7.352 ± 1.215, O-304; 6.192 ± 1.543) (Figure 4.38C). Hepatic gluconeogenic gene expression (*G6Pase, FBPase, PEPCK*) was assessed to measure diabetic hepatic gluconeogenesis post-O-304 treatment. No observed change with O-304 treatment was seen on *G6Pase* and *FBPase* gene expression (fold change in mRNA expression) (*G6Pase*: vehicle; 1.360 ± 0.4563, O-304; 1.324 ± 0.6780, *FBPase*: vehicle; 2.146 ± 0.8564, O-304; 0.5934 ± 0.08451, $p = 0.0846$) (Figure 4.38Di-ii). Although, a reduction in hepatic *PEPCK* gene expression was observed in diabetic rats that did not achieve statistical significance (fold change in mRNA expression) (Vehicle; 1.167 ± 0.1778, O-304; 0.6764 ± 0.1136, $p = 0.0581$) (Figure 4.38Di-iii).

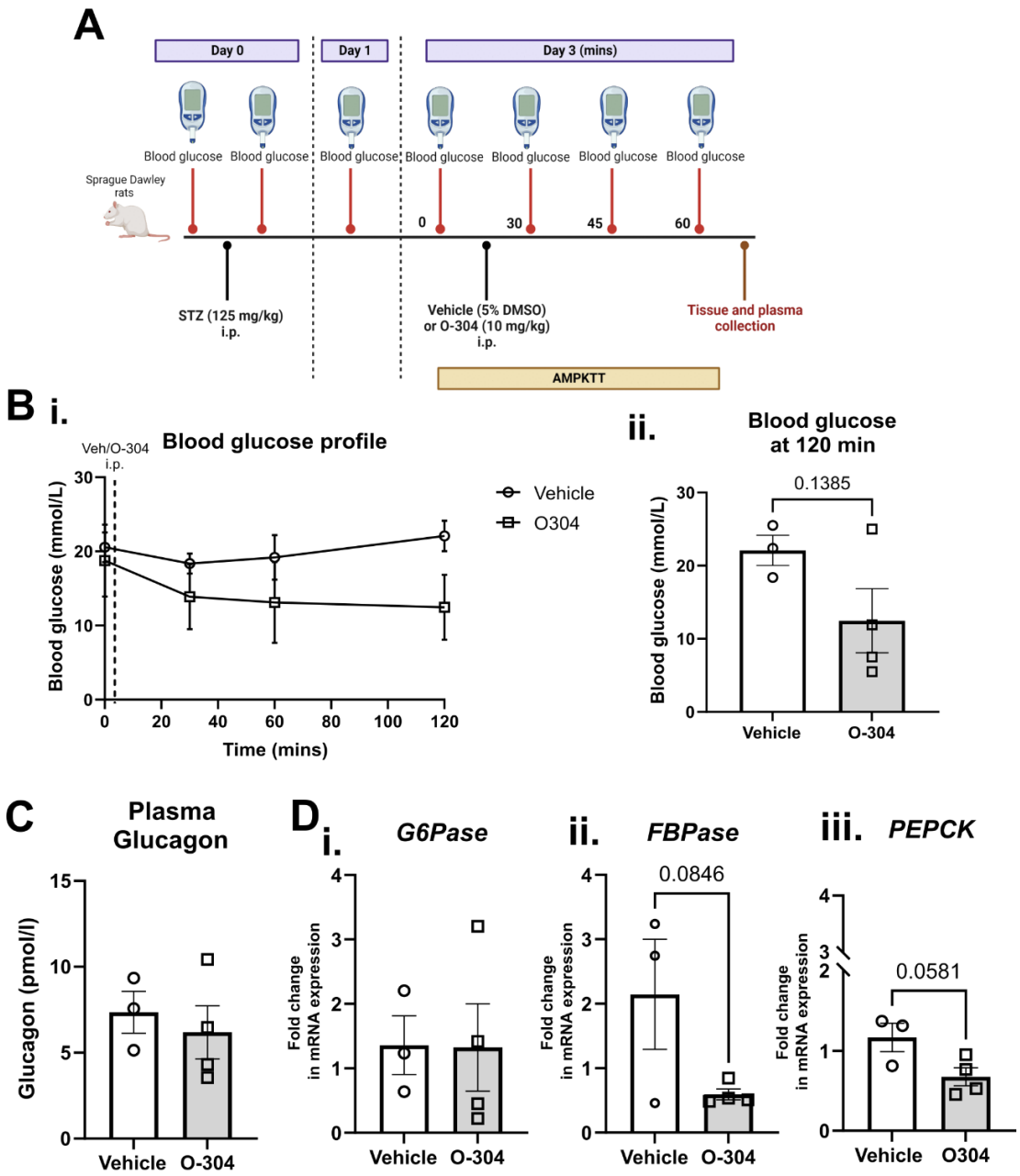

Figure 4.38: O-304 AMPK tolerance test (AMPK-TT, 10.0 mg/kg) in diabetic Sprague-Dawley rats.

A. Study design (post 5 h fast) **B. i**. Blood glucose profile during AMPK-TT, **ii.** blood glucose (mmol/l) at 120 min (Unpaired two-tailed t-test) **C.** Endpoint plasma glucagon profile measured by ELISA (Mercodia). **D.** Liver gluconeogenic **i.** *G6Pase* **ii**. *FBPase* **iii.** *PEPCK* gene expression, normalised to housekeeping genes *Hrpt, Rplp1* and *Sdha*, quantified by qPCR (Vehicle vs O-304) (n = 3 – 4, unpaired two-tailed t-test)

4.3 Discussion

Findings presented in this thesis determined the optimal [O-304] to stimulate downstream α-cell AMPK signalling for use in subsequent experiments. In this study, 10.0 µmol/l O-304 enhanced AMPKα Thr-172 phosphorylation but increases in ACC-Ser79 phosphorylation were observed at lower activator concentrations. Steneberg *et al.* 2018 indicated a concentration-dependent increase in AMPKα-Thr-172 and ACC-Ser-79 phosphorylation in various cell types from different key glucose-sensing and AMPK heterotrimer combination-expressing tissues, including skeletal muscle myotubes and hepatocyte (Steneberg *et al.* 2018). Importantly, the AMPK signalling cascade was activated upon O-304 application in islet-derived cells, including murine β-cell line, INS-1, and human islets at all [O-304] used (up to 10.0 µmol/l) (Steneberg *et al.* 2018). Both direct and indirect AMPK activators, A-769662 and metformin respectively, also can enhance downstream α-cell AMPK activation (Leclerc *et al.*, 2011). In these experiments, high activator concentrations were used (up to 500 µmol/l) in order to enhance α-cell AMPK signalling, increasing the likelihood of AMPKα Thr-172 phosphorylation through energy depletion by AMP-dependent binding to the AMPKγ subunit by LKB1-dependent Thr172 phosphorylation (Kim *et al.*, 2016; Ovens *et al.*, 2022; Sanders *et al.*, 2022). Therefore, 5.0 µmol/l O-304 (or otherwise stated) was used in most studies to not saturate AMPK activation.

O-304 increased α-cell glucose utilisation after high glucose reintroduction, not low glucose, in an SBI-sensitive manner. These data suggest O-304 enhanced α-cell glucose utilisation at high glucose concentrations, in an AMPK-dependent manner. Comparable to other allosteric AMPK activators (e.g., PF-793, SC4), O-304 enhanced insulin-independent glucose uptake in an AMPK-dependent manner in skeletal muscle myotubes (Steneberg *et al.*, 2018). In addition, O-304-enhanced muscle glucose uptake was similarly seen in T2DM rodent models (Steneberg *et al.*, 2018). Similarly, 991 enhanced isolated rat skeletal muscle and cultured human myotube glucose uptake (Lai *et al.*, 2014; Brown *et al.*, 2018). Albeit limited data is available, α-cells express GLUT transporters

(the level of isoform expression varies between species) required for glucose uptake. α-cell GLUT-1 mediated glucose transport is reportedly up to nine-times greater than that required for glucose utilisation (Heimberg *et al.*, 1996; Berger and Zdzieblo, 2020). Glucokinase activity is most likely driving this effect by integrating GLUT-mediated α-cell glucose uptake and glycolysis at high glucose availability (Basco *et al.*, 2018; Moede *et al.*, 2020; Bahl *et al.*, 2021). The current published evidence suggests AMPK activation drives cell-surface translocation of GLUT-4 transporter by activation of AS160 (Treebak *et al.*, 2006; Thong, Bilan and Klip, 2007). Therefore, this poses the question whether O-304 drives AMPK-dependent glucose utilisation by potentially increasing α-cell GLUT-4 transporter translocation, increasing α-cell glucose uptake and downstream glucose-limited glycolysis.

To ensure O-304 directly altered α-cell glycolysis, glycolytic end product lactate was measured. Interestingly, O-304 enhanced α-cell glycolytic flux and thus accelerated lactate secretion in both a glucose-dependent and AMPK-dependent manner. Human α-cells abundantly express LDHA (~ six times greater) compared to LDHB, where the latter is primarily localised to human β-cells (Moin *et al.*, 2020; Sanchez *et al.*, 2021; Cuozzo *et al.*, 2022). Recently, findings from Zaborska *et al.* 2020 found fluorescently labelled exogenous lactate can be imported into mouse α-cells, most likely due to monocarboxylate transporter (MCT) import (Zaborska *et al.*, 2020). Interestingly, exogenous lactate entry further hyperpolarised mouse α-cells by the opening of K_{ATP} channels, reducing $[Ca^{2+}]_i$ and concurrent inhibition of human and mouse glucagon secretion (Zaborska *et al.*, 2020). Other work has suggested a direct AMPK-LDH link to regulate cell function and fate. The genetic attenuation of AMPKα1 expression in myogenic precursor cells (MPCs) displayed increased extracellular lactate and LDH activity in both AMPKα1$^{-/-}$ knockout MPCs and muscle stem cells (MuSCs); corroborated by the opposite effect by increasing [991] activator application and thereby highlights a AMPK-LDH link to muscle cell function (Theret *et al.*, 2017). Together, these data suggest α-cell-derived lactate export is an autocrine electrophysiological regulator of downstream glucagon secretion. If so, it would be interesting to examine whether O-304-

dependent actions influence LDH activity and if so, impact α-cell electrical activity in intact islets.

Interestingly, O-304 did not affect human β-cell glucose utilisation. The aerobic-derived ATP production is largely favoured by β-cells compared to α-cells that primarily use anaerobic respiration (glycolysis) to generate ATP (Spégel and Mulder, 2020). This could partly be due to significantly lower LDH expression in β-cells compared to α-cells and lack of MCT-mediated lactate cell export; lowering ECAR-derived glycolysis values and lactate secretion (Zhao *et al.*, 2001; Moin *et al.*, 2020; Sanchez *et al.*, 2021; Cuozzo *et al.*, 2022). β-cell glycolysis-derived pyruvate production is therefore primarily shuttled into the mitochondria for oxidative respiration. It is important to note, AMPK activation by O-304 was not measured in this model. By measuring β-cell glucose-regulated mitochondrial metabolism, rather than glycolysis, is perhaps a more valuable indicator if O-304 can impact β-cell glucose utilisation in an AMPK-dependent manner.

These are, however, similarities between islet cell types on O-304's impact on cellular bioenergetics. In both α- and β-cells, O-304 enhanced basal ECAR and OCR in the absence of glucose (with α-cell changes being AMPK-dependent), suggesting that O-304 pushes rises in glycolysis and oxidative respiration through increasing use of alternative metabolic substrates. Cells were supplemented with metabolic substrates pyruvate and glutamine to maintain basal respiration and mitigate cellular stress. Therefore, evidence suggests rises in glucose-independent α-cell metabolism were partly by increased pyruvate shuttling (contributing to high ECAR/OCR) and glutamine-glutamate hydrolysis (high OCR by fuelling the Krebs' cycle). In this experimental paradigm, this speculation was rejected as there were no observed changes in acute α-cell glutamine and pyruvate utilisation with O-304 incubation. The absence of pyruvate and glutamine prior to injection, although, limited the O-304-induced increase in basal glycolytic respiration in addition to no change following AMPK inhibition. These data support an AMPK-independent action of O-304 in glutamine and pyruvate utilisation. It is important to consider whether

O-304-dependent influence on substrate utilisation is limited by complete metabolic substrate removal. For instance, the diminished production of ATP could be maximally activating AMPK and thereby stimulating α-cell ULK-1-sensitive autophagy. The reasoning being both α-cell ECAR and OCR appear to decline in complete substrate absence and shortly following post-substrate addition, indicating the α-cell metabolic demand for rapid ATP production to retain functionality and perhaps survival. Further research could adjust the experimental design to include metabolic supplements, such as normal [glucose] availability, to remove the possibility of accelerated cell autophagy and compromised function as a confounding variable.

These data were corroborated by a pilot study conducted by Dr. Ana Miguel Cruz, of whom examined alternative substrate utilisation (fructose and galactose) on α-cell bioenergetics. The cell extracellular medium contained pyruvate and glutamine, and similarly, basal OCR/ECAR was high following O-304 exposure prior to fructose supplementation. In the liver, fructose can cross the cell plasma membrane through GLUT-mediated transport (via GLUT-2 and GLUT-5) similarly to glucose, and is converted into glycolytic intermediate fructose-1-phosphate independently of glucokinase (Zhao and Keating, 2007; Dewdney *et al.*, 2020). Reduced glycolysis is sensed by lysosomal aldolase-fructose-1,6-bisphosphate (F-1,6-BP) signalling (Zhang *et al.*, 2017). This association regulates cell energy sensing by LKB1-induced phosphorylation of lysosomal-bound AMPK (Zhang *et al.*, 2017). In a previous study, O-304 failed to increase ACC and AMPK phosphorylation in HeLa cells, which lack LKB1 (Steneberg *et al.*, 2018). O-304 therefore requires upstream AMPK kinase LKB1 to sustain downstream AMPK signalling cascade activation. The current study found fructose introduction accelerated α-cell glycolysis by up to two-fold in the presence of O-304, which may suggest that both allosteric (glucose-deprivation) and exogenously activating AMPK (through LKB1, possibly by lysosomal surface-bound AMPK) increased α-cell fructose sensing by enhanced FBP-aldolase binding. In comparison to glucose, the magnitude of the increase in glycolysis as a result of fructose and galactose is relatively small (Figure 4.20). Additional evidence needs to clarify if glycolytic effects, as a result of O-

304, from alternative substrate utilisation are AMPK-sensitive and meaningful to α-cell physiology.

Furthermore, evidence postulated that O-304 augmented increases in OCR in a fructose concentration-dependent manner. This is most likely due to fructose increasing the glycolytic intermediate, pyruvate, and therefore substrate feed-through into oxidative metabolism. It is important to note that fructose-regulated oxidative respiration is different between each cell type/line dependent on concentration and length of exposure. For instance, high fructose concentrations (> 15 mmol/l) time-dependently increased rat myotube (L6) mitochondrial-generated ROS, possibly by mitochondrial membrane disruption and raised intracellular ROS in the HEK293 embryonic kidney cell line (Jaiswal *et al.*, 2015; Dornas *et al.*, 2017). Over more chronic fructose exposure (> 3 months) in rodent models*,* low fructose dose (10% fructose-fed) reduced cardiac electron transport chain complex I and II-derived ATP production and downstream oxygen consumption rates (Y.B. Zhang *et al.*, 2016). It is important to note that the classification of a high-fructose diet can vary between published work; with some studies annotating the diet as low fructose despite containing 50% of calories derived from fructose (Warren *et al.*, 2014; Taskinen, Packard and Borén, 2019; Mehta *et al.*, 2021). In humans, approximately 15 – 17% total energy intake is derived from fructose and associated sweeteners (Powell, Smith-Taillie and Popkin, 2016). Additional studies could examine whether O-304 enhanced fructose-dependent oxidative respiration in α-cells is retained over chronic fructose exposure and therefore could have a role in protecting α-cells from reduced mitochondrial efficiency associated with high-fructose diet/treatment (Mehta *et al.*, 2021).

High fructose diet, as mentioned, is linked to obesity and insulin resistance; with both comorbidities associated with type 2 diabetes and insulin resistance (Tappy and Le, 2010). How high fructose influences α-cell function is somewhat contradictory. For example, evidence postulated that high-fructose fed rodent islets had a reduction in glucagon-positive cells, but high-fructose fed mouse islets lack glucose-mediated suppression of glucagon secretion by enhancing

intracellular glucagon content (Topsakal *et al.*, 2016; Asghar *et al.*, 2017). These findings can be partially explained by attenuated paracrine control by lowered glucose-stimulated insulin secretion and α-cell area (Asghar *et al.*, 2017). Interestingly, high fructose-fed mouse islets displayed a reduction in glucose-stimulated oxygen consumption rate, but determination of α- or β-cell contribution has not been quantified (Asghar *et al.*, 2017). If high fructose-exposed islets have high glucose-stimulated glucagon secretion, could this be due to deficits in α-cell glucokinase activity and α-cell glucose-sensing, similarly demonstrated in hyperglucagonaemic glucokinase-knockout mice (Moede *et al.*, 2020)? Therefore, clarification is required as to whether O-304, by activating AMPK, can enhance fructose utilisation and improve α-cell glucose sensing, which is known to be dysregulated in T1DM.

As displayed, fructose glycolytic utilisation is greater compared to galactose Figure 4.19. Glycolytic metabolism derived from galactose yields no net ATP, compared to glucose that produces 2 net ATP (Marroquin *et al.*, 2007; Bonora *et al.*, 2012). The lack of glycolytic energy production from galactose is corroborated by other findings from published evidence where exposure to galactose (> 10 mmol/l) increased oxidative respiration in hepatocytes, chondrocytes, and human primary myotube differentiation, although the use of galactose as a mitochondrial fuel could be tissue-specific (Marroquin *et al.*, 2007; Aguer *et al.*, 2011; Elkalaf, Anděl and Trnka, 2013; Ohashi *et al.*, 2021). Certain tissues may therefore rely on galactose to fuel aerobic respiration. At the time of writing, there is no published literature in regard to α-cell galactose utilisation.

In addition, evidence provided here indicated that O-304 can enhance galactose-dependent glycolytic utilisation at high [galactose]. The basal galactose entry for glycolysis is minimal compared to fructose, which may suggest O-304 could enhance galactose transport into the cell and increasing glycolytic utilisation. Galactose is imported into the liver utilising GLUT-mediated transport, similarly to glucose (Coelho, Berry and Rubio-Gozalbo, 2015; Conte *et al.*, 2021). Therefore, as suggested previously, O-304 could increase

galactose utilisation by increasing AMPK-sensitive GLUT translocation and galactose intracellular availability, is a plausible idea for the observed effect on glycolysis. No change was observed in α-cell oxidative metabolism with acute galactose treatment in the absence of O-304, suggesting α-cell galactose is fuelling glycolytic-derived acidification, not pyruvate intermediates for oxidative respiration. Compared to glycolysis, O-304 similarly increased galactose-dependent α-cell oxidative metabolism. Human osteoarthritic chondrocytes, in response to galactose, increased AMPK Thr-172 phosphorylation and mitochondrial biogenesis marker PGC1α (Ohashi *et al.*, 2021). This poses the question, alongside the evidence provided in this thesis, whether galactose and O-304 enhanced PGC1α expression by AMPK activation and therefore enhanced mitochondrial capacity could be contributing to the observed α-cell oxidative respiration.

Galactose impact on blood glucose is yet, however, debated. Two studies conducted in 1979 found intravenous (i.v) galactose infusion in newborn babies increased blood glucose by 20% and in adult men only by 5% as much as glucose alone (Morgan, Wright and Marks, 1979; Pribylova and Kozlova, 1979). Galactose (50 g) ingestion stimulated an average small, yet significant, plasma glucose increase (0.8 mmol/l) at 30 min in healthy subjects, suggesting galactose has a low glycaemic index (Gannon, Khan and Nuttall, 2001). Whether galactose-driven glucose rises, if at all, are by direct pancreatic α-cell stimulation is yet unknown. A previous study suggested either galactose or N-acetylgalactosamine (a galactose metabolic derivative) linkages with proglucagon in rat islet extracts; suggesting possible direct galactose (or downstream metabolic substrate) regulation to glucagon processing (Patzelt and Weber, 1986). Supplementary work needs to clarify whether galactose can directly, or indirectly, control α-cell glucagon secretion.

Here, evidence suggested O-304 can reduce α-cell mitochondrial oxidative efficiency, independent of glucose and AMPK. This is demonstrated by enhanced inner mitochondrial membrane proton leak, reduced ATP-linked respiration and reduced total ATP. Similarly, other published findings using O-

304 (30 mg/kg)-exposed rats with testosterone propionate-induced benign prostatic hyperplasia (BPH) prostate tissue exhibited no significant trend for increased mitochondrial membrane potential and reduced mitochondrial size (Y. Li *et al.*, 2021b). The reduced mitochondrial function with O-304 exposure was further suggested with raised cytochrome C levels (Y. Li *et al.*, 2021b). O-304 increased mitochondrial number, most likely due to increased PGC1α expression (Y. Li *et al.*, 2021b). These findings were identical in BPH-rats infused with the PGC1α-activator, ZLN005 and in *SIRT3* (a PGC1α promoter) over-expressing rats (Y. Li *et al.*, 2021b). As stated, PGC1α is a master regulator of mitochondrial biogenesis by activating transcriptional factor expression associated with oxidative phosphorylation, Krebs cycle-related genes but also release of antioxidants (Bhalla *et al.*, 2011; Dominy and Puigserver, 2013; Tang *et al.*, 2020; Shen *et al.*, 2021). This poses the question whether O-304-increased mitochondrial inefficiency is driving increased SIRT-PGC1α axis, and if over a longer incubation period, could influence α-cell mitochondrial biogenesis to replace damaged mitochondria (mitophagy).

AMPK, as well as SIRT1, has been identified as a regulator of PGC1α transcript expression in pancreatic islets (Jaafar *et al.*, 2019). Here, O-304 enhanced α-cell mitochondrial proton leak and reduced ATP-coupled respiration, independently of AMPK, as findings were unaffected by both SBI (AMPK inhibitor) and glucose exposure. Similarly to O-304, salicylate is an allosteric and direct AMPK activator (Hawley *et al.*, 2012). In isolated rat mitochondria and cultured hepatocytes, salicylate (0.5 mmol/l) enhanced calcium-dependent mitochondrial permeability transition pore opening and cytochrome C release, although the authors did not examine AMPK (Battaglia, Salvi and Toninello, 2005). White adipose tissue derived from high fat diet (HFD) fed and O-304-exposed mice increased *Cox8b,* a component of cytochrome oxidase in the ETC (Steneberg *et al.*, 2018). Similarly, Hawley *et al.* 2012 suggested salicylate (> 10 mmol/l) increased HEK-293 oxygen consumption, similar to the mitochondrial protonophore dinitrophenol (DNP); suggesting like DNP, salicylate at a high concentration, is a mitochondrial proton uncoupler (Hawley *et al.*, 2012). Data indicated here found little effect on α-cell basal glycolysis and

oxidative respiration upon proton uncoupler (FCCP) treatment following O-304 exposure. This evidence could therefore postulate O-304 is a proton uncoupling agent, alongside the known efficacy as a robust AMPK activator.

Proton leak is common in highly metabolic cells; with 20% and 50% of hepatocytes and skeletal muscle (respectively) basal metabolic rate contributed by proton leak (Rolfe and Brand, 1996). Proton leak is primarily induced and regulated by uncoupling protein (UCP) opening, located on the inner mitochondrial membrane (IMM). There is a lack of published data investigating inducible α-cell proton leak and downstream function. Pancreatic α-cells in mouse islets and an α-cell line express high UCP-2 levels (Diao *et al.*, 2008). Both glucose-stimulated hyperpolarisation and mitochondrial membrane potential were increased in UCP-2 knockout α-cells and appeared to reduce glucagon secretion at low glucose (Diao *et al.*, 2008; Lee, Robson-Doucette and Wheeler, 2009; Allister *et al.*, 2013). Similarly, UCP-2-deficient diabetic mice had reduced blood glucose, supported by the reduced plasma glucagon secretion observed (Allister *et al.*, 2013). Furthermore, one study suggested UCP-2 is crucial for retaining α-cell viability in various cytotoxic and normal conditions (Diao *et al.*, 2008). This poses the question whether O-304 is enhancing UCP-2-dependent proton leak to control α-cell function and survival. More work is required to investigate the role of UCP-2-controlled proton leak in α-cell function.

Similarly to the increase in oxygen consumption following salicylate exposure, evidence from these studies could suggest O-304 can enhance non-mitochondrial oxygen consumption in an SBI-insensitive manner (Hawley *et al.*, 2012). Non-mitochondrial oxygen consumption is the remaining OCR after Rot/AA treatment. Sources of non-mitochondrial oxygen consumption include reactive oxygen species (ROS) generation, cyclooxygenase and NADPH oxidase activation (Dranka, Hill and Darley-Usmar, 2010; Hill *et al.*, 2012; Chacko *et al.*, 2014). Work described here suggested a concentration-dependent increase in α-cell ROS production with O-304 treatment, supporting the idea that O-304-derived non-mitochondrial oxygen consumption is derived

from increased ROS generation. O-304-enhanced ROS generation in α-cells is not necessarily a determinant for cell apoptosis. Evidence presented here suggested there was no change in α-cell viability with increasing O-304 treatment nor [glucose]. However, it was noted that complete αTC1.9 cell death (> 70%) was difficult to obtain (Figure 4.31). One study has suggested that human α-cells express higher levels of antioxidant enzymes (catalase and glutathione peroxidase; GPX) vs β-cell counterparts; perhaps an indication of α-cell protection against oxidative-mediated apoptosis (Miki *et al.*, 2018; Benkahla *et al.*, 2021). α-cell proton leak could be controlling downstream ROS levels and survival. Proton leak, uncoupled respiration and ROS production are all intrinsically regulated by a negative feedback mechanism whereby increases in ROS drive proton leak, and induced proton leak is a protective mechanism that can in turn limit ROS production (Brookes *et al.*, 1998; Echtay *et al.*, 2002). A greater ROS production and increased α-cell area were associated with deficient UCP-2 activity, compared to wild type (Lee, Robson-Doucette and Wheeler, 2009). Islets derived from aged mice characterised by a mitochondrial complex I deficiency (PolgA$^{mut/mut}$) had increased MitoP/MitoB (ROS and hydrogen peroxide indicator) in all peripheral tissues examined, including liver (Logan *et al.*, 2014). PolgA$^{mut/mut}$ aged islets were also found to have accelerated α-cell proliferation (Yu *et al.*, 2022). This evidence implies mitochondrial uncoupling, by O-304, could be an adaptive response to respond to the raised ROS production in the pancreatic α-cells.

There is a lack of evidence on whether α-cell's secrete ATP, but growing evidence suggests extracellular purinergic signalling can directly regulate α-cell glucagon secretion, especially as ATP is co-secreted with insulin from neighbouring β-cells (Richards-Williams *et al.*, 2008; Tudurí *et al.*, 2008). Here, evidence suggested O-304 exposure can reduce ATP-coupled respiration and ATP synthesis at the concentrations studied. This posed the question; is this due to accelerated ATP secretion? Evidence presented in this thesis, for the first time, demonstrates that αTC1.9 cells secrete ATP (similarly found in chapter 3) and increasing [O-304] treatment did not modify this. A reason behind this could be due to αTC1.9 cells sustaining intracellular ATP supply and

glucagon secretion. Published evidence reports purinergic receptors (namely A1 and P2X7) are expressed on the α-cell membrane (Chapal *et al.*, 1985; Petit *et al.*, 1996; Coutinho-Silva *et al.*, 2003; Grapengiesser *et al.*, 2006; Tudurí *et al.*, 2008). One study found purine nucleotides/nucleosides had efficacy at reducing mouse islet glucagon secretion and α-cell calcium oscillations (Tudurí *et al.*, 2008). It would be interesting to suggest that, similarly to β-cells, ATP is co-secreted with glucagon as either an autocrine, negative feedback mechanism or as a paracrine inhibitor of β-cell insulin secretion at low glucose.

Evidence presented here suggests O-304 could modulate glucagon secretion dependent on the model used. For instance, O-304 (5.0 µmol/l) increased αTC1.9 glucagon secretion two- to three-fold at both low and high [extracellular] glucose availability. Although pooled mouse *ex vivo* islets showed a non-statistically significant trend towards a reduction in islet glucagon secretion at low glucose following O-304 exposure, it is important to note high variability within the vehicle control. Additionally, it is important to note in this experiment, glucose-stimulated αTC1.9 glucagon secretion was not evident. For islets, the experimental design was refined to include a large decrease in extracellular [glucose] thought sufficient to stimulate glucagon secretion. A not statistical significant trend was seen for low glucose stimulated glucagon secretion in islets, albeit not significant, most likely due to data variation. Discrepancies may, therefore, lie between the lack of paracrine and cell-cell interactions in αTC1.9 cells, alongside differences between species islet architecture and the retention of α-cells on the islet periphery in *ex vivo* islets, which contribute to the variable glucagon secretion (Asadi and Dhanvantari, 2021).

Interestingly AMPK activator A-769662 treatment (500 µmol/l), similar to O-304, enhanced αTC1.9 glucagon secretion at 0 mmol/l and 17.0 mmol/l glucose and similarly to the methodology included in this thesis, included a large depletion of extracellular glucose (from basal; 10.0 mmol/l to 0 mmol/l) (Leclerc *et al.*, 2011). AMPK inhibitor (Compound C) exposure indicated a modest reduction in αTC1.9 glucagon secretion, but in this work, no combined AMPK activator and inhibitor experiment was conducted to demonstrate the AMPK-dependency of

the specified activator on αTC1.9 glucagon secretion. Prior evidence has indicated O-304 partially activates AMPK by LKB1-dependent signalling (Steneberg *et al.*, 2018). α-cell LKB1 knockout mice had reduced fasting plasma glucagon and ablated islet glucagon secretion at 3.0 mmol/l glucose (with a similar not statistical significant) trend seen in αAMPKα1 KO mice) (Sun *et al.*, 2015). Therefore, additional work will need to identify whether O-304 enhanced αTC1.9 glucagon secretion is AMPK-sensitive via and/or by upstream kinase (e.g., LKB1) activation.

Recent publications suggest α-cells not only intrinsically regulate glucagon secretion but also glucagon content under energy stress. The mTORC1 complex is a key regulator of cell proliferation and is inhibited by AMPK activation (Ling *et al.*, 2020). mTORC1 has previously been implicated as a regulator of α-cell proliferation in rapamycin-inhibited mTORC1 and, α-cell-specific Raptor knockout studies (Liu *et al.*, 2011; Solloway *et al.*, 2015; Bozadjieva *et al.*, 2017). Rapamycin-exposed αTC1.9 cells and mice demonstrate a reduction in glucagon protein/transcript expression and secretion (Bozadjieva *et al.*, 2017; Rajak *et al.*, 2021). Both cells and mice exposed to rapamycin displayed α-cell glucagon granules localised to lysosomes by lysosomal marker (LAMP1) co-staining, with the authors suggesting enhanced α-cell secretory granule lysosomal degradation (crinophagy) under energy-deprived conditions, including amino acid and insulin-induced hypoglycaemia (Rajak *et al.*, 2021). Similarly, α-Raptor KO mice had reduced fasting plasma glucagon, pancreatic glucagon content and heterozygous mice having reduced α-cell K_{ATP} activity (Bozadjieva *et al.*, 2017). In addition, O-304 increased microtubule-associated proteins 1A/1B light chain 3B (LC3B) puncta and autophagy in a human renal and rodent β-cell line (Steneberg *et al.*, 2018; Zhu *et al.*, 2022). These findings, altogether, suggest O-304 can regulate vesicle recycling in lysosomes to retain cell functionality.

A novel finding from this thesis indicated that O-304 exposure reduced glucagon content in a glucose-dependent manner in both mouse islets and αTC1.9 cells. As AMPK activation inhibits mTORC1 activity, it is possible that

O-304-reduced glucagon content is reflective of AMPK-mediated mTORC1-dependent glucagon degradation. This suggestion, however, cannot fully explain why O-304 enhanced αTC1.9 glucagon secretion, and therefore could suggest this action is AMPK-insensitive and a consequence of mitochondrial proton leak as described earlier. Mitochondrial proton leak, alongside uncoupled mitochondrial respiration, is most likely driving the increase in AMP/ADP:ATP. This evidence suggests that the diminished ATP inhibition of K_{ATP} channel activity, as a result of O-304 exposure, could sufficiently decrease α-cell membrane potential. The sustained membrane depolarisation and increased action potential height could limit the inactivation of voltage-gated calcium and sodium channels and thereby contribute to O-304 accelerating glucagon exocytosis. In addition, it would be interesting to examine whether the depletion in ATP, as a result of O-304, could be indicative of increased generation of α-cell second messengers, including cyclic AMP (cAMP). The accompanying low glucose-induced rise in $[cAMP]_I$ is a paracrine-independent stimulator of α-cell glucagon secretion (Tengholm and Gylfe, 2017; Yu *et al.*, 2019). cAMP can directly stimulate PKA-mediated glucagon granule exocytosis, and therefore provide a possible mechanism for the accelerated glucagon secretory response in isolated α-cells (Gromada *et al.*, 1997).

O-304 (10 mg/kg), which is brain-impermeable (T Edlund personal communication to C Beall) direct AMPK activator, was also used to investigate peripheral liver-α-cell regulation of blood glucose in diabetic (STZ) rats. A non-significant trend was observed towards a reduction in blood glucose at 120 min post-O-304 injection, however, the study was limited by both the number of experimental animals in each group and variable hyperglycaemia within the O-304 group. This trend, however, is supported by previous data in hyperglycaemic models conducted by Steneberg *et al.* 2018. Six-weeks of O-304 therapy/day reduced plasma blood glucose in two T2DM models (characterised by islet amyloid deposition and obesity) and fasting blood glucose in diet-obese mice (Steneberg *et al.*, 2018). Interestingly, compared to the study described in this chapter, O-304 took longer (~ 14 days) to reduce fasting blood glucose in obese mice and required multiple doses (Steneberg *et*

al., 2018). It would be interesting to investigate if recurrent, low dosing of O-304 in STZ-rats could significantly reduce hyperglycaemia by improving AMPK-dependent redox homeostasis in peripheral tissues, such as skeletal muscle, to thereby improve glucose clearance. Most importantly, these data are comparable to Phase IIa clinical trial data showing O-304 lowering fasting blood glucose in metformin-treated individuals with T2DM after 28-days treatment.

To investigate whether changes in blood glucose post-O-304 treatment was mediated by glucagon signalling, plasma glucagon was measured at the 120 min AMPK-TT endpoint. Data suggested no difference in plasma glucagon between the two groups, however a glucagon response can peak earlier than 120 min. This suggestion is seemingly corroborated in published work, whereby indirect AMPK activator, R481 (20 mg/kg) infusion enhanced peak plasma glucagon at 30 min sampling in a hyperinsulinaemic-hypoglycaemic rat study (Cruz *et al.*, 2021). Any direct changes in α-cell glucagon secretion would most likely be within 60 min, to rapidly counteract hypoglycaemia. Therefore, repeated blood sampling intervals during a 120 min AMPK-TT duration will exclude the possibility of a missed observation. This could be achieved by insertion of vascular catheters to limit pain and to reduce the impact of catecholamines on blood glucose measurements.

Additionally, measuring hepatic gluconeogenic gene expression allows us to determine whether the modest O-304-induced reduction in fasting blood glucose is due to reduced hepatic glucose production (indirectly/directly from glucagon signalling). No change in relative gene expression was observed in *FBPase* and *G6Pase*. However, O-304 exerted a near significant ($p = 0.05$) reduction in *PEPCK* gene expression. A power analysis calculation suggested this effect could achieve statistical significance, as only an $n = 6$ (increase of 2 – 3 animals from initial cohort) would be required to achieved significance. Contrary to the findings described here, O-304 treatment (10.0 µmol/l) did not influence substrate-derived hepatic glucose production in a previous study (Steneberg *et al.*, 2018). PEPCK is a hepatic enzyme required for gluconeogenesis; with reduced expression being an indicator of reduced

hepatic gluconeogenic capacity. It is surprising that O-304 only reduced expression of one gluconeogenic enzyme, as *PEPCK* and *G6Pase* are both controlled by CREB via rises in cAMP upon glucagon-mediated hepatic PKA signalling (He *et al.*, 2020). One study suggested AKT2, in the absence of insulin signalling, increased PEPCK expression (greater than G6Pase) by increasing CREB-phosphorylation and thereby “prime” the *PEPCK* promoter prior to glucagon stimulation (He *et al.*, 2020). The *PEPCK* promoter is regulated by AF2, unlike *G6P-ase* (Dashty, 2013). This evidence may suggest that basal *PEPCK* hepatic expression is already high in insulin-deficient STZ rats. Altogether, this evidence could suggest O-304 interferes with promoter binding to regulate *PEPCK* gene expression in STZ rats. Additional work needs to examine whether the pancreas-liver axis is modulated by O-304-enhanced AMPK activation in both a diabetic and healthy rodent model.

In conclusion, O-304-driven bioenergetic changes could be driven by α-cell UCP-2 opening. Figure 4.39 summarises how O-304-UCP-2 activity could be driving the key findings described here and the possible targets of O-304 in the α-cell. In addition, this chapter has discussed how O-304 increased α-cell bioenergetics and downstream glucagon secretion in a model-specific manner. O-304 is therefore as a potential therapeutic modulator of α-cell glucagon exocytosis, a process commonly dysregulated in both T1DM and T2DM. Finally, evidence provided here suggests that acute O-304 treatment have anti-hyperglycaemic effects in diabetic animals. Greater investigation is required to accurately determine how this may occur by examining other peripheral tissues, for instance, by examining any changes in glucose uptake in skeletal muscle.

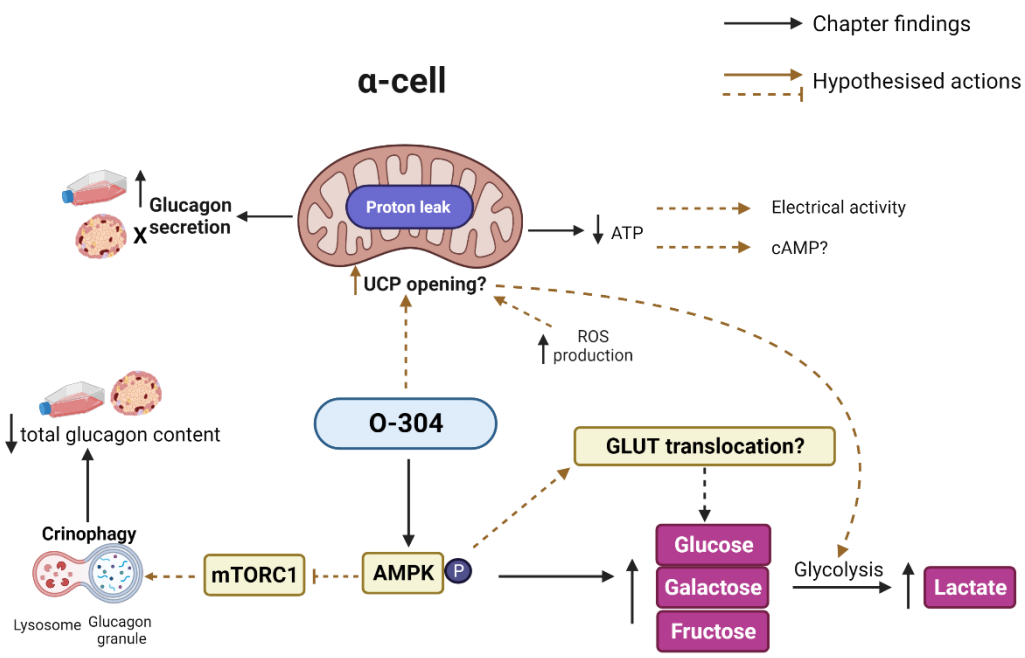

Figure 4.39: Summary of Chapter 4 findings and hypothesised actions of O-304.

O-304 stimulates α-cell AMPK activation and downstream glucose utilisation/lactate production in a glucose-sensitive manner. O-304 also increases proton leak and mitochondrial stress markers, alongside reduction in total ATP and increased ROS production. One hypothesis could be due to AMPK-independent and dependent actions of α-cell UCP-2 opening, driving the observed proton leak and reduced ATP-linked mitochondrial respiration. The depletion of ATP could be potentiating changes in α-cell electrical activity (i.e., K_{ATP} channel opening) and/or driving rises in intracellular cAMP; but this is yet to be examined. Increased UCP-2 activity has been shown to potentiate glycolysis by PFKFB2 activation, and drive glucagon secretion. Furthermore, in a model-specific manner, O-304 either increased or does not alter glucagon secretion. In both models, however, an observed glucose-dependent reduction in total glucagon content was observed by O-304 treatment. Hypothesised actions for this could be due to increased crinophagy of glucagon granules, dependent on AMPK-dependent mTORC1 inhibition, and therefore reducing total glucagon content. Created using Biorender.com.

Chapter 5

Characterisation of a novel AMPK activator, BI-9774, on pancreatic α-cell bioenergetics

5 Characterisation of a novel AMPK activator, BI-9774, on pancreatic α-cell bioenergetics

5.1 Introduction

5.1.1 Indirect AMPK activators

The previous chapter discussed the potential mechanistic targets of direct AMPK activator, O-304, and the therapeutic benefits in DM. There is large focus in the published literature on identifying anti-hyperglycaemic effects of direct AMPK activators from a skeletal muscle and liver perspective, but relatively little is explored on the potential impact and target on other key glucose-sensing tissues, such as the pancreatic islet.

Indirect AMPK activators, such as metformin, stimulate AMPK signalling by indirectly raising cell energy charge. One such mechanism by which metformin can do this is by mGPD inhibition. mGPD is the rate-limiting enzyme to sustain mitochondrial NAD^+/NADH and glycerol-3-phosphate shuttling, supplying electrons to oxidative respiration. Metformin, may therefore, increase [AMP:ATP] by the reducing transfer to the electron transport chain, with reduction in hepatic redox shuttling at least partially responsible for the reduction of AMPK-independent hepatic gluconeogenesis, albeit this is debated (Madiraju *et al.*, 2014; MacDonald *et al.*, 2021).

Studies using metformin have come under increasing scrutiny with regards to the activator concentration used in experiments. Most *in vitro* models use supra-physiological metformin concentrations (>1.0 mmol/l) to observe a reduction in hepatocyte glucose production, which consequently is not replicable in a clinical setting (Lamoia and Shulman, 2021). In addition, the discrepancies between the optimal concentration range of metformin in the blood is mainly attributed to differences in route of administration and pharmacokinetics in the liver/plasma (Hunter *et al.*, 2018). In addition, ~ 20% people with T2DM treated with metformin have nausea and additional gastrointestinal (GI) side-effects leading to 5.0% cessation of treatment (Kirpichnikov, McFarlane and Sowers, 2002;

Florez *et al.*, 2010; Wu, Horowitz and Rayner, 2017; Nabrdalik *et al.*, 2022). A recent meta-analysis study of randomised controlled trials found individuals with metformin-treated T2DM have increased risk of GI events compared to other anti-diabetic drugs (including SGLT2i and GLP-1RA's) and is most likely attributed to high OCT expression in other peripheral tissues, including the intestine (Wang *et al.*, 2002; Nabrdalik *et al.*, 2022). The abundant expression of OCT provides a mechanism behind metformin accumulation in the liver and the intestine, for example, and thereby potentiating adverse off-target effects. Furthermore, the clear differences in the gluconeogenic capability of metformin is at least partly based on acute or chronic exposure which is possibly attributed to the altered AMPK-dependent and -independent insulin release and thereby hepatic insulin-mediated action (Nguyen-Tu *et al.*, 2022). Likewise, providing a clear consensus if metformin-lowered hepatic gluconeogenesis is mediated by both indirect peripheral tissue actions and direct actions on the liver, dependent or independent of AMPK activation, is required. Collectively, these challenges highlight the need for higher efficacy AMPK activators to improve glucose homeostasis in DM to overcome the high discontinuation rates of biguanides, like metformin, in people with T2DM.

5.1.2 Direct AMPK activators

Small molecule AMPK activators have been developed by major pharmaceuticals to directly bind to the AMPK ADaM site and overcome obstacles associated with allosteric compounds (Jørgensen *et al.*, 2021). Most early allosteric AMPK activators have isoform-dependent action dependent on concentration used. Most recently SC-4 was identified to bind to not just α2/β1, but also β2-expressing tissues, with clinical implications in reducing hyperglycaemia (Ngoei *et al.*, 2018). Similarly, both PF-739 (β1 selective agonist) and MK-8722 (pan) activators have demonstrated improvements in glucose homeostasis in both rodent and primate T2DM models (Cokorinos *et al.*, 2017; Ngoei *et al.*, 2018). Although similar preclinical findings, isoform selectivity can be partly justified by activator structural differences. For instance, SC4 and MK-8722, but not PF-739, have a core ring-2 4'-nitrogen which may

allow stable β2 interaction (Cokorinos *et al.*, 2017; Myers *et al.*, 2017; Ngoei *et al.*, 2018; Steinberg and Carling, 2019) (**Error! Reference source not found.**). T he continued development of isoform selective direct activators provides tissue-specific targeting of AMPK in various pathogenic contexts.

A recent study, however, using MK-8772 identified critical questions with regards to clinical translatability of direct AMPK activators. Although findings demonstrated promising improvements to insulin-independent glucose homeostasis, chronic MK-8772 administration in non-human primates and rodents led to cardiac glycogen accumulation and hypertrophy (Myers *et al.*, 2017). On the contrary, a phase II clinical trial involving multiple O-304 doses, demonstrated significant blood glucose-lowering effects in both individuals with metformin-treated T2DM with additional improvements in cardiovascular function, including cardiac glycogen stores, to therefore act as a “exercise mimetic” (Steneberg *et al.*, 2018). The differences between activator action could also pose the question whether these opposing side effects could be due to different AMPK binding sites and subsequent tissue-specific effects.

5.1.3 BI-9774

Boehringer Ingelheim, the world-leading German pharmaceutical company, first financially backed pre-clinical AMPK agonists development in 2014 with Connexios Life Sciences. Pilot data suggested CNX-012-570 can lower hyperglycaemia and cholesterol in both diabetic and obese rodent models (Anil *et al.*, 2014). This early collaboration pioneered the development of BI-9774. Preliminary published findings (under the agonist name “compound 2”) found BI-9774 reduced rodent hyperglycaemia and increased AMPK activity (myoblasts, liver and human peripheral blood mononuclear cells; PBMCs) similarly to other direct AMPK activators (Grempler *et al.*, 2018). In particular, blood glucose was reduced in Zucker-Diabetic Fatty (ZDF) rats by ~ 30 % compared to the highest concentration tested (30 mg/kg), with little to no effect at lower doses (1.0 – 3.0 mg/kg) (Grempler *et al.*, 2018). In addition, similar to other direct small molecules, BI-9774 reportedly increased blood glucose uptake, and glucose tolerance in rodents (published product information). BI-9774 is a pan-AMPK activator that activates all AMPK isoform combinations with low EC_{50} and glucose transporter-4 (GLUT-4) translocation in rat myoblasts (

Table 5.1).

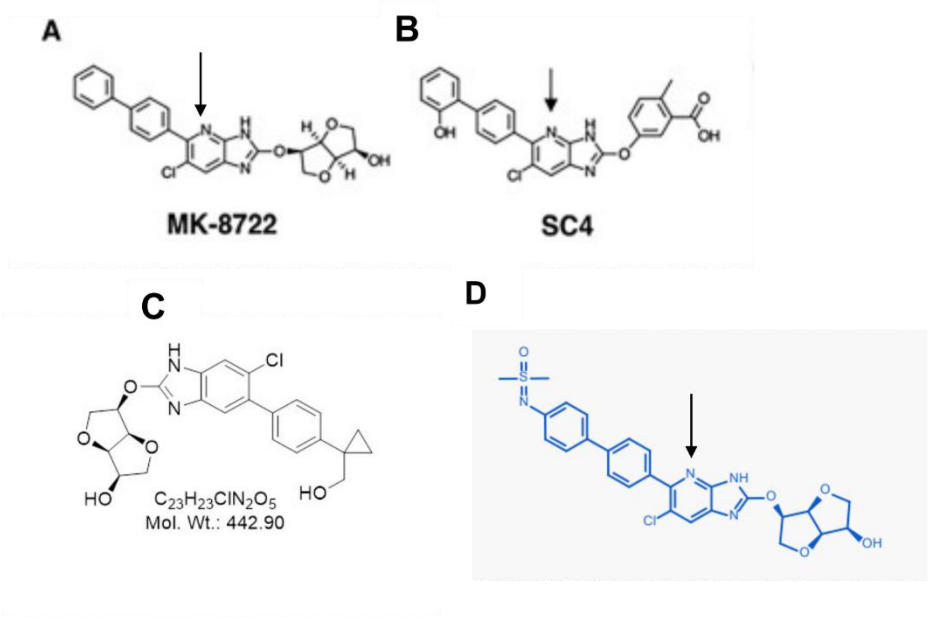

Figure 5.1: 2-D structure of several direct AMPK activators.

A. MK-8722, **B.** SC4, **C**. PF-739 and **D.** BI-9774 with arrows pointing to core ring-2 4' nitrogen group.

Table 5.1: BI-9774 EC_{50} for human AMPK isoform complex combinations *in vitro*.

Adapted from the BI-9774 profile provided by Boehringer Ingelheim (*AMPK Activator BI-9774*, no date)

AMPK isoform combination	BI-9774 (EC_{50}) (nmol/l)
Human AMPKα1β1γ1	64
Human AMPKα2β1γ1	88
Human AMPKα2β2γ2	15
Human AMPKα2β2γ3	24
Human AMPKα1β1γ3	84
Human AMPKα1β2γ2	41
Human AMPKα1β2γ3	12
GLUT4 translocation, L6 rat	8

Pharmacokinetic profiling of BI-9774 revealed both low potassium channel human ether-a-go-go related gene (hERG) inhibition (9.0% at 10.0 µmol/l *in vitro*), Madin-Darby canine kidney (MDCK) permeability (0.05 x 10^{-6} P_{app}a-b/b-a, 10^{-6} cm/s, at 1.0 µmol/l) and high MDCK efflux ratio suggesting a low risk of adverse cardiac side effects, blood-brain impermeability and cell drug efflux. AMPK activators ideally should have limited to no negative side effects on the cardiovascular system, unlike other activators such as MK-8722. Safety BI-9774 profiling in anesthetised rats (ZDF and Wistar) suggested BI-9774 lowered heart rate, however, clarification is needed with regards any concentration-dependent changes to animal heart glycogen deposition and weight (Grempler *et al.*, 2018). Collectively, these findings identify BI-9774 as a useful tool in investigating AMPK biology in whole-body and isolated cell models. In addition, investigating the direct actions of pan-AMPK activators, like BI-9774, on glucose-sensing cell function (such as the α-cells) can increase the knowledge and importance of AMPK regulation of glucose-dependent hormonal responses.

Given the evidence generated from other AMPK activators in previous chapters, the overarching hypothesis for this study is that BI-9774 will upregulate the AMPK signalling cascade and glycolytic rate without compromising mitochondrial oxidative respiration. Therefore, the following aims were addressed by using a wide BI-9774 concentration range to achieve sufficient direct, rather than AMP-mediated, AMPK activation for future studies;

1. Does BI-9774 stimulate α-cell AMPK signalling cascade activation?
2. Does BI-9774 alter α-cell glycolytic rate in a glucose-dependent manner?
3. If so, does BI-9774 modulate α-cell glycolysis without inhibiting mitochondrial oxygen consumption?

5.2 Results

5.2.1 BI-9774 increased AMPK signalling cascade activation in α-cells.

To assess whether BI-9774 enhanced α-cell AMPK activation, cells were exposed to BI-9774 (0 – 2.5 µmol/l) for 1 h in high glucose-containing (11.7 mmol/l) medium. AMPKα-Thr172 phosphorylation was not altered by increasing BI-9774 exposure (fold change in phosphorylation in comparison to vehicle) (100 nmol/l; 0.8797 ± 0.07409, 1.0 µmol/l; 1.124 ± 0.06249, 2.5 µmol/l; 1.260 ± 0.1396, *P = 0.1228*) (Figure 5.2B). ACC-Ser79 phosphorylation, however, was enhanced as a result of increasing [BI-9774] (fold change in phosphorylation in comparison to vehicle) (100 nmol/l; 2.312 ± 0.3772, 1.0 µmol/l; 3.290 ± 0.9547, *P = 0.0407,* 2.5 µmol/l; 3.787 ± 0.6651, *P = 0.0083*) (Figure 5.2C)

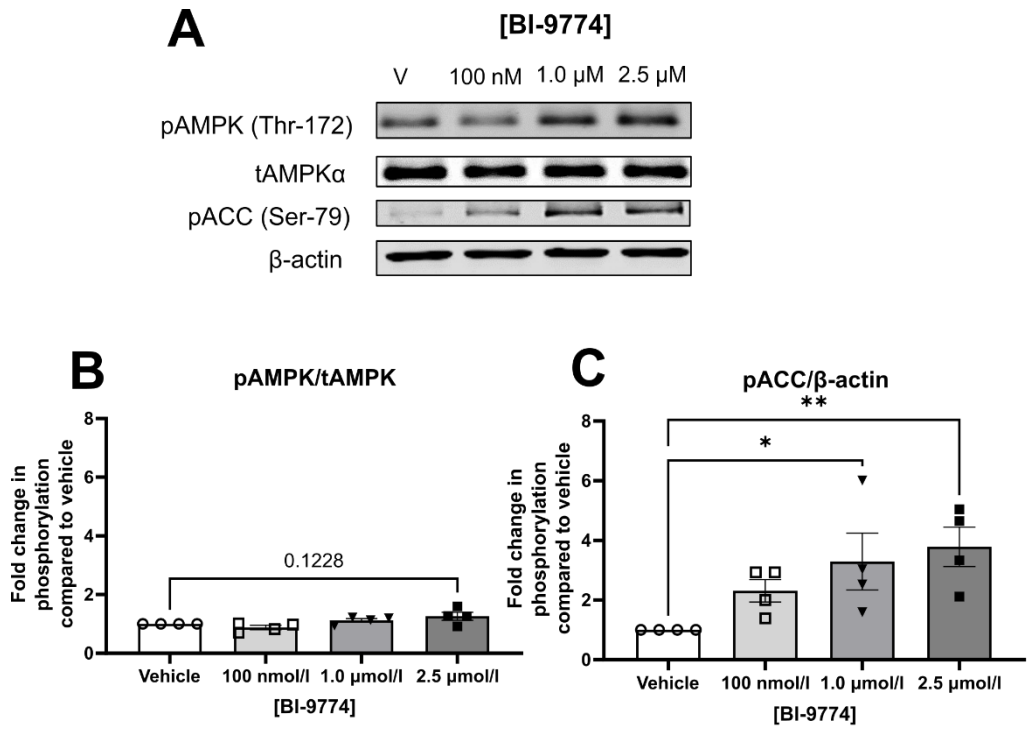

Figure 5.2: BI-9774 enhanced α-cell AMPK activity.

αTC1.9 cells were exposed to 100 nmol/l – 2.5 µmol/l [BI-9774] for 1 h in 11.7 mmol/l glucose-containing media. **A.** Representative immunoblotting images for phosphorylated AMPKα1/2 (pAMPK, Thr-172), total AMPKα1/2 (tAMPK), phosphorylated ACC (pACC, Ser-79) and beta-actin (β-actin). Densitometric analysis for **B.** pAMPK normalised to tAMPK and **C.** pACC normalised to β-actin displayed as fold change vs vehicle (One Way ANOVA with Dunnetts multiple comparison test, *P<0.05, **P<0.01)

5.2.2 BI-9774 pre-incubation did not influence α-cell glucose utilisation.

As shown in Chapter 4, O-304 pre-treatment enhanced α-cell glycolysis dependent on glucose availability. To evaluate whether BI-9774 will exert a similar potent influence on α-cell glycolysis, cells were exposed up to 10.0 µmol/l BI-9774 for 1 h in standard Seahorse XF DMEM medium.

BI-9774 (10.0 µmol/l) reduced α-cell basal ECAR in glucose-absent conditions, compared to vehicle (mpH/min/µg) (Vehicle; 2.637 ± 0.07875, 100 nmol/l; 2.425 ± 0.1096, 1.0 µmol/l; 2.560 ± 0.09184, 2.5 µmol/l; 2.432 ± 0.09184, 5.0 µmol/l; 2.723 ± 0.07775, 10.0 µmol/l; 2.274 ± 0.1124, *vehicle vs 10.0 µmol/l, P = 0.03*) (Figure 5.3A). This not statistically significant trend was similarly reflected in basal OCR (pmol/min/µg) (Vehicle; 40.57 ± 1.002, 100 nmol/l; 36.53 ± 1.487, 1.0 µmol/l; 40.13 ± 1.302, 2.5 µmol/l; 38.32 ± 1.233; 5.0 µmol/l; 42.79 ± 1.142, 10.0 µmol/l; 36.01 ± 1.125, *vehicle v 10.0 µmol/l, P = 0.0329*) (Figure 5.3B).

Following 0.5 mmol/l glucose reintroduction, $\Delta ECAR_{MAX}$ was not altered with [BI-9774] in comparison to vehicle (mpH/min/µg) (Vehicle; 1.470 ± 0.1143, 100 nmol/l; 1.402 ± 0.006630; 1.0 µmol/l, 1.542 ± 0.1121, 2.5 µmol/l; 1,448 ± 0.1019, 5.0 µmol/l; 1.471 ± 0.07473, 10.0 µmol/l; 1.335 ± 0.0828) (Figure 5.4Ai-ii).

After 5.5 mmol/l glucose injection, there was no significant difference in $\Delta ECAR_{MAX}$ compared to vehicle (mpH/min/µg) (Vehicle, 2.442 ± 0.1547; 100 nmol/l, 2.019 ± 0.1593, *vehicle vs 100 nmol/l, P = 0.1943*; 1.0 µmol/l; 2.133 ± 0.1896; 2.5 µmol/l; 2.285 ± 0.1223; 5.0 µmol/l; 2.492 ± 0.1374; 10.0 µmol/l; 2.348 ± 0.09056) (Figure 5.4Bi-ii).

In addition, $\Delta ECAR_{MAX}$ was not altered following high glucose (11.7 mmol/l) injection (mpH/min/µg) (Vehicle; 2.409 ± 0.1207, 100 nmol/l; 2.152 ± 0.2429, 1.0 µmol/l; 2.082 ± 0.1331, 2.5 µmol/l; 2.050 ± 0.09081, 5.0 µmol/l; 2.525 ± 0.1107, 10.0 µmol/l; 2.596 ± 0.1940) (Figure 5.4Ci-ii).

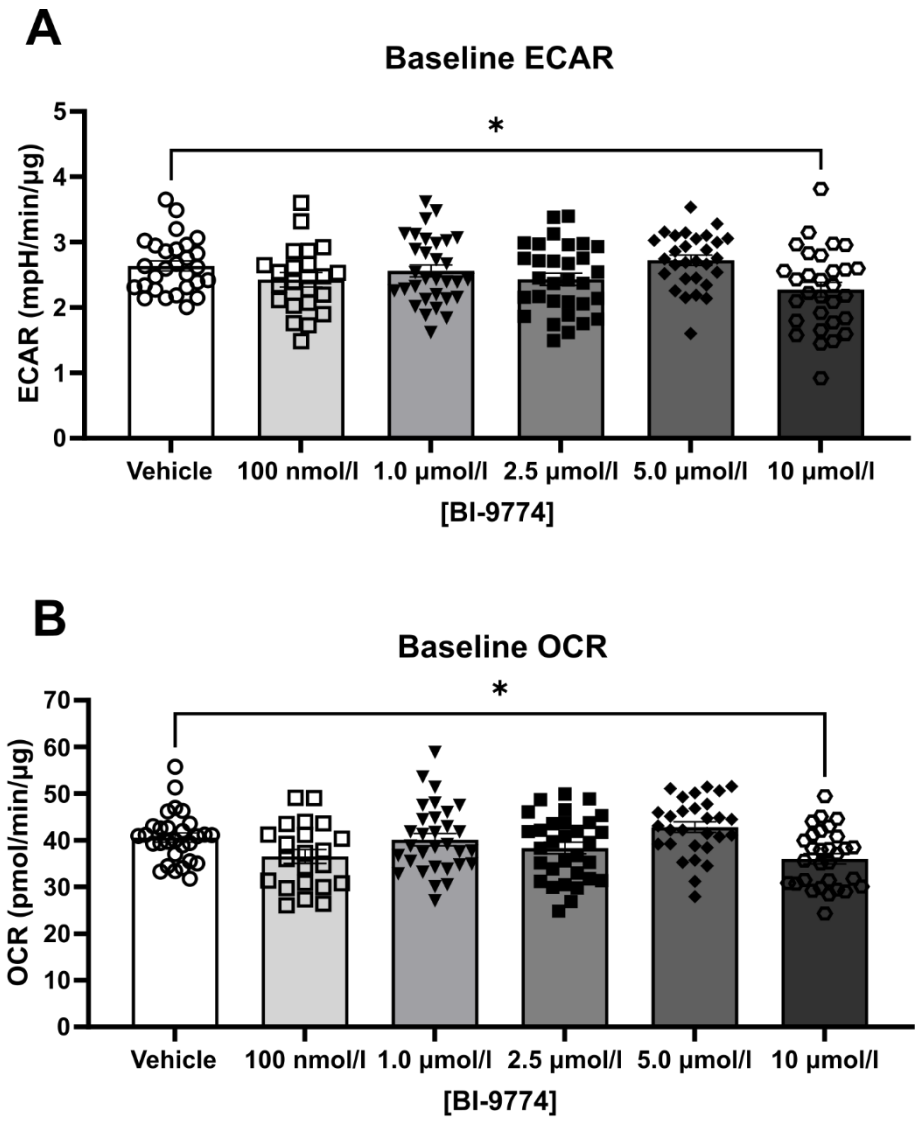

Figure 5.3: BI-9774 preincubation reduced basal extracellular acidification rate (ECAR) and oxidative metabolism in pancreatic α-cells.

αTC1.9 cells were preincubated with BI-9774 (0 – 10.0 µmol/l) for 1 h, in standard Seahorse XF DMEM media. **A.** Baseline extracellular acidification rate (ECAR) (mpH/min/µg) **B.** oxygen consumption rate (OCR) (pmol/min/µg) was calculated as an average of four measurements prior to glucose injection (One-Way ANOVA with Dunnetts multiple comparison test, *P<0.05, two individual plates).

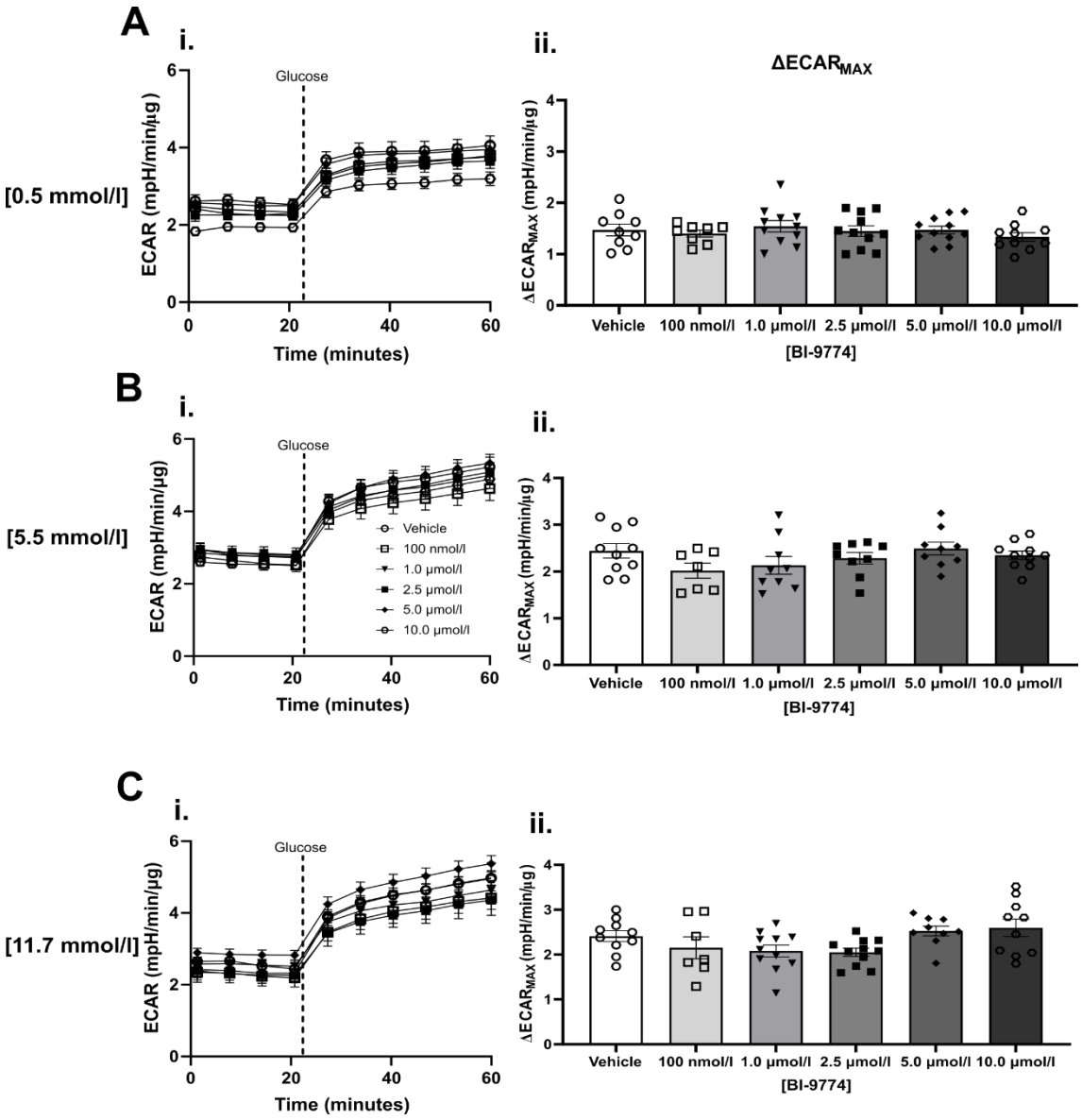

Figure 5.4: BI-9774 preincubation did not alter α-cell glucose utilisation.

αTC1.9 cells were preincubated with BI-9774 (0 – 10.0 µmol/l) for 1 h, in standard Seahorse XF DMEM media. **A - C i.** Representative traces depicting changes in extracellular acidification rate (ECAR) following glucose injection (0.5 - 11.7 mmol/l glucose) after ~ 20 min (mpH/min/µg). **A - C ii.** $\Delta ECAR_{MAX}$, or glucose utilisation, was calculated from maximum ECAR reading ($ECAR_{MAX}$) following glucose injection minus average ECAR readings at baseline (One Way ANOVA with Dunnetts multiple comparison test, n = 7 – 11, two individual plates)

5.2.3 Acute BI-9774 injection reduced α-cell glucose utilisation.

To confirm whether incubation time of BI-9774 was adequate to exert any influence on α-cell glucose utilisation, real-time ECAR/OCR measurements were recorded following BI-9774 acute injection (0 – 10.0 µmol/l) into the surrounding media.

Acute BI-9774 injection reduced α-cell basal ECAR in glucose-free conditions (mpH/min/µg) (Vehicle; 2.503 ± 0.1078; 100 nmol/l; 2.095 ± 0.05849, *P = 0.0392*; 1.0 µmol/l; 2.210 ± 0.08390, 2.5 µmol/l; 1.944 ± 0.08879, *P = 0.0027*; 5.0 µmol/l; 2.009 ± 0.07016, *P = 0.0010*; 10.0 µmol/l; 2.205 ± 0.09306, *P = 0.1337*) (Figure 5.5A). Similarly, BI-9774 acute injection reduced basal OCR in α-cells (pmol/min/µg) (Vehicle; 37.33 +/- 1.315, 100 nmol/l; 32.08 ± 0.7226, *vehicle vs 100 nmol/l, P = 0.0257*, 1.0 µmol/l; 33.91 ± 1.096, *vehicle vs 1.0 µmol/l, P = 0.2059*, 2.5 µmol/l; 33.17 ± 0.7725, 5.0 µmol/l; 32.07 ± 0.8974, *P = 0.0062*, 10.0 µmol/l; 34.34 ± 1.314) (Figure 5.5B).

After 0.5 mmol/l glucose injection, only BI-9774 (5.0 µmol/l) significantly attenuated $\Delta ECAR_{MAX}$ (mpH/min/µg) (Vehicle; 1.207 ± 0.08930; 100 nmol/l; 1.039 ± 0.05406; 1 µmol/l, 1.045 +/- 0.07718; 2.5 µmol/l;1.014 ± 0.05519, *P = 0.1661,* 5.0 µmol/l; 0.8913 ± 0.04609, *P = 0.0051*; 10.0 µmol/l; 0.9883 ± 0.07239, *P = 0.1004*) (Figure 5.6Ai-ii).

Post-5.5 mmol/l glucose injection, BI-9774 (5.0 µmol/l) reduced $\Delta ECAR_{MAX}$ (mpH/min/µg) (Vehicle; 2.068 ± 0.09712; 100 nmol/l, 1.777 ± 0.05368, *P = 0.0610*; 1.0 µmol/l; 2.031 ± 0.1345, 2.5 µmol/l, 1.763 ± 0.1354, *P = 0.0522*, 5.0 µmol/l; 1.711 ± 0.07256, *P = 0.0179,* 10.0 µmol/l; 1.821 ± 0.05094, *P = 0.1314*) (Figure 5.6Bi-ii).

After high (11.7 mmol/l) glucose injection, all [BI-9774] used lowered $\Delta ECAR_{MAX}$ (mpH/min/µg) (Vehicle; 2.548 ± 0.1197, *P = 0.0343*, 100 nmol/l; 2.141 ± 0.07466, *P = 0.0451*, 1.0 µmol/l; 2.157 ± 0.07404, *P = 0.0451*; 2.5 µmol/l; 1.830 ± 0.1450, *p < 0.0001*, 5.0 µmol/l; 1.949 ± 0.08462, *P = 0.0009*; 10.0 µmol/l; 2.010 ± 0.1345, *P = 0.0082*) (Figure 5.6Ci-ii).

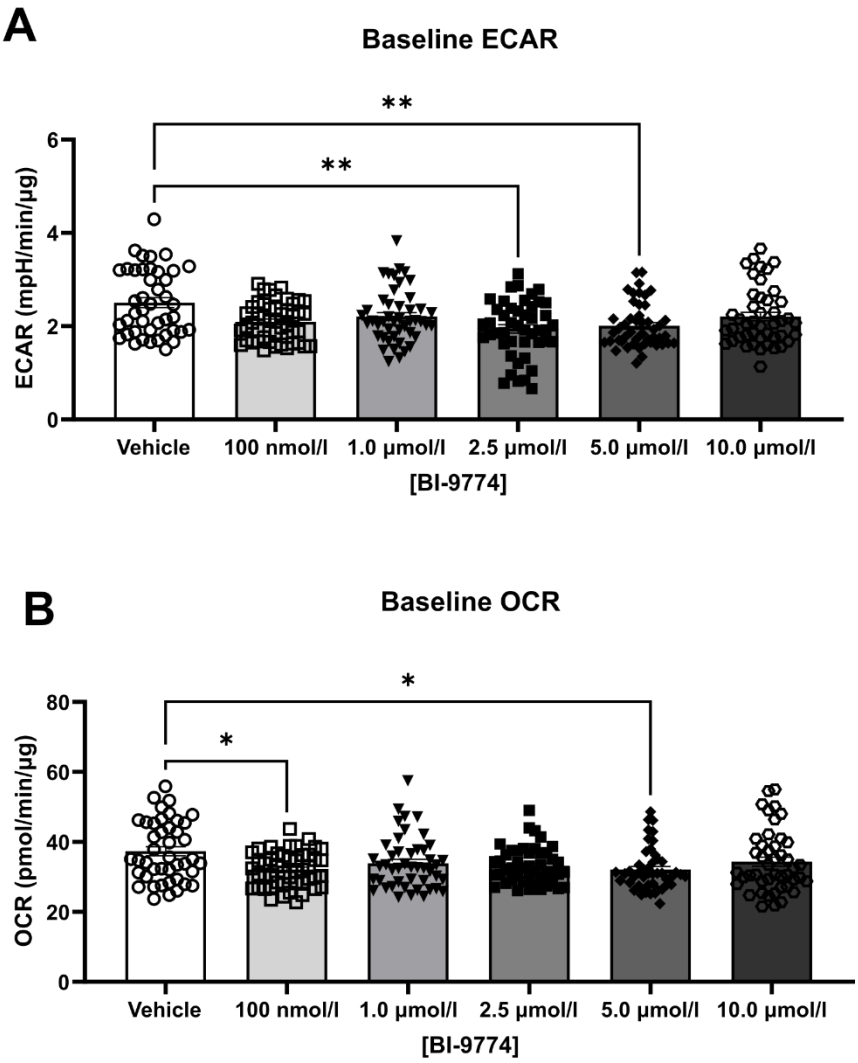

Figure 5.5: Acute BI-9774 injection reduced basal α-cell glycolysis and oxidative respiration.

αTC1.9 cells were acutely exposed to 0 – 10.0 µmol/l BI-9774 for ~ 20 minutes prior to glucose addition in standard Seahorse XF DMEM medium. **A.** Baseline extracellular acidification rate (ECAR) (mpH/min/µg) and **B.** oxygen consumption rate (OCR) (pmol/min/µg) measurements were calculated as an average of three measurements prior to glucose injection (Kruskal-Wallis test with Dunnetts multiple comparison test, n = 44 – 48, *P<0.05, **P<0.01, ***P<0.001, three individual plates)

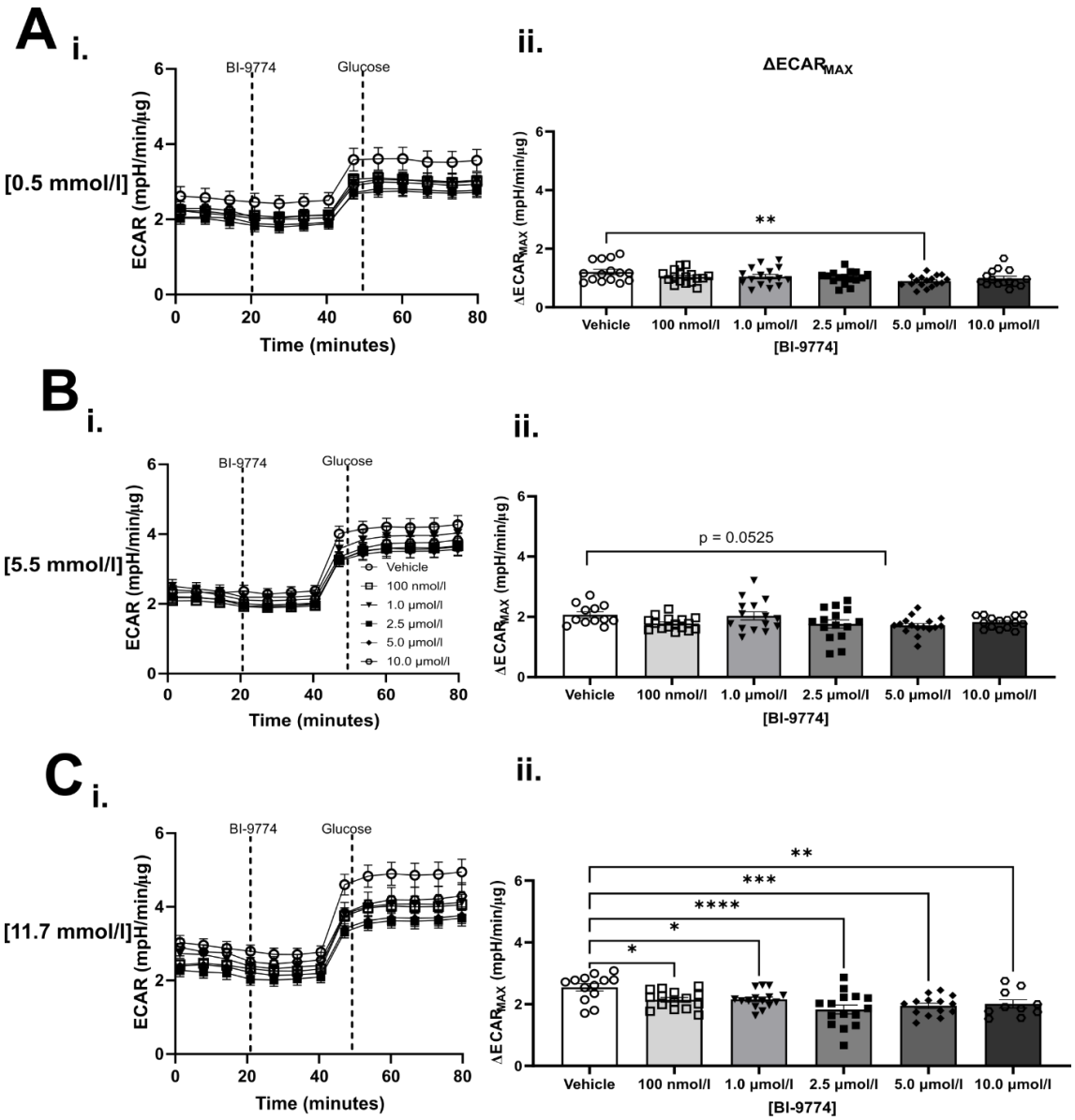

Figure 5.6: Acute BI-9774 injection attenuated α-cell glucose utilisation in a glucose-dependent manner.

A - C i. Representative traces depicting changes in αTC1.9 extracellular acidification rate (ECAR) following increasing [BI-9774] (100 nmol/l – 10.0 µmol/l) and subsequent glucose (0.5 – 11.7 mmol/l) injections into surrounding standard Seahorse XF DMEM medium at indicated time points (mpH/min/µg). **A - C ii.** $\Delta ECAR_{MAX}$, or glucose utilisation, calculated from maximum ECAR reading following glucose injection minus average ECAR readings following BI-9774 injection (n = 10 – 17, 0.5 – 11.7 mmol/l; One-Way ANOVA with Dunnett's multiple comparison test, *P<0.05, **P<0.01, ***P<0.001, ****P<0.0001, three individual plates).

5.3 Discussion

Prior evidence in this thesis has discussed O-304, another pan-AMPK activator, impact on AMPK activity and α-cell glucose metabolism. In addition, previous studies have reported other several AMPK activators, including AMP-mimetic AICAR and AMPKβ1-selective A-769662, have limited selectivity and wider off-target effects, partially attributed to rises in nucleotide levels (Hasenour *et al.*, 2014; Vlachaki Walker *et al.*, 2017). Therefore, this study characterised if BI-9774 exposure could activate the α-cell AMPK signalling cascade and the downstream metabolic effects.

5.3.1 Increasing [BI-9774] exposure activated downstream AMPK signalling cascade in α-cells.

Evidence presented in this chapter, following treatment with 100 nmol/l – 2.5 µmol/l BI-9774, suggested a concentration-dependent increase in ACC (Ser79) phosphorylation, but no significant change in Thr172 phosphorylation. These findings agree with the proposed binding site for BI-9774, whereby BI-9774 most likely binds to the AMPK allosteric drug and metabolite binding (ADaM) site on the AMPKα kinase domain. In addition, BI-9774 appears to have a lower half-maximal response (EC_{50}) for β2-containing complexes (

Table 5.1), suggesting β2 selectivity. Similarly, pan-AMPK activator SC-4 has selectivity for β2-containing AMPK complexes , specifically in skeletal muscle myotubes, by the colocalization to β2-Asp111 (Ngoei *et al.*, 2018). Both activators contain an core ring-2 4'-nitrogen, possibly contributing to β2 selectivity (Ngoei *et al.*, 2018). In this context, it is unlikely BI-9774 is increasing AMPK activity by binding to α-cell AMPK β2 as this subunit is not expressed in α-cells (as highlighted in Chapter 3). It is important to note that β2-selective small molecules are highly sought in restoring glucose homeostasis in DM, in order to precisely target β2-expressing tissues, such as skeletal muscle, and limit wide off-target effects. Further understanding on whether, and how, BI-9774 could regulate glucose-sensitive actions in other β2-containing tissues, such the pancreatic β-cell, is crucial in the preclinical research investigating BI-9774.

5.3.2 BI-9774 reduced α-cell glucose utilisation in a time and concentration-dependent manner.

As previously mentioned, BI-9774, has the capability to bind to all 12 AMPK heterotrimer complexes and modulate GLUT-4 translocation (

Table 5.1). Evidence from chapter 3 demonstrated α-cells express the GLUT-4 protein, and other pan-AMPK activators (i.e., O-304) stimulate α-cell glycolysis in an AMPK-dependent manner. In contrast to the initial hypothesis, preincubation of BI-9774 for ~ 1.5 h did not alter glucose utilisation at any given glucose concentration and it is unlikely any changes in GLUT expression/translocation will contribute to this. It is important to note that during BI-9774 preincubation, endogenous α-cell AMPK activation would be higher as a result of no extracellular glucose. Thereby, basal AMPK activity is most likely high by increased [AMP/ADP:ATP] binding for a sustained period of time, possibly limiting BI-9774 efficacy.

To address this, further experiments were conducted by acute BI-9774 injection ~ 20 min prior to glucose injection. All [BI-9774] attenuated glucose utilisation at the hyperglycaemic-like conditions. This could be an off-target effect, especially at high [BI9774] (10.0 µmol/l), by the inhibition (> 15%) of key receptors (sodium channels, purinergic P2X, muscimol-bound $GABA_A$ central activation) required for the control of α-cell activity and glucagon secretory responses to glucose (Grempler *et al.*, 2018). These findings, however, were surprising as it is widely known AMPK activation can phosphorylate PFKFB3 and thereby increase rate-limiting PFK-1 enzyme activity to accelerate glycolysis (Marsin *et al.*, 2000; Bando *et al.*, 2005). α-cell glucagon secretion is sensitive to small changes in glucose availability, and thereby additional studies are required to determine whether the BI-9774 mediated reduction in glucose utilisation is AMPK-dependent and impacts on downstream glucagon secretion.

In addition, basal ECAR and OCR were both reduced by BI-9774 exposure following acute and preincubation treatment. One theory could be that BI-9774 could mildly inhibit mGPD, similar to metformin. mGPD, as mentioned, is a mitochondrial redox shuttle, but has importance in linking both glycolysis and oxidative respiration. The oxidation of NADH in glycolysis aids the generation of glycerol-3-phosphate by the reduction of the glycolytic intermediate, dihydroxyacetone phosphate (DHAP) (Mráček, Drahota and Houštěk, 2013). This, in turn, generates electrons which can be transferred into the

mitochondrial electron transport chain by bound mGPD (Mráček, Drahota and Houštěk, 2013). mGPD inhibition would therefore attenuate both cytosolic and mitochondrial respiration by reducing mGPD-derived DHAP generation to feed into glycolysis, as well as reducing electron import into the mitochondria. This evidence is supported by the high mGPD expression localised to the pancreatic islet (MacDonald, 1981). mGPD activity and NAD/NADH redox generation have both a role in islet intracellular signalling and stimulus-secretion coupling, especially in β-cells (Eto *et al.*, 1999; Ravier *et al.*, 2000; Stamenkovic *et al.*, 2015). Additional BI-9774 titrations, at lower concentrations, are therefore required to see if the ECAR/OCR reduction in α-cells persist and to thereby limit any changes in nucleotide levels as result of metabolic inhibition.

Can BI-9774, as a pan-AMPK activator, activate different AMPK isoforms, dependent on nucleotide availability and subcellular localisation? Other AMPK activators, for instance, PT-1 (an indirect AMPK activator) can activate γ1-containing complexes, but not γ3 in muscle (Jensen *et al.*, 2015). In HEK-293 cells, however, PT-1 activates both γ1 and 3 complexes, suggesting differences in subcellular compartment AMPK activity dependent on tissue (Jensen *et al.*, 2015). In addition, AICAR acts as an AMP mimetic after cellular uptake and conversion into ZMP, binding to the AMPKγ subunit and therefore acts as a pro-drug allosteric AMPK activator (Višnjić *et al.*, 2021). Similarly to BI-9774, AICAR can attenuate hepatocyte glycolysis by reducing glucokinase-dependent glucose phosphorylation. This, in turn, reduced F2,6-BP generation, allosterically attenuating PFK-1 activation and downstream glycolytic substrate generation, albeit at least partially in an AMPK-independent manner (Vincent, Bontemps and Van Den Berghe, 1992; Guigas *et al.*, 2006; Vincent *et al.*, 2015). It is possible, in α-cells, that BI-9774 exposure could reduce glucokinase activity, and thereby limit pyruvate generation for mitochondrial respiration. It is unlikely, however, that BI-9774 acts as an indirect AMPK activator by complex I inhibition (e.g., R481), due to the little to no effect on α-cell AMPK Thr-172 phosphorylation, which would be observed as a result of increased $[AMP]_I$, and influence on both aerobic/anaerobic respiration.

5.3.3 Summary and future studies

To conclude, BI-9774 is a potent direct AMPK activator and has an inhibitory effect on glucose utilisation in α-cells at high glucose availability. Alongside evidence provided in this chapter, BI-9774 is the most selective small molecule tested in this thesis, based on the lack of AMPKα-Thr172 phosphorylation at lower concentrations. Future work will need to identify whether BI-9774 (100 nmol/l) could modulate α-cell nucleotide generation, to confirm direct binding to AMPK. If so, an additional concentration response study could be conducted (< 100 nmol/l) to determine **a.** the lowest [BI-9774] to enhance downstream AMPK activation **b.** whether the specified [BI-9774] can continue to exert similar reductions on α-cell glucose utilisation. These studies are key for characterising BI-9774 as a new, direct activator of AMPK and whether BI-9774 can be used to modulate α-cell glucagon secretion in DM.

Chapter 6

Investigation into the effects of recurrent low glucose (RLG) exposure on pancreatic α-cell function

6 Investigation into the effects of recurrent low glucose (RLG) exposure on pancreatic α-cell function

6.1 Introduction

Hypoglycaemia is a frequent complication of insulin-treated T1DM and advanced T2DM (Cryer, 2008; Rickels, 2019). Despite advances in disease management, such as the development of hybrid closed loop continuous glucose monitors (CGM) and insulin pumps, recurrent hypoglycaemic (RH) episodes continue to limit adequate glycaemic control in diabetes mellitus. For instance, in one study, > 30,000 individuals with T1DM with inadequate glycaemic control (HbA_{1C} > 9.0%) were correlated with increased severe hypoglycaemia incidence (Pettus *et al.*, 2019). Hypoglycaemia events, with increased disease duration, increase the risk of impaired cognitive performance, impaired awareness of hypoglycaemia (IAH), cardiovascular complications and, in turn, increased mortality (Kaur and Seaquist, 2023). Over time, RH episodes are exacerbated by and can lead to hypoglycaemia-associated autonomic failure (HAAF), which is commonly associated with impaired symptomatic hypoglycaemia awareness (Cryer, 2015). HAAF is associated with dysregulated peripheral counterregulatory hormone response to subsequent hypoglycaemic episodes, including both the α-cell glucagon secretion and the adrenal gland epinephrine response, to restore euglycaemia. The previous chapters (Chapter 3 – 5) covered the α-cell metabolic response following acute low glucose. Therefore, to investigate the α-cell metabolic and hormonal responses during/following RH in DM, α-cell function was measured following multiple episodes of low glucose over four days.

Central hypoglycaemia counter-regulation is controlled by the glucose-sensing regions of the brain including, but not limited to, the ventromedial hypothalamus (VMH) and surrounding glial cells (Borg *et al.*, 1997; Marty *et al.*, 2005). The VMH glucose-sensing cell population include glucose-excited (GE) and -inhibited (GI) neurones to synergistically respond to hyperglycaemia and hypoglycaemia respectively (Routh, 2010). Although the VMH neural

projections do not directly modulate sympathoadrenal counterregulatory response, it is well characterised VMH activation stimulates catecholamine release alongside raising plasma glucagon in response to hypoglycaemia (Garg, Chhina and Singh, 1978; Borg *et al.*, 1995; Stanley *et al.*, 2016).

Altered expression/activity of the glucose-sensing machinery contributes to the central adaptation to RH. Glucokinase (GCK), a key glucose sensor, is similarly expressed in GE neurones, with one bout of insulin-induced hypoglycaemia increasing VMH GCK mRNA expression (Kang *et al.*, 2008; Beall *et al.*, 2012). Increased hypothalamic glucose phosphorylation observed at low glucose in rats exposed to RH, implies increased hexokinase-1 (HK-1) activity following RH (Osundiji *et al.*, 2011). Intrinsically, inhibition of GCK dysregulated neuronal calcium flux and firing in the VMH (Yang *et al.*, 1999; Dunn-Meynell *et al.*, 2002; Kang *et al.*, 2004; Sanders, Dunn-Meynell and Levin, 2004). The pharmacological activation of GCK by local VMH drug delivery attenuated epinephrine and glucagon plasma levels during insulin-induced hypoglycaemia, inferring diminished hormone counter-regulatory responses (Levin *et al.*, 2008). This, partly, could be due to lack of GE hyperpolarisation observed *in vitro* to low glucose (Beall *et al.*, 2012). Collectively, these findings identify hypothalamic glucose-sensing adaptations after RH, perhaps contributing to altered downstream glycolysis.

The glucose-sensing kinase, AMPK, is similarly expressed in VMH neuronal populations (Alquier *et al.*, 2007). AMPKα2 subunit silencing diminished the low glucose-sensing behaviour in a mouse GE cell line; inferring dysregulated AMPK activation could contribute to diminished central glucose-sensing (Beall *et al.*, 2012). VMH AMPK silencing similarly diminished counterregulatory hormone responses at hypoglycaemia (McCrimmon *et al.*, 2008; Fan *et al.*, 2009). In addition, VMH AMPKα1/2 subunit expression were increased following RH, agreeing with more recent findings which similarly shown enhanced total VMH AMPK (but not pAMPK) levels following recurrent insulin-induced hypoglycaemia (RIIH) (Mandal *et al.*, 2017). Additionally, pharmacologically-activating AMPK, using local AICAR delivery into the VMH, increased

counterregulatory hormone levels in rats exposed to RH (McCrimmon *et al.*, 2006; Alquier *et al.*, 2007). Hypothalamic AICAR treatment enhanced the glucagon response, but not epinephrine, following both control and RH in T1DM rats; in which control rats are characterised by chronic hyperglycaemia (Fan *et al.*, 2009). It is important to note, however, caution should be taken when interpreting data using AICAR, due to multiple studies reporting various AMPK-independent actions on peripheral glucose homeostasis as detailed in Višnjić *et al.* 2021 review (Višnjić *et al.*, 2021).

Due to recurrent glucose deprivation, a suggested hypothesis for retaining glial and neuronal function includes the utilisation of alternative metabolic fuel sources as an adaptation of RH. Astrocytes are glucose-sensing; with activation being markedly increased upon fasting (Varela *et al.*, 2021). Astrocytes have increased PFKFB3 glycolytic enzyme expression compared to surrounding neuronal populations, suggesting a degree of metabolic flexibility under energy-stressed conditions (Almeida, Moncada and Bolaños, 2003). Human primary astrocytes (HPA) exposed to prior recurrent low glucose (RLG) episodes increased basal extracellular acidification rate (ECAR), an indicator of glycolysis; suggesting intrinsic glycolytic adaptations (Weightman Potter *et al.*, 2019). In addition, RLG-treated HPA cells had increased fatty acid oxidation (FAO) dependency, alongside enhanced mitochondrial proton leak, suggesting prior RLG bouts could induce a metabolic “switch” to sustain energy supply (Weightman Potter *et al.*, 2019). Recurrent glutamate bouts, a metabolic fuel for the Krebs cycle, attenuated mitochondrial dysfunction, associated with RLG exposure, dependent on rodent astrocytic population (Weightman Potter *et al.*, 2022). Therefore, these findings collectively suggest bioenergetic adaptations may occur, following prior bouts of low glucose, that could contribute to the defective central counterregulatory responses.

Alternative fuel adaptations, including lactate, could preserve glycolysis when glucose supply is low following intermittent bouts of low glucose. Lactate infusion during hypoglycaemia attenuated the epinephrine counterregulatory response, but improved cognitive function in people with T1DM (Maran *et al.*,

2000). Additionally, individuals with impaired awareness of hypoglycaemia (IAH) associated with T1DM had attenuated brain lactate levels compared to both healthy and individuals with T1DM with retained awareness (Wiegers *et al.*, 2016). Furthermore, the breakdown of astrocytic glycogen stores to glucose can be subsequently metabolised to lactate, to sustain neuronal activity (Wender *et al.*, 2000; Brown *et al.*, 2005). A rodent model of RH similarly had increased neuronal lactate uptake during hypoglycaemia compared to control, perhaps to retain some neuronal glycolytic metabolism which is diminished from prolonged reduction in glucose availability (Herzog *et al.*, 2013; Litvin, Clark and Fisher, 2013). Lactate could, therefore, serve as an inherent metabolic regulator of cell function following RH.

Research has largely focused on the central loss of glucose-sensitivity in individuals with RH. There is evidence to suggest intrinsic defects within other peripheral glucose-sensing organs, such as the pancreatic islet (Banarer, McGregor and Cryer, 2002). Both α- and β-cells express glucose-sensing machinery, similar to VMH GE and GI neurones, providing a compelling argument for alterations in intrinsic sensing mechanisms in islets contributing to RH episodes. T1DM and advanced T2DM are similarly associated with a loss of glucagon secretion in response to hypoglycaemia (Gerich *et al.*, 1973; Segel, Paramore and Cryer, 2002). Individuals with T1DM subjected to 3-months of hypoglycaemia avoidance displayed a raised glycaemic threshold for a glucagon response induced by hypoglycaemia (Fanelli *et al.*, 1993). In addition, hypoglycaemia monitoring restored both the magnitude of the epinephrine response and glycaemic threshold to hypoglycaemia (Fanelli *et al.*, 1993); possibly suggesting inherent α-cell defects in T1DM. Additionally, key identity and glucose-sensing genes had attenuated expression in purified T1DM human α-cells, suggesting lack of hypoglycaemia-induced excitability (Brissova *et al.*, 2018). A review conducted by Panzer *et al.* 2021 indicated the lack of, or defective, β-cells in diabetes mellitus may partially be responsible for this (Panzer and Caicedo, 2021). As the β-cell secretion of inhibitory factors (GABA, insulin) are attenuated during T1DM progression, this is hypothesised to limit α-cell membrane repolarisation and excitability to subsequent hypoglycaemic

stimuli (Panzer and Caicedo, 2021). δ-cell SST secretion, similarly to β-cells, suppresses glucagon secretion at high glucose by α-cell SSTR2/3 binding (Blodgett *et al.*, 2015; DiGruccio *et al.*, 2016). An intra-islet hypothesis for the defective RH glucagon secretion was demonstrated by SSTR2 antagonist treatment and restoration of counterregulatory glucagon response in diabetic and RH-treated rats (Yue *et al.*, 2012, 2013; Karimian *et al.*, 2013; Farhat *et al.*, 2022).These findings could suggest that δ-cell SST hypersecretion contribute to the diminished glucagon secretion in response to multiple hypoglycaemia episodes. To corroborate these findings, clinical efficacy of SSTR2 antagonists need to be therapeutically proven in T1DM. Defective autocrine α-cell signalling may contribute to the defective glucagon response in RH. Isolated α-cells from STZ-treated rats have an ablated calcium response to glutamate, an autocrine metabolic messenger co-secreted with glucagon (Panzer, Tamayo and Caicedo, 2022). Similarly, pharmacologically-activating ionotropic receptors enhanced glucagon secretion at low glucose in human pancreatic slices (Panzer, Tamayo and Caicedo, 2022). Collectively, these data suggest a highly plausible hypothesis for both paracrine and intrinsic autocrine defects that could contribute towards the defective α-cell glucagon response to hypoglycaemia in T1DM.

Oxidative phosphorylation gene expression appeared to be downregulated in $GADA^+$ human islets, where $GADA^+$ antibody is an early indicator of T1DM development (Doliba *et al.*, 2022). In addition, rate-limiting genes including GCK, LDH and PDH required for glycolysis were downregulated in $GADA^+$ α-cells (Doliba *et al.*, 2022). Glycolysis is also regulated by GCK activity in α-cells. Studies have suggested high-glucose dependent GCK activity is at least partially responsible for diminished α-cell glucagon secretion in rodent studies genetically and pharmacologically modulating *GCK* activity (Basco *et al.*, 2018; Moede *et al.*, 2020; Bahl *et al.*, 2021). Inserting an GCK-activating mutation, localised to the α-cells, attenuated HFD-associated increases in plasma glucagon after a glucose-tolerance test, although, no difference in fasted glycaemia was noted (Bahl *et al.*, 2021). Similarly, no studies to date have been

published examining whether α-cell glucose sensing changes following RH, identifying key gaps in knowledge, summarised in Figure 4.39.

In this chapter, α-cells exposed to prior bouts of RLG tested the overarching hypothesis that glycolytic capacity will be enhanced following RLG and is associated with attenuated low glucose-stimulated glucagon secretion. In addition, small molecules (R481/O-304) that enhance AMPK activity will partially restore the dysregulated metabolism in RLG-exposed α-cells. These hypothesises were examined in α-cells incubated up to four bouts of low glucose, for 3 h/day. Therefore, to examine α-cell bioenergetics and function following recurrent bouts of low glucose, studies aimed to address the following questions;

1. Do prior bouts of RLG induce glycolytic and oxidative adaptations in pancreatic α-cells?
2. Does the reintroduction of glucose alter α-cell glycolytic rate following RLG-exposure?

If α-cell metabolism is defective following RLG;

3. Is this contributed by defective α-cell AMPK activity?
4. Does this correspond to alterations in glucagon release?
5. And can pharmacologically activating AMPK, using O-304 and R481, restore dysregulated α-cell function following RLG?

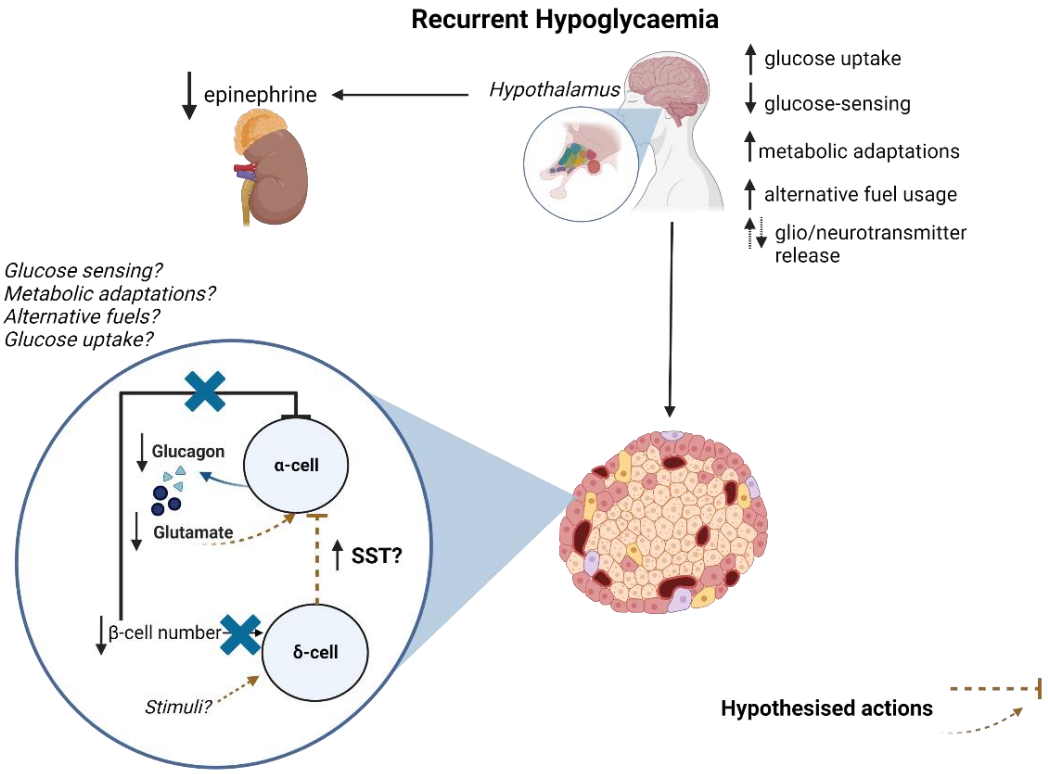

Figure 6.1: Schematic diagram illustrating gaps in knowledge on central/islet adaptations following recurrent hypoglycaemia (RH).

Hypothalamic adaptations in glucose uptake, glucose-sensing, metabolism resulting in changes in glial/neurotransmitter secretion are themes summarised in depth in recently published reviews and figure adapted from McCrimmon 2021 and McCrimmon 2022. Such adaptations have been shown to ameliorate the counterregulatory epinephrine response from the adrenal glands, as well as α-cell glucagon secretion in response to subsequent hypoglycaemic episodes. Most hypothesises justifying the attenuated counterregulatory response to hypoglycaemia are focused on diminished brain-autonomic nervous system response. However, there is increasing evidence to suggest defective intra-islet regulation of α-cell function, independently of central input, could contribute to diminished glucagon secretion in response to hypoglycaemia. Increased δ-cell area in STZ-treated rats has been observed, suggesting increased islet SST secretion, which may exacerbate the diminished glucagon secretion observed in RH (Orci *et al.* 1976). Similarly, reduced α-cell autocrine regulation (e.g., from glutamate) could exacerbate the diminished glucagon response to hypoglycaemia over time. Alongside attenuated β-cell paracrine feedback of glucagon secretion, it poses the question whether intrinsic α-cell defects are a direct consequence of RH. One hypothesis could suggest diminished α-cell glucose-sensing and metabolic reliance, similarly to the known hypothalamic adaptations, may contribute to the defective glucagon secretion observed. However, intrinsic mechanisms are yet to be fully elucidated. Created using Biorender.com.

6.2 Results

For all RLG experiments performed, the key comparisons were made between both control/antecedent low glucose, and acute low glucose/recurrent low glucose (RLG), with Table 6.1 describing number of prior bouts of low glucose.

Table 6.1: Frequency of low glucose bouts for each condition.

Condition	Bout of low glucose
Control	0
Acute Low Glucose	1
Antecedent	3
Recurrent Low Glucose (RLG)	4

6.2.1 Glycolytic rate during RLG exposure

To test the hypothesis that RLG exposure increased α-cell glycolysis at low and normal glucose, glycolytic rate assays were performed. In brief, cells were exposed to 3-days of 3 h bouts of either 0.5 (recurrent low glucose; RLG and antecedent low glucose) or 5.5 mmol/l (control and acute low glucose). On Day 4, cells were exposed to 0.5 (acute and RLG) or 5.5 mmol/l (control and antecedent low glucose)-containing standard Seahorse XF DMEM medium ± R481 (50 nmol/l) during degassing (1 h). For clarity and experimental question asked, data displayed in Figure 6.2/Figure 6.3 are the same vehicle groups illustrated in Figure 6.4/Figure 6.5, respectively, in order to examine two separate research questions. Statistical analysis, on the same groups, was therefore not duplicated in both Figure 6.4/Figure 6.5.

6.2.1.1 Prior bouts of low glucose increased key αTC1.9 glycolytic and oxidative parameters at low glucose.

RLG-exposed α-cells had > 2.0-fold higher basal glycolytic rate at recurrent low glucose compared to acute low glucose-treated cells (glycoPER pmol/min/µg) (Acute Low Glucose; 5.095 ± 0.5389, Recurrent Low Glucose; 10.80 ± 0.6868, *P < 0.0001)* (Figure 6.2C). Cells exposed to prior RLG bouts had enhanced compensatory glycolysis, following mitochondrial inhibition (pmol/min/µg) (Acute Low Glucose; 12.49 ± 0.7009, Recurrent Low Glucose; 22.09 ± 1.038, *P < 0.0001)* (Figure 6.2E). Increased glycolysis-derived acidification (% PER) was observed at low glucose, following RLG (Acute Low Glucose; 23.89 ± 2.066, Recurrent Low Glucose; 35.45 ± 1.428, *P < 0.0001*) (Figure 6.2D). In addition, basal OCR prior to injections was enhanced in cells exposed to prior RLG bouts (pmol/min/µg) (Acute Low Glucose; 32.54 ± 0.7168, Recurrent Low Glucose; 39.25 ± 1.278, *P < 0.0001*) (Figure 6.2F).

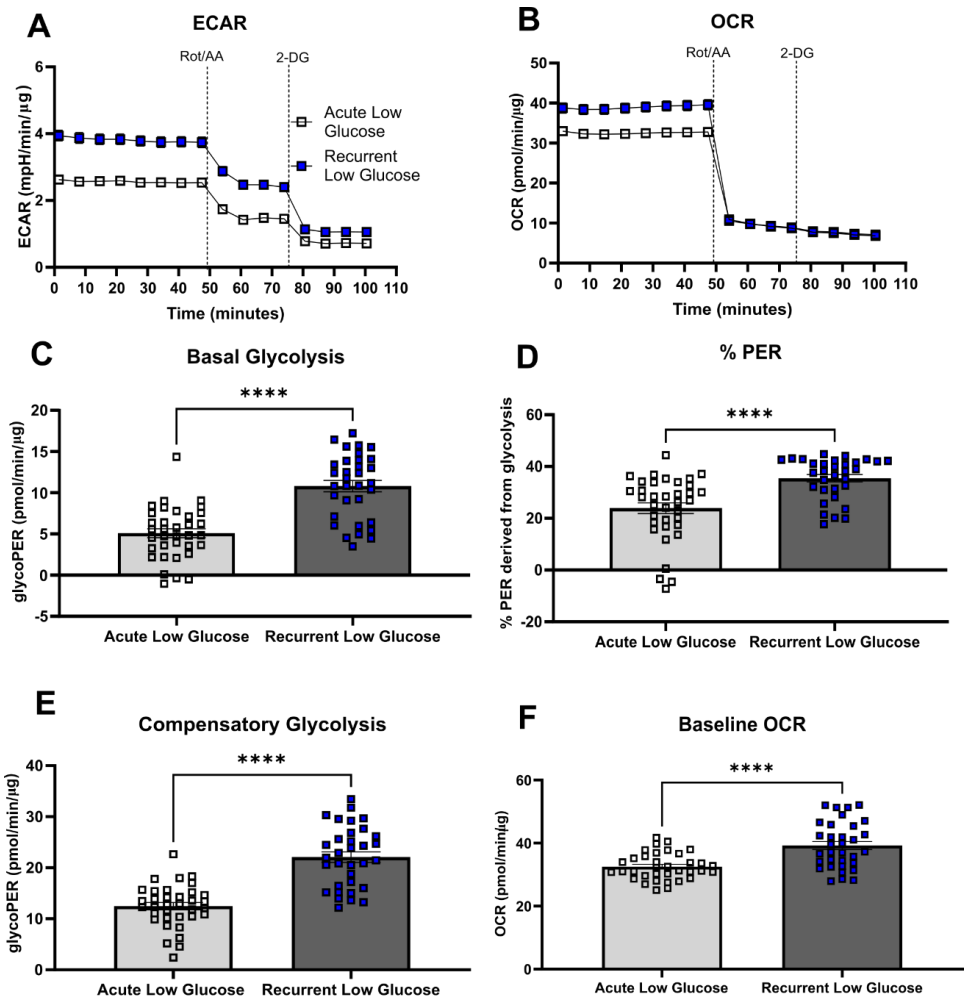

Figure 6.2: Recurrent low glucose (RLG) exposure enhanced α-cell glycolytic rate and compensatory glycolysis at low glucose.

αTC1.9 cells were incubated with either 5.5 mmol/l glucose (acute low glucose) or 0.5 mmol/l (recurrent low glucose, RLG) glucose for 3 days. On Day 4, cells were incubated with 0.5 mmol/l glucose for 1h before Seahorse XFe96 bioenergetic analysis. Cellular glycolytic proton efflux rate (glycoPER), a determinant of glycolysis, was measured after inhibition of oxidative respiration by rotenone/antimycin A (Rot/AA) injection and 2-deoxyglucose (2-DG) to subsequently inhibit glycolysis. **A.** Extracellular acidification rate (ECAR) and **B**. oxygen consumption rate (OCR) trace **C**. Basal glycolysis (Two-tailed unpaired t-test), **D.** Proton efflux rate derived from glycolysis (% PER) (Two-tailed Mann-Whitney test) **E.** Compensatory glycolysis (Two-tailed unpaired t-test), **F**. Baseline OCR (Unpaired two-tailed t-test) (n = 32 – 35, three separate plates, *P<0.05, **P<0.01, ***P<0.001, ****P<0.0001)

6.2.1.2 Antecedent low glucose attenuated αTC1.9 glycolytic reliance when recovered at normal glucose.

Prior bouts of low glucose attenuated α-cell basal glycolysis when recovered at normal glucose levels (antecedent low glucose), compared to control (glycoPER pmol/min/µg) (Control; 20.10 ± 1.323, Antecedent Low Glucose; 16.92 ± 0.7974, $P < 0.05$) (Figure 6.3C). Similarly, antecedent-treated α-cells had reduced glycolytic-derived acidification (% PER) (Control; 53.68 ± 1.880, Antecedent Low Glucose; 49.65 ± 0.8945, $P < 0.05$) (Figure 6.3D). α-cells exposed to antecedent low glucose and recovered at 5.5 mmol/l glucose showed no change in mitochondrial-induced compensatory glycolysis (pmol/min/µg) (Control; 70.81 ± 4.630, Antecedent Low Glucose; 70.81 ± 3.865, $P = 0.9997$) (Figure 6.3E). In addition, basal OCR was elevated in antecedent low glucose-treated cells (pmol/min/µg) (Control; 34.33 +/- 0.6437, Antecedent Low Glucose; 36.47 ± 0.8827, $P = 0.0566$) (Figure 6.3F).

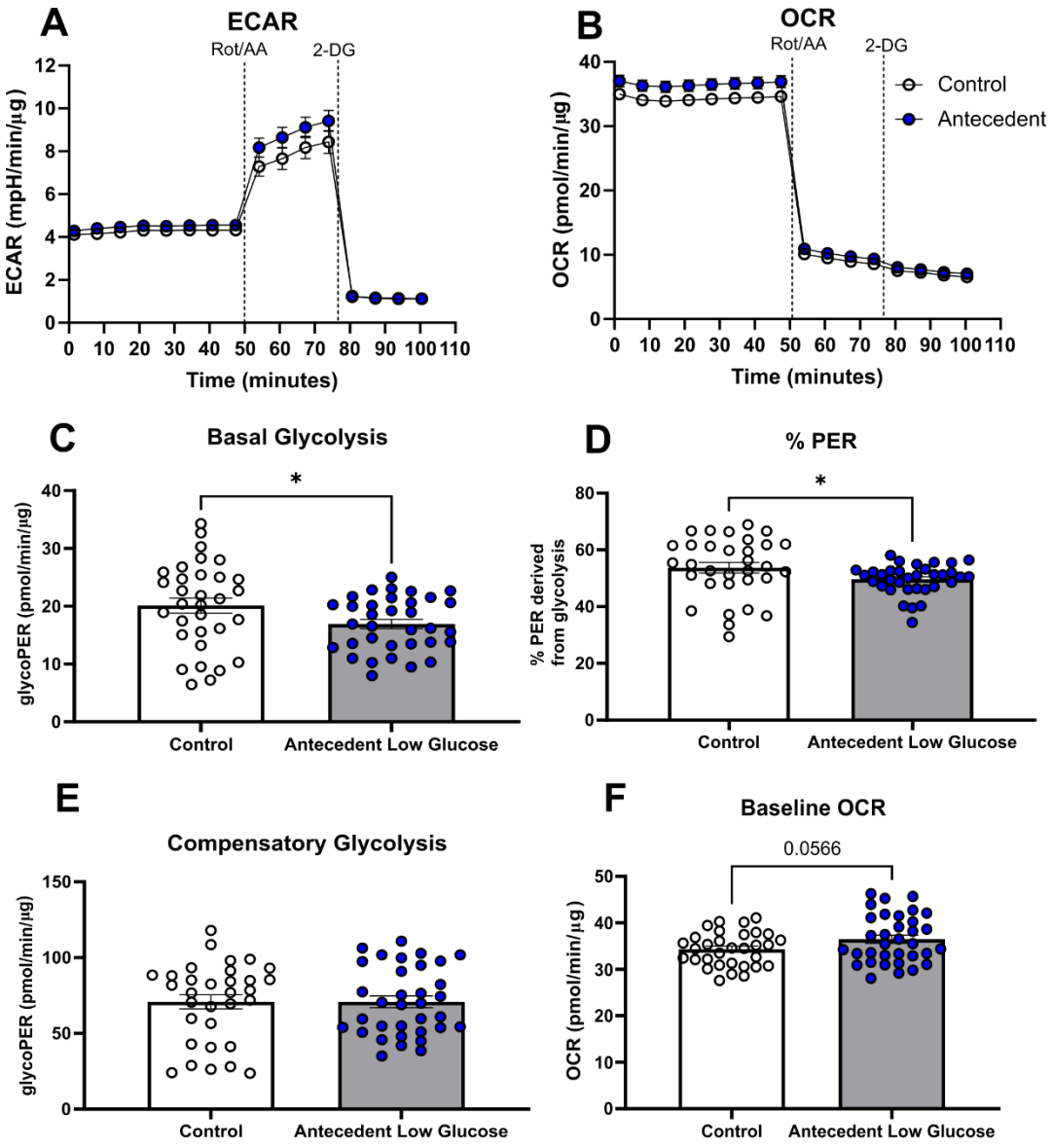

Figure 6.3: Antecedent low glucose attenuated α-cell glycolysis, but increased oxidative metabolism, at euglycaemic-like conditions.

αTC1.9 cells were incubated with either 5.5 mmol/l glucose (control) or 0.5 mmol/l (antecedent) glucose for 3 h episodes for 3 days. On Day 4, cells were incubated with 5.5 mmol/l glucose for 1 h before Seahorse XFe96 bioenergetic analysis. Cellular glycolytic proton efflux rate (glycoPER), a determinant of glycolysis, was measured after inhibition of oxidative respiration by rotenone/antimycin A (Rot/AA) injection and 2-deoxyglucose (2-DG) to subsequently inhibit glycolysis. **A.** Extracellular acidification rate (ECAR) and **B.** oxygen consumption rate (OCR) trace. **C.** Basal glycolysis (Two-tailed unpaired t-test), **D.** Proton efflux rate derived from glycolysis (%PER) (Mann-Whitney test) **E.** Compensatory glycolysis (Two-tailed unpaired t-test), **F.** Baseline OCR (Unpaired two-tailed t-test) (n = 32 – 34, three separate plates, *P<0.05)

6.2.1.3 R481 treatment enhanced α-cell glycolysis regardless of RLG-altered bioenergetics.

R481 increased αTC1.9 basal glycolysis at both acute low glucose and RLG conditions (Acute Low Glucose: vehicle; 5.095 ± 0.539, R481: 9.862 ± 0.543, *P < 0.0001,* Recurrent Low Glucose: Vehicle; 10.801 ± 0.687, R481; 15.510 ± 0.784, *P < 0.0001*) (Figure 6.4C). Similarly, R481 stimulated glycolysis-derived PER regardless of prior bouts of low glucose (Acute Low Glucose: vehicle; 23.606 ± 2.106, R481; 45.587 ± 1.765, *P < 0.0001,* Recurrent Low Glucose: vehicle; 35.449 ± 1.428, R481; 50.259 ± 1.376, *P < 0.0001*) (Figure 6.4D). Following Rot/AA-induced mitochondrial inhibition, R481 incubation did not increase compensatory glycolysis either in acute- or RLG-treated α-cells (Acute Low Glucose: Vehicle; 12.494 ± 0.701, R481; 13.746 ± 0.575, *Vehicle vs R481, P = 0.6779,* Recurrent Low Glucose: Vehicle; 22.088 ± 1.038, R481; 21.928 ± 0.892, *Vehicle vs R481, P = 0.9991, Acute Low Glucose R481 vs Recurrent Low Glucose R481, P < 0.0001*) (Figure 6.4E).

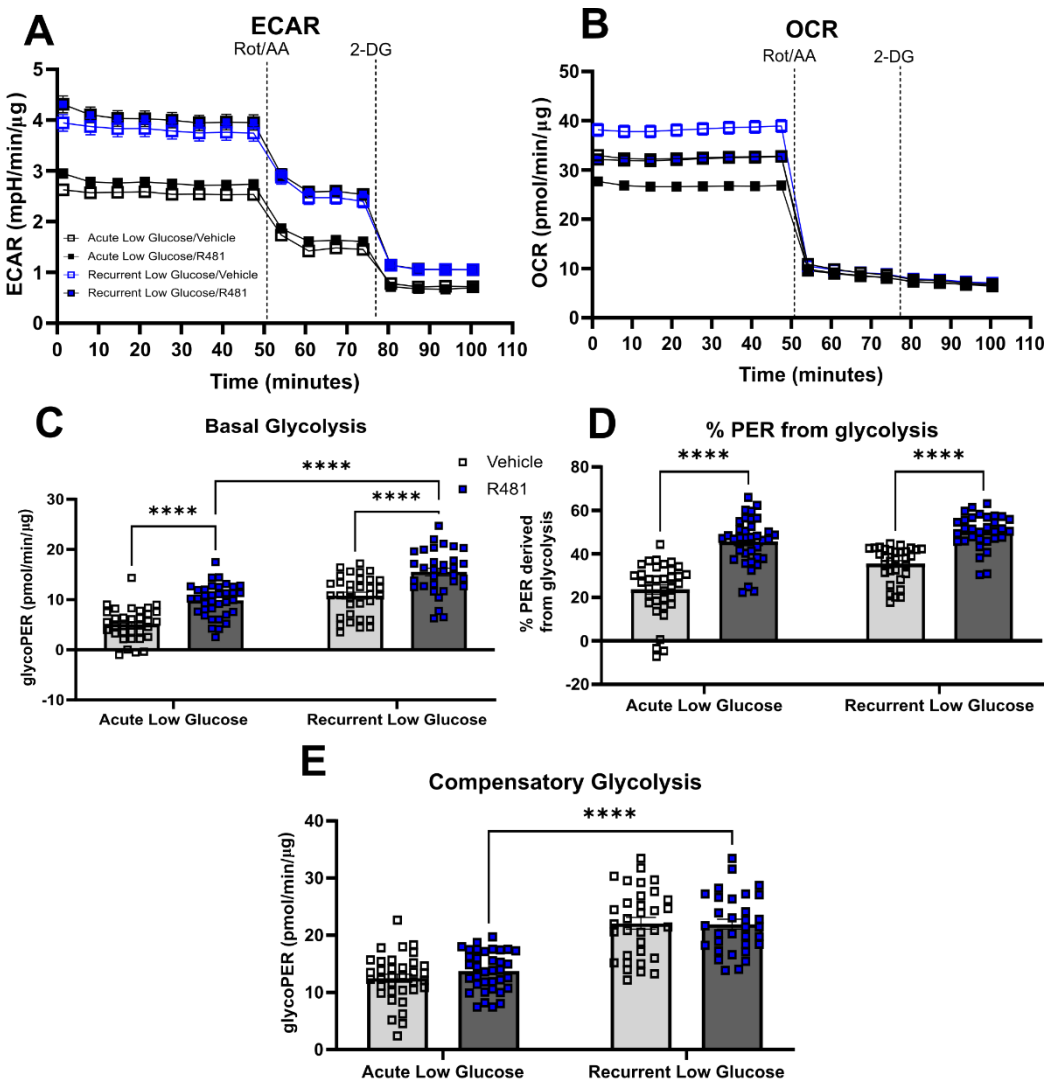

Figure 6.4: Recurrent low glucose (RLG) exposure increased α-cell R481-enhanced glycolytic rate at low glucose.

αTC1.9 cells were incubated with either 5.5 mmol/l glucose (control) or 0.5 mmol/l (antecedent) glucose for 3 h episodes for 3 days. On Day 4, cells were incubated with 0.5 mmol/l glucose ± R481 (50 nmol/l) for 1 h before Seahorse XFe96 bioenergetic analysis. Glycolytic proton efflux rate (glycoPER), a determinant of glycolysis, was measured after inhibition of oxidative respiration by rotenone/antimycin A (Rot/AA) injection and 2-deoxyglucose (2-DG) to subsequently inhibit glycolysis**. A.** Extracellular acidification rate (ECAR) and **B.** oxygen consumption rate (OCR) trace **C.** Basal glycolysis (Two-Way ANOVA with Tukey's multiple comparison test, ****P<0.0001) **D.** Proton efflux rate derived from glycolysis (%PER) (multiple Mann-Whitney tests with Holm-Šídák multiple comparison test) **E.** Compensatory glycolysis (Two-Way ANOVA with Tukey's multiple comparison test) (n = 32 – 35, three separate plates)

6.2.1.4 R481 treatment increased α-cell glycolysis regardless of antecedent low glucose.

R481 treatment enhanced αTC1.9 basal glycolysis after antecedent low glucose bouts and control at 5.5 mmol/l glucose (Control: vehicle; 20.101 ± 1.323, R481; 41.699 ± 2.066, $P < 0.0001$, Antecedent Low Glucose: vehicle; 16.924 ± 0.797, R481; 42.027 ± 1.334, $P < 0.0001$) (Figure 6.5C). This effect is observed in glycolytic-derived acidification measurements (Control: Vehicle; 53.681 ± 1.880, R481; 78.149 ± 1.104, $P < 0.0001$, Antecedent Low Glucose: Vehicle; 49.648 ± 0.894, R481; 77.472 ± 0.741, $P < 0.0001$) (Figure 6.5D). Additionally, R481 did not alter compensatory glycolysis in control or antecedent low glucose-treated α-cells (Control: Vehicle; 70.811 ± 4.630, R481; 70.210 ± 3.302, Antecedent Low Glucose: Vehicle; 70.814 ± 3.865, R481; 76.133 ± 4.399) (Figure 6.5E).

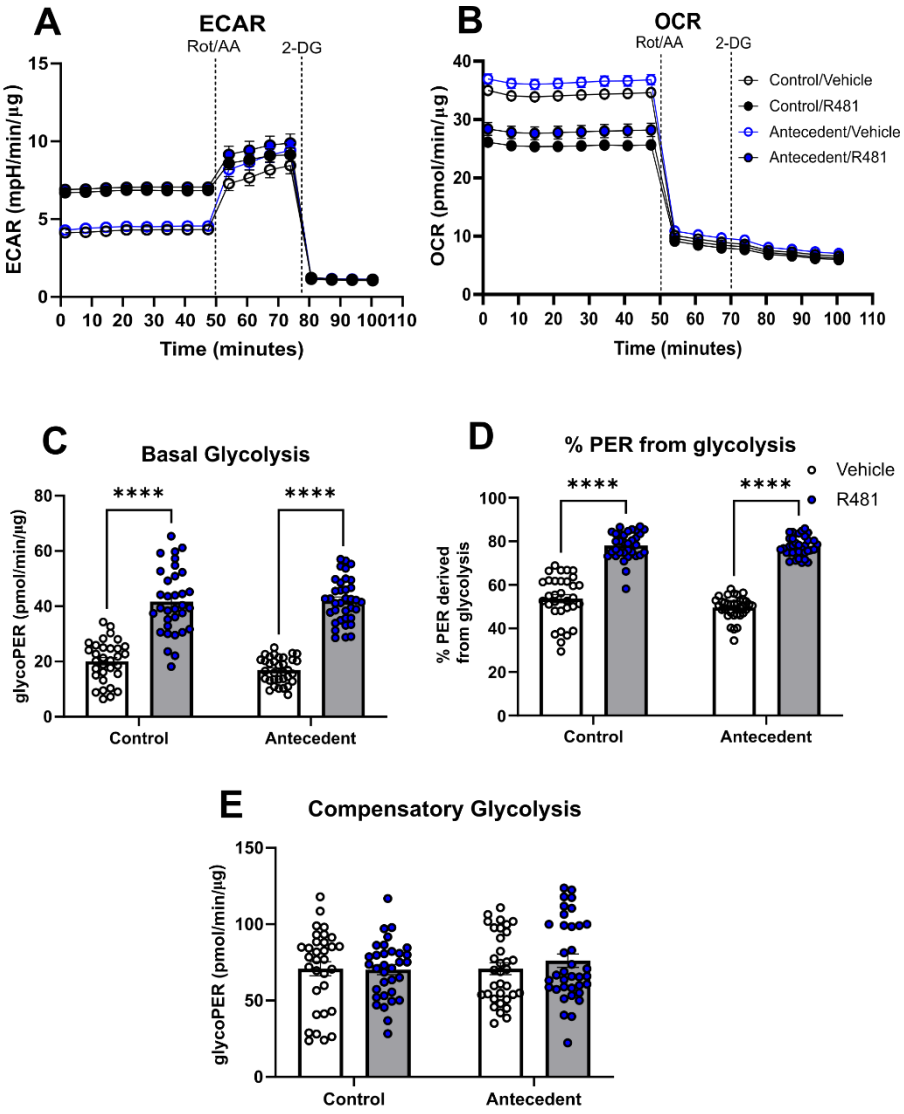

Figure 6.5: R481 enhanced α-cell glycolytic rate regardless of antecedent low glucose, at euglycaemic-like conditions.

αTC1.9 cells were incubated with either 5.5 mmol/l glucose (control) or 0.5 mmol/l (antecedent) glucose for 3 h episodes for 3 days. On Day 4, cells were incubated with 5.5 mmol/l glucose ± R481 (50 nmol/l) for 1h before Seahorse XFe96 bioenergetic analysis. Cellular glycolytic proton efflux rate (glycoPER), a determinant of glycolysis, was measured after inhibition of oxidative respiration by rotenone/antimycin A (Rot/AA) injection and 2-deoxyglucose (2-DG) to subsequently inhibit glycolysis. **A.** Extracellular acidification rate (ECAR) and **B.** oxygen consumption rate (OCR) trace **C.** Basal glycolysis (Two-Way ANOVA with Tukey's multiple comparison test, ****P<0.0001) **D.** Proton efflux rate derived from glycolysis (%PER) (multiple Mann-Whitney tests with Holm-Šídák multiple comparison test) **E.** Compensatory glycolysis (Two-Way ANOVA with Tukey's multiple comparison test) (n = 32 – 36, three separate plates)

6.2.2 Glycolytic protein expression

To examine AMPK pathway activation after prior bouts of low glucose, cells were exposed in accordance with a three-day RLG protocol referred to in Chapter 2. On Day 4, cells were preincubated in 5.5 mmol/l glucose-containing standard Seahorse XF DMEM medium ± R481 (50 nmol/l) for 1 h. Subsequently, cells were incubated in either 5.5 or 0.5 mmol/l glucose ± R481 for an additional 1 h and protein phosphorylation was quantified.

6.2.2.1 AMPK signalling cascade activation following RLG exposure.

No change was observed in AMPK phosphorylation after RLG compared to acute low glucose, regardless of R481 treatment (fold change in protein expression compared to control) (Acute low glucose: R481; 1.127 ± 0.022, Recurrent low glucose: vehicle; 0.875 ± 0.238, R481; 1.048 ± 0.269) (Figure 6.6Ci). Similarly, there was no change in ACC phosphorylation with either RLG or R481 treatment (fold change in protein expression compared to control) (Acute low glucose: R481; 1.364 ± 0.183, Recurrent low glucose: vehicle; 1.273 ± 0.305, R481; 1.551 ± 0.743) (Figure 6.6Cii).

Prior antecedent low glucose episodes did not alter α-cell AMPK phosphorylation compared to control, either with or without R481 treatment, at 5.5 mmol/l glucose (fold change in protein expression compared to control) (Control: R481; 1.271 ± 0.290, Antecedent: vehicle; 1.052 ± 0.061, R481; 1.373 ± 0.196) (Figure 6.6Bi). In addition, there was no observed difference in phosphorylation of ACC with either treatment (fold change in protein expression compared to control) (Control; R481: 1.509 ± 0.348, Antecedent: vehicle; 1.266 ± 0.307, R481; 1.646 ± 0.434) (Figure 6.6Bii).

6.2.2.2 GLUT-4 expression following RLG exposure.

To investigate whether there were any alterations in glucose transport, glucose transporter protein expression (GLUT-4) was examined. No changes in GLUT-4 protein expression were observed in RLG-treated cells compared to acute low glucose-treated cells, regardless of R481 treatment, at 0.5 mmol/l glucose (fold

change in protein expression compared to control) (Acute low glucose: R481; 1.095 ± 0.191, Recurrent Low Glucose: vehicle; 1.052 ± 0.207, R481; 1.057 ± 0.314) (Figure 6.6Ciii). Similarly, there were no significant differences between cells exposed to prior bouts of low glucose compared to control at 5.5 mmol/l (fold change in protein expression compared to control) (Control: R481: 1.095 ± 0.191, Antecedent: vehicle; 1.052 ± 0.207, R481; 1.057 ± 0.314) (Figure 6.6Biii).

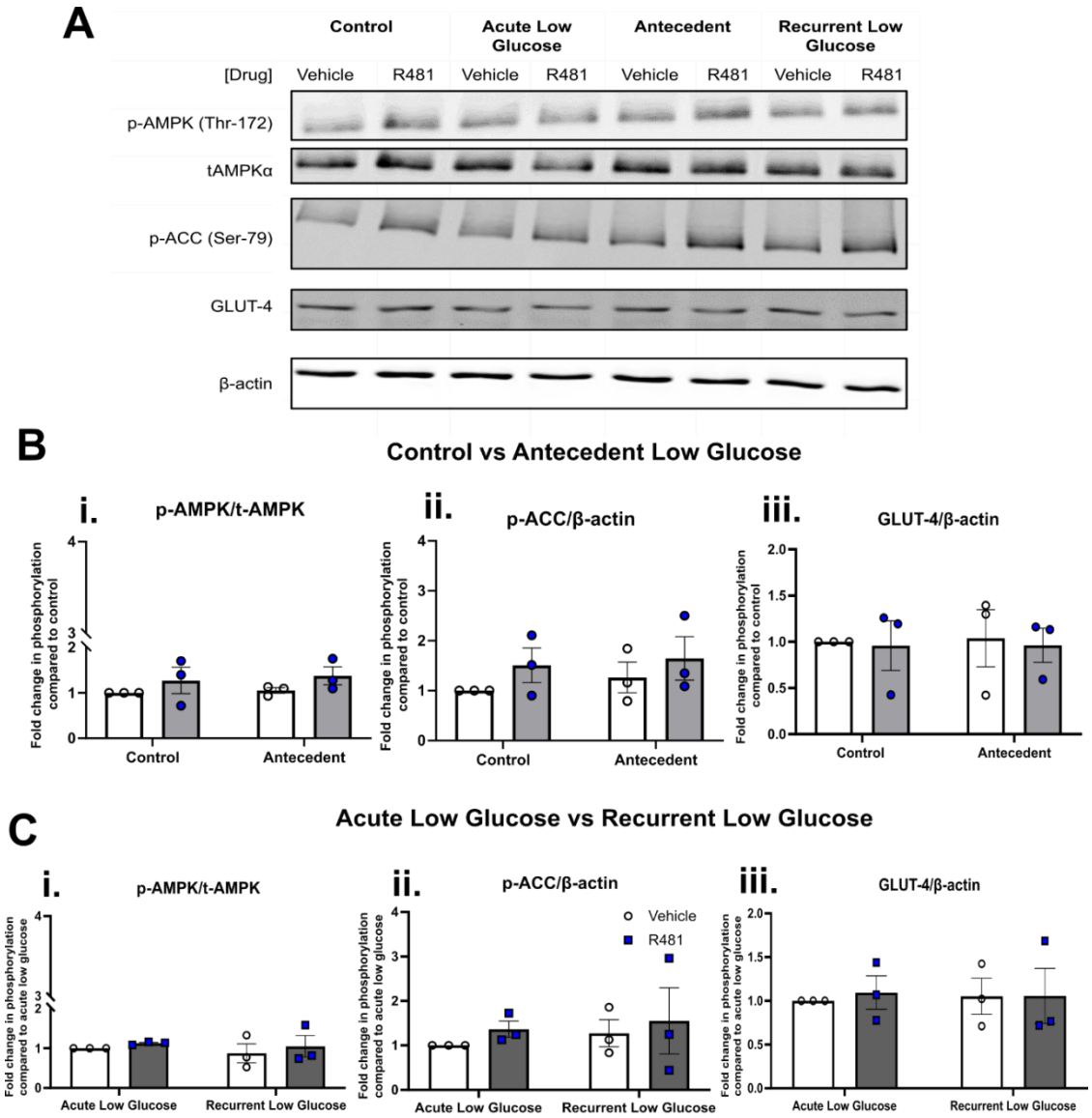

Figure 6.6: AMPK signalling cascade activation and GLUT-4 transporter expression after prior bouts of low glucose, ± R481 treatment.

αTC1.9 cells were exposed to 5.5 (Control, acute low glucose) or 0.5 (Antecedent and recurrent low glucose) mmol/l glucose over 3-days. On Day 4, cells were preincubated with standard Seahorse XF media containing 5.5 mmol/l glucose ± R481 (50 nmol/l) for 1 h. Cells were then exposed to either 0.5 (Acute low glucose, recurrent low glucose) or 5.5 (control, antecedent low glucose) mmol/l glucose for 1 h. **A.** Representative immunoblot for phosphorylated AMPKα1/2 (pAMPK, Thr172), total AMPKα1/2 (tAMPK), phosphorylated ACC (pACC, Ser79) and beta-actin (β-actin). Densitometric analysis for **B - C i.** pAMPK normalised to tAMPK and **B - C ii.** pACC normalised to β-actin and **B - C iii.** GLUT-4 normalised to β-actin (Two-Way ANOVA with Tukey's multiple comparison test, n = 3).

6.2.3 Glucose utilisation post-RLG exposure

To examine glycolytic reactivation following RLG exposure, on the fourth day of the RLG protocol, cells were exposed to 0.5 mmol/l glucose ± R481 (50 nmol/l) for 1 h during degassing. Media was removed, cells washed in standard Seahorse XF medium and replaced with fresh standard Seahorse XF DMEM medium containing no glucose supplementation ± R481 for a total ~ 92 min prior to bioenergetic analysis. For clarity and experimental question asked, data displayed in Figure 6.7 are vehicle groups displayed in Figure 6.8, in order to examine two separate research questions. Statistical analysis, on the same groups, was therefore not duplicated in Figure 6.8.

6.2.3.1 RLG-exposed α-cells had enhanced glucose recovery.

After acute 0.1 mmol/l glucose injection, no significant difference was observed in $\Delta ECAR_{MAX}$ in RLG- and acute low glucose-exposed α-cells (mpH/min/µg) (Acute Low Glucose; 0.2654 ± 0.03027, Recurrent Low Glucose; 0.3447 ± 0.03036, *P = 0.0738*) (Figure 6.7Ai-ii). No differences were similarly seen after 0.5 mmol/l glucose injection (mpH/min/µg) (Acute Low Glucose; 0.6523 ± 0.04795, Recurrent Low Glucose; 0.7746 ± 0.06478, *P = 0.1362*) (Figure 6.7Bi-ii). However, after 5.5 mmol/l glucose acute injection, RLG-treated α-cells had increased $\Delta ECAR_{MAX}$ compared to acute low glucose-treated α-cells (mpH/min/µg) (Acute Low Glucose; 1.173 ± 0.07140, Recurrent Low Glucose; 1.386 ± 0.05823, *P = 0.0254*) (Figure 6.7Ci-ii). Similarly, RLG-exposed α-cells increased $\Delta ECAR_{MAX}$ following high (11.7 mmol/l) glucose acute injection (mpH/min/µg) (Acute Low Glucose; 1.218 ± 0.1035, Recurrent Low Glucose; 1.491 ± 0.07818, *P = 0.038*) (Figure 6.7Di-ii).

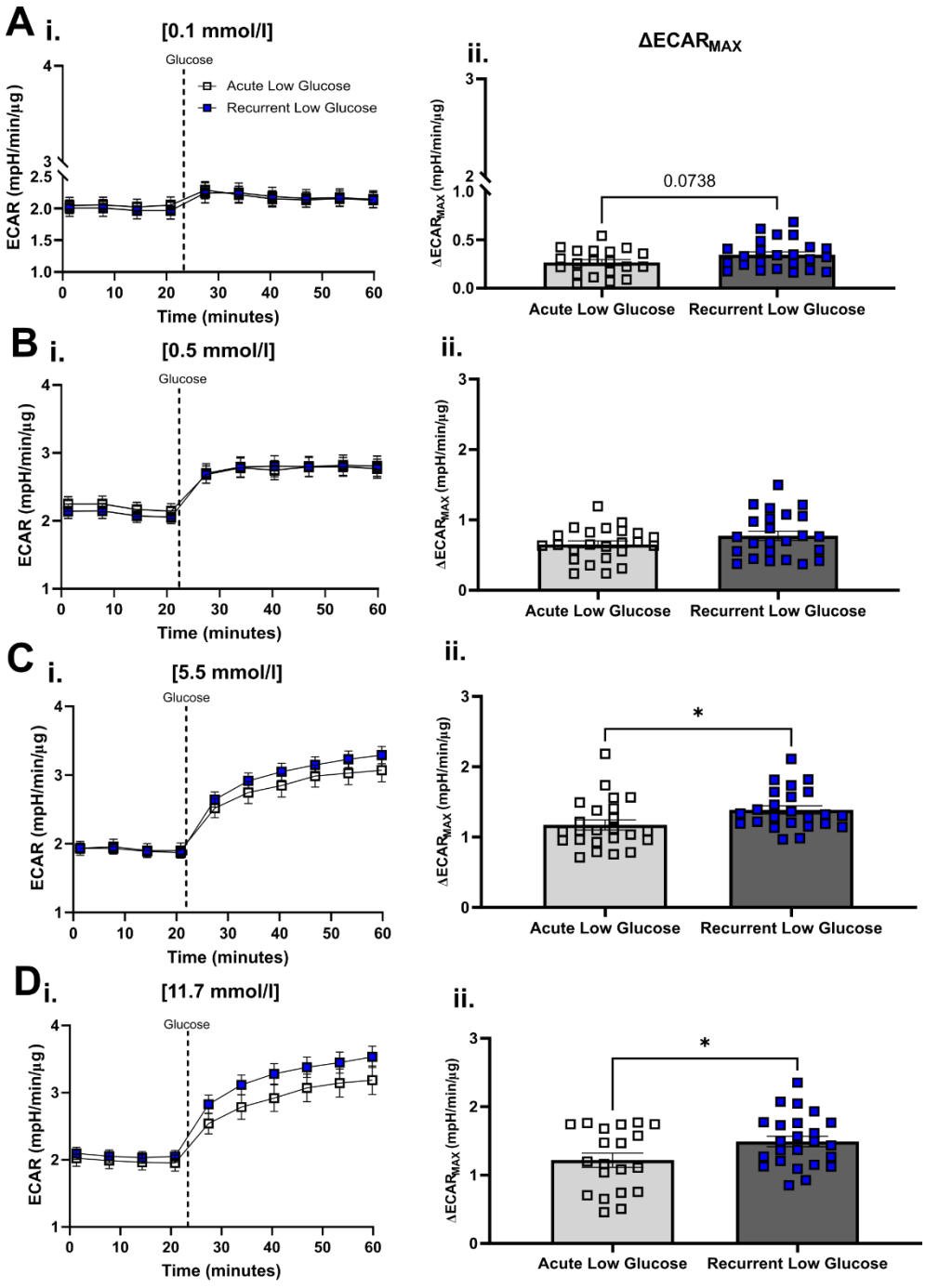

Figure 6.7: Recurrent low glucose (RLG)-exposed α-cells have enhanced glucose recovery.

αTC1.9 cells were exposed to 5.5 (acute low glucose) or 0.5 (Recurrent low glucose) mmol/l glucose over 3-days. On Day 4, cells were preincubated with standard Seahorse XF media ± 0.5 mmol/l glucose for 1 h. Media was then replaced with media containing no glucose prior to injection of **A i.** 0.1, **B i.** 0.5, **C i.** 5.5, **D i.** 11.7 mmol/l glucose. $\Delta ECAR_{MAX}$ was calculated (**A - D ii**.) from maximum ECAR reading minus average baseline ECAR measurements prior to injection (Unpaired two-tailed t-test, n = 20 – 24, *P<0.05)

6.2.3.2 R481 enhanced α-cell glucose recovery regardless of prior bouts of glucose.

R481 treatment did not alter α-cell $\Delta ECAR_{MAX}$ regardless of prior acute low glucose or RLG-treatment after 0.1 mmol/l glucose acute injection (Acute Low Glucose: vehicle; 0.265 ± 0.030, R481; 0.302 ± 0.037, Recurrent Low Glucose: vehicle; 0.345 ± 0.030, R481; 0.309 ± 0.034) (Figure 6.8Ai-ii). R481 incubation enhanced both RLG and acute low glucose-treated α-cells $\Delta ECAR_{MAX}$ after 0.5 mmol/l acute injection (mpH/min/µg) (Acute Low Glucose: vehicle; 0.652 ± 0.048, R481; 1.148 ± 0.094, *P = 0.0002,* Recurrent Low Glucose: vehicle; 0.775 ± 0.065, R481; 1.233 ± 0.122, *P = 0.0007)* (Figure 6.8Bi-ii). Similarly, R481 increased $\Delta ECAR_{MAX}$ after 5.5 mmol/l glucose acute injection in both prior low glucose conditions (mpH/min/µg) (Acute Low Glucose: vehicle; 1.173 ± 0.071, R481; 2.946 ± 0.160, *P < 0.0001,* Recurrent Low Glucose: vehicle; 1.386 ± 0.058, R481; 2.973 ± 0.243, *P < 0.0001*) (Figure 6.8Ci-ii). After 11.7 mmol/l glucose injection, R481 treatment increased $\Delta ECAR_{MAX}$ in prior acute low glucose and RLG-treated αTC1.9 cells (mpH/min/µg) (Acute Low Glucose: vehicle; 1.218 ± 0.103, R481; 3.331 ± 0.230, *P < 0.0001,* Recurrent Low Glucose: vehicle; 1.491 ± 0.078, R481; 3.541 ± 0.291, *P < 0.0001*) (Figure 6.8Di-ii).

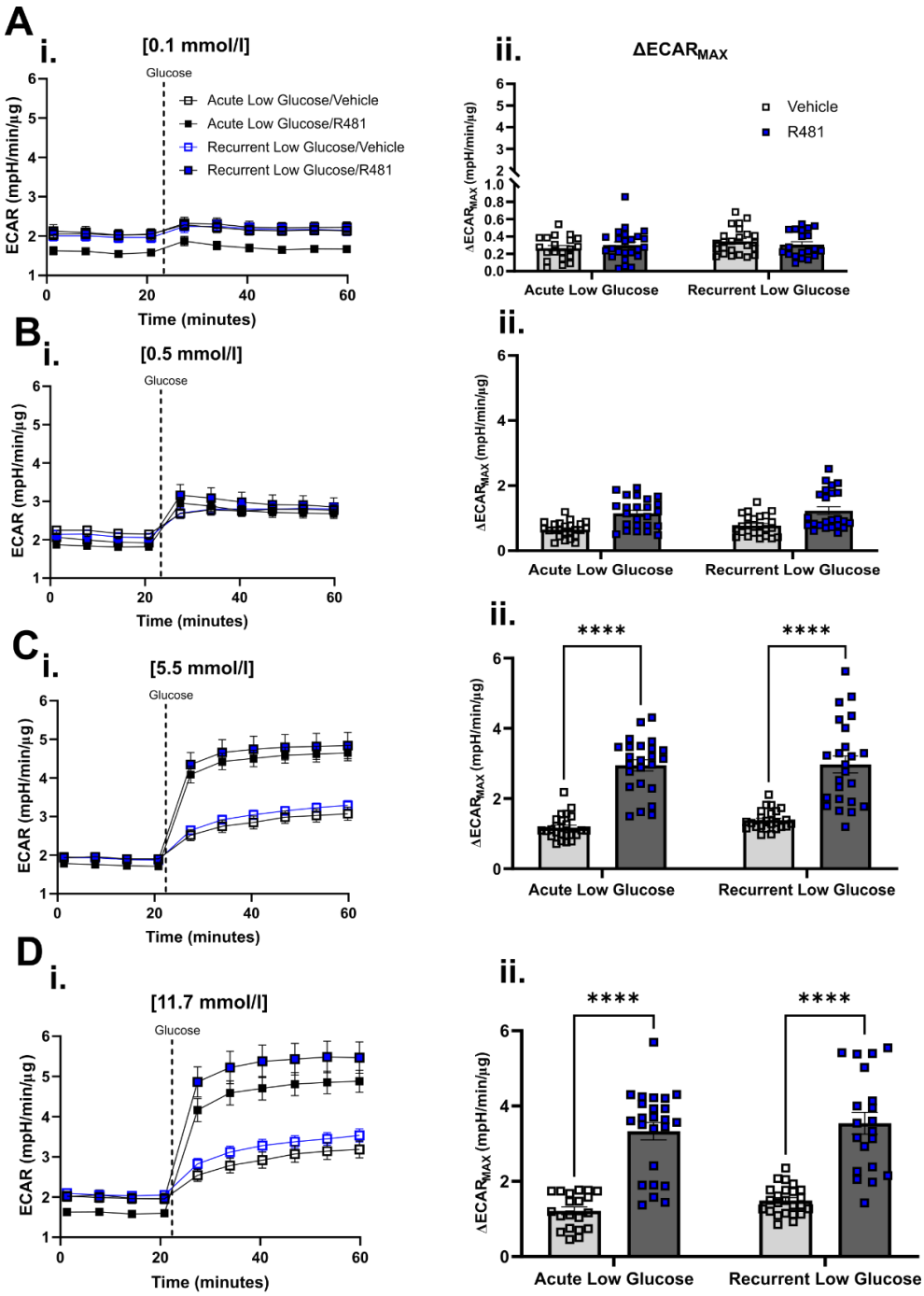

Figure 6.8: R481 enhanced α-cell glucose recovery regardless of prior low glucose bouts.

αTC1.9 cells were exposed to 5.5 (acute low glucose) or 0.5 (recurrent low glucose, RLG) mmol/l glucose over 3-days. On Day 4, cells were preincubated with standard Seahorse XF media containing 0.5 mmol/l glucose ± R481 (50 nmol/l) for 1 h. Media was then replaced with media containing no glucose ± R481 prior to injection of **A i**. 0.1, **B i**. 0.5, **C i.** 5.5, **D i**. 11.7 mmol/l glucose. $\Delta ECAR_{MAX}$ was calculated (**A-D ii**.) from maximum ECAR reading minus average baseline ECAR measurements prior to injection (Two-Way ANOVA with Tukey's multiple comparison test, n = 20 – 24, **P<0.01, ****P<0.0001)

6.2.4 Lactate secretion

Studies described in this chapter show that RLG exposure increased α-cell glycolysis. As lactate can be utilised as a metabolic fuel during energy stress, including RH-like conditions, this work investigated whether RLG could induce metabolic fuel adaptations during and post-bout of low glucose (Wender *et al.*, 2000; Brown *et al.*, 2005). Following three days of RLG protocol, on Day 4 acute low glucose and RLG-treated α-cells were both exposed to 0.5 mmol/l glucose for 1 h. Lactate secretion was analysed after extracellular lactate supernatant levels were normalised to total protein.

6.2.4.1 RLG did not alter α-cell L-lactate secretion at either low or normal glucose.

Lactate secretion was not altered following RLG at 0.5 mmol/l glucose (µM/µg) (Acute Low Glucose; 72.25 ± 14.40, Recurrent Low Glucose; 65.49 ± 5.091) (Figure 6.9). Similarly, antecedent low glucose-treated α-cells had no significant difference in lactate secretion compared to control (µM/µg) (Control: 74.97 ± 4.463, Antecedent; 65.90 ± 7.053) (Figure 6.10).

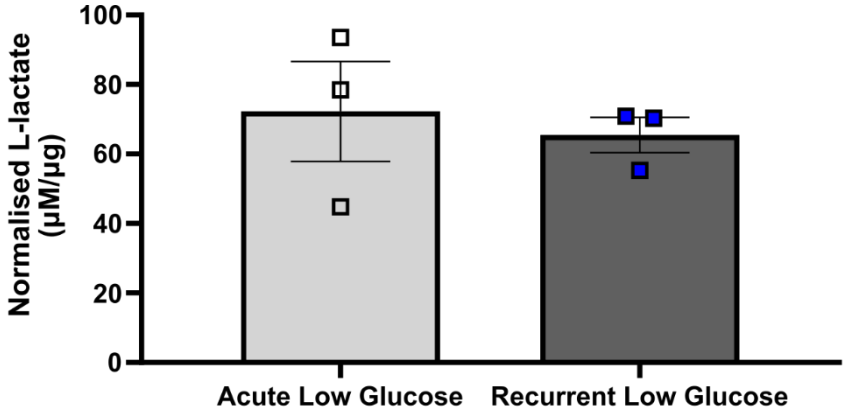

Figure 6.9: Recurrent low glucose (RLG)-exposed α-cells did not significantly alter L-lactate secretion at low glucose.

αTC1.9 cells were incubated with either 5.5 mmol/l glucose (acute low glucose) or 0.5 mmol/l (recurrent low glucose) for 3 h episodes for 3 days. On Day 4, cells were incubated with serum-free, 5.5 mmol/l glucose-containing media for 2 h and further incubated with 0.5 mmol/l glucose for 1 h. Supernatant L-lactate secretion (normalised to total protein) was measured using fluorescence-based L-lactate assay (Cayman Chemical) (Unpaired two-tailed t-test, n = 3)

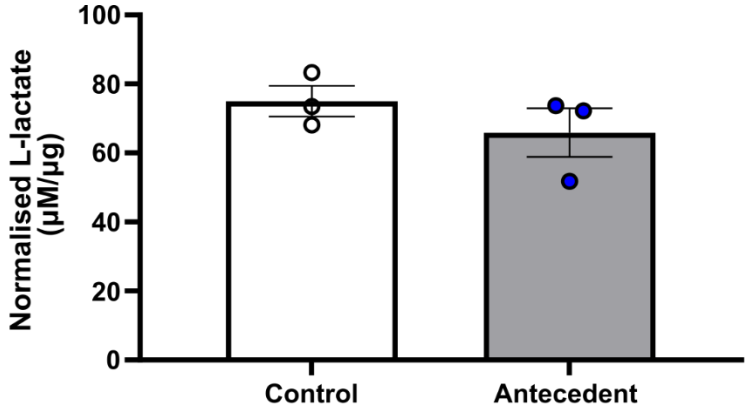

Figure 6.10: α-cell L-lactate secretion was unchanged following antecedent low glucose.

αTC1.9 cells were incubated with either 5.5 mmol/l glucose (control) or 0.5 mmol/l (antecedent) glucose for 3 h episodes for 3 days. On Day 4, cells were incubated with serum-free, 5.5 mmol/l glucose-containing media for 2 h and further incubated with 5.5 mmol/l glucose for 1 h. Supernatant L-lactate secretion (normalised to total protein) was measured using fluorescence-based L-lactate assay (Cayman Chemical) (Unpaired two-tailed t-test, n = 3).

6.2.4.2 Glucose recovery from prior bouts of low glucose did not alter α-cell L-lactate secretion.

Prior work has demonstrated RLG-exposed α-cells have increased glucose recovery at high [glucose]. To investigate if increased glucose recovery reflects enhanced lactate secretion derived from glycolysis, on Day 4 cells were exposed to an additional 1 h with either 0.5 or 11.7 mmol/l glucose.

Interestingly, increased RLG glucose recovery did not modulate α-cell lactate secretion, compared to acute low glucose (µM/µg) (0.5: acute low glucose; 58.419 ± 6.20; recurrent low glucose; 56.650 ± 2.218, 11.7: acute low glucose; 62.593 ± 6.451, recurrent low glucose; 57.769 ± 3.764) (Figure 6.11). Similarly, antecedent low glucose-exposed α-cells had no difference in L-lactate secretion derived from glycolytic reliance compared to control (µM/µg) (0.5: control; 64.002 ± 8.129, antecedent low glucose; 64.085 ± 6.775, 11.7: control; 63.121 ± 9.449, antecedent low glucose; 62.085 ± 4.526) (Figure 6.12).

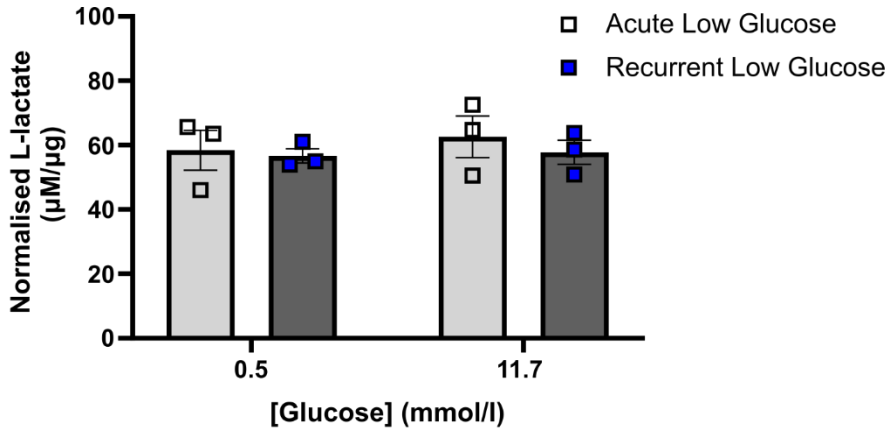

Figure 6.11: Recurrent low glucose (RLG) does not alter α-cell L-lactate secretion after glucose recovery.

αTC1.9 cells were incubated with either 5.5 mmol/l glucose (acute low glucose) or 0.5 mmol/l (recurrent low glucose) for 3 h episodes for 3 days. On Day 4, cells were incubated with serum-free, 5.5 mmol/l glucose-containing media for 2 h and further incubated with 0.5 mmol/l glucose for 1 h. Subsequently, cells were incubated in 0.5/11.7 mmol/l glucose for a further 1 h. Supernatant L-lactate secretion (normalised to total protein) was measured using fluorescence-based L-lactate assay (Cayman Chemical) (Two-Way ANOVA with Tukey's multiple comparisons test).

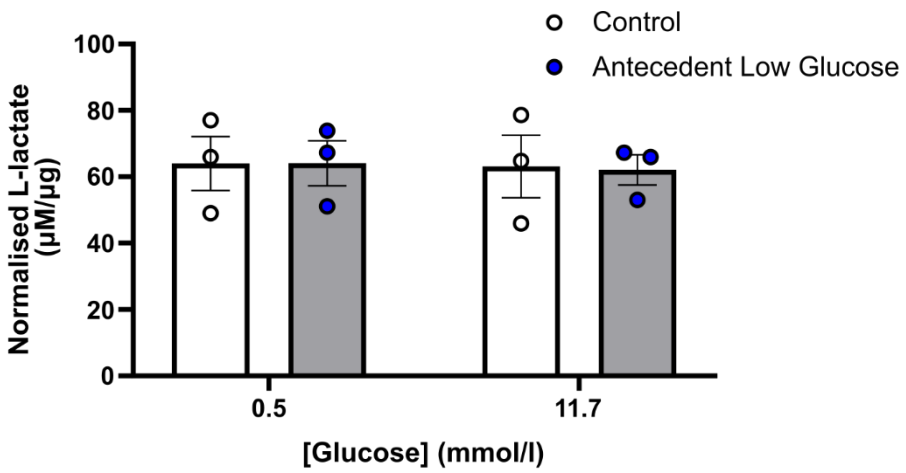

Figure 6.12: Antecedent low glucose did not alter α-cell glucose recovery in L-lactate secretion.

αTC1.9 cells were incubated with either 5.5 mmol/l glucose (control) or 0.5 mmol/l (antecedent) glucose for 3 h episodes for 3 days. On Day 4, cells were incubated with serum-free, 5.5 mmol/l glucose-containing media for 2 h and further incubated with 5.5 mmol/l glucose for 1 h. Subsequently, cells were recovered in 11.7 mmol/l or incubated with 0.5 mmol/l glucose for a further 1 h. Supernatant L-lactate secretion (normalised to total protein) was measured using fluorescence-based L-lactate assay (Cayman Chemical) (Two-Way ANOVA with Tukey's multiple comparisons test).

6.2.5 Total ATP (tATP) measurements

RLG induced α-cell glycolytic and mitochondrial adaptations, and therefore this study investigated if these bioenergetic adaptations result in an alteration in ATP production. For clarity and experimental question asked, Figure 6.13/Figure 6.14 are the stated vehicle groups illustrated in Figure 6.15/Figure 6.16 respectively. Repetitive statistical testing between both vehicle groups were therefore not displayed and analysed in Figure 6.15/Figure 6.16.

6.2.5.1 Recurrent low glucose (RLG) did not alter α-cell tATP levels at low glucose.

RLG exposure did not alter αTC1.9 tATP at low glucose (µmol/ml) (Acute Low Glucose; 1.386 ± 0.1387, Recurrent Low Glucose; 1.516 ± 0.1606) (Figure 6.13). However, prior bouts of low glucose significantly increased tATP compared to control at 5.5 mmol/l glucose (µmol/ml) (Control; 1.118 ± 0.1442, Antecedent; 1.584 ± 0.1030, *P = 0.0170)* (Figure 6.14).

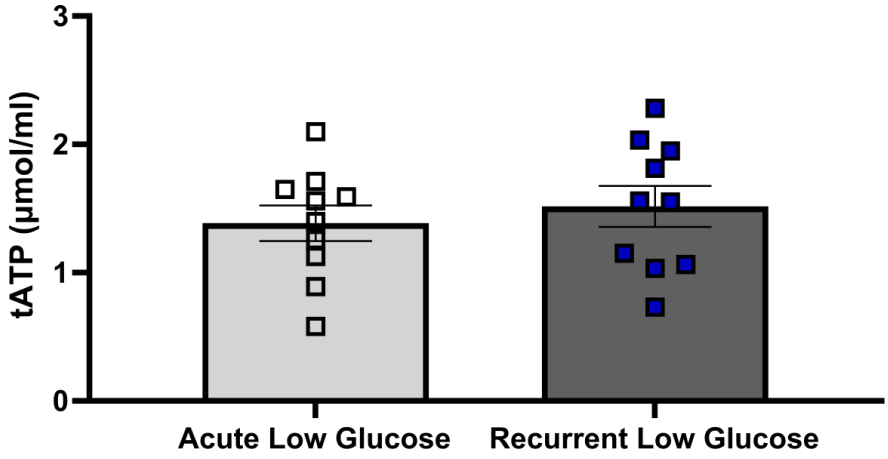

Figure 6.13: Recurrent low glucose (RLG)-treated α-cells have no change in total ATP (tATP) levels.

αTC1.9 cells were exposed to 0.5/5.5 mmol/l glucose over 3-days. On Day 4, cells were preincubated with phenol-free DMEM media containing 2.0 mmol/l L-glutamine, 2.5 mmol/l sodium pyruvate and 5.5 mmol/l glucose for total 2.5 h. Media was replaced by fresh 0.5 mmol/l glucose for an additional 30 min. tATP (µM/ml) was quantified using ATPliteTM luminescence assays (Two-tailed unpaired t-test, n = 10)

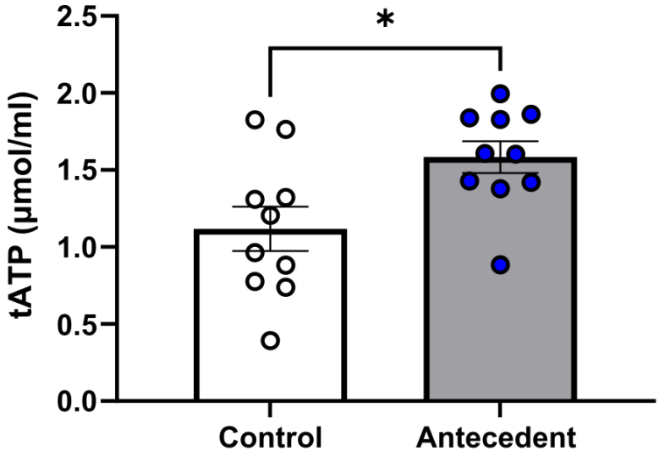

Figure 6.14: Antecedent low glucose enhanced basal α-cell total ATP (tATP) levels.

αTC1.9 cells were exposed to 0.5/5.5 mmol/l glucose over 3-days. On Day 4, cells were preincubated with phenol-free DMEM media containing 2.0 mmol/l L-glutamine, 2.5 mmol/l sodium pyruvate and 5.5 mmol/l glucose for total 2.5 h. Media was replaced by fresh 5.5 mmol/l glucose for an additional 30 min. Total ATP (µM/ml) was quantified using ATPlite^{TM} luminescence assays (Two-tailed unpaired t-test, n = 10, *P<0.05)

6.2.5.2 R481 treatment decreased total ATP (tATP) levels regardless of RLG in α-cells.

Cells were subsequently pre-treated with R481 (50 nmol/l) and substrate-containing (2.5 mmol/l pyruvate, 2.0 mmol/l glutamine, 5.5 mmol/l glucose) media for 30 min. Media was replaced with either 0.5/5.5 mmol/l glucose and metabolic substrate-containing media ± R481 for 30 min prior to measuring tATP.

R481 reduced tATP levels in both acute and RLG-treated α-cells at low glucose (µmol/ml) (Acute Low Glucose: vehicle; 1.386 ± 0.139, R481; 0.748 ± 0.137, *P = 0.0110,* Recurrent Low Glucose: vehicle; 1.516 ± 0.161, R481; 0.998 ± 0.172, *P = 0.0427*) (Figure 6.15). However, R481 treatment did not alter either α-cell tATP after antecedent low glucose at 5.5 mmol/l glucose (µmol/ml) (Control: vehicle; 1.118 ± 0.144, R481; 0.826 ± 0.117, Antecedent: vehicle; 1.584 ± 0.103, R481; 1.289 ± 0.153) (Figure 6.16).

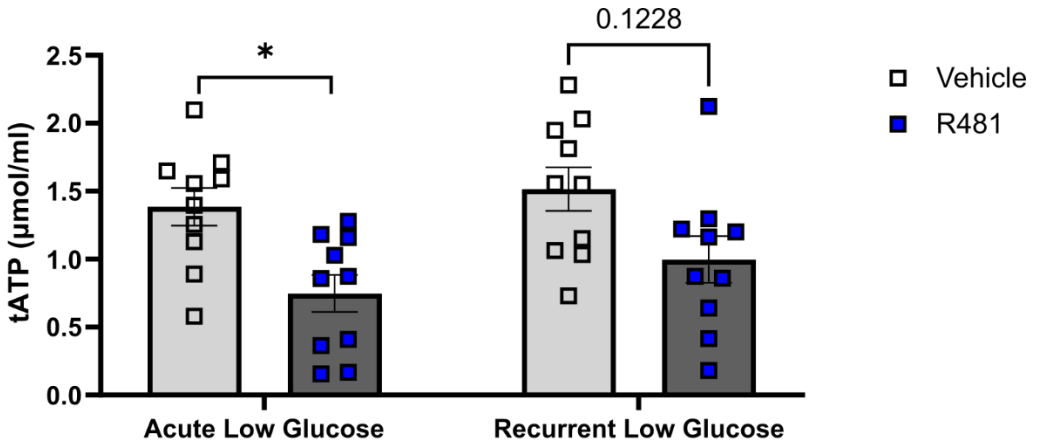

Figure 6.15: R481 treatment reduced total ATP (tATP) levels at low glucose in both acute and recurrent low glucose (RLG)-treated αTC1.9 cells.

αTC1.9 cells were exposed to 0.5 mmol/l glucose over 3-days. On Day 4, cells were preincubated with phenol-free DMEM media containing 2.0 mmol/l L-glutamine, 2.5 mmol/l sodium pyruvate and 5.5 mmol/l glucose for 2 h and preincubated ± R481 (50 nmol/l) for 30 min. Media was replaced by fresh 0.5 mmol/l glucose ± R481 (50 nmol/l) for an additional 30 min. tATP (µM/ml) was quantified using ATPlite™ luminescence assays (*P < 0.05, Two-Way ANOVA with Tukey's multiple comparisons test, n = 10)

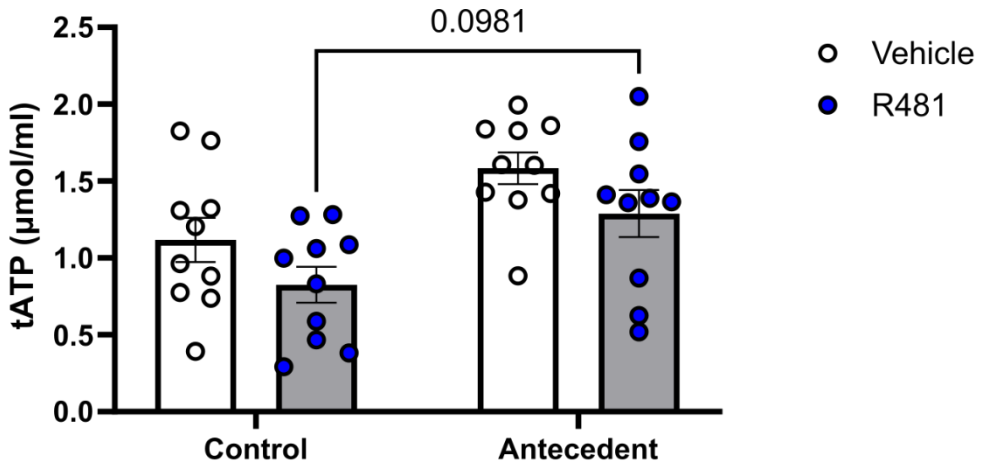

Figure 6.16: R481 did not alter α-cell total ATP (tATP) levels regardless of antecedent low glucose.

αTC1.9 cells were exposed to 5.5 mmol/l glucose over 3-days. On Day 4, cells were preincubated with phenol-free DMEM media containing 2.0 mmol/l L-glutamine, 2.5 mmol/l sodium pyruvate and 5.5 mmol/l glucose for 2 h and preincubated ± R481 (50 nmol/l) for 30 min. Media was replaced by fresh 5.5 mmol/l glucose ± R481 (50 nmol/l) for an additional 30 min. tATP (µM/ml) was quantified using ATPlite™ luminescence assays (Two-Way ANOVA with Tukey's multiple comparisons test, n = 10)

6.2.5.3 R481 treatment did not alter α-cell total ATP (tATP) levels after prior antecedent low glucose bouts.

To examine if the increased glucose recovery from RLG reflects enhanced ATP generation, following a three-day RLG protocol on Day 4, α-cells were exposed to 5.5 mmol/l glucose-containing media for 2 h. Cells were incubated with ± R481 (50 nmol/l), substrate- and 0.5 mmol/l glucose-containing media for 1 h. Cells were further incubated with 0.5 – 11.7 mmol/l glucose-containing media ± R481 (50 nmol/l) for 30 min and tATP was measured.

R481 did not affect tATP after α-cell glucose recovery following RLG exposure at any glucose availability (µmol/ml) (0.5: Acute Low Glucose; vehicle; 0.986 ± 0.332, R481; 0.492 ± 0.181, Recurrent Low Glucose; vehicle; 1.371 ± 0.420, R481; 0.479 ± 0.176) (5.5: Acute Low Glucose; vehicle; 1.304 ± 0.339, R481; 0.915 ± 0.191, Recurrent Low Glucose; vehicle; 1.398 ± 0.412, R481; 0.926 ± 0.366) (11.7: Acute Low Glucose; vehicle; 1.050 ± 0.236, R481; 0.816 ± 0.227, Recurrent Low Glucose; vehicle; 1.184 ± 0.303, R481; 0.599 ± 0.247) (Figure 6.17A-C).

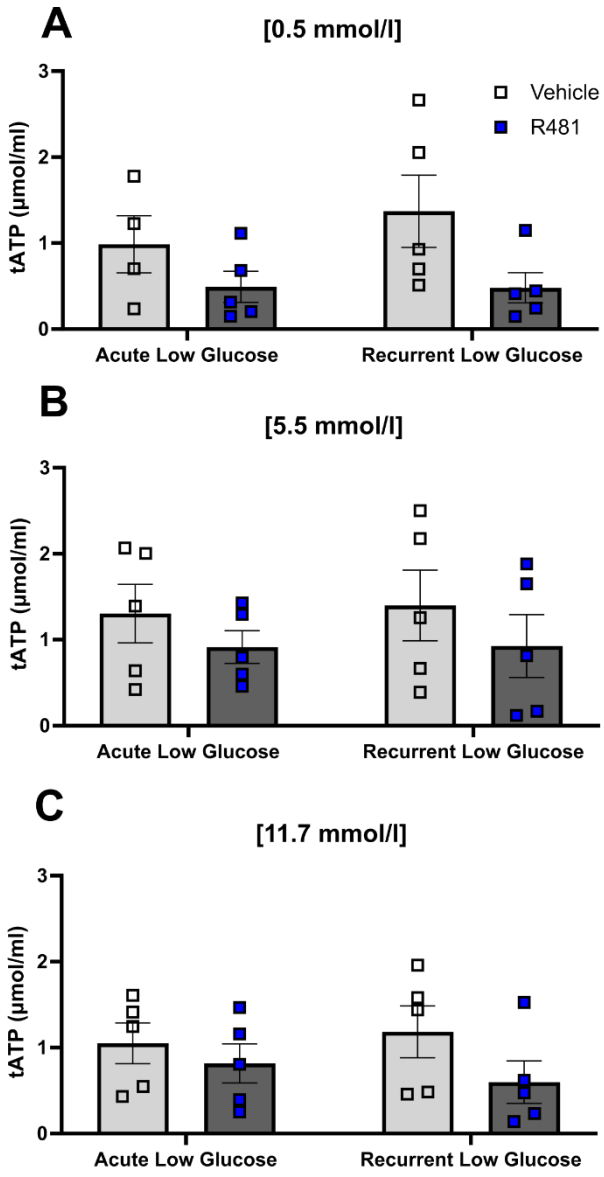

Figure 6.17: R481 did not alter total ATP (tATP) levels following glucose recovery in recurrent low glucose (RLG)-treated α-cells.

αTC1.9 cells were exposed to 0.5 mmol/l glucose over 3-days. On Day 4, cells were preincubated with phenol-free DMEM media containing 2.0 mmol/l L-glutamine, 2.5 mmol/l sodium pyruvate and 5.5 mmol/l glucose for 2 h. Cells were subsequently incubated 0.5 mmol/l ± R481 (50 nmol/l) for 1 h and media was replaced by fresh **A.** 0.5 (Two-Way ANOVA with Tukey's multiple comparison test), **B.** 5.5 (Multiple Mann-Whitney tests with Holm-Šídák's multiple comparison tests) and **C.** 11.7 mmol/l glucose (Two-Way ANOVA with Tukey's multiple comparison test) ± R481 (50 nmol/l) for an additional 30 min. tATP (µM/ml) was quantified using ATPlite™ luminescence assays (n = 5).

6.2.6 Glucagon secretion during RLG exposure

Recurrent hypoglycaemic episodes, over time, diminishes α-cell glucagon secretion required for glucose counter-regulation (Gerich *et al.*, 1973). To investigate if recurrent bouts of low glucose directly alter α-cell glucagon secretion, alongside direct metabolic adaptations, supernatants and lysates collected from 6.2.4. were used to measure glucagon secretion normalised to total glucagon content.

6.2.6.1 Recurrent low glucose (RLG) did not alter α-cell glucagon secretion.

α-cells, following RLG exposure, did not have altered glucagon secretion at low glucose (% secretion) (Acute Low Glucose; 0.7590 ± 0.1285, Recurrent Low Glucose; 1.006 ± 0.06068, *P = 0.120*) (Figure 6.18A). Similarly, no difference in total glucagon content was observed (µg) (Acute Low Glucose; 1.392 ± 0.2383, Recurrent Low Glucose; 1.269 ± 0.1024) (Figure 6.18B). No difference in glucagon secretion was observed after prior bouts of antecedent low glucose, recovered at 5.5 mmol/l glucose (% secretion) (Control; 1.044 ± 0.1946, Antecedent; 1.127 ± 0.1804) (Figure 6.19A). Additionally, total α-cell glucagon content was unaffected by prior bouts of antecedent low glucose (µg) (Control; 1.278 ± 0.2238, Antecedent; 1.269 ± 0.1091) (Figure 6.19B).

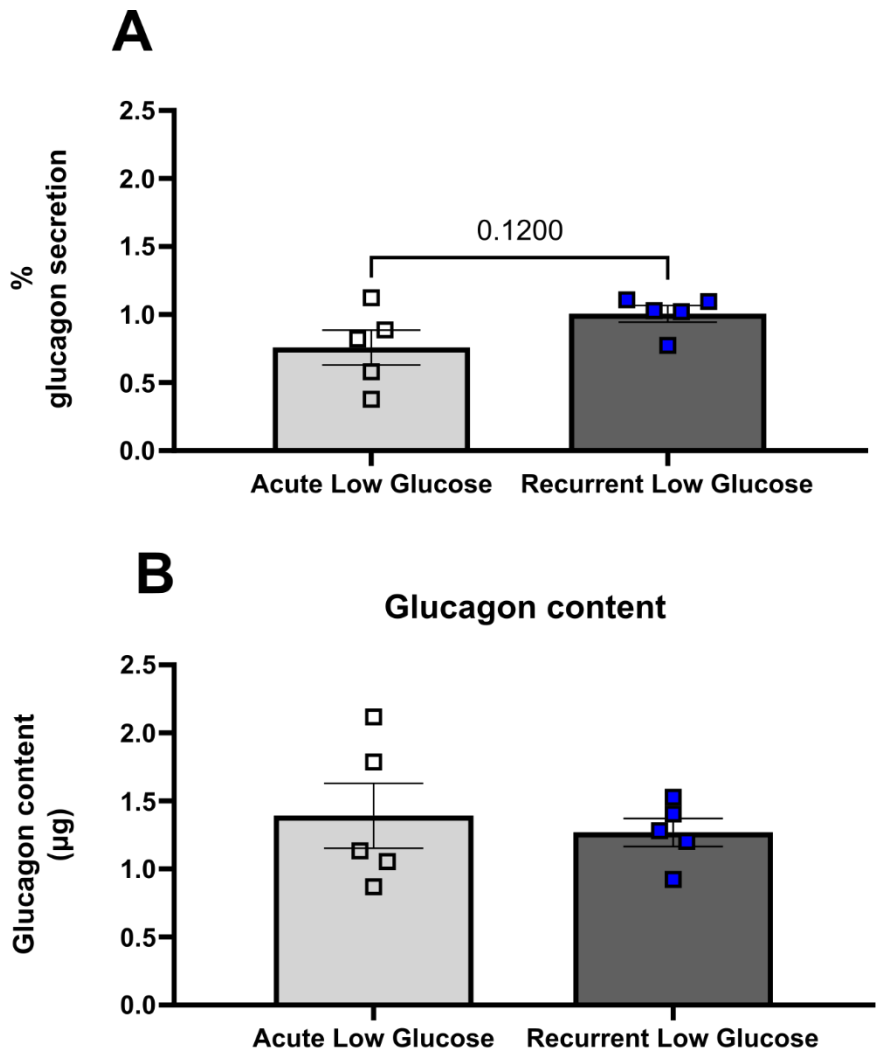

Figure 6.18: Recurrent low glucose (RLG) did not alter α-cell glucagon secretion at low glucose.

αTC1.9 cells were incubated with either 5.5 mmol/l glucose (acute low glucose) or 0.5 mmol/l (recurrent low glucose) for 3 h episodes for 3 days. On Day 4, cells were incubated with serum-free, 5.5 mmol/l glucose-containing media for 2h and further incubated with 0.5 mmol/l glucose for 1h. Subsequently, cells were recovered in 11.7 mmol/l or treated with 0.5 mmol/l glucose for a further 1 h. **A.** Normalised glucagon secretion and **B.** glucagon content were measured using Promega Lumit™ glucagon immunoassay (Unpaired two-tailed t-test)

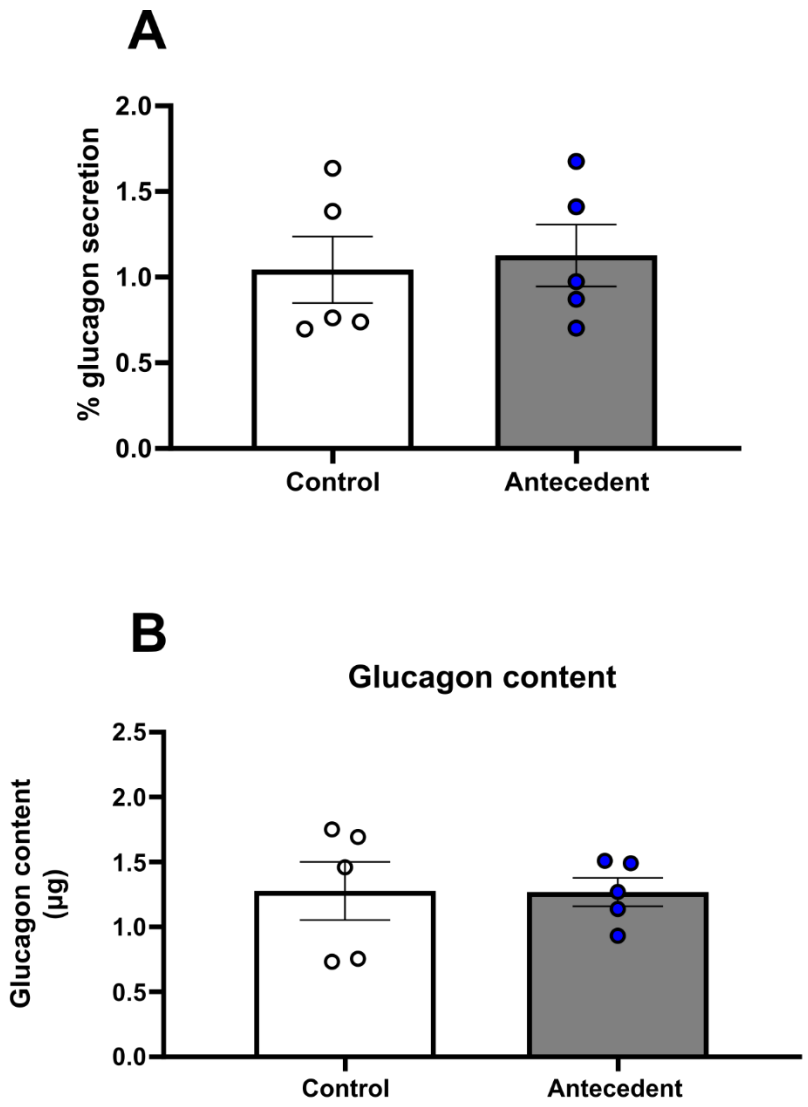

Figure 6.19: Antecedent low glucose did not alter α-cell glucagon secretion at 5.5 mmol/l glucose.

αTC1.9 cells were incubated with either 5.5 mmol/l glucose (control) or 0.5 mmol/l (antecedent) glucose for 3 h episodes for 3 days. On Day 4, cells were incubated with serum-free, 5.5 mmol/l glucose-containing media for 2h and further incubated with 5.5 mmol/l glucose for 1h. Subsequently, cells were recovered in 11.7 mmol/l or incubated with 0.5 mmol/l glucose for a further 1 h. **A.** Normalised glucagon secretion and **B**. glucagon content were measured using Promega Lumit™ glucagon immunoassay (Unpaired two-tailed t-test).

6.2.6.2 Glucagon secretion following glucose recovery.

To investigate if increased glucose recovery following RLG reflects an alteration to downstream α-cell glucagon secretion, following glucose treatment, cells were recovered in 0.5/11.7 mmol/l glucose for an additional 1 h.

6.2.6.3 Glucose recovery from prior bouts of low glucose did not alter αTC1.9 glucagon secretion.

Glucose recovery from RLG did not alter α-cell glucagon secretion (% secretion) (0.5: Acute Low Glucose; 2.238 ± 0.378, Recurrent Low Glucose; 2.432 ± 0.244, 11.7: Acute Low Glucose; 2.014 ± 0.341, Recurrent Low Glucose; 2.469 ± 0.262). This was reflected in no differences in glucagon content between all conditions (µg) (0.5: Acute Low Glucose; 0.112 ± 0.015, Recurrent Low Glucose; 0.115 ± 0.011, 11.7: Acute Low Glucose; 0.105 ± 0.002, Recurrent Low Glucose; 0.095 ± 0.008).

Glucose recovery from prior antecedent low glucose bouts similarly did not alter α-cell glucagon secretion (% secretion) (0.5: Control; 2.037 ± 0.158, Antecedent; 2.395 ± 0.136, 11.7: Control; 2.444 ± 0.101, Antecedent; 2.373 ± 0.203) (Figure 6.21A). Additionally, total glucagon content was not altered in all conditions (µg) (0.5: Control; 0.113 ± 0.012, Antecedent; 0.108 ± 0.006, 11.7: Control; 0.106 ± 0.007, Antecedent; 0.107 ± 0.009) (Figure 6.21B).

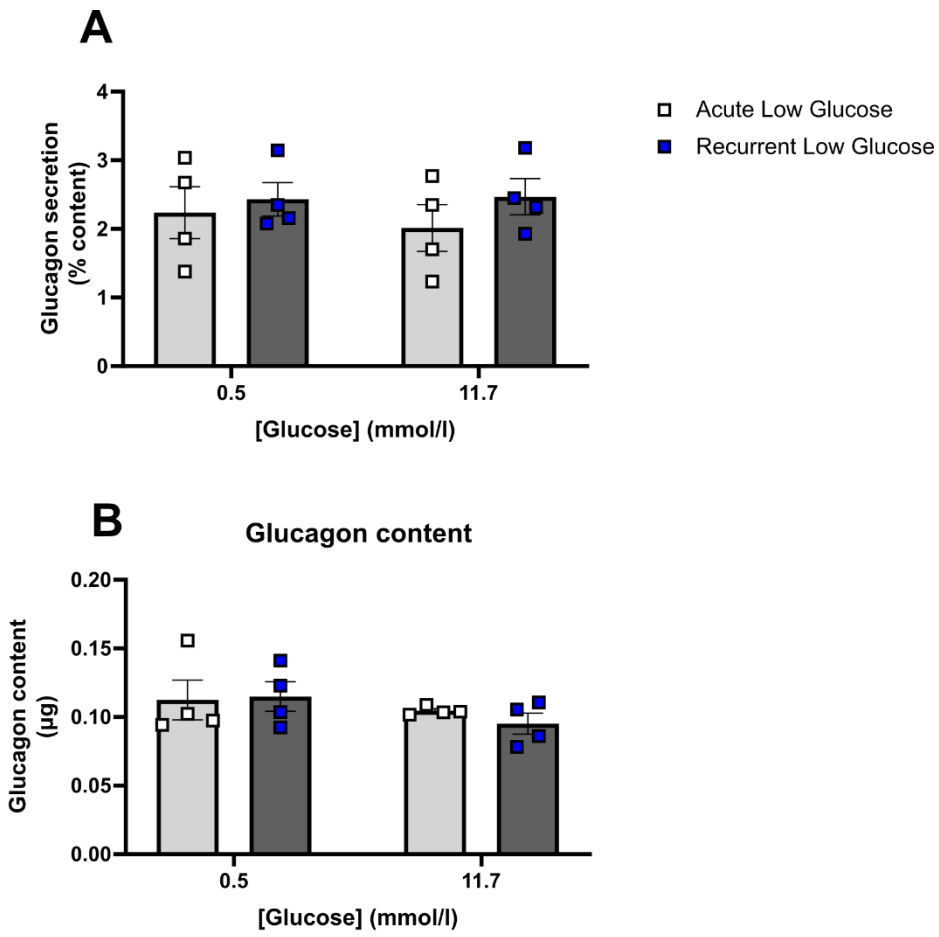

Figure 6.20: Glucose recovery did not alter α-cell glucagon secretion following prior recurrent bouts of low glucose.

αTC1.9 cells were incubated with either 5.5 mmol/l glucose (control) or 0.5 mmol/l (antecedent) glucose for 3 h episodes for 3 days. On Day 4, cells were incubated with serum-free, 5.5 mmol/l glucose-containing media for 2h and further exposed to 0.5 mmol/l glucose for 1 h. Subsequently, cells were recovered in 11.7 mmol/l or treated with 0.5 mmol/l glucose for a further 1 h. **A.** Normalised glucagon secretion and **B.** glucagon content were measured using Promega Lumit^{TM} glucagon immunoassay (Two-Way ANOVA with Tukey's multiple comparisons test).

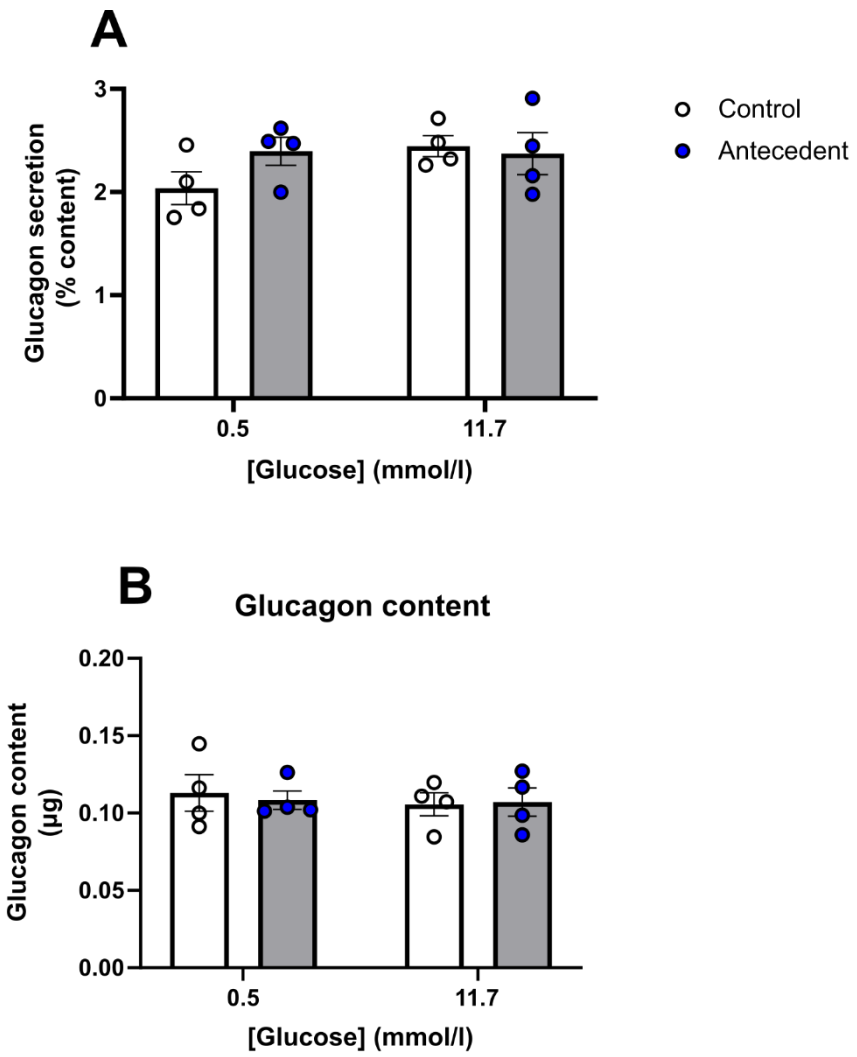

Figure 6.21: Antecedent low glucose did not alter α-cell glucagon secretion.

αTC1.9 cells were incubated with either 5.5 mmol/l glucose (control) or 0.5 mmol/l (antecedent) glucose for 3 h episodes for 3 days. On Day 4, cells were incubated with serum-free, 5.5 mmol/l glucose-containing media for 2 h and further exposed to 5.5 mmol/l glucose for 1 h. Subsequently, cells were recovered in 11.7 mmol/l or treated with 0.5 mmol/l glucose for a further 1 h**. A.** Normalised glucagon secretion and **B**. glucagon content were measured using Promega Lumit™ glucagon immunoassay (Two-Way ANOVA with Tukey's multiple comparisons test).

6.2.7 α-cell bioenergetics following recurrent AMPK inhibition

To determine whether prior bouts of low glucose increased glycolytic rate by intermittent AMPK activation, a pilot study was conducted by following the intermittent application of an AMPK inhibitor, SBI-0206965 (30.0 µmol/l) for 30 min in standard Seahorse XF DMEM medium containing 5.5 mmol/l glucose, prior to each low glucose bout (according to the RLG protocol) for three days. On Day 4, cells were pre-treated with SBI- for 30 min prior to being stimulated with 0.5 mmol/l glucose ± SBI for 1 h. In addition, to investigate if direct AMPK activator (O-304) continues to enhance α-cell bioenergetics after recurrent SBI treatment, O-304 (5.0 µmol/l) was acutely injected using the Seahorse XFe96 analyser prior to measuring glycolytic rate by mitochondrial inhibition (Rot/AA).

6.2.7.1 Intermittent AMPK inhibition attenuated α-cell basal bioenergetics at acute low glucose, but not RLG.

SBI-treatment attenuated α-cell basal glycolytic rate at acute low glucose (pmol/min/µg) (Control; 17.689 ± 0.666, SBI; 12.099 ± 0.679, $P < 0.0001$). However, the effect of recurrent SBI treatment on α-cell glycolysis was abolished in cells exposed to RLG (pmol/min/µg) (Control; 19.716 ± 0.885, SBI; 17.495 ± 0.948, $P = 0.129$) (Figure 6.22A).

Similarly, recurrent SBI- treatment diminished basal OCR at acute low glucose (pmol/min/µg) (Control; 32.087 ± 0.668, SBI; 26.630 ± 0.891, $P = 0.0005$). Although, recurrent SBI treatment did not modulate basal OCR in cells exposed to RLG treatment (pmol/min/µg) (Control; 33.860 ± 1.118, SBI; 31.684 ± 1.199) (Figure 6.22B).

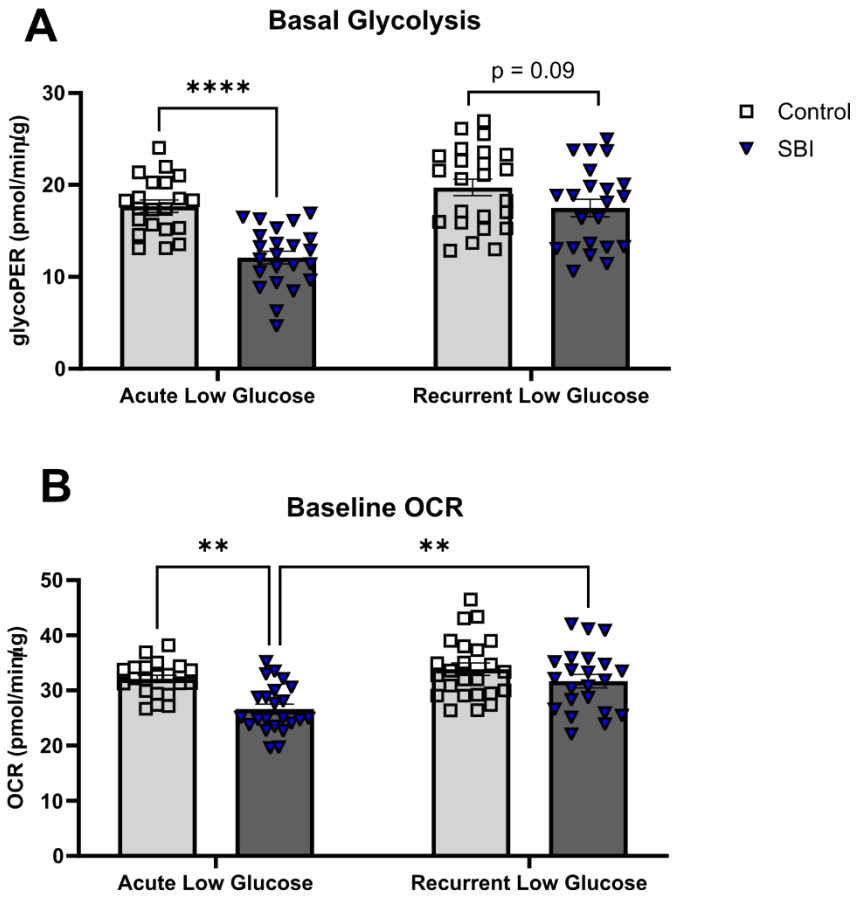

Figure 6.22: Intermittent SBI attenuated basal bioenergetics at acute low glucose, but not recurrent low glucose (RLG)-exposed α-cells.

αTC1.9 cells were preincubated ± 30 min SBI-0206965 (SBI, 30.0 µmol/l) in serum-free 5.5 mmol/l glucose-containing DMEM prior to a 3 h 0.5 mmol/l glucose stimulation (0.5 mmol/l glucose) for three-days. On Day 4, cells were preincubated ± 30 min SBI prior to a 1 h acute low glucose (0.5 mmol/l) stimulation ± SBI in standard Seahorse XF DMEM media. **A.** Basal glycolysis was calculated by glycolytic proton efflux rate (glycoPER, pmol/lmin/µg) (Multiple Mann-Whitney tests using Holm-Šídák multiple comparisons) and **B.** baseline mitochondrial respiration (OCR, pmol/min/µg) was calculated as the average OCR measurements prior to injection (Two-Way ANOVA with Tukey's multiple comparisons test) (n = 21 – 24, one plate, ***P<0.001, ****P<0.0001)

6.2.7.2 Intermittent AMPK inhibition did not influence O-304-induced αTC1.9 bioenergetic changes at acute low glucose.

To investigate if intermittent AMPK inhibition altered O-304-modulated bioenergetics in α-cells, both baseline glycolysis and oxidative respiration parameters were measured following acute O-304 injection. O-304 failed to alter glycolysis, although, recurrent SBI treatment attenuated basal glycolysis after O-304 treatment (pmol/min/µg) (-/-; 16.12 ± 0.9781, -/+; 17.88 ± 0.9053, +/-; 11.21 ± 0.7882, *-,+ vs ++; P = 0.1594,* +/+; 13.73 ± 0.7435, *-,+ vs +,+; P = 0.0076*) (Figure 6.23C). O-304 attenuated PER derived from glycolysis regardless of prior SBI treatment (%PER) (-/-; 53.27 ± 1.403, -/+; 44.09 ± 1.818, *-/- vs -/+, P = 0.0122,* +/-; 50.30 ± 2.899, +/+; 40.77 ± 1.342, *+/- vs +/+, P = 0.0057*) (Figure 6.23D). Additionally, O-304 continued to enhance ΔOCR_{MAX} in both recurrent SBI-treated and control cells (pmol/min/µg) (-/-; -0.5820 ± 0.09776, -/+; 15.59 ± 1.150, *-,- vs -,+; P = 0.0005,* +/-; -0.4688 ± 0.1363, +/+; 16.35 ± 0.7775, *+,- vs +,+; P = 0.0003*) (Figure 6.23E).

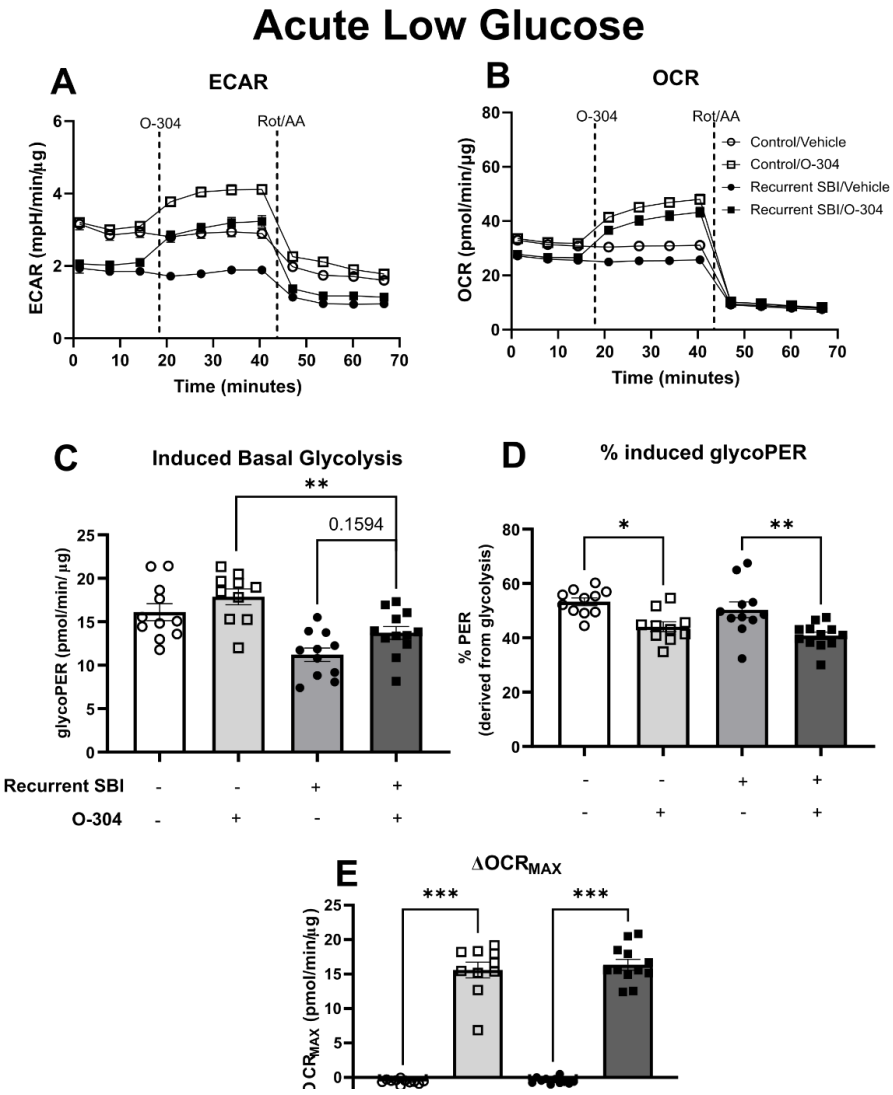

Figure 6.23: Recurrent SBI treatment attenuated O-304-induced glycolysis in α-cells.

αTC1.9 cells were incubated ± 3.5 h SBI-0206965 (SBI, 30.0 µmol/l) in serum-free 5.5 mmol/l glucose-containing DMEM for three-days. On Day 4, cells were preincubated ± 30 min SBI prior to a 1 h acute low glucose (0.5 mmol/l) stimulation ± SBI in standard Seahorse XF DMEM media. Cells were acutely stimulated ± O-304 (5.0 µmol/l) at ~ 17 min prior to mitochondrial inhibitor, rotenone/antimycin A, injection (Rot/AA, 0.5 µmol/l). Representative **A.** ECAR and **B.** OCR traces with **C**. induced basal glycolysis (glycoPER) contributed by acute O-304 injection (One-Way ANOVA with Tukey's multiple comparisons test) **D.** Induced PER derived from glycolysis (%glycoPER) (One-Way ANOVA with Tukey's multiple comparison test) **E**. ΔOCRMAX calculated by maximal OCR reading post-O-304 injection minus average baseline measurements (Kruskal-Wallis test with Dunn's multiple comparison test, n = 10 -11, one plate, **P<0.01, ***P<0.001)

6.2.7.3 Intermittent AMPK inhibition did not influence O-304-induced bioenergetic changes in RLG-treated α-cells.

O-304 did not modulate induced basal glycolysis, regardless of prior recurrent SBI or RLG bouts (pmol/min/µg) (-,-; 17.55 ± 1.199, -,+; 19.23 ± 1.034, +.-; 16.81 ± 1.208, +,+; 19.11 ± 1.371) (Figure 6.24C). RLG and/or recurrent SBI bouts did not influence O-304 modulated glycolytic-derived acidification (%PER) (-/-; 54.79 ± 1.488, -/+; 42.37 ± 1.672, *-/- vs -/+, P < 0.0001,* +/-; 53.94 ± 0.9018, +/+; 45.14 ± 1.491, *+/- vs +/+, P = 0.0007*) (Figure 6.24D). Similarly, O-304 increased oxidative respiration (ΔOCR_{MAX}) regardless of prior recurrent SBI and RLG bouts (pmol/min/µg) (-/-; -0.6770 ± 0.07858, -/+; 22.09 ± 1.425, *-/- vs -/+; P < 0.0001,* +/-; 0.1998 ± 0.1615, +/+; 20.25 ± 1.493, *+/- vs -/-, P < 0.0001*) (Figure 6.24E).

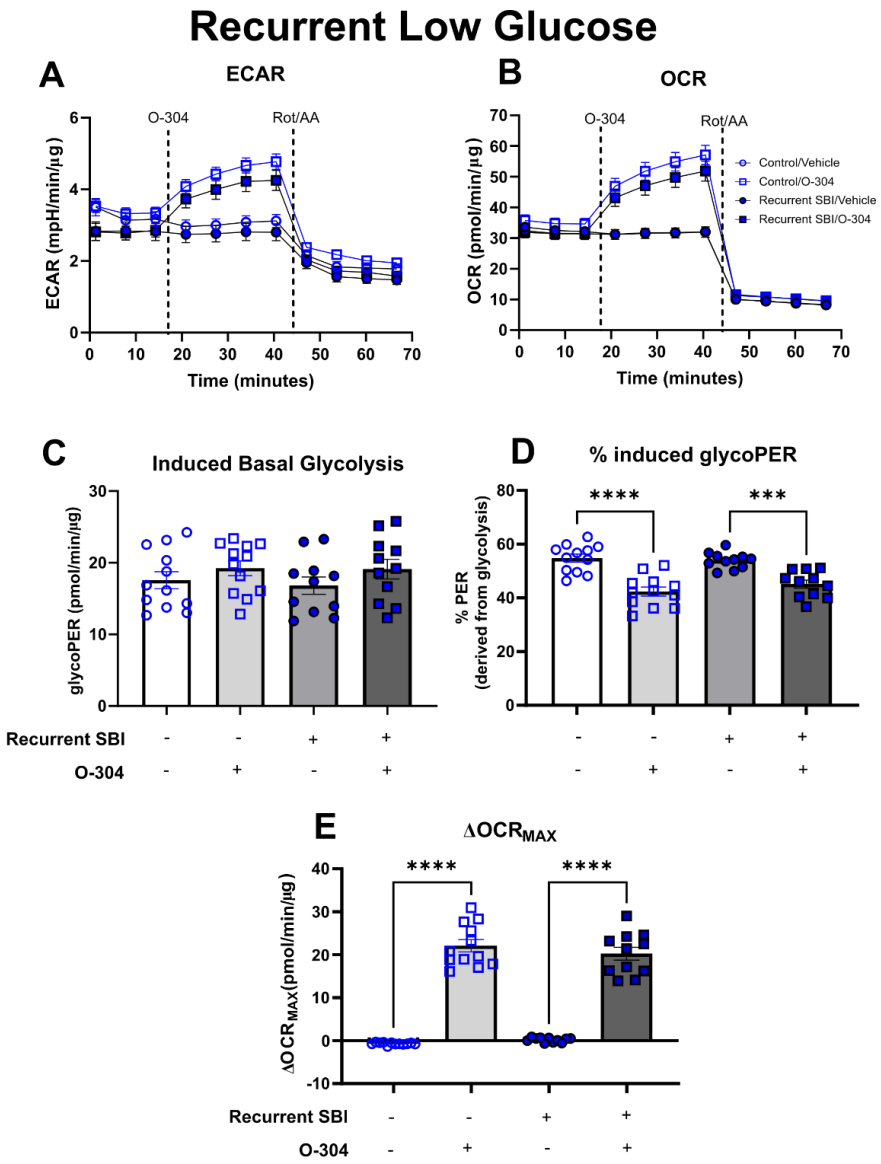

Figure 6.24: Intermittent SBI treatment did not influence O-304-induced bioenergetic changes in recurrent low glucose (RLG)-exposed α-cells.

αTC1.9 cells were preincubated ± 30 min SBI-0206965 (SBI, 30.0 µmol/l) in serum-free 5.5 mmol/l glucose-containing DMEM prior to a 3 h 0.5 mmol/l glucose stimulation (0.5 mmol/l glucose) for three-days. On Day 4, cells were preincubated ± 30 min SBI prior to a 1h acute low glucose (0.5 mmol/l) stimulation ± SBI in standard Seahorse XF media. Cells were acutely stimulated ± O-304 (5.0 µmol/l) at ~ 17 min prior to rotenone/antimycin A injection (Rot/AA, 0.5 µmol/l). Representative **A.** ECAR and **B.** OCR traces with **C**. Induced basal glycolysis derived from O-304 acute injection (Kruskal-Wallis test with Dunn's multiple comparisons test) **D**. induced glycolysis (% glycoPER) contributed by acute O-304 injection (One-Way ANOVA with Tukey's multiple comparison test) and **E**. ΔOCR_{MAX} calculated by maximal OCR reading post-O-304 injection minus average baseline measurements (One-Way ANOVA with Tukey's multiple comparison test, n = 10 -11, one plate, ***P<0.001, ****P<0.0001)

6.2.8 α-cell bioenergetics following recurrent AMPK activation

Recurrent hypoglycaemia is characterised by diminished central glucose-sensing thereby reducing autonomic control of α-cell glucagon secretion (Taborsky, Ahrén and Havel, 1998). The pharmacological and genetic manipulation of central AMPK activity demonstrate the importance of AMPK signalling to retain low glucose sensing (Beall *et al.*, 2012; McCrimmon, 2021). Therefore, to explore whether recurrent AMPK activation could ameliorate the observed metabolic adaptations following RLG, α-cells were incubated ± R481 (50 nmol/l) during each bout of low or normal glucose conditions for 3 h bouts for a total of 3 days, in accordance with standard RLG protocol. On Day 4, cells were exposed to 0.5 mmol/l glucose ± R481 for 1 h in standard Seahorse XF DMEM media. Glucose utilisation ($\Delta ECAR_{MAX}$) was measured following acute glucose injection.

6.2.8.1 Intermittent R481 treatment increased α-cell glucose utilisation after acute low glucose exposure.

Cells exposed to 3 prior bouts of R481 had enhanced basal ECAR (in glucose-free conditions) compared to vehicle; a not statistically significant trend similarly shown after four bouts of R481 incubations (mpH/min/µg) (0; 1.130 ± 0.1039, 1; 0.8408 ± 0.0936, *0 vs 1, P = 0.1202,* 3; 1.537 ± 0.08682, *0 vs 3, P = 0.0111,* 4; 1.156 ± 0.06656, *1 vs 4; P = 0.0692*) (Figure 6.25A). Increased basal OCR measurements were similarly seen after 4 R481 bouts compared to 1 (pmol/min/µg) (0; 23.13 ± 1.240, 1; 15.01 ± 0.8548, *0 vs 1, P < 0.0001,* 3; 27.03 ± 0.8987, *0 vs 3, P = 0.040,* 4; 20.64 ± 0.9596, *1 vs 4, P = 0.0014, 3 vs 4, P = 0.0002*) (Figure 6.25B). After 0.5 mmol/l glucose injection, four bouts of R481 enhanced $\Delta ECAR_{MAX}$ compared to one bout of R481 treatment (mpH/min/µg) (0; 0.4601 ± 0.07029, 1; 0.6425 ± 0.08750, 3; 0.5745 ± 0.05908, 4; 1.169 ± 0.08207, *1 vs 4, P = 0.0004, 3 vs 4, P = 0.0001*) (Figure 6.25Ci-ii). Four bouts of R481 treatment similarly increased 11.7 mmol/l glucose-stimulated $\Delta ECAR_{MAX}$ (mpH/min/µg) (0; 1.033 ± 0.1181, 1; 2.377 ± 0.3528, *0 vs 3, P = 0.0013,* 3; 1.558 ± 0.07692, 4; 3.479 ± 0.2291, *1 vs 4, P = 0.008, 3 vs 4, P < 0.0001*) (Figure 6.25Di-ii).

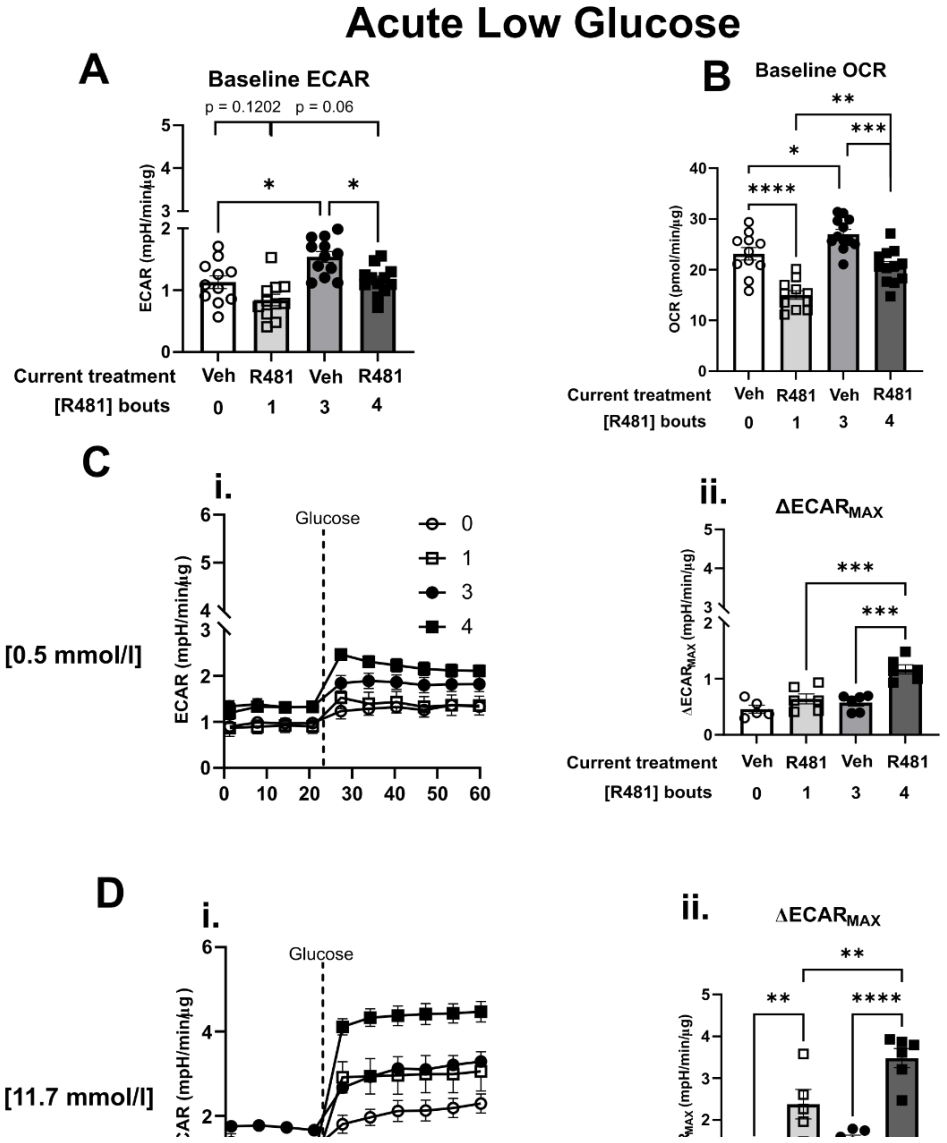

Figure 6.25: Repeated R481 treatment increased α-cell glucose utilisation, compared to acute R481 treatment, after acute low glucose.

αTC1.9 cells were exposed to 2 h total of serum free, 5.5 mmol/l glucose and 3h ± R481 (50 nmol/l) for three days. On Day 4, cells were incubated with 0.5 mmol/l glucose ± R481 in standard Seahorse XF DMEM medium for 1 h and replaced with media ± R481 in no glucose. **A.** Baseline ECAR and **B.** OCR (n = 11 -12) was calculated from average measurements prior to glucose injection at ~ 20 min. Glucose utilisation, calculated from representative ECAR traces (**C - D i**.), ($\Delta ECAR_{MAX}$) from maximum ECAR reading post-glucose injection subtracted from average baseline readings prior to injection (**C - D ii**.) (all One-Way ANOVA with Tukey's multiple comparison test, *P<0.05, **P<0.01, ***P<0.001, ****P<0.0001, n = 5 – 6, one plate)

6.2.8.2 Intermittent R481 treatment reduced glucose utilisation and oxidative respiration in RLG-exposed α-cells.

RLG-incubated α-cells, which were exposed to four bouts of recurrent R481 treatment had diminished ECAR compared to one and three bouts of R481 treatment (mpH/min/µg) (0; 1.854 ± 0.08410, 1; 1.340 ± 0.06133, *0 vs 1, P = 0.0021,* 3; 1.654 ± 0.1527, 4; 0.9714 ± 0.1007, *1 vs 4, P = 0.0458, 3 vs 4, P = 0.0002*) (Figure 6.26A). Similarly, four bouts of R481 treatment reduced basal OCR in comparison to one and three bouts of R481 treatment; with a significant reduction in basal OCR observed in recovered cells exposed to three prior bouts of R481 compared to control (pmol/min/µg) (0; 31.76 ± 1.180*,* 1; 20.79 ± 0.8053, *0 vs 1, P < 0.0001,* 3; 24.86 ± 1.084, 4; 15.41 ± 1.174, *1 vs 4, P = 0.0043, 3 vs 4, P < 0.0001*) (Figure 6.26B). After 0.5 mmol/l glucose acute injection, cells exposed to four bouts of R481 treatment had attenuated $\Delta ECAR_{MAX}$ compared to one acute R481 bout, and R481-stimulated $\Delta ECAR_{MAX}$ was not present (mpH/min/µg) (0; 0.6844 ± 0.07692, 1; 1.148 ± 0.06606, 3; 0.5654 ± 0.1047, 4; 0.5732 ± 0.06045) (Figure 6.26Ci-ii). Similarly, four recurrent R481 bouts attenuated 11.7 mmol/l glucose-stimulated $\Delta ECAR_{MAX}$ compared to one acute R481 bout, however, still retained R481-stimulated high glucose utilisation (mpH/min/µg) (0; 1.522 ± 0.08934, 1; 3.407 ± 0.1614, *0 vs 1, P < 0.0001,* 3; 1.109 ± 0.1298, 4; 1.939 ± 0.2797, *1 vs 4, P < 0.0001, 3 vs 4, P = 0.0207*) (Figure 6.26Di-ii).

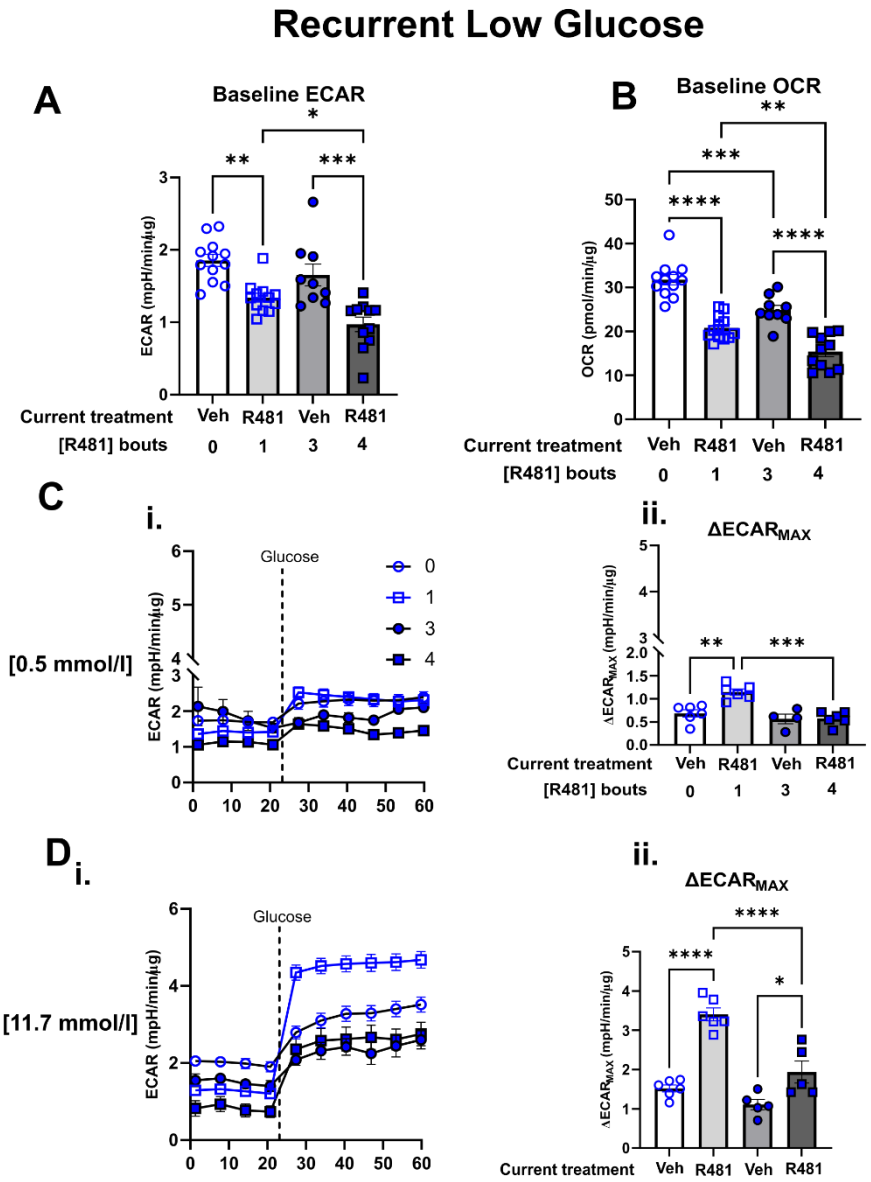

Figure 6.26 Intermittent R481 bouts attenuated glucose utilisation compared to acute R481 treatment in recurrent low glucose (RLG)-treated α-cells.

αTC1.9 cells were exposed to 2 h total of serum free, 5.5 mmol/l glucose and 3 h ± R481 (50 nmol/l) and 0.5 mmol/l glucose for three days. On Day 4, cells were incubated with 0.5 mmol/l glucose ± R481 in standard Seahorse XF medium for 1 h. **A.** Baseline ECAR and **B.** OCR (n = 10 - 12, One-Way ANOVA with Tukey's multiple comparison test) was calculated from average measurements prior to glucose injection at ~20 min. Glucose utilisation, calculated from representative ECAR traces (**C – D i.**) ($\Delta ECAR_{MAX}$) derived from maximum ECAR reading post-glucose injection (**C - D ii.** One-Way ANOVA with Tukey's multiple comparison test) subtracted from average baseline readings prior to injection (*P<0.05, **P<0.01, ***P<0.001, ****P<0.0001, n = 4 – 6, one plate)

6.3 Discussion

Within 5 years of diagnosis, nearly all individuals with T1DM have an inadequate glucagon counterregulatory response to hypoglycaemia (McCrimmon, 2008, 2022). This can partially be explained by the dysregulated central and autonomic control of α-cell glucagon secretion (Fan *et al.*, 2009). In addition, the glucagon response to hypoglycaemia is retained following autonomic blockade (in both dogs and humans), indicating peripheral-localised defects in counterregulatory signalling (Palmer *et al.*, 1976; Hilsted *et al.*, 1991; Gupta *et al.*, 1997). From an intra-islet perspective, tolbutamide-induced hypoglycaemia in islets diminished the glucagon counterregulatory response regardless of an intact autonomic response (Banarer, McGregor and Cryer, 2002). Furthermore, the inhibition of somatostatin (SST) receptor restored hypoglycaemia-induced plasma glucagon in both recurrent hypoglycaemia-treated and diabetic rats (Strowski *et al.*, 2000; Banarer, McGregor and Cryer, 2002; Yue *et al.*, 2012; Karimian *et al.*, 2013; Hoffman *et al.*, 2021). These published findings indicate both intra-islet and intrinsic α-cell dysfunction could contribute to the defective glucagon counter-regulation observed in T1DM (Gerich *et al.*, 1973). Therefore, subsequent studies investigated for the first time whether recurrent hypoglycaemic-like episodes could induce intrinsic metabolic adaptations which may contribute to dysregulated α-cell function.

Interestingly, α-cells exposed to RLG exhibited increased glycolytic rate and compensatory glycolysis at low glucose compared to the acute low glucose control; suggesting RLG increased α-cell glycolytic capacity in glucose-deprived conditions. This elevation in capacity, in which at low glucose there will be minimal glycolysis, could be as a result of either increased activity, or expression of key glycolytic enzymes. Other glucose-sensing cells, such as human primary astrocytes (HPA), have a similarly enhanced ECAR, an indicator of glycolysis, at euglycaemic-like glucose levels following RLG (Weightman Potter *et al.*, 2019). Unlike glial and neuronal cells, there is limited published evidence on whether α-cells contain alternative substrate “stores” to sustain glucagon secretion at low glucose, identifying an important research question

for further work (Briant *et al.*, 2018a). α-cells and islets both express hexokinase-1 (HK-1), a rate-limiting enzyme of glycolysis, which has a high glucose affinity and low V_{MAX} glucose saturation, meaning HK-1 has a low capacity for glucose phosphorylation (Heimberg *et al.*, 1996; Beall *et al.*, 2012). HK-1 is regulated by allosteric inhibition through its product (glucose-6-phosphate), providing the possibility of HK-1 regulating glycolysis especially in fasted conditions (Aleshin *et al.*, 1998). Although current work did not investigate α-cell HK-1 expression, it would be interesting in the future to explore whether increased HK-1 expression previously observed in T1DM human islets contribute to enhanced α-cell glycolytic capacity at low glucose following prior bouts of RLG (Nomoto *et al.*, 2020).

In addition, α-cells appear to have increased basal OCR at low glucose, following prior bouts of RLG. Such increased glycolytic capacity may also contribute towards the raised oxidative respiration at low glucose. Other studies showed pyruvate supplementation, in recurrent hypoglycaemic (RH) diabetic and acute hypoglycaemic rats, attenuated hypoglycaemia-associated neuronal degeneration and death (Suh *et al.*, 2005; Choi *et al.*, 2013). In addition, brain cortical mitochondria derived from recurrent insulin-induced hypoglycaemic rats (RIIH) had enhanced PDH and other associated Krebs cycle enzyme activity (Cardoso and Moreira, 2021). These findings could pose the question if increased pyruvate shuttling, by the PDH complex, into the Krebs cycle could sustain α-cell oxidative respiration as an adaptation to compensate for enhanced basal glycolysis and protect from cell death.

Pyruvate dehydrogenase kinase-4 (PDK4) phosphorylates and inhibits activation of the PDH complex to reduce pyruvate oxidation to acetyl Co-A (Attia *et al.*, 2010). PDK4 is a defined α-cell “marker”, with expression restricted to α-cells rather than β-cells (Akhmedov *et al.*, 2012). *PDK4* overexpression is linked to enhanced hepatic fatty acid oxidation (FAO) and cAMP accumulation, potentiating downstream gluconeogenesis (Park *et al.*, 2018). Pharmacological attenuation of PDK4 activity is therefore a key metabolic target in alleviating hyperglycaemia in DM. Interestingly, deficient *PDK4* expression reduced fasting

glycaemia in mice, by limiting gluconeogenic precursors and driving ketone body generation (Jeoung *et al.*, 2006; Jeoung and Harris, 2008; Zhao *et al.*, 2020). Therefore, is PDK4 activity diminished over time in α-cells exposed to RH? Furthermore, is impaired PDK4 activity possibly potentiating the increase in oxidative respiration observed in α-cells exposed to RLG? Relatively little is known about PDK4 involvement in α-cell function, and therefore poses an interesting question for further research into α-cell bioenergetics. In addition, no change in α-cell total ATP (tATP) was observed after prior bouts of RLG at low glucose, but this evidence cannot exclude the possibility that altered enzymatic activity in the ATP-creatine phosphate pathway could be sustaining α-cell ATP levels.

Although enhanced glycolysis at low glucose was observed in α-cells exposed to RLG, no changes in lactate secretion were observed either during or following glucose recovery; a not statistically significant trend similarly noted in RLG-exposed HPA studies (Weightman Potter *et al.*, 2019). Additional experiments, using several intermediate time points (up to 60 min), would be important in required to confirm these findings, to ensure any effects have not been missed. However, it is important to mention lactate can be bidirectionally metabolised back to pyruvate, which is preferentially mediated by the β-subunit of LDH, encoded by the *LDHB* gene (Nam, Sunhwa and Shin, 2016; Forkasiewicz *et al.*, 2020). Pancreatic α-cells express *LDHB*, albeit at a far lower expression level than *LDHA*, and in other cell types, the *LDHA*:*LDHB* isoenzyme ratio can be altered to facilitate a metabolic shift for energy demand (Nam, Sunhwa and Shin, 2016; Cuozzo *et al.*, 2022). Therefore, it would be interesting to investigate if there are any transcriptional alterations in *LDH* expression following RLG which could contribute towards to the increased oxidative metabolism observed.

After three prior bouts of low glucose and recovery at euglycaemic-like conditions (5.5 mmol/l glucose, “antecedent” low glucose), α-cells displayed a reduced basal glycolytic rate, alongside no changes in compensatory glycolysis but similarly elevated basal OCR. Likewise, findings from Weightman-Potter *et*

al. 2018 showed increased basal oxidative respiration in human astrocytes, at least partially contributed by the observed enhanced proton leak following RLG (Weightman Potter *et al.*, 2019). This cannot exclude the possibility that partial mitochondrial uncoupling, and hence proton leak, could be contributing towards the increased OCR/ECAR observed following RLG. Here, at least following antecedent low glucose episodes, α-cells displayed increased tATP levels and therefore could suggest sustained coupled oxidative respiration. In addition, pancreatic α-cells preferentially use oxidative respiration at low glucose, and glycolysis at high glucose to sustain the energy-demanding process of glucagon secretion (Grubelnik *et al.*, 2020b). As such, α-cells have the capability to metabolically "switch", likewise to astrocytes, facilitating a degree of flexibility in ATP generation (Grubelnik *et al.*, 2020b). It could therefore be hypothesised that RLG-exposed α-cells in euglycaemic-like conditions have a metabolic shift towards oxidative respiration, possibly to compensate for impaired ATP generation.

Chapter 3 previously showed αTC1.9 cells express glucose transporter, GLUT-4 protein. In these experimental studies, no differences were observed in α-cell GLUT-4 transporter expression following prior bouts of low glucose. The expression of other GLUT transporters (including GLUT-1 or 3) were not measured in these studies, and as such, cannot fully discount the hypothesis of enhanced GLUT-mediated glucose entry. No change in glycolytic enzymatic protein expression was similarly observed in human astrocytes following RLG (Weightman Potter *et al.*, 2019). However, protein expression changes cannot discount the hypothesis that there are either post-translational modifications or alteration to glycolytic enzyme subcellular localisation. De Jesus *et al.* 2022 identified in a mitochondrial-associated *HK-1* knockdown mouse model, that subcellular localisation of HK-1 can determine substrate fate in immune cell glycolysis and inflammatory markers, in which markers are similarly elevated in a diabetic immune cell model [(De Jesus *et al.*, 2022). The subcellular localisation of α-cell metabolic processes similarly appeared to be dysregulated in human islet amyloid polypeptide (hiAPP) diabetic mice (Wang *et al.*, 2021). These findings suggested a diminished glucose-dependent switch from

oxidative respiration to glycolysis, with fluorescence-lifetime image microscopy (FLIM) images suggesting oxidative phosphorylation (OXPHOS) signals, derived from NAD(P)H signals, were distributed throughout the cytoplasm rather than physiological localisation near the cell membrane (Wang *et al.*, 2021). Therefore, further studies could examine the localisation of glycolytic end-products and key glucose-sensing enzymes (for instance, AMPK) rather than endogenous protein expression, to measure any adaptations to metabolic fate following RLG.

Endogenous AMPK activation is stimulated by intracellular glucose deprivation and thereby serves as a sensor of glucose availability. These studies revealed no difference in α-cell AMPK activation between either antecedent or RLG-treated groups, similar to work from Weightman *et al.* 2019. The findings from Chapter 3 and 4 suggested pharmacological AMPK activation could augment α-cell glycolytic rate in an SBI-sensitive manner. To examine whether pharmacological activation of AMPK, using R481, could restore basal glycolysis following RLG, α-cells were acutely treated ± R481 during the final glucose bout. R481 treatment additively increased RLG-stimulated glycolysis and reliance at low glucose, indicating acute R481 treatment could potentiate α-cell glycolytic rate at low glucose. However, no additive changes were observed following antecedent low glucose and R481, perhaps highlighting R481 can only additively increase RLG-exposed α-cell glycolysis at low glucose, where endogenous AMPK activity would be greatest (at least in control). Further mechanistic detail is required on how R481 treatment induces these effects. Evidence indicated here showed acute R481 exposure did not enhance glucose transporter (GLUT-4) protein expression, which is expected due to short treatment time. Therefore, measuring glucose uptake is important to examine if the upregulated glycolysis observed in RLG with/without R481 is mediated by increased glucose import and intracellular glucose availability/utilisation. Preliminary findings, although not significant, suggested a trend in continued increases in AMPK activation following R481 treatment in all conditions (due to low statistical power). Defective central AMPK activity is thought to contribute towards recurrent hypoglycaemia. Studies using repetitive 2-DG/insulin

injections to mimic recurrent bouts of hypoglycaemia, increased arcuate nucleus and hypothalamic AMPKα1/2 activity (McCrimmon *et al.*, 2006; Alquier *et al.*, 2007). The reduction in central glucose-sensing activity is most likely contributed by glycogen supercompensation (Alquier *et al.*, 2007). As detailed before in Chapter 3, increased glycogen stores in islet cells, in particular β-cells, are associated with intra-islet dysfunction and pathology in T2DM (Brereton *et al.*, 2016). Similarly, pharmacologically activating AMPK using an indirect activator (AICAR) enhanced counterregulation in T1DM rodents(Fan *et al.*, 2009). Further work is therefore required to clarify whether pharmacological AMPK activation, by R481, can restore α-cell function following RLG.

Evidence presented here indicated R481 depleted α-cell tATP following acute low glucose exposure. A non-significant effect was similarly observed after RLG but can be considered underpowered, with power analysis calculations estimating an additional n = 5 would be required to test for statistical significance. A reduction in tATP, following R481 exposure, is a consequence of mild complex I inhibition and thereby reducing oxidative respiration; mimicking metformin (Cruz *et al.*, 2021). Other studies showed no change in intracellular ATP at high [R481] in a hypothalamic neuronal cell line, although this may reflect specific cell-specific differences in metabolism (Cruz *et al.*, 2021).

Post-RLG, α-cell glycolytic reactivation was measured following acute reintroduction of glucose (0.5 – 11.7 mmol/l), with RLG increasing both normoglycaemic and hyperglycaemia α-cell glucose utilisation following the final bout of low glucose, which may imply an increased glucose recovery and sustained ATP generation. Weightman-Potter *et al.* 2019 likewise found increased HPA glucose utilisation with no effect on intracellular ATP at only hyperglycaemic and euglycaemic-like conditions following a similar RLG protocol (Weightman Potter *et al.*, 2019). Recently, glucokinase expression and activity has been reported to regulate α-cell electrophysiological status and high glucose-induced suppression glucagon secretion (Basco *et al.*, 2018; Moede *et al.*, 2020; Bahl *et al.*, 2021). α-cell-specific *GCK* knockout mice had reduced α-cell ATP/ADP ratio and failed to suppress glucagon secretion at high glucose

(Basco *et al.*, 2018). Similarly, Moede *et al.* 2020 showed pharmacological activation of glucokinase attenuated glucagon release events in isolated rodent α-cells (Moede *et al.*, 2020). Likewise, genetic α-cell *GCK* activation in mice attenuated insulin-induced plasma glucagon and attenuated high fat diet (HFD)-associated hyperglucagonaemia (Bahl *et al.*, 2021). GK activity, unlike HK, is not inhibited by glucose-6-phosphate and has a lower glucose affinity with a high V_{MAX} (Sener *et al.*, 1985). In high glucose conditions (e.g., the fed-state), glucokinase is a well-characterised glucose sensor and coupling partner for β-cell glucose-stimulated insulin secretion (GSIS) (Matschinsky and Wilson, 2019; Haythorne *et al.*, 2022). It is plausible, therefore, that enhanced glycolytic capacity at high glucose could be mediated by increased glucokinase activity and/or expression in order to retain α-cell glucose sensitivity following RLG. Further studies could examine whether RLG-mediated glycolytic reactivation is maintained following pharmacological glucokinase inhibition (e.g., mannoheptulose).

Preliminary work was conducted to establish if intermittent AMPK inhibition, by applying SBI-0206965 (SBI) prior to each low glucose bout, would abolish the increase in glycolysis and oxidative respiration following RLG. Recurrent bouts of SBI attenuated α-cell glycolysis and oxidative metabolism at acute low glucose but failed to attenuate both parameters in cells exposed to prior bouts of RLG. One could postulate endogenous AMPK activity is diminished over the duration of the RLG protocol, perhaps compromising low glucose-sensitivity. As this was a pilot study, additional data are required to confirm this suggestion.

In addition, subsequent work investigated if intermittent inhibition of AMPK activity would prevent the increased glycolysis observed following O-304 treatment at acute low glucose and RLG. In this instance, acute O-304 injection most likely attenuated α-cell glycolysis in favour of enhancing mitochondrial oxidative respiration, with the increased ECAR post-injection could possibly be due to acidification derived from oxidative metabolism, not glycolysis. As recurrent SBI bouts did not attenuate these effects, one could suggest enhanced α-cell bioenergetics from acute O-304 treatment is AMPK-insensitive.

As demonstrated in chapter 3 and in studies described here, acute R481 incubation increased α-cell glucose utilisation, regardless of prior RLG bouts. To observe whether recurrent AMPK activator treatment could attenuate RLG-enhanced basal glycolysis, α-cells were exposed to intermittent bouts of R481 during each low glucose bout for 4 days. It is important to note that increased α-cell death was observed (not shown) following recurrent R481 treatment over the three days, especially in RLG + R481 groups. The increased cell death is most likely due mitochondrial accumulation and thereby sustained mitochondrial inhibition. Metformin, similarly to R481, mildly inhibits mitochondrial respiration and has been hypothesised (although debated) to accumulate in the mitochondrial matrix dependent on high mitochondrial membrane potential (Panfoli *et al.*, 2021; Feng *et al.*, 2022). Additional studies will therefore use lower [R481] in each bout to mitigate α-cell death.

In addition, this pilot study indicated four recurrent bouts of R481 additively enhanced glucose utilisation at low and high glucose at acute low glucose. In contrast, RLG and four intermittent bouts of R481 diminished α-cell glucose utilisation following glucose re-introduction. These data may infer multiple bouts of R481 treatment, could in fact further impair, rather than restore, α-cell glucose sensitivity following RLG. Multiple bouts of mitochondrial complex I inhibition, and possible drug accumulation, could most likely reduce α-cell redox state by increasing ROS production, impairing α-cell viability as seen in individuals with complex I deficiency (Pitkänen and Robinson, 1996; Sharma and Alonso, 2014). Furthermore, additional studies need to examine if intermittent α-cell AMPK activation, by small molecule direct activators (rather than mild complex I inhibitors), could restore α-cell glucose-sensitive glucagon secretion in RH. In a clinical setting, and if successful, recurrent AMPK activator exposure could increase glucagon response during a hypoglycaemia and prevent impaired counterregulatory responses to subsequent hypoglycaemic episodes observed in DM.

Glucagon secretion and content were measured to ascertain if RLG directly dysregulates α-cell glucagon secretion and/or content as a consequence of

observed metabolic changes. Here, both glucagon secretion and content, were unaffected by RLG or following glucose recovery. The disparity between depolarisation and glucose threshold for low glucose-stimulated glucagon secretion is mainly attributed to experimental model used. For instance, human α-cell sorted aggregates displayed a lack of suppression of glucagon secretion at high glucose, compared to islets and unsorted cells (Reissaus and Piston, 2017). In the same study, isolated α-cells failed to inhibit glucagon secretion in response to glibenclamide treatment; unlike islets and a mixed islet cell population (Reissaus and Piston, 2017).These findings are comparable to work using isolated mouse and human α-cells, which demonstrated impaired glucose-suppression of glucagon secretion, implying isolated α-cells could have impaired glucose-insensitive glucagon secretion (Reissaus and Piston, 2017). Furthermore, such studies have suggested that islet gap junction connectivity and paracrine regulation accounts for up to 23 % of high glucose-mediated suppression of glucagon secretion (Briant *et al.*, 2018b). As T1DM is associated with the impaired paracrine control of glucagon secretion, pharmacological inhibition of SSTR2a receptors on the α-cell is a potential therapeutic target for boosting glucagon secretion and thereby preventing subsequent hypoglycaemic episodes, from evidence previously described (Hoffman *et al.*, 2021; Farhat *et al.*, 2022). It is important to note the studies previously described here have used a mouse α-cell line in the absence of paracrine factors. In addition, published evidence suggested both PDK inhibition and catalytic pyruvate dehydrogenase phosphatase (PDP) viral overexpression in a mouse β-cell line enhanced PDH activity, in a glucose-dependent manner, but did not alter glucose-stimulated insulin secretion (Nicholls, Ainscow and Rutter, 2002). Here, as the author did not observe any changes to downstream glucagon secretion, albeit alongside clear α-cell bioenergetic adaptations, this poses the question if PDH activity is coupled to the islet secretory response? Drawing from published studies, α-cell dysfunction following RLG could be, at least partially, mediated by defective intra-islet signalling. Therefore, additional work should be performed in a more replete model of RH and in isolated islets to examine the external influence on α-cell adaptations in RH.

In summary, evidence provided in this study suggest intrinsic α-cell defects in glycolytic and mitochondrial respiration following recurrent hypoglycaemia-like conditions. One could speculate that these potent bioenergetic adaptations are, in part, contributed by increased pyruvate shuttling into the mitochondria, as well as increased glucose-sensing enzyme activity (Choi *et al.*, 2013). In addition, further work is required to examine if the altered compartmental association of key glucose-sensing, and rate-limiting glycolytic enzymes, including AMPK and HK, could contribute to the metabolic shift observed in RLG-exposed α-cells.

Chapter 7

The role of CFTR in both glucose homeostasis and cystic fibrosis-related diabetes (CFRD) pathogenesis

7 The role of CFTR in both glucose homeostasis and cystic fibrosis-related diabetes (CFRD) pathogenesis.

AMPK colocalises with the key ion channel, cystic fibrosis transmembrane receptor (CFTR), whereby AMPK acts as an inhibitor of CFTR function and hence limiting cAMP-dependent chloride (Cl^-) secretion (Walker *et al.*, 2003). Therefore, a literature review was conducted to assess the importance of CFTR in glucose homeostasis, the role of CFTR in pathophysiology, and potential glycaemic benefits for direct AMPK activation in cystic fibrosis (CF) and cystic fibrosis-related diabetes (CFRD).

7.1 CFTR structure and regulation

CFTR is an ATP-gated anion channel responsible for mediating Cl^- and bicarbonate diffusion across apical epithelial membranes (Moran, 2010). CFTR channels display a conserved ABC channel architecture, consisting of two transmembrane domains (TMD1 and TMD2), comprising of six transmembrane helices and two nucleotide binding domains (NBD1 and NBD2) (Csanády, Vergani and Gadsby, 2019).

CFTR channel uniquely links TMD1-NBD1 and TMD2-NBD2 through a regulatory (R) domain (Cheng *et al.*, 1991; Farinha *et al.*, 2016). CFTR channel activity relies on post-translational NBD1/2 ATP hydrolysis and protein kinase regulation to shift CFTR open-closed state (Anderson *et al.*, 1991; Farinha *et al.*, 2016). cAMP-dependent protein kinase A (PKA) activation predominantly controls CFTR channel gating by phosphorylating multiple R-domain sites, which is possibly enhanced by protein kinase C (PKC) (Chappe *et al.*, 2003; Farkas *et al.*, 2020). Importantly, AMPK phosphorylates the serine inhibitory sites (Ser-737 and Ser-768) in the R domain to reduce CFTR-mediated Cl^- channel efflux (Hallows *et al.*, 2000; Kongsuphol *et al.*, 2009a) (summarised in Figure 7.1, adapted from Farinha and Canato, 2016).

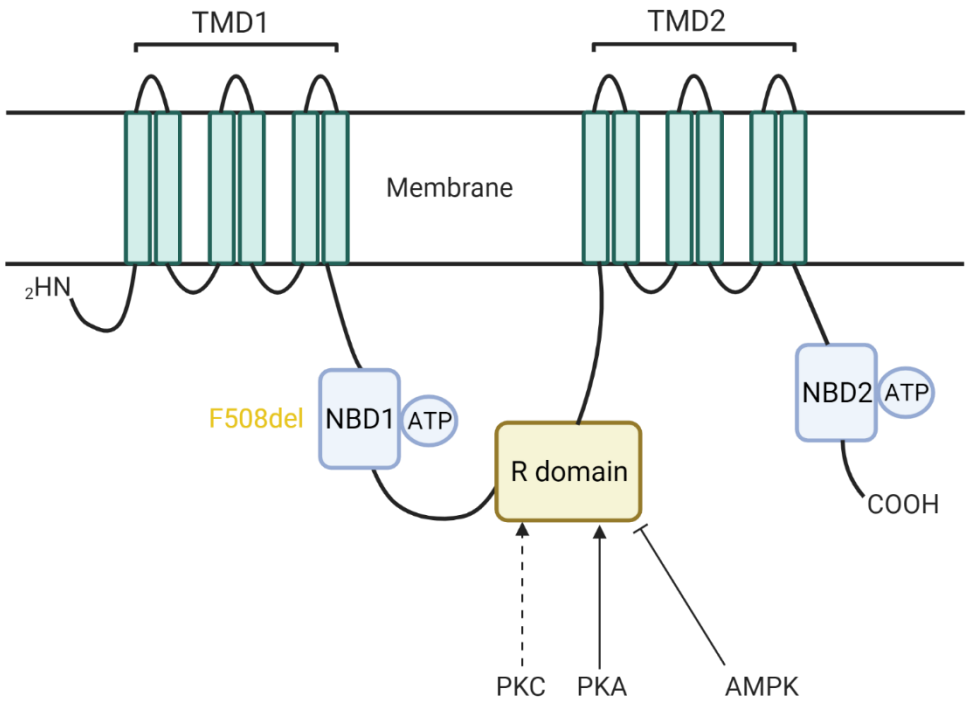

Figure 7.1: CFTR structure and kinase regulation.

CFTR channel comprises of two transmembrane spanning domains (TSD1/TSD2) and two nucleotide binding domains (NBD1/2). Linking NBD1 and NBD2 is the unique regulatory (R) domain, which influences NBD1/2 ATP hydrolysis and CFTR channel opening probability. CFTR channel activity depends largely on R-domain phosphorylation at multiple amino acid residues by PKA and possibly PKC activation. Similarly, AMPK promotes the CFTR closed state and hence reduces CFTR-mediated chloride ion secretion. The dashed line indicates a hypothesised action. Created using Biorender.com.

7.2 *CFTR* mutations

As of 2022, over 400 CF-causing *CFTR* variants have been identified to be pathogenic, according to the Clinical and Functional Translation of CFTR (CFTR2) database (*CFTR2 Variant List History*, no date). Such *CFTR* variants have been "traditionally" classified into six classes, as shown in Figure 7.2, to develop personalised medicine for specific cystic fibrosis (CF) genotypes (Zielenski and Tsui, 1995; Veit *et al.*, 2016). It is important to note that traditional *CFTR* variant categorisation excludes *CFTR* mutations that could exert combinatory effects within the cell (e.g., DF508) (Du, Sharma and Lukacs, 2005). In Caucasian populations, > 80% CF chromosomes contain a deletion of phenylalanine at residue 508 (DF508) (Cheng *et al.*, 1990; Lucotte, Hazout and De Braekeleer, 1995; Riordan, 2008; Lukacs and Verkman, 2012). DF508 CFTR mutations are associated with a high diabetes incidence and pancreatic insufficiency within CF individuals (Ahmed *et al.*, 2003; Adler *et al.*, 2008; Norris *et al.*, 2019) (Figure 7.2). To further understand these mechanisms, this literature review will evaluate the importance of CFTR activity in intrinsic cellular physiology and how CFTR activity can contribute to whole-body glucose homeostasis. Furthermore, this review will assess current research discussing how defective CFTR activity (focusing primarily on DF508 CFTR mutation) can influence the impaired glucose tolerance (IGT) observed in CF individuals and cystic fibrosis-related diabetes (CFRD) pathogenesis.

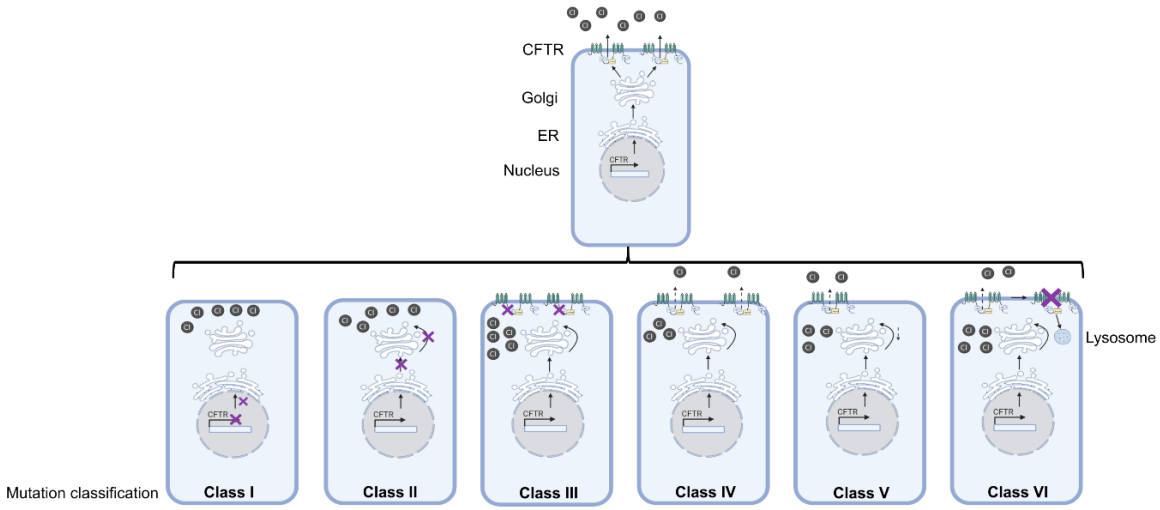

CFTR defect	Protein synthesis	Protein trafficking	Limited CFTR gating	Reduced CFTR conductance	Reduced protein synthesis and/or trafficking	Plasma membrane CFTR instability
CFTR channel function	Minimal			Residual		
Clinical phenotype	Severe			Less-severe		
Mutation prevalence in European individuals with CF (%)	~ 16.4 %	> 80 %	3.9 %	3.3 %	3.0 %	?
Risk of pancreatic insufficiency	High	High	High	Low	Low	High
Diabetes risk	High	High	Moderate	Moderate	Low	-
Example genotypes	G542X W1282X	DF508	G551D	R117H	A455E	4326delTC

Figure 7.2: Traditional classification of CFTR mutations.

Typically, class I CFTR mutations display a more severe clinical phenotype than class IV. Genotype classification is based around CFTR trafficking, maturation and functionality as shown. DF508 is in red as it is the mutant primarily discussed in the following literature review. Adapted from Ahmed et al., 2003; Adler et al., 2008; Norris et al., 2019. Created using Biorender.com.

7.3 CFTR, CFRD and the pancreatic α-cell

Current literature discussing CFTR expression in pancreatic α-cells is controversial. Recent studies have shown *CFTR* mRNA and protein expression within rodent α-cells; with clear glucagon and CFTR co-localisation on the islet periphery (Boom *et al.*, 2007; Edlund *et al.*, 2017; W.Q. Huang *et al.*, 2017). Furthermore, CFTR and glucagon immunoreactivity can co-localise on the plasma membrane on isolated human α-cells (Boom *et al.*, 2007; Edlund *et al.*, 2017). Also, following data reanalysis from findings from Segerstolpe *et al.*, 2016 , one single-cell RNA sequencing (scRNA-seq) study suggested human α-cells have the third greatest *CFTR* RNA expression within the pancreas (Lam *et al.*, 2020). In contrast, no colocalisation of *CFTR* RNA was observed within glucagon-positive α-cells in isolated ferret islets or isolated human α-cells (Sun *et al.*, 2017; Hart *et al.*, 2018).

In the last decade, however, there has been substantial interest in whether CFTR can intrinsically modulate α-cell glucagon secretion. *Ex vivo* and *in vivo* DF508 *CFTR* mouse models show up to 3.0-fold greater glucagon secretion and fasted plasma glucagon respectively (W.Q. Huang *et al.*, 2017; Wen Qing Huang *et al.*, 2017; Edlund *et al.*, 2019). Isolated human islets treated with a CFTR inhibitor similarly secreted excessive glucagon secretion under low glucose (Edlund *et al.*, 2017). Furthermore, overexpressing CFTR in an α-cell line reduced low glucose-dependent glucagon secretion (W.Q. Huang *et al.*, 2017). Therefore, one would expect defective *CFTR* to increase the likelihood of hyperglucagonaemia in CF individuals. One study supported this, for instance individuals with CF and IGT had diminished suppression of glucagon secretion after oral glucose tolerance test (OGTT) (Lanng *et al.*, 1993; Armaghanian *et al.*, 2020). Such findings pose the question; can changes in CFTR channel activity, seen in CF, modulate α-cell glucagon secretion?

Recent evidence suggests CFTR channel activity could enhance low glucose-dependent α-cell depolarisation and consequently glucagon secretion. CFTR inhibitor exposure abolished cAMP-dependent Cl^- efflux, suggesting the

presence of CFTR-mediated Cl^- currents within human and mouse α-cells (Edlund *et al.*, 2017; W.Q. Huang *et al.*, 2017). In human islets, application of putative CFTR blockers appeared not to alter CFTR single-channel current, open probability or affect depolarisation-induced glucagon secretion. Discrepancies in data may possibly be attributed to the small study sample number (Edlund *et al.*, 2017). Furthermore, over-expressing CFTR promoted a hyperpolarised α-cell resting membrane potential *in vitro*, especially following high glucose exposure. Also, DF508 mutant mouse islets exhibited greater changes in membrane potential at low glucose (W.Q. Huang *et al.*, 2017). Previous studies have shown intracellular calcium $[Ca^{2+}]_i$ changes can regulate CFTR channel activity by both PKC-dependent and independent changes, alongside cAMP-dependent PKA activation (Billet and Hanrahan, 2013; Billet *et al.*, 2013). In DF508 mouse islets, low glucose-stimulated increases in $[Ca^{2+}]_i$ appeared to be further enhanced (W.Q. Huang *et al.*, 2017). Similarly, CFTR inhibitor application potentiated $[Ca^{2+}]_i$ in an *CFTR*-overexpressing α-cell line (Wen Qing Huang *et al.*, 2017). These data imply α-cell CFTR activity suppresses the low glucose-dependent increase in $[Ca^{2+}]_i$ required for depolarisation-regulated glucagon secretion by hyperpolarising the α-cell membrane.

Furthermore, if CFTR activity could modulate α-cell depolarisation-induced glucagon secretion, could CFTR activity directly modulate glucagon granule exocytosis? Whether CFTR-mediated suppression of calcium influx is a direct mechanism through voltage-gated Ca^{2+} channel opening, or by downstream cAMP-dependent exocytosis is unclear. Application of putative CFTR inhibitor ,CFTRinh172, attenuated both cAMP-enhanced glucagon secretion and α-cell membrane capacitance in mouse islets, but not the former in human islets (Edlund *et al.*, 2017). This finding suggests CFTR activity propagates cAMP-induced granule exocytosis in a species-dependent manner, possibly due to the differences in α-cell proportion in the islet. Regardless, additional clarification is required to determine whether this effect is glucose-dependent, as initial experiments were completed at euglycaemic levels of glucose.

Findings in an α-cell line imply CFTR could regulate glucagon secretion at the transcriptional level (Edlund *et al.*, 2017; Wen Qing Huang *et al.*, 2017). Prohormone convertase-2 (PC-2) transcription and glucagon-encoding gene expression depend on CREB, Pax6 transcriptional factors and phospho-CREB/CRE binding (Knepel, Chafitz and Habener, 1990; Steiner, 1998; Katz *et al.*, 2009). In α-cells, CFTR over-expression both reduced CREB phosphorylation and pro-glucagon protein expression (Wen Qing Huang *et al.*, 2017). Furthermore, PC2 expression was increased in both DF508 mouse mutant and CFTRinh172-treated mouse islets, which could suggest CFTR activity influences glucagon post-translational processing most likely mediated by $[cAMP]_i$ (Wen Qing Huang *et al.*, 2017). However, CF neonatal ferret islets had attenuated *GCG* mRNA expression compared to non-CF controls, this perhaps highlights age discrepancies between experimental models (Sun *et al.*, 2017). In addition, pro-glucagon cleavage can be indirectly affected by CFTR-mediated changes in Ca^{2+} flux, but this requires study in greater detail in a human model (Wen Qing Huang *et al.*, 2017).

But does glucose directly regulate CFTR activity within the α-cell? CFTR is activated upon glucose stimulation and increases in intracellular nucleotides (ATP/cAMP) (Cliff, Schoumacher and Frizzell, 1992; Berger, Ikuma and Welsh, 2005; Edlund *et al.*, 2014; Guo *et al.*, 2014). Application of the CFTR inhibitor, GlyH, attenuated high glucose-induced mouse whole α-cell currents (W.Q. Huang *et al.*, 2017). Similarly, subsequently exposing from high to low glucose-containing medium increased intracellular concentration of Cl^- in CFTR-overexpressing mouse α-cells (W.Q. Huang *et al.*, 2017). These data could suggest α-cell CFTR open probability is regulated in a glucose-sensitive manner to negatively inhibit glucagon secretion. CFTR channel activity can also control downstream cAMP-induced glucagon secretion but also is directly regulated by intracellular cAMP levels. Forskolin, a cAMP-increasing agent, enhanced glucagon secretion but putative CFTR inhibitor application propagated further cAMP-induced glucagon secretion at low and high glucose in human islets (Edlund *et al.*, 2017). However, in mouse islets, CFTR inhibition affected cAMP-induced glucagon secretion and whole-cell currents at low glucose or glucose

absence respectively, which possibly reflects species-specific differences (Edlund *et al.*, 2017; W.Q. Huang *et al.*, 2017).

Recent findings from *in vitro/ex vivo* studies suggest CFTR activity could negatively regulate glucagon secretion by inhibiting K_{ATP} channel opening (W.Q. Huang *et al.*, 2017). Although the importance is still debated, low glucose mildly increases K_{ATP} channel opening enough to permit voltage-gated Na^+ and Ca^{2+} channel activity, thereby facilitating calcium-dependent glucagon secretion (Quan Zhang *et al.*, 2013). How α-cell K_{ATP} channel activity regulates glucagon secretion is covered in greater depth in a recent review from Zhang *et al.*, 2020. More recently, studies have postulated that CFTR may enhance K_{ATP} channel opening within the α-cell. Overexpressing CFTR and glibenclamide-mediated inhibition of K_{ATP} channel activity in an α-cell line further increased depolarisation and α-cell current following low glucose (W.Q. Huang *et al.*, 2017). Additionally, downregulating K_{ATP} channel activity (by SUR1) recovered CFTR-mediated inhibition of glucagon secretion, with only modest glucose-sensitive changes in both an α-cell line and DF508 rodent models (W.Q. Huang *et al.*, 2017). Altogether, this study could indicate glucose-stimulated CFTR channel activity further potentiates K_{ATP} channel conductance and opening to suppress glucagon secretion greater than glucose-dependent closure of K_{ATP} channels.

K_{ATP} channel-dependent depolarisation can regulate CFTR channel activity in α-cells. Depolarisation-induced glucagon secretion requires low K_{ATP} channel conductance (~ 70 pS) and only a small change (~ 10mV) change in α-cell membrane potential (Zhang, Dou and Rorsman, 2020). By adapting Watts and Sherman mathematical α-cell model, CFTR current relies on glucose-regulated K_{ATP} channel conductance to modulate mouse α-cell membrane potential for glucagon secretion (Watts and Sherman, 2014; Edlund *et al.*, 2017). In reducing K_{ATP} conductance and therefore reducing open K_{ATP} channels (recapitulating high glucose), inhibiting CFTR currents reduces action potential height and increases firing frequency (Watts and Sherman, 2014; Edlund *et al.*, 2017). With a further increase in K_{ATP} channel opening (similar to 1.0 mmol/l glucose), the

firing frequency is increased with CFTR inhibition (Edlund *et al.*, 2017). But CFTR current appears to completely silence α-cell electrical activity with an additional small increase in K_{ATP} conductance, with this effect abolished following application of a putative CFTR inhibitor (Edlund *et al.*, 2017). How CFTR does this is still unclear in α-cell physiology. In other cell types, CFTR-regulated ATP-sensitive K^+ channel opening may be through a PKA-mediated switch (Lu *et al.*, 2006). Both studies, therefore, suggest "adaptive" CFTR opening in either regulating or being regulated by K_{ATP} channel activity to control glucagon secretion (Edlund *et al.*, 2017; W.Q. Huang *et al.*, 2017).

Interestingly, current research suggest α-cells are retained or increased during cystic fibrosis (CF) or cystic fibrosis-related diabetes (CFRD); with up to a 15% increase in glucagon-positive α-cells in islets (Löhr *et al.*, 1989; Uc *et al.*, 2015; Bogdani *et al.*, 2017; Hart *et al.*, 2018). One study found greater glucagon:total pancreatic tissue area staining in both CF and CFRD patients compared to control (Iannucci *et al.*, 1984; Hull *et al.*, 2018). In contrast, another study found no immunochemical difference in total islet staining between control and CF or CFRD human islets (Abdul-Karim *et al.*, 1986). Study differences in quantitative analysis may contribute to these differences (i.e., comparing cell composition changes in relation to islet area or pancreatic area).

How does increased α-cell islet contribution relate to clinical observations seen in CFRD/CF? Fasting plasma glucagon levels range from no change to reduced in individuals with CF (Moran *et al.*, 1991; Sheikh *et al.*, 2017). Additionally, hypoglycaemia has become a more recognised, but still unexplained, symptom in people with CF and often observed hours following oral glucose tolerance testing (OGTT) (Hirsch *et al.*, 2013; Aitken *et al.*, 2020). One study suggested reactive hypoglycaemia does not increase likelihood of CFRD development, but these data included individuals with already diagnosed CFRD (Mannik *et al.*, 2018). CF individuals with no history of CFRD showed unchanged plasma glucagon either with or without hypoglycaemia after 180 min OGTT and mixed-meal tolerance testing (Lanng *et al.*, 1993; Aitken *et al.*, 2020; Kilberg *et al.*, 2020a). Whereas plasma glucose concentrations were significantly reduced

after 135 min OGTT, fasting adrenaline concentrations appear to be 22% higher in CF patients with hypoglycaemia (Aitken *et al.*, 2020). In addition, a recent study by Kilberg *et al.* 2020b included a longer OGTT time period (180 min) to examine both early and late-stage counterregulatory responses to glycaemia in exocrine-insufficient CF and healthy individuals both with or without a reactive hypoglycaemia episode ($Hypo^+$) (Kilberg *et al.*, 2020b). CF $Hypo^+$ glucagon response within 30 min of OGTT was increased, alongside lower insulin, compared to the control $Hypo^+$ group (Kilberg *et al.*, 2020b). However, 120 – 180 min post-stimulus, CF $Hypo^+$ had no delayed increase in glucagon secretory response alongside higher plasma insulin and glucose; indicating an over-suppression of glucagon secretion (Kilberg *et al.*, 2020b). These data, in total, indicate several mechanisms for dysregulated postprandial counterregulation. First, the dysregulated autonomic (i.e., adrenaline) and paracrine (i.e., insulin) feedback may play a part in early and late postprandial glucagon secretion. Second, as plasma insulin at 120 – 180 min OGTT was unchanged between CF $Hypo^+$ vs CF control, this finding suggests intrinsic defects within the α-cell contribute to the diminished glucagon secretion in response to hypoglycaemia. These findings, altogether, could suggest the diminished counter-regulatory α-cell glucagon secretory response to hypoglycaemia in CF patients.

In addition, the authors note that the majority of all CF individuals studied, of whom developed hypoglycaemia, had exocrine insufficiency. This finding, which agrees with several other studies, have suggested CF exocrine insufficiency is associated with reduced glucagon secretion following hypoglycaemia and amino-acid stimulation respectively (Moran *et al.*, 1991; Sheikh *et al.*, 2017; Aitken *et al.*, 2020). Interestingly, preliminary data found 71% of hypoglycaemic CF individuals had a homozygous DF508 mutation compared to 30.8% CF without hypoglycaemia (Battezzati *et al.*, 2007; Armaghanian *et al.*, 2016). These data could imply diminished exocrine sufficiency, alongside lack of CFTR-associated α-cell function, defective glucagon secretion, IGT and islet dysfunction may cumulatively contribute to the development of CFRD.

Altogether, this evidence suggests CFTR negatively regulates cAMP- and glucose-dependent glucagon secretion by tightly controlling α-cell electrical activity to prevent pathological glucagon secretion. However, further work is required to understand these intrinsic mechanisms in greater detail and how they correspond to CFRD clinical phenotypes.

7.4 CFTR, CFRD and the pancreatic β-cell

Since 2007, there has been considerable research interest in whether CFTR may influence intrinsic β-cell function. Isolated rodent β-cells and cell lines all show low *CFTR* mRNA and protein expression in comparison to "non-beta cells" and minimal *CFTR* RNA co-localisation within human islets and ferret pancreata (Boom *et al.*, 2007; Edlund *et al.*, 2014; Ntimbane *et al.*, 2016; Sun *et al.*, 2017; Fulvio *et al.*, 2020; White *et al.*, 2020). In addition, islet single-cell RNA analysis of existing data sets showed *CFTR* expression within a low proportion of human β-cells (~ 1.4 – 5.0% >1 reads per kilobase of transcript per million mapped reads, RPKM, per cell) (Hart *et al.*, 2018). Therefore, the reported functional CFTR expression on the β-cell is widely variable between different experimental analyses, which most likely corresponds to the high transcriptional heterogeneity within different β-cell "pools" and inter-species variation in islet composition (Baron *et al.*, 2016; Farack *et al.*, 2019).

Using animal models with associated defective CFTR activity has aided the understanding around CFTR-mediated downstream regulation of β-cell insulin secretion. Unlike α-cell glucagon secretion, previous findings suggest CFTR activity can enhance β-cell insulin secretion (Edlund *et al.*, 2014, 2019; Guo *et al.*, 2014). Mice with whole-body expression of the DF508 *CFTR* mutation displayed significantly attenuated glucose-stimulated insulin secretion (GSIS), agreeing with data similarly observed in both CF neonatal ferret islets and *CFTR*-knockdown β-cell lines (Guo *et al.*, 2014; Ntimbane *et al.*, 2016; Sun *et al.*, 2017). After pharmacological CFTR inhibition, both mouse and human islets resulted in reduced cAMP-, GLP-1- and GSIS (Edlund *et al.*, 2014; Sun *et al.*, 2017; Fulvio *et al.*, 2020). However, β-cell-specific *CFTR* deletion did not influence cAMP-dependent, GSIS nor overall glucose homeostasis in mice, therefore contrasting with global *CFTR* mutant findings (Hart *et al.*, 2018). Interestingly, *CFTR* knockout ferret islets had increased *SLC2A1* mRNA expression, coding for β-cell specific GLUT-1 transporter implying CFTR-GLUT1 interactions could influence glucose transport (Sun *et al.*, 2017). However, this link would need further investigation.

Similarly to α-cells, recent evidence could imply insulin secretion is governed by changes in β-cell electrical activity modulated by CFTR opening. Reducing CFTR activity in immortalised β-cell lines and primary DF508 mouse β-cells attenuated glucose-stimulated depolarisation, with reduced action potential bursts respectively (Guo *et al.*, 2014). Importantly, the glucose-regulated K_{ATP} channel closure within the β-cell is crucial for controlling depolarisation and hence insulin release (Ashfield *et al.*, 1999; Gribble *et al.*, 2003). Pharmacological CFTR inhibition similarly reduced both glibenclamide-induced β-cell membrane depolarisation, and CFTR activity, requiring a larger current injection in patch-clamped RINmF5 cells to initiate an action potential (Guo *et al.*, 2014). Similarly, insulin secretion is defective CFTR neonatal ferret islets (Sun *et al.*, 2017). Defective CFTR activity did not change the amount of secreted insulin, but unlike wild-type islets, diazoxide (K_{ATP} opener) did not reduce total islet insulin content (Sun *et al.*, 2017). These findings suggest β-cell insulin secretory mechanisms in CF ferret islets are “normal” but total insulin content contained in intracellular granules is reduced; possibly contributed by defective insulin processing (Sun *et al.*, 2017). Therefore, unlike α-cell regulation of CFTR by K_{ATP} opening, β-cell CFTR channel activity may instead be indirectly influenced by K_{ATP} channel closure to potentiate GSIS, thereby stabilising β-cell electrical activity and resting membrane potential. This, in turn, emphasises the complex interplay between K_{ATP} channel activity and other ionic channels on islet hormone secretion.

CFTR can regulate other cAMP-activated Cl^- channels to enhance glucose-dependent β-cell depolarisation. Application of DIDS, a CFTR-insensitive Cl^- channel blocker, provides evidence for a small CFTR current but also DIDS-sensitive cAMP-enhanced Cl^- current within human and mouse islets (Edlund *et al.*, 2014). These data may suggest β-cells contain high cAMP-enhanced Cl^- current dependent and independent on CFTR opening. In epithelial tissues, it is well-known that cAMP-dependent CFTR activity requires ANO1, a voltage and calcium-activated Cl^- channel, for cellular Cl^- transport (Benedetto *et al.*, 2017). Both AO1, a selective ANO1 blocker, and GlyH additively attenuated GLP-1 and high GSIS in human islets, with a similar trend observed in mouse islets (Edlund

et al., 2014). CFTR could, at least partly, interact with ANO1 activity to regulate downstream GSIS (Edlund *et al.*, 2014).

Whether CFTR regulates calcium-modulated depolarisation within the β-cell is relatively undetermined. CFTR inhibition (by GlyH or CFTRInh-172) did not affect the calcium current in both isolated human and mouse β-cells (Sun *et al.*, 2017). However, neonatal *CFTR* knockout ferret islets had high $[Ca^{2+}]_i$ at low glucose and a lack of high glucose-stimulated increase $[Ca^{2+}]_i$ (Sun *et al.*, 2017). Furthermore, application of CFTRInh-172 inhibitor reduced total islet insulin secretion but ameliorated glucose-stimulated calcium uptake in both WT and CF neonatal ferrets (Sun *et al.*, 2017). Similarly, CFTR inhibition reduced glucose-stimulated Fura-2 $[Ca^{2+}]_i$ increases, oscillations and insulin secretion in the RIN5mF cell line and DF508 mutant mice (Guo *et al.*, 2014). In addition, CFTRInh-172 did not affect directly affect slow-activating $[Ca^{2+}]$ currents in isolated mouse and human β-cells at low glucose (Edlund *et al.*, 2014). Importantly, there should be caution when interpreting the above data. Application of CFTRInh-172 inhibitor further reduced glucose-dependent $[Ca^{2+}]$ flux, and insulin secretion in *CFTR* knockout ferret islets, identifying (as mentioned in a recent literature review by Norris *et al.*, 2019 that high CFTR inhibitor concentrations could have off-target effects on the mitochondria, independent of CFTR channel inhibition (Sun *et al.*, 2017; Norris *et al.*, 2019). Therefore, it is still unclear whether CFTR opening could influence $[Ca^{2+}]$-induced β-cell depolarisation and would need further clarification to eliminate any off-target inhibitor effects.

cAMP-stimulated Cl^- currents, possibly arising from CFTR-ANO1 interactions, have a distinct role independent from β-cell membrane depolarisation. Mouse islet studies showed CFTR inhibition diminished insulin secretion, at low glucose, independently of cAMP/K^+-induced depolarisation (Edlund *et al.*, 2014). Furthermore, pharmacological blocking of CFTR activity in mouse and human β-cells resulted in depleted depolarisation-induced granule exocytosis; corresponding to high CFTR and syntaxin plasma membrane co-localisation (Edlund *et al.*, 2014). In addition, transmission electron microscopy (TEM)

identified a reduced granule surface density, ~ 20% reduction in granule number and ATP-independent granule exocytosis within β-cells in mouse DF508 islets (Edlund *et al.*, 2019). These data correspond to the diminished intracellular insulin content previously shown in CF models (Fontés *et al.*, 2015; Sun *et al.*, 2017). One explanation suggests that CFTR activity may regulate fusion vesicular protein functionality to enhance insulin secretion, but this requires further study. DIDS application inhibited insulin secretion, suggesting the CFTR-ANO1 interaction could potentiate cAMP-dependent insulin exocytosis in mouse β-cells (Edlund *et al.*, 2014). However, ANO1-specific inhibition in human β-cells is required to determine this conclusion confidently.

DF508-CFTR misprocessing contributes to human and animal CF phenotypes. Similarly, defective β-cell CFTR activity may decrease GSIS through abnormal insulin processing (Edlund *et al.*, 2019). As previously mentioned, K_{ATP} channel-dependent hyperpolarisation failed to alter insulin content in CF ferret islets, in contrast to healthy islets, suggesting defective K_{ATP}-sensitive insulin processing (Sun *et al.*, 2017). Intravenous glucose tolerance tests showed high plasma proinsulin: insulin content after 60 min, but not in the fasted-state in DF508 pig models, similarly indicating reduced glucose-stimulated insulin processing (Uc *et al.*, 2015). In addition, individuals with CF and pancreatic insufficiency had increased fasting and hyperglycaemia-induced proinsulin:c-peptide ratio (Sheikh *et al.*, 2017). For insulin exocytosis, granule priming in mouse β-cells requires a low granular pH in response to cAMP and glucose stimuli (Davidson, Rhodes and Hutton, 1988; Barg *et al.*, 2001). CFTR inhibition, however, increased intragranular pH, demonstrating insulin granule priming and granule acidification require Cl^- ion influx, as shown in knockout models (Barg *et al.*, 2001). Therefore, it is reasonable to suggest cAMP-enhanced CFTR-ANO1 channel interaction could provide intracellular Cl^- ions for granule Cl^- channel influx, increasing pH-dependent granule acidification, aiding β-cell proinsulin processing and priming in response to glucose stimuli. These data would correspond to the delayed first-phase insulin secretion seen in glucose tolerance tests in both CF animal models and humans (Sheikh *et al.*, 2017; Sun *et al.*, 2017; Nyirjesy *et al.*, 2018). In people with CF and moderate

glucose tolerance, a delayed decreased peak glucose-stimulated first-phase insulin secretion may contribute to the development and association of the CFRD clinical phenotype (Cucinotta *et al.*, 1994; Tofé *et al.*, 2005; Mohan *et al.*, 2009; Sheikh *et al.*, 2017).

A recent review covered, in-depth, the idea that β-cell insulin release and electrophysiological state is heterogenous. This, in part, is driven by master "hub" cells ("pacemakers"), with a distinct β-cell signature to control neighbouring β-cells functionality and demonstrated in pathophysiological and physiological contexts (Fulvio *et al.*, 2020). CFTR expression in the β-cell is similarly heterogenous, with expression being differentially localised dependent on class of CFTR mutation (Fulvio *et al.*, 2020). Interestingly, the same study showed only 16 % of β-cells are electrically responsive to cAMP at high glucose, with approximately double the percentage at low glucose (Fulvio *et al.*, 2020). These findings suggest the known β-cell heterogeneity could contribute to the widely contrasting published findings on CFTR expression and role in β-cell electrical state.

Exocrine pancreatic decline promotes islet remodelling and β-cell dysfunction through increased islet oxidative and inflammatory stress. High immune cell infiltration and intra-islet pro-inflammatory cytokine (IL-1β, TNF-α, IL-6) secretion has been reported in both CF and CFRD human islets, although it is a debated observation in CF animal models (Fontés *et al.*, 2015; Hart *et al.*, 2018; Khan *et al.*, 2019). As the pancreatic β-cell is highly susceptible to ER stress, similar to most secretory cells, misfolded CFTR protein and pro-inflammatory cytokine accumulation persistently activates intracellular ER-stress pathways, such as NF-κB (Knorre *et al.*, 2002). This, in turn, perhaps increases reactive oxygen species (ROS) generation, and deficient β-cell insulin secretion to trigger apoptosis to further perpetuate dysregulated glucose homeostasis.

If this is the case, are β-cells lost during CF and CFRD? Early studies showed a reduction in insulin-stained islet area in both CF and CFRD human islets, with two studies reporting ~ 50 - 65% reduction in CF and CFRD insulin-stained islet

area (Bogdani *et al.*, 2017; Hart *et al.*, 2018). More recent, larger studies are controversial. One study observed a significant decrease in insulin-positive islet areas in adult and young CF tissues (Bogdani *et al.*, 2017). In contrast, other studies found no difference in the insulin-stained area:pancreatic area between controls and CF/CFRD human islets (Hull *et al.*, 2018). The discrepancy lies between how studies are normalising β-cell area, as overlooking β-cell mass compared to overall pancreatic area disregards any relative changes in β-cell size within the islet, as identified in a young CF ferret model (Olivier *et al.*, 2012). However, current research implies β-cell loss occurs at a young age, with severe β-cell damage and pro-inflammatory cytokine islet infiltration appearing to be highly prevalent in younger CF patients influencing CFRD development (Bogdani *et al.*, 2017). *CFTR* mutation severity may not affect the reduction seen in young CF β-cell loss, but individuals with DF508 mutation are ~ 20 times more likely to develop CFRD (Koch *et al.*, 2001; Bogdani *et al.*, 2017). More recently, a large genome-wide association study (GWAS) indicated the genetic risk may govern the age of onset when CFRD may develop and is strongly associated with CFRD with polygenic risk scores for type 2 diabetes mellitus (T2DM)-related β-cell dysfunction, including insulin secretion and possibly apoptosis (Aksit *et al.*, 2020).

Collectively, although requiring further investigation, these data suggest early intrinsic defects within CFTR-defective β-cells could contribute to worsened glucose tolerance in CF patients, and therefore CFRD progression (Iannucci *et al.*, 1984; Soejima and Landing, 1986).

7.5 CFTR expression in other islet cells and relevance to CF/CFRD.

7.5.1 δ-Cells

Although less characterised than α- or β-cells, somatostatin (SST)-secreting δ-cells are crucial in endocrine and paracrine islet regulation of glucose homeostasis (Rorsman and Huising, 2018; Arrojo e Drigo *et al.*, 2019). As previously mentioned, defective CFTR can lead to abnormal islet hormone secretion, which thus poses the question of a potential role of CFTR within the δ-cell for glucose-stimulated somatostatin secretion. Although there are limited published data, human islets and ferret SST-stained islets showed both minimal *CFTR* mRNA expression and CFTR-SST-positive co-localisation (Boom *et al.*, 2007; Edlund *et al.*, 2017; Sun *et al.*, 2017). Interestingly, human CF islets appear to have increased or unchanged intra-islet SST-staining compared to non-CF controls (Iannucci *et al.*, 1984; Abdul-Karim *et al.*, 1986; Löhr *et al.*, 1989; Meacham *et al.*, 1993; Bogdani *et al.*, 2017; Rotti *et al.*, 2018; Edlund *et al.*, 2019). CFRD SST-staining is less characterised; with some findings indicating no difference between CF and CFRD SST staining in human islets (Abdul-Karim *et al.*, 1986; Hull *et al.*, 2018). In contrast, an older study suggested individuals with CFRD had increased arginine-stimulated SST secretion (Meacham *et al.*, 1993). Altogether, there is a lack of evidence to suggest δ-cells express and intrinsically require endogenous CFTR activity to contribute to both physiological and CF/CFRD-retained SST secretion.

The retained SST secretion during CF/CFRD may provide a hypothesis for the dysregulated α- and β-cell hormone secretion. Recent islet mathematical models suggest mouse δ-cells and β-cells are electrically coupled, where both hormone secretory responses control α-cell activity and each other (Briant *et al.*, 2018b). With regards to CFTR and SST secretion, one study showed glucose- and cAMP-induced SST secretion was attenuated by both GlyH and CFTRInh-172 CFTR inhibition in mouse islets, possibly due to diminished insulin/urocortin-3 release which are known potentiators of SST secretion (Edlund *et al.*, 2017). Similarly, depolarisation- and cAMP-induced SST secretion was attenuated with individual application of ANO1 and CFTR

inhibitors in mouse islets (Edlund *et al.*, 2017). On the contrary, DF508 mouse islets had significantly enhanced SST secretion at all [glucose] which, in part, could be an attempt to limit excessive glucagon secretion at low glucose (Edlund *et al.*, 2019). It is important to highlight the study discrepancies could be contributed to by length of islet incubation (e.g., 15 – 60 min). Furthermore, due to glucose-independent actions of excessive SST secretion following CFTR ablation/inhibition, the paracrine regulation of SST secretory response cannot rule out any intrinsic CFTR-dependent defects in δ-cell signalling.

7.5.2 PP cells

Feeding stimulates islet PP-cells to secrete pancreatic polypeptide (PP) to regulate digestion, but PP-cell function has been relatively unexplored in CF/CFRD (Schmidt *et al.*, 2005). Undetectable PP-cell *CFTR* RNA expression and no change in PP secretion was observed after CFTR inhibitor application in ferrets, but it is currently unknown in human PP-cells (Sun *et al.*, 2017). However, increased PP-stained area has been noted in CF/CFRD human islets (Löhr *et al.*, 1989; Bogdani *et al.*, 2017; Hull *et al.*, 2018). Findings from one study suggests PP-cell area appears to be variable in young individuals with CF. CF islets either had unchanged or reduced PP islet staining, with human islets from individuals with CFRD demonstrating decreased PP-cell area compared to CF islets (Nousia-Arvanitakis *et al.*, 1985; Hull *et al.*, 2018). In addition, individuals with CF have demonstrated a lack of PP response to feeding (Allen *et al.*, 1983). On the other hand, one study indicated exocrine-insufficient CF individuals have increased insulin-stimulated PP levels compared to exocrine-sufficient CF (Moran *et al.*, 1991). These data are surprising as chronic pancreatitis, a complication of CF, is characterised by continuously low PP levels associated with pancreatic islet loss and both exocrine/endocrine pancreatic insufficiency (Milnerowicz and Śliwińska-Mosson, 2017).

In summary, one could speculate the observed altered PP cell function and number may be as a result or contribute to CFRD development, most likely due

to extrinsic factors, such as local pancreatic inflammation, rather than intrinsic dysregulated CFTR signalling within the PP-cell. A summary of hypothesised downstream consequences resulting from defective CFTR expression in islet cells is illustrated in Figure 7.3.

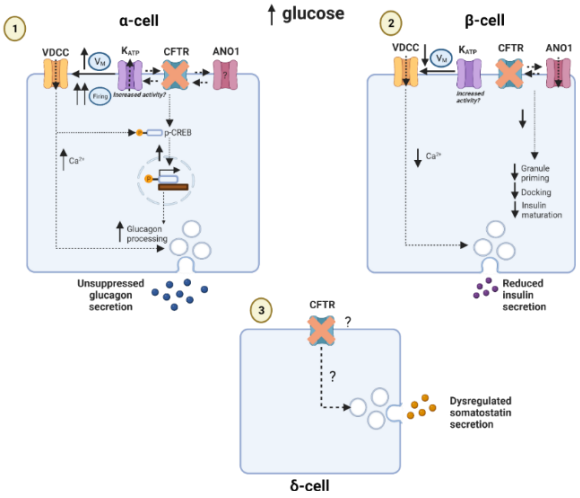

Figure 7.3: Hypothesised islet cell dysfunction resulting from defective CFTR expression.

(1) It has been previously hypothesised CFTR could exert downstream effects through being regulated, or regulating, K_{ATP} channel-induced depolarisation. At high glucose, defective CFTR activity could, although speculative, further increase glucagon secretion by enhancing K_{ATP} channel activity. By doing so, increased action potential (AP) amplitude increased calcium entry by voltage-dependent calcium channel (VDCC) activation. A small previous study shown overexpressing CFTR within an α-cell line reduced pro-glucagon, PC2 and p-CREB protein expression, possibly suggesting CFTR could negatively regulate pro-glucagon processing within α-cells. Increased α-cell $[Ca^{2+}]_i$ in response to CFTR inhibition could directly potentiate CREB phosphorylation and thereby increase glucagon processing in the α-cell. Therefore, CFTR-defective alpha-cells may have elevated depolarisation-induced glucagon secretion and processing. **(2)** In β-cells, DF508 CFTR mutant mouse islets had defective pro-insulin cleavage/processing and therefore reducing mature insulin secretion. Previous work suggests CFTR regulates ANO1-induced chloride influx, and ANO1-dependent insulin granule exocytosis. Moreover, defective CFTR mouse β-cells shown reduced insulin granule docking and exocytosis. These findings collectively suggest defective CFTR-ANO1-dependent interactions may ameliorate insulin granule priming, maturation, and plasma membrane docking. It is not known if CFTR interacts with ANO1 in α-cells. Similarly, it would be interesting to propose increased K_{ATP} channel activity in the β-cell could attenuate VDCC opening and calcium entry. Dysregulated CFTR intrinsic signalling may contribute to the enhanced glucagon secretion and augmented first-phase insulin secretion contributing to hyperglycaemia seen in CF and CFRD patients. **(3)** Interestingly, some studies report somatostatin (SST) staining appears to be increased in CF individuals. In addition, published literature indicate dysregulated islet SST secretion. Little is known if intrinsic defects in CFTR signalling within the δ-cell could contribute to this phenotype, alongside altered intra-islet paracrine signalling from neighbouring β- and α-cells. Dashed lines indicate hypothesised actions. Created using Biorender.com.

7.6 CFTR and exocrine pancreas

The majority of pancreatic CFTR expression is localised to the ductal epithelium lining both the rodent and human exocrine pancreas (Marino *et al.*, 1991; Sun *et al.*, 2017; Hart *et al.*, 2018). CFTR activity maintains ductal pH by regulating the apical HCO_3/Cl^- transport gradient and therefore acinar cell digestive enzyme secretion (Saint-Criq and Gray, 2017). The insufficient CFTR-dependent electrolyte and pancreatic enzyme secretion in the duct, as a result of defective CFTR activity, can lead to exocrine pancreatic insufficiency characterised in ~85% CF patients (Durie, 1989; Saint-Criq and Gray, 2017). The abundant CFTR exocrine expression suggests endocrine islet dysfunction may be secondary to the changes in the exocrine pancreas, and thereby responsible for potentiating the development of CFRD (Sun *et al.*, 2017). This suggestion is plausible as cells lining the ductal epithelium have topographical, frequent association with cells in the islets of Langerhans throughout the pancreas (Madden and Sarras, 1989; Bertelli *et al.*, 2001; Bertelli and Bendayan, 2005; Hai Lu Zhao *et al.*, 2008).

One such hypothesis suggests the loss of CFTR functionality within the exocrine tissue results in pancreas remodelling and paracrine-mediated islet dysfunction seen in CF; independent of CFTR-intrinsic islet defects (Sun *et al.*, 2017; Hart *et al.*, 2018). Findings suggest hyperglycaemia is associated with high pancreatic inflammation, fibrosis and β-cell loss in a young CF ferret model, similarly to the known dysregulated glucose homeostasis phenotype seen in young CF children (Yi *et al.*, 2016a, 2016b; Rotti *et al.*, 2018). It is well-established that CF is associated with early exocrine inflammation, activating the production of exocrine pro-inflammatory cytokines (e.g., IL-1β/IL-6) secretion (Sun *et al.*, 2017; Hart *et al.*, 2018). Islet immune infiltration, therefore, can aid a localised and systemic pancreatic inflammatory response which is a well-described characteristic of CFRD development (Hart *et al.*, 2018; Hull *et al.*, 2018). Furthermore, high amyloid deposition could exacerbate the inflammatory milieu, a common hallmark of T2DM (Couce *et al.*, 1996). Although still documented in CF, human CFRD islets appear to have greater

amyloid deposits than both young and adult CF islets, further characterising CFRD as an advanced clinical complication of CF (Iannucci *et al.*, 1984; Couce *et al.*, 1996; Bogdani *et al.*, 2017; Hart *et al.*, 2018; Hull *et al.*, 2018). In addition, heightened metalloproteinase (MMP) expression may enhance islet remodelling, such as MMP-7, to respond to the peak pancreatic inflammation observed in CF ferrets (Rotti *et al.*, 2018). These data could argue that early exocrine pancreatic insufficiency consequently promotes the later defective β-cell function and compromised glucose tolerance, driving CFRD progression (Yi *et al.*, 2016b; Rotti *et al.*, 2018).

Interestingly, the pancreatic islet cells are not completely lost in CFRD-diagnosed individuals, and therefore the “bystander hypothesis” cannot fully explain the dysregulated endocrine function associated with CFRD (Iannucci *et al.*, 1984; Soejima and Landing, 1986; Couce *et al.*, 1996; Bogdani *et al.*, 2017; Yoon, 2017; Hull *et al.*, 2018). This finding therefore asks the question if, and by what mechanism, are islet-cells adapting to the inflammatory pancreatic environment seen in CF/CFRD? Ductal-cell precursors can transdifferentiate into β-cells to respond to islet inflammation and propagate β-cell regeneration (Solar *et al.*, 2009; Uzan *et al.*, 2009; Li *et al.*, 2010; Mingfeng Zhang *et al.*, 2016). In one study, young CF human β-cells had low positivity for proliferation and/or ductal markers compared to control, suggesting an early reduction in β-cell area may be through altered proliferation and ductal neogenesis rather than β-cell apoptosis (Bogdani *et al.*, 2017). However, increased proliferative immune staining in both ductal and insulin-positive cells were noted during and after peak exocrine inflammation in CF ferrets (Rotti *et al.*, 2018). Similarly, β-cell differentiation and maturation gene markers in *CFTR* knockout neonatal ferret islets were upregulated (Sun *et al.*, 2017). An increase in ductal transdifferentiation into β-cells could be a “rescue” attempt to alleviate hyperglycaemia seen in exocrine-inflamed CF ferrets, a postprandial clinical observation in CFRD patients (Rotti *et al.*, 2018). In addition, CFTR inhibition may upregulate islet cell number through increasing the ductal/acinar-cell progenitor pool in young rodent models, highlighting the possible CFTR role in reducing ductal to islet cell differentiation (Rotti *et al.*, 2018). Whether ductal

trans-differentiation to other endocrine cell types occurs in CFRD is still unclear but could pose an attractive therapeutic opportunity in regenerating the diminished β-cell number contributing to CFRD development.

Exocrine inflammation may activate resident endocrine and exocrine pancreatic stellate cells (PSCs) by contributing to extensive fibrotic deposition and islet remodelling seen in CF ferret models (Sun *et al.*, 2017; Rotti *et al.*, 2018). Not only are PSCs involved in islet fibrosis, but these cells influence glucose intolerance and reduced islet survival as seen in T2DM (Zha *et al.*, 2014; Zang *et al.*, 2015; Lee *et al.*, 2017). In co-culture, PSCs increased islet insulin release over short periods, and with chronic exposure, increasing islet-cell death (Zang *et al.*, 2015) (Figure 7.4). More studies are required to evaluate PSCs intra-islet distribution and role in CFRD-related islet remodelling.

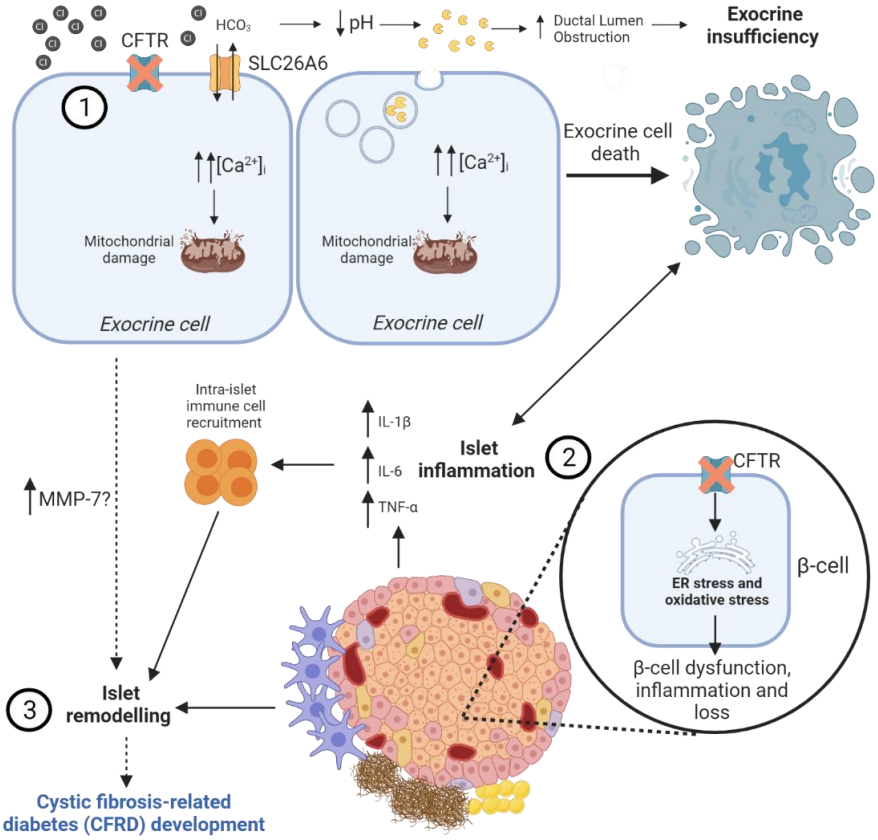

Figure 7.4: Suggested intra-islet and exocrine *CFTR* defects, contribution to β-cell dysfunction and CFRD development.

(1) Defective ductal cell CFTR activity reduces fluid secretion, lowering pH in the ductal lumen. Class II *CFTR* mutations (e.g. DF508) promote $[Ca^{2+}]_i$ overload in exocrine cells, resulting in mitochondrial damage and therefore further impaired bicarbonate and fluid secretion. Consequently, reduced digestive protein washout and increased protein concentration further elevates the likelihood of protein precipitation and thus ductal obstruction. Ductal obstruction promotes exocrine cell death, inflammation, fibrosis and adipose tissue replacement characterising CF "exocrine insufficiency". **(2)** One hypothesis suggests exocrine "bystander damage" mediates β-cell dysfunction in CFRD by enhanced islet remodelling and inflammation. β-cell ER accumulation of misfolded CFTR proteins could enhance intra-islet inflammation, further propagating ER and oxidative stress-mediated β-cell loss. β-cell cytokine secretion (TNF-α. IL-6, IL-1β) could accelerate intra-islet inflammation and immune cell recruitment seen in $CD45^+$ stained CFRD islets. **(3)** CFRD human and *CFTR* mutant non-human islets can be surrounded by both high amyloid deposition and activated pancreatic stellate cells which are embedded within deposited adipose tissue. Alongside possible elevated islet markers, these characteristics could be evident of high islet remodelling during CF, contributing to CFRD islet pathogenesis. It is important to note islets, and β-cells, are not completely destroyed during CFRD. One hypothesis suggested ductal-islet cell trans-differentiation could replenish the β-cells destroyed and retain some β-cell mass in CF and CFRD islets. Created using Biorender.com.

7.7 An Emerging Field: GLP-1 and CFTR regulation within the pancreatic islets

Abnormal gastrointestinal glucagon-like peptide-1 (GLP-1) secretion in CF/CFRD may contribute to dysregulated islet hormone secretion. GLP-1 stimulates β-cell insulin secretion and inhibits glucagon secretion in response to hyperglycaemia (Mojsov, Weir and Habener, 1987; Zhang *et al.*, 2019). Whether active GLP-1 secretion is altered in CF and CFRD, however, is not fully clear. After mixed meal testing (MMT), low or unchanged active GLP-1 concentrations have been shown in people with CF and CFRD (Kuo *et al.*, 2011; Hillman *et al.*, 2012; Kelly *et al.*, 2019). This may be a mechanism for postprandial hyperglycaemia in CFRD, but most likely does not contribute to the OGTT-induced hypoglycaemia in CFRD (Aitken *et al.*, 2020). Furthermore, in one study, plasma GLP-1 was increased in individuals with pancreatic-sufficient CF, identifying local and systemic differences in how pancreatic sufficiency may influence digestion in CF (Sheikh *et al.*, 2017). However, this is still disputed, with a small study demonstrating elevated active peak GLP-1 secretion after OGTT in individuals with CF and CFRD (Armaghanian *et al.*, 2020). Similarly, other published findings found a significant increase in total GLP-1 after 60 min OGTT in individuals with CFRD and CF, but CFRD individuals had abolished incretin-dependent increase in insulin secretion when compared to healthy and CF individuals (Frost *et al.*, 2019). Therefore, these findings could suggest reduced incretin sensitivity and secretion, in part, contribute to the diminished β-cell insulin secretory response to a glucose stimulus.

Currently, there is a significant focus on short-acting GLP-1 agonist therapy to improve β-cell insulin secretion in CFRD (Ode *et al.*, 2019)**.** GLP-1 analogues are already used for T2DM management and may have utility in CFRD (Phillips *et al.*, 2015; Geyer *et al.*, 2019). For instance, GLP-1 receptor agonist treatment reduced postprandial hyperglycaemia in young individuals with CF and IGT, which is possibly mediated by slowed gastric emptying (Perano *et al.*, 2014; Moheet and Moran, 2017). Furthermore, pancreatic enzyme replacement therapy (PERT) enhanced GLP-1 secretion in pancreatic-insufficient individuals

with CF in one study after a high-fat meal (Perano *et al.*, 2014). In contrast, after mixed meal tolerance testing (MMTT), individuals with PERT-supplemented pancreatic insufficiency had a lower, early GLP-1 increase compared to control (Sheikh *et al.*, 2017). The utility of incretin agonists in CFRD therefore requires further clarification. However, caveats to potential pharmacotherapies are discussed later.

7.8 Phenotypic challenges in examining the effect of *CFTR* mutations in the pancreas.

Understanding CFRD pathogenesis, until relatively recently, has been challenging due to insufficient animal models that fully recapitulate the severe CF pancreatic pathology seen in humans (Guilbault *et al.*, 2007; Tuggle *et al.*, 2014; Rosen *et al.*, 2018). Unlike CF/CFRD in humans, mouse whole-body or β-cell specific *CFTR* knockout and mutant (DF508) models do not develop the significant exocrine disease associated with CF; with considerable discrepancies in OGTT blood glucose findings (Lanng *et al.*, 1993; Fontés *et al.*, 2015; Hart *et al.*, 2018). In contrast, *CFTR* knockout ferrets and pigs do develop CF-associated exocrine pancreatic disease spontaneously *in utero,* and after birth, respectively (Rogers *et al.*, 2008; Sun *et al.*, 2014). Both porcine and ferret models have greater CFTR amino acid similarity to humans (> 90%) compared to rodent models, providing a reason for these similar phenotypes (Ostedgaard *et al.*, 2007; Fisher *et al.*, 2012). Furthermore, these models have relative sparing of islet mass, dysregulated insulin secretion and age-dependent dysregulation of glucose homeostasis, which phenotypes are similarly observed in individuals with CF (Olivier *et al.*, 2012; Sun *et al.*, 2014, 2017; Uc *et al.*, 2015; Rotti *et al.*, 2018). These models highlight a potential avenue for greater reproducibility in CF research.

7.9 CFTR in the brain

The brain contains glucose sensing neurons, akin to the α- and β-cells of the pancreas, termed glucose-inhibited (GI) and glucose-excited (GE) neurones, respectively (Shimazu and Minokoshi, 2017). These glucose sensing neurones play an important role in maintaining glucose homeostasis, contributing to glucose tolerance and preventing hypoglycaemia (Miki *et al.*, 2001; Shimazu and Minokoshi, 2017). This is under the control of a number of brain regions including (but not limited to) the hypothalamus, nucleus of the solitary tract (NTS), bed nucleus of the striata terminalis and the parabrachial nucleus (PBN) (Roh, Song and Kim, 2016). Importantly, is CFTR expressed in the glucose sensing neurons and does CFTR influence neuronal activity? Importantly, in the rat brain, CFTR expression has been reported in regions involved in glucose homeostasis including the BNST, PBN, NTS and paraventricular nucleus of the hypothalamus (Mulberg *et al.*, 1995). CFTR expression has also been confirmed in the human hypothalamus (Guo *et al.*, 2009). Few studies have reported functional contributions of CFTR to glucose sensing but importantly, two studies have demonstrated a role of CFTR in coupling changes in glucose levels to neuronal outputs. Exposure of rat ventromedial hypothalamus GI neurons, which contribute to the prevention of hypoglycaemia, to low glucose levels increased AMP-activated protein kinase (AMPK) phosphorylation leading to downstream phosphorylation and inhibition of CFTR (Song and Routh, 2006; Murphy *et al.*, 2009). Moreover, maintaining CFTR in the open position using gemflibrozil, prevented the depolarisation induced by low glucose, suggesting CFTR-mediated Cl^- influx contributes to the inhibition of GI neurons (Murphy *et al.*, 2009). AMPK has been reported to reduce cAMP-mediated Cl^- secretion in epithelial cells and to directly interact with and inhibit cAMP-stimulated CFTR activity (Hallows *et al.*, 2000; Walker *et al.*, 2003). Given that CFTR activity maintains GI neurons in a more hyperpolarised state, what is the likely consequence of CFTR mutations on whole body glucose counterregulation? No studies have investigated the effect of brain CFTR modulation on the counterregulatory response to hypoglycaemia, however, loss or reduction in a hyperpolarising current would likely result in more depolarised GI neurons, a

signal that could enhance CRR. Hypoglycaemia occurs in people with CF, for example, during OGTT, rates of reactive hypoglycaemia were 15% and fasting hypoglycaemia were 14% in people with CF (Battezzati *et al.*, 2007). For a recent detailed review of clinical aspects of hypoglycaemia in CF see Moheet *et al.*, 2019. Therefore, the glucose variation seen in CF and CFRD may contribute to the increased mortality and morbidity, discussed in more detail below.

7.10 Glucose variation, ER stress and CFTR function: do these factors contribute to CF disease progression?

Does hypoglycaemia worsen or accelerate CF progression? As mentioned above, CFTR can be inhibited by the energy sensing kinase AMPK (Hallows *et al.*, 2000; Kongsuphol *et al.*, 2009a). This kinase is activated by an increase in the AMP/ATP ratio, which occurs during energy stress including hypoglycaemia (Hardie, Carling and Carlson, 1998). This raises the possibility that hypoglycaemia in CF/CFRD may activate AMPK to further reduce CFTR function. In a gastric cancer cell line, nutrient starvation decreased cell surface localisation and total expression of CFTR, an effect mimicked by pharmacological activation of AMPK using AICAR (Zhu *et al.*, 2018). Moreover, breath glucose has been measured in CF and non-CF participants and found to change in line with glycaemia, indicating that hyperglycaemia results in increased respiratory glucose levels and this is exacerbated in CFRD (Baker *et al.*, 2007). This would be expected to suppress AMPK activation, permitting CFTR activity. If frequent hypoglycaemia occurs in CF and CFRD, it is plausible this could activate AMPK in CFTR-expressing tissues to attenuate CFTR activity or cell surface expression as previously suggested (Hallows *et al.*, 2003; Zhu *et al.*, 2018). This is complicated by the observation that dysfunctional CFTR can increase AMPK activity in airway epithelial cells *in vitro*, a response thought to mitigate inflammation (Hallows *et al.*, 2006). Whether this occurs *in vivo* when hyperglycaemia is present has not been investigated. However, both hyperglycaemia and hypoglycaemia have additional effects on cellular function that may impact CFTR. For example, both high and low glucose levels can induce endoplasmic reticulum (ER) stress in a number of tissues (Ikesugi *et al.*, 2009; Back and Kaufman, 2012; Zhong *et al.*, 2012; Iurlaro *et al.*, 2017). Importantly, the DF508 mutation has a misfolded protein structure and is retained within the ER-Golgi apparatus leading to reduced trafficking and surface protein expression (Gilbert *et al.*, 1998; Lukacs and Verkman, 2012). Moreover, airway bacterial infection and inflammation drives ER stress in CF and the presence of the mutant protein also increases expression of the unfolded protein response (UPR) (Kerbiriou *et al.*, 2007; Ribeiro and Boucher,

2010). Therefore, it is plausible that glucose variation could alter both AMPK activity and induce ER stress to directly and indirectly reduce CFTR function.

7.11 Pharmacological treatments for CFRD: opportunities and potential contraindications.

Ivacaftor is a CFTR opener that increases ion flow in patients with low CFTR activity and lumacaftor is a drug that improves CFTR folding, trafficking and cell surface expression (Van Goor *et al.*, 2009). See Habib *et al.*, 2019 for a comprehensive analysis of recent clinical trials involving novel, pharmacological CFTR regulators. The remainder of this section will discuss opportunities and potential pitfalls with emerging treatments for CFRD and how these could impact clinical outcomes not directly related to glucose control.

At present, insulin is still the main therapeutic intervention to control blood glucose in CFRD (Moran *et al.*, 2010). This is largely because metformin, the most widely used drug in T2DM has some unfavourable characteristics. For instance, metformin therapy can increase the risk for lactic acidosis and on commencement of treatment can lead to gastrointestinal (GI) distress and short-term weight loss, which in CF therapeutics, perhaps could exacerbate the clinical CF phenotype (Defronzo *et al.*, 2016). Despite this, metformin-related lactic acidosis has a relatively low incidence in T2DM therapy (Salpeter *et al.*, 2010). Interestingly, relating to CF, preclinical data suggests that metformin can activate AMPK in the lung, which could reduce CFTR activity (Tang *et al.*, 2021). For example, metformin can activate AMPK in myofibroblasts related to idiopathic lung fibrosis and reverse fibrosis in a mouse model in an AMPK-dependent manner (Rangarajan *et al.*, 2018; Kheirollahi *et al.*, 2019). This study also demonstrated that AMPK activity was lower in patients with idiopathic pulmonary fibrosis (IPF) (Rangarajan *et al.*, 2018). In contrast, metformin has also been reported to activate AMPK in a rat model to reduce lung damage (Wu *et al.*, 2019). A similar mechanism has been reported in renal cysts, where metformin-induced AMPK activation regulated CFTR activity to attenuate cystogenesis (Takiar *et al.*, 2011). Currently, a phase II clinical trial is being conducted to assess the effectiveness of metformin therapy to improve CFTR channel functionality in individuals with CFRD and therefore highlights the putative efficacy of AMPK activator therapy in CFRD (*Effects of Metformin on*

Airway Ion Channel Dysfunction in Cystic Fibrosis-related Diabetes, no date). However, metformin also has significant anti-inflammatory benefits not related to the effect of the drug on glucose control or via the activation of AMPK, as highlighted in a recent review (Cameron *et al.*, 2016; Kristófi, Endocrinology and 2021, 2021). The anti-inflammatory actions of AMPK activation could be a putative therapeutic target in CF, which clinical phenotype is characterised by high tissue inflammation. For instance, the activation of AMPK by AICAR downregulated secretion of inflammatory mediators in DF508 epithelial cells (Hallows *et al.*, 2006). In addition, ADaM site-binding and direct AMPK activators have anti-hyperglycaemic actions in T2DM models, which may have clinical relevance in also attenuating hyperglycaemia and thus hyperglycaemia-exacerbated islet inflammation, characteristic in CFRD development (Cokorinos *et al.*, 2017; Steneberg *et al.*, 2018).

As suggested above, GLP-1 receptor agonists (RAs) are widely used for the treatment of diabetes and recent data from the SURPASS clinical trial suggests that patients taking Tirzepatide drug lose between 7.0 – 9.5 kg body weight (Rosenstock *et al.*, 2021). This effect is less desirable in CFRD, where maintaining a healthy BMI can be challenging (Zemel *et al.*, 2000). GLP-1 RA's can modulate AMPK activity (Andreozzi *et al.*, 2016; R. Li *et al.*, 2021a). Exenatide increases AMPK activity in a number of tissues including skeletal muscle, cultured hepatocytes, cardiomyocytes and endothelial cells (Svegliati-Baroni *et al.*, 2011; Andreozzi *et al.*, 2016; Wei *et al.*, 2016; Xiaotian *et al.*, 2016). Importantly, GLP-1 receptors are found in lung tissue in rodents and humans and although GLP-1R-mediated activation of AMPK has not been reported in CFTR-expressing cells in the lung, it will be important to examine going forward whether the GLP-1R agonists alter pulmonary exacerbations in CF over the longer term (Wei and Mojsov, 1996; Romaní-Pérez *et al.*, 2013).

7.12 Concluding remarks

In conclusion, this review has highlighted the possibility for intrinsic CFTR-dependent defects in key glucose-sensing tissues in which, collectively, could contribute to worsened glucose counterregulation observed in CFRD. It is important to note this is most likely additive from indirect, exocrine-mediated alterations in islet morphology and function observed in CF/CFRD. An interesting research question going forward is if the altered glucose homeostasis observed in CFRD is partially mediated by defective counterregulatory responses to blood glucose in CFRD, due to the ubiquitous expression of CFTR in human tissues. If so, it raises the possibility that small molecule activators of AMPK, as mentioned, could be useful in restoring both central and peripheral glucose homeostasis, alongside reducing sustained inflammation in CF. In addition, this review has highlighted several barriers to understanding the mechanisms behind CFRD development. The likelihood of CFRD development is potentiated by the class of CFTR mutation an individual with CF has, and with the majority of studies focusing on the most common Class II genotypic variant (DF508), it limits study applicability to, for instance, Class I mutations which similarly have differential CFTR function and increased diabetes risk (Adler *et al.*, 2008). That being said, understanding the therapeutic actions of CFTR pharmacological modulators on pancreatic islet hormonal secretion can potentially restore glucose homeostasis that is commonly dysregulated in CF and CFRD.

Chapter 8

General discussion and concluding remarks

8 General discussion and concluding remarks

Impaired hormonal secretory responses from the pancreatic islet are associated with profound glucose variability seen in diabetes mellitus (DM) and complications from pre-existing chronic conditions (e.g., CFRD). The glucagon-secreting α-cells in DM exhibit dysregulated glucagon release following hypoglycaemia and hyperglycaemia. Similarly, CFRD development is associated with impaired glucagon secretion in response to glucose (Edlund *et al.*, 2019; Aitken *et al.*, 2020). There is a lack of clear consensus on how α-cells intrinsically regulate glucagon secretion in response to extracellular glucose. By understanding α-cell physiology, one can identify possible therapeutic targets to modulate counterregulatory glucagon release. Therefore, this thesis examined the involvement of the critical glucose sensor, AMPK, on α-cell function and characterised the downstream actions of pharmacological activation of AMPK in glucose-dependent responses in the α-cell. Furthermore, this thesis explored the role of AMPK activity in CFRD, using literature-based sources.

8.1 Key findings

8.1.1 Chapter 3

Previous data suggested pharmacological AMPK activation by indirect activator, metformin, can stimulate the α-cell glucagon secretory response (Leclerc *et al.*, 2011). A new and more potent metformin-like AMPK activator, similarly enhanced plasma glucagon levels during hyperinsulinaemic-hypoglycaemic clamp studies in healthy rodents (Cruz *et al.*, 2021). In this thesis, R481 increased α-cell AMPK activity by, most likely, allosteric activation by rises in $[AMP]_I$. In addition, elevated AMPK activity by R481 increased αTC1.9 glycolytic rate and lactate secretion. A particularly novel finding from this thesis suggested AMPK activation could mediate metabolic switching in glucose-deprived conditions when exposed to saturated fatty acids (FAs) to possibly sustain α-cell function. These findings, altogether, infer AMPK is a potent regulator of α-cell metabolism, especially in nutrient depleted conditions. Interestingly, R481-

induced bioenergetic changes did not influence downstream glucagon secretion, which could be mediated by mild complex I inhibition.

8.1.2 Chapter 4

O-304 is an allosteric AMPK activator previously demonstrated to lower hyperglycaemia and reduce cardiovascular complications in humans with metformin-treated T2DM (Steneberg *et al.*, 2018). In particular, O-304 exposure can directly increase islet insulin secretory response and limit β-cell stress in a T2DM mouse model (Steneberg *et al.*, 2018; López-Pérez *et al.*, 2021). Evidence from this chapter corroborated the findings from chapter 3 using R481, whereby exposure to O-304 enhanced α-cell glycolytic rate. In addition, similarly to R481, O-304 increased lactate secretion. These findings, altogether, emphasise the role of AMPK in α-cell glycolysis and lactate generation.

Contrasting the evidence from R481, O-304 differentially regulated glucagon secretion and content, dependent on experimental model and glucose availability. A reduction in glucagon content, by O-304, could be driven by AMPK mediated mTORC1 inhibition leading to glucagon granule crinophagy. O-304 was also found to be an anti-hyperglycaemic agent in insulin-deficient diabetic rats, possibly by reducing gluconeogenic gene expression, similar to the study findings by Steneberg *et al.*, 2018. To compare and contrast, R481 may not have the same effect on α-cell glucagon secretion due to differences in mechanism of action. Mild complex I inhibition can reduce NADH oxidation and ROS production (Vranas *et al.*, 2021). In this chapter, increased ROS production by O-304, most likely by UCP-2 opening, is most likely contributing to the exaggerated glucagon secretory response in αTC1.9 cells and as R481 does not affect α-cell ROS production, this implies a potential difference between the two activators in effect on glucagon secretion. Whether O-304-stimulated glucagon secretion in the αTC1.9 cells is an AMPK-mediated effect is yet to be determined. The differential effects on α-cell glucagon secretion following O-304 or R481 exposure are illustrated in Figure 8. 1.

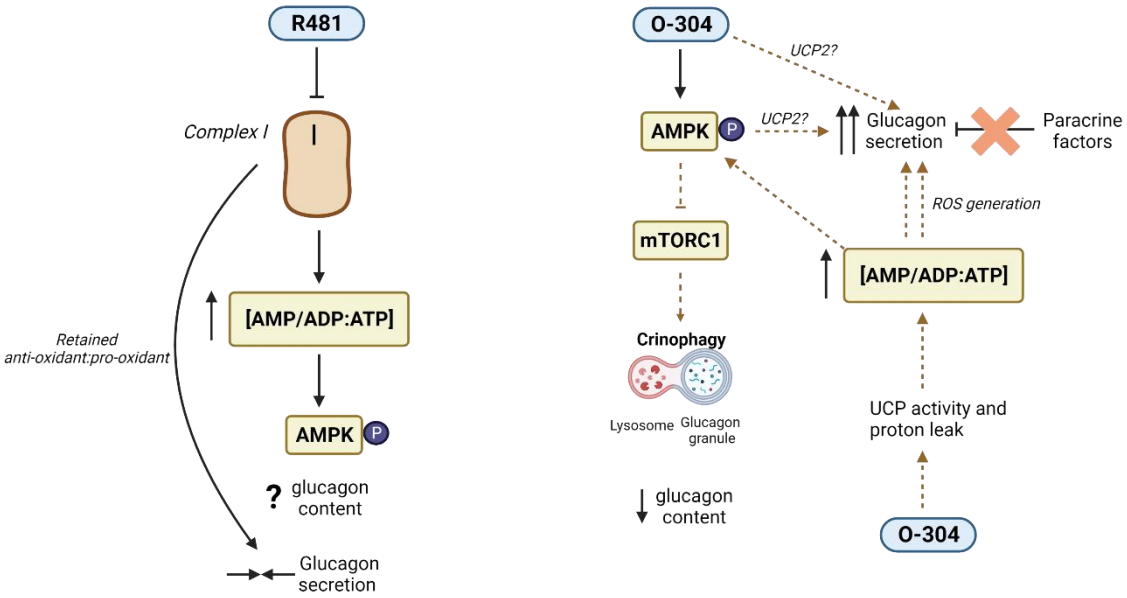

Figure 8. 1: The hypothesised, differential effects of R481 and O-304 on glucagon secretion and content.

Both O-304 and R481 seemingly have differential actions on α-cell function. Putative mechanisms may include, but are not limited to; changes in nucleotide ratio, glucagon secretion and mitochondrial function (reactive oxygen species; ROS, uncoupling protein; UCP). Created using Biorender.com.

8.1.3 Chapter 5

As mentioned, both AMPK activators, R481 and O-304, increased α-cell glycolysis alongside, or dependent on, the modulation of mitochondrial oxidative respiration. Findings in chapter 5 therefore briefly characterised if a new glucose-lowering allosteric pan-AMPK activator, BI-9774, could alter α-cell AMPK activity independent of changes to mitochondrial respiration. Unlike O-304, BI-9774 attenuated basal oxidative respiration and glycolysis in glucose-free conditions. In contrast to both R481 and O-304, BI-9774 exposure reduced α-cell glycolysis at high glucose. The differences between BI-9774 and O-304 as both are pan-AMPK activators, on α-cell glucose utilisation could be reflective of both direct and indirect actions on AMPK and thereby differential impact on downstream metabolic targets. In addition, AMPK activators could activate different combinations of AMPK isoenzymes in the α-cell, dependent on concentration used. Therefore, it is important to clarify the binding site of BI-9774 on AMPK, by using AMPK-ablated tissues, to accurately determine whether the bioenergetic actions of BI-9774 are AMPK-mediated.

8.1.4 Chapter 6

Over time, recurrent bouts of hypoglycaemia blunt the glucagon response to low blood glucose (Gerich *et al.*, 1973). Studies have focused on the defective central control of autonomic glucagon secretion (Heller and Cryer, 1991). α-cells express the necessary glucose-sensing machinery (including AMPK, GCK, HK, PKFKB3, K_{ATP}*)*, similarly to hypothalamic neurones, to regulate glucagon secretion dependent on glycaemic status (Acreman and Zhang, 2022). Here recurrent low glucose may suppress α-cell AMPK activity and contribute to dysregulated α-cell bioenergetics and thereby glucagon response to hypoglycaemia. Data suggest that during low glucose, RLG significantly increased α-cell glycolytic capacity and enhanced mitochondrial respiration. In addition, RLG raised α-cell glucose metabolism following reintroduction of high glucose.This may be mediated by increased expression, activity or sub-compartmental colocalisation of key rate-limiting glycolytic enzymes, GCK and

HK, driving glucose-dependent bioenergetic alterations, which require further investigation. In contrast, no changes were observed in α-cell glucagon secretion following RLG. The loss of extrinsic regulation (i.e., intra-islet factors, autonomic innervation) could thereby contribute towards the defective glucagon secretory responses commonly seen in recurrent hypoglycaemia. In summary, findings in chapter 6 provide evidence of intrinsic changes to α-cell glucose sensing following recurrent low glucose exposure.

8.1.5 Chapter 7

CFRD, a complication of cystic fibrosis (CF), affects up to 50% of CF individuals > 30 years old (Moheet and Moran, 2017). Although CFRD shares clinical phenotypes of both T1DM and T2DM, it is considered distinct. CFRD, unlike T1DM, is not characterised by autoimmune β-cell destruction but diagnosis is similarly associated with diminished cell mass and insulin deficiency (Brennan *et al.*, 2004). Similarly to T2DM aetiology, individuals with CFRD can develop insulin resistance and chronic hyperglycaemia (Lanng *et al.*, 1994). Therefore, a literature review was conducted to assess the contribution and interplay of glucose-sensing tissues in CFRD .

Previous studies have shown heterogenous *CFTR* expression in both α- and β-cells (Fulvio *et al.*, 2020). Impaired islet hormone secretion, possibly due to defective *CFTR* expression, could contribute to reactive hypoglycaemia commonly observed in CF individuals, alongside worsened glucose tolerance and exocrine insufficiency to further potentiate the development of CFRD (Moran *et al.*, 1991; Edlund *et al.*, 2017; Haliloglu *et al.*, 2017). In addition, alterations in whole-body glucose homeostasis could exacerbate CFRD progression, with evidence suggesting dysregulated central autonomic and incretin control of islet hormone secretion further impairs glucose tolerance in CF (Aitken *et al.*, 2020; Kilberg *et al.*, 2020a). In addition, a suggestion, albeit speculative, could imply defective CFTR activity in central hypothalamic neurones contribute to the dysregulated counterregulatory hormone secretion commonly seen in CF (Guo *et al.*, 2009).

There are several thoughts for consideration in future research into understanding CFRD development. As previously discussed in chapter 7, exocrine insufficiency is a large contributor to islet remodelling and worsened glucose tolerance in CF (Bogdani *et al.*, 2017). The extent of pancreatic insufficiency varies between experimental model used. DF508 mice, for instance, do not exhibit extensive pancreatic disease, as discussed in greater depth in Wilschanski and Novak, 2013. On the contrary, CF pigs and ferrets develop an extensive exocrine inflammatory phenotype in early life similar to individuals with CF (Uc *et al.*, 2015; Yi *et al.*, 2016a; Norris *et al.*, 2019). It is important to consider this species-species variation in CFRD development. Islet architecture differs between rodents and humans, but at the time of writing, no published studies have compared ferret nor pig islet architecture to human islets. Comparing both species' islet architecture is important to investigate if any differences in distribution of endocrine cells within the islet could contribute to discrepancies in defective islet hormone secretion in CF animals.

The role of intracellular energy sensing in the control of islet hormone secretion, in the context of CFRD development, has to date been understudied. Evidence suggests the α-subunit of AMPK can bind to CFTR to attenuate PKA-sensitive CFTR activity (Hallows *et al.*, 2000; Kongsuphol *et al.*, 2009a). Functionally, the AMPK inhibitor compound C failed to reduce CFTR-mediated chloride transport in AMPKα1 knockout epithelial tissues (nose, trachea and colon), indicating AMPK-CFTR dependency in whole-body chloride ion secretion (Kongsuphol *et al.*, 2009b). Chloride channels (VRAC/SWELL1, ANO1/2) are expressed in glucose-sensing β-cells and regulate depolarisation-induced insulin secretion as a result of high glucose exposure (Thompson and Satin, 2021). This could suggest that low energy status, as a consequence of glucose deprivation, could enhance endogenous AMPK, inhibiting CFTR activity and limiting insulin secretion at low glucose. It is not known whether dysregulated AMPK activity is linked to diminished islet CFTR function and/or hormone secretion in islets, indicating an area for further investigation. In addition, evidence from this literature review suggested the possible therapeutic application of novel AMPK

activators to alleviate inflammation associated with hyperglycaemia in CF and CFRD.

The key bioenergetic and glucagon findings from pharmacological, AMPK activator-focused chapters (chapter 3 – 5) are summarised in Table 8.1.

Table 8.1: Summary of key bioenergetic and glucagon findings from this thesis.

Arrows pointing up represent increased effect, with arrows point down represent reduced effect. Question mark (?) indicates question has not been studied, and two horizontal arrows pointing to each other represent no change.

	Model	R481	O-304	BI-9774
Glycolysis	αTC1.9	↑	↑	↓
Lactate	αTC1.9	↑	↑	?
Mitochondrial respiration	αTC1.9	↓	↑	↓
Fatty acid oxidation (FAO)	αTC1.9	↑	?	?
Glucagon secretion	αTC1.9	→ ←	↑	?
	Islet	→ ←	→ ←	?
Glucagon content	αTC1.9	?	↓	?
	Islet	→ ←	↓	?

8.2 Uncoupling protein-2 (UCP-2) and AMPK: a therapeutic target in metabolic diseases?

UCP-2 is an uncoupling protein localised on the mitochondrial membrane and upon activation, drives proton leak to alleviate oxidative stress (Tian *et al.*, 2018). The importance of UCP-2 is not exclusively limited to maintaining a tightly regulated antioxidant system. In pancreatic islets, UCP-2 positively regulates the glucagon secretory response to low glucose, whereby UCP-2 negatively regulates glucose-stimulated insulin secretion (GSIS), indicating UCP-2 could be integral for coupling glucose-sensitive secretory responses in peripheral tissues (Zhang *et al.*, 2001; Allister *et al.*, 2013).

Single nucleotide polymorphisms (SNPs) in the *UCP-2* gene are associated with increased risk of obesity and T2DM (Jia *et al.*, 2009). Obese-diabetic mouse models have upregulated β-cell UCP-2 expression, associated with diminished glucose-sensing in response to hyperglycaemia and thereby contributing to dysfunctional GSIS (Zhang *et al.*, 2001, 2006; Joseph *et al.*, 2002). These findings highlight UCP-2 as a crucial “controller” of physiological glucose counterregulation and glucose sensing, with dysregulated expression, at least partly, contributing towards the uncontrolled hyperglycaemia in diabetes.

AMPK, as a crucial regulator of energy homeostasis, can regulate UCP-2 dependent bioenergetics in certain tissues. For instance, AMPK activity in orexigenic neurones stimulated UCP-2 activity to sustain bioenergetic capacity in response to the hunger hormone, ghrelin (Andrews *et al.*, 2008). In addition, constitutive AMPKα2 activation similarly increased UCP-2 activity, and thereby enhanced hepatic FAO by limiting ACC-dependent inhibition in fasted conditions (Foretz *et al.*, 2005). Furthermore, AICAR increased UCP-2 activity in endothelial cells by reducing oxidative stress (Kim *et al.*, 2008). Therefore, can pharmacologically increasing AMPK activity diminish UCP-2-dependent islet dysfunction associated with DM? Evidence from chapter 3 shows AMPK activator R481 can stimulate α-cell FAO in glucose-deprived conditions, and

FAO has previously been reported to sustain glucagon secretion at low glucose (Briant *et al.*, 2018a). In addition, AMPK/UCP-2 interaction could sustain adequate glucose-sensing in both β-cells and hypothalamic cells (Beall *et al.*, 2010, 2012). Although, in α-cells, R481 did not enhance glucagon secretion. As R481 is an indirect activator of AMPK in the α-cell, one can postulate this effect is most likely not UCP-2 mediated. In contrast, O-304 enhanced α-cell mitochondrial uncoupling and glucagon secretion. If this is mediated by UCP-2 activity has not been determined but could highlight a potential pharmacological target to promote glucagon secretion in hypoglycaemia.

It would be interesting to postulate the blunted glucose sensitivity in response to hypoglycaemia commonly associated with T1DM is due to attenuated UCP-2 activity. Chapter 6 findings suggest recurrent hypoglycaemic-like conditions increased oxidative respiration, possibly driven by increased oxidative stress and attenuated UCP-2 activity; but this is yet to be clarified (Kato *et al.*, 2019; Languren *et al.*, 2019). Both UCP-2 and AMPK activity can influence glucose-sensing and thereby VMH neuronal activity, indicating the potential importance of AMPK/UCP-2 interactions in regulating peripheral glucose homeostasis (Yang *et al.*, 2010; Toda *et al.*, 2016).

Congenital hyperinsulinism (CHI), similar to T1DM, is associated with recurrent, severe hypoglycaemic episodes caused by excessive and uninhibited β-cell insulin secretion (Banerjee *et al.*, 2019; Wakeling *et al.*, 2022). Interestingly, published data showed 2.4 % of 211 individuals with CHI had a *UCP2* inactivating mutation (González-Barroso *et al.*, 2008; Ferrara *et al.*, 2017). OGTT-associated hypoglycaemia is similarly seen in some individuals with CFRD > 3 h post-OGTT, as highlighted in chapter 7, with possible links to both defective α-cell glucose-sensing and excessive paracrine inhibition of glucagon secretion (Kilberg *et al.*, 2020b). This evidence suggests the attenuated UCP-2 activity could be associated with defective glucose-sensing, in response to hypoglycaemia, in CFRD and CHI, involving excessive insulin secretion and imperfect insulin therapy respectively.

8.3 Insight into pharmacologically modulating AMPK activity

The identification of an allosteric drug and metabolite (ADaM) site in between α- and β-subunits by activators 991 and A-769662 led to the design of new, pan-AMPK activators to specifically bind to this region (Xiao *et al.*, 2013; Calabrese *et al.*, 2014). Compounds which bind to the ADaM site commonly have preferential selectivity towards a β-isoform, particularly β1, thereby providing therapeutic promise in precisely targeting AMPK activity in alleviating metabolic disease. For instance, A-769662 and 991 preferentially bind to β1-containing complexes, within a certain concentration, most likely via Ser-108 phosphorylation (Sanders *et al.*, 2007; Xiao *et al.*, 2013). The liver abundantly express AMPK β1, with A-769662 and 991 activators having potent AMPKβ1-Ser108 dependent influence on hepatic lipogenesis, triglyceride generation (Cool *et al.*, 2006; Boudaba *et al.*, 2018). Similarly, long chain fatty-acyl coenzyme A (LCFA-CoA) selectively bind to the β1 ADaM site to regulate hepatocyte fatty acid oxidation (FAO) (Pinkosky *et al.*, 2020). Thereby, pharmacologically targeting β1 provides significant promise in lowering hepatic-related complications, such as steatosis and NAFLD, commonly associated in T2DM. Some ADaM site-binding compounds bind to both AMPK β1 and β2 dependent on activator concentration used, therefore, there is need for tissue-selective β2 activators**.** SC4 selectively binds to the AMPK β2 ADaM site and has preferential binding to α2-containing complexes, indicating SC4 could have therapeutic outcomes by improving skeletal muscle glucose uptake in T2DM (Ngoei *et al.*, 2018; Ovens *et al.*, 2022). Furthermore, pilot data collected suggested the AMPK β1 isoform is primarily expressed the mouse islet, with expression of β2 protein most likely being restricted to the β-cell; corresponding with published findings (Scott *et al.*, 2015). By developing specific isoform ADaM-site activators provides promising opportunities and selectivity to precisely target different AMPK heterotrimeric complex combinations in a variety of glucose-sensing tissues.

As metformin is commonly prescribed for treating T2DM, it would be an attractive therapeutic opportunity to see if dual AMPK therapy could maximise

AMPK-dependent modulation of blood glucose. Both A-769662 and AICAR co-stimulation further drive AMPK activity by limiting α-subunit dephosphorylation and additively attenuating hepatocyte lipogenesis, a complication of T2DM and NAFLD (Ducommun *et al.*, 2014). From a whole-body perspective, individuals with T2DM already receiving metformin therapy displayed further reduced fasting plasma glucose and insulin resistance following 28-day treatment with O-304, compared to metformin alone (Steneberg *et al.*, 2018). O-304 combination therapy, alongside allosteric activators, may provide additive beneficial actions especially for individuals with T2DM already prescribed metformin to attenuate hyperglycaemia. The mechanism of action of O-304 is thought to be preventing α Thr-172 dephosphorylation, similar to A-769662, and the compound's impact on AMPK activity is dependent on the presence of the upstream kinase, LKB1 (Steneberg *et al.*, 2018). As the binding site for O-304 is currently unknown (similar to BI-9774), it would be interesting to see if O-304, in addition to LKB1-dependent actions, can selectively bind to a β1 or β2-specific AMPK ADaM site to regulate AMPK activity (Göransson *et al.*, 2007). In addition, it would be interesting to investigate if low [O-304], alongside another allosteric activator (e.g., brain permeable activator R481) could maximally stimulate AMPK activity and consequently retain both central and peripheral glucose-sensing in T1DM, but this idea is largely speculative.

Studies from this thesis used the AMPK inhibitor SBI-0206965 (SBI) to fully determine AMPK-sensitive bioenergetics. SBI was originally identified as a highly potent inhibitor of autophagy initiator, ULK-1, signalling cascade (Egan *et al.*, 2015). AMPK activation stimulates ULK-1-dependent autophagy, in addition to ULK-1-dependent phosphorylation of AMPK β Ser-108 site (Egan *et al.*, 2011; Dite *et al.*, 2018). Additive and individual stimulation of AMPKα Thr-172 phosphorylation was observed with SBI exposure in chapter 4, alongside O-304 treatment, whilst downstream AMPK activity was attenuated. This phenomenon is similarly observed in mouse embryonic fibroblasts (MEFs) and other cell types (Egan *et al.*, 2015; Dite *et al.*, 2018). SBI could promote these additive contradictory effects by binding to the α-kinase domain and effectively "disconnecting" α- and β-subunits, thereby attenuating downstream AMPK

activity (Dite *et al.*, 2018; Ahwazi *et al.*, 2021). In this thesis, SBI was deemed the most selective inhibitor at the time of study commencement. Future studies will use BAY-3827 as a higher-selective AMPK inhibitor used at low concentrations (IC_{50}; up to 15.0 nmol/l) (Ahwazi *et al.*, 2021).

8.4 Study limitations

It is important to highlight key general limitations encompassed throughout this thesis, that have not been covered in the discussion in each chapter. As the majority of the studies were conducted in *in vitro* monolayer cell models, it may not fully recapitulate islet cell functionality in a whole-body, *in vivo* context and thereby limit glucose-sensitive glucagon secretory responses. For instance, pancreatic islets are surrounded by a highly vascularised “matrix” alongside nerve endings to control islet blood flow, glucose sensitivity, and hormone secretion (Rodriguez-Diaz *et al.*, 2011b; Papas *et al.*, 2019). Neither *ex vivo* isolated islets, nor αTC1.9 cells, retain extra-pancreatic innervation and is therefore important to further corroborate findings in whole-body, *in vivo* models. Similarly, α-cells are retained in an islet, and rely at least partly on negative feedback regulation from other endocrine cell types to control glucose-sensitive hormone secretion (Nyman *et al.*, 2010; Bonner-Weir, Sullivan and Weir, 2015). Islet secretory studies conducted in this thesis, in addition to studies involving αTC1.9, overcome this limitation. In addition, pancreatic islets collected were derived from CD1 mice, in which there are known species differences in cell mass and architecture between rodent and human islets (Cabrera *et al.*, 2006). For instance, α-cells are primarily localised to the periphery in mouse islets in a “core and mantle” structure; however, endocrine cells within human islets are more randomly distributed throughout the islet (Brissova *et al.*, 2005; Bonner-Weir, Sullivan and Weir, 2015). Similarly, rodent islets have up to 20 % proportion of α-cells whereas human islets contain up to double that proportion of α-cells, comprising up to 40% of islet area, alongside known islet to islet heterogeneity being evident in published literature (Cabrera *et al.*, 2006; Bonner-Weir, Sullivan and Weir, 2015). Species heterogeneity, alongside known architectural differences, is also observed in the differential

glucose transporter expression on islet endocrine subtypes, and furthermore, in understanding DM pathogenesis, for example in CFRD, as previously reviewed in chapter 7 (De Vos *et al.*, 1995). Altogether, additional studies are important to corroborate findings generated from this thesis in both rodent *in vivo* and human islet models to recapitulate a "full" glucose-sensing model. Greater availability of published opensource datasets, including RNAseq (Sandberg Lab and bioimaging banks, Pancreatlas^{TM}), collected from human pancreata, provides a wealth of opportunities in understanding human islet physiology and pathophysiology where pancreatic tissue is limited (*Sandberg Lab Tool: Pancreas*, no date; Segerstolpe *et al.*, 2016; Saunders *et al.*, 2020).

8.5 Final conclusion

In conclusion, evidence from this thesis highlighted the role of AMPK activity in metabolically controlling downstream α-cell functionality in both physiological and pathophysiological contexts. Interestingly, since DM was classified as a "bihormonal" disorder in 1975, consensus has not yet been attained on how the α-cell intrinsically responds to changes in blood glucose (Unger and Orci, 1975). The findings discussed in this thesis suggest that α-cells have the capacity to metabolically adapt in pathophysiological contexts where substrates are restricted and therefore widening the current knowledge of intrinsic α-cell dynamics in health and disease. In addition, themes and evidence from this thesis emphasised the complex and pleiotropic metabolic targets of AMPK activators in the α-cell, suggesting the differing applicability in both hyperglycaemic and hypoglycaemic contexts. Investigating if these effects are replicable in other glucose-sensing tissues is crucial in the therapeutic relevance of novel, direct AMPK activators and understanding whole-body dysregulated glucose homeostasis observed in DM.

Chapter 9

Appendices

9 Appendices

9.1 Appendix A

Table 9.1: Liver gluconeogenic gene chromosomal profile and referenced housekeeping genes.

	Gene	Full gene name	Species	Chromosomal location	Catalogue number and assay identification (ID)
Target genes	*Fbp2/**FBPase***	*Fructose-1,6-bisphosphatase 2*	Rat	Chr.17: 372554 - 389918 on Build Rnor_6.0	4331182 - Rn00678065_m1
	*Pck1/GTP, PCK, PEPCK-C, **Pepck**, RATPEPCK*	*Phosphoenolpyruvate carboxylkinase 1 (soluble)*	Rat	Chr.3: 171213936 - 171219885 on Build Rnor_6.0	4331182 - Rn01529014_m1
	*G6pc/**G6Pase***	*Glucose-6-phosphatase, catalytic subunit*	Rat	Chr.10: 89286009 - 89296213 on Build Rnor_6.0	4331182 - Rn00689876_m1
Housekeeping genes	*Hprt1/Hgprtase*	*hypoxanthine phosphoribosyltransferase 1*	Rat	Chr.X: 158196640 - 158228815 on Build Rnor_6.0	4331182 - Rn01527840_m1
	Sdha	*succinate dehydrogenase complex, subunit A, flavoprotein (Fp)*	Rat	Chr.1: 31545631 - 31570601 on Build Rnor_6.0	4331182 - Rn00590475_m1
	Rplp1	*ribosomal protein, large, P1*	Rat	Chr.8: 66862143 - 66863476 on Build Rnor_6.0	4331182 - Rn03467157_gH

Chapter 10

Bibliography

10 Bibliography

’T Hart, L.M. *et al.* (2000) ‘Reduced second phase insulin secretion in carriers of a sulphonylurea receptor gene variant associating with Type II diabetes mellitus’, *Diabetologia*, 43(4), pp. 515–519. Available at: https://doi.org/10.1007/S001250051337/METRICS.

Abdul-Karim, F.W. *et al.* (1986) ‘Islets of Langerhans in adolescents and adults with cystic fibrosis. A quantitative study.’, *Archives of Pathology & Laboratory Medicine*, 110(7), pp. 602–606. Available at: https://europepmc.org/article/med/2872872 (Accessed: 7 April 2023).

Acreman, S. and Zhang, Q. (2022) ‘Regulation of α-cell glucagon secretion: The role of second messengers’, *Chronic Diseases and Translational Medicine*, 8(1), pp. 7–18. Available at: https://doi.org/10.1016/J.CDTM.2021.06.001/ASSET/D32551F1-4B8D-4D62-AEB9-8DD2B903FE72/ASSETS/GRAPHIC/2095-882X-08-01-003-F001.PNG.

Adler, A.I. *et al.* (2008) ‘Genetic Determinants and Epidemiology of Cystic Fibrosis–Related DiabetesResults from a British cohort of children and adults’, *Diabetes Care*, 31(9), pp. 1789–1794. Available at: https://doi.org/10.2337/DC08-0466.

Agilent Technologies Seahorse XF Buffer Factor Protocol Quick Reference Guide (no date).

Agilent Technologies Seahorse XF Cell Mito Stress Test Kit User Guide 103015-100 (no date). Available at: https://www.agilent.com/cs/library/usermanuals/public/XF_Cell_Mito_Stress_Test_Kit_User_Guide.pdf (Accessed: 19 April 2023).

Agilent Technologies Seahorse XF Glycolytic Rate Assay Kit User Guide (no date). Available at: https://www.agilent.com/cs/library/usermanuals/public/103344-400.pdf (Accessed: 19 April 2023).

Aguer, C. *et al.* (2011) ‘Galactose enhances oxidative metabolism and reveals mitochondrial dysfunction in human primary muscle cells’, *PloS one*, 6(12). Available at: https://doi.org/10.1371/JOURNAL.PONE.0028536.

Ahmad, M., Wolberg, A. and Kahwaji, C.I. (2022) ‘Biochemistry, Electron Transport Chain’, *StatPearls* [Preprint]. Available at: https://www.ncbi.nlm.nih.gov/books/NBK526105/ (Accessed: 11 April 2023).

Ahmed, N. *et al.* (2003) ‘Molecular consequences of cystic fibrosis transmembrane regulator (CFTR) gene mutations in the exocrine pancreas’, *Gut*, 52(8), pp. 1159–1164. Available at: https://doi.org/10.1136/GUT.52.8.1159.

Ahwazi, D. *et al.* (2021) ‘Investigation of the specificity and mechanism of action of the ULK1/AMPK inhibitor SBI-0206965’, *Biochemical Journal*, 478(15), pp. 2977–2997. Available at: https://doi.org/10.1042/BCJ20210284.

Aitken, M.L. *et al.* (2020) ‘Impaired counterregulatory responses to hypoglycaemia following oral glucose in adults with cystic fibrosis’, *Diabetologia*, 63(5), pp. 1055–1065. Available at: https://doi.org/10.1007/S00125-020-05096-6/FIGURES/4.

Akhmedov, D. *et al.* (2012) ‘Pyruvate dehydrogenase E1α phosphorylation is induced by glucose but does not control metabolism-secretion coupling in INS-1E clonal β-cells’, *Biochimica et Biophysica Acta (BBA) - Molecular Cell Research*, 1823(10), pp. 1815–1824. Available at: https://doi.org/10.1016/J.BBAMCR.2012.07.005.

Akil, A.A.S. *et al.* (2021) ‘Diagnosis and treatment of type 1 diabetes at the dawn of the personalized medicine era’, *Journal of Translational Medicine 2021 19:1*, 19(1), pp. 1–19. Available at: https://doi.org/10.1186/S12967-021-02778-6.

Aksit, M.A. *et al.* (2020) ‘Genetic Modifiers of Cystic Fibrosis-Related Diabetes Have Extensive Overlap With Type 2 Diabetes and Related Traits’, *The Journal of Clinical Endocrinology & Metabolism*, 105(5), pp. 1401–1415. Available at:

https://doi.org/10.1210/CLINEM/DGZ102.

Aledavood, E. *et al.* (2019) ‘Understanding the Mechanism of Direct Activation of AMP-Kinase: Toward a Fine Allosteric Tuning of the Kinase Activity’, *Journal of Chemical Information and Modeling*, 59(6), pp. 2859–2870. Available at: https://doi.org/10.1021/ACS.JCIM.8B00890/ASSET/IMAGES/LARGE/CI-2018-008905_0010.JPEG.

Aleshin, A.E. *et al.* (1998) ‘The mechanism of regulation of hexokinase: new insights from the crystal structure of recombinant human brain hexokinase complexed with glucose and glucose-6-phosphate’, *Structure*, 6(1), pp. 39–50. Available at: https://doi.org/10.1016/S0969-2126(98)00006-9.

Allen, J.M. *et al.* (1983) ‘Adult Cystic stic Fibrosis: Postprandial Response of Gut Regulatory Peptides’, *Gastroenterology*, 85(6), pp. 1379–1383. Available at: https://doi.org/10.1016/S0016-5085(83)80021-3.

Allister, E.M. *et al.* (2013) ‘UCP2 Regulates the Glucagon Response to Fasting and Starvation’, *Diabetes*, 62(5), pp. 1623–1633. Available at: https://doi.org/10.2337/DB12-0981.

Almaça, J. *et al.* (2016) ‘Human Beta Cells Produce and Release Serotonin to Inhibit Glucagon Secretion from Alpha Cells’, *Cell Reports*, 17(12), pp. 3281–3291. Available at: https://doi.org/10.1016/J.CELREP.2016.11.072.

Almeida, A., Moncada, S. and Bolaños, J.P. (2003) ‘Nitric oxide switches on glycolysis through the AMP protein kinase and 6-phosphofructo-2-kinase pathway’, *Nature Cell Biology 2003 6:1*, 6(1), pp. 45–51. Available at: https://doi.org/10.1038/ncb1080.

Alquier, T. *et al.* (2007) ‘Role of Hypothalamic Adenosine 5′-Monophosphate-Activated Protein Kinase in the Impaired Counterregulatory Response Induced by Repetitive Neuroglucopenia’, *Endocrinology*, 148(3), pp. 1367–1375. Available at: https://doi.org/10.1210/EN.2006-1039.

American Diabetes Association (2019) ‘6. Glycemic targets: Standards of

medical care in diabetesd2019', *Diabetes Care*, 42(Supplement_1), pp. S61–S70. Available at: https://doi.org/10.2337/dc19-S006.

American Diabetes Association Professional Practice Committee (2022a) '9. Pharmacologic Approaches to Glycemic Treatment: Standards of Medical Care in Diabetes—2022', *Diabetes Care*, 45(Supplement_1), pp. S125–S143. Available at: https://doi.org/10.2337/dc22-S009.

American Diabetes Association Professional Practice Committee (2022b) 'Classification and Diagnosis of Diabetes: Standards of Medical Care in Diabetes—2022', *Diabetes Care*, 45(Supplement_1), pp. S17–S38. Available at: https://doi.org/10.2337/DC22-S002.

AMPK Activator BI-9774 (no date). Available at: https://www.opnme.com/sites/default/files/opnMe_M2O_profile_AMPK_BI-9774.pdf (Accessed: 20 April 2023).

Andersen, D.H. (1938) 'Cystic fibrosis of the pancreas and its relation to celiac disease: a clinical and pathologic study', *American Journal of Diseases of Children*, 56(2), pp. 344–399. Available at: https://doi.org/10.1001/ARCHPEDI.1938.01980140114013.

Anderson, M.P. *et al.* (1991) 'Nucleoside triphosphates are required to open the CFTR chloride channel', *Cell*, 67(4), pp. 775–784. Available at: https://doi.org/10.1016/0092-8674(91)90072-7.

Anderson, R.J. *et al.* (2001) 'The prevalence of comorbid depression in adults with diabetes: a meta-analysis', *Diabetes care*, 24(6), pp. 1069–1078. Available at: https://doi.org/10.2337/DIACARE.24.6.1069.

Andersson, L.E. *et al.* (2015) 'Characterization of Stimulus-Secretion Coupling in the Human Pancreatic EndoC-βH1 Beta Cell Line', *PLOS ONE*, 10(3), p. e0120879. Available at: https://doi.org/10.1371/JOURNAL.PONE.0120879.

Andreozzi, F. *et al.* (2016) 'The GLP-1 receptor agonists exenatide and liraglutide activate Glucose transport by an AMPK-dependent mechanism',

Journal of Translational Medicine, 14(1), pp. 1–13. Available at: https://doi.org/10.1186/S12967-016-0985-7/FIGURES/8.

Andrews, Z.B. *et al.* (2008) 'UCP2 mediates ghrelin's action on NPY/AgRP neurons by lowering free radicals', *Nature*, 454(7206), p. 846. Available at: https://doi.org/10.1038/NATURE07181.

Anello, M. *et al.* (2005) 'Functional and morphological alterations of mitochondria in pancreatic beta cells from type 2 diabetic patients', *Diabetologia*, 48(2), pp. 282–289. Available at: https://doi.org/10.1007/S00125-004-1627-9/FIGURES/5.

Anil, T.M. *et al.* (2014) 'CNX-012-570, a direct AMPK activator provides strong glycemic and lipid control along with significant reduction in body weight; studies from both diet-induced obese mice and db/db mice models', *Cardiovascular Diabetology*, 13(1), p. 27. Available at: https://doi.org/10.1186/1475-2840-13-27.

Arden, C. *et al.* (2008) 'A role for PFK-2/FBPase-2, as distinct from fructose 2,6-bisphosphate, in regulation of insulin secretion in pancreatic beta-cells', *The Biochemical journal*, 411(1), pp. 41–51. Available at: https://doi.org/10.1042/BJ20070962.

Armaghanian, N. *et al.* (2016) 'Hypoglycaemia in cystic fibrosis in the absence of diabetes: A systematic review', *Journal of Cystic Fibrosis*, 15(3), pp. 274–284. Available at: https://doi.org/10.1016/J.JCF.2016.02.012.

Armaghanian, N. *et al.* (2020) 'Hypoglycemia in cystic fibrosis during an extended oral glucose tolerance test', *Pediatric Pulmonology*, 55(12), pp. 3391–3399. Available at: https://doi.org/10.1002/PPUL.25081.

Arrojo e Drigo, R. *et al.* (2019) 'Structural basis for delta cell paracrine regulation in pancreatic islets', *Nature Communications*, 10(1). Available at: https://doi.org/10.1038/S41467-019-11517-X.

Asadi, F. and Dhanvantari, S. (2021) 'Pathways of Glucagon Secretion and

Trafficking in the Pancreatic Alpha Cell: Novel Pathways, Proteins, and Targets for Hyperglucagonemia', *Frontiers in Endocrinology*, 12, p. 1236. Available at: https://doi.org/10.3389/FENDO.2021.726368/BIBTEX.

Asghar, Z.A. *et al.* (2017) 'Reduced islet function contributes to impaired glucose homeostasis in fructose-fed mice', *American Journal of Physiology - Endocrinology and Metabolism*, 312(2), pp. E109–E116. Available at: https://doi.org/10.1152/AJPENDO.00279.2016/ASSET/IMAGES/LARGE/ZH10021777040005.JPEG.

Ashfield, R. *et al.* (1999) 'Identification of the high-affinity tolbutamide site on the SUR1 subunit of the K(ATP) channel.', *Diabetes*, 48(6), pp. 1341–1347. Available at: https://doi.org/10.2337/DIABETES.48.6.1341.

Attia, R.R. *et al.* (2010) 'Regulation of Pyruvate Dehydrogenase Kinase 4 (PDK4) by Thyroid Hormone: ROLE OF THE PEROXISOME PROLIFERATOR-ACTIVATED RECEPTOR γ COACTIVATOR (PGC-1α)', *Journal of Biological Chemistry*, 285(4), pp. 2375–2385. Available at: https://doi.org/10.1074/JBC.M109.039081.

Back, S.H. and Kaufman, R.J. (2012) 'Endoplasmic Reticulum Stress and Type 2 Diabetes', *Annual review of biochemistry*, 81, p. 767. Available at: https://doi.org/10.1146/ANNUREV-BIOCHEM-072909-095555.

Bădescu, S. V. *et al.* (2016) 'The association between Diabetes mellitus and Depression', *Journal of Medicine and Life*, 9(2), p. 120. Available at: /pmc/articles/PMC4863499/ (Accessed: 10 April 2023).

Bahl, V. *et al.* (2021) 'Genetic activation of α-cell glucokinase in mice causes enhanced glucose-suppression of glucagon secretion during normal and diabetic states', *Molecular Metabolism*, 49, p. 101193. Available at: https://doi.org/10.1016/J.MOLMET.2021.101193.

Bähr, I. *et al.* (2012) 'GLUT4 in the endocrine pancreas - Indicating an impact in pancreatic islet cell physiology?', *Hormone and Metabolic Research*, 44(6), pp.

442–450. Available at: https://doi.org/10.1055/s-0032-1306335.

Bailey, S.J., Ravier, M.A. and Rutter, G.A. (2007) ‘Glucose-Dependent Regulation of γ-Aminobutyric Acid (GABAA) Receptor Expression in Mouse Pancreatic Islet α-Cells’, *Diabetes*, 56(2), pp. 320–327. Available at: https://doi.org/10.2337/DB06-0712.

Baker, E.H. *et al.* (2007) ‘Hyperglycemia and cystic fibrosis alter respiratory fluid glucose concentrations estimated by breath condensate analysis’, *Journal of Applied Physiology*, 102(5), pp. 1969–1975. Available at: https://doi.org/10.1152/JAPPLPHYSIOL.01425.2006/ASSET/IMAGES/LARGE/ZDG0050772670003.JPEG.

Balázs, A. and Mall, M.A. (2019) ‘Mucus obstruction and inflammation in early cystic fibrosis lung disease: Emerging role of the IL-1 signaling pathway’, *Pediatric Pulmonology*, 54(S3), pp. S5–S12. Available at: https://doi.org/10.1002/PPUL.24462.

Balram, A., Thapa, S. and Chatterjee, S. (2022) ‘Glycosphingolipids in Diabetes, Oxidative Stress, and Cardiovascular Disease: Prevention in Experimental Animal Models’, *International Journal of Molecular Sciences 2022, Vol. 23, Page 15442*, 23(23), p. 15442. Available at: https://doi.org/10.3390/IJMS232315442.

Baltrusch, S. *et al.* (2006) ‘Improved Metabolic Stimulus for Glucose-Induced Insulin Secretion through GK and PFK-2/FBPase-2 Coexpression in Insulin-Producing RINm5F Cells’, *Endocrinology*, 147(12), pp. 5768–5776. Available at: https://doi.org/10.1210/EN.2006-0694.

Banarer, S., McGregor, V.P. and Cryer, P.E. (2002) ‘Intraislet Hyperinsulinemia Prevents the Glucagon Response to Hypoglycemia Despite an Intact Autonomic Response’, *Diabetes*, 51(4), pp. 958–965. Available at: https://doi.org/10.2337/DIABETES.51.4.958.

Banday, M.Z., Sameer, A.S. and Nissar, S. (2020) ‘Pathophysiology of

diabetes: An overview', *Avicenna Journal of Medicine*, 10(4), p. 174. Available at: https://doi.org/10.4103/AJM.AJM_53_20.

Bando, H. *et al.* (2005) 'Phosphorylation of the 6-Phosphofructo-2-Kinase/Fructose 2,6-Bisphosphatase/PFKFB3 Family of Glycolytic Regulators in Human Cancer', *Clinical Cancer Research*, 11(16), pp. 5784–5792. Available at: https://doi.org/10.1158/1078-0432.CCR-05-0149.

Banerjee, I. *et al.* (2019) 'Therapies and outcomes of congenital hyperinsulinism-induced hypoglycaemia', *Diabetic Medicine*, 36(1), pp. 9–21. Available at: https://doi.org/10.1111/DME.13823.

Banting, F.G. and Best, C.H. (1922) 'The internal secretion of the pancreas', *The Journal of Laboratory and Clinical Medicine* [Preprint]. Available at: https://academic.oup.com/nutritionreviews/article/45/4/55/1917696 (Accessed: 11 April 2023).

Barg, S. *et al.* (2001) 'Priming of insulin granules for exocytosis by granular Cl(-) uptake and acidification', *Journal of cell science*, 114(Pt 11), pp. 2145–2154. Available at: https://doi.org/10.1242/JCS.114.11.2145.

Baron, M. *et al.* (2016) 'A Single-Cell Transcriptomic Map of the Human and Mouse Pancreas Reveals Inter- and Intra-cell Population Structure', *Cell Systems*, 3(4), pp. 346-360.e4. Available at: https://doi.org/10.1016/J.CELS.2016.08.011.

Basco, D. *et al.* (2018) 'α-cell glucokinase suppresses glucose-regulated glucagon secretion', *Nature Communications 2018 9:1*, 9(1), pp. 1–9. Available at: https://doi.org/10.1038/s41467-018-03034-0.

Basu, A. *et al.* (1993) 'Persisting Mortality in Diabetic Ketoacidosis', *Diabetic Medicine*, 10(3), pp. 282–284. Available at: https://doi.org/10.1111/J.1464-5491.1993.TB00060.X.

Battaglia, V., Salvi, M. and Toninello, A. (2005) 'Oxidative stress is responsible for mitochondrial permeability transition induction by salicylate in liver

mitochondria', *Journal of Biological Chemistry*, 280(40), pp. 33864–33872. Available at: https://doi.org/10.1074/jbc.M502391200.

Battezzati, A. *et al.* (2007) 'Spontaneous hypoglycemia in patients with cystic fibrosis', *European Journal of Endocrinology*, 156(3), pp. 369–376. Available at: https://doi.org/10.1530/EJE.1.02344.

Bayliss, J.A. *et al.* (2016) 'Ghrelin-AMPK Signaling Mediates the Neuroprotective Effects of Calorie Restriction in Parkinson's Disease', *Journal of Neuroscience*, 36(10), pp. 3049–3063. Available at: https://doi.org/10.1523/JNEUROSCI.4373-15.2016.

Beall, C. *et al.* (2010) 'Loss of AMP-activated protein kinase alpha2 subunit in mouse beta-cells impairs glucose-stimulated insulin secretion and inhibits their sensitivity to hypoglycaemia', *The Biochemical journal*, 429(2), pp. 323–333. Available at: https://doi.org/10.1042/BJ20100231.

Beall, C. *et al.* (2012) 'Mouse hypothalamic GT1-7 cells demonstrate AMPK-dependent intrinsic glucose-sensing behaviour', *Diabetologia*, 55(9), pp. 2432–2444. Available at: https://doi.org/10.1007/S00125-012-2617-Y/FIGURES/7.

Beiroa, D. *et al.* (2014) 'GLP-1 Agonism Stimulates Brown Adipose Tissue Thermogenesis and Browning Through Hypothalamic AMPK', *Diabetes*, 63(10), pp. 3346–3358. Available at: https://doi.org/10.2337/DB14-0302.

Benedetto, R. *et al.* (2017) 'Epithelial Chloride Transport by CFTR Requires TMEM16A', *Scientific Reports*, 7(1). Available at: https://doi.org/10.1038/s41598-017-10910-0.

Benkahla, M.A. *et al.* (2021) 'HLA class I hyper-expression unmasks beta cells but not alpha cells to the immune system in pre-diabetes', *Journal of autoimmunity*, 119, p. 102628. Available at: https://doi.org/10.1016/J.JAUT.2021.102628.

Benner, C. *et al.* (2014) 'The transcriptional landscape of mouse beta cells compared to human beta cells reveals notable species differences in long non-

coding RNA and protein-coding gene expression', *BMC Genomics*, 15(1), p. 620. Available at: https://doi.org/10.1186/1471-2164-15-620.

Berger, A.L., Ikuma, M. and Welsh, M.J. (2005) 'Normal gating of CFTR requires ATP binding to both nucleotide-binding domains and hydrolysis at the second nucleotide-binding domain', *Proceedings of the National Academy of Sciences of the United States of America*, 102(2), pp. 455–460. Available at: https://doi.org/10.1073/PNAS.0408575102.

Berger, C. and Zdzieblo, D. (2020) 'Glucose transporters in pancreatic islets', *Pflugers Archiv*, 472(9), p. 1249. Available at: https://doi.org/10.1007/S00424-020-02383-4.

Bertelli, E. *et al.* (2001) 'Association between islets of Langerhans and pancreatic ductal system in adult rat. Where endocrine and exocrine meet together?', *Diabetologia*, 44(5), pp. 575–584. Available at: https://doi.org/10.1007/S001250051663.

Bertelli, E. and Bendayan, M. (2005) 'Association between endocrine pancreas and ductal system. More than an epiphenomenon of endocrine differentiation and development?', *Journal of Histochemistry and Cytochemistry*, 53(9), pp. 1071–1086. Available at: https://doi.org/10.1369/JHC.5R6640.2005/ASSET/IMAGES/LARGE/10.1369_JHC.5R6640.2005-FIG2.JPEG.

Bhalla, K. *et al.* (2011) 'PGC1α promotes tumor growth by inducing gene expression programs supporting lipogenesis', *Cancer Research*, 71(21), pp. 6888–6898. Available at: https://doi.org/10.1158/0008-5472.CAN-11-1011/649989/AM/PGC1-PROMOTES-TUMOR-GROWTH-BY-INDUCING-GENE.

Bieri, M. *et al.* (2012) 'AMP-Activated Protein Kinase β-Subunit Requires Internal Motion for Optimal Carbohydrate Binding', *Biophysical Journal*, 102(2), pp. 305–314. Available at: https://doi.org/10.1016/J.BPJ.2011.12.012.

Billet, A. *et al.* (2013) ‘Role of Tyrosine Phosphorylation in the Muscarinic Activation of the Cystic Fibrosis Transmembrane Conductance Regulator (CFTR)’, *The Journal of Biological Chemistry*, 288(30), p. 21815. Available at: https://doi.org/10.1074/JBC.M113.479360.

Billet, A. and Hanrahan, J.W. (2013) ‘The secret life of CFTR as a calcium-activated chloride channel’, *Journal of Physiology*, 591(21), pp. 5273–5278. Available at: https://doi.org/10.1113/JPHYSIOL.2013.261909.

Birk, J.B. and Wojtaszewski, J.F.P. (2006) ‘Predominant alpha2/beta2/gamma3 AMPK activation during exercise in human skeletal muscle’, *The Journal of physiology*, 577(Pt 3), pp. 1021–1032. Available at: https://doi.org/10.1113/JPHYSIOL.2006.120972.

Bisgaard Bengtsen, M., Møller, N. and Bengtsen, M.B. (2022) ‘Experimentally Induced Hypoglycemia-associated Autonomic Failure in Humans: Determinants, Designs, and Drawbacks’, *Journal of the Endocrine Society*, 6(10). Available at: https://doi.org/10.1210/JENDSO/BVAC123.

Blodgett, D.M. *et al.* (2015) ‘Novel Observations From Next-Generation RNA Sequencing of Highly Purified Human Adult and Fetal Islet Cell Subsets’, *Diabetes*, 64(9), pp. 3172–3181. Available at: https://doi.org/10.2337/DB15-0039.

Bodansky, H.J. *et al.* (1992) ‘Evidence for an environmental effect in the aetiology of insulin dependent diabetes in a transmigratory population.’, *BMJ : British Medical Journal*, 304(6833), p. 1020. Available at: https://doi.org/10.1136/BMJ.304.6833.1020.

Boddu, S.K., Aurangabadkar, G. and Kuchay, M.S. (2020) ‘New onset diabetes, type 1 diabetes and COVID-19’, *Diabetes & Metabolic Syndrome: Clinical Research & Reviews*, 14(6), pp. 2211–2217. Available at: https://doi.org/10.1016/J.DSX.2020.11.012.

Boden, G. and Chen, X. (1999) ‘Effects of fatty acids and ketone bodies on

basal insulin secretion in type 2 diabetes.', *Diabetes*, 48(3), pp. 577–583. Available at: https://doi.org/10.2337/DIABETES.48.3.577.

Bogdani, M. *et al.* (2017) 'Structural abnormalities in islets from very young children with cystic fibrosis may contribute to cystic fibrosis-related diabetes', *Scientific reports*, 7(1). Available at: https://doi.org/10.1038/S41598-017-17404-Z.

Boldison, J. and Wong, F.S. (2016) 'Immune and Pancreatic β Cell Interactions in Type 1 Diabetes', *Trends in endocrinology and metabolism: TEM*, 27(12), pp. 856–867. Available at: https://doi.org/10.1016/J.TEM.2016.08.007.

Bonner-Weir, S., Sullivan, B.A. and Weir, G.C. (2015) 'Human Islet Morphology Revisited: Human and Rodent Islets Are Not So Different After All', *Journal of Histochemistry and Cytochemistry*, 63(8), p. 604. Available at: https://doi.org/10.1369/0022155415570969.

Bonora, M. *et al.* (2012) 'ATP synthesis and storage', *Purinergic Signalling*, 8(3), p. 343. Available at: https://doi.org/10.1007/S11302-012-9305-8.

Boom, A. *et al.* (2007) 'Expression and localization of cystic fibrosis transmembrane conductance regulator in the rat endocrine pancreas', *Endocrine*, 32(2), pp. 197–205. Available at: https://doi.org/10.1007/S12020-007-9026-X/FIGURES/5.

Borg, M.A. *et al.* (1997) 'Local ventromedial hypothalamus glucose perfusion blocks counterregulation during systemic hypoglycemia in awake rats', *The Journal of clinical investigation*, 99(2), pp. 361–365. Available at: https://doi.org/10.1172/JCI119165.

Borg, W.P. *et al.* (1995) 'Local ventromedial hypothalamus glucopenia triggers counterregulatory hormone release', *Diabetes*, 44(2), pp. 180–184. Available at: https://doi.org/10.2337/DIAB.44.2.180.

Boß, M. *et al.* (2016) 'AMPK-independent inhibition of human macrophage ER stress response by AICAR', *Scientific Reports 2016 6:1*, 6(1), pp. 1–10.

Available at: https://doi.org/10.1038/srep32111.

Boudaba, N. *et al.* (2018) 'AMPK Re-Activation Suppresses Hepatic Steatosis but its Downregulation Does Not Promote Fatty Liver Development', *EBioMedicine*, 28, pp. 194–209. Available at: https://doi.org/10.1016/J.EBIOM.2018.01.008.

Bozadjieva, N. *et al.* (2017) 'Loss of mTORC1 signaling alters pancreatic α cell mass and impairs glucagon secretion', *The Journal of Clinical Investigation*, 127(12), pp. 4379–4393. Available at: https://doi.org/10.1172/JCI90004.

Bradford, M.M. (1976) 'A rapid and sensitive method for the quantitation of microgram quantities of protein utilizing the principle of protein-dye binding', *Analytical Biochemistry*, 72(1–2), pp. 248–254. Available at: https://doi.org/10.1016/0003-2697(76)90527-3.

Brass, E.P. and Hoppel, C.L. (2015) 'Mitochondria as targets of drug toxicity: Lessons from the R118 phase I experience', *Clinical Pharmacology & Therapeutics*, 98(5), pp. 464–466. Available at: https://doi.org/10.1002/CPT.160.

Brennan, A.L. *et al.* (2004) 'Clinical importance of cystic fibrosis-related diabetes', *Journal of Cystic Fibrosis*, 3(4), pp. 209–222. Available at: https://doi.org/10.1016/J.JCF.2004.08.001.

Brereton, M.F. *et al.* (2014) 'Reversible changes in pancreatic islet structure and function produced by elevated blood glucose', *Nature Communications 2014 5:1*, 5(1), pp. 1–11. Available at: https://doi.org/10.1038/ncomms5639.

Brereton, M.F. *et al.* (2016) 'Hyperglycaemia induces metabolic dysfunction and glycogen accumulation in pancreatic β-cells', *Nature Communications 2016 7:1*, 7(1), pp. 1–15. Available at: https://doi.org/10.1038/ncomms13496.

Briant, L.J.B. *et al.* (2018a) 'CPT1a-Dependent Long-Chain Fatty Acid Oxidation Contributes to Maintaining Glucagon Secretion from Pancreatic Islets', *Cell Reports*, 23(11), pp. 3300–3311. Available at:

https://doi.org/10.1016/j.celrep.2018.05.035.

Briant, L.J.B. *et al.* (2018b) ‘δ-cells and β-cells are electrically coupled and regulate α-cell activity via somatostatin’, *Journal of Physiology*, 596(2), pp. 197–215. Available at: https://doi.org/10.1113/JP274581.

Brissova, M. *et al.* (2005) ‘Assessment of human pancreatic islet architecture and composition by laser scanning confocal microscopy’, *Journal of Histochemistry and Cytochemistry*, 53(9), pp. 1087–1097. Available at: https://doi.org/10.1369/jhc.5C6684.2005.

Brissova, M. *et al.* (2018) ‘α Cell Function and Gene Expression Are Compromised in Type 1 Diabetes’, *Cell Reports*, 22(10), pp. 2667–2676. Available at: https://doi.org/10.1016/j.celrep.2018.02.032.

Brookes, P.S. *et al.* (1998) ‘Peroxynitrite and brain mitochondria: Evidence for increased proton leak’, *Journal of Neurochemistry*, 70(5), pp. 2195–2202. Available at: https://doi.org/10.1046/J.1471-4159.1998.70052195.X.

Brown, A.E. *et al.* (2018) ‘Pharmacological activation of AMPK and glucose uptake in cultured human skeletal muscle cells from patients with ME/CFS’, *Bioscience Reports*, 38(3). Available at: https://doi.org/10.1042/BSR20180242/57494.

Brown, A.M. *et al.* (2005) ‘Astrocyte glycogen metabolism is required for neural activity during aglycemia or intense stimulation in mouse white matter’, *Journal of Neuroscience Research*, 79(1–2), pp. 74–80. Available at: https://doi.org/10.1002/JNR.20335.

Brun, T. *et al.* (2020) ‘AMPK Profiling in Rodent and Human Pancreatic Beta-Cells under Nutrient-Rich Metabolic Stress’, *International Journal of Molecular Sciences*, 21(11). Available at: https://doi.org/10.3390/IJMS21113982.

Brunelle, J.L. and Green, R. (2014) ‘One-dimensional SDS-Polyacrylamide Gel Electrophoresis (1D SDS-PAGE)’, *Methods in Enzymology*, 541, pp. 151–159. Available at: https://doi.org/10.1016/B978-0-12-420119-4.00012-4.

Bultot, L. *et al.* (2016) ‘Benzimidazole derivative small-molecule 991 enhances AMPK activity and glucose uptake induced by AICAR or contraction in skeletal muscle’, *American Journal of Physiology - Endocrinology and Metabolism*, 311(4), pp. E706–E719. Available at: https://doi.org/10.1152/AJPENDO.00237.2016/ASSET/IMAGES/LARGE/ZH10151676530007.JPEG.

Burrack, A.L., Martinov, T. and Fife, B.T. (2017) ‘T cell-mediated beta cell destruction: Autoimmunity and alloimmunity in the context of type 1 diabetes’, *Frontiers in Endocrinology*, 8, p. 343. Available at: https://doi.org/10.3389/fendo.2017.00343.

Cabrera, O. *et al.* (2006) ‘The unique cytoarchitecture of human pancreatic islets has implications for islet cell function’, *Proceedings of the National Academy of Sciences*, 103(7), pp. 2334–2339. Available at: https://doi.org/10.1073/pnas.0510790103.

Cabrera, O. *et al.* (2008) ‘Glutamate Is a Positive Autocrine Signal for Glucagon Release’, *Cell Metabolism*, 7(6), pp. 545–554. Available at: https://doi.org/10.1016/J.CMET.2008.03.004.

Calabrese, M.F. *et al.* (2014) ‘Structural Basis for AMPK Activation: Natural and Synthetic Ligands Regulate Kinase Activity from Opposite Poles by Different Molecular Mechanisms’, *Structure*, 22(8), pp. 1161–1172. Available at: https://doi.org/10.1016/J.STR.2014.06.009.

Calella, P. *et al.* (2018) ‘Cystic fibrosis, body composition, and health outcomes: a systematic review’, *Nutrition (Burbank, Los Angeles County, Calif.)*, 55–56, pp. 131–139. Available at: https://doi.org/10.1016/J.NUT.2018.03.052.

Cameron, A.R. *et al.* (2016) ‘Anti-Inflammatory Effects of Metformin Irrespective of Diabetes Status’, *Circulation Research*, 119(5), pp. 652–665. Available at: https://doi.org/10.1161/CIRCRESAHA.116.308445/-/DC1.

Cameron, A.R. *et al.* (2018) ‘Metformin selectively targets redox control of

complex I energy transduction', *Redox Biology*, 14, pp. 187–197. Available at: https://doi.org/10.1016/J.REDOX.2017.08.018.

Campbell, E. *et al.* (2014) 'Fructose-Induced Hypertriglyceridemia: A Review', *Nutrition in the Prevention and Treatment of Abdominal Obesity*, pp. 197–205. Available at: https://doi.org/10.1016/B978-0-12-407869-7.00019-2.

Cappel, D.A. *et al.* (2019) 'Pyruvate-Carboxylase-Mediated Anaplerosis Promotes Antioxidant Capacity by Sustaining TCA Cycle and Redox Metabolism in Liver', *Cell Metabolism*, 29(6), pp. 1291-1305.e8. Available at: https://doi.org/10.1016/J.CMET.2019.03.014.

Cardoso, S. and Moreira, P.I. (2021) 'Insulin-induced recurrent hypoglycemia up-regulates glucose metabolism in the brain cortex of chemically induced diabetic rats', *International Journal of Molecular Sciences*, 22(24), p. 13470. Available at: https://doi.org/10.3390/IJMS222413470/S1.

Carling, D. (2017) 'AMPK signalling in health and disease', *Current Opinion in Cell Biology*, 45, pp. 31–37. Available at: https://doi.org/10.1016/J.CEB.2017.01.005.

Cerf, M.E. (2013) 'Beta cell dysfunction and insulin resistance', *Frontiers in Endocrinology*, 4(MAR), p. 37. Available at: https://doi.org/10.3389/FENDO.2013.00037/BIBTEX.

CFTR2 Variant List History (no date). Available at: https://cftr2.org/mutations_history (Accessed: 6 April 2023).

Chacko, B.K. *et al.* (2014) 'The Bioenergetic Health Index: a new concept in mitochondrial translational research', *Clinical Science*, 127, pp. 367–373. Available at: https://doi.org/10.1042/CS20140101.

Chapal, J. *et al.* (1985) 'Evidence for an A2-subtype adenosine receptor on pancreatic glucagon secreting cells.', *British Journal of Pharmacology*, 86(3), p. 565. Available at: https://doi.org/10.1111/J.1476-5381.1985.TB08932.X.

Chappe, V. *et al.* (2003) ‘Phosphorylation of protein kinase C sites in NBD1 and the R domain control CFTR channel activation by PKA’, *The Journal of Physiology*, 548(Pt 1), p. 39. Available at: https://doi.org/10.1113/JPHYSIOL.2002.035790.

Charron, M.J. and Vuguin, P.M. (2015) ‘Lack of glucagon receptor signaling and its implications beyond glucose homeostasis’, *Journal of Endocrinology*, 224(3), pp. R123–R130. Available at: https://doi.org/10.1530/JOE-14-0614.

Chen, Q., Shen, Y. and Zheng, J. (2021) ‘A review of cystic fibrosis: Basic and clinical aspects’, *Animal Models and Experimental Medicine*, 4(3), pp. 220–232. Available at: https://doi.org/10.1002/AME2.12180.

Cheng, S.H. *et al.* (1990) ‘Defective intracellular transport and processing of CFTR is the molecular basis of most cystic fibrosis’, *Cell*, 63(4), pp. 827–834. Available at: https://doi.org/10.1016/0092-8674(90)90148-8.

Cheng, S.H. *et al.* (1991) ‘Phosphorylation of the R domain by cAMP-dependent protein kinase regulates the CFTR chloride channel’, *Cell*, 66(5), pp. 1027–1036. Available at: https://doi.org/10.1016/0092-8674(91)90446-6.

Choi, B.Y. *et al.* (2013) ‘Pyruvate Administration Reduces Recurrent/Moderate Hypoglycemia-Induced Cortical Neuron Death in Diabetic Rats’, *PLOS ONE*, 8(11), p. e81523. Available at: https://doi.org/10.1371/JOURNAL.PONE.0081523.

Choi, Y., Abdelmegeed, M.A. and Song, B.J. (2017) ‘Diet high in fructose promotes liver steatosis and hepatocyte apoptosis in C57BL/6J female mice: Role of disturbed lipid homeostasis and increased oxidative stress’, *Food and chemical toxicology : an international journal published for the British Industrial Biological Research Association*, 103, p. 111. Available at: https://doi.org/10.1016/J.FCT.2017.02.039.

Christensen, M. *et al.* (2011) ‘Glucose-Dependent Insulinotropic Polypeptide: A Bifunctional Glucose-Dependent Regulator of Glucagon and Insulin Secretion in

Humans', *Diabetes*, 60(12), p. 3103. Available at: https://doi.org/10.2337/DB11-0979.

Cliff, W.H., Schoumacher, R.A. and Frizzell, R.A. (1992) 'cAMP-activated Cl channels in CFTR-transfected cystic fibrosis pancreatic epithelial cells', *The American journal of physiology*, 262(5 Pt 1). Available at: https://doi.org/10.1152/AJPCELL.1992.262.5.C1154.

Coelho, A.I., Berry, G.T. and Rubio-Gozalbo, M.E. (2015) 'Galactose metabolism and health', *Current Opinion in Clinical Nutrition and Metabolic Care*, 18(4), pp. 422–427. Available at: https://doi.org/10.1097/MCO.0000000000000189.

Cokorinos, E.C. *et al.* (2017) 'Activation of Skeletal Muscle AMPK Promotes Glucose Disposal and Glucose Lowering in Non-human Primates and Mice', *Cell Metabolism*, 25(5), pp. 1147-1159.e10. Available at: https://doi.org/10.1016/J.CMET.2017.04.010.

Conte, F. *et al.* (2021) 'Galactose in human metabolism, glycosylation and congenital metabolic diseases: Time for a closer look', *Biochimica et Biophysica Acta (BBA) - General Subjects*, 1865(8), p. 129898. Available at: https://doi.org/10.1016/J.BBAGEN.2021.129898.

Cool, B. *et al.* (2006) 'Identification and characterization of a small molecule AMPK activator that treats key components of type 2 diabetes and the metabolic syndrome', *Cell Metabolism*, 3(6), pp. 403–416. Available at: https://doi.org/10.1016/j.cmet.2006.05.005.

Cooper, J.D. *et al.* (2008) 'Meta-analysis of genome-wide association study data identifies additional type 1 diabetes loci', *Nature genetics*, 40(12), p. 1399. Available at: https://doi.org/10.1038/NG.249.

Couce, M. *et al.* (1996) 'Diabetes mellitus in cystic fibrosis is characterized by islet amyloidosis', *The Journal of clinical endocrinology and metabolism*, 81(3), pp. 1267–1272. Available at: https://doi.org/10.1210/JCEM.81.3.8772610.

Coughlan, K.A. *et al.* (2014) ‘AMPK activation: A therapeutic target for type 2 diabetes?’, *Diabetes, Metabolic Syndrome and Obesity: Targets and Therapy*, 7, pp. 241–253. Available at: https://doi.org/10.2147/DMSO.S43731.

Coutinho-Silva, R. *et al.* (2003) ‘P2X and P2Y purinoceptor expression in pancreas from streptozotocin-diabetic rats’, *Molecular and Cellular Endocrinology*, 204(1–2), pp. 141–154. Available at: https://doi.org/10.1016/S0303-7207(03)00003-0.

Cruz, A.M. (2019) *The integrated physiology of glucose homeostasis: regulation by extracellular and intracellular nucleotide sensors*. University of Exeter.

Cruz, A.M. *et al.* (2021) ‘Brain Permeable AMP-Activated Protein Kinase Activator R481 Raises Glycaemia by Autonomic Nervous System Activation and Amplifies the Counterregulatory Response to Hypoglycaemia in Rats’, *Frontiers in Endocrinology*, 12, p. 1630. Available at: https://doi.org/10.3389/FENDO.2021.697445/BIBTEX.

Cryer, P.E. (2001) ‘Hypoglycemia-associated autonomic failure in diabetes’, *American Journal of Physiology - Endocrinology and Metabolism*, 281(6), pp. E1115-21. Available at: https://doi.org/10.1152/ajpendo.2001.281.6.e1115.

Cryer, P.E. (2004) ‘Diverse Causes of Hypoglycemia-Associated Autonomic Failure in Diabetes’, *https://doi.org/10.1056/NEJMra031354*, 350(22), pp. 2272–2279. Available at: https://doi.org/10.1056/NEJMRA031354.

Cryer, P.E. (2005) ‘Mechanisms of Hypoglycemia-Associated Autonomic Failure and Its Component Syndromes in Diabetes’, *Diabetes*, 54(12), pp. 3592–3601. Available at: https://doi.org/10.2337/DIABETES.54.12.3592.

Cryer, P.E. (2008) ‘The barrier of hypoglycemia in diabetes’, *Diabetes*, 57(12), pp. 3169–3176. Available at: https://doi.org/10.2337/DB08-1084.

Cryer, P.E. (2010) ‘Hypoglycemia in type 1 diabetes mellitus’, *Endocrinology and Metabolism Clinics of North America*, 39(3), pp. 641–654. Available at: https://doi.org/10.1016/j.ecl.2010.05.003.

Cryer, P.E. (2015) ‘Hypoglycemia-Associated Autonomic Failure in Diabetes: Maladaptive, Adaptive, or Both?’, *Diabetes*, 64, p. 2571. Available at: https://doi.org/10.2337/db15-0331.

Csanády, L., Vergani, P. and Gadsby, D.C. (2019) ‘Structure, gating, and regulation of the CFTR anion channel’, *Physiological Reviews*, 99(1), pp. 707–738. Available at: https://doi.org/10.1152/PHYSREV.00007.2018/ASSET/IMAGES/LARGE/Z9J00011928970006.JPEG.

Cucinotta, D. *et al.* (1994) ‘First-phase insulin response to intravenous glucose in cystic fibrosis patients with different degrees of glucose tolerance’, *Journal of Pediatric Endocrinology and Metabolism*, 7(1), pp. 13–18. Available at: https://doi.org/10.1515/JPEM.1994.7.1.13/MACHINEREADABLECITATION/RIS.

Cullen, K.S. *et al.* (2014) ‘Glucagon induces translocation of glucokinase from the cytoplasm to the nucleus of hepatocytes by transfer between 6-phosphofructo 2-kinase/fructose 2,6-bisphosphatase-2 and the glucokinase regulatory protein’, *Biochimica et Biophysica Acta*, 1843(6), p. 1123. Available at: https://doi.org/10.1016/J.BBAMCR.2014.02.006.

Cuozzo, F. *et al.* (2022) ‘High-resolution glucose fate-mapping reveals LDHB-dependent lactate production by human pancreatic β cells’, *bioRxiv*, p. 2022.12.21.521364. Available at: https://doi.org/10.1101/2022.12.21.521364.

Cusi, K. *et al.* (2021) ‘Efficacy and safety of PXL770, a direct AMP kinase activator, for the treatment of non-alcoholic fatty liver disease (STAMP-NAFLD): a randomised, double-blind, placebo-controlled, phase 2a study’, *The Lancet Gastroenterology and Hepatology*, 6(11), pp. 889–902. Available at: https://doi.org/10.1016/S2468-1253(21)00300-9.

Cystic Fibrosis Trust (2022) ‘UK Cystic Fibrosis Registry 2021 Annual Data Report’.

Czech, M.P. (1985) ‘The nature and regulation of the insulin receptor: structure and function’, *Annual review of physiology*, 47(1), pp. 357–381. Available at: https://doi.org/10.1146/ANNUREV.PH.47.030185.002041.

Dagon, Y. *et al.* (2012) ‘p70S6 Kinase Phosphorylates AMPK on Serine 491 to Mediate Leptin’s Effect on Food Intake’, *Cell Metabolism*, 16(1), pp. 104–112. Available at: https://doi.org/10.1016/J.CMET.2012.05.010.

Dai, X.Q. *et al.* (2022) ‘Heterogenous impairment of α cell function in type 2 diabetes is linked to cell maturation state’, *Cell Metabolism*, 34(2), pp. 256-268.e5. Available at: https://doi.org/10.1016/J.CMET.2021.12.021.

Danielle Dean, E. (2020) ‘A Primary Role for α-Cells as Amino Acid Sensors’, *Diabetes*, 69(4), pp. 542–549. Available at: https://doi.org/10.2337/DBI19-0021.

Dasgupta, B. *et al.* (2023) ‘The AMPK β2 Subunit Is Required for Energy Homeostasis during Metabolic Stress’, *https://doi.org/10.1128/MCB.05853-11*, 32(14), pp. 2837–2848. Available at: https://doi.org/10.1128/MCB.05853-11.

Dash, S. *et al.* (2018) ‘Evaluation of the specific effects of intranasal glucagon on glucose production and lipid concentration in healthy men during a pancreatic clamp’, *Diabetes, Obesity and Metabolism*, 20(2), pp. 328–334. Available at: https://doi.org/10.1111/DOM.13069.

Dashty, M. (2013) ‘A quick look at biochemistry: Carbohydrate metabolism’, *Clinical Biochemistry*, 46(15), pp. 1339–1352. Available at: https://doi.org/10.1016/J.CLINBIOCHEM.2013.04.027.

Davidson, H.W., Rhodes, C.J. and Hutton, J.C. (1988) ‘Intraorganellar calcium and pH control proinsulin cleavage in the pancreatic beta cell via two distinct site-specific endopeptidases’, *Nature*, 333(6168), pp. 93–96. Available at: https://doi.org/10.1038/333093A0.

DeBalsi, K.L. *et al.* (2014) ‘Targeted Metabolomics Connects Thioredoxin-interacting Protein (TXNIP) to Mitochondrial Fuel Selection and Regulation of Specific Oxidoreductase Enzymes in Skeletal Muscle’, *The Journal of Biological*

Chemistry, 289(12), p. 8106. Available at: https://doi.org/10.1074/JBC.M113.511535.

Defronzo, R. *et al.* (2016) 'Metformin-associated lactic acidosis: Current perspectives on causes and risk', *Metabolism*, 65(2), pp. 20–29. Available at: https://doi.org/10.1016/J.METABOL.2015.10.014.

Defronzo, R.A. and Tripathy, D. (2009) 'Skeletal Muscle Insulin Resistance Is the Primary Defect in Type 2 Diabetes'. Available at: https://doi.org/10.2337/dc09-S302.

Demetriades, C., Plescher, M. and Teleman, A.A. (2016) 'Lysosomal recruitment of TSC2 is a universal response to cellular stress', *Nature Communications*, 7. Available at: https://doi.org/10.1038/NCOMMS10662.

Detaille, D. *et al.* (2002) 'Obligatory role of membrane events in the regulatory effect of metformin on the respiratory chain function', *Biochemical Pharmacology*, 63(7), pp. 1259–1272. Available at: https://doi.org/10.1016/S0006-2952(02)00858-4.

Dewdney, B. *et al.* (2020) 'A Sweet Connection? Fructose's Role in Hepatocellular Carcinoma', *Biomolecules 2020, Vol. 10, Page 496*, 10(4), p. 496. Available at: https://doi.org/10.3390/BIOM10040496.

Dholariya, S.J. and Orrick, J.A. (2022) 'Biochemistry, Fructose Metabolism', *StatPearls* [Preprint]. Available at: https://www.ncbi.nlm.nih.gov/books/NBK576428/ (Accessed: 31 March 2023).

Diao, J. *et al.* (2008) 'UCP2 is highly expressed in pancreatic α-cells and influences secretion and survival', *Proceedings of the National Academy of Sciences of the United States of America*, 105(33), pp. 12057–12062. Available at: https://doi.org/10.1073/PNAS.0710434105/SUPPL_FILE/0710434105SI.PDF.

DiGruccio, M.R. *et al.* (2016) 'Comprehensive alpha, beta and delta cell transcriptomes reveal that ghrelin selectively activates delta cells and promotes

somatostatin release from pancreatic islets', *Molecular metabolism*, 5(7), pp. 449–458. Available at: https://doi.org/10.1016/J.MOLMET.2016.04.007.

DiMeglio, L.A., Evans-Molina, C. and Oram, R.A. (2018) 'Type 1 diabetes', *Lancet (London, England)*, 391(10138), p. 2449. Available at: https://doi.org/10.1016/S0140-6736(18)31320-5.

Dite, T.A. *et al.* (2018) 'AMP-activated protein kinase selectively inhibited by the type II inhibitor SBI-0206965', *Journal of Biological Chemistry*, 293(23), pp. 8874–8885. Available at: https://doi.org/10.1074/JBC.RA118.003547/ATTACHMENT/61D3CB3A-159B-451D-863F-9555F694BA39/MMC1.PDF.

Dogliotti, G. *et al.* (2017) 'Membrane-binding and activation of LKB1 by phosphatidic acid is essential for development and tumour suppression', *Nature Communications 2017 8:1*, 8(1), pp. 1–12. Available at: https://doi.org/10.1038/ncomms15747.

Doliba, N.M. *et al.* (2022) 'α Cell dysfunction in islets from nondiabetic, glutamic acid decarboxylase autoantibody–positive individuals', *The Journal of Clinical Investigation*, 132(11). Available at: https://doi.org/10.1172/JCI156243.

Doménech, E. *et al.* (2015) 'AMPK and PFKFB3 mediate glycolysis and survival in response to mitophagy during mitotic arrest', *Nature cell biology*, 17(10), pp. 1304–1316. Available at: https://doi.org/10.1038/NCB3231.

Dominy, J.E. and Puigserver, P. (2013) 'Mitochondrial biogenesis through activation of nuclear signaling proteins', *Cold Spring Harbor perspectives in biology*, 5(7). Available at: https://doi.org/10.1101/CSHPERSPECT.A015008.

Dorajoo, R. *et al.* (2017) 'Single-cell transcriptomics of East-Asian pancreatic islets cells', *Scientific Reports*, 7(1). Available at: https://doi.org/10.1038/S41598-017-05266-4.

Dornas, W.C. *et al.* (2017) 'Oxidative stress causes hypertension and activation of nuclear factor-κB after high-fructose and salt treatments', *Scientific reports*, 7.

Available at: https://doi.org/10.1038/SREP46051.

Dranka, B.P., Hill, B.G. and Darley-Usmar, V.M. (2010) 'Mitochondrial reserve capacity in endothelial cells: The impact of nitric oxide and reactive oxygen species', *Free Radical Biology and Medicine*, 48(7), pp. 905–914. Available at: https://doi.org/10.1016/J.FREERADBIOMED.2010.01.015.

Du, K., Sharma, M. and Lukacs, G.L. (2005) 'The DeltaF508 cystic fibrosis mutation impairs domain-domain interactions and arrests post-translational folding of CFTR', *Nature structural & molecular biology*, 12(1), pp. 17–25. Available at: https://doi.org/10.1038/NSMB882.

Duca, L.M. *et al.* (2017) 'Diabetic Ketoacidosis at Diagnosis of Type 1 Diabetes Predicts Poor Long-term Glycemic Control', *Diabetes Care*, 40(9), pp. 1249–1255. Available at: https://doi.org/10.2337/DC17-0558.

Ducommun, S. *et al.* (2014) 'Enhanced activation of cellular AMPK by dual-small molecule treatment: AICAR and A769662', *Am J Physiol Endocrinol Metab*, 306, pp. 688–696. Available at: https://doi.org/10.1152/ajpendo.00672.2013.-AMP-activated.

Dufour, S. *et al.* (2009) 'Regulation of net hepatic glycogenolysis and gluconeogenesis by epinephrine in humans', *American Journal of Physiology - Endocrinology and Metabolism*, 297(1), p. E231. Available at: https://doi.org/10.1152/AJPENDO.00222.2009.

Dunn-Meynell, A.A. *et al.* (2002) 'Glucokinase Is the Likely Mediator of Glucosensing in Both Glucose-Excited and Glucose-Inhibited Central Neurons', *Diabetes*, 51(7), pp. 2056–2065. Available at: https://doi.org/10.2337/DIABETES.51.7.2056.

Durie, P.R. (1989) 'The pathophysiology of the pancreatic defect in cystic fibrosis', *Acta paediatrica Scandinavica. Supplement*, 363(363), pp. 41–44. Available at: https://doi.org/10.1111/APA.1989.78.S363.41.

Echtay, K.S. *et al.* (2002) 'Superoxide activates mitochondrial uncoupling

proteins', *Nature*, 415(6867), pp. 96–99. Available at: https://doi.org/10.1038/415096A.

Edlund, A. *et al.* (2014) 'CFTR and Anoctamin 1 (ANO1) contribute to cAMP amplified exocytosis and insulin secretion in human and murine pancreatic beta-cells', *BMC medicine*, 12(1). Available at: https://doi.org/10.1186/1741-7015-12-87.

Edlund, A. *et al.* (2017) 'CFTR is involved in the regulation of glucagon secretion in human and rodent alpha cells', *Scientific Reports*, 7(1). Available at: https://doi.org/10.1038/S41598-017-00098-8.

Edlund, A. *et al.* (2019) 'Defective exocytosis and processing of insulin in a cystic fibrosis mouse model', *Journal of Endocrinology*, 241(1), pp. 45–57. Available at: https://doi.org/10.1530/JOE-18-0570.

Effects of Metformin on Airway Ion Channel Dysfunction in Cystic Fibrosis-related Diabetes (no date). Available at: https://clinicaltrials.gov/ct2/show/NCT04530383 (Accessed: 7 April 2023).

Egan, D.F. *et al.* (2011) 'Phosphorylation of ULK1 (hATG1) by AMP-activated protein kinase connects energy sensing to mitophagy', *Science*, 331(6016), pp. 456–461. Available at: https://doi.org/10.1126/SCIENCE.1196371/SUPPL_FILE/EGAN-SOM.PDF.

Egan, D.F. *et al.* (2015) 'Small Molecule Inhibition of the Autophagy Kinase ULK1 and Identification of ULK1 Substrates', *Molecular cell*, 59(2), pp. 285–297. Available at: https://doi.org/10.1016/J.MOLCEL.2015.05.031.

Ehrmann, D. *et al.* (2020) 'Risk factors and prevention strategies for diabetic ketoacidosis in people with established type 1 diabetes', *The Lancet Diabetes & Endocrinology*, 8(5), pp. 436–446. Available at: https://doi.org/10.1016/S2213-8587(20)30042-5.

El-Mir, M.Y. *et al.* (2000) 'Dimethylbiguanide inhibits cell respiration via an indirect effect targeted on the respiratory chain complex I', *Journal of Biological*

Chemistry, 275(1), pp. 223–228. Available at: https://doi.org/10.1074/jbc.275.1.223.

El, K. *et al.* (2021) 'GIP mediates the incretin effect and glucose tolerance by dual actions on α cells and β cells', *Science Advances*, 7(11). Available at: https://doi.org/10.1126/SCIADV.ABF1948/SUPPL_FILE/ABF1948_SM.PDF.

Elkalaf, M., Anděl, M. and Trnka, J. (2013) 'Low Glucose but Not Galactose Enhances Oxidative Mitochondrial Metabolism in C2C12 Myoblasts and Myotubes', *PLOS ONE*, 8(8), p. e70772. Available at: https://doi.org/10.1371/JOURNAL.PONE.0070772.

Elksnis, A. *et al.* (2019) 'Heterogeneity of metabolic defects in type 2 diabetes and its relation to reactive oxygen species and alterations in beta-cell mass', *Frontiers in Physiology*, 10(FEB), p. 107. Available at: https://doi.org/10.3389/FPHYS.2019.00107/BIBTEX.

Elliott, A.D., Ustione, A. and Piston, D.W. (2015) 'Somatostatin and insulin mediate glucose-inhibited glucagon secretion in the pancreatic α-cell by lowering cAMP', *American Journal of Physiology - Endocrinology and Metabolism*, 308(2), pp. E130–E143. Available at: https://doi.org/10.1152/AJPENDO.00344.2014.

Epstein, R.J., Watson, J. V. and Smith, P.J. (1988) 'Subpopulation analysis of drug-induced cell-cycle delay in human tumor cells using 90° light scatter', *Cytometry*, 9(4), pp. 349–358. Available at: https://doi.org/10.1002/CYTO.990090412.

Erion, K.A. *et al.* (2015) 'Chronic exposure to excess nutrients left-shifts the concentration dependence of glucose-stimulated insulin secretion in pancreatic β-cells', *Journal of Biological Chemistry*, 290(26), pp. 16191–16201. Available at: https://doi.org/10.1074/jbc.M114.620351.

Eto, K. *et al.* (1999) 'Role of NADH shuttle system in glucose-induced activation of mitochondrial metabolism and insulin secretion', *Science*, 283(5404), pp.

981–985. Available at: https://doi.org/10.1126/SCIENCE.283.5404.981.

Ewald, N. *et al.* (2012) ‘Prevalence of diabetes mellitus secondary to pancreatic diseases (type 3c)’, *Diabetes/Metabolism Research and Reviews*, 28(4), pp. 338–342. Available at: https://doi.org/10.1002/DMRR.2260.

Fadini, G.P. *et al.* (2011) ‘Characteristics and outcomes of the hyperglycemic hyperosmolar non-ketotic syndrome in a cohort of 51 consecutive cases at a single center’, *Diabetes Research and Clinical Practice*, 94(2), pp. 172–179. Available at: https://doi.org/10.1016/J.DIABRES.2011.06.018.

Fan, X. *et al.* (2009) ‘Hypothalamic AMP-activated protein kinase activation with AICAR amplifies counterregulatory responses to hypoglycemia in a rodent model of type 1 diabetes’, *American Journal of Physiology - Regulatory Integrative and Comparative Physiology*, 296(6). Available at: https://doi.org/10.1152/AJPREGU.90600.2008.

Fanelli, C.G. *et al.* (1993) ‘Meticulous Prevention of Hypoglycemia Normalizes the Glycemic Thresholds and Magnitude of Most of Neuroendocrine Responses to, Symptoms of, and Cognitive Function During Hypoglycemia in intensively Treated Patients With Short-Term IDDM’, *Diabetes*, 42, pp. 1683–89. Available at: http://diabetesjournals.org/diabetes/article-pdf/42/11/1683/359623/42-11-1683.pdf (Accessed: 28 March 2023).

Farack, L. *et al.* (2019) ‘Transcriptional Heterogeneity of Beta Cells in the Intact Pancreas The proportion of extreme cells increases in insulin-resistant animals’. Available at: https://doi.org/10.1016/j.devcel.2018.11.001.

Farhat, R. *et al.* (2022) ‘ZT-01: A novel somatostatin receptor 2 antagonist for restoring the glucagon response to hypoglycaemia in type 1 diabetes’, *Diabetes, Obesity and Metabolism*, 24(5), pp. 908–917. Available at: https://doi.org/10.1111/DOM.14652.

Farinha, C.M. *et al.* (2016) ‘Regulatory crosstalk by protein kinases on CFTR trafficking and activity’, *Frontiers in Chemistry*, 4(JAN), p. 1. Available at:

https://doi.org/10.3389/FCHEM.2016.00001/BIBTEX.

Farinha, C.M. and Canato, S. (2016) ‘From the endoplasmic reticulum to the plasma membrane: mechanisms of CFTR folding and trafficking’, *Cellular and Molecular Life Sciences 2016 74:1*, 74(1), pp. 39–55. Available at: https://doi.org/10.1007/S00018-016-2387-7.

Farkas, B. *et al.* (2020) ‘Discovering the chloride pathway in the CFTR channel’, *Cellular and Molecular Life Sciences*, 77(4), pp. 765–778. Available at: https://doi.org/10.1007/S00018-019-03211-4/FIGURES/7.

Farrell, P.M. *et al.* (2017) ‘Diagnosis of Cystic Fibrosis: Consensus Guidelines from the Cystic Fibrosis Foundation’, *The Journal of pediatrics*, 181S, pp. S4-S15.e1. Available at: https://doi.org/10.1016/J.JPEDS.2016.09.064.

Feng, J. *et al.* (2022) ‘Mitochondria as an important target of metformin: The mechanism of action, toxic and side effects, and new therapeutic applications’, *Pharmacological Research*, 177, p. 106114. Available at: https://doi.org/10.1016/J.PHRS.2022.106114.

Ferrara, C.T. *et al.* (2017) ‘Novel Hypoglycemia Phenotype in Congenital Hyperinsulinism Due to Dominant Mutations of Uncoupling Protein 2’, *The Journal of Clinical Endocrinology & Metabolism*, 102(3), pp. 942–949. Available at: https://doi.org/10.1210/JC.2016-3164.

Fisher, J.T. *et al.* (2012) ‘Comparative Processing and Function of Human and Ferret Cystic Fibrosis Transmembrane Conductance Regulator’, *The Journal of Biological Chemistry*, 287(26), p. 21673. Available at: https://doi.org/10.1074/JBC.M111.336537.

Florez, H. *et al.* (2010) ‘Impact of Metformin-Induced Gastrointestinal Symptoms on Quality of Life and Adherence in Patients with Type 2 Diabetes’, © *Postgraduate Medicine*, 122(2), pp. 112–120. Available at: https://doi.org/10.3810/pgm.2010.03.2128.

Fontés, G. *et al.* (2015) ‘The ΔF508 Mutation in the Cystic Fibrosis

Transmembrane Conductance Regulator Is Associated With Progressive Insulin Resistance and Decreased Functional β-Cell Mass in Mice', *Diabetes*, 64(12), pp. 4112–4122. Available at: https://doi.org/10.2337/DB14-0810.

Forbes, J.M. and Cooper, M.E. (2013) 'Mechanisms of diabetic complications', *Physiological Reviews*, 93(1), pp. 137–188. Available at: https://doi.org/10.1152/PHYSREV.00045.2011/ASSET/IMAGES/LARGE/Z9J00111326440008.JPEG.

Foretz, M. *et al.* (2005) 'Short-Term Overexpression of a Constitutively Active Form of AMP-Activated Protein Kinase in the Liver Leads to Mild Hypoglycemia and Fatty Liver', *Diabetes*, 54(5), pp. 1331–1339. Available at: https://doi.org/10.2337/DIABETES.54.5.1331.

Foretz, M. *et al.* (2010) 'Metformin inhibits hepatic gluconeogenesis in mice independently of the LKB1/AMPK pathway via a decrease in hepatic energy state', *The Journal of Clinical Investigation*, 120(7). Available at: https://doi.org/10.1172/JCI40671.

Forkasiewicz, A. *et al.* (2020) 'The usefulness of lactate dehydrogenase measurements in current oncological practice', *Cellular and Molecular Biology Letters*, 25(1), pp. 1–14. Available at: https://doi.org/10.1186/S11658-020-00228-7/TABLES/1.

Franklin, I. *et al.* (2005) 'β-Cell Secretory Products Activate α-Cell ATP-Dependent Potassium Channels to Inhibit Glucagon Release', *Diabetes*, 54(6), pp. 1808–1815. Available at: https://doi.org/10.2337/DIABETES.54.6.1808.

Frier, B.M. (2014) 'Hypoglycaemia in diabetes mellitus: Epidemiology and clinical implications', *Nature Reviews Endocrinology*. Nature Publishing Group, pp. 711–722. Available at: https://doi.org/10.1038/nrendo.2014.170.

Frost, F. *et al.* (2019) 'Loss of incretin effect contributes to postprandial hyperglycaemia in cystic fibrosis-related diabetes', *Diabetic Medicine*, 36(11), pp. 1367–1374. Available at: https://doi.org/10.1111/DME.14121.

Fruehwald-Schultes, B. *et al.* (2001) ‘Metformin Does Not Adversely Affect Hormonal and Symptomatic Responses to Recurrent Hypoglycemia’, *The Journal of Clinical Endocrinology & Metabolism*, 86(9), pp. 4187–4192. Available at: https://academic.oup.com/jcem/article/86/9/4187/2848697 (Accessed: 4 April 2023).

Fu, A. *et al.* (2015) ‘LKB1 couples glucose metabolism to insulin secretion in mice’, *Diabetologia*, 58(7), pp. 1513–1522. Available at: https://doi.org/10.1007/S00125-015-3579-7/FIGURES/7.

Fulvio, M. Di *et al.* (2020) ‘Heterogeneous expression of CFTR in insulin-secreting β-cells of the normal human islet’, *PLOS ONE*, 15(12), p. e0242749. Available at: https://doi.org/10.1371/JOURNAL.PONE.0242749.

Galsgaard, K.D. *et al.* (2018) ‘Disruption of glucagon receptor signaling causes hyperaminoacidemia exposing a possible liver-alpha-cell axis’, *American Journal of Physiology - Endocrinology and Metabolism*, 314(1), pp. E93–E103. Available at: https://doi.org/10.1152/AJPENDO.00198.2017/ASSET/IMAGES/LARGE/ZH10111778190007.JPEG.

Gannon, M.C., Khan, M.A. and Nuttall, F.Q. (2001) ‘Glucose Appearance Rate After the Ingestion of Galactose’. Available at: https://doi.org/10.1053/meta.2001.19442.

Garcia, D. and Shaw, R.J. (2017) ‘AMPK: Mechanisms of Cellular Energy Sensing and Restoration of Metabolic Balance’, *Molecular cell*, 66(6), pp. 789–800. Available at: https://doi.org/10.1016/J.MOLCEL.2017.05.032.

Garg, S.K., Chhina, G.S. and Singh, B. (1978) ‘Topographic localisation of insulinogenic and insulinoprival areas in the hypothalamus’, *Experientia*, 34(9), pp. 1237–1238. Available at: https://doi.org/10.1007/BF01922980.

Geddes, J. *et al.* (2008) ‘Prevalence of impaired awareness of hypoglycaemia in adults with type 1 diabetes’, *Diabetic Medicine*, 25(4), pp. 501–504. Available

at: https://doi.org/10.1111/j.1464-5491.2008.02413.x.

Gee, K.R. *et al.* (2002) ‘Detection and imaging of zinc secretion from pancreatic, β-cells using a new fluorescent zinc indicator’, *Journal of the American Chemical Society*, 124(5), pp. 776–778. Available at: https://doi.org/10.1021/JA011774Y/SUPPL_FILE/JA011774Y_S.PDF.

Geidl-Flueck, B. *et al.* (2021) ‘Fructose- and sucrose- but not glucose-sweetened beverages promote hepatic de novo lipogenesis: A randomized controlled trial’, *Journal of Hepatology*, 75(1), pp. 46–54. Available at: https://doi.org/10.1016/j.jhep.2021.02.027.

Gelling, R.W. *et al.* (2003) ‘Lower blood glucose, hyperglucagonemia, and pancreatic α cell hyperplasia in glucagon receptor knockout mice’, *Proceedings of the National Academy of Sciences of the United States of America*, 100(3), p. 1438. Available at: https://doi.org/10.1073/PNAS.0237106100.

Gerich, J.E. *et al.* (1973) ‘Lack of Glucagon Response to Hypoglycemia in Diabetes: Evidence for an Intrinsic Pancreatic Alpha Cell Defect’, *Science*, 182(4108), pp. 171–173. Available at: https://doi.org/10.1126/SCIENCE.182.4108.171.

Gerich, J.E. *et al.* (2001) ‘Renal GluconeogenesisIts importance in human glucose homeostasis’, *Diabetes Care*, 24(2), pp. 382–391. Available at: https://doi.org/10.2337/DIACARE.24.2.382.

Geyer, M.C. *et al.* (2019) ‘Exenatide corrects postprandial hyperglycaemia in young people with cystic fibrosis and impaired glucose tolerance: A randomized crossover trial’, *Diabetes, Obesity and Metabolism*, 21(3), pp. 700–704. Available at: https://doi.org/10.1111/DOM.13544.

Gilbert, A. *et al.* (1998) ‘ΔF508 CFTR Localizes in the Endoplasmic Reticulum–Golgi Intermediate Compartment in Cystic Fibrosis Cells’, *Experimental Cell Research*, 242(1), pp. 144–152. Available at: https://doi.org/10.1006/EXCR.1998.4101.

Gillespie, K.M. *et al.* (2004) 'The rising incidence of childhood type 1 diabetes and reduced contribution of high-risk HLA haplotypes', *Lancet (London, England)*, 364(9446), pp. 1699–1700. Available at: https://doi.org/10.1016/S0140-6736(04)17357-1.

Gilon, P. (2020) 'The role of α-cells in islet function and glucose homeostasis in health and type 2 diabetes', *Journal of Molecular Biology* [Preprint]. Available at: https://doi.org/10.1016/J.JMB.2020.01.004.

Givan, A.L. (2011) 'Flow Cytometry: An Introduction', *Methods in Molecular Biology*, 699, pp. 1–29. Available at: https://doi.org/10.1007/978-1-61737-950-5_1/FIGURES/15_1.

Glechner, A. *et al.* (2018) 'Effects of lifestyle changes on adults with prediabetes: A systematic review and meta-analysis', *Primary Care Diabetes*, 12(5), pp. 393–408. Available at: https://doi.org/10.1016/J.PCD.2018.07.003.

González-Barroso, M.M. *et al.* (2008) 'Mutations in UCP2 in Congenital Hyperinsulinism Reveal a Role for Regulation of Insulin Secretion', *PLoS ONE*, 3(12), p. 3850. Available at: https://doi.org/10.1371/JOURNAL.PONE.0003850.

Van Goor, F. *et al.* (2009) 'Rescue of CF airway epithelial cell function in vitro by a CFTR potentiator, VX-770', *Proceedings of the National Academy of Sciences of the United States of America*, 106(44), p. 18825. Available at: https://doi.org/10.1073/PNAS.0904709106.

Göransson, O. *et al.* (2007) 'Mechanism of action of A-769662, a valuable tool for activation of AMP-activated protein kinase', *Journal of Biological Chemistry*, 282(45), pp. 32549–32560. Available at: https://doi.org/10.1074/jbc.M706536200.

Gosmanov, A.R., Gosmanova, E.O. and Kitabchi, A.E. (2021) 'Hyperglycemic Crises: Diabetic Ketoacidosis and Hyperglycemic Hyperosmolar State', *Acute Endocrinology*, pp. 119–147. Available at: https://doi.org/10.1007/978-1-60327-177-6_6.

Gottlieb, P.A. *et al.* (2012) 'No relation between cystic fibrosis-related diabetes and type 1 diabetes autoimmunity', *Diabetes care*, 35(8), p. e57. Available at: https://doi.org/10.2337/DC11-2327.

Gowans, G.J. *et al.* (2013) 'AMP Is a True Physiological Regulator of AMP-Activated Protein Kinase by Both Allosteric Activation and Enhancing Net Phosphorylation', *Cell Metabolism*, 18(4), p. 556. Available at: https://doi.org/10.1016/J.CMET.2013.08.019.

Graf, R. and Klessen, C. (1981) 'Glycogen in Pancreatic Islets of Steroid Diabetic Rats Carbohydrate Histochemical Detection and Localization Using an Immunocytochemical Technique *', *Histochemistry* [Preprint].

Granados, A. *et al.* (2021) 'The association between body composition, leptin levels and glucose dysregulation in youth with cystic fibrosis', *Journal of Cystic Fibrosis*, 20(5), pp. 796–802. Available at: https://doi.org/10.1016/J.JCF.2021.06.004.

Grapengiesser, E. *et al.* (2006) 'Glucose Induces Glucagon Release Pulses Antisynchronous with Insulin and Sensitive to Purinoceptor Inhibition', *Endocrinology*, 147(7), pp. 3472–3477. Available at: https://doi.org/10.1210/EN.2005-1431.

Gregory, G.A. *et al.* (2022) 'Global incidence, prevalence, and mortality of type 1 diabetes in 2021 with projection to 2040: a modelling study', *The lancet. Diabetes & endocrinology*, 10(10), pp. 741–760. Available at: https://doi.org/10.1016/S2213-8587(22)00218-2.

Gregory, J.M. *et al.* (2019) 'Iatrogenic Hyperinsulinemia, Not Hyperglycemia, Drives Insulin Resistance in Type 1 Diabetes as Revealed by Comparison With GCK-MODY (MODY2)', *Diabetes*, 68(8), pp. 1565–1576. Available at: https://doi.org/10.2337/DB19-0324.

Gregory, J.M., Cherrington, A.D. and Moore, D.J. (2020) 'The Peripheral Peril: Injected Insulin Induces Insulin Insensitivity in Type 1 Diabetes', *Diabetes*,

69(5), p. 837. Available at: https://doi.org/10.2337/DBI19-0026.

Grempler, R. *et al.* (2018) ‘Discovery and translation of a target engagement marker for AMP-activated protein kinase (AMPK)’, *PLOS ONE*, 13(5), p. e0197849. Available at: https://doi.org/10.1371/JOURNAL.PONE.0197849.

Gribble, F.M. *et al.* (2003) ‘A Novel Glucose-Sensing Mechanism Contributing to Glucagon-Like Peptide-1 Secretion From the GLUTag Cell Line’, *Diabetes*, 52(5), pp. 1147–1154. Available at: https://doi.org/10.2337/DIABETES.52.5.1147.

Gromada, J. *et al.* (1997) ‘Adrenaline stimulates glucagon secretion in pancreatic A-cells by increasing the Ca2+ current and the number of granules close to the L-type Ca2+ channels’, *The Journal of general physiology*, 110(3), pp. 217–228. Available at: https://doi.org/10.1085/JGP.110.3.217.

Gromada, J. *et al.* (2001) ‘Somatostatin inhibits exocytosis in rat pancreatic α-cells by Gi2-dependent activation of calcineurin and depriming of secretory granules’, *The Journal of Physiology*, 535(2), pp. 519–532. Available at: https://doi.org/10.1111/J.1469-7793.2001.00519.X.

Gross, K.C. and Acosta, P.B. (1991) ‘Fruits and vegetables are a source of galactose: implications in planning the diets of patients with galactosaemia’, *Journal of inherited metabolic disease*, 14(2), pp. 253–258. Available at: https://doi.org/10.1007/BF01800599.

Grubelnik, V. *et al.* (2020a) ‘Mitochondrial Dysfunction in Pancreatic Alpha and Beta Cells Associated with Type 2 Diabetes Mellitus’, *Life*, 10(12), pp. 1–16. Available at: https://doi.org/10.3390/LIFE10120348.

Grubelnik, V. *et al.* (2020b) ‘Modelling of dysregulated glucagon secretion in type 2 diabetes by considering mitochondrial alterations in pancreatic α-cells’, *Royal Society Open Science*, 7(1). Available at: https://doi.org/10.1098/RSOS.191171.

Gugliucci, A. (2016) ‘Fructose surges damage hepatic adenosyl-

monophosphate-dependent kinase and lead to increased lipogenesis and hepatic insulin resistance', *Medical Hypotheses*, 93, pp. 87–92. Available at: https://doi.org/10.1016/J.MEHY.2016.05.026.

Guigas, B. *et al.* (2006) '5-Aminoimidazole-4-carboxamide-1-beta-D-ribofuranoside and metformin inhibit hepatic glucose phosphorylation by an AMP-activated protein kinase-independent effect on glucokinase translocation', *Diabetes*, 55(4), pp. 865–874. Available at: https://doi.org/10.2337/DIABETES.55.04.06.DB05-1178.

Guilbault, C. *et al.* (2007) 'Cystic fibrosis mouse models', *American journal of respiratory cell and molecular biology*, 36(1), pp. 1–7. Available at: https://doi.org/10.1165/RCMB.2006-0184TR.

Guo, J.H. *et al.* (2014) 'Glucose-induced electrical activities and insulin secretion in pancreatic islet 2-cells are modulated by CFTR', *Nature Communications*, 5(1), pp. 1–10. Available at: https://doi.org/10.1038/ncomms5420.

Guo, Y. *et al.* (2009) 'Expression and Distribution of Cystic Fibrosis Transmembrane Conductance Regulator in Neurons of the Human Brain', *Journal of Histochemistry and Cytochemistry*, 57(12), p. 1113. Available at: https://doi.org/10.1369/JHC.2009.953455.

Gupta, V. *et al.* (1997) 'The defective glucagon response from transplanted intrahepatic pancreatic islets during hypoglycemia is transplantation site-determined', *Diabetes*, 46(1), pp. 28–33. Available at: https://doi.org/10.2337/DIAB.46.1.28.

Habib, A.R.R. *et al.* (2019) 'A Systematic Review of the Clinical Efficacy and Safety of CFTR Modulators in Cystic Fibrosis', *Scientific Reports 2019 9:1*, 9(1), pp. 1–9. Available at: https://doi.org/10.1038/s41598-019-43652-2.

Haliloglu, B. *et al.* (2017) 'Hypoglycemia is common in children with cystic fibrosis and seen predominantly in females', *Pediatric Diabetes*, 18(7), pp. 607–

613. Available at: https://doi.org/10.1111/PEDI.12470.

Hallows, K.R. *et al.* (2000) ‘Inhibition of cystic fibrosis transmembrane conductance regulator by novel interaction with the metabolic sensor AMP-activated protein kinase’, *The Journal of Clinical Investigation*, 105(12), pp. 1711–1721. Available at: https://doi.org/10.1172/JCI9622.

Hallows, K.R. *et al.* (2003) ‘Regulation of channel gating by AMP-activated protein kinase modulates cystic fibrosis transmembrane conductance regulator activity in lung submucosal cells’, *Journal of Biological Chemistry*, 278(2), pp. 998–1004. Available at: https://doi.org/10.1074/jbc.M210621200.

Hallows, K.R. *et al.* (2006) ‘Up-regulation of AMP-activated kinase by dysfunctional cystic fibrosis transmembrane conductance regulator in cystic fibrosis airway epithelial cells mitigates excessive inflammation’, *Journal of Biological Chemistry*, 281(7), pp. 4231–4241. Available at: https://doi.org/10.1074/jbc.M511029200.

Hamilton, A. *et al.* (2018) ‘Adrenaline Stimulates Glucagon Secretion by Tpc2-Dependent Ca2+ Mobilization From Acidic Stores in Pancreatic α-Cells’, *Diabetes*, 67(6), pp. 1128–1139. Available at: https://doi.org/10.2337/DB17-1102.

Hardie, D.G. (2018) ‘Keeping the home fires burning†: AMP-activated protein kinase’, *Journal of The Royal Society Interface*, 15(138). Available at: https://doi.org/10.1098/RSIF.2017.0774.

Hardie, D.G. and Alessi, D.R. (2013) ‘LKB1 and AMPK and the cancer-metabolism link - ten years after’, *BMC Biology*, 11(1), pp. 1–11. Available at: https://doi.org/10.1186/1741-7007-11-36/FIGURES/5.

Hardie, D.G., Carling, D. and Carlson, M. (1998) ‘The AMP-activated/SNF1 protein kinase subfamily: metabolic sensors of the eukaryotic cell?’, *Annual review of biochemistry*, 67, pp. 821–855. Available at: https://doi.org/10.1146/ANNUREV.BIOCHEM.67.1.821.

Hardie, D.G. and Lin, S.C. (2017) ‘AMP-activated protein kinase – not just an energy sensor’, *F1000Research*, 6. Available at: https://doi.org/10.12688/F1000RESEARCH.11960.1.

Hardy, A.B. *et al.* (2011) ‘Regulation of glucagon secretion by zinc: lessons from the β cell-specific Znt8 knockout mouse model’, *Diabetes, Obesity and Metabolism*, 13(SUPPL. 1), pp. 112–117. Available at: https://doi.org/10.1111/J.1463-1326.2011.01451.X.

Hart, N.J. *et al.* (2018) ‘Cystic fibrosis–related diabetes is caused by islet loss and inflammation’, *JCI Insight*, 3(8). Available at: https://doi.org/10.1172/JCI.INSIGHT.98240.

Hasenour, C.M. *et al.* (2014) ‘5-Aminoimidazole-4-carboxamide-1-β-D-ribofuranoside (AICAR) effect on glucose production, but not energy metabolism, is independent of hepatic AMPK in vivo’, *Journal of Biological Chemistry*, 289(9), pp. 5950–5959. Available at: https://doi.org/10.1074/jbc.M113.528232.

Hassan, R.H., Bourron, O. and Hajduch, E. (2014) ‘Defect of insulin signal in peripheral tissues: Important role of ceramide’, *World Journal of Diabetes*, 5(3), p. 244. Available at: https://doi.org/10.4239/WJD.V5.I3.244.

Hauke, S. *et al.* (2022) ‘ATP is an essential autocrine factor for pancreatic β-cell signaling and insulin secretion’, *Physiological Reports*, 10(1), p. e15159. Available at: https://doi.org/10.14814/PHY2.15159.

Hawley, S.. *et al.* (2003) ‘Complexes between the LKB1 tumor suppressor, STRAD alpha/beta and MO25 alpha/beta are upstream kinases in the AMP-activated protein kinase cascade’, *Journal of biology*, 2(4), p. 28. Available at: https://doi.org/10.1186/1475-4924-2-28.

Hawley, S.A. *et al.* (1996) ‘Characterization of the AMP-activated protein kinase kinase from rat liver and identification of threonine 172 as the major site at which it phosphorylates AMP-activated protein kinase’, *The Journal of biological*

chemistry, 271(44), pp. 27879–27887. Available at: https://doi.org/10.1074/JBC.271.44.27879.

Hawley, S.A. *et al.* (2010) 'Use of Cells Expressing γ Subunit Variants to Identify Diverse Mechanisms of AMPK Activation', *Cell Metabolism*, 11(6), p. 554. Available at: https://doi.org/10.1016/J.CMET.2010.04.001.

Hawley, S.A. *et al.* (2012) 'The ancient drug salicylate directly activates AMP-activated protein kinase', *Science (New York, N.Y.)*, 336(6083), p. 918. Available at: https://doi.org/10.1126/SCIENCE.1215327.

Haythorne, E. *et al.* (2019) 'Diabetes causes marked inhibition of mitochondrial metabolism in pancreatic β-cells', *Nature Communications 2019 10:1*, 10(1), pp. 1–17. Available at: https://doi.org/10.1038/s41467-019-10189-x.

Haythorne, E. *et al.* (2022) 'Altered glycolysis triggers impaired mitochondrial metabolism and mTORC1 activation in diabetic β-cells', *Nature Communications 2022 13:1*, 13(1), pp. 1–19. Available at: https://doi.org/10.1038/s41467-022-34095-x.

He, L. *et al.* (2020) 'Regulation of basal expression of hepatic PEPCK and G6Pase by AKT2', *Biochemical Journal*, 477(5), pp. 1021–1031. Available at: https://doi.org/10.1042/BCJ20190570.

Hearne, A. *et al.* (2020) 'Oligomycin-induced proton uncoupling', *Toxicology in Vitro*, 67. Available at: https://doi.org/10.1016/J.TIV.2020.104907.

Heimberg, H. *et al.* (1995) 'Differences in glucose transporter gene expression between rat pancreatic alpha- and beta-cells are correlated to differences in glucose transport but not in glucose utilization', *The Journal of biological chemistry*, 270(15), pp. 8971–8975. Available at: https://doi.org/10.1074/JBC.270.15.8971.

Heimberg, H. *et al.* (1996) 'The glucose sensor protein glucokinase is expressed in glucagon-producing α-cells', *Proceedings of the National Academy of Sciences of the United States of America*, 93(14), pp. 7036–7041. Available

at: https://doi.org/10.1073/PNAS.93.14.7036.

Heller, S.R. *et al.* (2007) ‘Risk of hypoglycaemia in types 1 and 2 diabetes: Effects of treatment modalities and their duration’, *Diabetologia*, 50(6), pp. 1140–1147. Available at: https://doi.org/10.1007/S00125-007-0599-Y/TABLES/4.

Heller, S.R. (2017) ‘Glucose Concentrations of Less Than 3.0 mmol/L (54 mg/dL) Should Be Reported in Clinical Trials: A Joint Position Statement of the American Diabetes Association and the European Association for the Study of Diabetes’, *Diabetes Care*, 40(1), pp. 155–157. Available at: https://doi.org/10.2337/DC16-2215.

Heller, S.R. and Cryer, P.E. (1991) ‘Reduced Neuroendocrine and Symptomatic Responses to Subsequent Hypoglycemia After 1 Episode of Hypoglycemia in Nondiabetic Humans’, *Diabetes*, 40(2), pp. 223–226. Available at: https://doi.org/10.2337/DIAB.40.2.223.

Herzig, S. and Shaw, R.J. (2018) ‘AMPK: guardian of metabolism and mitochondrial homeostasis’, *Nature reviews. Molecular cell biology*, 19(2), p. 121. Available at: https://doi.org/10.1038/NRM.2017.95.

Herzog, R.I. *et al.* (2013) ‘Lactate preserves neuronal metabolism and function following antecedent recurrent hypoglycemia’, *The Journal of Clinical Investigation*, 123(5), pp. 1988–1998. Available at: https://doi.org/10.1172/JCI65105.

Hill, B.G. *et al.* (2012) ‘Integration of cellular bioenergetics with mitochondrial quality control and autophagy’, *Biological Chemistry*, 393(12), pp. 1485–1512. Available at: https://doi.org/10.1515/HSZ-2012-0198/MACHINEREADABLECITATION/RIS.

Hillman, M. *et al.* (2012) ‘Reduced levels of active GLP-1 in patients with cystic fibrosis with and without diabetes mellitus’, *Journal of Cystic Fibrosis*, 11(2), pp. 144–149. Available at: https://doi.org/10.1016/J.JCF.2011.11.001.

Hilsted, J. *et al.* (1991) ‘Plasma glucagon and glucose recovery after hypoglycemia: The effect of total autonomic blockade’, *Acta Endocrinologica (Norway)*, 125(4), pp. 466–469. Available at: https://doi.org/10.1530/ACTA.0.1250466.

Hirsch, I.B. *et al.* (2013) ‘Hypoglycemia in adults with cystic fibrosis during oral glucose tolerance testing’, *Diabetes care*, 36(8). Available at: https://doi.org/10.2337/DC12-1859.

Hoffman, E.G. *et al.* (2021) ‘Somatostatin Receptor Antagonism Reverses Glucagon Counterregulatory Failure in Recurrently Hypoglycemic Male Rats’, *Endocrinology*, 162(12), pp. 1–11. Available at: https://doi.org/10.1210/ENDOCR/BQAB189.

Holden, H.M., Rayment, I. and Thoden, J.B. (2003) ‘Structure and Function of Enzymes of the Leloir Pathway for Galactose Metabolism’, *Journal of Biological Chemistry*, 278(45), pp. 43885–43888. Available at: https://doi.org/10.1074/jbc.R300025200.

Holman, N. *et al.* (2020) ‘Risk factors for COVID-19-related mortality in people with type 1 and type 2 diabetes in England: a population-based cohort study’, *The Lancet Diabetes and Endocrinology*, 8(10), pp. 823–833. Available at: https://doi.org/10.1016/S2213-8587(20)30271-0.

Holst, J.J. and Albrechtsen, N.J.W. (2019) ‘Methods and Guidelines for Measurement of Glucagon in Plasma’, *International Journal of Molecular Sciences*, 20(21). Available at: https://doi.org/10.3390/IJMS20215416.

Honzawa, N., Fujimoto, K. and Kitamura, T. (2019) ‘Cell Autonomous Dysfunction and Insulin Resistance in Pancreatic α Cells’, *International Journal of Molecular Sciences 2019, Vol. 20, Page 3699*, 20(15), p. 3699. Available at: https://doi.org/10.3390/IJMS20153699.

Hu, M. *et al.* (2019) ‘AMPK Inhibition Suppresses the Malignant Phenotype of Pancreatic Cancer Cells in Part by Attenuating Aerobic Glycolysis’, *Journal of*

Cancer, 10(8), p. 1870. Available at: https://doi.org/10.7150/JCA.28299.

Huang, Wen Qing *et al.* (2017) 'Abnormal CFTR affects glucagon production by islet a cells in cystic fibrosis and polycystic ovarian syndrome', *Frontiers in Physiology*, 8(NOV), p. 835. Available at: https://doi.org/10.3389/FPHYS.2017.00835/FULL.

Huang, W.Q. *et al.* (2017) 'Glucose-Sensitive CFTR Suppresses Glucagon Secretion by Potentiating KATP Channels in Pancreatic Islet α Cells', *Endocrinology*, 158(10), pp. 3188–3199. Available at: https://doi.org/10.1210/EN.2017-00282.

Huising, M.O. *et al.* (2010) 'CRFR1 is expressed on pancreatic β cells, promotes β cell proliferation, and potentiates insulin secretion in a glucose-dependent manner', *Proceedings of the National Academy of Sciences of the United States of America*, 107(2), p. 912. Available at: https://doi.org/10.1073/PNAS.0913610107.

Hull, R.L. *et al.* (2018) 'Islet interleukin-1β immunoreactivity is an early feature of cystic fibrosis that may contribute to β-cell failure', *Diabetes Care*, 41(4), pp. 823–830. Available at: https://doi.org/10.2337/DC17-1387/-/DC1.

Hunter, R.W. *et al.* (2018) 'Metformin reduces liver glucose production by inhibition of fructose-1-6-bisphosphatase', *Nature Medicine 2018 24:9*, 24(9), pp. 1395–1406. Available at: https://doi.org/10.1038/s41591-018-0159-7.

Hurley, R.L. *et al.* (2005) 'The Ca2+/calmodulin-dependent protein kinase kinases are AMP-activated protein kinase kinases', *Journal of Biological Chemistry*, 280(32), pp. 29060–29066. Available at: https://doi.org/10.1074/jbc.M503824200.

Iannucci, A. *et al.* (1984) 'Endocrine pancreas in cystic fibrosis: an immunohistochemical study', *Human pathology*, 15(3), pp. 278–284. Available at: https://doi.org/10.1016/S0046-8177(84)80191-4.

IDF Diabetes Atlas (2013) *IDF Diabetes, 6th Edition*.

IDF Diabetes Atlas (2015) *IDF Diabetes, 7th edition*. Available at: https://diabetesatlas.org/atlas/seventh-edition/ (Accessed: 10 April 2023).

Idowu, A.O. *et al.* (2022) '10-Year Risk of Developing Type 2 Diabetes Mellitus: A Survey of Rural Communities in Southern Nigeria: West Afr J Med. 2022 Nov 30; 39 (11): 1113', *wajmed.com*, 39(11). Available at: https://wajmed.com/ojs3.3__wajm/index.php/wajmed/article/view/292 (Accessed: 10 April 2023).

Ikesugi, K. *et al.* (2009) 'Induction of Endoplasmic Reticulum Stress in Retinal Pericytes by Glucose Deprivation', *http://dx.doi.org/10.1080/02713680600966785*, 31(11), pp. 947–953. Available at: https://doi.org/10.1080/02713680600966785.

Iurlaro, R. *et al.* (2017) 'Glucose Deprivation Induces ATF4-Mediated Apoptosis through TRAIL Death Receptors', *Molecular and Cellular Biology*, 37(10). Available at: https://doi.org/10.1128/MCB.00479-16.

Jaafar, R. *et al.* (2019) 'MTORC1-to-AMPK switching underlies βcell metabolic plasticity during maturation and diabetes', *Journal of Clinical Investigation*, 129(10), pp. 4124–4137. Available at: https://doi.org/10.1172/JCI127021.

Jacques-Silva, M.C. *et al.* (2010) 'ATP-gated P2X3 receptors constitute a positive autocrine signal for insulin release in the human pancreatic beta cell.', *Proceedings of the National Academy of Sciences of the United States of America*, 107(14), pp. 6465–6470. Available at: https://doi.org/10.1073/PNAS.0908935107.

Jaiswal, N. *et al.* (2015) 'Fructose-induced ROS generation impairs glucose utilization in L6 skeletal muscle cells'. Available at: https://doi.org/10.3109/10715762.2015.1031662.

Jakovljevic, N.K. *et al.* (2021) 'Targeting Mitochondria in Diabetes', *International Journal of Molecular Sciences 2021, Vol. 22, Page 6642*, 22(12), p. 6642. Available at: https://doi.org/10.3390/IJMS22126642.

Janah, L. *et al.* (2019) ‘Glucagon Receptor Signaling and Glucagon Resistance’, *International Journal of Molecular Sciences*, 20(13). Available at: https://doi.org/10.3390/IJMS20133314.

Janež, A. *et al.* (2020) ‘Insulin Therapy in Adults with Type 1 Diabetes Mellitus: a Narrative Review’, *Diabetes Therapy*, 11(2), p. 387. Available at: https://doi.org/10.1007/S13300-019-00743-7.

Janikiewicz, J. *et al.* (2015) ‘Islet β-cell failure in type 2 diabetes - Within the network of toxic lipids’, *Biochemical and Biophysical Research Communications*, 460(3), pp. 491–496. Available at: https://doi.org/10.1016/J.BBRC.2015.03.153.

Janzen, N.R., Whitfield, J. and Hoffman, N.J. (2018) ‘Interactive Roles for AMPK and Glycogen from Cellular Energy Sensing to Exercise Metabolism’, *International Journal of Molecular Sciences*, 19(11). Available at: https://doi.org/10.3390/IJMS19113344.

Jaspers, R.T. *et al.* (2017) ‘Exercise, fasting, and mimetics: toward beneficial combinations?’, *The FASEB Journal*, 31(1), pp. 14–28. Available at: https://doi.org/10.1096/FJ.201600652R.

Jenkins, Y. *et al.* (2013) ‘AMPK Activation through Mitochondrial Regulation Results in Increased Substrate Oxidation and Improved Metabolic Parameters in Models of Diabetes’, *PLOS ONE*, 8(12), p. e81870. Available at: https://doi.org/10.1371/JOURNAL.PONE.0081870.

Jensen, T.E. *et al.* (2015) ‘PT-1 selectively activates AMPK-γ 1 complexes in mouse skeletal muscle, but activates all three γ subunit complexes in cultured human cells by inhibiting the respiratory chain’, *Biochem. J*, 467, pp. 461–472. Available at: https://doi.org/10.1042/BJ20141142.

Jeon, S.M. (2016) ‘Regulation and function of AMPK in physiology and diseases’, *Experimental & Molecular Medicine 2016 48:7*, 48(7), pp. e245–e245. Available at: https://doi.org/10.1038/emm.2016.81.

Jeoung, N.H. *et al.* (2006) ‘Role of pyruvate dehydrogenase kinase isoenzyme 4 (PDHK4) in glucose homoeostasis during starvation’, *Biochemical Journal*, 397(Pt 3), p. 417. Available at: https://doi.org/10.1042/BJ20060125.

Jeoung, N.H. and Harris, R.A. (2008) ‘Pyruvate dehydrogenase kinase-4 deficiency lowers blood glucose and improves glucose tolerance in diet-induced obese mice’, *American Journal of Physiology - Endocrinology and Metabolism*, 295(1), pp. 46–54. Available at: https://doi.org/10.1152/AJPENDO.00536.2007/ASSET/IMAGES/LARGE/ZH10070853420003.JPEG.

De Jesus, A. *et al.* (2022) ‘Hexokinase 1 cellular localization regulates the metabolic fate of glucose’, *Molecular Cell*, 82(7), pp. 1261-1277.e9. Available at: https://doi.org/10.1016/J.MOLCEL.2022.02.028.

Jia, J.J. *et al.* (2009) ‘The polymorphisms of UCP2 and UCP3 genes associated with fat metabolism, obesity and diabetes’, *Obesity Reviews*, 10(5), pp. 519–526. Available at: https://doi.org/10.1111/J.1467-789X.2009.00569.X.

Jiang, S. *et al.* (2020) ‘Diabetic-induced alterations in hepatic glucose and lipid metabolism: The role of type 1 and type 2 diabetes mellitus’, *Molecular Medicine Reports*, 22(2), p. 603. Available at: https://doi.org/10.3892/MMR.2020.11175.

Johanns, M. *et al.* (2022) ‘Inhibition of basal and glucagon-induced hepatic glucose production by 991 and other pharmacological AMPK activators’, *Biochemical Journal*, 479(12), pp. 1317–1336. Available at: https://doi.org/10.1042/BCJ20220170.

Johanns, M., Hue, L. and Rider, M.H. (2023) ‘AMPK inhibits liver gluconeogenesis: fact or fiction?’, *Biochemical Journal*, 480(1), pp. 105–125. Available at: https://doi.org/10.1042/BCJ20220582.

Johnson, J.D. (2021) ‘On the causal relationships between hyperinsulinaemia, insulin resistance, obesity and dysglycaemia in type 2 diabetes’, *Diabetologia*,

64(10), pp. 2138–2146. Available at: https://doi.org/10.1007/S00125-021-05505-4/TABLES/1.

Jones, B. *et al.* (2018) ‘Control of insulin secretion by GLP-1’, *Peptides*, 100, pp. 75–84. Available at: https://doi.org/10.1016/J.PEPTIDES.2017.12.013.

Jørgensen, N.O. *et al.* (2021) ‘Direct small molecule ADaM-site AMPK activators reveal an AMPKγ3-independent mechanism for blood glucose lowering’, *Molecular Metabolism*, 51, p. 101259. Available at: https://doi.org/10.1016/J.MOLMET.2021.101259.

Joseph, J.W. *et al.* (2002) ‘Uncoupling protein 2 knockout mice have enhanced insulin secretory capacity after a high-fat diet’, *Diabetes*, 51(11), pp. 3211–3219. Available at: https://doi.org/10.2337/DIABETES.51.11.3211.

Kailey, B. *et al.* (2012) ‘SSTR2 is the functionally dominant somatostatin receptor in human pancreatic β- and α-cells’, *American Journal of Physiology - Endocrinology and Metabolism*, 303(9). Available at: https://doi.org/10.1152/AJPENDO.00207.2012.

Kang, L. *et al.* (2004) ‘Physiological and Molecular Characteristics of Rat Hypothalamic Ventromedial Nucleus Glucosensing Neurons’, *Diabetes*, 53(3), pp. 549–559. Available at: https://doi.org/10.2337/DIABETES.53.3.549.

Kang, L. *et al.* (2008) ‘Prior hypoglycemia enhances glucose responsiveness in some ventromedial hypothalamic glucosensing neurons’, *American Journal of Physiology - Regulatory Integrative and Comparative Physiology*, 294(3), pp. 784–792. Available at: https://doi.org/10.1152/AJPREGU.00645.2007/ASSET/IMAGES/LARGE/ZH60030862050004.JPEG.

Kaprio, J. *et al.* (1992) ‘Concordance for type 1 (insulin-dependent) and type 2 (non-insulin-dependent) diabetes mellitus in a population-based cohort of twins in Finland’, *Diabetologia*, 35(11), pp. 1060–1067. Available at: https://doi.org/10.1007/BF02221682.

Karabiyik, C. *et al.* (2021) ‘Glucose starvation induces autophagy via ULK1-mediated activation of PIKfyve in an AMPK-dependent manner’, *Developmental Cell*, 56(13), pp. 1961-1975.e5. Available at: https://doi.org/10.1016/J.DEVCEL.2021.05.010.

Karalliedde, J. and Gnudi, L. (2016) ‘Diabetes mellitus, a complex and heterogeneous disease, and the role of insulin resistance as a determinant of diabetic kidney disease’, *Nephrology, dialysis, transplantation : official publication of the European Dialysis and Transplant Association - European Renal Association*, 31(2), pp. 206–213. Available at: https://doi.org/10.1093/NDT/GFU405.

Karimian, N. *et al.* (2013) ‘Somatostatin Receptor Type 2 Antagonism Improves Glucagon Counterregulation in Biobreeding Diabetic Rats’, *Diabetes*, 62(8), pp. 2968–2977. Available at: https://doi.org/10.2337/DB13-0164.

Kato, A. *et al.* (2019) ‘Recurrent short-term hypoglycemia and hyperglycemia induce apoptosis and oxidative stress via the ER stress response in immortalized adult mouse Schwann (IMS32) cells’, *Neuroscience Research*, 147, pp. 26–32. Available at: https://doi.org/10.1016/J.NEURES.2018.11.004.

Katz, L.S. *et al.* (2009) ‘Pax6 Regulates the Proglucagon Processing Enzyme PC2 and Its Chaperone 7B2’, *Molecular and Cellular Biology*, 29(8), pp. 2322–2334. Available at: https://doi.org/10.1128/MCB.01543-08/SUPPL_FILE/SUPPLEMENTARY_TABLES.PDF.

Kaul, K., Apostolopoulou, M. and Roden, M. (2015) ‘Insulin resistance in type 1 diabetes mellitus’, *Metabolism*, 64(12), pp. 1629–1639. Available at: https://doi.org/10.1016/J.METABOL.2015.09.002.

Kaur, J. and Seaquist, E.R. (2023) ‘Hypoglycaemia in type 1 diabetes mellitus: risks and practical prevention strategies’, *Nature Reviews Endocrinology* |, 19, pp. 177–186. Available at: https://doi.org/10.1038/s41574-022-00762-8.

Kawamori, D. *et al.* (2009) ‘Insulin Signaling in α Cells Modulates Glucagon

Secretion In Vivo', *Cell Metabolism*, 9(4), pp. 350–361. Available at: https://doi.org/10.1016/J.CMET.2009.02.007.

Kelly, A. *et al.* (2019) 'Islet hormone and incretin secretion in cystic fibrosis after four months of ivacaftor therapy', *American Journal of Respiratory and Critical Care Medicine*, 199(3), pp. 342–351. Available at: https://doi.org/10.1164/RCCM.201806-1018OC/SUPPL_FILE/DISCLOSURES.PDF.

Kelly, R.P. *et al.* (2015) 'Short-term administration of the glucagon receptor antagonist LY2409021 lowers blood glucose in healthy people and in those with type 2 diabetes', *Diabetes, Obesity and Metabolism*, 17(4), pp. 414–422. Available at: https://doi.org/10.1111/DOM.12446.

Kerbiriou, M. *et al.* (2007) 'Coupling cystic fibrosis to endoplasmic reticulum stress: Differential role of Grp78 and ATF6', *Biochimica et Biophysica Acta (BBA) - Molecular Basis of Disease*, 1772(11–12), pp. 1236–1249. Available at: https://doi.org/10.1016/J.BBADIS.2007.10.004.

Kerem, B.S. *et al.* (1989) 'Identification of the Cystic Fibrosis Gene: Genetic Analysis', *Science*, 245(4922), pp. 1073–1080. Available at: https://doi.org/10.1126/SCIENCE.2570460.

Khan, D. *et al.* (2019) 'Short-term CFTR inhibition reduces islet area in C57BL/6 mice', *Scientific Reports 2019 9:1*, 9(1), pp. 1–11. Available at: https://doi.org/10.1038/s41598-019-47745-w.

Khan, S. *et al.* (2014) 'Autocrine activation of P2Y1 receptors couples Ca2+ influx to Ca2+ release in human pancreatic beta cells', *Diabetologia*, 57(12), pp. 2535–2545. Available at: https://doi.org/10.1007/S00125-014-3368-8/FIGURES/8.

Kheirollahi, V. *et al.* (2019) 'Metformin induces lipogenic differentiation in myofibroblasts to reverse lung fibrosis', *Nature Communications 2019 10:1*, 10(1), pp. 1–16. Available at: https://doi.org/10.1038/s41467-019-10839-0.

Kilberg, M.J. *et al.* (2020a) ‘Dysregulated insulin in pancreatic insufficient cystic fibrosis with post-prandial hypoglycemia’, *Journal of Cystic Fibrosis*, 19(2), pp. 310–315. Available at: https://doi.org/10.1016/J.JCF.2019.07.006.

Kilberg, M.J. *et al.* (2020b) ‘Hypoglycemia and Islet Dysfunction Following Oral Glucose Tolerance Testing in Pancreatic-Insufficient Cystic Fibrosis’, *J Clin Endocrinol Metab*, 105(10), pp. 3179–3189. Available at: https://doi.org/10.1210/clinem/dgaa448.

Kilimnik, G. *et al.* (2010) ‘Intraislet production of GLP-1 by activation of prohormone convertase 1/3 in pancreatic α-cells in mouse models of -cell regeneration.’, *Islets*, 2(3), pp. 149–155. Available at: https://doi.org/10.4161/ISL.2.3.11396.

Kim, J. *et al.* (2016) ‘AMPK activators: mechanisms of action and physiological activities’, *Experimental & Molecular Medicine 2016 48:4*, 48(4), pp. e224–e224. Available at: https://doi.org/10.1038/emm.2016.16.

Kim, J.E. *et al.* (2008) ‘AMP-Activated Protein Kinase Activation by 5-Aminoimidazole-4-carboxamide-1-β-D-ribofuranoside (AICAR) Inhibits Palmitate-Induced Endothelial Cell Apoptosis Through Reactive Oxygen Species Suppression’, *Journal of Pharmacological Sciences*, 106(3), pp. 394–403. Available at: https://doi.org/10.1254/JPHS.FP0071857.

Kirpichnikov, D., McFarlane, S.I. and Sowers, J.R. (2002) ‘Metformin: An update’, *Annals of Internal Medicine*, 137(1), pp. 25–33. Available at: https://doi.org/10.7326/0003-4819-137-1-200207020-00009.

Klaff, L.J. and Taborsky, G.J. (1987) ‘Pancreatic somatostatin is a mediator of glucagon inhibition by hyperglycemia’, *Diabetes*, 36(5), pp. 592–596. Available at: https://doi.org/10.2337/DIAB.36.5.592.

Knepel, W., Chafitz, J. and Habener, J.F. (1990) ‘Transcriptional Activation of the Rat Glucagon Gene by the Cyclic AMP-Responsive Element in Pancreatic Islet Cells’, *Molecular and Cellular Biology*, 10, pp. 6799–6804. Available at:

https://doi.org/10.1128/mcb.10.12.6799-6804.1990.

Knorre, A. *et al.* (2002) 'DeltaF508-CFTR causes constitutive NF-kappaB activation through an ER-overload response in cystic fibrosis lungs', *Biological chemistry*, 383(2), pp. 271–282. Available at: https://doi.org/10.1515/BC.2002.029.

Knudsen, J.G. *et al.* (2019) 'Dysregulation of Glucagon Secretion by Hyperglycemia-Induced Sodium-Dependent Reduction of ATP Production', *Cell Metabolism*, 29(2), p. 430. Available at: https://doi.org/10.1016/J.CMET.2018.10.003.

Koay, A. *et al.* (2010) 'AMPK β subunits display isoform specific affinities for carbohydrates', *FEBS Letters*, 584(15), pp. 3499–3503. Available at: https://doi.org/10.1016/J.FEBSLET.2010.07.015.

Kobayashi, H. *et al.* (2004) 'Expression of glucose transporter 4 in the human pancreatic islet of Langerhans', *Biochemical and Biophysical Research Communications*, 314(4), pp. 1121–1125. Available at: https://doi.org/10.1016/J.BBRC.2004.01.010.

Koch, C. *et al.* (2001) 'European Epidemiologic Registry of Cystic Fibrosis (ERCF): Comparison of Major Disease Manifestations Between Patients With Different Classes of Mutations on Behalf of the Investigators of the ERCF', *Pediatric Pulmonology*, 31, pp. 1–12. Available at: https://doi.org/10.1002/1099-0496.

Kola, B. *et al.* (2005) 'Cannabinoids and Ghrelin Have Both Central and Peripheral Metabolic and Cardiac Effects via AMP-activated Protein Kinase', *Journal of Biological Chemistry*, 280(26), pp. 25196–25201. Available at: https://doi.org/10.1074/JBC.C500175200.

Komatsu, M. *et al.* (2013) 'Glucose-stimulated insulin secretion: A newer perspective', *Journal of Diabetes Investigation*, 4(6), pp. 511–516. Available at: https://doi.org/10.1111/JDI.12094.

Kongsuphol, P. *et al.* (2009a) ‘Mechanistic Insight into Control of CFTR by AMPK’, *Journal of Biological Chemistry*, 284(9), pp. 5645–5653. Available at: https://doi.org/10.1074/JBC.M806780200.

Kongsuphol, P. *et al.* (2009b) ‘Regulation of Cl- secretion by AMPK in vivo’, *Pflugers Archiv European Journal of Physiology*, 457(5), pp. 1071–1078. Available at: https://doi.org/10.1007/S00424-008-0577-3/FIGURES/6.

Kopietz, F. *et al.* (2021) ‘A-769662 inhibits adipocyte glucose uptake in an AMPK-independent manner’, *The Biochemical journal*, 478(3), pp. 633–646. Available at: https://doi.org/10.1042/BCJ20200659.

Kramer, N.B. *et al.* (2021) ‘Glucagon Resistance and Decreased Susceptibility to Diabetes in a Model of Chronic Hyperglucagonemia’, *Diabetes*, 70(2), pp. 477–491. Available at: https://doi.org/10.2337/DB20-0440.

Krieger, J.P., Langhans, W. and Lee, S.J. (2015) ‘Vagal mediation of GLP-1’s effects on food intake and glycemia’, *Physiology & Behavior*, 152, pp. 372–380. Available at: https://doi.org/10.1016/J.PHYSBEH.2015.06.001.

Kristófi, R., Endocrinology, J.E.-J. of and 2021, undefined (2021) ‘Metformin as an anti-inflammatory agent: a short review’, *scholar.archive.org* [Preprint]. Available at: https://doi.org/10.1530/JOE-21-0194.

Kuo, P. *et al.* (2011) ‘Gastric Emptying, Incretin Hormone Secretion, and Postprandial Glycemia in Cystic Fibrosis—Effects of Pancreatic Enzyme Supplementation’, *The Journal of Clinical Endocrinology & Metabolism*, 96(5), pp. E851–E855. Available at: https://doi.org/10.1210/JC.2010-2460.

Laemmli, U.K. (1970) ‘Cleavage of Structural Proteins during the Assembly of the Head of Bacteriophage T4’, *Nature 1970 227:5259*, 227(5259), pp. 680–685. Available at: https://doi.org/10.1038/227680a0.

Laguna, T.A., Nathan, B.M. and Moran, A. (2010) ‘Managing diabetes in cystic fibrosis’, *Obesity and Metabolism*, 12, pp. 858–864. Available at: https://doi.org/10.1111/j.1463-1326.2010.01250.x.

Lai, Y.C. *et al.* (2014) ‘A small-molecule benzimidazole derivative that potently activates AMPK to increase glucose transport in skeletal muscle: comparison with effects of contraction and other AMPK activators’, *Biochemical Journal*, 460(3), pp. 363–375. Available at: https://doi.org/10.1042/BJ20131673.

Lam, A.T.N. *et al.* (2020) ‘Increased expression of anion transporter SLC26A9 delays diabetes onset in cystic fibrosis’, *The Journal of Clinical Investigation*, 130(1), pp. 272–286. Available at: https://doi.org/10.1172/JCI129833.

Lamoia, T.E. and Shulman, G.I. (2021) ‘Cellular and Molecular Mechanisms of Metformin Action’, *Endocrine Reviews*, 42(1), pp. 77–96. Available at: https://doi.org/10.1210/ENDREV/BNAA023.

Languren, G. *et al.* (2019) ‘Recurrent moderate hypoglycemia exacerbates oxidative damage and neuronal death leading to cognitive dysfunction after the hypoglycemic coma’, *Journal of Cerebral Blood Flow & Metabolism*, 39(5), p. 808. Available at: https://doi.org/10.1177/0271678X17733640.

Lanng, S. *et al.* (1993) ‘Pancreas and gut hormone responses to oral glucose and intravenous glucagon in cystic fibrosis patients with normal, impaired, and diabetic glucose tolerance’, *Acta Endocrinologica (Norway)*, 128(3), pp. 207–214. Available at: https://doi.org/10.1530/ACTA.0.1280207.

Lanng, S. *et al.* (1994) ‘Insulin sensitivity and insulin clearance in cystic fibrosis patients with normal and diabetic glucose tolerance’, *Clinical Endocrinology*, 41(2), pp. 217–223. Available at: https://doi.org/10.1111/J.1365-2265.1994.TB02533.X.

Laybutt, D.R. *et al.* (2007) ‘Endoplasmic reticulum stress contributes to beta cell apoptosis in type 2 diabetes’, *Diabetologia*, 50(4), pp. 752–763. Available at: https://doi.org/10.1007/S00125-006-0590-Z/TABLES/2.

Leclerc, I. *et al.* (2011) ‘AMP-activated protein kinase regulates glucagon secretion from mouse pancreatic alpha cells’, *Diabetologia*, 54(1), pp. 125–134. Available at: https://doi.org/10.1007/s00125-010-1929-z.

Lee, E. *et al.* (2017) ‘A role of pancreatic stellate cells in islet fibrosis and β-cell dysfunction in type 2 diabetes mellitus’, *Biochemical and biophysical research communications*, 485(2), pp. 328–334. Available at: https://doi.org/10.1016/J.BBRC.2017.02.082.

Lee, Jieun *et al.* (2016) ‘Hepatic fatty acid oxidation restrains systemic catabolism during starvation’, *Cell reports*, 16(1), p. 201. Available at: https://doi.org/10.1016/J.CELREP.2016.05.062.

Lee, S.C., Robson-Doucette, C.A. and Wheeler, M.B. (2009) ‘Uncoupling protein 2 regulates reactive oxygen species formation in islets and influences susceptibility to diabetogenic action of streptozotocin’, *Journal of Endocrinology*, 203(1), pp. 33–43. Available at: https://doi.org/10.1677/JOE-09-0117.

Lee, Y. *et al.* (2004) ‘Hyperleptinemia prevents lipotoxic cardiomyopathy in acyl CoA synthase transgenic mice’, *Proceedings of the National Academy of Sciences of the United States of America*, 101(37), pp. 13624–13629. Available at: https://doi.org/10.1073/PNAS.0405499101/ASSET/0FE60BB3-2CBF-4958-BB4E-869F1AC2EF41/ASSETS/GRAPHIC/ZPQ0370459510005.JPEG.

Lee, Young H. *et al.* (2016) ‘Glucagon is the key factor in the development of diabetes’, *Diabetologia*, 59(7), pp. 1372–1375. Available at: https://doi.org/10.1007/S00125-016-3965-9/TABLES/2.

Leibiger, B. *et al.* (2012) ‘Glucagon regulates its own synthesis by autocrine signaling’, *Proceedings of the National Academy of Sciences of the United States of America*, 109(51), pp. 20925–20930. Available at: https://doi.org/10.1073/PNAS.1212870110/SUPPL_FILE/PNAS.201212870SI.PDF.

Levin, B.E. *et al.* (2008) ‘Ventromedial Hypothalamic Glucokinase Is an Important Mediator of the Counterregulatory Response to Insulin-Induced Hypoglycemia’. Available at: https://doi.org/10.2337/db07-1755.

Li, H. *et al.* (2018) ‘The first pediatric case of glucagon receptor defect due to

biallelic mutations in GCGR is identified by newborn screening of elevated arginine', *Molecular Genetics and Metabolism Reports*, 17, p. 46. Available at: https://doi.org/10.1016/J.YMGMR.2018.09.006.

Li, R. *et al.* (2021) 'GLP-1-Induced AMPK Activation Inhibits PARP-1 and Promotes LXR-Mediated ABCA1 Expression to Protect Pancreatic β-Cells Against Cholesterol-Induced Toxicity Through Cholesterol Efflux', *Frontiers in Cell and Developmental Biology*, 9. Available at: https://doi.org/10.3389/FCELL.2021.646113/FULL.

Li, W.C. *et al.* (2010) 'Activation of pancreatic-duct-derived progenitor cells during pancreas regeneration in adult rats', *Journal of Cell Science*, 123(16), pp. 2792–2802. Available at: https://doi.org/10.1242/JCS.065268.

Li, Y. *et al.* (2021) 'SIRT3 affects mitochondrial metabolic reprogramming via the AMPK-PGC-1α axis in the development of benign prostatic hyperplasia'. Available at: https://doi.org/10.1002/pros.24208.

Li, Y.Y. *et al.* (2013) 'Novel small-molecule AMPK activator orally exerts beneficial effects on diabetic db/db mice', *Toxicology and Applied Pharmacology*, 273(2), pp. 325–334. Available at: https://doi.org/10.1016/J.TAAP.2013.09.006.

Liang, J. *et al.* (2015) 'Myristoylation confers noncanonical AMPK functions in autophagy selectivity and mitochondrial surveillance', *Nature Communications 2015 6:1*, 6(1), pp. 1–14. Available at: https://doi.org/10.1038/ncomms8926.

Ling, N.X.Y. *et al.* (2020) 'mTORC1 directly inhibits AMPK to promote cell proliferation under nutrient stress', *Nature metabolism*, 2(1), p. 41. Available at: https://doi.org/10.1038/S42255-019-0157-1.

Lipovka, Y. and Konhilas, J.P. (2015) 'AMP-Activated Protein Kinase Signalling in Cancer and Cardiac Hypertrophy', *Cardiovascular pharmacology: open access*, 4(3). Available at: https://doi.org/10.4172/2329-6607.1000154.

Litvin, M., Clark, A.L. and Fisher, S.J. (2013) 'Recurrent hypoglycemia: boosting

the brain's metabolic flexibility', *The Journal of Clinical Investigation*, 123(5), pp. 1922–1924. Available at: https://doi.org/10.1172/JCI69796.

Liu, J. *et al.* (2022) 'Low- and middle-income countries demonstrate rapid growth of type 2 diabetes: an analysis based on Global Burden of Disease 1990–2019 data', *Diabetologia*, 65(8), p. 1339. Available at: https://doi.org/10.1007/S00125-022-05713-6.

Liu, Z. *et al.* (2011) 'Insulin and Glucagon Regulate Pancreatic α-Cell Proliferation', *PLoS ONE*, 6(1), p. 16096. Available at: https://doi.org/10.1371/JOURNAL.PONE.0016096.

Livak, K.J. and Schmittgen, T.D. (2001) 'Analysis of relative gene expression data using real-time quantitative PCR and the 2(-Delta Delta C(T)) Method', *Methods (San Diego, Calif.)*, 25(4), pp. 402–408. Available at: https://doi.org/10.1006/METH.2001.1262.

Logan, A. *et al.* (2014) 'In vivo levels of mitochondrial hydrogen peroxide increase with age in mtDNA mutator mice', *Aging Cell*, 13(4), pp. 765–768. Available at: https://doi.org/10.1111/ACEL.12212.

Löhr, M. *et al.* (1989) 'Cystic fibrosis associated islet changes may provide a basis for diabetes - An immunocytochemical and morphometrical study', *Virchows Archiv A Pathological Anatomy and Histopathology*, 414(2), pp. 179–185. Available at: https://doi.org/10.1007/BF00718598.

Longuet, C. *et al.* (2013) 'Liver-specific disruption of the murine glucagon receptor produces α-cell hyperplasia: evidence for a circulating α-cell growth factor', *Diabetes*, 62(4), pp. 1196–1205. Available at: https://doi.org/10.2337/DB11-1605.

López-Pérez, A. *et al.* (2021) 'Pan-AMPK activator O304 prevents gene expression changes and remobilisation of histone marks in islets of diet-induced obese mice', *Scientific Reports 2021 11:1*, 11(1), pp. 1–13. Available at: https://doi.org/10.1038/s41598-021-03567-3.

Los, E. and Wilt, A.S. (2023) ‘Diabetes Mellitus Type 1 In Children’, *StatPearls* [Preprint]. Available at: https://www.ncbi.nlm.nih.gov/books/NBK441918/ (Accessed: 10 April 2023).

Low Wang, C.C., Galinkin, J.L. and Hiatt, W.R. (2015) ‘Toxicity of a novel therapeutic agent targeting mitochondrial complex I’, *Clinical Pharmacology and Therapeutics*, 98(5), pp. 551–559. Available at: https://doi.org/10.1002/CPT.178.

Lu, M. *et al.* (2006) ‘CFTR is required for PKA-regulated ATP sensitivity of Kir1.1 potassium channels in mouse kidney’, *Journal of Clinical Investigation*, 116(3), pp. 797–807. Available at: https://doi.org/10.1172/JCI26961.

Lucotte, G., Hazout, S. and De Braekeleer, M. (1995) ‘Complete map of cystic fibrosis mutation DF508 frequencies in Western Europe and correlation between mutation frequencies and incidence of disease’, *Human Biology* [Preprint]. Available at: https://www.jstor.org/stable/41465429 (Accessed: 6 April 2023).

Lukacs, G.L. and Verkman, A.S. (2012) ‘CFTR: folding, misfolding and correcting the ΔF508 conformational defect’, *Trends in molecular medicine*, 18(2), p. 81. Available at: https://doi.org/10.1016/J.MOLMED.2011.10.003.

Ma, X. *et al.* (2005) ‘Glucagon stimulates exocytosis in mouse and rat pancreatic alpha-cells by binding to glucagon receptors’, *Molecular endocrinology (Baltimore, Md.)*, 19(1), pp. 198–212. Available at: https://doi.org/10.1210/ME.2004-0059.

Ma, Y. *et al.* (2018) ‘Recurrent hypoglycemia inhibits the counterregulatory response by suppressing adrenal activity’, *The Journal of Clinical Investigation*, 128(9), pp. 3866–3871. Available at: https://doi.org/10.1172/JCI91921.

Ma, Z.A., Zhao, Z. and Turk, J. (2012) ‘Mitochondrial dysfunction and β-cell failure in type 2 diabetes mellitus’, *Experimental diabetes research*, 2012. Available at: https://doi.org/10.1155/2012/703538.

Maahs, D.M. *et al.* (2010) ‘Chapter 1: Epidemiology of Type 1 Diabetes’, *Endocrinology and metabolism clinics of North America*, 39(3), p. 481. Available at: https://doi.org/10.1016/J.ECL.2010.05.011.

MacDonald, M.J. (1981) ‘High content of mitochondrial glycerol-3-phosphate dehydrogenase in pancreatic islets and its inhibition by diazoxide.’, *Journal of Biological Chemistry*, 256(16), pp. 8287–8290. Available at: https://doi.org/10.1016/S0021-9258(19)68840-X.

MacDonald, M.J. *et al.* (2021) ‘Metformin’s Therapeutic Efficacy in the Treatment of Diabetes Does Not Involve Inhibition of Mitochondrial Glycerol Phosphate Dehydrogenase’, *Diabetes*, 70(7), pp. 1575–1580. Available at: https://doi.org/10.2337/DB20-1143.

Madden, M.E. and Sarras, M.P. (1989) ‘The pancreatic ductal system of the rat: cell diversity, ultrastructure, and innervation’, *Pancreas*, 4(4), pp. 472–485. Available at: https://doi.org/10.1097/00006676-198908000-00013.

Madiraju, A.K. *et al.* (2014) ‘Metformin suppresses gluconeogenesis by inhibiting mitochondrial glycerophosphate dehydrogenase’, *Nature*, 510(7506), p. 542. Available at: https://doi.org/10.1038/NATURE13270.

Malaisse, W.J. (2016) ‘Role of glycogen metabolism in pancreatic islet beta cell function’, *Diabetologia*, 59(11), pp. 2489–2491. Available at: https://doi.org/10.1007/S00125-016-4092-3/METRICS.

Mandal, S.K. *et al.* (2017) ‘Role of hindbrain adenosine 5′-monophosphate-activated protein kinase (AMPK) in hypothalamic AMPK and metabolic neuropeptide adaptation to recurring insulin-induced hypoglycemia in the male rat’, *Neuropeptides*, 66, pp. 25–35. Available at: https://doi.org/10.1016/J.NPEP.2017.08.001.

Mannik, L.A. *et al.* (2018) ‘Prevalence of hypoglycemia during oral glucose tolerance testing in adults with cystic fibrosis and risk of developing cystic fibrosis-related diabetes’, *Journal of cystic fibrosis : official journal of the*

European Cystic Fibrosis Society, 17(4), pp. 536–541. Available at: https://doi.org/10.1016/J.JCF.2018.03.009.

Maran, A. *et al.* (2000) 'Brain function rescue effect of lactate following hypoglycaemia is not an adaptation process in both normal and Type I diabetic subjects', *Diabetologia*, 43(6), pp. 733–741. Available at: https://doi.org/10.1007/S001250051371/METRICS.

Marangou, A.G. *et al.* (1986) 'Metabolic consequences of prolonged hyperinsulinemia in humans. Evidence for induction of insulin insensitivity', *Diabetes*, 35(12), pp. 1383–1389. Available at: https://doi.org/10.2337/DIAB.35.12.1383.

Le Marchand, S.J. and Piston, D.W. (2010) 'Glucose Suppression of Glucagon Secretion: METABOLIC AND CALCIUM RESPONSES FROM α-CELLS IN INTACT MOUSE PANCREATIC ISLETS*', *The Journal of Biological Chemistry*, 285(19), p. 14389. Available at: https://doi.org/10.1074/JBC.M109.069195.

Marcinko, K. *et al.* (2015) 'The AMPK activator R419 improves exercise capacity and skeletal muscle insulin sensitivity in obese mice', *Molecular Metabolism*, 4(9), pp. 643–651. Available at: https://doi.org/10.1016/J.MOLMET.2015.06.002.

De Marinis, Y.Z. *et al.* (2010) 'GLP-1 inhibits and adrenaline stimulates glucagon release by differential modulation of N- and L-type Ca2+ channel-dependent exocytosis', *Cell metabolism*, 11(6), p. 543. Available at: https://doi.org/10.1016/J.CMET.2010.04.007.

Marino, C.R. *et al.* (1991) 'Localization of the cystic fibrosis transmembrane conductance regulator in pancreas.', *The Journal of Clinical Investigation*, 88(2), pp. 712–716. Available at: https://doi.org/10.1172/JCI115358.

Marroquin, L.D. *et al.* (2007) 'Circumventing the Crabtree Effect: Replacing Media Glucose with Galactose Increases Susceptibility of HepG2 Cells to Mitochondrial Toxicants', *Toxicological Sciences*, 97(2), pp. 539–547. Available

at: https://doi.org/10.1093/TOXSCI/KFM052.

Marshall, B.C. *et al.* (2005) ‘Epidemiology of cystic fibrosis-related diabetes’, *The Journal of Pediatrics*, 146(5), pp. 681–687. Available at: https://doi.org/10.1016/J.JPEDS.2004.12.039.

Marsin, A.S. *et al.* (2000) ‘Phosphorylation and activation of heart PFK-2 by AMPK has a role in the stimulation of glycolysis during ischaemia’, *Current Biology*, 10(20), pp. 1247–1255. Available at: https://doi.org/10.1016/S0960-9822(00)00742-9.

Marsin, A.S. *et al.* (2002) ‘The stimulation of glycolysis by hypoxia in activated monocytes is mediated by AMP-activated protein kinase and inducible 6-phosphofructo-2-kinase’, *Journal of Biological Chemistry*, 277(34), pp. 30778–30783. Available at: https://doi.org/10.1074/jbc.M205213200.

Martín-Timón, I. and Cañizo-Gómez, F.J. del (2015) ‘Mechanisms of hypoglycemia unawareness and implications in diabetic patients’, *World Journal of Diabetes*, 6(7), p. 912. Available at: https://doi.org/10.4239/WJD.V6.I7.912.

Marty, N. *et al.* (2005) ‘Regulation of glucagon secretion by glucose transporter type 2 (glut2) and astrocyte-dependent glucose sensors’, *The Journal of Clinical Investigation*, 115. Available at: https://doi.org/10.1172/JCI26309.

Massa, L. *et al.* (2004) ‘Interaction of 6-Phosphofructo-2-Kinase/Fructose-2,6-Bisphosphatase (PFK-2/FBPase-2) With Glucokinase Activates Glucose Phosphorylation and Glucose Metabolism in Insulin-Producing Cells’, *Diabetes*, 53(4), pp. 1020–1029. Available at: https://doi.org/10.2337/DIABETES.53.4.1020.

Mathew, T.K. and Tadi, P. (2022) ‘Blood Glucose Monitoring’, *Medical Devices and Systems*, pp. 66-1-66–10. Available at: https://doi.org/10.5005/jp/books/12651_10.

Matschinsky, F.M. and Wilson, D.F. (2019) ‘The central role of glucokinase in glucose homeostasis: A perspective 50 years after demonstrating the presence

of the enzyme in islets of Langerhans', *Frontiers in Physiology*, 10(MAR), p. 148. Available at: https://doi.org/10.3389/FPHYS.2019.00148/BIBTEX.

McCoy, R.G. *et al.* (2012) 'Increased Mortality of Patients With Diabetes Reporting Severe Hypoglycemia', *Diabetes Care*, 35(9), p. 1897. Available at: https://doi.org/10.2337/DC11-2054.

McCrimmon, R. (2008) 'The mechanisms that underlie glucose sensing during hypoglycaemia in diabetes', *Diabetic Medicine*, 25(5), pp. 513–522. Available at: https://doi.org/10.1111/J.1464-5491.2008.02376.X.

McCrimmon, R.J. *et al.* (2006) 'Activation of AMP-Activated Protein Kinase Within the Ventromedial Hypothalamus Amplifies Counterregulatory Hormone Responses in Rats With Defective Counterregulation', *Diabetes*, 55(6), pp. 1755–1760. Available at: https://doi.org/10.2337/DB05-1359.

McCrimmon, R.J. *et al.* (2008) 'Key Role for AMP-Activated Protein Kinase in the Ventromedial Hypothalamus in Regulating Counterregulatory Hormone Responses to Acute Hypoglycemia', *Diabetes*, 57(2), pp. 444–450. Available at: https://doi.org/10.2337/DB07-0837.

McCrimmon, R.J. (2021) 'Consequences of recurrent hypoglycaemia on brain function in diabetes', *Diabetologia*, 64(5), p. 971. Available at: https://doi.org/10.1007/S00125-020-05369-0.

McCrimmon, R.J. (2022) 'Remembrance of things past: The consequences of recurrent hypoglycaemia in diabetes', *Diabetic Medicine*, 39(12), p. e14973. Available at: https://doi.org/10.1111/DME.14973.

McIntyre, H.D. *et al.* (1991) 'Metformin increases insulin sensitivity and basal glucose clearance in type 2 (non-insulin dependent) diabetes mellitus', *Australian and New Zealand journal of medicine*, 21(5), pp. 714–719. Available at: https://doi.org/10.1111/J.1445-5994.1991.TB01375.X.

Meacham, L.R. *et al.* (1993) 'Preservation of somatostatin secretion in cystic fibrosis patients with diabetes.', *Archives of Disease in Childhood*, 68(1), p. 123.

Available at: https://doi.org/10.1136/ADC.68.1.123.

Medici, F. *et al.* (1999) 'Concordance rate for type II diabetes mellitus in monozygotic twins: actuarial analysis', *Diabetologia*, 42(2), pp. 146–150. Available at: https://doi.org/10.1007/S001250051132.

Meek, T.H. *et al.* (2015) 'Evidence That in Uncontrolled Diabetes, Hyperglucagonemia Is Required for Ketosis but Not for Increased Hepatic Glucose Production or Hyperglycemia', *Diabetes*, 64(7), p. 2376. Available at: https://doi.org/10.2337/DB14-1562.

Mehta, R. *et al.* (2021) 'Exogenous exposure to dihydroxyacetone mimics high fructose induced oxidative stress and mitochondrial dysfunction', *Environmental and Molecular Mutagenesis*, 62(3), pp. 185–202. Available at: https://doi.org/10.1002/EM.22425.

Meloni, A.R. *et al.* (2013) 'GLP-1 receptor activated insulin secretion from pancreatic β-cells: mechanism and glucose dependence', *Diabetes, Obesity & Metabolism*, 15(1), p. 15. Available at: https://doi.org/10.1111/J.1463-1326.2012.01663.X.

Merrins, M.J. *et al.* (2012) 'Phosphofructo-2-kinase/Fructose-2,6-bisphosphatase Modulates Oscillations of Pancreatic Islet Metabolism', *PLoS ONE*, 7(4). Available at: https://doi.org/10.1371/JOURNAL.PONE.0034036.

Merz, K.E. and Thurmond, D.C. (2020) 'Role of Skeletal Muscle in Insulin Resistance and Glucose Uptake', *Comprehensive Physiology*, 10(3), p. 785. Available at: https://doi.org/10.1002/CPHY.C190029.

Van Der Meulen, T. *et al.* (2015) 'Urocortin3 mediates somatostatin-dependent negative feedback control of insulin secretion', *Nature Medicine 2015 21:7*, 21(7), pp. 769–776. Available at: https://doi.org/10.1038/nm.3872.

Miki, A. *et al.* (2018) 'Divergent antioxidant capacity of human islet cell subsets: A potential cause of beta-cell vulnerability in diabetes and islet transplantation', *PLOS ONE*, 13(5), p. e0196570. Available at:

https://doi.org/10.1371/JOURNAL.PONE.0196570.

Miki, T. *et al.* (2001) 'ATP-sensitive K+ channels in the hypothalamus are essential for the maintenance of glucose homeostasis', *Nature neuroscience*, 4(5), pp. 507–512. Available at: https://doi.org/10.1038/87455.

Miller, R.A. *et al.* (2013) 'Biguanides suppress hepatic glucagon signalling by decreasing production of cyclic AMP', *Nature*, 494(7436), pp. 256–260. Available at: https://doi.org/10.1038/nature11808.

Milnerowicz, H. and Śliwińska-Mosson, M. (2017) 'Distribution of Pancreatic Polypeptide-secreting Endocrine Cells in Nondiabetic and Diabetic Cases', *Applied Immunohistochemistry and Molecular Morphology*, 25(6), pp. 422–431. Available at: https://doi.org/10.1097/PAI.0000000000000310.

Minokoshi, Y. *et al.* (2002) 'Leptin stimulates fatty-acid oxidation by activating AMP-activated protein kinase', *Nature 2002 415:6869*, 415(6869), pp. 339–343. Available at: https://doi.org/10.1038/415339a.

Mir-Coll, J. *et al.* (2016) 'Genetic models rule out a major role of beta cell glycogen in the control of glucose homeostasis', *Diabetologia*, 59(5), pp. 1012–1020. Available at: https://doi.org/10.1007/S00125-016-3871-1/FIGURES/7.

Miranda, C. *et al.* (2022) 'Gap junction coupling and islet delta-cell function in health and disease', *Peptides*, 147, p. 170704. Available at: https://doi.org/10.1016/J.PEPTIDES.2021.170704.

Mitchelhill, K.I. *et al.* (1997) 'Posttranslational modifications of the 5'-AMP-activated protein kinase β1 subunit', *Journal of Biological Chemistry*, 272(39), pp. 24475–24479. Available at: https://doi.org/10.1074/jbc.272.39.24475.

Mitrakou, A. *et al.* (2010) 'Role of Reduced Suppression of Glucose Production and Diminished Early Insulin Release in Impaired Glucose Tolerance', *http://dx.doi.org/10.1056/NEJM199201023260104*, 326(1), pp. 22–29. Available at: https://doi.org/10.1056/NEJM199201023260104.

Mobasseri, M. *et al.* (2020) ‘Prevalence and incidence of type 1 diabetes in the world: a systematic review and meta-analysis’, *Health promotion perspectives*, 10(2), pp. 98–115. Available at: https://doi.org/10.34172/HPP.2020.18.

Moede, T. *et al.* (2020) ‘Glucokinase intrinsically regulates glucose sensing and glucagon secretion in pancreatic alpha cells’, *Scientific Reports 2020 10:1*, 10(1), pp. 1–11. Available at: https://doi.org/10.1038/s41598-020-76863-z.

Mohan, K. *et al.* (2009) ‘Mechanisms of glucose intolerance in cystic fibrosis’, *Diabetic Medicine*, 26(6), pp. 582–588. Available at: https://doi.org/10.1111/J.1464-5491.2009.02738.X.

Moheet, A. *et al.* (2019) ‘Hypoglycemia in cystic fibrosis: Prevalence, impact and treatment’, *Journal of Cystic Fibrosis*, 18, pp. S19–S24. Available at: https://doi.org/10.1016/J.JCF.2019.08.004.

Moheet, A. and Moran, A. (2017) ‘CF-related diabetes: Containing the metabolic miscreant of cystic fibrosis’, *Pediatric pulmonology*, 52(S48), pp. S37–S43. Available at: https://doi.org/10.1002/PPUL.23762.

Moheet, A. and Moran, A. (2022) ‘New Concepts in the Pathogenesis of Cystic Fibrosis–Related Diabetes’, *The Journal of Clinical Endocrinology & Metabolism*, 107(6), pp. 1503–1509. Available at: https://doi.org/10.1210/CLINEM/DGAC020.

Moin, A.S.M. *et al.* (2020) ‘Pancreatic alpha-cell mass across adult human lifespan’, *European Journal of Endocrinology*, 182(2). Available at: https://doi.org/10.1530/EJE-19-0844.

Mojsov, S., Weir, G.C. and Habener, J.F. (1987) ‘Insulinotropin: Glucagon-like peptide I (7-37) co-encoded in the glucagon gene is a potent stimulator of insulin release in the perfused rat pancreas’, *Journal of Clinical Investigation*, 79(2), pp. 616–619. Available at: https://doi.org/10.1172/JCI112855.

Moonira, T. *et al.* (2020) ‘Metformin lowers glucose 6-phosphate in hepatocytes by activation of glycolysis downstream of glucose phosphorylation’, *Journal of*

Biological Chemistry, 295(10), pp. 3330–3346. Available at: https://doi.org/10.1074/JBC.RA120.012533.

Moran, A. *et al.* (1991) 'Pancreatic endocrine function in cystic fibrosis', *The Journal of Pediatrics*, 118(5), pp. 715–723. Available at: https://doi.org/10.1016/S0022-3476(05)80032-0.

Moran, A. *et al.* (2010) 'Clinical Care Guidelines for Cystic Fibrosis–Related Diabetes: A position statement of the American Diabetes Association and a clinical practice guideline of the Cystic Fibrosis Foundation, endorsed by the Pediatric Endocrine Society', *Diabetes Care*, 33(12), p. 2697. Available at: https://doi.org/10.2337/DC10-1768.

Moran, O. (2010) 'Model of the cAMP activation of chloride transport by CFTR channel and the mechanism of potentiators', *Journal of Theoretical Biology*, 262(1), pp. 73–79. Available at: https://doi.org/10.1016/J.JTBI.2009.08.032.

Moreira, P.I. (2014) 'Metformin in the diabetic brain: friend or foe?', *Annals of Translational Medicine*, 2(6), p. 54. Available at: https://doi.org/10.3978/J.ISSN.2305-5839.2014.06.10.

De Morentin, P.B.M. *et al.* (2011) 'Hypothalamic AMP-activated protein kinase as a mediator of whole body energy balance', *Reviews in Endocrine and Metabolic Disorders 2011 12:3*, 12(3), pp. 127–140. Available at: https://doi.org/10.1007/S11154-011-9165-5.

Morgan, L.M., Wright, J.W. and Marks, V. (1979) 'The Effect of Oral Galactose on GIP and Insulin Secretion in Man', *Diabetologia*, 16, pp. 235–239.

Morrison, K.R. *et al.* (2022) 'An AMPKα2-specific phospho-switch controls lysosomal targeting for activation', *Cell Reports*, 38(7), p. 110365. Available at: https://doi.org/10.1016/J.CELREP.2022.110365.

Mortera, R.R., Bains, Y. and Gugliucci, A. (2019) 'Fructose at the crossroads of the metabolic syndrome and obesity epidemics', *Frontiers in Bioscience - Landmark*, 24(2), pp. 186–211. Available at:

https://doi.org/10.2741/4713/4713/FIG7.JPG.

Mráček, T., Drahota, Z. and Houštěk, J. (2013) ‘The function and the role of the mitochondrial glycerol-3-phosphate dehydrogenase in mammalian tissues’, *Biochimica et Biophysica Acta (BBA) - Bioenergetics*, 1827(3), pp. 401–410. Available at: https://doi.org/10.1016/J.BBABIO.2012.11.014.

Mulberg, A.E. *et al.* (1995) ‘Expression and localization of the cystic fibrosis transmembrane conductance regulator mRNA and its protein in rat brain’, *The Journal of clinical investigation*, 96(1), pp. 646–652. Available at: https://doi.org/10.1172/JCI118080.

Müller, W.A., Faloona, G.R. and Unger, R.H. (1973) ‘Hyperglucagonemia in diabetic ketoacidosis: Its prevalence and significance’, *The American Journal of Medicine*, 54(1), pp. 52–57. Available at: https://doi.org/10.1016/0002-9343(73)90083-1.

Munday, M.R. *et al.* (1988) ‘Identification by amino acid sequencing of three major regulatory phosphorylation sites on rat acetyl-CoA carboxylase’, *European Journal of Biochemistry*, 175(2), pp. 331–338. Available at: https://doi.org/10.1111/J.1432-1033.1988.TB14201.X.

Muneer, M. (2021) ‘Hypoglycaemia’, *Advances in Experimental Medicine and Biology*, 1307, pp. 43–69. Available at: https://doi.org/10.1007/5584_2020_534/TABLES/10.

Murlin, J.R. *et al.* (1923) ‘Aqueous extracts of pancreas: I. influence on the carbohydrate metabolism of depancreatized animals’, *Journal of Biological Chemistry*, 56(1), pp. 253–296. Available at: https://doi.org/10.1016/S0021-9258(18)85619-8.

Murphy, B.A. *et al.* (2009) ‘AMP-activated protein kinase and nitric oxide regulate the glucose sensitivity of ventromedial hypothalamic glucose-inhibited neurons’, *American Journal of Physiology - Cell Physiology*, 297(3), p. C750. Available at: https://doi.org/10.1152/AJPCELL.00127.2009.

Myers, R.W. *et al.* (2017) ‘Systemic pan-AMPK activator MK-8722 improves glucose homeostasis but induces cardiac hypertrophy’, *Science (New York, N.Y.)*, 357(6350), pp. 507–511. Available at: https://doi.org/10.1126/SCIENCE.AAH5582.

Nabrdalik, K. *et al.* (2022) ‘Gastrointestinal adverse events of metformin treatment in patients with type 2 diabetes mellitus: A systematic review, meta-analysis and meta-regression of randomized controlled trials’, *Frontiers in Endocrinology*, 13, p. 2166. Available at: https://doi.org/10.3389/FENDO.2022.975912/BIBTEX.

Nagy, L. *et al.* (2018) ‘Glycogen phosphorylase inhibition improves beta cell function’, *British Journal of Pharmacology*, 175(2), p. 301. Available at: https://doi.org/10.1111/BPH.13819.

Nam, K.S., Sunhwa, O.H. and Shin, I. (2016) ‘Ablation of CD44 induces glycolysis-to-oxidative phosphorylation transition via modulation of the c-Src–Akt–LKB1–AMPKα pathway’, *Biochemical Journal*, 473(19), pp. 3013–3030. Available at: https://doi.org/10.1042/BCJ20160613.

Nederstigt, C. *et al.* (2019) ‘Associated auto-immune disease in type 1 diabetes patients: a systematic review and meta-analysis’, *European Journal of Endocrinology*, 180(2), pp. 135–144. Available at: https://doi.org/10.1530/EJE-18-0515.

Neopane, K. *et al.* (2022) ‘Blocking AMPK β1 myristoylation enhances AMPK activity and protects mice from high-fat diet-induced obesity and hepatic steatosis’, *Cell Reports*, 41(12). Available at: https://doi.org/10.1016/J.CELREP.2022.111862.

Newman, B. *et al.* (1987) ‘Concordance for type 2 (non-insulin-dependent) diabetes mellitus in male twins’, *Diabetologia*, 30(10), pp. 763–768. Available at: https://doi.org/10.1007/BF00275741.

Ngoei, K.R.W. *et al.* (2018) ‘Structural Determinants for Small-Molecule

Activation of Skeletal Muscle AMPK α2β2γ1 by the Glucose Importagog SC4', *Cell Chemical Biology*, 25(6), pp. 728-737.e9. Available at: https://doi.org/10.1016/J.CHEMBIOL.2018.03.008.

Nguyen-Tu, M.S. *et al.* (2022) 'Opposing effects on regulated insulin secretion of acute vs chronic stimulation of AMP-activated protein kinase', *Diabetologia*, 65(6), pp. 997–1011. Available at: https://doi.org/10.1007/S00125-022-05673-X/FIGURES/6.

Nicholls, L.I., Ainscow, E.K. and Rutter, G.A. (2002) 'Glucose-stimulated insulin secretion does not require activation of pyruvate dehydrogenase: Impact of adenovirus-mediated overexpression of PDH kinase and PDH phosphate phosphatase in pancreatic islets', *Biochemical and Biophysical Research Communications*, 291(4), pp. 1081–1088. Available at: https://doi.org/10.1006/BBRC.2002.6567.

Nishitani, S. *et al.* (2002) 'Leucine promotes glucose uptake in skeletal muscles of rats', *Biochemical and Biophysical Research Communications*, 299(5), pp. 693–696. Available at: https://doi.org/10.1016/S0006-291X(02)02717-1.

Noblet, B. *et al.* (2021) 'Dual regulation of TxNIP by ChREBP and FoxO1 in liver', *iScience*, 24(3), p. 102218. Available at: https://doi.org/10.1016/J.ISCI.2021.102218.

Nolan, C.J. *et al.* (2015) 'Insulin resistance as a physiological defense against metabolic stress: implications for the management of subsets of type 2 diabetes', *Diabetes*, 64(3), pp. 673–686. Available at: https://doi.org/10.2337/DB14-0694.

Nolan, C.J. and Prentki, M. (2019) 'Insulin resistance and insulin hypersecretion in the metabolic syndrome and type 2 diabetes: Time for a conceptual framework shift', *Diabetes & vascular disease research*, 16(2), pp. 118–127. Available at: https://doi.org/10.1177/1479164119827611.

Nolfi-Donegan, D., Braganza, A. and Shiva, S. (2020) 'Mitochondrial electron

transport chain: Oxidative phosphorylation, oxidant production, and methods of measurement', *Redox Biology*, 37, p. 101674. Available at: https://doi.org/10.1016/J.REDOX.2020.101674.

Nomoto, H. *et al.* (2020) 'Activation of the HIF1α/PFKFB3 stress response pathway in beta cells in type 1 diabetes', *Diabetologia*, 63(1), pp. 149–161. Available at: https://doi.org/10.1007/S00125-019-05030-5/FIGURES/6.

Norris, A.W. *et al.* (2019) 'Survival in a bad neighborhood: pancreatic islets in cystic fibrosis', *The Journal of endocrinology*, 241(1), pp. R35–R50. Available at: https://doi.org/10.1530/JOE-18-0468.

Norris, J.M., Johnson, R.K. and Stene, L.C. (2020) 'Type 1 diabetes—early life origins and changing epidemiology', *The Lancet Diabetes & Endocrinology*, 8(3), pp. 226–238. Available at: https://doi.org/10.1016/S2213-8587(19)30412-7.

Nousia-Arvanitakis, S. *et al.* (1985) 'Pancreatic polypeptide in cystic fibrosis.', *Archives of Pathology & Laboratory Medicine*, 109(8), pp. 722–726. Available at: https://europepmc.org/article/med/3893382 (Accessed: 7 April 2023).

Ntimbane, T. *et al.* (2016) 'CFTR silencing in pancreaticβ-cells reveals a functional impact on glucose-stimulated insulin secretion and oxidative stress response', *American Journal of Physiology - Endocrinology and Metabolism*, 310(3), pp. E200–E212. Available at: https://doi.org/10.1152/AJPENDO.00333.2015/ASSET/IMAGES/LARGE/ZH10021675030005.JPEG.

Nyirjesy, S.C. *et al.* (2018) 'β-Cell secretory defects are present in pancreatic insufficient cystic fibrosis with 1-hour oral glucose tolerance test glucose ≥155 mg/dL'. Available at: https://doi.org/10.1111/pedi.12700.

Nyman, L.R. *et al.* (2010) 'Glucose-dependent blood flow dynamics in murine pancreatic islets in vivo', *American Journal of Physiology - Endocrinology and Metabolism*, 298(4), pp. 807–814. Available at:

https://doi.org/10.1152/AJPENDO.00715.2009/SUPPL_FILE/FIGS1.PDF.

O'Carroll, A.M. *et al.* (2008) 'Vasopressin potentiates corticotropin-releasing hormone-induced insulin release from mouse pancreatic β-cells', *The Journal of Endocrinology*, 197(2), p. 231. Available at: https://doi.org/10.1677/JOE-07-0645.

O'Neill, H.M., Holloway, G.P. and Steinberg, G.R. (2013) 'AMPK regulation of fatty acid metabolism and mitochondrial biogenesis: Implications for obesity', *Molecular and Cellular Endocrinology*, 366(2), pp. 135–151. Available at: https://doi.org/10.1016/J.MCE.2012.06.019.

Oakhill, J.S. *et al.* (2010) 'β-Subunit myristoylation is the gatekeeper for initiating metabolic stress sensing by AMP-activated protein kinase (AMPK)', *Proceedings of the National Academy of Sciences of the United States of America*, 107(45), pp. 19237–19241. Available at: https://doi.org/10.1073/PNAS.1009705107/-/DCSUPPLEMENTAL/PNAS.1009705107_SI.PDF.

Ode, K.L. *et al.* (2019) 'Cystic fibrosis related diabetes: Medical management', *Journal of Cystic Fibrosis*, 18, pp. S10–S18. Available at: https://doi.org/10.1016/J.JCF.2019.08.003.

Ohashi, Y. *et al.* (2021) 'Metabolic reprogramming in chondrocytes to promote mitochondrial respiration reduces downstream features of osteoarthritis', *Scientific Reports 2021 11:1*, 11(1), pp. 1–16. Available at: https://doi.org/10.1038/s41598-021-94611-9.

Olesen, H. V. *et al.* (2020) 'Cystic fibrosis related diabetes in Europe: Prevalence, risk factors and outcome; Olesen et al', *Journal of Cystic Fibrosis*, 19(2), pp. 321–327. Available at: https://doi.org/10.1016/J.JCF.2019.10.009.

Oligschlaeger, Y. *et al.* (2016) 'The interaction between AMPKβ2 and the PP1-targeting subunit R6 is dynamically regulated by intracellular glycogen content', *Biochemical Journal*, 473(7), pp. 937–947. Available at:

https://doi.org/10.1042/BJ20151035.

Olivier, A.K. *et al.* (2012) ‘Abnormal endocrine pancreas function at birth in cystic fibrosisferrets’, *The Journal of Clinical Investigation*, 122(10), p. 3755. Available at: https://doi.org/10.1172/JCI60610.

Olivier, S., Foretz, M. and Viollet, B. (2018) ‘Promise and challenges for direct small molecule AMPK activators’, *Biochemical Pharmacology*, 153, pp. 147–158. Available at: https://doi.org/10.1016/J.BCP.2018.01.049.

Olofsson, C.S. *et al.* (2004) ‘Palmitate stimulation of glucagon secretion in mouse pancreatic α-cells results from activation of L-type calcium channels and elevation of cytoplasmic calcium’, *Diabetes*, 53(11), pp. 2836–2843. Available at: https://doi.org/10.2337/diabetes.53.11.2836.

Olpin, S.E. (2004) ‘Implications of impaired ketogenesis in fatty acid oxidation disorders’, *Prostaglandins Leukotrienes and Essential Fatty Acids*, 70(3), pp. 293–308. Available at: https://doi.org/10.1016/j.plefa.2003.06.003.

Opara, E.C. and Go, V.L.W. (1991) ‘Influence of gastric inhibitory polypeptide (GIP) and glucose on the regulation of glucagon secretion by pancreatic alpha cells’, *Regulatory Peptides*, 32(2), pp. 65–73. Available at: https://doi.org/10.1016/0167-0115(91)90035-F.

Ostedgaard, L.S. *et al.* (2007) ‘Processing and function of CFTR-ΔF508 are species-dependent’, *Proceedings of the National Academy of Sciences of the United States of America*, 104(39), pp. 15370–15375. Available at: https://doi.org/10.1073/PNAS.0706974104/SUPPL_FILE/06974FIG7.PDF.

Osundiji, M.A. *et al.* (2011) ‘Recurrent hypoglycemia increases hypothalamic glucose phosphorylation activity in rats’, *Metabolism: clinical and experimental*, 60(4), p. 550. Available at: https://doi.org/10.1016/J.METABOL.2010.05.009.

Otonkoski, T. *et al.* (2007) ‘Physical Exercise–Induced Hypoglycemia Caused by Failed Silencing of Monocarboxylate Transporter 1 in Pancreatic β Cells’, *American Journal of Human Genetics*, 81(3), p. 467. Available at:

https://doi.org/10.1086/520960.

Ovens, A.J. *et al.* (2022) ‘Structure-function analysis of the AMPK activator SC4 and identification of a potent pan AMPK activator’, *Biochemical Journal*, 479(11), pp. 1181–1204. Available at: https://doi.org/10.1042/BCJ20220067.

Owen, M.R., Doran, E. and Halestrap, A.P. (2000) ‘Evidence that metformin exerts its anti-diabetic effects through inhibition of complex 1 of the mitochondrial respiratory chain.’, *Biochemical Journal*, 348(Pt 3), p. 607. Available at: https://doi.org/10.1042/0264-6021:3480607.

Padilla-Martínez, F. *et al.* (2020) ‘Systematic Review of Polygenic Risk Scores for Type 1 and Type 2 Diabetes’, *International Journal of Molecular Sciences*, 21(5). Available at: https://doi.org/10.3390/IJMS21051703.

Palmer, J.P. *et al.* (1976) ‘Glucagon response to hypoglycemia in sympathectomized man’, *The Journal of clinical investigation*, 57(2), pp. 522–525. Available at: https://doi.org/10.1172/JCI108305.

Panfoli, I. *et al.* (2021) ‘The Hormetic Effect of Metformin: “Less Is More”?’, *International Journal of Molecular Sciences 2021, Vol. 22, Page 6297*, 22(12), p. 6297. Available at: https://doi.org/10.3390/IJMS22126297.

Panzer, J.K. and Caicedo, A. (2021) ‘Targeting the Pancreatic α-Cell to Prevent Hypoglycemia in Type 1 Diabetes’, *Diabetes*, 70(12), pp. 2721–2732. Available at: https://doi.org/10.2337/DBI20-0048.

Panzer, J.K., Tamayo, A. and Caicedo, A. (2022) ‘Restoring glutamate receptor signaling in pancreatic alpha cells rescues glucagon responses in type 1 diabetes’, *Cell Reports*, 41(11), p. 111792. Available at: https://doi.org/10.1016/J.CELREP.2022.111792.

Papas, K.K. *et al.* (2019) ‘Oxygenation strategies for encapsulated islet and beta cell transplants’, *Advanced Drug Delivery Reviews*, 139, pp. 139–156. Available at: https://doi.org/10.1016/J.ADDR.2019.05.002.

Parikh, H. *et al.* (2007) ‘TXNIP Regulates Peripheral Glucose Metabolism in Humans’, *PLoS Medicine*, 4(5), pp. 0868–0879. Available at: https://doi.org/10.1371/JOURNAL.PMED.0040158.

Park, B.Y. *et al.* (2018) ‘PDK4 Deficiency Suppresses Hepatic Glucagon Signaling by Decreasing cAMP Levels’, *Diabetes*, 67(10), pp. 2054–2068. Available at: https://doi.org/10.2337/DB17-1529.

Park, H.J. *et al.* (2020) ‘The essential role of fructose-1,6-bisphosphatase 2 enzyme in thermal homeostasis upon cold stress’, *Experimental & Molecular Medicine 2020 52:3*, 52(3), pp. 485–496. Available at: https://doi.org/10.1038/s12276-020-0402-4.

Parker, J.C. *et al.* (2002) ‘Glycemic control in mice with targeted disruption of the glucagon receptor gene’, *Biochemical and Biophysical Research Communications*, 290(2), pp. 839–843. Available at: https://doi.org/10.1006/bbrc.2001.6265.

Patel, M.S. *et al.* (2014) ‘The pyruvate dehydrogenase complexes: Structure-based function and regulation’, *Journal of Biological Chemistry*, 289(24), pp. 16615–16623. Available at: https://doi.org/10.1074/JBC.R114.563148.

Patwari, P. *et al.* (2006) ‘The Interaction of Thioredoxin with Txnip: EVIDENCE FOR FORMATION OF A MIXED DISULFIDE BY DISULFIDE EXCHANGE’, *Journal of Biological Chemistry*, 281(31), pp. 21884–21891. Available at: https://doi.org/10.1074/JBC.M600427200.

Patzelt, C. and Weber, B. (1986) ‘Early O-glycosidic glycosylation of proglucagon in pancreatic islets: an unusual type of prohormonal modification.’, *The EMBO journal*, 5(9), pp. 2103–2108. Available at: https://doi.org/10.1002/J.1460-2075.1986.TB04472.X.

Pederson, R.A. and Brown, J.C. (1978) ‘Interaction of Gastric Inhibitory Polypeptide, Glucose, and Arginine on Insulin and Glucagon Secretion from the Perfused Rat Pancreas’, *Endocrinology*, 103(2), pp. 610–615. Available at:

https://doi.org/10.1210/ENDO-103-2-610.

Pelgrom, L.R., van der Ham, A.J. and Everts, B. (2016) ‘Analysis of TLR-induced metabolic changes in dendritic cells using the seahorse XFe96 extracellular flux analyzer’, *Methods in Molecular Biology*, 1390, pp. 273–285. Available at: https://doi.org/10.1007/978-1-4939-3335-8_17.

Perano, S.J. *et al.* (2014) ‘Pancreatic Enzyme Supplementation Improves the Incretin Hormone Response and Attenuates Postprandial Glycemia in Adolescents With Cystic Fibrosis: A Randomized Crossover Trial’, *The Journal of Clinical Endocrinology & Metabolism*, 99(7), pp. 2486–2493. Available at: https://doi.org/10.1210/JC.2013-4417.

Pernicova, I. and Korbonits, M. (2014) ‘Metformin-mode of action and clinical implications for diabetes and cancer’, *NATURE REVIEWS | ENDOCRINOLOGY*, 10, pp. 143–156. Available at: https://doi.org/10.1038/nrendo.2013.256.

Petit, P. *et al.* (1996) ‘Purinergic Receptors and Metabolic Function’, 39, pp. 413–425. Available at: https://doi.org/10.1002/(SICI)1098-2299(199611/12)39:3/4.

Pettus, J.H. *et al.* (2019) ‘Incidences of Severe Hypoglycemia and Diabetic Ketoacidosis and Prevalence of Microvascular Complications Stratified by Age and Glycemic Control in U.S. Adult Patients With Type 1 Diabetes: A Real-World Study’, *Diabetes Care*, 42(12), pp. 2220–2227. Available at: https://doi.org/10.2337/DC19-0830.

Phillips, L.K. *et al.* (2015) ‘Gastric emptying and glycaemia in health and diabetes mellitus’, *Nature reviews. Endocrinology*, 11(2), pp. 112–128. Available at: https://doi.org/10.1038/NRENDO.2014.202.

Pingitore, A. *et al.* (2017) ‘Dynamic Profiling of Insulin Secretion and ATP Generation in Isolated Human and Mouse Islets Reveals Differential Glucose Sensitivity’, *Cellular Physiology and Biochemistry*, 44(4), pp. 1352–1359.

Available at: https://doi.org/10.1159/000485532.

Pinkosky, S.L. *et al.* (2020) 'Long-chain fatty acyl-CoA esters regulate metabolism via allosteric control of AMPK β1 isoforms', *Nature Metabolism 2020 2:9*, 2(9), pp. 873–881. Available at: https://doi.org/10.1038/s42255-020-0245-2.

Pinti, M. V. *et al.* (2019) 'Mitochondrial dysfunction in type 2 diabetes mellitus: An organ-based analysis', *American Journal of Physiology - Endocrinology and Metabolism*, 316(2), pp. E268–E285. Available at: https://doi.org/10.1152/AJPENDO.00314.2018/ASSET/IMAGES/LARGE/ZH10021980260002.JPEG.

Piro, S. *et al.* (2010) 'Palmitate Affects Insulin Receptor Phosphorylation and Intracellular Insulin Signal in a Pancreatic α-Cell Line', *Endocrinology*, 151(9), pp. 4197–4206. Available at: https://doi.org/10.1210/EN.2009-1472.

Pitkänen, S. and Robinson, B.H. (1996) 'Mitochondrial Superoxide Radicals and MnSOD Mitochondrial Complex I Deficiency Leads to Increased Production of Superoxide Radicals and Induction of Superoxide Dismutase', *J. Clin. Invest*, 98(2), pp. 345–351.

Pompili, M. *et al.* (2009) 'Quality of Life and Suicide Risk in Patients With Diabetes Mellitus', *Psychosomatics*, 50(1), pp. 16–23. Available at: https://doi.org/10.1176/APPI.PSY.50.1.16.

Pontiroli, A.E. *et al.* (1989) 'Intranasal Glucagon as Remedy for Hypoglycemia: Studies in Healthy Subjects and Type I Diabetic Patients', *Diabetes Care*, 12(9), pp. 604–609. Available at: https://doi.org/10.2337/DIACARE.12.9.604.

Pontiroli, A.E. and Tagliabue, E. (2019) 'Therapeutic Use of Intranasal Glucagon: Resolution of Hypoglycemia', *International Journal of Molecular Sciences*, 20(15). Available at: https://doi.org/10.3390/IJMS20153646.

Powell, E.S., Smith-Taillie, L.P. and Popkin, B.M. (2016) 'Added Sugars Intake Across the Distribution of US Children and Adult Consumers: 1977-2012',

Journal of the Academy of Nutrition and Dietetics, 116(10), pp. 1543-1550.e1. Available at: https://doi.org/10.1016/J.JAND.2016.06.003.

Powers, A.C. *et al.* (1990) 'Proglucagon processing similar to normal islets in pancreatic alpha-like cell line derived from transgenic mouse tumor', *Diabetes*, 39(4), pp. 406–414. Available at: https://doi.org/10.2337/DIAB.39.4.406.

Del Prato, S. *et al.* (1994) 'Effect of sustained physiologic hyperinsulinaemia and hyperglycaemia on insulin secretion and insulin sensitivity in man', *Diabetologia*, 37(10), pp. 1025–1035. Available at: https://doi.org/10.1007/BF00400466.

Pribylova, J. and Kozlova, J. (1979) 'Glucose and Galactose Infusions in Newborns of Diabetic and Healthy Mothers', *Biol. Neonate*, 36, pp. 193–197.

Pullen, T.J. *et al.* (2010) 'Identification of genes selectively disallowed in the pancreatic islet', *http://dx.doi.org/10.4161/isl.2.2.11025*, 2(2), pp. 89–95. Available at: https://doi.org/10.4161/ISL.2.2.11025.

Qayyum, N. *et al.* (2021) 'Molecular Sciences Role of Thioredoxin-Interacting Protein in Diseases and Its Therapeutic Outlook', *Int. J. Mol. Sci* [Preprint]. Available at: https://doi.org/10.3390/ijms22052754.

Qi, X. and Tester, R.F. (2019) 'Fructose, galactose and glucose – In health and disease', *Clinical Nutrition ESPEN*, 33, pp. 18–28. Available at: https://doi.org/10.1016/J.CLNESP.2019.07.004.

Qian, W.J. *et al.* (2000) 'Detection of secretion from single pancreatic β-cells using extracellular fluorogenic reactions and confocal fluorescence microscopy', *Analytical Chemistry*, 72(4), pp. 711–717. Available at: https://doi.org/10.1021/AC991085T/ASSET/IMAGES/LARGE/AC991085TF00007.JPEG.

Quesada, I. *et al.* (2008) 'Physiology of the pancreatic α-cell and glucagon secretion: Role in glucose homeostasis and diabetes', *Journal of Endocrinology*, 199(1), pp. 5–19. Available at: https://doi.org/10.1677/JOE-08-0290.

van Raalte, D.H. and Verchere, C.B. (2017) ‘Improving glycaemic control in type 2 diabetes: Stimulate insulin secretion or provide beta-cell rest?’, *Diabetes, Obesity and Metabolism*, 19(9), pp. 1205–1213. Available at: https://doi.org/10.1111/DOM.12935.

Rabuazzo, A.M. *et al.* (1997) ‘Hexokinase Shift to Mitochondria Is Associated With an Increased Sensitivity to Glucose in Rat Pancreatic Islets’, *Diabetes*, 46(7), pp. 1148–1152. Available at: https://doi.org/10.2337/DIAB.46.7.1148.

Rahier, J., Goebbels, R.M. and Henquin, J.C. (1983) ‘Cellular composition of the human diabetic pancreas’, *Diabetologia*, 24(5), pp. 366–371. Available at: https://doi.org/10.1007/BF00251826.

Rajak, S. *et al.* (2021) ‘MTORC1 inhibition drives crinophagic degradation of glucagon’, *Molecular Metabolism*, 53, p. 101286. Available at: https://doi.org/10.1016/J.MOLMET.2021.101286.

Rangarajan, S. *et al.* (2018) ‘Metformin reverses established lung fibrosis in a bleomycin model’, *Nature medicine*, 24(8), p. 1121. Available at: https://doi.org/10.1038/S41591-018-0087-6.

Ravassard, P. *et al.* (2011) ‘A genetically engineered human pancreatic β cell line exhibiting glucose-inducible insulin secretion’, *The Journal of Clinical Investigation*, 121(9), p. 3589. Available at: https://doi.org/10.1172/JCI58447.

Ravier, M.A. *et al.* (2000) ‘The oscillatory behavior of pancreatic islets from mice with mitochondrial glycerol-3-phosphate dehydrogenase knockout’, *Journal of Biological Chemistry*, 275(3), pp. 1587–1593. Available at: https://doi.org/10.1074/jbc.275.3.1587.

Ravier, M.A. and Rutter, G.A. (2005) ‘Glucose or Insulin, but not Zinc Ions, Inhibit Glucagon Secretion From Mouse Pancreatic α-Cells’, *Diabetes*, 54(6), pp. 1789–1797. Available at: https://doi.org/10.2337/DIABETES.54.6.1789.

Reaven, G.M. *et al.* (1987) ‘Documentation of hyperglucagonemia throughout the day in nonobese and obese patients with noninsulin-dependent diabetes

mellitus', *The Journal of clinical endocrinology and metabolism*, 64(1), pp. 106–110. Available at: https://doi.org/10.1210/JCEM-64-1-106.

Reaven, G.M. (1988) 'Banting lecture 1988. Role of insulin resistance in human disease', *Diabetes*, 37(12), pp. 1595–1607. Available at: https://doi.org/10.2337/DIAB.37.12.1595.

Redondo, M.J. *et al.* (2008) 'Concordance for Islet Autoimmunity among Monozygotic Twins', *https://doi.org/10.1056/NEJMc0805398*, 359(26), pp. 2849–2850. Available at: https://doi.org/10.1056/NEJMC0805398.

Regina, C.C., Mu'ti, A. and Fitriany, E. (2022) 'Diabetes Mellitus Type 2', *Verdure: Health Science Journal*, 3(1), pp. 8–17. Available at: https://www.ncbi.nlm.nih.gov/books/NBK513253/ (Accessed: 10 April 2023).

Reissaus, C.A. and Piston, D.W. (2017) 'Reestablishment of Glucose Inhibition of Glucagon Secretion in Small Pseudoislets', *Diabetes*, 66(4), pp. 960–969. Available at: https://doi.org/10.2337/DB16-1291.

Ribalet, B. and Eddlestone, G.T. (1995) 'Characterization of the G protein coupling of a somatostatin receptor to the K+ATP channel in insulin-secreting mammalian HIT and RIN cell lines.', *The Journal of Physiology*, 485(Pt 1), p. 73. Available at: https://doi.org/10.1113/JPHYSIOL.1995.SP020713.

Ribeiro, C.M.P. and Boucher, R.C. (2010) 'Role of Endoplasmic Reticulum Stress in Cystic Fibrosis–Related Airway Inflammatory Responses', *Proceedings of the American Thoracic Society*, 7(6), p. 387. Available at: https://doi.org/10.1513/PATS.201001-017AW.

Richards-Williams, C. *et al.* (2008) 'Extracellular ATP and zinc are co-secreted with insulin and activate multiple P2X purinergic receptor channels expressed by islet beta-cells to potentiate insulin secretion', *Purinergic Signalling*, 4(4), p. 393. Available at: https://doi.org/10.1007/S11302-008-9126-Y.

Richter, M.M. *et al.* (2022) 'The Liver–α-Cell Axis in Health and in Disease', *Diabetes*, 71(9), pp. 1852–1861. Available at: https://doi.org/10.2337/DBI22-

0004.

Rickels, M.R. (2019) ‘Hypoglycemia-associated autonomic failure, counterregulatory responses, and therapeutic options in type 1 diabetes’, *Annals of the New York Academy of Sciences*, 1454(1), pp. 68–79. Available at: https://doi.org/10.1111/NYAS.14214.

Riordan, J.R. *et al.* (1989) ‘Identification of the Cystic Fibrosis Gene: Cloning and Characterization of Complementary DNA’, *Science*, 245(4922), pp. 1066–1073. Available at: https://doi.org/10.1126/SCIENCE.2475911.

Riordan, J.R. (2008) ‘CFTR Function and Prospects for Therapy’, *https://doi.org/10.1146/annurev.biochem.75.103004.142532*, 77, pp. 701–726. Available at: https://doi.org/10.1146/ANNUREV.BIOCHEM.75.103004.142532.

Rix, I. *et al.* (2019) ‘Glucagon Physiology’, *Canadian Journal of Diabetes*, 34(3), pp. 187–188. Available at: https://doi.org/10.1016/S1499-2671(10)43015-4.

Rizza, R.A. *et al.* (1985) ‘Production of insulin resistance by hyperinsulinaemia in man’, *Diabetologia*, 28(2), pp. 70–75. Available at: https://doi.org/10.1007/BF00279918/METRICS.

Rodriguez-Diaz, R. *et al.* (2011a) ‘Alpha cells secrete acetylcholine as a non-neuronal paracrine signal priming beta cell function in humans’, *Nature Medicine 2011 17:7*, 17(7), pp. 888–892. Available at: https://doi.org/10.1038/nm.2371.

Rodriguez-Diaz, R. *et al.* (2011b) ‘Innervation patterns of autonomic axons in the human endocrine pancreas’, *Cell metabolism*, 14(1), pp. 45–54. Available at: https://doi.org/10.1016/J.CMET.2011.05.008.

Rodriguez-Diaz, R. *et al.* (2020) ‘The Local Paracrine Actions of the Pancreatic α-Cell’, *Diabetes*, 69(4), pp. 550–558. Available at: https://doi.org/10.2337/DBI19-0002.

Roep, B.O. *et al.* (2020) ‘Type 1 diabetes mellitus as a disease of the β-cell (do

not blame the immune system?)', *Nature Reviews Endocrinology 2020 17:3*, 17(3), pp. 150–161. Available at: https://doi.org/10.1038/s41574-020-00443-4.

Rogers, C.S. *et al.* (2008) 'Disruption of the CFTR gene produces a model of cystic fibrosis in newborn pigs', *Science (New York, N.Y.)*, 321(5897), pp. 1837–1841. Available at: https://doi.org/10.1126/SCIENCE.1163600.

Roh, E., Song, D.K. and Kim, M.-S. (2016) 'Emerging role of the brain in the homeostatic regulation of energy and glucose metabolism', *Experimental & Molecular Medicine*, 48, p. 216. Available at: https://doi.org/10.1038/emm.2016.4.

Rolfe, D.F.S. and Brand, M.D. (1996) 'Contribution of mitochondrial proton leak to skeletal muscle respiration and to standard metabolic rate', *https://doi.org/10.1152/ajpcell.1996.271.4.C1380*, 271(4 40-4). Available at: https://doi.org/10.1152/AJPCELL.1996.271.4.C1380.

Romaní-Pérez, M. *et al.* (2013) 'Pulmonary GLP-1 receptor increases at birth and exogenous GLP-1 receptor agonists augmented surfactant-protein levels in litters from normal and nitrofen-treated pregnant rats', *Endocrinology*, 154(3), pp. 1144–1155. Available at: https://doi.org/10.1210/EN.2012-1786.

Rommens, J.M. *et al.* (1989) 'Identification of the Cystic Fibrosis Gene: Chromosome Walking and Jumping', *Science*, 245(4922), pp. 1059–1065. Available at: https://doi.org/10.1126/SCIENCE.2772657.

Rorsman, P. and Huising, M.O. (2018) 'The somatostatin-secreting pancreatic δ-cell in health and disease', *Nature reviews. Endocrinology*, 14(7), p. 404. Available at: https://doi.org/10.1038/S41574-018-0020-6.

Rosen, B.H. *et al.* (2018) 'Animal and model systems for studying cystic fibrosis', *Journal of Cystic Fibrosis*, 17(2), pp. S28–S34. Available at: https://doi.org/10.1016/J.JCF.2017.09.001.

Rosenberg, M., Azevedo, N.F. and Ivask, A. (2019) 'Propidium iodide staining underestimates viability of adherent bacterial cells', *Scientific Reports 2019 9:1*,

9(1), pp. 1–12. Available at: https://doi.org/10.1038/s41598-019-42906-3.

Rosenfalck, A.M. *et al.* (1992) ‘Nasal glucagon in the treatment of hypoglycaemia in type 1 (insulin-dependent) diabetic patients’, *Diabetes Research and Clinical Practice*, 17(1), pp. 43–50. Available at: https://doi.org/10.1016/0168-8227(92)90042-P.

Rosenstock, J. *et al.* (2021) ‘Efficacy and safety of a novel dual GIP and GLP-1 receptor agonist tirzepatide in patients with type 2 diabetes (SURPASS-1): a double-blind, randomised, phase 3 trial’, *Lancet (London, England)*, 398(10295), pp. 143–155. Available at: https://doi.org/10.1016/S0140-6736(21)01324-6.

Ross, F.A., Jensen, T.E. and Hardie, D.G. (2016) ‘Differential regulation by AMP and ADP of AMPK complexes containing different γ subunit isoforms’, *Biochemical Journal*, 473(2), pp. 189–199. Available at: https://doi.org/10.1042/BJ20150910.

Rotti, P.G. *et al.* (2018) ‘Pancreatic and Islet Remodeling in Cystic Fibrosis Transmembrane Conductance Regulator (CFTR) Knockout Ferrets’, *The American Journal of Pathology*, 188(4), p. 876. Available at: https://doi.org/10.1016/J.AJPATH.2017.12.015.

Routh, V.H. (2010) ‘Glucose Sensing Neurons in the Ventromedial Hypothalamus’, *Sensors (Basel, Switzerland)*, 10(10), p. 9002. Available at: https://doi.org/10.3390/S101009002.

Roy, T. and Lloyd, C.E. (2012) ‘Epidemiology of depression and diabetes: a systematic review’, *Journal of affective disorders*, 142 Suppl(SUPPL.). Available at: https://doi.org/10.1016/S0165-0327(12)70004-6.

Rui, L. (2014) ‘Energy Metabolism in the Liver’, *Comprehensive Physiology*, 4(1), p. 177. Available at: https://doi.org/10.1002/CPHY.C130024.

Said, E.A. *et al.* (2022) ‘The AMPK activator A-769662 inhibits human TASK3 potassium channels in an AMPK-independent manner’, *bioRxiv*, p.

2022.05.24.493214. Available at: https://doi.org/10.1101/2022.05.24.493214.

Saint-Criq, V. and Gray, M.A. (2017) ‘Role of CFTR in epithelial physiology’, *Cellular and Molecular Life Sciences*, 74(1), p. 93. Available at: https://doi.org/10.1007/S00018-016-2391-Y.

Sakakibara, R. *et al.* (1997) ‘Characterization of a human placental fructose-6-phosphate, 2-kinase/fructose-2,6-bisphosphatase’, *Journal of biochemistry*, 122(1), pp. 122–128. Available at: https://doi.org/10.1093/OXFORDJOURNALS.JBCHEM.A021719.

Sakamoto, K. *et al.* (2005) ‘Deficiency of LKB1 in skeletal muscle prevents AMPK activation and glucose uptake during contraction’, *The EMBO Journal*, 24(10), p. 1810. Available at: https://doi.org/10.1038/SJ.EMBOJ.7600667.

Salpeter, S.R. *et al.* (2008) ‘Meta-analysis: Metformin Treatment in Persons at Risk for Diabetes Mellitus’, *The American Journal of Medicine*, 121(2), pp. 149-157.e2. Available at: https://doi.org/10.1016/J.AMJMED.2007.09.016.

Salpeter, S.R. *et al.* (2010) ‘Risk of fatal and nonfatal lactic acidosis with metformin use in type 2 diabetes mellitus’, *Cochrane Database of Systematic Reviews*, 2017(12). Available at: https://doi.org/10.1002/14651858.CD002967.PUB3/MEDIA/CDSR/CD002967/REL0003/CD002967/IMAGE_N/NCD002967-CMP-002-03.PNG.

Salt, I.P. *et al.* (1998) ‘AMP-activated protein kinase is activated by low glucose in cell lines derived from pancreatic β cells, and may regulate insulin release’, *Biochemical Journal*, 335(3), pp. 533–539. Available at: https://doi.org/10.1042/BJ3350533.

Samuel, V.T. and Shulman, G.I. (2016) ‘The pathogenesis of insulin resistance: integrating signaling pathways and substrate flux’, *The Journal of Clinical Investigation*, 126(1), p. 12. Available at: https://doi.org/10.1172/JCI77812.

Sanchez, P.K.M. *et al.* (2021) ‘LDHA is enriched in human islet alpha cells and upregulated in type 2 diabetes’, *Biochemical and Biophysical Research*

Communications, 568, pp. 158–166. Available at: https://doi.org/10.1016/J.BBRC.2021.06.065.

Sandberg Lab Tool: Pancreas (no date). Available at: https://sandberglab.se/tool/pancreas/ (Accessed: 10 April 2023).

Sanders, M.J. *et al.* (2007) 'Defining the Mechanism of Activation of AMP-activated Protein Kinase by the Small Molecule A-769662, a Member of the Thienopyridone Family', *Journal of Biological Chemistry*, 282(45), pp. 32539–32548. Available at: https://doi.org/10.1074/JBC.M706543200.

Sanders, M.J. *et al.* (2022) 'Natural (dihydro)phenanthrene plant compounds are direct activators of AMPK through its allosteric drug and metabolite–binding site', *Journal of Biological Chemistry*, 298(5), p. 101852. Available at: https://doi.org/10.1016/J.JBC.2022.101852.

Sanders, N.M., Dunn-Meynell, A.A. and Levin, B.E. (2004) 'Third Ventricular Alloxan Reversibly Impairs Glucose Counterregulatory Responses'. Available at: http://diabetesjournals.org/diabetes/article-pdf/53/5/1230/647168/zdb00504001230.pdf (Accessed: 28 March 2023).

Sanz, P., Rubio, T. and Garcia-Gimeno, M.A. (2013) 'AMPKbeta subunits: more than just a scaffold in the formation of AMPK complex', *The FEBS Journal*, 280(16), pp. 3723–3733. Available at: https://doi.org/10.1111/FEBS.12364.

Sapra, A. and Bhandari, P. (2022) 'Diabetes Mellitus', *StatPearls* [Preprint]. Available at: https://www.ncbi.nlm.nih.gov/books/NBK551501/ (Accessed: 10 April 2023).

Saunders, D.C. *et al.* (2020) 'Pancreatlas: Applying an Adaptable Framework to Map the Human Pancreas in Health and Disease', *Patterns*, 1(8), p. 100120. Available at: https://doi.org/10.1016/J.PATTER.2020.100120.

Sautin, Y.Y. *et al.* (2023) 'Phosphatidylinositol 3-Kinase-Mediated Effects of Glucose on Vacuolar H+-ATPase Assembly, Translocation, and Acidification of Intracellular Compartments in Renal Epithelial Cells',

https://doi.org/10.1128/MCB.25.2.575-589.2005, 25(2), pp. 575–589. Available at: https://doi.org/10.1128/MCB.25.2.575-589.2005.

Van Schaftingen, E. *et al.* (1982) 'A Kinetic Study of Pyrophosphate: Fructose-6-Phosphate Phosphotransferase from Potato Tubers', *European Journal of Biochemistry*, 129(1), pp. 191–195. Available at: https://doi.org/10.1111/J.1432-1033.1982.TB07039.X.

Schmidt, P.T. *et al.* (2005) 'A role for pancreatic polypeptide in the regulation of gastric emptying and short-term metabolic control', *The Journal of clinical endocrinology and metabolism*, 90(9), pp. 5241–5246. Available at: https://doi.org/10.1210/JC.2004-2089.

Schuit, F. *et al.* (1997) 'Metabolic Fate of Glucose in Purified Islet Cells: GLUCOSE-REGULATED ANAPLEROSIS IN β CELLS', *Journal of Biological Chemistry*, 272(30), pp. 18572–18579. Available at: https://doi.org/10.1074/JBC.272.30.18572.

Schwartz, G.J. and Blouet, C. (2011) 'Nutrient-Sensing Hypothalamic TXNIP Links Nutrient Excess to Energy Imbalance in Mice', *Journal of Neuroscience*, 31(16), pp. 6019–6027. Available at: https://doi.org/10.1523/JNEUROSCI.6498-10.2011.

Scotet, V., L'hostis, C. and Férec, C. (2020) 'The Changing Epidemiology of Cystic Fibrosis: Incidence, Survival and Impact of the CFTR Gene Discovery', *Genes*, 11(6). Available at: https://doi.org/10.3390/GENES11060589.

Scott, J.W. *et al.* (2014) 'Small Molecule Drug A-769662 and AMP Synergistically Activate Naive AMPK Independent of Upstream Kinase Signaling', *Chemistry & Biology*, 21(5), pp. 619–627. Available at: https://doi.org/10.1016/J.CHEMBIOL.2014.03.006.

Scott, J.W. *et al.* (2015) 'Inhibition of AMP-Activated Protein Kinase at the Allosteric Drug-Binding Site Promotes Islet Insulin Release', *Chemistry & Biology*, 22(6), pp. 705–711. Available at:

https://doi.org/10.1016/J.CHEMBIOL.2015.05.011.

Segel, S.A., Paramore, D.S. and Cryer, P.E. (2002) ‘Hypoglycemia-associated autonomic failure in advanced type 2 diabetes’, *Diabetes*, 51(3), pp. 724–733. Available at: https://doi.org/10.2337/DIABETES.51.3.724.

Segerstolpe, Å. *et al.* (2016) ‘Single-Cell Transcriptome Profiling of Human Pancreatic Islets in Health and Type 2 Diabetes’, *Cell Metabolism*, 24(4), pp. 593–607. Available at: https://doi.org/10.1016/J.CMET.2016.08.020.

Sekine, N. *et al.* (1994) ‘Low lactate dehydrogenase and high mitochondrial glycerol phosphate dehydrogenase in pancreatic beta-cells. Potential role in nutrient sensing.’, *Journal of Biological Chemistry*, 269(7), pp. 4895–4902. Available at: https://doi.org/10.1016/S0021-9258(17)37629-9.

Sellick, C.A., Campbell, R.N. and Reece, R.J. (2008) ‘Chapter 3 Galactose Metabolism in Yeast—Structure and Regulation of the Leloir Pathway Enzymes and the Genes Encoding Them’, *International Review of Cell and Molecular Biology*, 269, pp. 111–150. Available at: https://doi.org/10.1016/S1937-6448(08)01003-4.

Sener, A. *et al.* (1985) ‘Anomeric specificity of hexokinase and glucokinase activities in liver and insulin-producing cells.’, *Biochemical Journal*, 230(2), p. 345. Available at: https://doi.org/10.1042/BJ2300345.

Seo, S. *et al.* (2008) ‘Acute Effects of Glucagon-Like Peptide-1 on Hypothalamic Neuropeptide and AMP Activated Kinase Expression in Fasted Rats’, *Endocrine Journal*, 55(5), pp. 867–874.

Sha, W., Hu, F. and Bu, S. (2020) ‘Mitochondrial dysfunction and pancreatic islet β-cell failure (Review)’, *Experimental and Therapeutic Medicine*, 20(6), pp. 1–1. Available at: https://doi.org/10.3892/ETM.2020.9396.

Sharma, R. and Tiwari, S. (2021) ‘Renal gluconeogenesis in insulin resistance: A culprit for hyperglycemia in diabetes’, *World Journal of Diabetes*, 12(5), p. 556. Available at: https://doi.org/10.4239/WJD.V12.I5.556.

Sharma, R.B. and Alonso, L.C. (2014) ‘Lipotoxicity in the pancreatic beta cell: Not just survival and function, but proliferation as well?’, *Current Diabetes Reports*, 14(6), p. 492. Available at: https://doi.org/10.1007/s11892-014-0492-2.

Sheikh, S. *et al.* (2017) ‘Reduced β-cell secretory capacity in pancreatic-insufficient, but not pancreatic-sufficient, cystic fibrosis despite normal glucose tolerance’, *Diabetes*, 66(1), pp. 134–144. Available at: https://doi.org/10.2337/DB16-0394/-/DC1.

Shen, L. *et al.* (2021) ‘PGC1α regulates mitochondrial oxidative phosphorylation involved in cisplatin resistance in ovarian cancer cells via nucleo-mitochondrial transcriptional feedback’, *Experimental Cell Research*, 398(1), p. 112369. Available at: https://doi.org/10.1016/J.YEXCR.2020.112369.

Shimazu, T. and Minokoshi, Y. (2017) ‘Systemic Glucoregulation by Glucose-Sensing Neurons in the Ventromedial Hypothalamic Nucleus (VMH)’, *Journal of the Endocrine Society*, 1(5), pp. 449–459. Available at: https://doi.org/10.1210/JS.2016-1104.

da Silva Rosa, S.C. *et al.* (2020) ‘Mechanisms of muscle insulin resistance and the cross-talk with liver and adipose tissue’, *Physiological reports*, 8(19). Available at: https://doi.org/10.14814/PHY2.14607.

Da Silva Xavier, G. *et al.* (2000) ‘Role of AMP-activated protein kinase in the regulation by glucose of islet beta cell gene expression’, *Proceedings of the National Academy of Sciences of the United States of America*, 97(8), p. 4023. Available at: https://doi.org/10.1073/PNAS.97.8.4023.

Da Silva Xavier, G. (2018) ‘The Cells of the Islets of Langerhans’, *Journal of Clinical Medicine 2018, Vol. 7, Page 54*, 7(3), p. 54. Available at: https://doi.org/10.3390/JCM7030054.

Slucca, M. *et al.* (2010) ‘ATP-Sensitive K+ Channel Mediates the Zinc Switch-Off Signal for Glucagon Response During Glucose Deprivation’, *Diabetes*, 59(1), pp. 128–134. Available at: https://doi.org/10.2337/DB09-1098.

Smith, P.A., Sellers, L.A. and Humphrey, P.P.A. (2001) ‘Somatostatin activates two types of inwardly rectifying K+ channels in MIN-6 cells’, *The Journal of Physiology*, 532(Pt 1), p. 127. Available at: https://doi.org/10.1111/J.1469-7793.2001.0127G.X.

Soejima, K. and Landing, B.H. (1986) ‘Pancreatic islets in older patients with cystic fibrosis with and without diabetes mellitus: morphometric and immunocytologic studies’, *Pediatric pathology*, 6(1), pp. 25–46. Available at: https://doi.org/10.3109/15513818609025923.

Solar, M. *et al.* (2009) ‘Pancreatic exocrine duct cells give rise to insulin-producing beta cells during embryogenesis but not after birth’, *Developmental cell*, 17(6), pp. 849–860. Available at: https://doi.org/10.1016/J.DEVCEL.2009.11.003.

Solloway, M.J. *et al.* (2015) ‘Glucagon Couples Hepatic Amino Acid Catabolism to mTOR-Dependent Regulation of α-Cell Mass’, *Cell reports*, 12(3), pp. 495–510. Available at: https://doi.org/10.1016/J.CELREP.2015.06.034.

Solomou, A. *et al.* (2015) ‘The zinc transporter Slc30a8/ZnT8 is required in a subpopulation of pancreatic α;-cells for hypoglycemia-induced glucagon secretion’, *Journal of Biological Chemistry*, 290(35), pp. 21432–21442. Available at: https://doi.org/10.1074/JBC.M115.645291.

Song, Q. *et al.* (2020) ‘The emerging roles of vacuolar-type ATPase-dependent Lysosomal acidification in neurodegenerative diseases’, *Translational Neurodegeneration 2020 9:1*, 9(1), pp. 1–14. Available at: https://doi.org/10.1186/S40035-020-00196-0.

Song, Z. and Routh, V.H. (2006) ‘Recurrent hypoglycemia reduces the glucose sensitivity of glucose-inhibited neurons in the ventromedial hypothalamus nucleus’, *American journal of physiology. Regulatory, integrative and comparative physiology*, 291(5). Available at: https://doi.org/10.1152/AJPREGU.00148.2006.

De Souza Almeida Matos, A.L. *et al.* (2019) ‘Allosteric regulation of AMP-activated protein kinase by adenylate nucleotides and small-molecule drugs’, *Biochemical Society Transactions*, 47(2), pp. 733–741. Available at: https://doi.org/10.1042/BST20180625.

Spégel, P. and Mulder, H. (2020) ‘Metabolomics Analysis of Nutrient Metabolism in β-Cells’, *Journal of Molecular Biology*, 432(5), pp. 1429–1445. Available at: https://doi.org/10.1016/J.JMB.2019.07.020.

Sprague, J.E. and María Arbeláez, A. (2011) ‘Glucose Counterregulatory Responses to Hypoglycemia’, *Pediatr Endocrinol Rev*, 9(1), pp. 463–475.

Stamenkovic, J.A. *et al.* (2015) ‘Inhibition of the malate-aspartate shuttle in mouse pancreatic islets abolishes glucagon secretion without affecting insulin secretion’, *Biochem. J*, 468, pp. 49–63. Available at: https://doi.org/10.1042/BJ20140697.

Stanley, S.A. *et al.* (2016) ‘Bidirectional electromagnetic control of the hypothalamus regulates feeding and metabolism’, *Nature 2016 531:7596*, 531(7596), pp. 647–650. Available at: https://doi.org/10.1038/nature17183.

Stedman, M. *et al.* (2020) ‘Cost of hospital treatment of type 1 diabetes (T1DM) and type 2 diabetes (T2DM) compared to the non-diabetes population: a detailed economic evaluation’, *BMJ Open*, 10(5), p. e033231. Available at: https://doi.org/10.1136/BMJOPEN-2019-033231.

Steele, C. *et al.* (2004) ‘Insulin Secretion in Type 1 Diabetes’, *Diabetes*, 53(2), pp. 426–433. Available at: https://doi.org/10.2337/DIABETES.53.2.426.

Steinberg, G.R. and Carling, D. (2019) ‘AMP-activated protein kinase: the current landscape for drug development’, *Nature Reviews Drug Discovery 2019 18:7*, 18(7), pp. 527–551. Available at: https://doi.org/10.1038/s41573-019-0019-2.

Steinberg, G.R., Rush, J.W.E. and Dyck, D.J. (2003) ‘AMPK expression and phosphorylation are increased in rodent muscle after chronic leptin treatment’,

American Journal of Physiology - Endocrinology and Metabolism, 284(3 47-3). Available at: https://doi.org/10.1152/AJPENDO.00318.2002/ASSET/IMAGES/LARGE/H10331195004.JPEG.

Steiner, D.F. (1998) 'The proprotein convertases', *Current opinion in chemical biology*, 2(1), pp. 31–39. Available at: https://doi.org/10.1016/S1367-5931(98)80033-1.

Steneberg, P. *et al.* (2018) 'PAN-AMPK activator O304 improves glucose homeostasis and microvascular perfusion in mice and type 2 diabetes patients', *JCI insight*, 3(12). Available at: https://doi.org/10.1172/JCI.INSIGHT.99114.

Strowski, M.Z. *et al.* (2000) 'Somatostatin Inhibits Insulin and Glucagon Secretion via Two Receptor Subtypes: An in Vitro Study of Pancreatic Islets from Somatostatin Receptor 2 Knockout Mice', *Endocrinology*, 141(1), pp. 111–117. Available at: https://doi.org/10.1210/ENDO.141.1.7263.

Stumvoll, M. *et al.* (1995) 'Metabolic effects of metformin in non-insulin-dependent diabetes mellitus', *The New England journal of medicine*, 333(9), pp. 550–554. Available at: https://doi.org/10.1056/NEJM199508313330903.

Suga, T. *et al.* (2019) 'SGLT1 in pancreatic α cells regulates glucagon secretion in mice, possibly explaining the distinct effects of SGLT2 inhibitors on plasma glucagon levels', *Molecular metabolism*, 19, pp. 1–12. Available at: https://doi.org/10.1016/J.MOLMET.2018.10.009.

Suh, S.W. *et al.* (2005) 'Pyruvate Administered After Severe Hypoglycemia Reduces Neuronal Death and Cognitive Impairment', *Diabetes*, 54, pp. 1452–1458. Available at: http://diabetesjournals.org/diabetes/article-pdf/54/5/1452/380247/zdb00505001452.pdf (Accessed: 29 March 2023).

Sun, G. *et al.* (2015) 'LKB1 and AMPKα1 are required in pancreatic alpha cells for the normal regulation of glucagon secretion and responses to hypoglycemia', *Molecular Metabolism*, 4(4), pp. 277–286. Available at:

https://doi.org/10.1016/j.molmet.2015.01.006.

Sun, H. *et al.* (2021) ‘IDF Diabetes Atlas: Global, regional and country-level diabetes prevalence estimates for 2021 and projections for 2045’, *Diabetes Research and Clinical Practice*, 183. Available at: https://doi.org/10.1016/J.DIABRES.2021.109119.

Sun, X. *et al.* (2014) ‘Gastrointestinal pathology in juvenile and adult CFTR-knockout ferrets’, *The American journal of pathology*, 184(5), pp. 1309–1322. Available at: https://doi.org/10.1016/J.AJPATH.2014.01.035.

Sun, X. *et al.* (2017) ‘CFTR Influences Beta Cell Function and Insulin Secretion Through Non-Cell Autonomous Exocrine-Derived Factors’, *Endocrinology*, 158(10), p. 3325. Available at: https://doi.org/10.1210/EN.2017-00187.

Svegliati-Baroni, G. *et al.* (2011) ‘Glucagon-like peptide-1 receptor activation stimulates hepatic lipid oxidation and restores hepatic signalling alteration induced by a high-fat diet in nonalcoholic steatohepatitis’, *Liver International*, 31(9), pp. 1285–1297. Available at: https://doi.org/10.1111/J.1478-3231.2011.02462.X.

Svendsen, B. *et al.* (2018) ‘Insulin Secretion Depends on Intra-islet Glucagon Signaling’, *Cell Reports*, 25(5). Available at: https://doi.org/10.1016/j.celrep.2018.10.018.

Svendsen, B. and Holst, J.J. (2021) ‘Paracrine regulation of somatostatin secretion by insulin and glucagon in mouse pancreatic islets’, *Diabetologia*, 64(1), pp. 142–151. Available at: https://doi.org/10.1007/S00125-020-05288-0/FIGURES/4.

Swisa, A. *et al.* (2015) ‘Loss of Liver Kinase B1 (LKB1) in Beta Cells Enhances Glucose-stimulated Insulin Secretion Despite Profound Mitochondrial Defects’, *Journal of Biological Chemistry*, 290(34), pp. 20934–20946. Available at: https://doi.org/10.1074/JBC.M115.639237.

Tabák, A.G. *et al.* (2012) ‘Prediabetes: A high-risk state for developingdiabetes’,

Lancet, 379(9833), p. 2279. Available at: https://doi.org/10.1016/S0140-6736(12)60283-9.

Taborsky, G.J., Ahrén, B. and Havel, P.J. (1998) 'Autonomic mediation of glucagon secretion during hypoglycemia: implications for impaired alpha-cell responses in type 1 diabetes.', *Diabetes*, 47(7), pp. 995–1005. Available at: https://doi.org/10.2337/DIABETES.47.7.995.

Taegtmeyer, H. *et al.* (2013) 'Insulin resistance protects the heart from fuel overload in dysregulated metabolic states', *American journal of physiology. Heart and circulatory physiology*, 305(12). Available at: https://doi.org/10.1152/AJPHEART.00854.2012.

Taïb, B. *et al.* (2013) 'Glucose regulates hypothalamic long-chain fatty acid metabolism via AMP-activated kinase (AMPK) in neurons and astrocytes', *Journal of Biological Chemistry*, 288(52), pp. 37216–37229. Available at: https://doi.org/10.1074/jbc.M113.506238.

Takatani, T. *et al.* (2021) 'Insulin receptor substrate 1 (IRS1), but not IRS2, plays a dominant role in regulating pancreatic alpha cell function in mice', *Journal of Biological Chemistry*, 296, p. 100646. Available at: https://doi.org/10.1016/j.jbc.2021.100646.

Takiar, V. *et al.* (2011) 'Activating AMP-activated protein kinase (AMPK) slows renal cystogenesis', *Proceedings of the National Academy of Sciences of the United States of America*, 108(6), pp. 2462–2467. Available at: https://doi.org/10.1073/PNAS.1011498108/SUPPL_FILE/PNAS.201011498SI.PDF.

Talley, J.T. and Mohiuddin, S.S. (2023) 'Biochemistry, Fatty Acid Oxidation', *StatPearls* [Preprint]. Available at: https://www.ncbi.nlm.nih.gov/books/NBK556002/ (Accessed: 11 April 2023).

Tan, J. *et al.* (2022) 'Oxygen is a critical regulator of cellular metabolism and function in cell culture', *bioRxiv*, p. 2022.11.29.516437. Available at:

https://doi.org/10.1101/2022.11.29.516437.

Tang, C.-J. *et al.* (2021) ‘Metformin prevents PFKFB3-related aerobic glycolysis from enhancing collagen synthesis in lung fibroblasts by regulating AMPK/mTOR pathway’, *Experimental and Therapeutic Medicine*, 21(6), pp. 1–8. Available at: https://doi.org/10.3892/ETM.2021.10013.

Tang, C. *et al.* (2020) ‘Mitochondrial quality control in kidney injury and repair’, *Nature Reviews Nephrology 2020 17:5*, 17(5), pp. 299–318. Available at: https://doi.org/10.1038/s41581-020-00369-0.

Tappy, L. and Le, K.A. (2010) ‘Metabolic effects of fructose and the worldwide increase in obesity’, *Physiological Reviews*, 90(1), pp. 23–46. Available at: https://doi.org/10.1152/PHYSREV.00019.2009/ASSET/IMAGES/LARGE/Z9J00011025290007.JPEG.

Taskinen, M.R., Packard, C.J. and Borén, J. (2019) ‘Dietary Fructose and the Metabolic Syndrome’, *Nutrients*, 11(9). Available at: https://doi.org/10.3390/NU11091987.

Tengholm, A. (2014) ‘Purinergic P2Y1 receptors take centre stage in autocrine stimulation of human beta cells’, *Diabetologia*, 57(12), pp. 2436–2439. Available at: https://doi.org/10.1007/S00125-014-3392-8/METRICS.

Tengholm, A. and Gylfe, E. (2017) ‘cAMP signalling in insulin and glucagon secretion’, *Diabetes, Obesity and Metabolism*, 19, pp. 42–53. Available at: https://doi.org/10.1111/DOM.12993.

Tesfaye, N. and Seaquist, E.R. (2010) ‘Neuroendocrine Responses to Hypoglycemia’, *Annals of the New York Academy of Sciences*, 1212, p. 12. Available at: https://doi.org/10.1111/J.1749-6632.2010.05820.X.

The Small molecule AMPK activator O304 acts as an oral PCSK9 inhibitor - Betagenon AB (2015). Available at: https://news.cision.com/betagenon-ab/r/the-small-molecule-ampk-activator-o304-acts-as-an-oral-pcsk9-inhibitor,c9716333 (Accessed: 11 April 2023).

Theret, M. *et al.* (2017) ‘AMPKα1-LDH pathway regulates muscle stem cell self-renewal by controlling metabolic homeostasis’, *The EMBO Journal*, 36(13), pp. 1946–1962. Available at: https://doi.org/10.15252/EMBJ.201695273.

Thielen, L.A. *et al.* (2020) ‘Identification of an Anti-diabetic, Orally Available Small Molecule that Regulates TXNIP Expression and Glucagon Action’, *Cell Metabolism*, 32(3), pp. 353-365.e8. Available at: https://doi.org/10.1016/j.cmet.2020.07.002.

Thieu, V.T. *et al.* (2020) ‘Treatment and prevention of severe hypoglycaemia in people with diabetes: Current and new formulations of glucagon’, *Diabetes, Obesity and Metabolism*, 22(4), pp. 469–479. Available at: https://doi.org/10.1111/DOM.13941.

Thompson, B. and Satin, L.S. (2021) ‘Beta-Cell Ion Channels and Their Role in Regulating Insulin Secretion’, *Comprehensive Physiology*, 11(4), pp. 1–21. Available at: https://doi.org/10.1002/CPHY.C210004.

Thong, F.S.L., Bilan, P.J. and Klip, A. (2007) ‘The Rab GTPase-Activating Protein AS160 Integrates Akt, Protein Kinase C, and AMP-Activated Protein Kinase Signals Regulating GLUT4 Traffic’, *Diabetes*, 56(2), pp. 414–423. Available at: https://doi.org/10.2337/DB06-0900.

Thornton, C., Snowden, M.A. and Carling, D. (1998) ‘Identification of a novel AMP-activated protein kinase β subunit isoform that is highly expressed in skeletal muscle’, *Journal of Biological Chemistry*, 273(20), pp. 12443–12450. Available at: https://doi.org/10.1074/jbc.273.20.12443.

Tian, X.Y. *et al.* (2018) ‘Uncoupling protein 2 in cardiovascular health and disease’, *Frontiers in Physiology*, 9(AUG), p. 1060. Available at: https://doi.org/10.3389/FPHYS.2018.01060/BIBTEX.

To, M.S. *et al.* (2010) ‘Mitochondrial uncoupler FCCP activates proton conductance but does not block store-operated Ca(2+) current in liver cells’, *Archives of biochemistry and biophysics*, 495(2), pp. 152–158. Available at:

https://doi.org/10.1016/J.ABB.2010.01.004.

Toda, C. *et al.* (2016) ‘UCP2 Regulates Mitochondrial Fission and Ventromedial Nucleus Control of Glucose Responsiveness’, *Cell*, 164(5), pp. 872–883. Available at: https://doi.org/10.1016/J.CELL.2016.02.010.

Tofé, S. *et al.* (2005) ‘Insulin-secretion abnormalities and clinical deterioration related to impaired glucose tolerance in cystic fibrosis’, *European Journal of Endocrinology*, 152(2), pp. 241–247. Available at: https://doi.org/10.1530/EJE.1.01836.

Tomic, D., Shaw, J.E. and Magliano, D.J. (2022) ‘The burden and risks of emerging complications of diabetes mellitus’, *Nature Reviews Endocrinology 2022 18:9*, 18(9), pp. 525–539. Available at: https://doi.org/10.1038/s41574-022-00690-7.

Topsakal, S. *et al.* (2016) ‘Alpha lipoic acid attenuates high-fructose-induced pancreatic toxicity’, *Pancreatology*, 16(3), pp. 347–352. Available at: https://doi.org/10.1016/J.PAN.2016.03.001.

Traba, J. *et al.* (2016) ‘An Optimized Protocol to Analyze Glycolysis and Mitochondrial Respiration in Lymphocytes’, *Journal of Visualized Experiments : JoVE*, 2016(117), p. 54918. Available at: https://doi.org/10.3791/54918.

Treebak, J.T. *et al.* (2006) ‘AMPK-Mediated AS160 Phosphorylation in Skeletal Muscle Is Dependent on AMPK Catalytic and Regulatory Subunits’, *Diabetes*, 55(7), pp. 2051–2058. Available at: https://doi.org/10.2337/DB06-0175.

Tsonkova, V.G. *et al.* (2018) ‘The EndoC-βH1 cell line is a valid model of human beta cells and applicable for screenings to identify novel drug target candidates’, *Molecular Metabolism*, 8, p. 144. Available at: https://doi.org/10.1016/J.MOLMET.2017.12.007.

Tudurí, E. *et al.* (2008) ‘Inhibition of Ca2+ signaling and glucagon secretion in mouse pancreatic α-cells by extracellular ATP and purinergic receptors’, *American Journal of Physiology - Endocrinology and Metabolism*, 294(5).

Available at: https://doi.org/10.1152/AJPENDO.00641.2007/SUPPL_FILE/TUDURI_ET_AL_SUPPLEMENTAL_FIG_4.PDF.

Tuggle, K.L. *et al.* (2014) 'Characterization of Defects in Ion Transport and Tissue Development in Cystic Fibrosis Transmembrane Conductance Regulator (CFTR)-Knockout Rats', *PLOS ONE*, 9(3), p. e91253. Available at: https://doi.org/10.1371/JOURNAL.PONE.0091253.

Uc, A. *et al.* (2015) 'Glycaemic regulation and insulin secretion are abnormal in cystic fibrosis pigs despite sparing of islet cell mass', *Clinical science (London, England : 1979)*, 128(2), pp. 131–142. Available at: https://doi.org/10.1042/CS20140059.

UK Prospective Diabetes Study (UKPDS) Group (1998) 'Intensive blood-glucose control with sulphonylureas or insulin compared with conventional treatment and risk of complications in patients with type 2 diabetes (UKPDS 33)', *The Lancet*, 352(9131), pp. 837–853. Available at: https://doi.org/10.1016/S0140-6736(98)07019-6.

Unger, R.H. *et al.* (1959) 'Glucagon Antibodies and Their Use for Immunoassay for Glucagon.', *https://doi.org/10.3181/00379727-102-25338*, 102(3), pp. 621–623. Available at: https://doi.org/10.3181/00379727-102-25338.

Unger, R.H. and Orci, L. (1975) 'The essential role of glucagon in the pathogenesis of diabetes mellitus', *Lancet (London, England)*, 1(7897), pp. 14–16. Available at: https://doi.org/10.1016/S0140-6736(75)92375-2.

Unnikrishnan, R. *et al.* (2017) 'Type 2 Diabetes: Demystifying the Global Epidemic', *Diabetes*, 66(6), pp. 1432–1442. Available at: https://doi.org/10.2337/DB16-0766.

Uzan, B. *et al.* (2009) 'Mechanisms of KGF mediated signaling in pancreatic duct cell proliferation and differentiation', *PloS one*, 4(3). Available at: https://doi.org/10.1371/JOURNAL.PONE.0004734.

Varela, L. *et al.* (2021) ‘Hunger-promoting AgRP neurons trigger an astrocyte-mediated feed-forward autoactivation loop in mice’, *The Journal of Clinical Investigation*, 131(10). Available at: https://doi.org/10.1172/JCI144239.

Vega-Monroy, M.-L.L. de la *et al.* (2011) ‘Beta-Cell Function and Failure in Type 1 Diabetes’, *Type 1 Diabetes - Pathogenesis, Genetics and Immunotherapy* [Preprint]. Available at: https://doi.org/10.5772/22089.

Veit, G. *et al.* (2016) ‘From CFTR biology toward combinatorial pharmacotherapy: Expanded classification of cystic fibrosis mutations’, *Molecular Biology of the Cell*, 27(3), pp. 424–433. Available at: https://doi.org/10.1091/MBC.E14-04-0935.

Vergari, E. *et al.* (2019) ‘Insulin inhibits glucagon release by SGLT2-induced stimulation of somatostatin secretion’, *Nature Communications 2019 10:1*, 10(1), pp. 1–11. Available at: https://doi.org/10.1038/s41467-018-08193-8.

Vial, G., Detaille, D. and Guigas, B. (2019) *Role of Mitochondria in the Mechanism(s) of Action of Metformin*, *Frontiers in Endocrinology*. Frontiers Media S.A. Available at: https://doi.org/10.3389/fendo.2019.00294.

Vieira, E., Liu, Y.J. and Gylfe, E. (2004) ‘Involvement of α1 and β-adrenoceptors in adrenaline stimulation of the glucagon-secreting mouse α-cell’, *Naunyn-Schmiedeberg’s Archives of Pharmacology*, 369(2), pp. 179–183. Available at: https://doi.org/10.1007/S00210-003-0858-5/FIGURES/5.

Vincent, E.E. *et al.* (2015) ‘Differential effects of AMPK agonists on cell growth and metabolism’, *Oncogene*, 34, pp. 3627–3639. Available at: https://doi.org/10.1038/onc.2014.301.

Vincent, F., Bontemps, F. and Van Den Berghe, G. (1992) ‘Inhibition of glycolysis by 5-amino-4-imidazolecarboxamide riboside in isolated rat hepatocytes’, *Biochem. J*, 281, pp. 267–272. Available at: http://portlandpress.com/biochemj/article-pdf/281/1/267/605137/bj2810267.pdf (Accessed: 4 April 2023).

Viollet, B. *et al.* (2010) ‘AMPK inhibition in health and disease’, *Critical Reviews in Biochemistry and Molecular Biology*, 45(4), p. 276. Available at: https://doi.org/10.3109/10409238.2010.488215.

Višnjić, D. *et al.* (2021) ‘AICAr, a Widely Used AMPK Activator with Important AMPK-Independent Effects: A Systematic Review’, *Cells 2021, Vol. 10, Page 1095*, 10(5), p. 1095. Available at: https://doi.org/10.3390/CELLS10051095.

Vlachaki Walker, J.M. *et al.* (2017) ‘AMP-activated protein kinase (AMPK) activator A-769662 increases intracellular calcium and ATP release from astrocytes in an AMPK-independent manner’, *Diabetes, obesity & metabolism*, 19(7), pp. 997–1005. Available at: https://doi.org/10.1111/DOM.12912.

De Vos, A. *et al.* (1995) ‘Human and rat beta cells differ in glucose transporter but not in glucokinase gene expression’, *The Journal of clinical investigation*, 96(5), pp. 2489–2495. Available at: https://doi.org/10.1172/JCI118308.

Vranas, M. *et al.* (2021) ‘Structural Basis for Inhibition of ROS-Producing Respiratory Complex I by NADH-OH’, *Angewandte Chemie - International Edition*, 60(52), pp. 27277–27281. Available at: https://doi.org/10.1002/ANIE.202112165.

Wakeling, M.N. *et al.* (2022) ‘Non-coding variants disrupting a tissue-specific regulatory element in HK1 cause congenital hyperinsulinism’, *Nature Genetics 2022 54:11*, 54(11), pp. 1615–1620. Available at: https://doi.org/10.1038/s41588-022-01204-x.

Walker, J. *et al.* (2003) ‘Activation of AMP-activated protein kinase reduces cAMP-mediated epithelial chloride secretion’, *American journal of physiology. Gastrointestinal and liver physiology*, 285(5). Available at: https://doi.org/10.1152/AJPGI.00077.2003.

Wang, D.-S. *et al.* (2002) ‘Involvement of organic cation transporter 1 in hepatic and intestinal distribution of metformin’, *The Journal of pharmacology and experimental therapeutics*, 302(2), pp. 510–515. Available at:

https://doi.org/10.1124/JPET.102.034140.

Wang, M.Y. *et al.* (2015) ‘Glucagon receptor antibody completely suppresses type 1 diabetes phenotype without insulin by disrupting a novel diabetogenic pathway’, *Proceedings of the National Academy of Sciences of the United States of America*, 112(8), pp. 2503–2508. Available at: https://doi.org/10.1073/PNAS.1424934112/ASSET/25A3EF67-DE25-4B79-86D6-BE5E8BD64003/ASSETS/GRAPHIC/PNAS.1424934112FIG03.JPEG.

Wang, Z. *et al.* (2021) ‘Live-cell imaging of glucose-induced metabolic coupling of β and α cell metabolism in health and type 2 diabetes’, *Communications Biology*, 4(1). Available at: https://doi.org/10.1038/S42003-021-02113-1.

Warren, B.E. *et al.* (2014) ‘Early mitochondrial dysfunction in glycolytic muscle, but not oxidative muscle, of the fructose-fed insulin-resistant rat’, *American Journal of Physiology - Endocrinology and Metabolism*, 306(6), pp. 658–667. Available at: https://doi.org/10.1152/AJPENDO.00511.2013.

Watts, M. and Sherman, A. (2014) ‘Modeling the pancreatic α-cell: dual mechanisms of glucose suppression of glucagon secretion’, *Biophysical journal*, 106(3), pp. 741–751. Available at: https://doi.org/10.1016/J.BPJ.2013.11.4504.

Wei, R. *et al.* (2016) ‘Exenatide exerts direct protective effects on endothelial cells through the AMPK/Akt/eNOS pathway in a GLP-1 receptor-dependent manner’, *American Journal of Physiology - Endocrinology and Metabolism*, 310(11), pp. E947–E957. Available at: https://doi.org/10.1152/AJPENDO.00400.2015/ASSET/IMAGES/LARGE/ZH10111675760006.JPEG.

Wei, Y. and Mojsov, S. (1996) ‘Distribution of GLP-1 and PACAP receptors in human tissues’, *Acta Physiologica Scandinavica*, 157(3), pp. 355–357. Available at: https://doi.org/10.1046/J.1365-201X.1996.42256000.X.

Weightman Potter, P.G. *et al.* (2019) ‘Basal fatty acid oxidation increases after recurrent low glucose in human primary astrocytes’, *Diabetologia*, 62(1), p. 187.

Available at: https://doi.org/10.1007/S00125-018-4744-6.

Weightman Potter, P.G. *et al.* (2022) 'Glutamate Prevents Altered Mitochondrial Function Following Recurrent Low Glucose in Hypothalamic but Not Cortical Primary Rat Astrocytes', *Cells*, 11(21), p. 3422. Available at: https://doi.org/10.3390/CELLS11213422/S1.

Wender, R. *et al.* (2000) 'Astrocytic Glycogen Influences Axon Function and Survival during Glucose Deprivation in Central White Matter', *The Journal of Neuroscience*, 20(18), p. 6804. Available at: https://doi.org/10.1523/JNEUROSCI.20-18-06804.2000.

Wendt, A. and Eliasson, L. (2020) *Pancreatic α-cells – The unsung heroes in islet function*, *Seminars in Cell and Developmental Biology*. Elsevier Ltd. Available at: https://doi.org/10.1016/j.semcdb.2020.01.006.

Weyer, C. *et al.* (1999) 'The natural history of insulin secretory dysfunction and insulin resistance in the pathogenesis of type 2 diabetes mellitus', *The Journal of clinical investigation*, 104(6), pp. 787–794. Available at: https://doi.org/10.1172/JCI7231.

Whicher, C.A., O'Neill, S. and Holt, R.I.G. (2020) 'Diabetes in the UK: 2019', *Diabetic medicine : a journal of the British Diabetic Association*, 37(2), pp. 242–247. Available at: https://doi.org/10.1111/DME.14225.

White, M.G. *et al.* (2020) 'In Situ Analysis Reveals That CFTR Is Expressed in Only a Small Minority of β-Cells in Normal Adult Human Pancreas', *The Journal of Clinical Endocrinology & Metabolism*, 105(5), pp. 1366–1374. Available at: https://doi.org/10.1210/CLINEM/DGZ209.

Wiegers, E.C. *et al.* (2016) 'Brain Lactate Concentration Falls in Response to Hypoglycemia in Patients With Type 1 Diabetes and Impaired Awareness of Hypoglycemia', *Diabetes*, 65(6), pp. 1601–1605. Available at: https://doi.org/10.2337/DB16-0068.

Wilschanski, M. and Novak, I. (2013) 'The Cystic Fibrosis of Exocrine

Pancreas', *Cold Spring Harbor Perspectives in Medicine*, 3(5). Available at: https://doi.org/10.1101/CSHPERSPECT.A009746.

Woods, A. *et al.* (2017) 'Liver-Specific Activation of AMPK Prevents Steatosis on a High-Fructose Diet', *Cell Reports*, 18(13), p. 3043. Available at: https://doi.org/10.1016/J.CELREP.2017.03.011.

Wu, L. *et al.* (2019) 'Metformin Activates the Protective Effects of the AMPK Pathway in Acute Lung Injury Caused by Paraquat Poisoning', *Oxidative Medicine and Cellular Longevity*, 2019. Available at: https://doi.org/10.1155/2019/1709718.

Wu, L., Fritz, J.D. and Powers, A.C. (1998) 'Different Functional Domains of GLUT2 Glucose Transporter Are Required for Glucose Affinity and Substrate Specificity*This work was supported by grants from the Department of Veterans Affairs Research Service (Career Development Award and Merit Review Award), a fellowship award from the Juvenile Diabetes Foundation International (to L.W.), and the Vanderbilt Diabetes Research and Training Center (NIH Grant DK-20593).', *Endocrinology*, 139(10), pp. 4205–4212. Available at: https://doi.org/10.1210/ENDO.139.10.6245.

Wu, N. *et al.* (2013) 'AMPK-Dependent Degradation of TXNIP upon Energy Stress Leads to Enhanced Glucose Uptake via GLUT1', *Molecular Cell*, 49(6), pp. 1167–1175. Available at: https://doi.org/10.1016/J.MOLCEL.2013.01.035.

Wu, T., Horowitz, M. and Rayner, C.K. (2017) 'New insights into the anti-diabetic actions of metformin: from the liver to the gut', *Expert review of gastroenterology & hepatology*, 11(2), pp. 157–166. Available at: https://doi.org/10.1080/17474124.2017.1273769.

Wuttke, A., Idevall-Hagren, O. and Tengholm, A. (2013) 'P2Y1 receptor-dependent diacylglycerol signaling microdomains in β cells promote insulin secretion', *The FASEB Journal*, 27(4), pp. 1610–1620. Available at: https://doi.org/10.1096/FJ.12-221499.

Xiao, B. *et al.* (2011) ‘Structure of mammalian AMPK and its regulation by ADP’, *Nature 2011 472:7342*, 472(7342), pp. 230–233. Available at: https://doi.org/10.1038/nature09932.

Xiao, B. *et al.* (2013) ‘Structural basis of AMPK regulation by small molecule activators’, *Nature Communications*, 4. Available at: https://doi.org/10.1038/NCOMMS4017.

Xiaotian, L. *et al.* (2016) ‘Exenatide Activates the APPL1-AMPK-PPARα Axis to Prevent Diabetic Cardiomyocyte Apoptosis’, *Journal of diabetes research*, 2016. Available at: https://doi.org/10.1155/2016/4219735.

Xu, E. *et al.* (2006) ‘Intra-islet insulin suppresses glucagon release via GABA-GABAA receptor system’, *Cell metabolism*, 3(1), pp. 47–58. Available at: https://doi.org/10.1016/J.CMET.2005.11.015.

Yamada, H. *et al.* (2001) ‘Ca2+-Dependent Exocytosis of l-Glutamate by αTC6, Clonal Mouse Pancreatic α-Cells’, *Diabetes*, 50(5), pp. 1012–1020. Available at: https://doi.org/10.2337/DIABETES.50.5.1012.

Yan, Y. *et al.* (2018) ‘Structure and Physiological Regulation of AMPK’, *International Journal of Molecular Sciences 2018, Vol. 19, Page 3534*, 19(11), p. 3534. Available at: https://doi.org/10.3390/IJMS19113534.

Yan, Y. *et al.* (2019) ‘Structures of AMP-activated protein kinase bound to novel pharmacological activators in phosphorylated, non-phosphorylated, and nucleotide-free states’, *The Journal of Biological Chemistry*, 294(3), p. 953. Available at: https://doi.org/10.1074/JBC.RA118.004883.

Yang, C.S. *et al.* (2010) ‘Hypothalamic AMP-activated protein kinase regulates glucose production’, *Diabetes*, 59(10), pp. 2435–2443. Available at: https://doi.org/10.2337/DB10-0221.

Yang, J., Kalhan, S.C. and Hanson, R.W. (2009) ‘What Is the Metabolic Role of Phosphoenolpyruvate Carboxykinase?’, *The Journal of Biological Chemistry*, 284(40), p. 27025. Available at: https://doi.org/10.1074/JBC.R109.040543.

Yang, X.-J. *et al.* (1999) ‘Hypothalamic Glucose Sensor Similarities to and Differences From Pancreatic-Cell Mechanisms’, *DIABETES*, 48. Available at: http://diabetesjournals.org/diabetes/article-pdf/48/9/1763/364914/10480606.pdf (Accessed: 28 March 2023).

Yi, Y. *et al.* (2016a) ‘A transient metabolic recovery from early life glucose intolerance in cystic fibrosis ferrets occurs during pancreatic remodeling’, *Endocrinology*, 157(5), pp. 1852–1865. Available at: https://doi.org/10.1210/EN.2015-1935/SUPPL_FILE/EN-15-1935.PDF.

Yi, Y. *et al.* (2016b) ‘Abnormal glucose tolerance in infants and young children with cystic fibrosis’, *American Journal of Respiratory and Critical Care Medicine*, 194(8), pp. 974–980. Available at: https://doi.org/10.1164/RCCM.201512-2518OC/SUPPL_FILE/DISCLOSURES.PDF.

Yki-Järvinen, H. (1997) ‘Acute and Chronic Effects of Hyperglycaemia on Glucose Metabolism: Implications for the Development of New Therapies’. Available at: https://doi.org/10.1002/(SICI)1096-9136(199708)14:3.

Yong, H.L. and White, M.F. (2004) ‘Insulin receptor substrate proteins and diabetes’, *Archives of pharmacal research*, 27(4), pp. 361–370. Available at: https://doi.org/10.1007/BF02980074.

Yoon, J.C. (2017) ‘Evolving Mechanistic Views and Emerging Therapeutic Strategies for Cystic Fibrosis–Related Diabetes’, *Journal of the Endocrine Society*, 1(11), pp. 1386–1400. Available at: https://doi.org/10.1210/JS.2017-00362.

Yu, E. and Sharma, S. (2022) ‘Cystic Fibrosis’, *StatPearls* [Preprint]. Available at: https://www.ncbi.nlm.nih.gov/books/NBK493206/ (Accessed: 10 April 2023).

Yu, Q. *et al.* (2019) ‘Glucose controls glucagon secretion by directly modulating cAMP in alpha cells’, *Diabetologia*, 62(7), pp. 1212–1224. Available at: https://doi.org/10.1007/S00125-019-4857-6/FIGURES/6.

Yu, X. *et al.* (2004) ‘Leptinomimetic effects of the AMP kinase activator AICAR

in leptin-resistant rats: Prevention of diabetes and ectopic lipid deposition', *Diabetologia*, 47(11), pp. 2012–2021. Available at: https://doi.org/10.1007/S00125-004-1570-9/FIGURES/7.

Yu, X. *et al.* (2022) 'Mitochondrial complex I subunit deficiency promotes pancreatic α-cell proliferation', *Molecular Metabolism*, 60. Available at: https://doi.org/10.1016/J.MOLMET.2022.101489.

Yuan, S. and Larsson, S.C. (2020) 'An atlas on risk factors for type 2 diabetes: a wide-angled Mendelian randomisation study', *Diabetologia*, 63(11), pp. 2359–2371. Available at: https://doi.org/10.1007/S00125-020-05253-X/FIGURES/2.

Yuan, T. *et al.* (2019) 'Effects of metformin on metabolism of white and brown adipose tissue in obese C57BL/6J mice', *Diabetology and Metabolic Syndrome*, 11(1), pp. 1–10. Available at: https://doi.org/10.1186/S13098-019-0490-2/FIGURES/4.

Yue, J.T.Y. *et al.* (2012) 'Somatostatin receptor type 2 antagonism improves glucagon and corticosterone counterregulatory responses to hypoglycemia in streptozotocin-induced diabetic rats', *Diabetes*, 61(1), pp. 197–207. Available at: https://doi.org/10.2337/DB11-0690.

Yue, J.T.Y. *et al.* (2013) 'Amelioration of Hypoglycemia Via Somatostatin Receptor Type 2 Antagonism in Recurrently Hypoglycemic Diabetic Rats', *Diabetes*, 62(7), p. 2215. Available at: https://doi.org/10.2337/DB12-1523.

Zaborska, K.E. *et al.* (2020) 'Lactate activation of α-cell KATP channels inhibits glucagon secretion by hyperpolarizing the membrane potential and reducing Ca2+ entry', *Molecular Metabolism*, 42, p. 101056. Available at: https://doi.org/10.1016/J.MOLMET.2020.101056.

Zang, G. *et al.* (2015) 'Activated pancreatic stellate cells can impair pancreatic islet function in mice', *Upsala journal of medical sciences*, 120(3), pp. 169–180. Available at: https://doi.org/10.3109/03009734.2015.1032453.

Ždralević, M. *et al.* (2018) 'Double genetic disruption of lactate dehydrogenases

A and B is required to ablate the “Warburg effect” restricting tumor growth to oxidative metabolism’, *The Journal of Biological Chemistry*, 293(41), p. 15947. Available at: https://doi.org/10.1074/JBC.RA118.004180.

Zemel, B.S. *et al.* (2000) ‘Longitudinal relationship among growth, nutritional status, and pulmonary function in children with cystic fibrosis: Analysis of the Cystic Fibrosis Foundation National CF Patient Registry’, *The Journal of Pediatrics*, 137(3), pp. 374–380. Available at: https://doi.org/10.1067/MPD.2000.107891.

Zha, M. *et al.* (2014) ‘Isolation and characterization of islet stellate cells in rat’, *Islets*, 6(2), pp. e28701-1-e28701-7. Available at: https://doi.org/10.4161/ISL.28701.

Zhang, C.S. *et al.* (2014) ‘The lysosomal v-ATPase-ragulator complex is a common activator for AMPK and mTORC1, acting as a switch between catabolism and anabolism’, *Cell Metabolism*, 20(3), pp. 526–540. Available at: https://doi.org/10.1016/j.cmet.2014.06.014.

Zhang, C.S. *et al.* (2017) ‘Fructose-1,6-bisphosphate and aldolase mediate glucose sensing by AMPK’, *Nature 2017 548:7665*, 548(7665), pp. 112–116. Available at: https://doi.org/10.1038/nature23275.

Zhang, C.Y. *et al.* (2001) ‘Uncoupling protein-2 negatively regulates insulin secretion and is a major link between obesity, β cell dysfunction, and type 2 diabetes’, *Cell*, 105(6), pp. 745–755. Available at: https://doi.org/10.1016/S0092-8674(01)00378-6.

Zhang, C.Y. *et al.* (2006) ‘Genipin inhibits UCP2-mediated proton leak and acutely reverses obesity- and high glucose-induced beta cell dysfunction in isolated pancreatic islets’, *Cell metabolism*, 3(6), pp. 417–427. Available at: https://doi.org/10.1016/J.CMET.2006.04.010.

Zhang, Mingfeng *et al.* (2016) ‘Growth factors and medium hyperglycemia induce Sox9+ ductal cell differentiation into β cells in mice with reversal of

diabetes', *Proceedings of the National Academy of Sciences of the United States of America*, 113(3), pp. 650–655. Available at: https://doi.org/10.1073/PNAS.1524200113/SUPPL_FILE/PNAS.201524200SI.PDF.

Zhang, Quan *et al.* (2013) 'Role of KATP channels in glucose-regulated glucagon secretion and impaired counterregulation in type 2 diabetes', *Cell Metabolism*, 18(6), pp. 871–882. Available at: https://doi.org/10.1016/j.cmet.2013.10.014.

Zhang, Q., Dou, H. and Rorsman, P. (2020) '"Resistance is futile?" – paradoxical inhibitory effects of KATP channel closure in glucagon-secreting α-cells', *The Journal of Physiology*, 598(21), pp. 4765–4780. Available at: https://doi.org/10.1113/JP279775.

Zhang, Y. *et al.* (2019) 'GLP-1 Receptor in Pancreatic α-Cells Regulates Glucagon Secretion in a Glucose-Dependent Bidirectional Manner', *Diabetes*, 68(1), pp. 34–44. Available at: https://doi.org/10.2337/DB18-0317.

Zhang, Y.B. *et al.* (2016) 'High fructose causes cardiac hypertrophy via mitochondrial signaling pathway', *American Journal of Translational Research*, 8(11), p. 4869. Available at: /pmc/articles/PMC5126329/ (Accessed: 2 April 2023).

Zhang, Ya Lin *et al.* (2013) 'AMP as a Low-Energy Charge Signal Autonomously Initiates Assembly of AXIN-AMPK-LKB1 Complex for AMPK Activation', *Cell Metabolism*, 18(4), pp. 546–555. Available at: https://doi.org/10.1016/J.CMET.2013.09.005.

Zhao, C. *et al.* (2001) 'Expression and Distribution of Lactate/Monocarboxylate Transporter Isoforms in Pancreatic Islets and the Exocrine Pancreas', *Diabetes*, 50(2), pp. 361–366. Available at: https://doi.org/10.2337/DIABETES.50.2.361.

Zhao, F.-Q. and Keating, A.F. (2007) 'Functional Properties and Genomics of Glucose Transporters', *Current Genomics*, 8(2), p. 113. Available at:

https://doi.org/10.2174/138920207780368187.

Zhao, Hai Lu *et al.* (2008) 'Topographical associations between islet endocrine cells and duct epithelial cells in the adult human pancreas', *Clinical endocrinology*, 69(3), pp. 400–406. Available at: https://doi.org/10.1111/J.1365-2265.2008.03190.X.

Zhao, Ying *et al.* (2008) 'Both Gi and Go heterotrimeric G proteins are required to exert the full effect of norepinephrine on the β-Cell KATP channel', *Journal of Biological Chemistry*, 283(9), pp. 5306–5316. Available at: https://doi.org/10.1074/jbc.M707695200.

Zhao, Y. *et al.* (2010) 'Noradrenaline inhibits exocytosis via the G protein βγ subunit and refilling of the readily releasable granule pool via the αi1/2 subunit', *Journal of Physiology*, 588(18), pp. 3485–3498. Available at: https://doi.org/10.1113/JPHYSIOL.2010.190090.

Zhao, Y. *et al.* (2020) 'PDK4-Deficiency Reprograms Intrahepatic Glucose and Lipid Metabolism to Facilitate Liver Regeneration in Mice', *Hepatology Communications*, 4(4), pp. 504–517. Available at: https://doi.org/10.1002/HEP4.1484.

Zheng, Y., Ley, S.H. and Hu, F.B. (2017) 'Global aetiology and epidemiology of type 2 diabetes mellitus and its complications', *Nature Reviews Endocrinology 2017 14:2*, 14(2), pp. 88–98. Available at: https://doi.org/10.1038/nrendo.2017.151.

Zhong, T. *et al.* (2016) 'Metformin alters DNA methylation genome-wide via the H19/SAHH axis', *Oncogene 2017 36:17*, 36(17), pp. 2345–2354. Available at: https://doi.org/10.1038/onc.2016.391.

Zhong, Y. *et al.* (2012) 'Activation of Endoplasmic Reticulum Stress by Hyperglycemia Is Essential for Müller Cell–Derived Inflammatory Cytokine Production in Diabetes', *Diabetes*, 61(2), pp. 492–504. Available at: https://doi.org/10.2337/DB11-0315.

Zhou, G. *et al.* (2001) ‘Role of AMP-activated protein kinase in mechanism of metformin action’, *Journal of Clinical Investigation*, 108(8), pp. 1167–1174. Available at: https://doi.org/10.1172/JCI13505.

Zhu, L. *et al.* (2018) ‘Involvement of AMP-activated Protein Kinase (AMPK) in Regulation of Cell Membrane Potential in a Gastric Cancer Cell Line’, *Scientific Reports*, 8(1), p. 6028. Available at: https://doi.org/10.1038/S41598-018-24460-6.

Zhu, M. *et al.* (2022) ‘AMPK Activator O304 Protects Against Kidney Aging Through Promoting Energy Metabolism and Autophagy’, *Frontiers in Pharmacology*, 13, p. 574. Available at: https://doi.org/10.3389/FPHAR.2022.836496/BIBTEX.

Zielenski, J. and Tsui, L.-C. (1995) ‘CYSTIC FIBROSIS: GENOTYPIC AND PHENOTYPIC VARIATIONS’, *Annu. Rev. Genetics*, 29, pp. 777–784. Available at: www.annualreviews.org (Accessed: 6 April 2023).

Zierath, J.R. and Kawano, Y. (2003) ‘The effect of hyperglycaemia on glucose disposal and insulin signal transduction in skeletal muscle’, *Best Practice & Research Clinical Endocrinology & Metabolism*, 17(3), pp. 385–398. Available at: https://doi.org/10.1016/S1521-690X(03)00040-X.

Zolin, A. *et al.* (2018) ‘Cystic Fibrosis Mortality in Childhood. Data from European Cystic Fibrosis Society Patient Registry’, *International Journal of Environmental Research and Public Health*, 15(9). Available at: https://doi.org/10.3390/IJERPH15092020.

Zu, X. *et al.* (2013) ‘Chemical Genetics of Acetyl-CoA Carboxylases’, *Molecules 2013, Vol. 18, Pages 1704-1719*, 18(2), pp. 1704–1719. Available at: https://doi.org/10.3390/MOLECULES18021704.